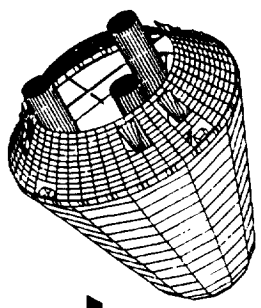


P. 392

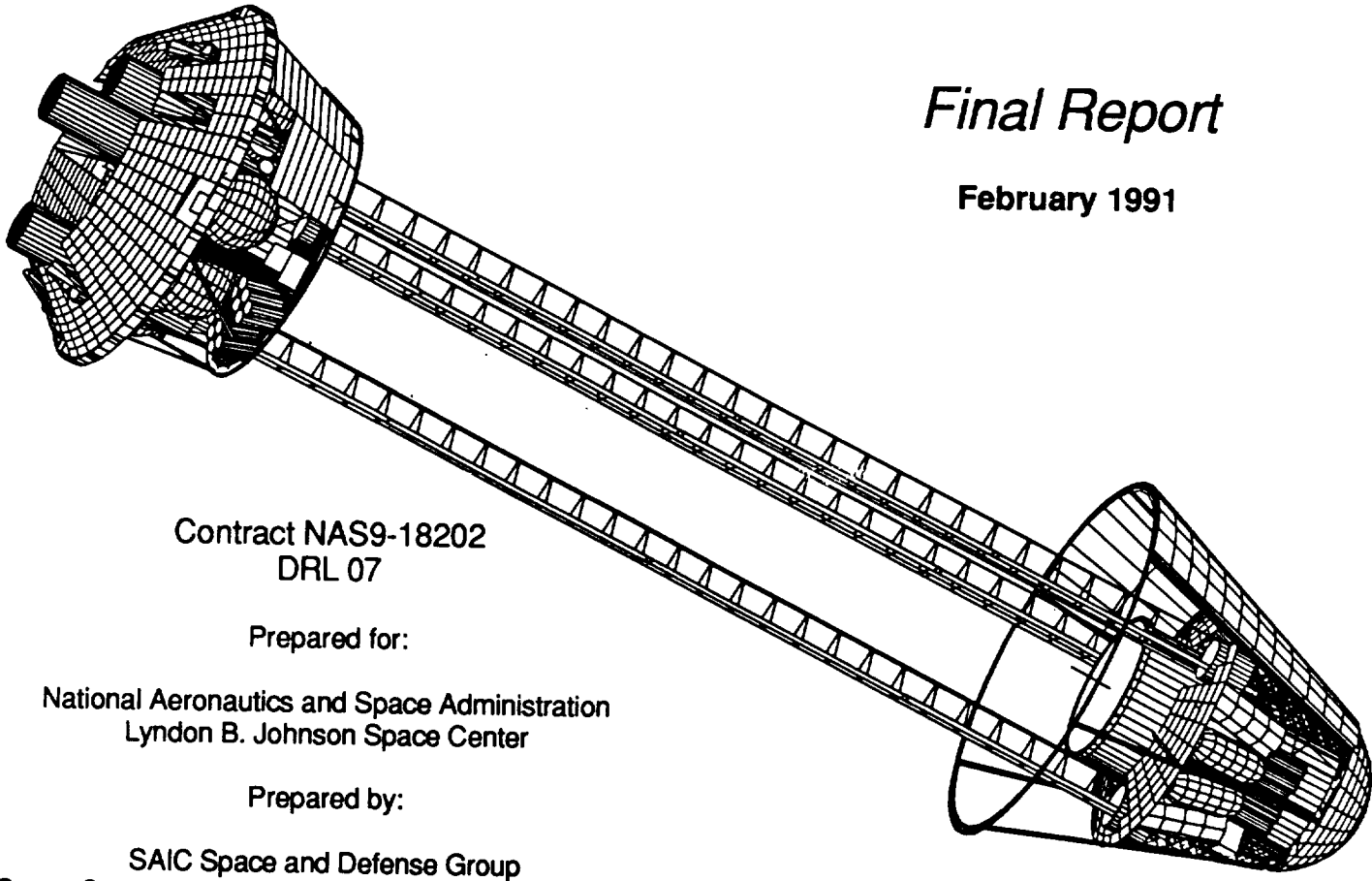
RRS-037
330317



Reusable Reentry Satellite (RRS) System Design Study

Final Report

February 1991



Contract NAS9-18202
DRL 07

Prepared for:

National Aeronautics and Space Administration
Lyndon B. Johnson Space Center

Prepared by:

SAIC Space and Defense Group
Space Systems Integration and Development Division



- Allied Signal
- Astro Aerospace
- ITHACO
- Honeywell
- COR Aerospace
- Microcraft
- Eagle Engineering
- Krug International

Science Applications International Corporation

21151 Western Avenue • Torrance, California 90501-1724 • (213) 781-9022

(NASA-CR-197897) REUSABLE REENTRY
SATELLITE (RRS) SYSTEM DESIGN STUDY
Final Report (Science Applications
International Corp.) 292 p

NO3-14733

Unclass

TOR4.8/10.5

FOREWORD

The overall RRS Phase B Study objective is to design a relatively inexpensive satellite to access space for extended periods of time, with eventual recovery of experiments on Earth. The RRS will be capable of: 1) being launched by a variety of expendable launch vehicles, 2) operating in low-earth orbit as a free-flying unmanned laboratory, and 3) executing an independent atmospheric reentry and soft landing. The RRS will be designed to be refurbished and reused up to three times a year for a period of 10 years. The expected principal use for such a system is research on the effects of variable gravity (0-1.5 g) and radiation on small animals, plants, lower life forms, tissue samples, and materials processes.

The Final Report, in conjunction with the Summary Reports referenced herein, provides a description of the SAIC design and analysis which investigated various hardware options available for fulfilling the NASA RRS requirements using the proposed SAIC concept. Concepts considered emphasized off-the-shelf technology, adequate margins of capability, high reliability, maintainability, cost effectiveness, and compatibility with existing support networks. From these studies, a synergistic preliminary design was developed that can uniquely support a wide range of NASA Life Sciences objectives through use of existing technology and space-proven hardware. Key vehicle features include:

- A highly controllable, multi-redundant control/propulsion approach that can ensure public safety during CONUS operations.
- A solar array implementation that can nominally provide an indefinite 100 to 200 watts of payload power (over 300 watts in a sun-synchronous orbit), eliminating the mission constraints imposed by a stored energy system.
- A low vehicle shielding level to facilitate exposure to the full space radiation spectrum.
- A flexible operating configuration to permit variable experimentation within and among various missions.
- A low Coriolis, uniform gravitational environment, for specimens up to at least Group 3 nonhuman primates (squirrel monkeys and similar species).
- A launch vehicle adaptor approach that permits low risk use of space-proven Delta hardware and technology for either single or dual launches.

The SAIC RRS design effort was led by the Space System Integration and Development Division of SAIC's Space and Defense Group, Torrance, California. The project consisted of a series of contract-identified trade studies led by Mr. Bob Curtis, followed by a preliminary design effort led by Mr. Howard Hayden. The satellite design was developed under a team approach in

which SAIC personnel experienced in satellite development and subsystem technologies led both the overall design effort and the individual design tasks, with specialized contractor/vendor support used as needed for specific hardware applications (Figure i). The overall effort involved numerous SAIC personnel (Table i) from various SAIC divisions who had specific experience applicable to the project. The Fairchild Space support (manufacturing, reliability and cost areas, as well as other valuable observations), was led by Mr. Marty Nachman of the Torrance, California, office. Mr. Michael Richardson of the NASA/JSC New Initiatives Office provided the RRS objectives and policy guidance for the NAS 9-18202 contract.

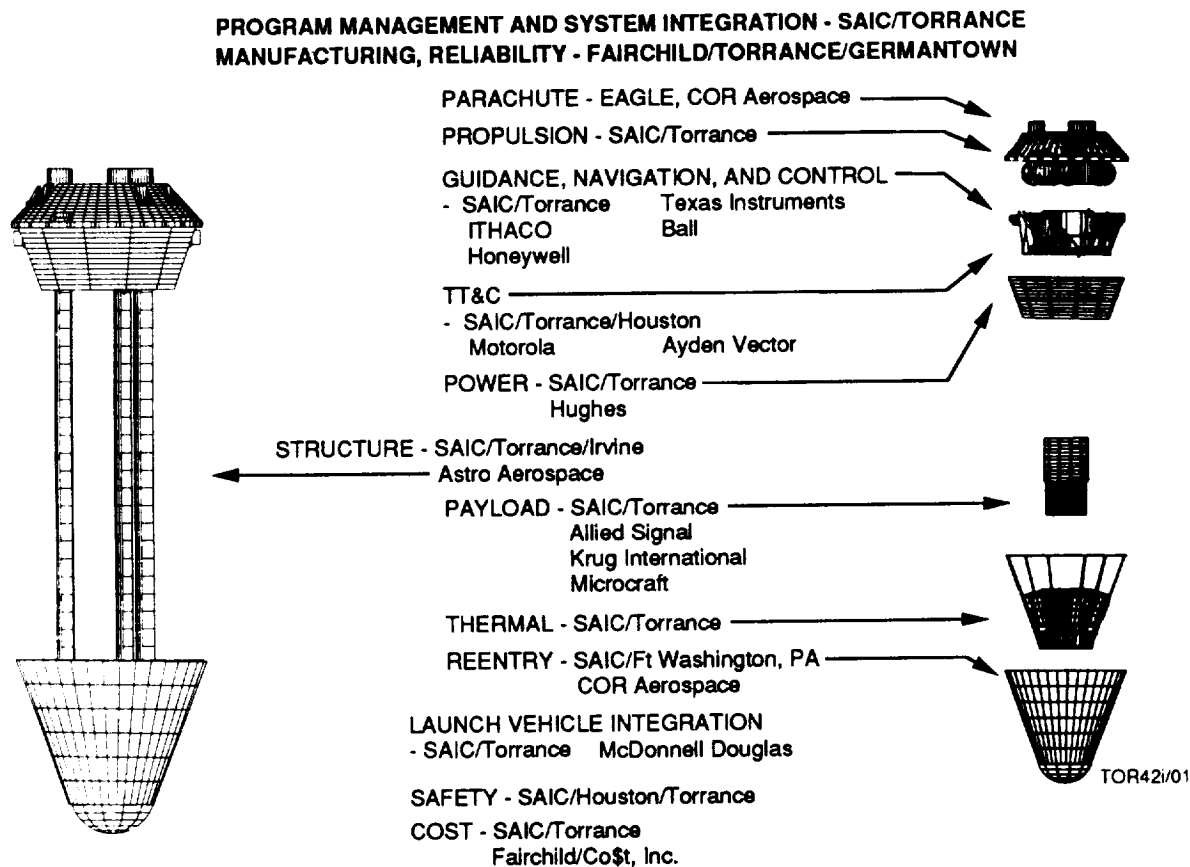


Figure i. SAIC Phase B Design Team

Table i. SAIC Design Team

Manager, Preliminary Design – Howard Hayden
Manager, Trade Studies – Bob Curtis

System Engineer – Howard Hayden
Lead Vehicle Engineer – Steve Apfel
Lead Payload Engineer – Scott Heppner
Life Sciences Advisors – Bill Haynes, Carl Reichwein

System Engineering – Hayden, Norton Rodman, Apfel, Ed Schwarzbein
Payload – Heppner, Hayden, Apfel, Haynes, Larry Anderson, Craig Fox
Safety – Tom Janicik, Apfel, Dan Martens
Structures – Apfel, Bill Loomis
Electrical Power – Rodman, Mark Matossian, Apfel, Hayden
Propulsion – Apfel, Chris Scheil
GNC – Hayden, Scott Bell
TT&C – Tom Stewart, Hayden, Fox
Thermal – Clark Wallace
Reentry – Sid Weinberg, Wallace, Curtis
Recovery – Apfel, Curtis
Cost Estimation – Mike Niggel, Hayden

And the Torrance publications personnel who, under the guidance of
Barbara Barrett, turned a mass of paper into a quality product.

CONTENTS

Section	Page
FOREWORD	i
1.0 INTRODUCTION	1-1
1.1 Background.....	1-1
1.2 Purpose	1-1
2.0 REQUIREMENTS	2-1
2.1 Formal Requirements Documentation	2-2
2.2 System Requirements	2-3
2.3 Design Implications.....	2-5
3.0 EVENT SYNOPSIS	3-1
4.0 STUDY RESULTS	4-1
4.1 Approach.....	4-1
4.2 Trade Studies Summary.....	4-2
4.2.1 SOW Directed Trade Studies	4-2
4.2.2 Preliminary Design Support.....	4-7
5.0 OPERATIONS CONCEPTS	5-1
5.1 Pre-Operations	5-3
5.1.2 Pre-Operations Phase.....	5-5
5.2 Mission Operations	5-5
5.2.1 Vehicle Operations.....	5-5
5.2.2 Ground Operations	5-19
5.3 Refurbishment.....	5-21
6.0 CONFIGURATION	6.0-1
6.1 Program Risk.....	6.1-2
6.1.1 Operational Risk	6.1-2
6.1.2 Developmental Risk	6.1-5
6.1.3 Cost/Schedule Risk.....	6.1-9
6.1.4 Overall Assessment.....	6.1-10
6.2 Rodent Module.....	6.2-1
6.2.1 Operation.....	6.2-2
6.2.2 Requirements.....	6.2-7
6.2.3 Trade Study Summary	6.2-9
6.2.4 Baseline Design	6.2-15
6.2.5 RRV Support.....	6.2-51

CONTENTS (Cont.)

Section	Page
6.3 Structures Subsystem	6.3-1
6.3.1 Operation.....	6.3-1
6.3.2 Requirements.....	6.3-2
6.3.3 Trade Study Summary	6.3-3
6.3.4 Baseline Design	6.3-45
6.3.5 Control, Command and Telemetry.....	6.3-45
6.3.6 Structure Test.....	6.3-46
6.3.7 Conclusions	6.4-1
6.4 Reentry Thermal Protection Subsystem.....	6.4-1
6.4.1 Introduction.....	6.4-1
6.4.2 Modeling Tool.....	6.4-1
6.4.3 Model.....	6.4-2
6.4.4 Assumptions.....	6.4-6
6.4.5 Results	6.4-6
6.4.6 Conclusions	6.5-1
6.5 Propulsion	6.5-1
6.5.1 Functional Operation	6.5-3
6.5.2 Requirements.....	6.5-5
6.5.3 Trade Study Summary	6.5-7
6.5.4 Baseline Design	6.5-13
6.5.5 Command and Control	6.5-14
6.5.6 Test	6.5-14
6.5.7 Manufacturing	6.5-14
6.5.8 Refurbishment.....	6.5-14
6.5.9 Conclusions	6.6-1
6.6 Guidance, Navigation and Control (GNC)	6.6-1
6.6.1 Operations Timeline Support.....	6.6-6
6.6.2 Design Requirements.....	6.6-6
6.6.3 Trade Studies.....	6.6-12
6.6.4 GNC Baseline Design.....	6.6-78
6.6.5 Control Requirements	6.6-78
6.6.6 Special Testing	6.6-80
6.6.7 Manufacturing	6.6-80
6.6.8 Refurbishment.....	6.7-1
6.7 Telemetry, Tracking, and Command (TT&C) Subsystem.....	6.7-1
6.7.1 Operations Timeline Support.....	6.7-1
6.7.2 Design Requirements.....	6.7-13
6.7.3 RRS TT&C Subsystems.....	6.7-13

CONTENTS (Cont.)

Section	Page
6.8 Power	6.8-1
6.8.1 Operations	6.8-1
6.8.2 Requirements	6.8-2
6.8.3 Trade Study Summary	6.8-3
6.8.4 Baseline Description	6.8-4
6.8.5 Command and Control	6.8-40
6.8.6 Test	6.8-40
6.8.7 Manufacture	6.8-40
6.8.8 Refurbishment	6.8-41
6.9 Thermal Control Subsystem (TCS)	6.9-1
6.9.1 Operations	6.9-1
6.9.2 Requirements	6.9-1
6.9.3 Trade Study Summary	6.9-1
6.9.1 Thermal Subsystem Requirements	6.9-2
6.9.4 Baseline Design	6.9-3
6.9.5 Command and Control	6.9-32
6.10 Recovery	6.10-1
6.10.1 Operations	6.10-1
6.10.2 Requirements	6.10-1
6.10.3 Trade Study Summary	6.10-1
6.10.4 Baseline Design	6.10-4
6.10.5 Command and Control	6.10-6
7.0 COST SUMMARY	7-1
7.1 Scalability	7-1
7.2 Approach	7-3
7.3 Summary	7-3
8.0 CONCLUSIONS AND RECOMMENDATIONS	7-1
8.1 Key Features	7-1
8.2 Conclusions	7-4
8.3 Recommendations	7-5
8.4 Summary	7-5

FIGURES

Figure		Page
i	SAIC Phase B Design Team.....	ii
2-1	RRS Specification Tree.....	2-3
2-2	RRS Functional Flow	2-4
4.1	Modular Manufacturing and Refurbishment Concept.....	4-4
4-2	Variable Mid-Deck Locker Capacity	4-6
4-3	Free Space Radiation Exposure	4-6
4-4	RRS Mission Risk Overview.....	4-8
5-1	Launch Vehicle Options.....	5-6
5-2	Launch Vehicle Candidate.....	5-7
5-3	Scaled Vehicle Configurations.....	5-8
5-4	Pre-Operations Checkout.....	5-9
5-5	Vehicle Operations	5-10
5-6	Launch Pad Sequence	5-11
5-7	Launch.....	5-12
5-8	GNC Launch Phase.....	5-13
5-9	Pre-Mission Checkout.....	5-14
5-10	Extended Vehicle – Microgravity.....	5-15
5-11	Extended Vehicle – Artificial Gravity	5-16
5-12	Reentry Preparation.....	5-16
5-13	De-Orbit Operations.....	5-17
5-14	Terminal Operations	5-18
5-15	Manufacturing and Refurbishment Flow.....	5-24
6-1	Primary RRS Characteristics	6.0-3
6-2	Modular Manufacturing and Refurbishment Concept.....	6.0-4
6-3	SAIC Fractional Gravity Approach.....	6.0-4
6-4	Ground Checkout and Experimentation Control	6.0-5
6-5	Free Space Radiation Exposure	6.0-6
6-6	Variable Mid-Deck Locker Capacity	6.0-7
6-7	Payload Module Scaling.....	6.0-8
6-8	Scaled Vehicle Configurations.....	6.0-9
6.1-1	Risk Mitigation - A Total Program Approach.....	6.1-1
6.1-2	RRS Mission Risk Overview.....	6.1-3
6.1-3	GNC Design Priorities	6.1-4
6.1-4	Minimal Risk CONUS Recovery Flight.....	6.1-6
6.1-5	Schedules Assurance Program	6.1-11
6.2-1	Ground Checkout and Experimentation Control	6.2-5
6.2-2	Ground Control Experiment Module	6.2-6
6.2-3	SAIC Fractional Approach.....	6.2-10
6.2-4	Payload Module Comparison.....	6.2-13
6.2-5	Variable Mid-Deck Locker Capacity	6.2-14
6.2-6	Payload Module Designed to Accommodate Other Science Payloads	6.2-14
6.2-7	Payload Module Scaling.....	6.2-16
6.2-8	RM Configuration.....	6.2-17
6.2-9	Baseline Energy Requirement	6.2-18

FIGURES (Cont.)

Figure		Page
6.2-10	Cage Requirements	6.2-20
6.2-11	Cage Features.....	6.2-21
6.2-12	Impact of Consumables on Rodent Module Weight	6.2-23
6.2-13	EM Assembly.....	6.2-26
6.2-14	Potential Cage Configurations.....	6.2-27
6.2-15	Utility Core Detail.....	6.2-28
6.2-16	Variable Mid-Deck Locker Capacity	6.2-29
6.2-17	RAHF Drinking Water System.....	6.2-32
6.2-18	Fully Integrated Support Module.....	6.2-36
6.2-19	Pressure Vessel (With EM Access Cover Removed)	6.2-37
6.2-20	Rodent Module Instrumentation.....	6.2-41
6.2-21	RRS Video Surveillance.....	6.2-43
6.2-22	RRS Passive Environmental Control	6.2-49
6.3-1	RRS Vehicle – Launch Configuration	6.3-4
6.3-2	RRS Retracted Configuration.....	6.3-4
6.3-3	Propulsion Submodule Structure (Top View)	6.3-6
6.3-4	Propulsion Submodule (3D View).....	6.3-6
6.3-5	DM Command Submodule.....	6.3-8
6.3-6	Command Submodule Dimensions	6.3-8
6.3-7	DM Prior to MM Mating and AFT Solar Array Installation	6.3-9
6.3-8	Deployed Module	6.3-10
6.3-9	Nose Submodule.....	6.3-11
6.3-10	Impact Attenuation System Installation.....	6.3-11
6.3-11	Water Landing Option.....	6.3-13
6.3-12	Water Landing Flotation Collar.....	6.3-14
6.3-13	RRV - Water Landing Flotation Collar Inflated	6.3-14
6.3-14	Gore Section Heat Shield Submodule	6.3-15
6.3-15	Typical Intermediate Frame Cross-Section.....	6.3-15
6.3-16	Honeycomb Heat Shield Substrate Dimensions.....	6.3-16
6.3-17	Substrate 3D View	6.3-16
6.3-18	Main Module Basic Structure.....	6.3-18
6.3-19	Shear Panel Dimensions.....	6.3-18
6.3-20	Carrier Module Structure.....	6.3-19
6.3-21	Main Module Side View.....	6.3-19
6.3-22	Main Module Top View	6.3-20
6.3-23	Carrier Structure With Heat Shield.....	6.3-20
6.3-24	Electronics and ECLSS Tank Installation	6.3-21
6.3-25	Main Module With ECLSS Tanks Installed.....	6.3-21
6.3-26	Main Module With Cover Installed	6.3-22
6.3-27	Relative Structural Deformation Results.....	6.3-25
6.3-28	Structural Deformation Results.....	6.3-25
6.3-29	Astromast Schematic.....	6.3-28
6.3-30	RM Installation - Exploded View	6.3-29
6.3-31	Payload Attachment.....	6.3-29
6.3-32	Payload ICD Mechanical Top View.....	6.3-30
6.3-33	Lower Payload Support Bracket	6.3-31
6.3-34	Detailed Fluid and Power Connections.....	6.3-31

FIGURES (Cont.)

Figure		Page
6.3-35	Fluid and Power Connection Location	6.3-32
6.3-36	Fluid and Power Connection Access Top View	6.3-33
6.3-37	Launch Vehicle Installation Single Spacecraft	6.3-34
6.3-38	Delta Interface Single RRS Launch	6.3-35
6.3-39	Delta Launch Vehicle Mechanical Interface Single RRS Launch	6.3-35
6.3-40	Launch Vehicle Interface (RRV)	6.3-36
6.3-41	Detail View RRV Launch Vehicle Interface Area.....	6.3-36
6.3-42	RRV Deployment From Delta Launch Vehicle	6.3-37
6.3-43	Dual-Launch System.....	6.3-38
6.3-44	15-Rodent Module	6.3-41
6.3-45	12-Rodent Configuration.....	6.3-43
6.3-46	9-Rodent Module Configuration	6.3-44
6.3-47	6-Rodent Module Configuration	6.3-47
6.4-1	RRS Aeroshell Model	6.4-2
6.4-2	Reentry Model Trajectories-A	6.4-4
6.4-3	Reentry Model Trajectories-B	6.4-5
6.4-4	Net Heating Rates Trajectories 1A, 2A, and 3A- Vehicle Nosetip	6.4-7
6.4-5	Results - Heat Shield Thickness Requirements.....	6.4-9
6.5-1	RRS Propulsion Schematic	6.5-8
6.5-2	Propulsion Electrical Schematic	6.5-9
6.5-3	Hamilton Standard Main Maneuver Thruster	6.5-11
6.5-4	Hamilton Standard ACS Thruster.....	6.5-12
6.6-1	GNC Orbital Flight – Extended μ G.....	6.6-3
6.6-2	Extended Vehicle – Artificial Gravity	6.6-4
6.6-3	GNC Recovery – De-Orbit.....	6.6-5
6.6-4	Typical GPS Performance	6.6-7
6.6-5	TI AN/PSN-9 RRS Configuration – A Space Capable Precision Pointing GPS Receiver.....	6.6-9
6.6-6	TI AN/PSN-9 Field Test Data – Geometry (DOP) and Multipath Effects.....	6.6-10
6.6-7	TI AN/PSN-9 Field Test Data – Multiple Antenna Configurations	6.6-11
6.6-8	GNC Launch Phase.....	6.6-14
6.6-9	Architecture	6.6-16
6.6-10	GNC Design Priorities	6.6-16
6.6-11	Attitude Control Configuration	6.6-17
6.6-12	GPS-Based Attitude Control Feasibility.....	6.6-20
6.6-13	GNC Operating Configuration – Recovery Phase - De-Orbit.....	6.6-21
6.6-14	De-Orbit Propulsion Control.....	6.6-22
6.6-15	Attitude Control Sensor Geometry	6.6-24
6.6-16	Satellite Configuration.....	6.6-26
6.6-17	Disturbance Environment	6.6-27
6.6-18	RRS GNC Configuration Microgravity Mode.....	6.6-28
6.6-19	RRS GNC Configuration Microgravity With Thermal Roll	6.6-29
6.6-20	RRS GNC Configuration Artificial Gravity Mode.....	6.6-30
6.6-21	RRS GNC Configuration IMU Alignment.....	6.6-32
6.6-22	RRS GNC Configuration Major Maneuvers.....	6.6-33
6.6-23	Gravity Gradient Stabilized Mode With Yaw Rotation	6.6-34

FIGURES (Cont.)

Figure		Page
6.6-24	Spin Stabilized Mode – 1.5 G	6.6-35
6.6-25	Three-Axis Gravity Gradient Stabilized – Typical Capture Performance.....	6.6-36
6.6-26	Three-Axis Gravity Gradient Stabilized – Typical Steady-State Performance ...	6.6-37
6.6-27	GNC Artificial Gravity Control – Ithaco Scanwheels	6.6-38
6.6-28	GPS/Scanwheel Sensor Geometry.....	6.6-40
6.6-29	Anticipated GPS Antenna Performance – Ball Communications Systems Division Antenna	6.6-41
6.6-30	Ball 2267 MHz Bifilar Helix Data – 12" Diameter, 12 Degree Conical Ground Plane	6.6-42
6.6-31	Honeywell Ring Laser Gyro Assembly (RLGA)	6.6-45
6.6-32	RLGA Sensor Configuration	6.6-46
6.6-33	RLGA Performance.....	6.6-47
6.6-34	GNC Microgravity Control – Magnetometer, Torquerods and Momentum Wheels	6.6-48
6.6-35	SANDAC V Architecture.....	6.6-51
6.6-36	SANDAC V Mechanical Design.....	6.6-52
6.6-37	Target System General Operation Sequence	6.6-55
6.6-38	Typical Gateway Configuration	6.6-56
6.6-39	Hawk Task State Diagram	6.6-63
6.6-40	SANDAC V Software Development System	6.6-67
6.6-41	SANDAC V Software Creation Process	6.6-69
6.6-42	Debugging Equipment Configuration.....	6.6-71
6.7-1	TDRSS/User Spacecraft Configuration	6.7-4
6.7-2	NASA Space Network (1992).....	6.7-5
6.7-3	Air Force Space Network (1992)	6.7-6
6.7-4	Air Force Satellite Control Network	6.7-7
6.7-5	DRM-1 Ground Trace – NASA Space Network.....	6.7-8
6.7-6	DRM-2 Ground Trace – NASA Space Network.....	6.7-8
6.7-7	DRM-3 Ground Trace – NASA Space Network.....	6.7-9
6.7-8	DRM-1 Ground Trace – Air Force Space Network.....	6.7-10
6.7-9	DRM-2 Ground Trace – Air Force Space Network.....	6.7-10
6.7-10	DRM-3 Ground Trace – Air Force Space Network.....	6.7-11
6.7-11	TDRSS Coverage Versus Altitude and Inclination.....	6.7-12
6.7-12	RRS Communications Subsystem.....	6.7-13
6.7-13	TDRSS Forward and Return Service Frequency Plan.....	6.7-16
6.7-14	Space Network Elements and Interfaces	6.7-17
6.7-15	NASA Standard TDRSS User Transponder Functional Block Diagram.....	6.7-18
6.7-16	TT&C Antenna	6.7-19
6.7-17	Antenna Orientation.....	6.7-20
6.7-18	Telemetry System	6.7-21
6.8-1	Deployed Module With AFT Array Dimensions (Inches).....	6.8-5
6.8-2	Power System Schematics	6.8-7
6.8-3	Power Generation Capability for a Gravity Gradient Mission.....	6.8-9
6.8-4	Power Generation Capability for an Artificial Gravity Mission	6.8-10
6.8-5	Array Performance Profile Per Rotation Artificial Gravity/Worst Case Orbit....	6.8-11
6.8-6	Battery Cycling Profile Artificial Gravity/Worst Case Orbit	6.8-12
6.8-7	Nickel Hydrogen Battery Cell	6.8-13

FIGURES (Cont.)

Figure		Page
6.8-8	Cell Energy Capacity Versus Temperature.....	6.8-13
6.8-9	Battery Charge Controller.....	6.8-14
6.8-10	Battery Charge Controller Block Diagram	6.8-16
6.8-11	Housekeeping Power Supply.....	6.8-18
6.8-12	Strain Gage Amplifier	6.8-18
6.8-13	Battery Pressure Monitor Circuit.....	6.8-19
6.8-14	Current Sensor	6.8-19
6.8-15	BBC Telemetry Accuracy Over Temperature	6.8-21
6.8-16	Battery Discharge Controller.....	6.8-22
6.8-17	Single Battery Discharge Controller String Functional Block Diagram.....	6.8-23
6.8-18	Housekeeping Power Supply.....	6.8-24
6.8-19	Soft Start Circuit	6.8-25
6.8-20	Gate Drive Circuit.....	6.8-26
6.8-21	Regulation Control Circuit	6.8-26
6.8-22	Timing Diagram.....	6.8-27
6.8-23	Output Power Diode Fault Detect Circuit.....	6.8-28
6.8-24	BDC Overvoltage Protect Circuit.....	6.8-28
6.8-25	Battery Current Sharing Circuit	6.8-30
6.8-26	Bus Voltage Limiter Block Diagram	6.8-32
6.8-27	Detailed Schematic, Bus Voltage Limiter Circuit.....	6.8-34
6.8-28	MM Power Distribution Unit	6.8-35
6.8-29	DM Power Distribution Unit.....	6.8-35
6.8-30	Concept for Software Controlled Switch.....	6.8-36
6.8-31	Schematic Diagram of Astromast Power Transmission	6.8-39
6.9-1	Payload Module ECLSS Heat Exchanger TCS Coolant Loop and.....	6.9-6
6.9-2	Payload Module ECLSS Heat Exchanger Thermal Control Subsystem.....	6.9-6
6.9-3	Subdivision of Aeroshell Radiator Into 12 Equivalent Panels	6.9-8
6.9-4	Detail of Aeroshell Radiator Panel Model	6.9-8
6.9-5	ECLSS Heat Exchanger TCS Coolant Loop Fluid Network Model	6.9-9
6.9-6	ECLSS Heat Exchanger TCS Pump Characteristic Curve	6.9-10
6.9-7	Orbital Geometry and Vehicle Orientation and Rotation Modes	6.9-12
6.9-8	Total Absorbed Flux (Solar + Albedo + Earth IR) at Radiator Panel 1 Surface During One Orbital Period for DRM-3, Vernal/Autumnal Equinox and DRM-5, Summer Solstice With Vehicle Normal and Axial Rotation Rates of 7.0 and 0.14 rpm, Respectively.....	6.9-14
6.9-9	Fluid Network Hydraulic Response	6.9-15
6.9-10	Coolant Thermal Response	6.9-15
6.9-11	Aeroshell Surface and Coolant Thermal Response, DRM-3 and DRM-5	6.9-17
6.9-12	RRS Extended Module Model.....	6.9-20
6.9-13	DRM-3 Orbital Geometry and RRS Vehicle Orientation Considered in Extended Module Solar Array Thermal Response Analysis	6.9-21
6.9-14	Extended Module Solar Array Thermal Response for DRM-3 Orbit.....	6.9-21
6.9-15	Extended Module Solar Array Thermal Response for DRM-3	6.9-23
6.9-16	Extended Module Model Electrical Network Analog	6.9-23
6.9-17	Total Absorbed Flux (Solar + Albedo + Earth IR) at Extended Module Aft Cover Surface During One Orbital Period for DRM-3, Vernal/Autumnal Equinox, Normal Rotation and Gravity Gradient Vehicle Orientations.....	6.9-26

FIGURES (Cont.)

Figure		Page
6.9-18	Total Absorbed Flux (Solar + Albedo + Earth IR) at Extended Module Aft Cover Surface During One Orbital Period for DRM-5, Summer Solstice, Normal Rotation and Gravity Gradient Vehicle Orientations	6.9-27
6.9-19	Predicted Temperature Response of Extended Module for DRM-3, Vernal/Autumnal Equinox, Normal Rotation and Gravity Gradient Vehicle Orientations	6.9-28
6.9-20	Predicted Temperature Response of Extended Module for DRM-5, Summer Solstice, Normal Rotation and Gravity Gradient Vehicle Orientations	6.9-30
6.9-21	Microgravity Preferred Orientation.....	6.9-31
6.9-22	Water Storage Tank Locations Within Forward Module	6.9-31
6.10-1	Recovery Sequency.....	6.10-4
7-1	Relative Scaled Vehicle Cost.....	7-2
8-1	Key SAIC Design Features	8-2

TABLES

Table		Page
i	SAIC Design Team.....	iii
2-1	RRS Program.....	2-1
2-2	RRS SRD Applicable Documents.....	2-2
2-3	RRS Subsystem Distribution	2-4
3-1	Part I Synopsis	3-1
3-2	Part II Synopsis	3-2
5-1	Key Operations Considerations.....	5-1
5-2	RRS System Requirements Document Mission Operations Definitions	5-2
5-3	Expanded RRS Mission Operations Definitions.....	5-3
5-4	RRS Design Reference Missions.....	5-4
5-5	NASA LifeSat Mission Planning.....	5-4
5-6	RRS Recovery Timelines.....	5-22
5-7	RRS Recovery Options.....	5-23
6-1	SAIC Design Philosophy.....	6.0-1
6-2	Design Constraints	6.0-2
6-3	Design Approach	6.0-10
6-4	Key SAIC RRS Design Features.....	6.0-10
6.2-1	Payload Module Environments Comparison.....	6.2-12
6.2-2	Power Budget for Payload Module	6.2-19
6.2-3	Payload Components - Weights	6.2-24
6.2-4	Payload Mass and Power.....	6.2-25
6.2-5	Lighting.....	6.2-34
6.2-6	Environmental Control/Life Support System	6.2-46
6.2-7	Alternative Carbon Dioxide Removal Methods	6.2-47
6.3-1	Structure Subsystem.....	6.3-2
6.3-2	RRV Structural Design Assumptions	6.3-5
6.3-3	Astromast Characteristics.....	6.3-23
6.3-4	Astromast Loads Summary	6.3-24
6.3-5	Astromast Design.....	6.3-27
6.3-6	Mass Properties Launch Configuration.....	6.3-39
6.3-7	Extended Vehicle Mass Properties	6.3-40
6.3-8	15-Rodent Mass and Power.....	6.3-42
6.3-9	12-Rodent Mass and Power.....	6.3-43
6.3-10	9-Rodent Mass and Power	6.3-44
6.3-11	6-Rodent Mass and Power	6.3-47
6.4-1	ESM 1004 AP Thermophysical Properties.....	6.4-3
6.4-2	ESM Thickness Requirements and Total Predicted Recession.....	6.4-8
6.5-1	Propellant Budget DRM-1 - Blowdown.....	6.5-2
6.5-2	RRS Design Reference Missions.....	6.5-4
6.5-3	Propulsion Study Considerations	6.5-5
6.5-4	First Cut Propulsion System Trades	6.5-6
6.5-5	Liquid/Propellant Trades	6.5-6
6.5-6	Propulsion Subsystem Interface Support.....	6.5-13

TABLES

Table	Page
6.6-1 RRS Unique GPS Applications – Safety and Cost Driven.....	6.6-8
6.6-2 GPS Attitude Determination – Adaptation of Ground Proven Technology.....	6.6-12
6.6-3 GNC On-Orbit Operations	6.6-15
6.6-4 GNC Functional Allocation	6.6-18
6.6-5 GNC Performance Summary	6.6-25
6.6-6 System Configuration Considerations	6.6-53
6.6-7 SANDAC V Features	6.6-54
6.6-8 GATEWAY Host-Target Interface	6.6-57
6.6-9 Satellite Dynamic/Environmental Considerations.....	6.6-60
6.6-10 Hawk Services.....	6.6-63
6.6-11 Summary of GATAR Functions.....	6.6-65
6.6-12 Standard SANDAC V Tool Set.....	6.6-68
6.6-13 The Assembler Package	6.6-68
6.6-14 GATAR Capabilities	6.6-72
6.6-15 GATAR Symbolic Debugging.....	6.6-72
6.6-16 Software Sizing and Timing	6.6-75
6.6-17 GNC Interface Support.....	6.6-77
6.6-18 GNC Mass and Power Summary	6.6-78
6.6-19 Guidance and Control Mass and Power	6.6-79
6.7-1 RRS Design Reference Mission Set Definition	6.7-2
6.7-2 TT&C Design Requirements.....	6.7-2
6.7-3 Contact History Summary.....	6.7-12
6.7-4 Recommended TT&C Configuration Summary	6.7-14
6.7-5 TT&C Weight and Power Budget.....	6.7-14
6.7-6 Vehicle Event Correlation	6.7-22
6.7-7 Module Monitoring.....	6.7-22
6.7-8 Experiment Monitoring	6.7-23
6.7-9 Activity Monitoring (per cage).....	6.7-23
6.7-10 Image Recording	6.7-23
6.7-11 MMP-900 PCM Encoder Configuration for the PM.....	6.7-24
6.7-12 Aydin Vector MMP-900 Micro PCM Encoder.....	6.7-25
6.7-13 RRS MMP-900 Micro-Modular PCM Architecture	6.7-26
6.8-1 Power Trade Summary	6.8-2
6.8-2 Power Subsystem Interface Support.....	6.8-5
6.8-3 Main Module and Deployed Module Power Budgets	6.8-8
6.8-4 Selectable Battery Cell End-of-Charge Pressure Levels	6.8-15
6.8-5 Battery Charge Termination Options.....	6.8-20
6.8-6 Main Module Power Distribution Switch Requirements.....	6.8-36
6.8-7 Deployed Module Power Distribution Switch Requirements	6.8-37
6.9-1 Thermal Subsystem Requirements	6.9-2
6.9-2 RRS Design Reference Missions.....	6.9-2
6.9-3 ECLSS Heat Exchanger TCS Coolant Loop Fluid Network Components.....	6.9-10
6.9-4 DRM-3, Vernal/Autumnal Equinox and DRM-5, Summer Solstice Orbit Definitions.....	6.9-13
6.9-5 PM ECLSS TCS Weight Budget.....	6.9-16
6.9-6 Extended Module Model Electrical Network Analog Nodal Descriptions	6.9-24
6.9-7 Thermal Subsystem Mass and Power.....	6.9-33
6.9-8 Telemetry Measurements	6.9-33

TABLES

Table	Page
6.10-1 Preliminary Screening of Landing Systems.....	6.10-2
6.10-2 Landing System Downselect.....	6.10-2
6.10-3 Source Data from Parachute Industry.....	6.10-3
6.10-4 Terminal Reentry Mass and Power.....	6.10-5
7-1 Key Ground Rules and Assumptions.....	7-1
7-2 Price H Cost Estimating Approach.....	7-3
7-3 RRS Subsystem Quantities (Definitions).....	7-4
7-4 Pre-Calibration Price H Results (\$M).....	7-5
7-5 LCC Summary.....	7-5
8-1 Propulsion System Trade.....	8-3
8-2 Conclusions.....	8-4
8-3 Recommendations.....	8-5
8-4 Summary	8-6

ACRONYMS

AC	Attitude Control
ACRV	Assured Crew Return Vehicle
AEM	Animal Enclosure Module
AFSCN	Air Force Space Control Network
BCC	Battery Charge Controller
BVL	Bus Voltage Limiter
CD	Configuration Database
CG	Center of Gravity
CMOS	Complementary Metal Oxide Semiconductor
CP	Cage Processor
CP	Center of Pressure
CSA	Canadian Space Agency
CSR	Cost and Schedule Risk
DASS	Data Acquisition and Storage System
DDL	Device Data Language
DGPS	Differential Global Positioning System
DM	Deployed Module
DMA	Direct Memory Access
DOD	Department of Defense
DOP	Dilution of Precision
DOT	Department of Transportation
DP	Data Processor
DRA	Development Risk Assessment
DRM	Design Reference Mission
DSP	Deep Space Network
EBF	European Space Agency Microgravity Botany Facility
EBM	ESA Botany Module
ECLSS	Environmental Control Life Support System
ELV	Expandable Launch Vehicle
EM	Experiment Module
EPROM	Electrically Programmable Read Only Memory
ERP	Emergency Recovery Process
ESA	European Space Agency
ESM	Silicone Elastomer

ETR	Eastern Test Range
ETV	Engineering Test Vehicle
FMECA	Failure Modes and Effects Criticality Assessments
GCEM	Ground Control Experiment Module
GN	Ground Network
GNC	Guidance, Navigation, and Control
GPS	Global Positioning System
GTM	Ground Test Module
HCI	Horizon Crossing Indicator
HEOH	Habitat/Experiment Data Handling
HVDC	High Voltage Direct Current
I/O	Input/Output
IMU	Inertial Measurement Unit
IP	Image Processor
IR&D	Independent Research and Development
IUS	Inertial Upper Stage
JSC	Johnson Space Center
LV	Launch Vehicle
LVA	Launch Vehicle Adapter
MADS	Magnetic Acquisition De-Spin System
MIB	Medical Information Bus
MILA	Merritt Island Launch Area
MM	Main Module
MPU	Microprocessing Unit
NASA	National Aeronautics and Space Administration
NDM	Nut Deployment Mechanism
NGT	NASA Ground Terminal
OS	Operating System
OSN	Orbital Space Network
PHA	Payload Hazard Analyses
PI	Principal Investigator
PM	Payload Module
PME	Payload Module Emulator
PWM	Pulse Width Modulator
RAHF	Research Animal Holding Facility
RAM	Random Access Memory

RM	Rodent Module
RMOAD	Reference Mission Operational Analysis Document
ROM	Read Only Memory
RRS	Reusable Reentry Satellite
RRV	Reusable Reentry Vehicle
SAP	Schedule Assurance Program
SCSI	Small Computer Systems Interface
SEP	Spherical Error Probable
SLAPEM	System-Level Ablation Penetration Erosion Model
SM	Support Module
SN	Space Network
SNL	Sandia National Laboratory
SRD	Systems Requirement Document
STDN	Space Tracking and Data Network
TASC	Thermal Analyzer for System Components
TCS	Thermal Control System
TDRSS	Telemetry and Data Relay Satellite System
TI	Texas Instruments
TT&C	Telemetry, Tracking, and Command
VAFB	Vandenberg Air Force Base
VDU	Valve Driver Unit
VE	Vehicle Emulator
WSMR	White Sands Missile Range
WTR	Western Test Range

1.0 INTRODUCTION

1.1 Background

The Reusable Reentry Satellite (RRS) is intended to provide investigators in several biological disciplines with a relatively inexpensive method to access space for up to 60 days with eventual recovery on Earth. The RRS will permit totally intact, relatively soft, recovery of the vehicle, system refurbishment, and reflight with new and varied payloads. The RRS is to be capable of three reflights per year over a 10-year program lifetime. The RRS vehicle will have a large and readily accessible volume near the vehicle center of gravity for the Payload Module (PM) containing the experiment hardware. The vehicle is configured to permit the experimenter late access to the PM prior to launch and rapid access following recovery.

The RRS will operate in one of two modes:

- a. As a free-flying spacecraft in orbit, and will be allowed to drift in attitude to provide an acceleration environment of less than 10^{-5} g. The acceleration environment during orbital trim maneuvers will be less than 10^{-3} g.
- b. As an artificial gravity system, which spins at controlled rates to provide an artificial gravity of up to 1.5 Earth g.

The RRS system will be designed to be rugged, easily maintained, and economically refurbishable for the next flight. Some systems may be designed to be replaced rather than refurbished, if cost effective and capable of meeting the specified turnaround time. The minimum time between recovery and reflight will be approximately 60 days.

The PMs will be designed to be relatively autonomous, with experiments that require few commands and limited telemetry. Mass data storage will be accommodated in the PM. The hardware development and implementation phase is currently expected to start in 1991 with a first launch in late 1993.

1.2 Purpose

The National Aeronautics and Space Administration (NASA) contracted with SAIC to perform a Phase B study to provide a preliminary design of the RRS concept. Numerous trade and design studies were performed to refine the SAIC RRS concept into a design that satisfies the NASA requirements and is viable. The purpose of this Final Report is to summarize the overall effort with emphasis on the functional and preliminary design description of the vehicle and each subsystem.

2.0 REQUIREMENTS

The overall objectives and requirements for the RRS Phase B effort (Table 2-1) are in the November 23, 1988, RRS System Design Study Statement of Work. The primary objective was to attain a viable preliminary design for the RRS and associated Ground Control Experiment Module, including both system and payload interface requirements. Other objectives specifically included analyses of operations, refurbishment, system interface, development planning, and cost considerations. The intent was to optimize the basic Phase A design through a series of configuration/scaling, recovery, refurbishment, electrical power, TT&C, Thermal, and payload interface trade studies and develop a reference design for use in defining the Phase C/D effort.

Table 2-1. RRS Program

OBJECTIVE
<ul style="list-style-type: none">• PROVIDE LIFE SCIENCES INVESTIGATORS A RELATIVELY INEXPENSIVE, FREQUENT ACCESS TO SPACE FOR EXTENDED PERIODS OF TIME WITH EVENTUAL SATELLITE RECOVERY ON EARTH
GENERAL REQUIREMENTS
<ul style="list-style-type: none">• THE RRS WILL:<ul style="list-style-type: none">- Provide On-Orbit Laboratory for Research on Biological and Materials Processes- Be Launched on a Number of Expendable Launch Vehicles- Operate in Low-Earth Orbit as a Free-Flying Unmanned Laboratory- Provide Semi-Autonomous Atmospheric Reentry and Soft Landing in Continental U.S.
SPECIFIC REQUIREMENTS
<ul style="list-style-type: none">• MAXIMUM ORBITAL STAY OF 60 DAYS• 3 REFLIGHTS PER YEAR OVER 10-YEAR PROGRAM LIFE• ATTITUDE CONTROL<ul style="list-style-type: none">- 3-Axis Stabilized- Artificial Gravity (up to 1.5 g)- Free Flyer• RUGGED AND EASILY MAINTAINABLE<ul style="list-style-type: none">- Off-the-Shelf Components• MODULAR DESIGN<ul style="list-style-type: none">- Satellite Bus<ul style="list-style-type: none">- Nominal Satellite Functions (Thermal, Power, etc.)- Payload Module<ul style="list-style-type: none">- Rodent Module- General Biology Module- ESA Microgravity Botany Facility- Materials Processing Experiments

2.1 Formal Requirements Documentation

The requirements for the system (vehicle and Rodent Module) are contained in Reference A which in turn contained a list (Table 2-2) of 13 applicable documents primarily concerning payload requirements. The key payload documents included the National Institutes of Health (NIH) guide for laboratory animals (Table 2-2, Item h) and the following LifeSat Science Working Group facility requirements (References B, C, D) and Hq NASA LifeSat Level I, Phase B science and technical requirements (Reference E) documentation.

Table 2-2. RRS SRD Applicable Documents

(a)	NASA Technical Memorandum TM-82473, "Terrestrial Environment (Climatic) Criteria Guidelines for Use in Aerospace Vehicle Development, 1982 Revision."
(b)	NASA Technical Memorandum TM-78119, "Space and Planetary Environment Criteria Guidelines for Use in Space Vehicle Development, 1982 Revision."
(c)	General Biology Module Specification.
(d)	ESA Botany Module Specification. TBS
(e)	NASA Basic Safety Manual, NGB 1700.1 (V1-A).
(f)	NASA Technical Memorandum TM-101043 "A Conceptual Design Study of the Reusable Reentry Satellite," October 1988, NASA Ames Research Center.
(g)	"LifeSat – An International Biological Satellite Program, Science, Uniqueness, Necessity," May 1988, NASA Ames Research Center.
(h)	Guide for Care and Use of Laboratory Animals, U.S. Department of Health and Human Services, Public Health Service, National Institutes of Health, NIH Publication No. 85-23, Revised 1985.
(i)	Animal Welfare Act of 1966 as amended, 7 U.S.C. 2131 et seq.
(j)	Environmental and Special Senses, In: Methods of Animal Experimentation, Vol. IV, W. I. Gay, ed., Academic Press, 1973.
(k)	Housing to Control Research Variables, In: The Laboratory Rat, Vol. I, H. J. Baker et al., eds., Academic Press, 1973.
(l)	Federation of American Societies for Experimental Biology (FASEB) Biological Handbooks.
(m)	Nutrient Requirements of Laboratory Animals, 3rd ed., Number 10, National Academy of Sciences, 1978.

References:

- A. Reusable Reentry Satellite (RRS) System Requirements Document (SRD), November 23, 1988.
- B. Rodent Module, Facility Science Requirements Document, September 9, 1988.
- C. Plant Payload, Facility Science Requirements Document, September 8, 1988.
- D. General Biology Payload, Facility Science Requirements Document, September 9, 1988.
- E. LifeSat Reusable Reentry Satellite (RRS), Level I Phase B, Science and Technical Requirements Document (STRD), December 2, 1988.

2.2 System Requirements

The system requirements for the RRS are documented in a set of specifications (Figure 2-1) which began as a total implementation of the requirements contained in the RRS SRD. These basic requirements were then modified to reflect the more detailed design requirements as the preliminary design evolved. The multiple specification approach was taken since the RRV and PM are intended to be developed by independent organizations based on a firm interface specification which is to be the same for all versions of the payload module. The specification organization also reflects the requirement that all RRS external support (ELV and ground command and control) will be with the RRV (Figure 2-2). The organization of the PM and RRV specifications are by subsystem (Table 2-3) to simplify the requirements allocation and the audit trail through the modular design.

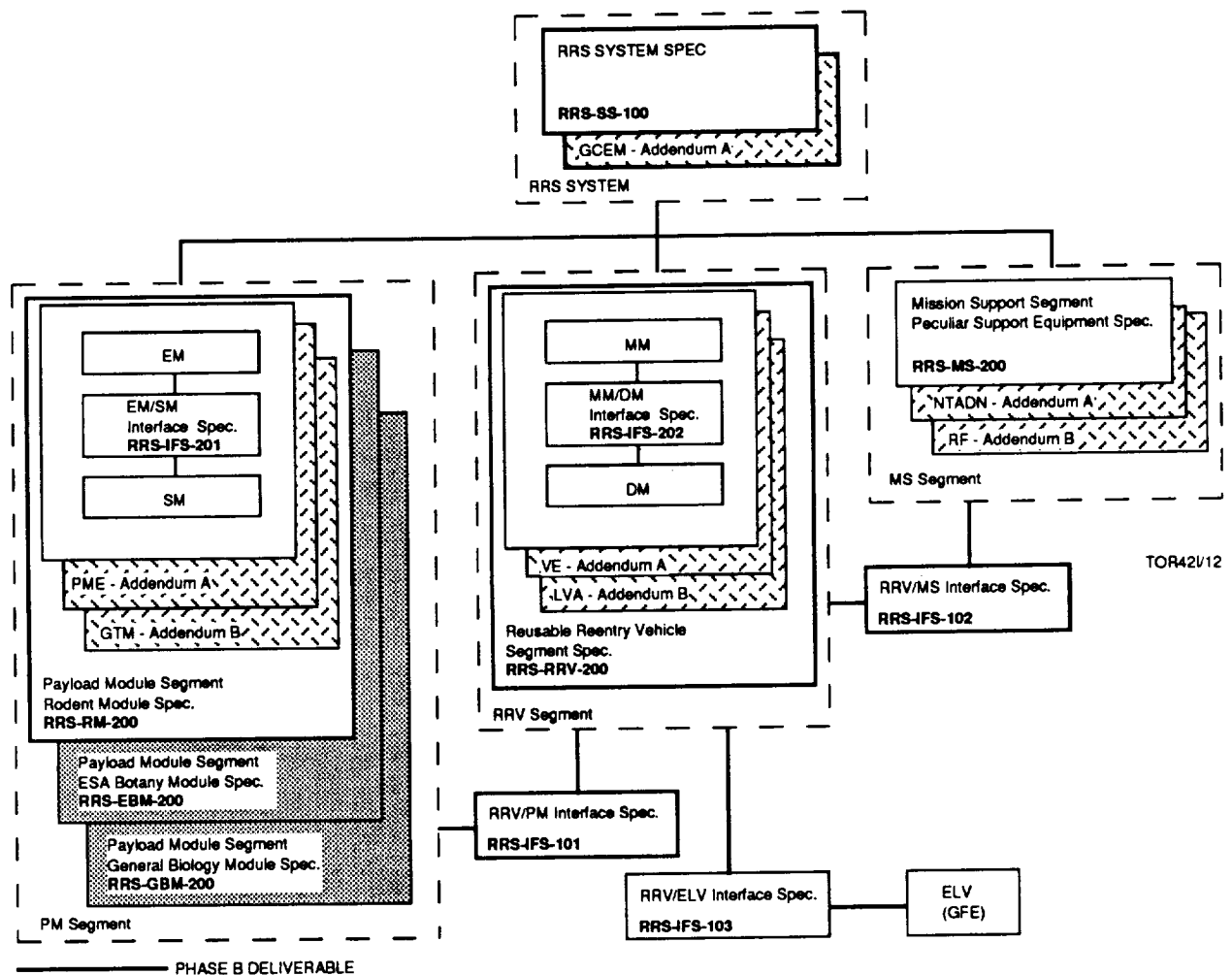


Figure 2-1. RRS Specification Tree

- ALL PM SUPPORT VIA THE RRV

- Prelaunch Checkout
- On-Orbit Operations
- Recovery Operations

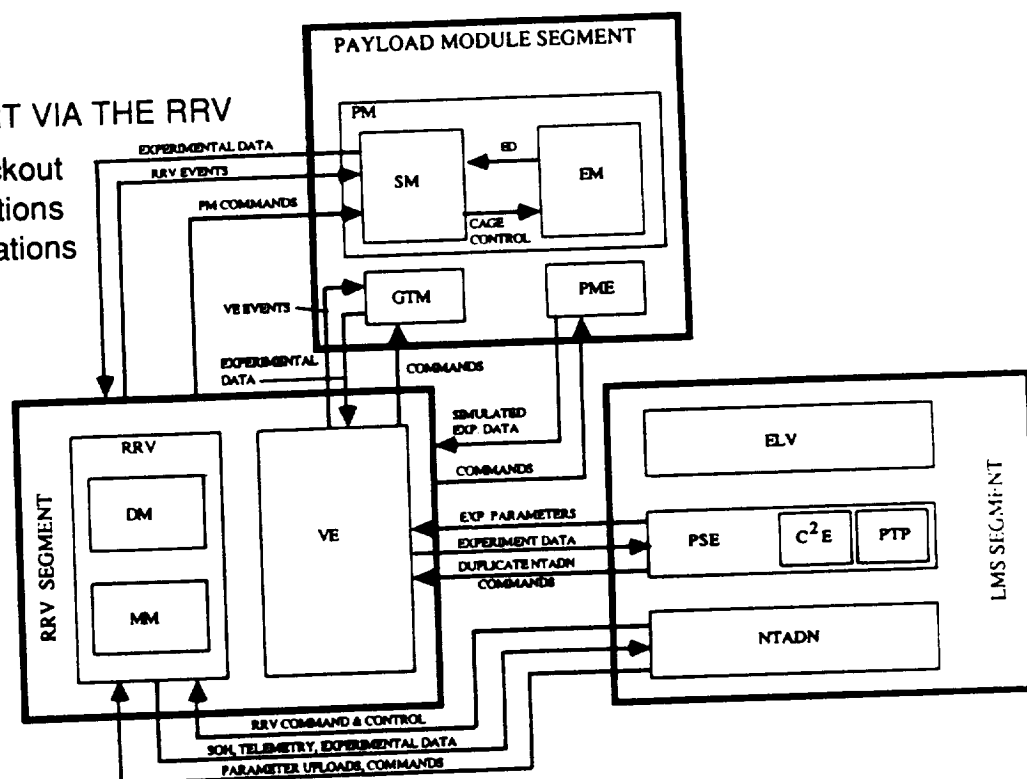


Figure 2-2. RRS Functional Flow

Table 2-3. RRS Subsystem Distribution

- SYSTEM SPECIFICATION ORGANIZED BY MODULE/SUBSYSTEM
- SUBSYSTEM SPECIFICATIONS ORGANIZED BY SUBSYSTEM/MODULE

Subsystem	Main Module	Deployed Module (Cont. Assy.)	Deployed Module (Prop. Assy.)	Payload Module	LV Adaptor
Propulsion	—	—	De-Orbit Attitude Cont.	—	Gas Deploy
GNC	GPS Rec/Ant IMU (1) Dual MWheel	Control System IMU (2) Dual MWheel GPS System Magnetic System Scanner System	GPS Ant (3)	—	—
TT&C	Data Interface SOH TLM	Com/Cmd/Dec SOH TLM Data Handling Memory	Antenna	Data Module SOH TLM Camera System	Booster TLM
Power	Conv/Control Batteries	Conv/Cont Batteries Solar Array	—	Conv/Cont Lighting	Deploy Control
Reentry	Heat Shield	—	—	—	—
Thermal	Radiator	Passive	Passive	HE/R/P/Ctl	—
Structure	Primary	Primary Astromast	Primary	Pressure Vess. Cage Assy.	Primary RRV Interface
ECLSS	Storage	—	—	ECLSS	—
Recovery	—	—	Parachute Deploy Mech.	—	—
Harness	Power, Control and Data	Power, Control and Data	Power, Control and Data	Power, Control and Data	Power, Control and Data

The specifications delivered as part of the Phase B effort are:

- RRS-SS-100 RRS System Specification
- RRS-RM-200 Payload Module Segment Rodent Module Specification
- RRS-RRV-200 Reusable Reentry Vehicle Segment Specification
- RRS-IFS-101 RRV/PM Interface Specification

The EM/SM, MM/DM, RRV/ELV, and RRV/MS (NATDN) interfaces, which do not have Phase B IFS documentation requirements, are described in Section 6 of this report.

2.3 Design Implications

Several primary requirements, specific and inferred, have either driven or constrained the configuration and internal design of the RRS. Several other issues, not explicitly addressed in the requirements documentation, are equally critical in achieving the desired system performance as described by NASA during the Phase B effort. More specifically:

a. Design Drivers

1. Animal Welfare (SRD Paragraph 4.3.2.2). The 99% probability of successful healthy recovery of experimental animals, combined with the long periods of no contact (SOW Para 3.2.6), drives a fail operational architecture for any failure critical to the health or successful recovery of the animals (Appendix D).
2. Public Safety (SRD Paragraph 3.1.7, 3.2.1 and 3.2.10). Public safety, although not explicitly defined in the SRD, involves two equally critical considerations:
 - (a) CONUS Recovery. Neither the 3-sigma footprint requirement of Paragraph 3.1.7, nor the 0.99% animal welfare requirement, will result in performance that fulfills the typical 1 in 1,000,000 launch base safety requirement. The need to preclude any single-point failure which would result in an impact significantly outside the CONUS 12x60 km landing footprint, thereby creating a major public hazard, drives the use of an autonomous, no single-point, multi-failure tolerant recovery process. A companion consideration is the impact the only other real alternative, a water recovery, has on PM access and refurbishment, and the associated program costs.

(b) **Uncontrolled Reentry.** Although there is a small probability of death, injury and/or significant damage from an uncontrolled reentry, the reentry of any space debris of any significant size is a public safety concern. The RRS program can create such debris from either of two causes, total failure of the vehicle on orbit or any portion of the vehicle deliberately left behind. More specifically:

(1) **Basic Vehicle.** The nature of the RRV is that a dead vehicle will sooner or later reenter intact with a massive kinetic energy release at impact. The need to preclude this failure mode drives the use of vehicle redundancy and automatic load shed capability to ensure the option for a manual initiated, wide ocean area impact is virtually guaranteed.

(2) **Jettisoned Debris (SOW Paragraph 3.1.2.3b).** Although the probability of intact reentry and the size of any jettisoned structure would likely be smaller than the basic vehicle, the full assurance of public safety requires, in descending order of design impact and magnitude of testing, either a controlled wide ocean area reentry, a guaranteed burn-up during reentry, or no jettisoning. Furthermore, since the system intent is multiple, short duration missions, a design that leaves significant debris in orbit has the potential for creating significant on-orbit operational safety restrictions unless all missions are flown in significantly different orbits.

3. **Total Power (SRD Paragraph 3.3.2.4d).** Although the current power per rodent-day is approximately the same as the original 45 kilowatt-hour (kWh) for a 12-rodent, 24-day mission, the nearly factor of 4 increase in total payload power required to support the 18-rodent, 60-day mission is a major design driver.

b. Design Constraints

1. **Payload Compatibility (Reference A, Paragraphs 2.0, 3.1.3, and 4.0).** The 18-rodent, 60-day requirement, in conjunction with the NIH laboratory animal guide (Table 2 - 2), and the requirement to be compatible with a 35-inch diameter botanical payload essentially sets the minimum weight, power and dimensions requirements for PM support. The 1080 rodent-day requirement, a factor of 3.75 greater than the 12x24 Phase A concept originally identified in the SOW as the

minimum requirement, is understood to be driven by the statistical sampling level required to ensure valid experimental results.

2. **Payload Access (SRD Paragraphs 3.2.2.3 and 3.2.5.1).** The 4-hour prelaunch and 2-hour post-landing access requirements, while not a major constraint on the vehicle, are significant in the operations process.
3. **Flight Experiment Control (SRD Paragraph 4.9.1).** The ground control experiment performs the dual function of ground control and the calibration of the existing extensive ground test database with space experimentation. In the case of calibration, the space experiment needs to replicate the ground test gravity environment as precisely and uniformly as possible so that any gravity-driven differences in ground and microgravity results can be correctly assessed.

c. Additional Requirements

1. **Dual Launch.** The dual launches included in the current RMOAD planning, but not the basic SOW/SRD, are clearly a major requirement and should be specified if the overall life cycle cost is to be minimized.
2. **Radiation Experimentation.** The need for galactic radiation experimentation for long duration manned missions requires an orbit that will maximize the galactic to near-earth proton/electron radiation ratio. This ratio should be specified so that the combined effects of apogee time, orbit precession and vehicle shielding on the radiation exposure, and the vehicle propulsion, can be optimized for a minimum energy orbit (not totally beyond the earth's radiation belts) with acceptable (maximum G, thermal) reentry opportunities.

3.0 EVENT SYNOPSIS

This effort was initiated by award of contract NAS 9-18202, a Firm-Fixed-Price Level-of-Effort for the Reusable Reentry Satellite, to SAIC on July 12, 1989. The contract award was based upon the SAIC proposal submitted in response to the January 10, 1989 NASA/JSC competitive RFP 9-BE2-23-8-48P. The Statement of Work structured the system design study into two 6-month efforts, Part I for system, subsystem, interface, and operational trade studies and Part II for completion of the reference design and associated specification/planning/cost data.

Part I was initiated with a kickoff proposal overview briefing to the NASA LifeSat Science Working Group (LSWG) held in lieu of the DRL-01 kickoff meeting and included the briefings and deliveries in Table 3-1.

Table 3-1. Part I Synopsis

Meetings:	
12 Jul 89	LSWG System Design Study Briefing
24 Oct 89	LSWG Interim Status Review
28 Nov 89	Interim Status Review
08 Feb 90	Midterm Review
15 Feb 90	LSWG Midterm Update
Deliveries:	
Summary Reports	
Launch Tradeoff	
Reentry Dispersion Analysis	
Recovery Tradeoff Study	
Propulsion System Trade Study	
Power System Trade Study	
Thermal Control Trade Study	
Payload Module	
Configuration Trade Study	
Telemetry, Tracking and Command Tradeoff Study	
Preliminary Life Cycle Cost Estimate	
Preliminary Hazard Analysis	

Part II was initiated following the receipt of the NASA/JSC post-Part I requirements update and included the briefings and deliveries in Table 3-2.

Table 3-2. Part II Synopsis

Meetings:	
06 Jun 90	Non-Advocate Review Concept Overview
02 Nov 90	Final Review
Deliveries:	
Final Report	
Appendices:	RRV Manufacturing Plan Rodent Module Manufacturing Plan Payload Hazard Analysis Preliminary Reliability Assessment
Specifications	
RRS-SS-100	System Specification for the Reusable Reentry Satellite
RRS-VS-200	Segment Specification for the Vehicle Segment of the Reusable Reentry Satellite
RRS-PS-200	Segment Specification for the Payload Segment of the Reusable Reentry Satellite
System Cost Estimates Document	

4.0 STUDY RESULTS

This NASA Phase B study effort was initiated to provide further definition of the RRS concept and to develop a preliminary design. The effort included numerous tradeoff studies with appropriate depth of analysis to clarify and document the viability of each approach. The system needed to be rugged, easily maintained, and economically refurbishable for the next flight. Some subsystems were designed to be replaced, rather than refurbished, if system replacement is cost effective and able to meet specified turnaround time. The hardware development and implementation schedule used in the trade studies is based on a program start in 1991 with a first launch in late 1993. The system and operations were developed to the degree necessary to provide a complete description of the designs and functional specifications.

4.1 Approach

Although the series of trade studies performed were done primarily during Part I, an extended effort was required in Part II as part of the overall preliminary design effort. The study results are documented in a series of trade study Summary Reports and/or the Final Report, depending upon the level of detail. In general, the individual Summary Reports emphasize design options while the Final Report is primarily oriented toward the preliminary design.

The Summary Report analyses were performed in accordance with the direction contained in the RRS Statement of Work and the System Requirements Document (SRD) and responses to those requirements are listed in each report. Although the individual analyses and studies did not necessarily lend themselves to be documented in exactly the same manner, the following general outline was used for all reports:

- Purpose
- Groundrules and Assumptions
- Analysis Methodology
- Analysis Results
- Conclusions
- Recommendations

The following individual summary reports have been published:

RRS-021 March 1990	Launch Tradeoff Study
RRS-022 March 1990	Recovery Tradeoff Study
RRS-023 March 1990	Reentry Dispersion Analysis
RRS-024 April 1990	Payload Module
RRS-025 February 1991	Telemetry, Tracking & Command (TT&C) Coverage Tradeoff Study
RRS-026 April 1990	Propulsion System Trade Study
RRS-027 April 1990	Thermal Control Trade Study
RRS-028 May 1990	Power System Trade Study
RRS-042 December 1990	Configuration Trade Study

4.2 Trade Studies Summary

With few exceptions, trade studies did not significantly alter the proposed SAIC design concept. The most significant changes are retention of the propulsion system for reentry and reversal of the direction of the main thruster firing. Both changes were made to reduce program risk. Of the trade studies summarized below, those summarized in paragraph 4.2.1 were done specifically in response to Paragraph 3.1.2 of the SOW. Those summarized in paragraph 4.2.2 are additional studies done in support of the SAIC Part II design effort.

4.2.1 SOW Directed Trade Studies

The following tradeoff studies were directed as part of the Part I effort by Paragraph 3.1.2 of the SOW. Although most of the information in the Summary Reports is still valid, some refinements occurred during the Part II design effort. These refinements are discussed in this Final Report, and are included in the following summaries.

4.2.1.1 Configuration (Section 6.0, 6.4; SOW Paragraph 3.1.2.1). The Configuration Trade Study, documented in RRS-042 and updated in this report, addressed the shape and internal configuration of the basic vehicle, and scaled the configuration for a range of payload capabilities. The final conclusion was that, while the vehicle could be scaled for a range of launch vehicles, the suggested preliminary design, which can be launched single or dual on either the Delta or Atlas, is the most cost effective from a life sciences viewpoint. The smaller versions of the RRV do not have the payload capacity to accommodate the RM requirements or the EBF. Furthermore, the limited volume would severely limit off-the-shelf equipment and/or the redundancy needed to ensure public safety. The 15 g maximum reentry load did not significantly influence vehicle design.

4.2.1.2 Launch (Section 5.0; SOW Paragraph 3.1.2.2). The Launch Vehicle Trade Study, documented in RRS-021 and updated in this report, was initially based on the assumption that there is a wide range of potential launch vehicles that would allow cost optimization. In fact, the potentially less expensive launches are not less expensive, on a scientific payoff basis, unless the experiments in the potential payload are sufficiently different that flying them together causes a costly integration task. For example, if 18 experiments (rodents) must be flown to get the required data, and flying them together in a single launch is not a major integration problem, flying them in smaller sets (e.g., 3 launches of 6 each) on some of the proposed boosters is the more costly program approach, assuming current requirements (e.g., detailed documentation, S-level parts, etc.) must be complied with. Conversely, if the lesser requirements are acceptable, and the requirements on the existing boosters comparably decreased, the current booster cost could probably be substantially reduced.

4.2.1.3 Recovery (Sections 6.4, 6.10; SOW Paragraph 3.1.2.3). The recovery trades involved several of the above trade studies (Configuration (RRS-042), Recovery (RRS-022) and Dispersion (RRS-023) and were expanded to include considerations for a water landing during Part II. Although variants on the basic reentry body were considered, significant variation from the basic sphere/cone was rejected because the basic shape performed acceptably and any significant variation would involve high development cost. The pre-deorbit jettison of any portion of the vehicle was rejected to preclude space debris being an issue for any significant use of the vehicle and the design impact of ensuring debris would not cause a public hazard on reentry. Similarly, the original intent to drop the propulsion subsystem was eliminated for the lack of a safe up-range impact zone on all potential orbits. Although the vehicle can be sealed adequately for water recovery, and a preliminary water recovery design was established (Section 6.3), the recovery force cost is not justified if a safe CONUS landing is possible. Although a crushable

nose was the design selected for landing shock attenuation, the water landing system uses a nose deployable flotation system that could also be considered for shock attenuation. Similarly, while the conventional parachute meets performance requirements and is, therefore, less expensive, the vehicle is designed to provide automated control, to a gliding parachute design, to allow use of such a parachute whenever the device becomes fully qualified. Meeting the 2 hour post-recovery access time did not pose any significant safety issues.

4.2.1.4 Refurbishment (Appendix A; SOW Paragraph 3.1.2.4). Since refurbishment is in essence a selective re-manufacturing process, the refurbishment trades were done in conjunction with the manufacturing analyses and published as part of the Manufacturing Plan (Appendix B). Both the initial manufacturing and the refurbishment schedules benefited from the parallel integration/test process inherent in the SAIC modularized (Figure 4-1) design philosophy.

OBJECTIVE: PARALLEL PROCESSING OPERATIONS TO SAVE SCHEDULE AND COST

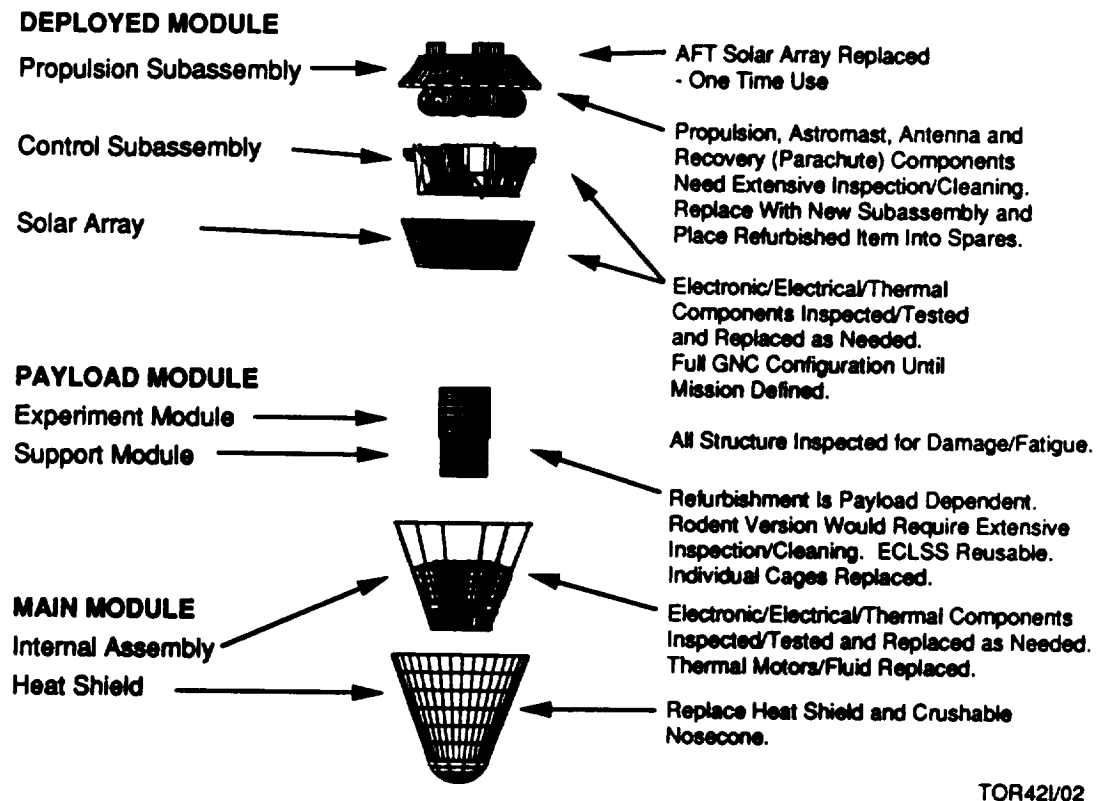


Figure 4.1. Modular Manufacturing and Refurbishment Concept

4.2.1.5 Electrical Power (Section 6.8; SOW Paragraph 3.1.2.5). Since the severe power limitations of a stored energy system (batteries or fuel cells) became evident early in the Power Trade Studies (RRS-028), the study primarily involved the estimation of the solar array power available for SAIC's rotating vehicle concept. The actual power system trades were done in Part II, and are included in this report. A jettisoned power subsystem is not required, and is not recommended because of the associated space debris and safety issues.

4.2.1.6 Telemetry, Command and Tracking (Section 6.7; SOW Paragraph 3.1.2.6). The TT&C Coverage Trade Study (RRS-025) defined the available ground station communications, and the projected twice-a-day contact is adequate for normal, unattended operations. However, since off-the-shelf components are available that can service both ground and TDRSS links, use of a low-data-rate TDRSS for visibility into critical operations (e.g., de-orbit burn) and "sick bird" contingency support is recommended.

4.2.1.7 Thermal Control (Section 6.9; SOW Paragraph 3.1.2.7). The Thermal Trade Study (RRS-027) primarily addresses the payload heat rejection issue. The use of a heat shield radiator and the SAIC common g ("inverted") launch configuration allows the vehicle to be adequately cooled during pre-launch simply by providing pad cooling air to the Launch Vehicle Adapter (LVA). A preliminary thermal analysis was done for all operating modes. A "thermal reservoir" concept is used to ensure payload thermal control for critical periods such as post-landing to external thermal support connection.

4.2.1.8 Payload Module Interface (Section 6.2; SOW Paragraph 3.1.2.8). The Payload Module (RM) Trade Study (RRS-024) primarily addresses the RM configuration, and provides additional detail concerning the internal configuration. The centralized payload core design provides the capability to fly up to six mid-deck lockers, in a near-uniform gravitational environment, without locker modification (Figure 4-2), and provides free-space radiation exposure (Figure 4-3) for a significant portion of the experimental volume. Shock/vibration/thermal isolation and electrical/thermal/command/data interfaces were developed and defined in the RRV/RM interface specification (RRS-IFS-101).

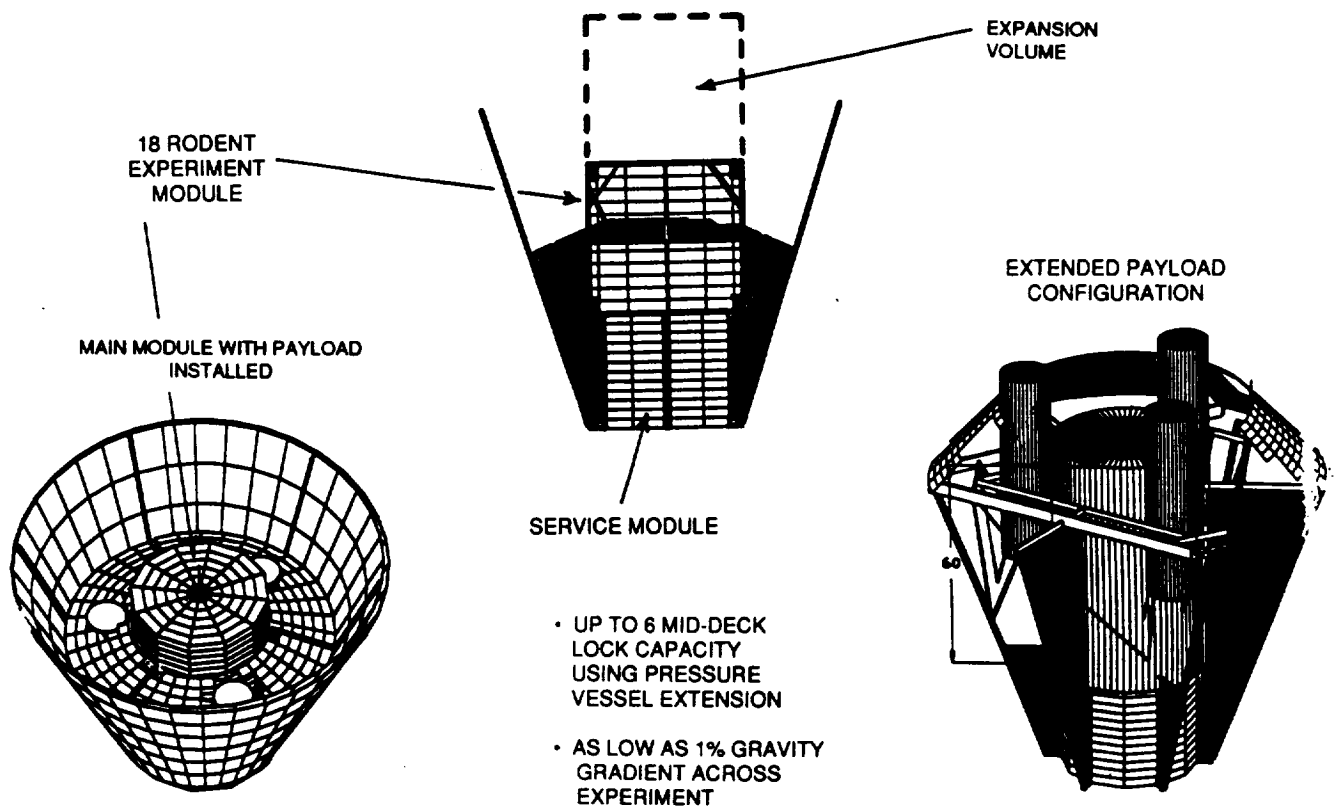


Figure 4-2. Variable Mid-Deck Locker Capacity

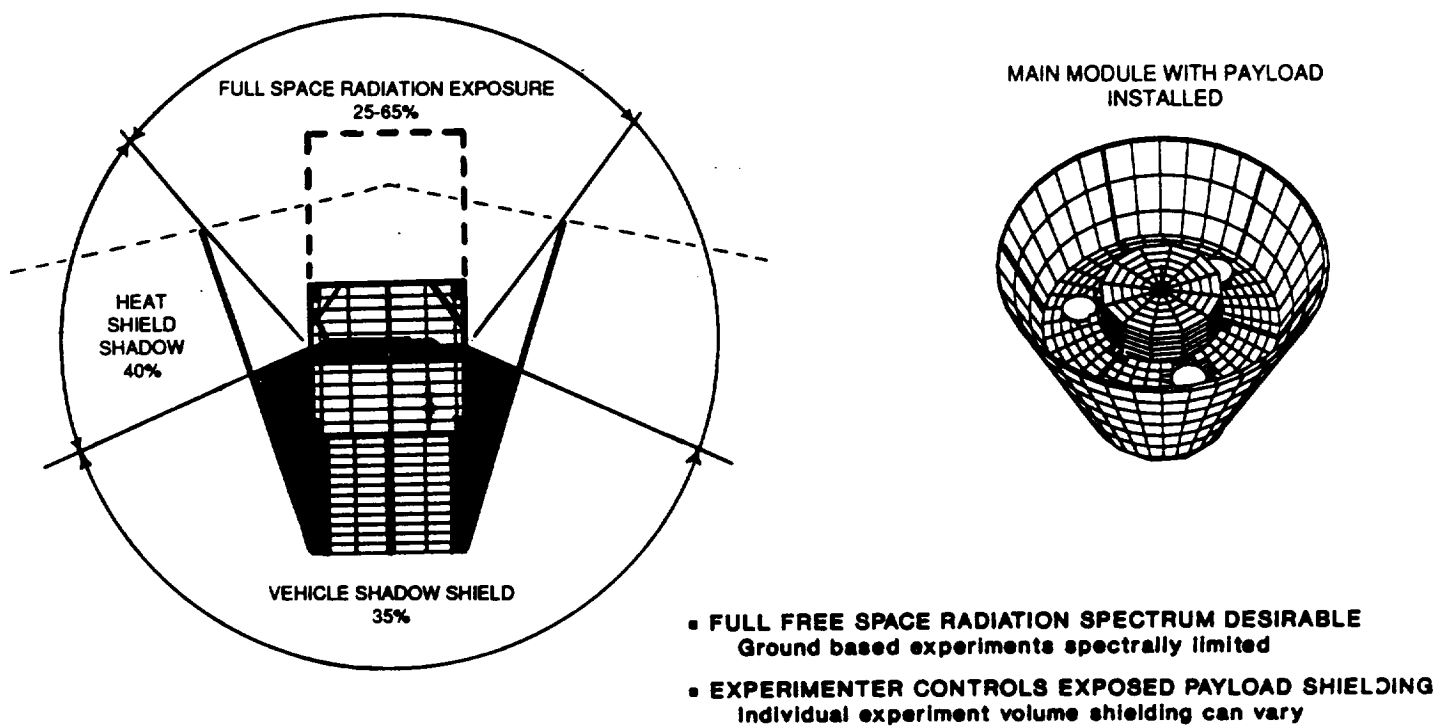


Figure 4-3. Free Space Radiation Exposure

4.2.2 Preliminary Design Support

The following trade studies were not required by the SOW, but were considered a necessary part of the evolution of the SAIC concept. Of these, only the propulsion subsystem results were published as a separate summary report. The other results are an integral part of this report.

4.2.2.1 Risk (Section 6.1). The overall mission profile (Figure 4-4) was analyzed to determine what mission risks required specific attention during the Part II preliminary design phase. This included Preliminary Payload Hazard Analyses (PHA) and Failure Modes and Effects Criticality Assessments (FMECA) (Appendix C), as well as the detailed propulsion/GNC analyses needed for the public safety assessment.

4.2.2.2 Propulsion (Section 6.5). This trade study (RRS-026) was driven by the need to ensure a fail operational de-orbit process for public safety. The approach also provides the means to have multi-orbit vehicle missions.

4.2.2.3 Structure (Section 6.3). The deployable tri-mast structure was analyzed by Astro Aerospace, manufacturer of the proposed Astromast, SAIC structures designers, and an independent structural consultant to ensure viability of the tri-mast concept. These results indicate sufficient design margin for safe operation out to 100 feet, and the dual retraction concept eliminates concern for a single-point retraction failure. The tri-mast assembly is almost fully deployment redundant and retraction tridundant. These studies are discussed in Section 6.3.

4.2.2.4 GNC (Section 6.6). The GNC design was investigated in detail (Figure 6.1-3) to ensure a fail operational capability for critical operations. Special attention was paid to the processor architecture and software development issues to ensure a highly reliable operation and minimize software development risk. These studies are discussed in Section 6.6.

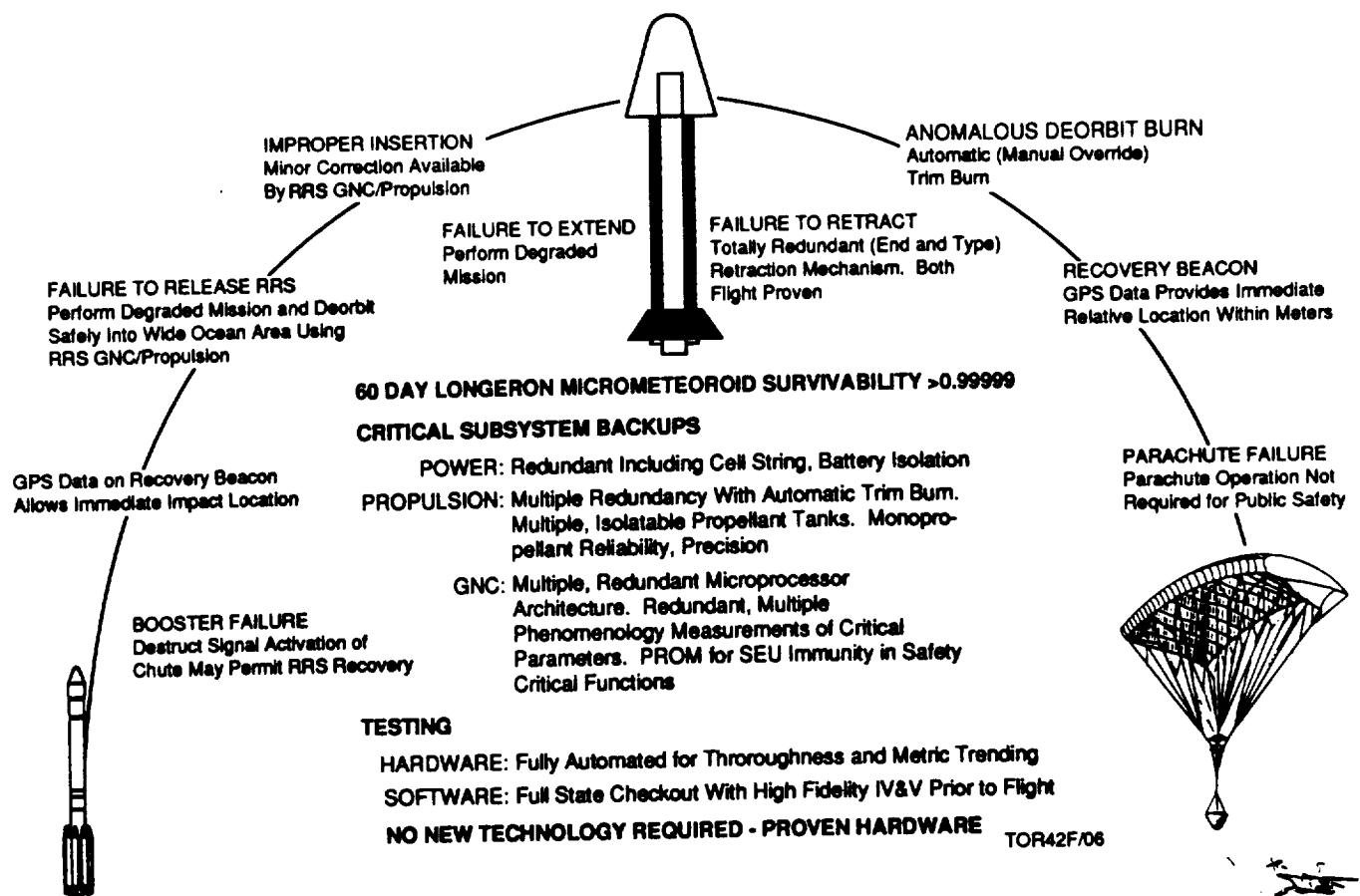


Figure 4-4. RRS Mission Risk Overview

5.0 OPERATIONS CONCEPTS

The concept of operations must clearly define the key operational considerations if they are to influence the system design sufficiently to ensure fulfillment of the overall mission objectives. In the case of the RRS (Table 5-1), there are three key considerations to be addressed if the program is to provide NASA with an efficient, recoverable access to space for unmanned experimentation.

Table 5-1. Key Operations Considerations

PUBLIC SAFETY <ul style="list-style-type: none">- Unattended, "Fail Operational" CONUS Reentry Process
RELIABLE, SCIENCE FRIENDLY ENVIRONMENT <ul style="list-style-type: none">- Minimum Integrate-to-Launch Timeline- Late Pre-Launch Access- Efficient On-Orbit Anomaly Identification/Resolution- Rapid Post-Recovery Access
MINIMUM OPERATIONS AND MAINTENANCE (O&M) SUPPORT <ul style="list-style-type: none">- Independent RRS Ephemeris Determination- Minimum Non-Payload Ground Crew Support- Pre-launch, On-Orbit, Recovery

The first consideration – safety – is primarily a design issue (which is discussed extensively in other sections of this report) since the actual operations can influence safety only to the extent that the design provides for a capability for influence. Although the overall safety of the RRS, the flight experiments, ground personnel, the public, and the prevention of property damage and damage to ground and flight hardware are all important, the issue of public safety is the overriding consideration. This issue, an integral part of the commercial licensing issues being addressed by the Department of Transportation (DOT) Office of Commercial Space Transportation (OCST), was a Congressional consideration in the 1988 amendments to the Commercial Space Launch Act of 1984. The DOT/OCST discussions, primarily driven by the NASA-funded Commercial Transporter (COMET) program, could make RRS safety a significant issue outside of the NASA process. This could be especially significant if there is any intent to ultimately convert the RRS to a commercial operation. If not addressed from the beginning, the potential for mandatory redesign to meet evolving requirements represent a, if not the, major cost/schedule risk for the RRS program.

The remaining considerations are best discussed within the overall context of the RRS operations as defined in the RRS System Requirements Document (Table 5-2). These definitions have been refined into somewhat greater detail (Table 5-3) to facilitate the Phase B preliminary design effort. The discussion will be in three parts: Pre-operations, Mission Operations, and Refurbishment.

Table 5-2. RRS System Requirements Document Mission Operations Definitions

An RRS mission consists of all activities (payload selection, integration, orbital operations, recovery, data retrieval), including ground control experiments, which relate to a single launch. Specific mission operations are defined as follows:	
Event	Operation
MISSION INITIATION	<u>Pre-Launch Phase</u> : Consists of payload selection, mission planning, experiment verification, and biocompatibility testing, integration, and launch site activities.
LIFTOFF	<u>Launch Phase</u> : Liftoff (first motion) to RRS separation
ORBIT INSERTION	<u>Orbital Flight</u> : Begins upon insertion (RRS separation) and concludes with first de-orbit command.
	<u>Recovery Phase</u> : Composed of De-orbit, Reentry and Terminal Phases
DE-ORBIT COMMAND for	De-orbit Phase: First de-orbit command to aerodynamically reoriented reentry.
ALIGNED FOR REENTRY	Reentry Phase: End of de-orbit to pilot chute deployment.
PILOT CHUTE DEPLOYMENT	Terminal Phase: From pilot chute deployment to impact.
IMPACT	<u>Post-Recovery Phase</u> : Impact to experiment and data delivered to PI, and simultaneous ground control experiments completed.
MISSION COMPLETE	<u>Refurbishment</u> : The disassembly, inspection, cleaning and repair necessary to return the RRV and PM hardware to flightworthy condition.
GROUND TESTS	<u>Ground Control Experiment</u> : Tests which (1) verify the experiment design, (2) verify the hardware biocompatibility and performance, and (3) serve as controls for the flight experiments.

Table 5-3. Expanded RRS Mission Operations Definitions

Event	Operation
MISSION INITIATION	<p><u>Pre-Launch Phase</u>: Composed of Pre-Operations and Launch Base Phases.</p> <p>Pre-Operations Phase: Payload selection, mission planning, experiment verification, and biocompatibility testing.</p> <p>Launch Base Phase: RRV/PM integration and launch site activities.</p>
LIFTOFF	<u>Launch Phase</u> : Liftoff to RRS separation
ORBIT INSERTION	<p><u>Orbital Flight</u>: Begins upon RRS separation and concludes with first de-orbit command.</p> <ul style="list-style-type: none"> - Pre-Mission Checkout - Mission Operations - Pre-Reentry Preparations <p><u>Recovery Phase</u>: Composed of De-orbit, Reentry and Terminal Phases</p>
DE-ORBIT COMMAND	De-orbit Phase: First de-orbit command to aerodynamically reoriented for reentry.
ALIGNED FOR REENTRY	Reentry Phase: End of de-orbit to pilot chute deployment.
PILOT CHUTE DEPLOYMENT	Terminal Phase: From pilot chute deployment to impact.
IMPACT	<u>Post-Recovery Phase</u> : Impact to experiment and data delivered to PI, and simultaneous ground control experiments completed.
MISSION COMPLETE	<u>Refurbishment</u> : The disassembly, inspection, cleaning and repair necessary to return the RRV/PM hardware to flightworthy condition.
GROUND TESTS	<u>Ground Control Experiment</u> . Tests to (1) verify the experiment design, (2) verify the hardware biocompatibility and performance, and (3) serve as a flight experiment control.

5.1 Pre-Operations

The Pre-Launch Phase, as defined in the RRS SRD, begins with the initiation of a given mission and includes both Pre-Operations and Launch Base phases. In reality, several payload missions are likely to be processed in parallel and the actual launch sequence determined well into the program after visibility is gained into the developmental problems of each of the payloads.

Since the SRD only established altitude/inclination limits, a set of Design Reference Missions (DRMs; Table 5-4) was established and information on the probable sequence of payloads (Table 5-5) was assessed. This assessment indicated that shared launches are to be

Table 5-4. RRS Design Reference Missions

• SEVEN DRMs REVIEWED FOR RRS APPLICATIONS:

DRM #	Character	Inclination	Altitude km (nm)	Orbit Type	Launch Site	Recovery Site
1*	Land Recovery	33.83°	350 (189)	Circ	ETR	WSMR
2*	High Altitude	33.83°	900 (486)	Circ	ETR	WSMR
3*	High Inclination	98°	897 (484)	Circ, Int	WTR	WSMR
4	Integer Orbit	35.65°	479 (259)	Circ, Int	ETR	WSMR
5	Water Recovery	28.5°	350 (189)	Circ	ETR	Water (ETR, WTR, Gulf)
6	Dual Altitude	33.8°	350-900	Circ	ETR	WSMR
7	High Altitude	33.8°	≤GTO	Elliptical	ETR	WSMR

• Primary DRMs

Abbreviations:

DRM	Design Reference Missions	WTR	Western Test Range
Circ	Circular	WSMR	White Sands Missile Range
Int	Integer	Gulf	Gulf of Mexico
ETR	Eastern Test Range		

Table 5-5. NASA LifeSat Mission Planning

Phase	Date	Orbit	Duration	Experiment
<i>Initial Phase</i>	Dec 1994	90/800 km	≤30 days	Cells, etc. (+ comp. satell.)
	Dec 1995	34/250	30-60	Cells, etc.
		34/500+	30-60	Cells, etc.
	Sep 1996	34/500+	45	Plants
		34/500+	45-60	Cells, etc.
	Jun 1997	90/200x30K	>60	Lower order organisms
	or	90/250	>60	Lower order organisms
		90/250	>60	Lower order organisms
	Dec 1997	90/ellip	30-60	Rodents/LOO (+comp. satell.)
<i>Second Phase</i>	<97 H-II	34/250	30	Micr-g bioprocess
	<98 Ariane	polar/250	45	Plants
	1999	34/250	30	Squirrel Monkey
	2000	polar/250	>60	Radiation Countermeasures

considered with first launch opportunity. Furthermore, the information indicated that 6 of the first 8 RRSs may be launched on first 5 boosters (1/2/2/2/1), with second launch placing vehicles in two different orbits. When the mission information was integrated with the potential launch options (Figure 5-1), the Delta and Atlas, two launch-proven vehicles, were clearly the primary candidates (Figure 5-2). Consideration was also given to scaling the vehicle (Figure 5-3) to fly a smaller payload on a smaller, theoretically less expensive, booster. However, the results supported the dual launch of the larger vehicle as the most cost-effective approach.

5.1.2 Pre-Operations Phase

The Pre-Operations Phase involves the selection of the payload for a given flight, the mission planning for that flight, the verification of the experiment's operation and any biocompatibility testing that may be required. The key operational consideration is to allow the payload selection to be as close as possible to launch site operations, minimizing the compounding of already costly payload problems with cost/schedule impact on the RRV effort. To minimize potential integration risks, payload and vehicle emulators (Figure 5-4) have been included in the program to validate RRV/PM compatibility prior to shipment to the launch site.

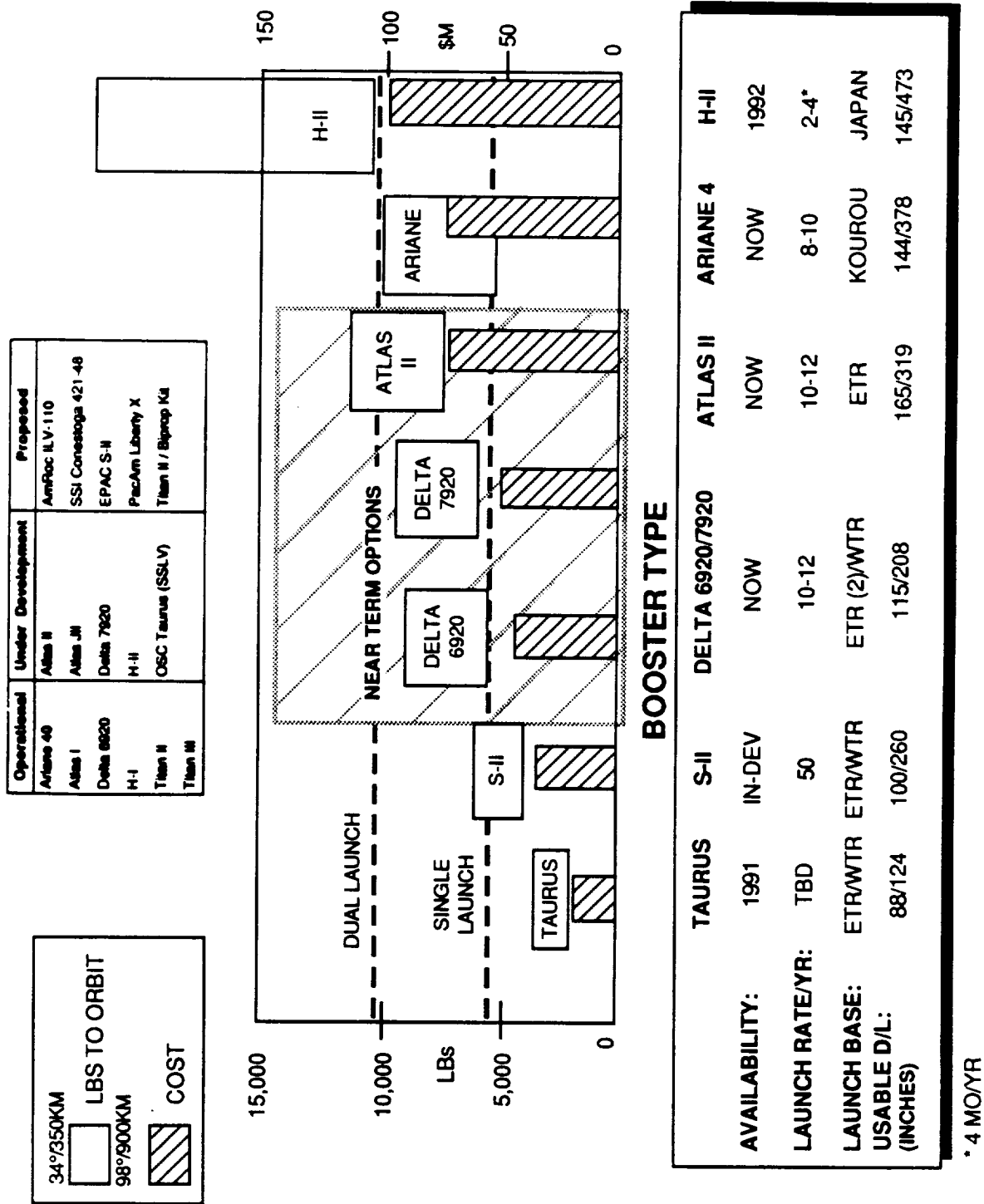
5.2 Mission Operations

Mission operations are driven by the vehicle's on-orbit mission profile and supported by appropriate ground operations. The key consideration is to minimize the cost of the ground support by making the vehicle operations as independent as possible.

5.2.1 Vehicle Operations

Vehicle operations (Figure 5-5) include all five operational phases: Launch Base, Launch, Orbital Flight, Recovery, and Post-Recovery. Of these, Launch Base, Orbital Flight, and Post-Recovery have the most important "Science Friendly" considerations. All vehicle operations, including the de-orbit burn, are sufficiently autonomous to preclude the need for TDRSS coverage. However, ground control visibility into selected operations (e.g., de-orbit burns, tri-mast operations) will probably be requested to ensure positive human control of critical operations.

















5.2.1.1 Launch Base Phase. The Launch Base Processing involves the RRV/PM integration and all other launch site activities. The key considerations are minimizing the Integrate-to-Launch Timeline and the provision for late Pre-Launch Access, the latter being driven






TOR42A/36

* 4 MO/YR

Figure 5-1. Launch Vehicle Options

VEHICLE	CAPABILITY (POUNDS)	
	350 km Circular 33.8°	833 km Circular 98.7°
Delta 6920	8,200 	Marginal  +
Delta 7920	10,600 	 +
Atlas I	11,000 	7,100 
Atlas II	13,000 	9,100  +
Atlas II AS (4 Castors)	Excessive Capability 	10,000  + 
Titan II	5,000 	Not Usable
Titan II (10 Solids)	9,500 	5,700 
Titan II (2 LRBs)	Excessive Capability	12,000  + 

 Single Launch
 Tandem Launch
 + Secondary Payload

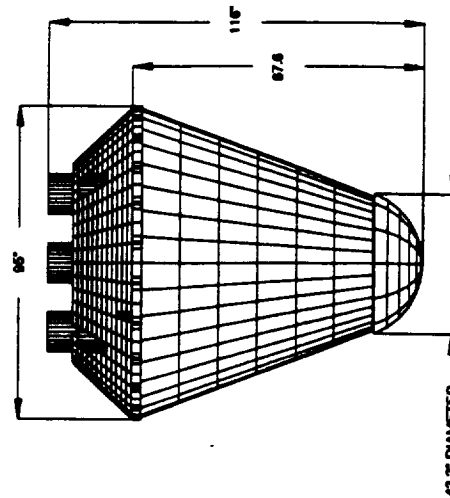
TOR42F/31

Figure 5-2. Launch Vehicle Candidate

SMALLER VEHICLES HAVE REDUCED REDUNDANCY, INCREASED
SAFETY RISK FOR CONUS RECOVERY

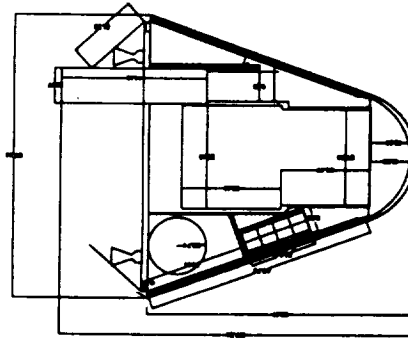
SIGNIFICANT NEW/MODIFIED HARDWARE DEVELOPMENT INCREASED
COST/SCHEDULE RISK LOSS OF SPACE QUALIFIED HERITAGE

RRV EXTERNAL DIMENSIONS

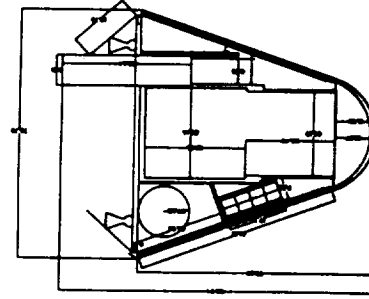


600 GM RODENTS

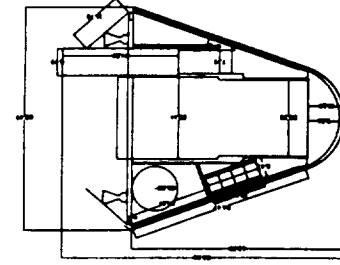
WEIGHT	18
POWER	3944
BASE DIAMETER	245
LENGTH	95
WEIGHT/RAT	116
2/DELTA	219



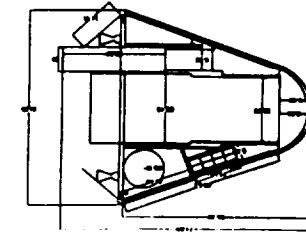
15
3602
204
88
107
240



12
3046
156
77
94
254



9
2495
125
68
84
277

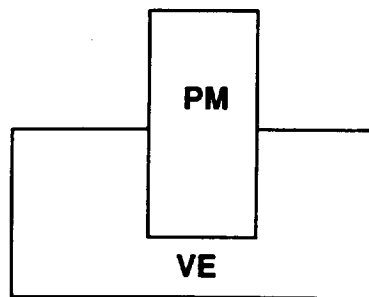


6
2135
98
61
75
356
≤1/TAURUS

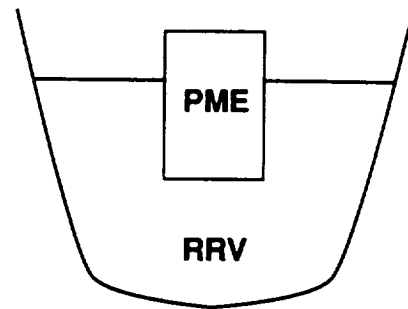
TOR42/18

Figure 5-3. Scaled Vehicle Configurations

- VARIED PAYLOADS REQUIRES TIGHT INTERFACE CONTROL AND POSITIVE VALIDATION PROCESS
 - Payload Provides PM Emulator (PME)
 - RRS Provides Vehicle Emulator (VE)
 - PME/VE Test Provides Initial Interface Validation



- VE Provides Positive Validation of RRV/PM Interface and Capability for Early Integrated Test of Flight PM



- PME Provides Interface for Assembly/Refurbishment Testing and the Capability for Preliminary Integrated Systems Test

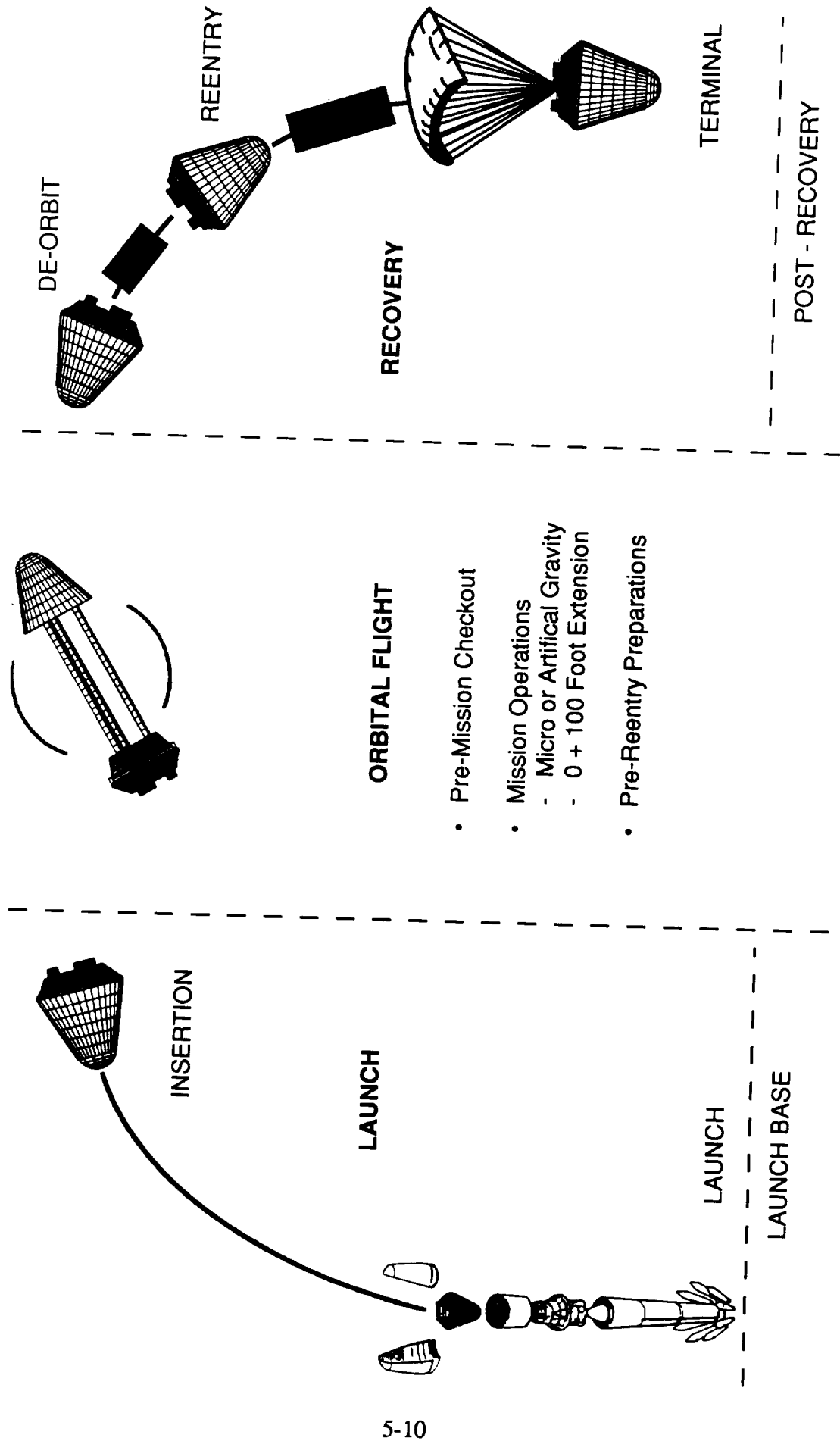
TOR42E/13

Figure 5-4. Pre-Operations Checkout

by the requirement to permit final experiment installation at up to T-12 hours and closeout as late as T-4 hours. Further complicating the process is the need to be able process two payloads for a single launch. The Launch Vehicle Adapter approach (Section 6.3) selected by SAIC allows parallel processing of the payloads (Figure 5-6) at the launch base, but requires additional detailed analyses to confirm the actual achievable timeline for the dual payload.

5.2.1.2 Launch Phase. The Launch Phase (Figure 5-7) begins with liftoff (first motion) and continues to RRS separation. SAIC's proposed use of GPS allows immediate determination of the RRS orbit without any ground support beyond telemetry reception and provides the ability for immediate vehicle attitude control (Figure 5-8).

5.2.1.3 Orbital Flight. The Orbital Phase begins upon insertion (RRS separation) and concludes with first de-orbit command. The original program requirements were for a mission duration from a few up to a maximum of 60 days at altitudes from 350 to 900 km and inclinations



TOR4211/13

Figure 5-5. Vehicle Operations

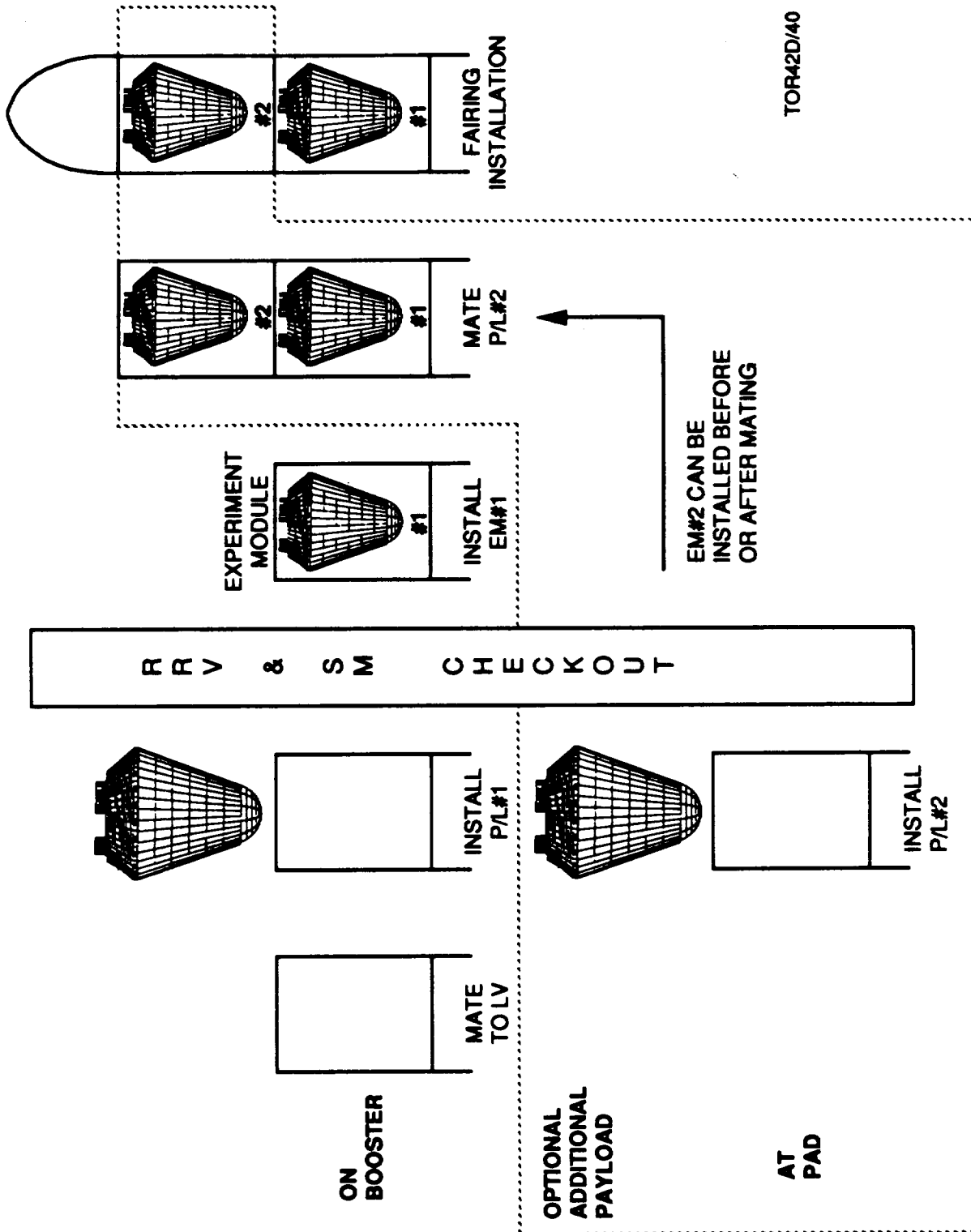
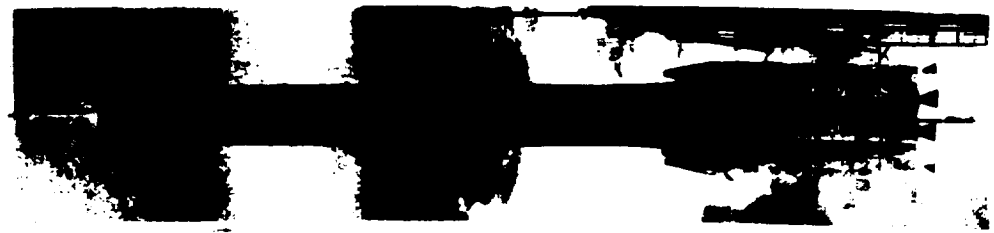
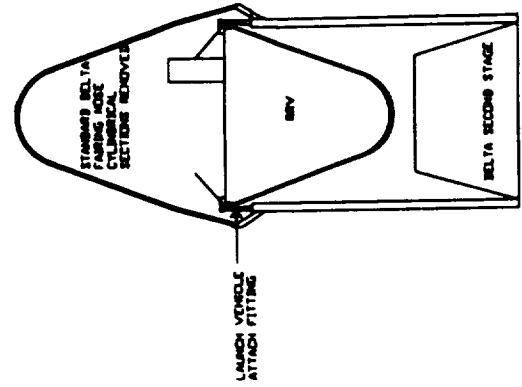


Figure 5-6. Launch Pad Sequence



- Vehicle Mounted Nose Down for Access Launch/OP/ Reentry G Load



- Use of Delta Nose Cone and Interstage Saves Development Cost

- Thermal and Power Interfaces Provide for Extended Prelaunch and Post Recovery Operations

- Module Emulators Provide for Early RRV/PM Interface Test and Validation
- Minimize Risk of Expensive Test/Launch Slips

- Delta Provides Proven Launch Capability
- Atlas Can Provide Enhanced Capability With Same Basic Interface

TOR42E/05

Figure 5-7. Launch

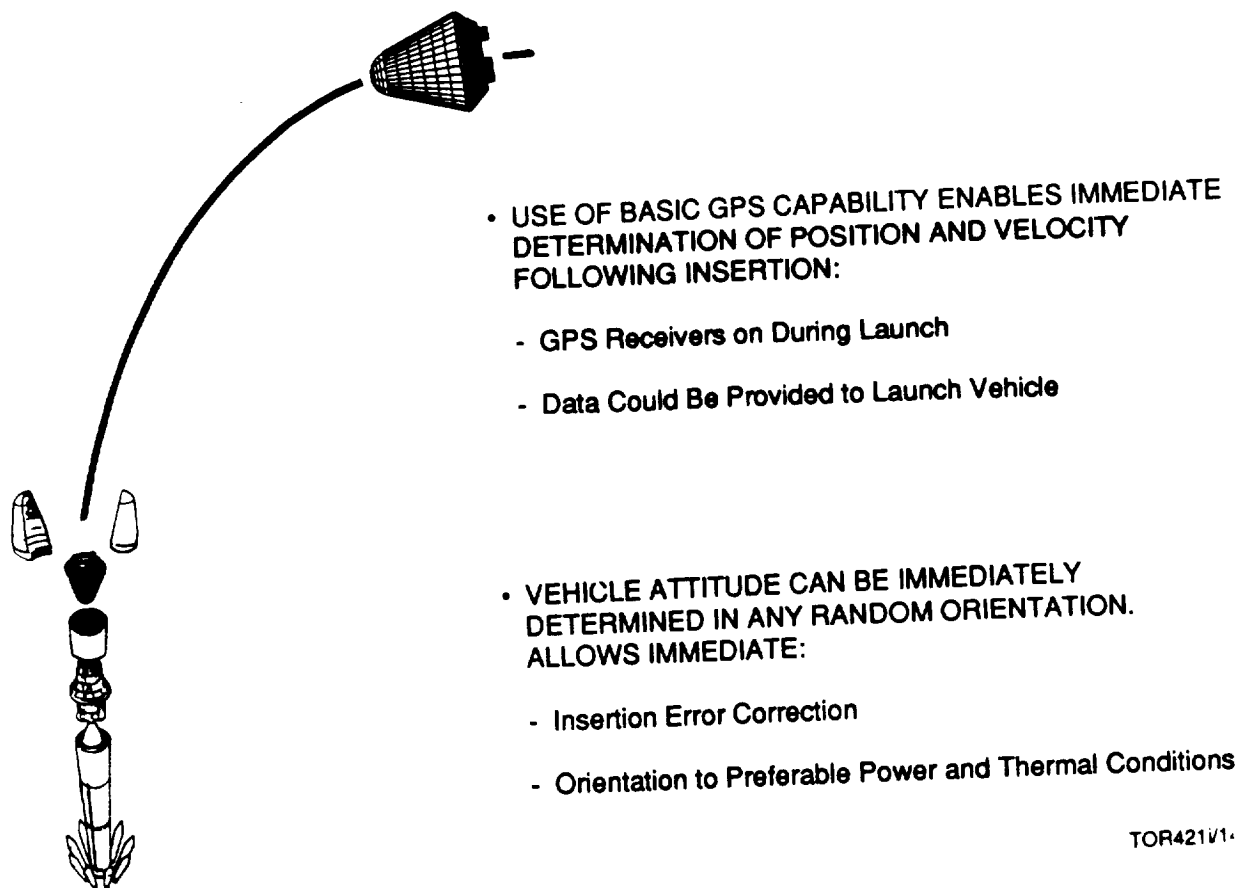


Figure 5-8. GNC Launch Phase

from 34 to 98 degrees. However, current NASA planning (Table 5-5) includes missions varying from 250-km circular at 34-degree inclination to a 200x30000 km orbit at 90-degree inclination, and missions from ≤ 30 to > 60 days. A payload capacity of approximately 1000 pounds is required to fulfill the RM requirement to fly 18 600-gm rats for 60 days (1080 rodent-days, up 375% from the original 288 rodent-day requirement). The key consideration is to provide an efficient means of on-orbit anomaly identification and resolution.

5.2.1.3.1 Pre-Mission Checkout. The initial on-orbit objective is to determine if the vehicle arrived without damage and is capable of performing the intended mission (Figure 5-9). The Pre-Mission Checkout is performed in the closed configuration to allow immediate recovery with minimal activity if problems exist. The final step of the Pre-Mission checkout is the extension of the deployable tri-mast to the appropriate length. Although the extension of the tri-mast is fully automatic and self-safing in the event of failure, TDRSS tracking support will probably be scheduled to provide ground control visibility into the operation.

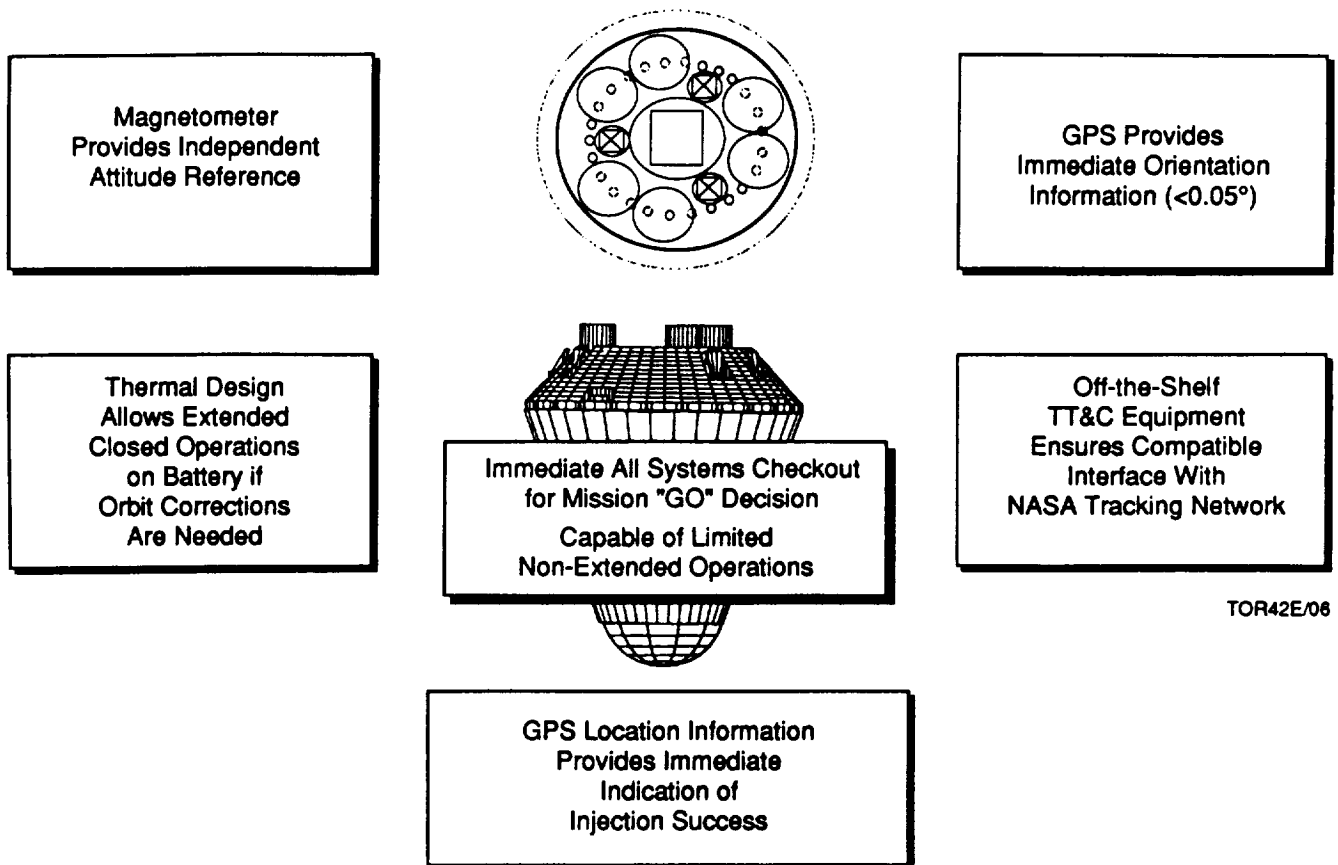


Figure 5-9. Pre-Mission Checkout

5.2.1.3.2 Mission Operations. The system must be capable of providing a gravity environment which can vary from microgravity (10^{-3} g maximum with $\leq 10^{-5}$ g $\geq 95\%$ of the time) to artificial gravity (0.1 g to 1.5 g (1.0 g for animals) controlled to $\pm 10\%$) within a single flight. Although the SRD PM requirements do not include simultaneous micro and artificial gravity experimentation, the EBM, which can be configured to use a centrifuge for artificial gravity independent of the RRV, has the potential capability for simultaneous experimentation.

- a. **Microgravity.** Microgravity operations (Figure 5-10) will normally be in a "free-flight" mode initially positioned for the best thermal/power capability for a given mission orbital profile (Section 6.8). Ground contact requirements will be driven by the payload requirement for experiment control. Daily contact (twice daily is available without TDRSS; see TT&C Coverage Summary Report) is adequate to ensure vehicle safety in the event of an RRV anomaly since the RRV operation will automatically configure the vehicle into a safe mode in accordance with a preplanned priority. Momentum wheels will be used to cancel the angular momentum generated by any internal rotating devices and/or any thermal rotisserie required for thermal balance.

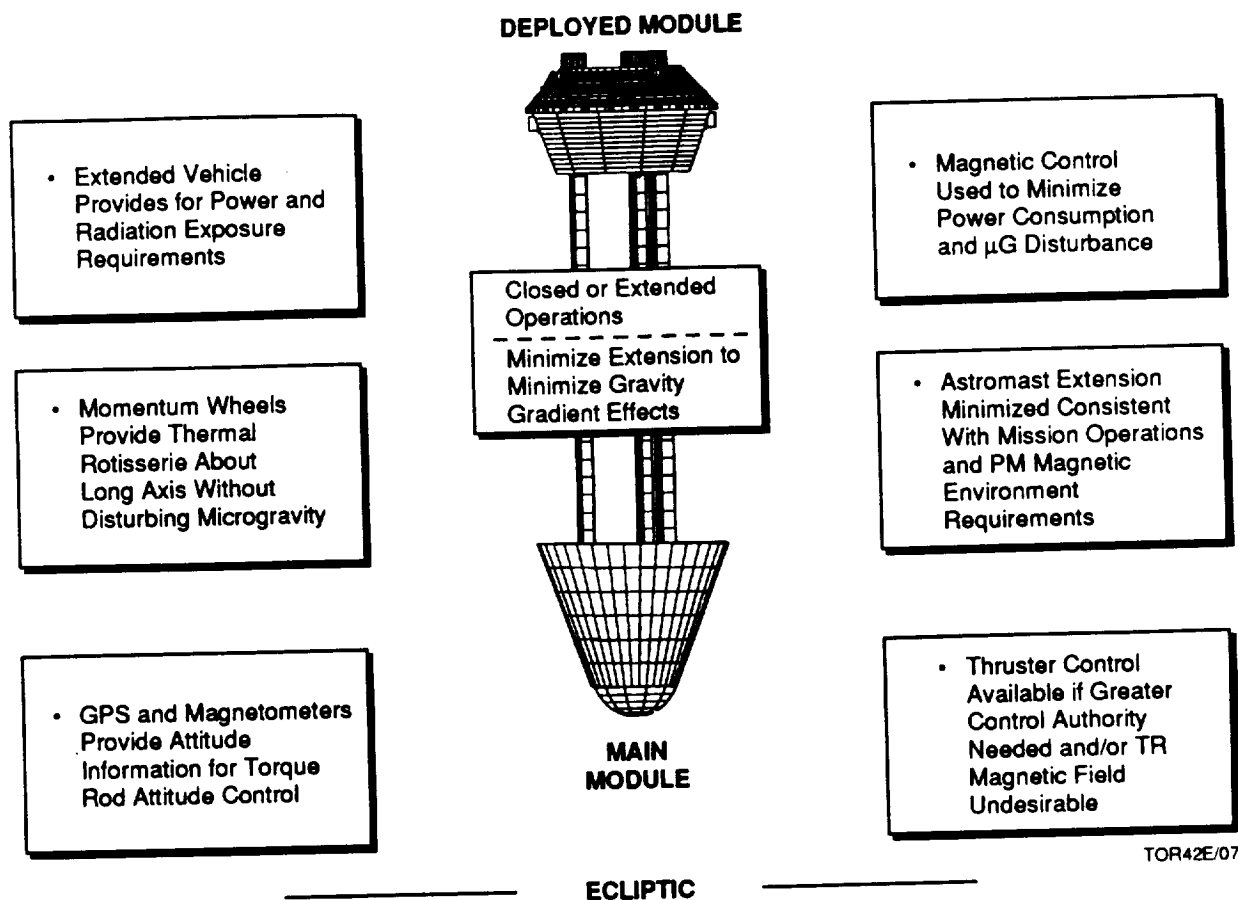


Figure 5-10. Extended Vehicle – Microgravity

b. Artificial Gravity. Artificial gravity operations (Figure 5-11) will be initiated after initial checkout at the appropriate extension length in the microgravity mode. The vehicle is oriented for operation in the desired spin plane with momentum wheels used to create the necessary preferential inertia. The spin-up is done under IMU control using thrusters. The twice daily available coverage should be adequate if the full multi-redundant IMU control is used. For power limited missions, the control system redundancy can be powered down and more frequent checks made via TDRSS to ensure mission safety. The vehicle will be despun into the microgravity mode at the end of the gravity mission.

5.2.1.3.3 Pre-Reentry Preparations. Reentry preparations (Figure 5-12) begin in the extended mode and include the retraction of the tri-mast. The IMU calibration and initiation of the tri-mast retraction will normally be scheduled during a ground pass, with TDRSS access scheduled for visibility into retraction operations.

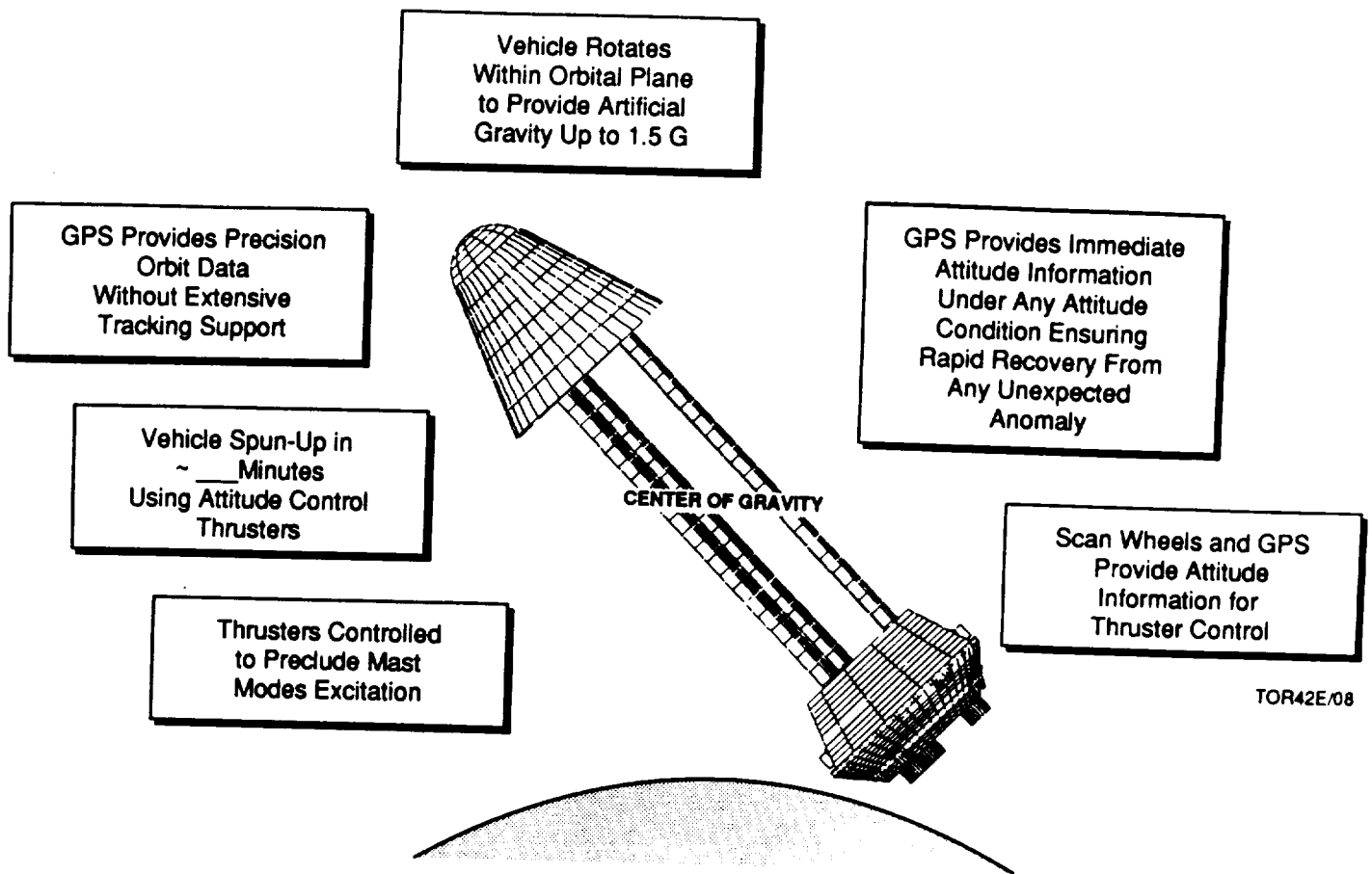


Figure 5-11. Extended Vehicle – Artificial Gravity

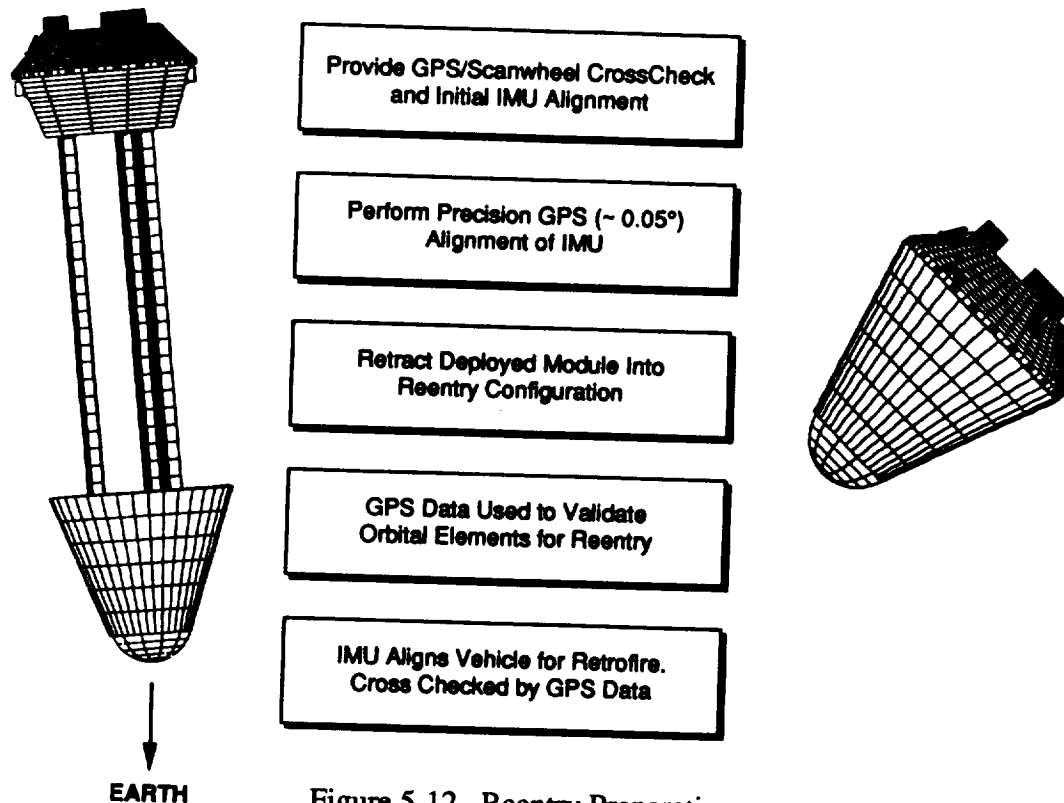


Figure 5-12. Reentry Preparation

5.2.1.4 Recovery Phase. The Recovery Phase includes the De-orbit, Reentry, and Terminal Phases of the On-Orbit operations. Although defined as distinct phases, once the vehicle is committed to de-orbit, the RRV will automatically perform all required functions without need for human intervention. In fact, while ground control visibility into the operations via TDRSS will probably be scheduled, any attempt at human intervention in the process is more likely to create than cure a problem.

5.2.1.4.1 De-orbit Phase. De-orbit operations (Figure 5-13) begin with the first de-orbit command and continue through aerodynamic reorientation for reentry. The operation is a "fail operational" process that is totally under IMU control, using GPS measurements for performance assurance.

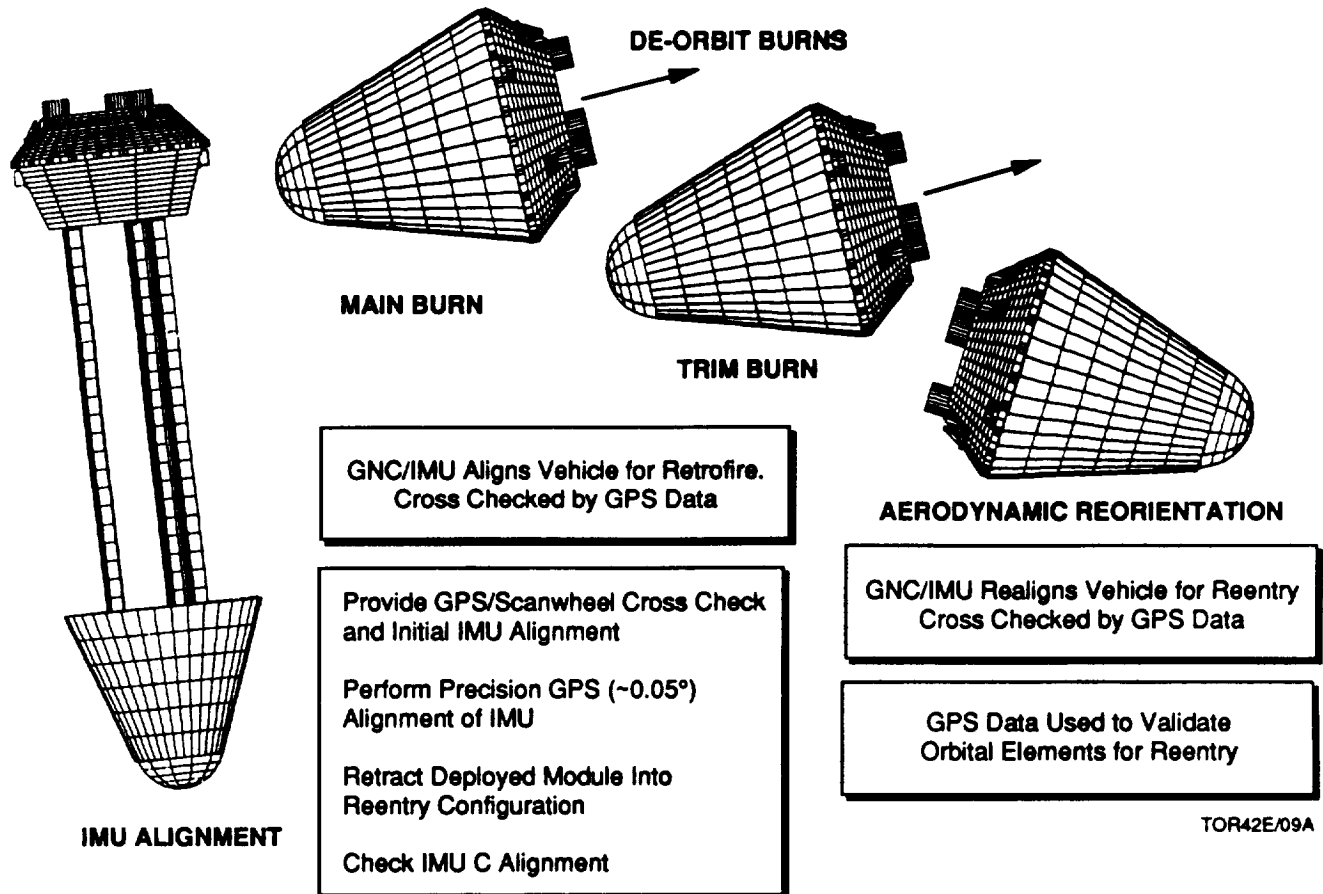


Figure 5-13. De-Orbit Operations

5.2.1.4.2 Reentry Phase. This is a totally autonomous phase which begins following the last de-orbit trim burn and continues until deployment of the pilot parachute. The deployment of the pilot parachute will be enabled at a preset time and activated by IMU control with a timer backup. GPS data will be used by the GNC to crosscheck the IMU operation. The reentry deacceleration shall not exceed 15 g axial nor TBD lateral.

5.2.1.4.3 Terminal Phase. The terminal phase (Figure 5-14) is from pilot chute deployment to landing. The RRS shall have a near-vertical descent from an altitude of at least 60,000 feet with a 3-sigma impact dispersion of no more than ± 6 km crossrange and ± 30 km downrange. The atmospheric braking shall not exceed 2 g axial. Impact shall not exceed 10 g any axis.

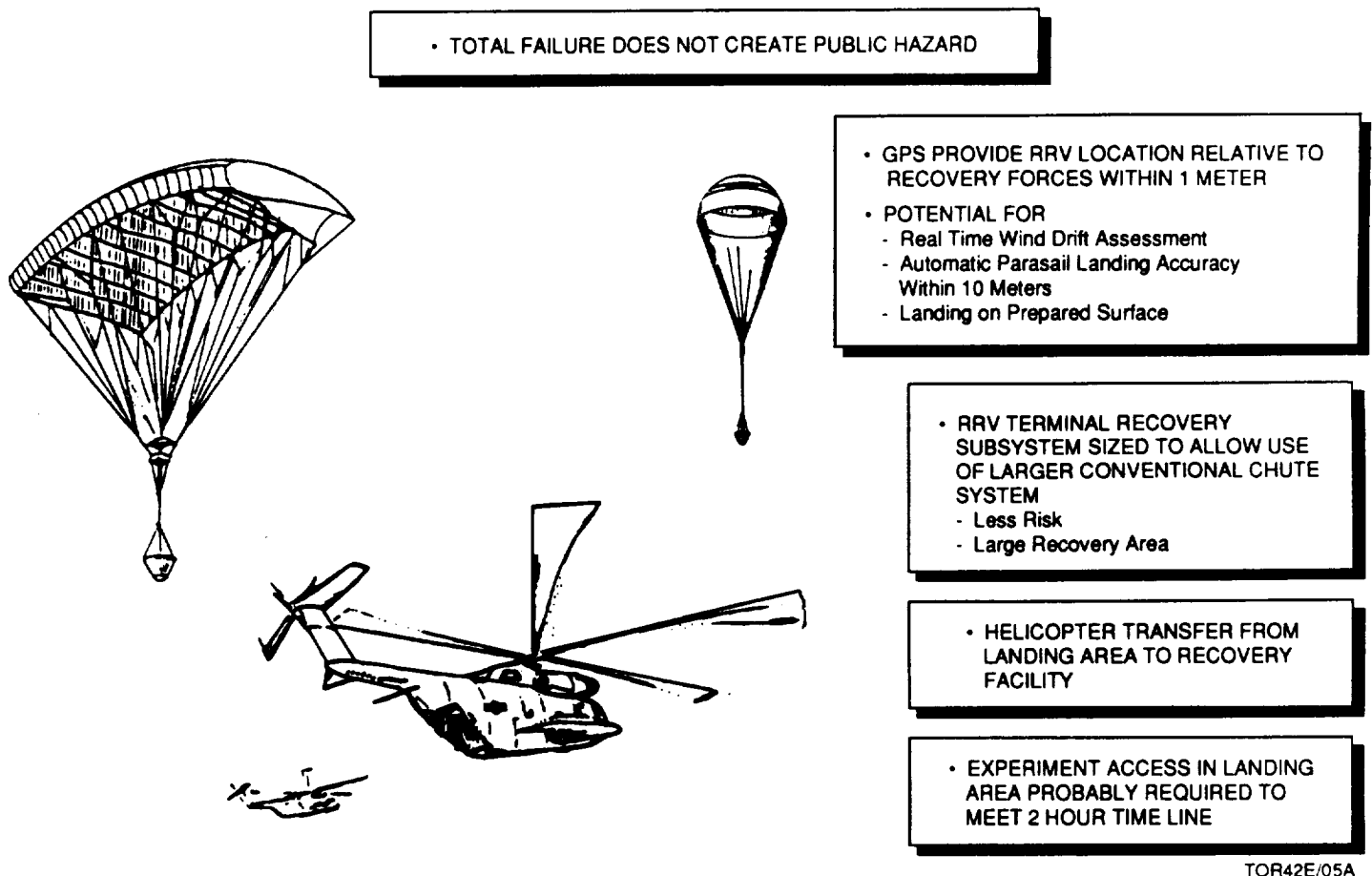


Figure 5-14. Terminal Operations

5.2.1.5 Post-Recovery Phase. The Post-Recovery Phase begins with the vehicle landing and continues until the experiment and data are delivered to the PI and simultaneous ground control experiments are completed. The primary consideration is rapid post-recovery access. Physical access to the PM and removal of the flight animals shall be ≤ 2 hours, with thermal/electrical support via Ground Support Equipment (GFE) within 60 minutes of touchdown, and delivery of the RRS to the post-recovery facility within 2 hours. Actual estimates of the recovery timelines (Tables 5-6 and 5-7) indicate that the 2-hour requirement can be met except under unusual recovery circumstances. Removal of the EM at either landing site was considered, but the cost of providing the environmental protection for such operations in the general White Sands area makes the approach sufficiently impractical that Option 4 is not recommended.

5.2.2 Ground Operations

5.2.2.1 Ground Control Experiment Module (GCEM). The objective of establishing a GCEM capability is to:

- a. Verify the experiment design
- b. Verify the hardware biocompatibility and performance
- c. Serve as controls for the flight experiments

All of the above require an operation as close to on-orbit conditions as possible. This in turn requires:

- a. Payload Module (PM) that functionally replicates the flight PM
- b. Vehicle Emulator (VE) that functionally replicates the operating environment of the PM
- c. Operator's console and associated GSE that both emulates the normal ground control interface and provides non-TT&C access to the:
 - (1) Vehicle mass memory
 - (2) PM control/data bus

The key to the success of the GCEM operation is the degree of fidelity of the PM environment. The vehicle emulation should, for example, provide the same power system characteristics as the actual vehicle if the true system response is to be validated. The same is true for the data bus used for control/data. Similarly, the PM environment should replicate the 1 g on-orbit conditions to validate gravity sensitive orbital operations (e.g., fluid and debris flow, filter action, etc.)

5.2.2.2 Mission Control. Since the RRS is not envisioned to be a real-time operation, and the GPS data will preclude any need for extensive tracking, Mission Control (MC) for the RRS will be a limited operation except during critical operations and or "sick vehicle" operations. Actual MC operations can be performed from any location having the real-time access needed for NATDN operations.

5.2.2.2.1 Mission Control Architecture. To minimize development and training cost, mission control for the RRS should replicate the console/GSE used for system testing and GCEM operations as close as possible. This approach also minimizes the amount of unique software development and ensures significant real operational test time on the software before it is committed to critical on-orbit use. Furthermore, because of the short duration of the RRS operational passes, the GSE should include enough of the GCEM equipment to permit validation of TT&C operations before the command/upload is released for use in a given pass.

5.2.2.2.2 Operations. RRS operations are expected to fall into one of four categories: launch support, normal on-orbit operations, "sick bird" operations, and critical maneuver control.

- a. **Launch Support.** Although all RRS operations will be conducted autonomously, the mission controller is expected to want real-time visibility into the operation. Since the need is for visibility into the operation, not a detailed data flow, the data available via the low-data-rate TDRSS link will be sufficient. Sufficient command will be available via TDRSS to "safe" the system if an anomaly occurs.
- b. **Normal Operations.** Normal support will consist of two or less 8- to 10-minute passes per day depending upon the mission. The short duration of the pass requires an efficient operation using a pre-validated pass plan and command sequence. Downlinked data will be recorded for post-pass processing with minimal real-time visibility other than a basic State-of-Health display on the RRS MC console.

- c. **"Sick Bird" Operations.** Whenever a significant anomaly occurs, the mission controller is expected to want extended real-time visibility into the on-orbit operation. Although the primary data dumps will be during the ground passes, there is a real-time need for safing the system and configuring the vehicle to obtain the necessary data for ground analysis. Adequate data/command capability for this type of operation will be available via the low-data-rate TDRSS link.
- d. **Critical Maneuver Control.** Although all RRS operations can be conducted autonomously, certain critical operations (e.g., tri-mast operations, de-orbit burns, etc.), the mission controller is expected to want the visibility into the operation. Since the need is for visibility into the operation, not a detailed data flow, the data available via the low-data-rate TDRSS link will be sufficient. Sufficient command will be available via TDRSS to "safe" the system if an anomaly occurs.

5.3 Refurbishment

The refurbishment cycle, which is defined in the SRD as the disassembly, inspection, cleaning, and repair necessary to return the RRV and PM hardware to flightworthy condition, actually begins with the RRV servicing that occurs during the recovery phase and includes transporting the vehicle to the refurbishment facility. The cycle (Figure 5-15), which is based upon the RRV manufacturing process and is discussed in Appendix A, is required to have the RRV ready for integration with another PM within 60 days of recovery from the prior mission.

Table 5-6. RRS Recovery Timelines

Activity	Time (min)	Uncertainty	
		Operational	Design
RRV Landing Landing contact until personnel arrive	5	10	10
Hazard Inspection and Safing Propellant leak check, visual inspection, safe pyros, open circuit breakers	10	10	5
RRV Transportation Sling Installation Connect sling attachments, recover parachute	5	5	10
RRV Positioning and Stabilization Position crane and transporter, attach sling, lift RRV onto cradle, secure RRV, recover parachutes	10	10	10
Helicopter Transfer Engage sling/harness, transport, position on arrival, disengage sling/harness	40	15	10
Transfer to Post-Recovery Facility Attach restraints, move to facility, install work platforms	10	5	5
Recovery System Canister Removal Position workstands, disconnect and cap wiring, remove structural fasteners, manually remove canister	10	5	5
PM Interface Disconnection Disengage power, disconnect interfaces, cap connectors, remove structural fasteners	10	10	20
PM Removal and Transfer Position crane, attach cable to PM, extract PM from RRS, transfer PM to GCEM support cart, install fasteners, reconnect interfaces, turn on power and GSE support	20	10	20
Access to EM Remove cover to PM, attach lift cable, remove animal cage	10	5	5

TOR42F/03

Table 5-7. RRS Recovery Options

Option 1 - Helicopter return of the RRV and EM access in the Post-Recovery Facility

Option 2 - Helicopter return of the RRV with PM removal on facility apron and EM access in the Post-Recovery Facility

Option 3 - PM removal at the landing site with helicopter transfer of the PM and EM access in the Post-Recovery Facility

Option 4 - EM removal at landing site and EM access at landing site

Activity		Options			
		1	2	3	4
RRV Landing		①	①	①	
Hazard Inspection and Safing		②	②	②	
RRV Transportation Sling Installation		③	③		
RRV Positioning and Stabilization				③	
Helicopter Transfer		④	④		⑦
Transfer to Post-Recovery Facility		⑤	⑥	⑧	
Recovery System Canister Removal		⑥	⑤	④	
PM Interface Disconnection			⑥	⑤	
PM Removal and Transfer			⑦	⑥	
Access to EM		⑦	⑧	⑨	⑨
Recovery to Northrop Strip	Baseline Time =	0.833 hr. (50 min)	1.333 hr. (80 min)	1.417 hr. (85 min)	
	Uncertainty =	0.401 hr. (24.5 min)	0.667 hr. (40 min)	0.667 hr. (40.9 min)	
	Probable Time =	1.234 hr. (74.5 min)	2.000 hr. (120 min)	2.085 hr. (125.9 min)	
General White Sands Recovery	Baseline Time =	1.500 hr. (90 min)	2.000 hr. (120 min)	2.083 hr. (125 min)	
	Uncertainty =	0.501 hr. (30.4 min)	0.718 hr. (43.9 min)	0.735 hr. (44.7 min)	
	Probable Time =	2.001 hr. (120.4 min)	2.718 hr. (163.9 min)	2.818 hr. (169.7 min)	

TOR42F/04

6.0 CONFIGURATION

This section discusses the baseline design of the SAIC RRS configuration. The discussion begins with a quick overview of the design, then addresses the operational and developmental risks, and finally provides details of each module/subsystem. The intent is to identify and describe the design logic and drivers in addition to providing a compilation of design details.

The SAIC approach is driven by the philosophy (Table 6-1) that the vehicle design should be responsive to the critical safety and science mission requirements, and that the affordability and operational efficiency of the program need not suffer in order to meet those requirements. This approach is founded on the basic belief that program development risk (technical and cost) is best minimized by applying existing component level technology in a manner that maximizes testability and nonserial scheduling. Furthermore, while space qualified components using S-level parts may be ideal for long duration space operations, use of such items should not be allowed to drive cost and schedule risk if less costly and readily available components exist that have proven capability for the projected mission environment and duration. This is especially true for a short mission, refurbishable vehicle such as RRS where redundancy in design is already driven by CONUS recovery fail operational requirements.

Table 6-1. SAIC Design Philosophy

#1	SAFETY <ul style="list-style-type: none">- CONUS Recovery- Fail Operational/Redundant Systems
#2	MEET SCIENCE REQUIREMENTS <ul style="list-style-type: none">- 0-1.5 g With Negligible Gravity Gradient and Coriolis- 18 Rodent/60 Day Mission- Quick Access to Payload- Multiple Payload Accommodation
#3	AFFORDABLE DESIGN <ul style="list-style-type: none">- Minimal Development Risk- Off-the-Shelf Technology Where Possible- Innovation Where Advantageous
#4	MINIMIZE OPERATIONAL SUPPORT <ul style="list-style-type: none">- Use Existing Ground Support Resources- Minimize Refurbishment

Given the SAIC design philosophy, the NASA requirements did not create any significant design constraints (Table 6-2). Instead, generalized mission objectives that were described as important by NASA, but not quantified in the SRD, became the key items to be considered in the design to the extent that they did not drive the design. For example:

- The vehicle shielding should be minimized to provide maximum experimental flexibility for radiation experimentation.
- Ground control and on-orbit experiments should be absolutely identical, with the exception of the space radiation environment, to provide a true cross calibration that would clearly reveal unexpected space effects.
- The vehicle should support up to six mid-deck lockers to be consistent with RMOAD planning.
- There should be no nonstructural single point failure anywhere in the de-orbit to landing recovery process that could create a public hazard.

Table 6-2. Design Constraints

<ul style="list-style-type: none"> • NASA RRS SYSTEM REQUIREMENTS DOCUMENT <ul style="list-style-type: none"> - Did Not Create Design Problems, Flexible - Did Not Drive Cost • FLEXIBLE OPERATIONS <ul style="list-style-type: none"> - Controllable Radiation Exposure - Uniform Payload Environment <ul style="list-style-type: none"> - Exact 1G Ground Control Experiment - Simple STS Mid-Deck Locker Use - Fail Operational Reentry for White Sands Landing • BOOSTER – USE OF PROVEN BOOSTER HARDWARE <ul style="list-style-type: none"> - Single Launch – Delta to All Orbits <ul style="list-style-type: none"> - Adaptor Utilizes Existing Delta Hardware - Dual Launch <ul style="list-style-type: none"> - Delta to Lower Orbits/Inclinations - Atlas to High Orbits/Inclinations

Similarly, if the intent of the program is really long-term recoverable access to space, booster considerations should cover the full RMOAD mission spectrum (including dual launches), emphasizing payload per unit life cycle costs. While any potential development cost risk should be minimized, that minimization should be in balance with and not override long-term operational savings.

The primary characteristics of the SAIC design are shown in Figures 6-1 and 6-2. The three module, multiassembly configuration allows science accommodation and cost/schedule risk minimization to be synergistic instead of competitive. The Deployed Module (DM) provides for the basic host satellite functions while the Main Module (MM) is the primary reentry vehicle body and contains the Payload Module (PM). These modules further divide into subassemblies that can be manufactured and refurbished in parallel to save cost and time.

Although the mast is perceptively a major risk, multiple analyses have shown that the SAIC tri-mast approach is a viable design that provides multiple performance enhancements. Although the minimization of payload Coriolis effects (Figure 6-3) was the initial driver in the mast oriented design, the full 100 foot extension is only needed for low fractional gravity experimentation. A much shorter extension is sufficient for the critical 1 G earth comparative experimentation (~20 feet) and an even shorter extension (~10 feet) can generally provide the module separation necessary for the solar power and radiation exposure capabilities. More specifically, the mast configuration provides for:

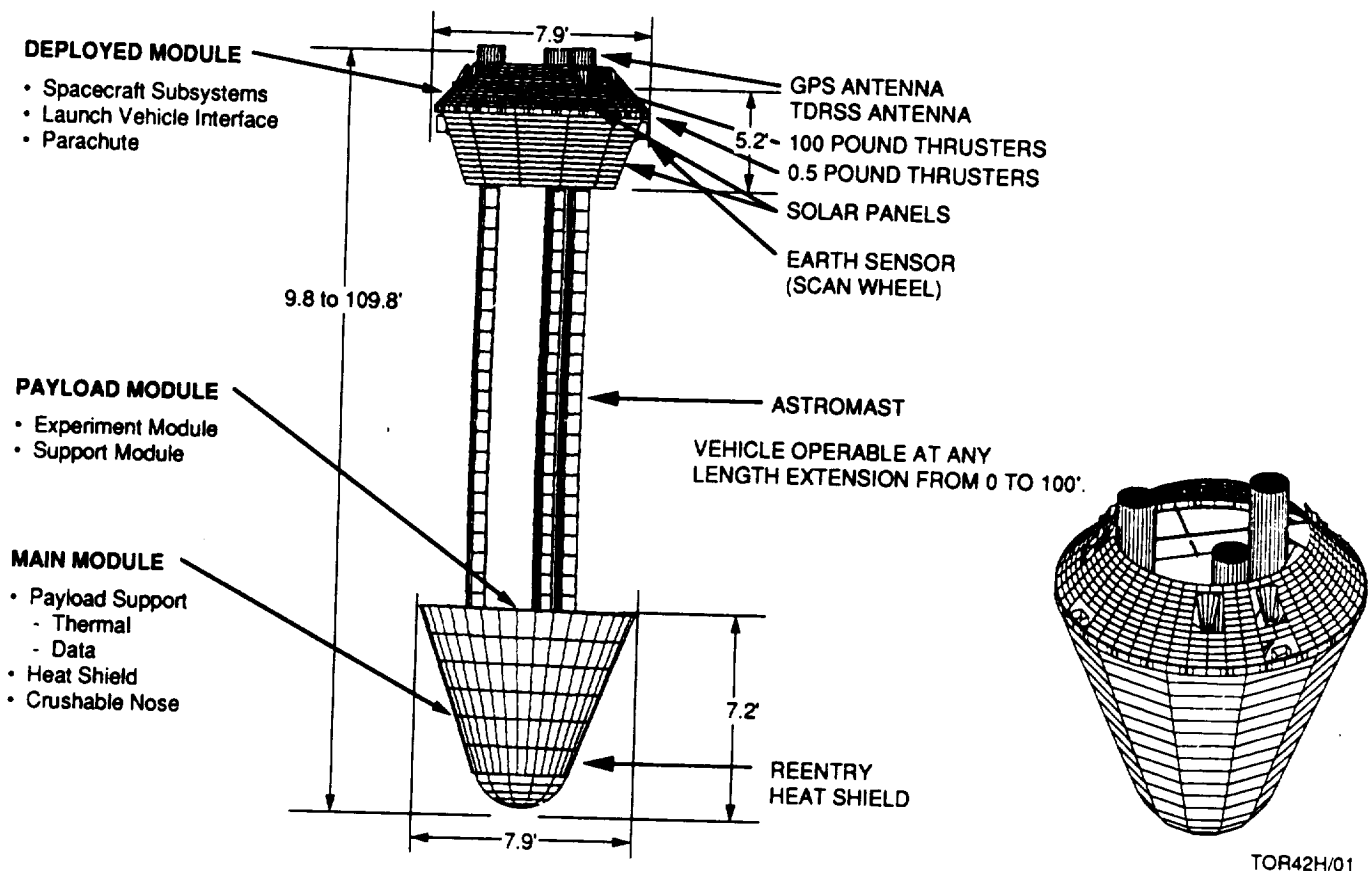
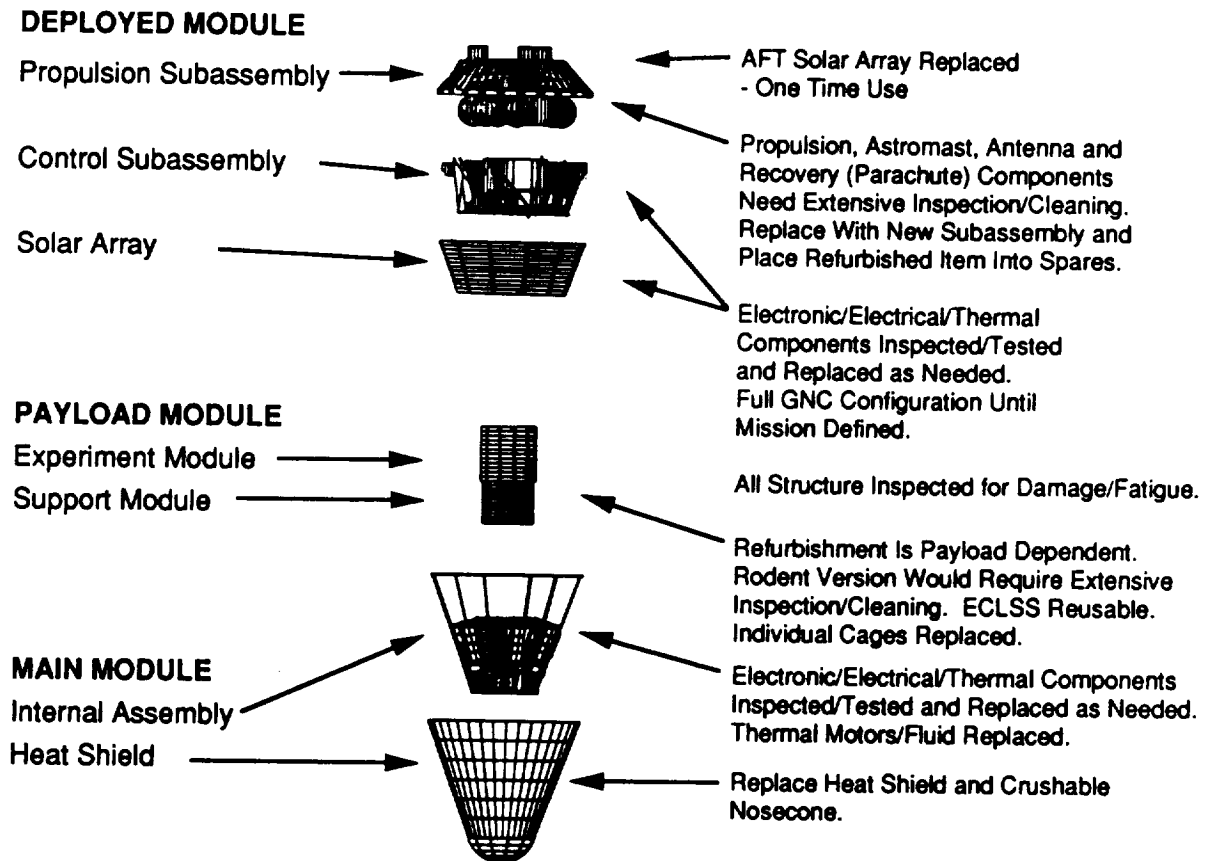


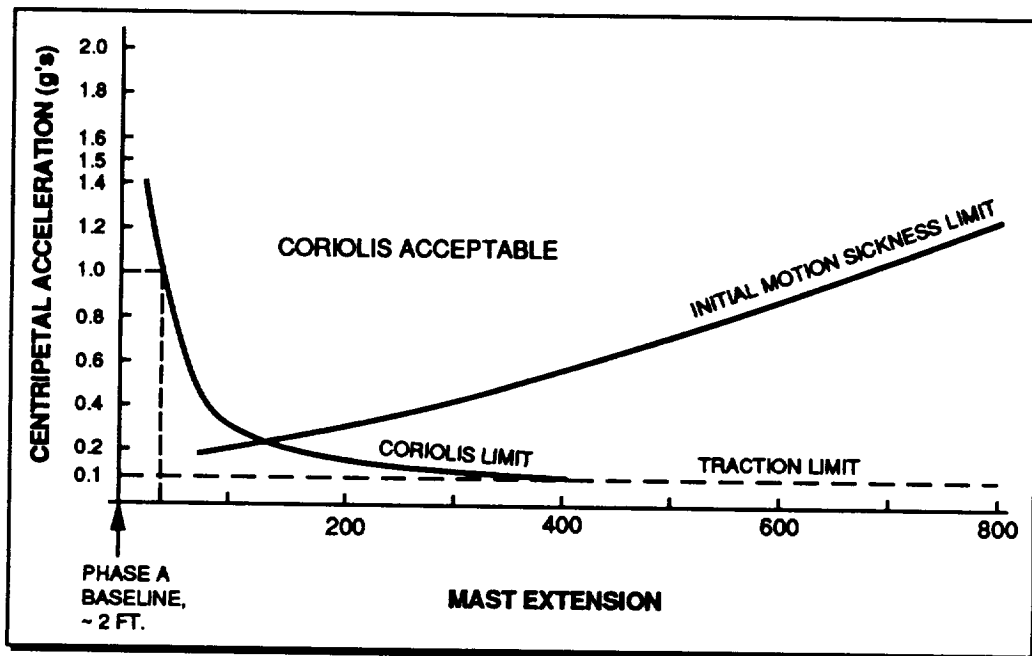
Figure 6-1. Primary RRS Characteristics

OBJECTIVE: PARALLEL PROCESSING OPERATIONS TO SAVE SCHEDULE AND COST



TOR421/02

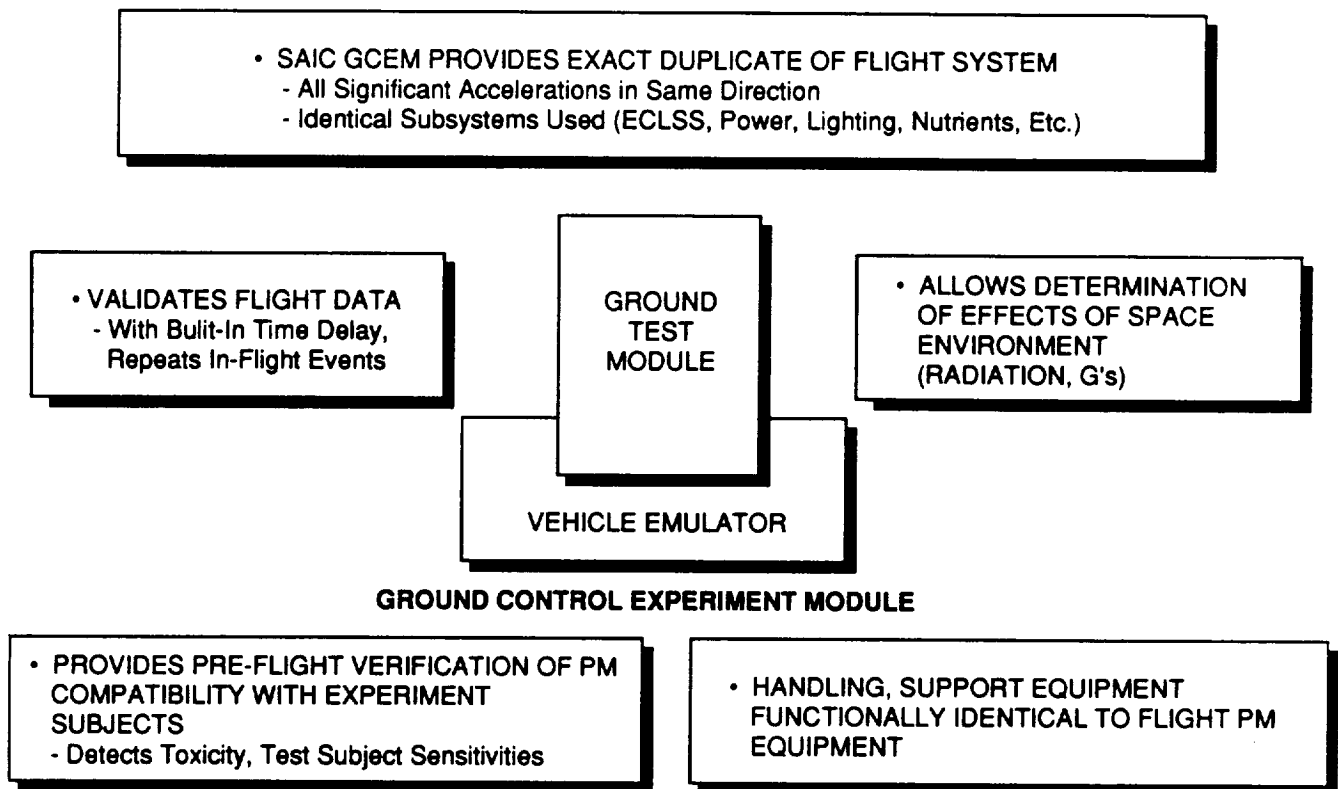
Figure 6-2. Modular Manufacturing and Refurbishment Concept



DERIVED FROM: "PHYSICAL CONSIDERATIONS OF ARTIFICIAL GRAVITY" TOR42B/01a
D. B. CRAMER, "TETHER IN SPACE" WORKSHOP, JUNE 1983

Figure 6-3. SAIC Fractional Gravity Approach

- A near uniform payload volume gravitational environment.
- Exact replication of the orbital gravity environment (Figure 6-4) in a ground control experiment.
- Use of the solar arrays to eliminate stored energy capacity (batteries or otherwise) as a major mission limiting factor for both total power and mission duration.
- Virtually hemispherical free space radiation exposure (Figure 6-5) that puts the experimenter in almost total control of the radiation spectrum.
- Experimentation with the full six mid-deck lockers capacity used in the RMOAD planning (Figure 6-6).



TOR42E/04

Figure 6-4. Ground Checkout and Experimentation Control

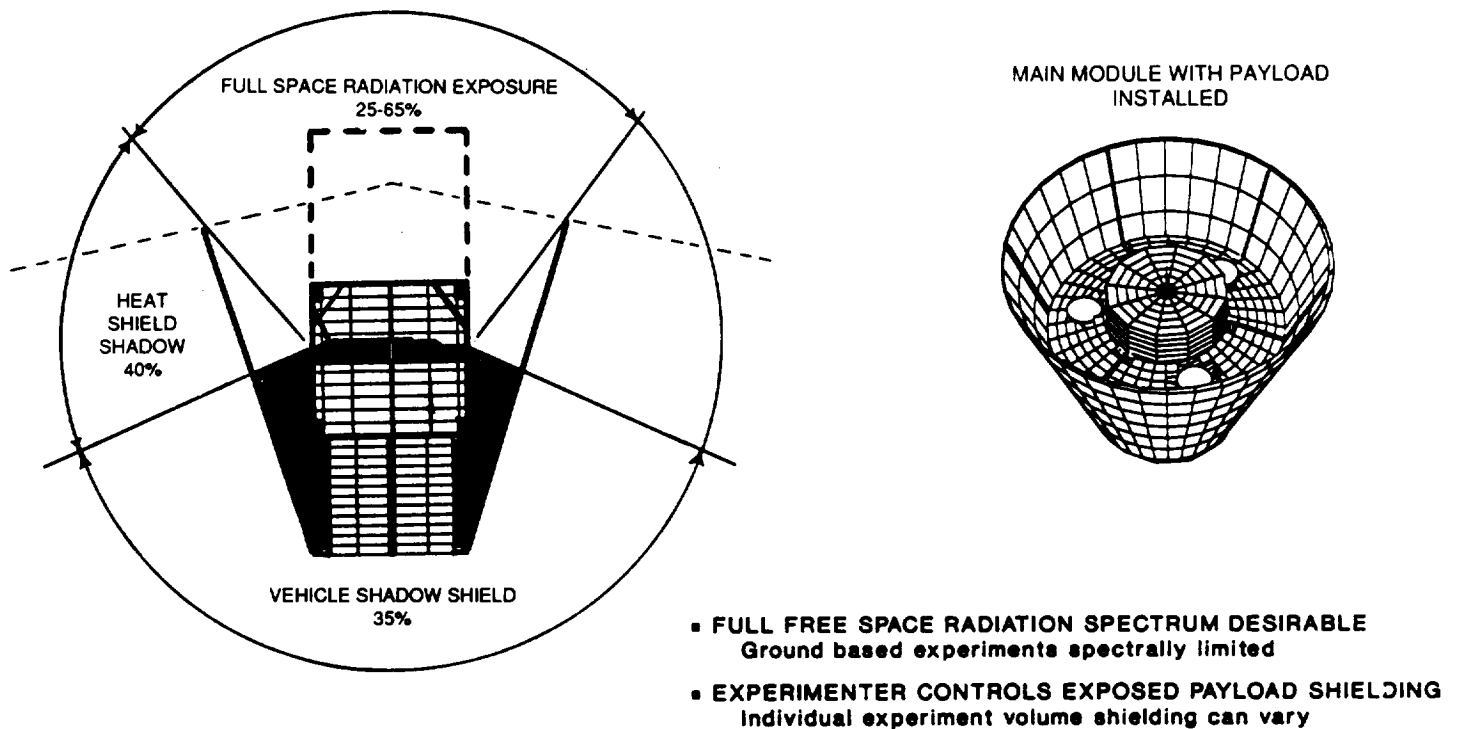


Figure 6-5. Free Space Radiation Exposure

The centralized payload volume also allows the payload module scaling (Figure 6-7) that would be necessary for potential scaled down vehicle configurations (Figure 6-8). However, while the scaled down approach may be attractive for possible use on the Taurus, the weight-per-unit payload, and therefore cost per unit payload, increases by about two-thirds for only about a 50% per launch cost savings. This is in addition to the nearly a factor of 2 increase in science cost if the full 18 rats must be flown to obtain the necessary experimental statistics.

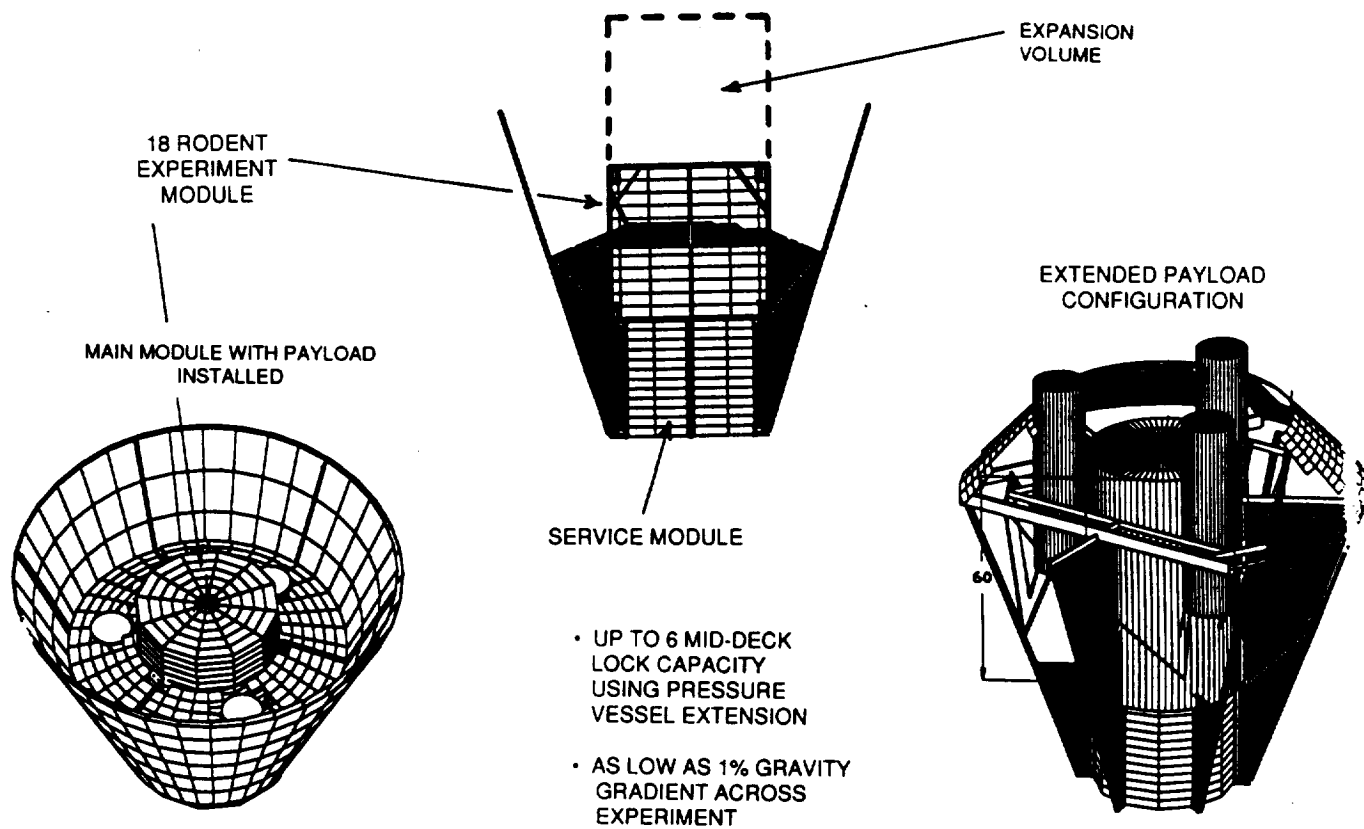


Figure 6-6. Variable Mid-Deck Locker Capacity

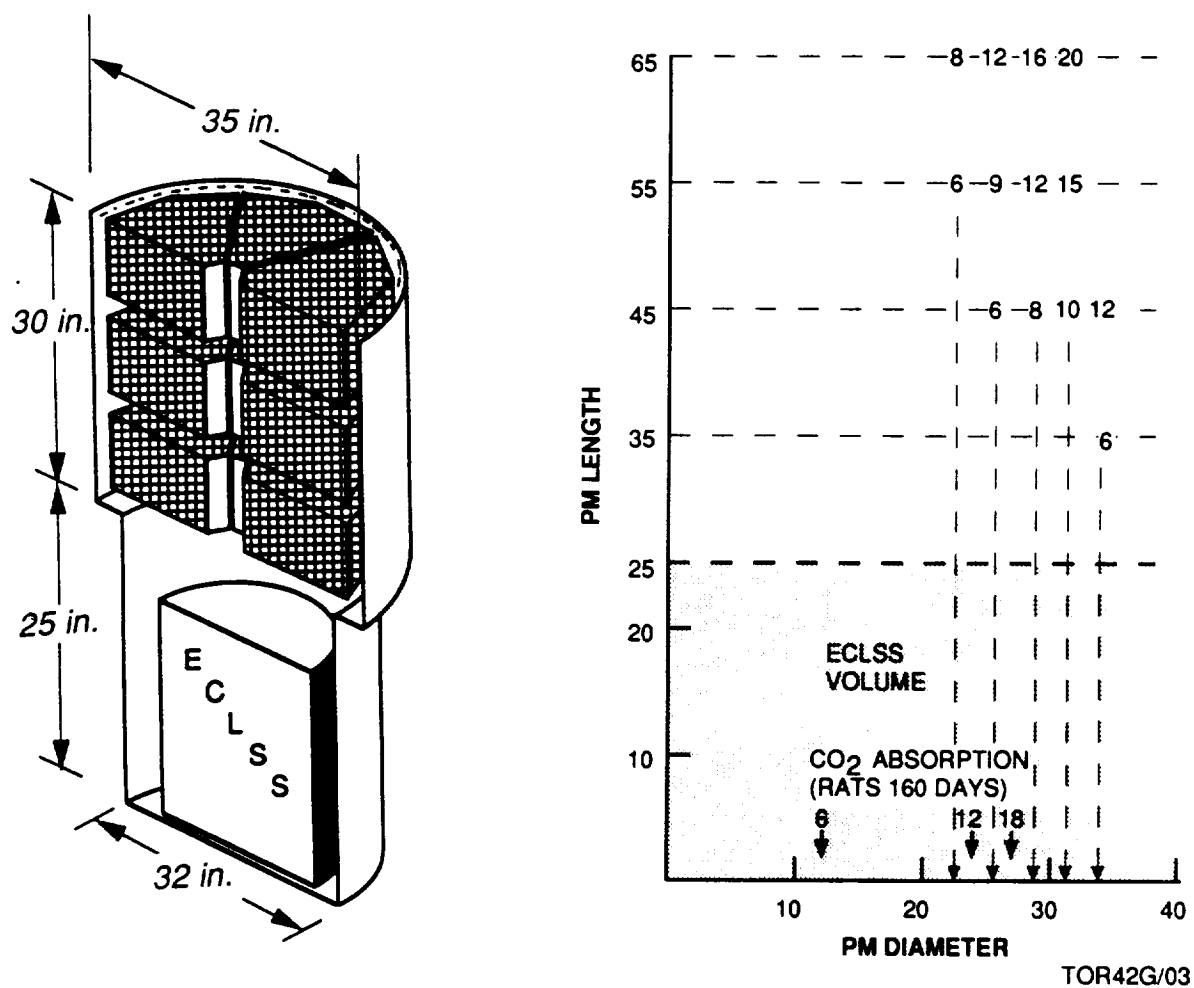


Figure 6-7. Payload Module Scaling

SMALLER VEHICLES HAVE REDUCED REDUNDANCY, INCREASED
SAFETY RISK FOR CONUS RECOVERY

SIGNIFICANT NEW/MODIFIED HARDWARE DEVELOPMENT INCREASED
COST/SCHEDULE RISK LOSS OF SPACE QUALIFIED HERITAGE

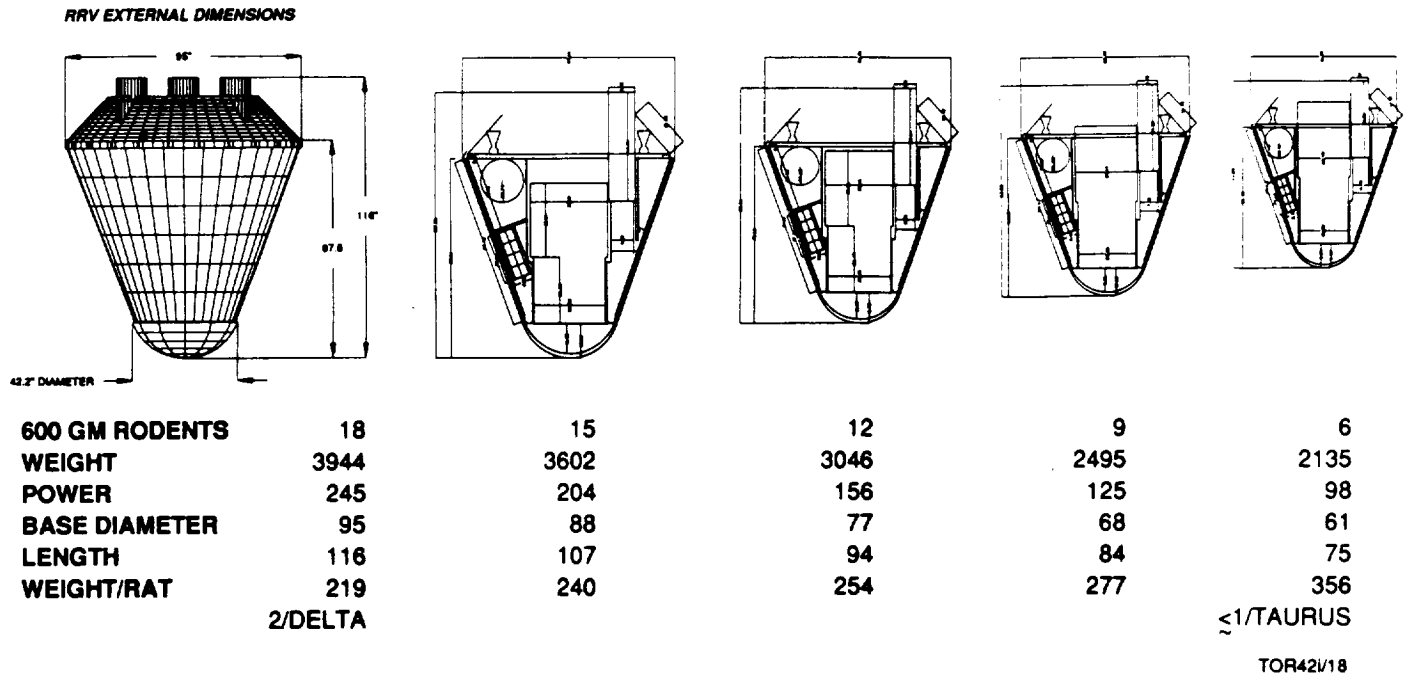


Figure 6-8. Scaled Vehicle Configurations

In summary, the SAIC design approach (Table 6-3) emphasizes public safety and science accommodation, with the use of the deployable tri-mast being a key element in the vehicle's unique performance capabilities. The following sections will discuss in greater detail the design features (Table 6-4) that make the SAIC design a unique approach for low risk, flexible, space experimentation.

Table 6-3. Design Approach

<ul style="list-style-type: none"> • PUBLIC SAFETY <ul style="list-style-type: none"> - Fail Operational Reentry Operations <ul style="list-style-type: none"> - Multiple Failure Tolerant - Liquid, Multi-burn Multi-Thruster Design • SCIENCE REQUIREMENTS <ul style="list-style-type: none"> - Flexible Operations <ul style="list-style-type: none"> - Radiation Exposure - Uniform Payload Environment - Large Unrestricted Volume - Long-Term Mission Power • VEHICLE <ul style="list-style-type: none"> - Astromast – Multi-Failure Tolerant <ul style="list-style-type: none"> - Provides Operational Flexibility <ul style="list-style-type: none"> • Environment, Coriolis, Power • Exact On-Orbit Ground Test Environment
--

Table 6-4. Key SAIC RRS Design Features
– Low Risk Flexible Space Experimentation –

<ul style="list-style-type: none"> • VEHICLE <ul style="list-style-type: none"> - Highly Controllable, Multi-Redundant Control/Propulsion Approach <ul style="list-style-type: none"> - Ensures Public Safety During CONUS Operations - Provides Minimal Risk Initial Operations Orbit - Solar Array Power <ul style="list-style-type: none"> - Up to 407 Watts Available (Mission Dependent) - Eliminates the Mission Constraints Imposed by a Stored Energy System - Single/Dual Launch Vehicle Adaptor <ul style="list-style-type: none"> - Minimizes Risk Through Use of Proven Delta Hardware/Technology - Simplifies Satellite Interface/Access/Deployment • PAYLOAD <ul style="list-style-type: none"> - Low Vehicle Shielding, Gravity Gradient and Coriolis Levels <ul style="list-style-type: none"> - Allows Gravitational Experimentation in Maximum Space Radiation Spectrum - Flexible Operating Configuration <ul style="list-style-type: none"> - Permits Variable Experimentation Within/Among Various Missions - Permits Specimen Configurations From 18 Rats to Group 2 Nonhuman Primates

6.1 Program Risk

The risks that face a program such as the RRS involve both operational and developmental considerations. Although not totally separable, if the operational risk is unacceptable, the program is not viable no matter how low the developmental risk can be perceived. Similarly, if the system is to provide long-term, cost-effective access to space, the vehicle's scientific flexibility/utility and program life-cycle cost should be carefully balanced with the developmental risk. SAIC has, therefore, taken a carefully balanced approach (Figure 6.1-1) in which some developmental risk is considered acceptable if significant operational risk mitigation can be achieved.

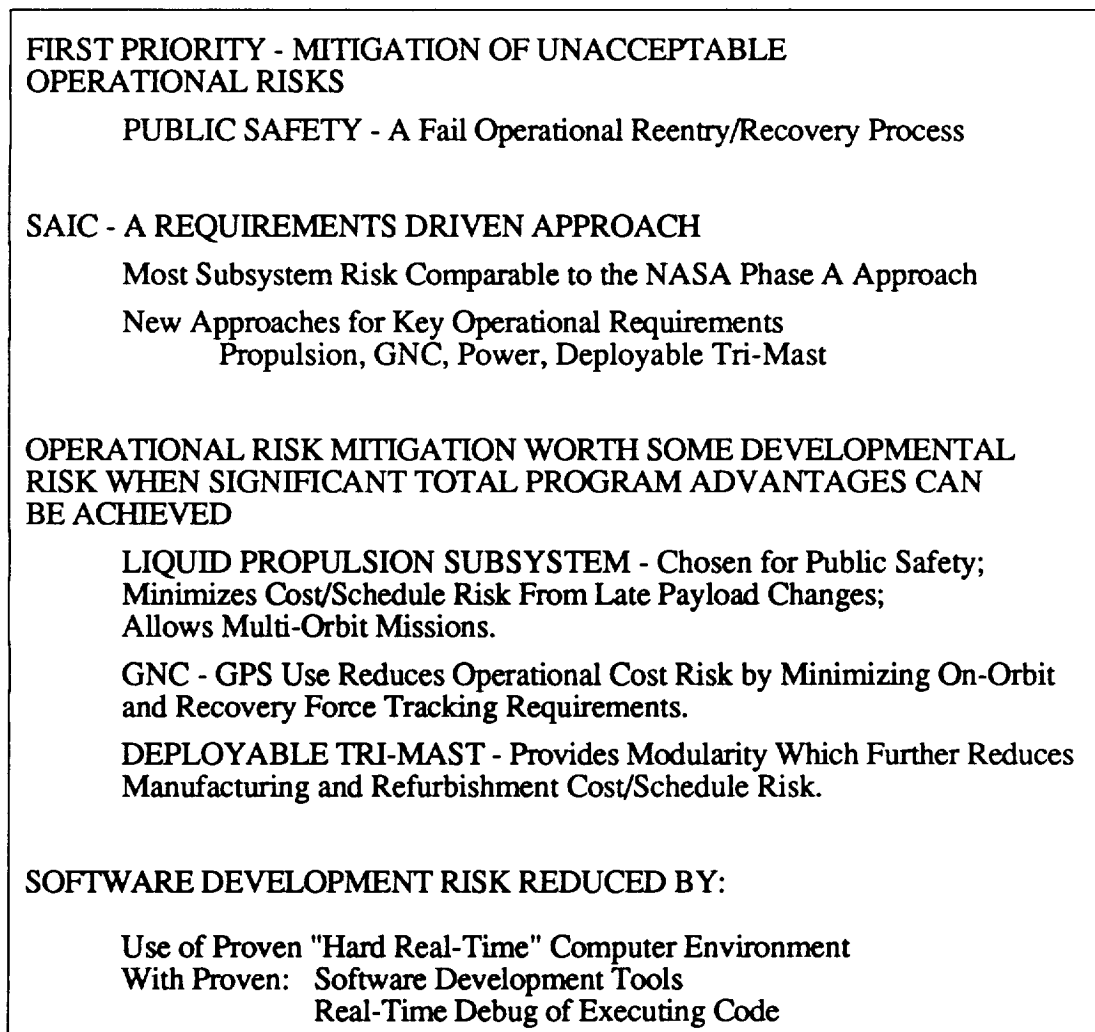


Figure 6.1-1. Risk Mitigation - A Total Program Approach

The SAIC approach to a safe CONUS recovery is a good example of such considerations. If a CONUS recovery is required by the RRS to achieve scientific objectives and minimize operational cost, public safety must be the premier risk mitigation issue in system design. Once committed to a CONUS recovery, the system must be able to identify and mitigate any single-point failure without ground intervention if that failure can result in a landing outside of the designated safe recovery area. Similarly, no single point failure should be permitted that could ultimately result in the uncontrolled reentry of a "dead" vehicle into a populated area. The result was the decision to use multi-element liquid propulsion and control subsystems that use proven components and technology to ensure a "fail operational" reentry process.

6.1.1 Operational Risk

The foundation of the operational risk assessment is the efforts documented in the Payload Hazard Analysis (Appendix C) and Preliminary Reliability Assessment (Appendix D). The mission functions were assessed from launch to landing (Figure 6.1-2) and each subsystem analyzed for failure modes and their criticality.

In general, the redundant architecture approach, which is discussed detail at the subsystem level, results in a configuration that meets the SRD reliability requirements without creating a major vehicle weight impact. Similarly, the use of existing components provides a heritage that significantly contributes to the credibility of the reliability assessment. The individual subsystem Failure Mode Effects and Criticality Assessments (FMECAs) are included in Appendix C.

Various approaches have been used to mitigate potential operational risks from launch through landing. More specifically, the key elements of mission success include:

- a. **Launch Operations.** A preliminary analysis of the launch hazards indicates that use of a destruct charge in the RRS would: 1) create a debris pattern that is a greater hazard than the vehicle itself, and 2) significantly complicate and enhance the ground crew hazard during the post-landing recovery process. Furthermore, depending upon the time of powered flight termination, the recovery subsystem could potentially provide a means of safe payload recovery. Although the RRS Emergency Recovery Process (ERP), conceptually described in the Launch Vehicle Interface portion of the Structures section, is clearly not a guarantee of safe recovery, the process could potentially mitigate the less than 0.99 probability of booster flight success sufficiently to achieve the required (SRD) 0.99 probability of safe recovery for the entire mission. The RRS alone currently meets the requirement.

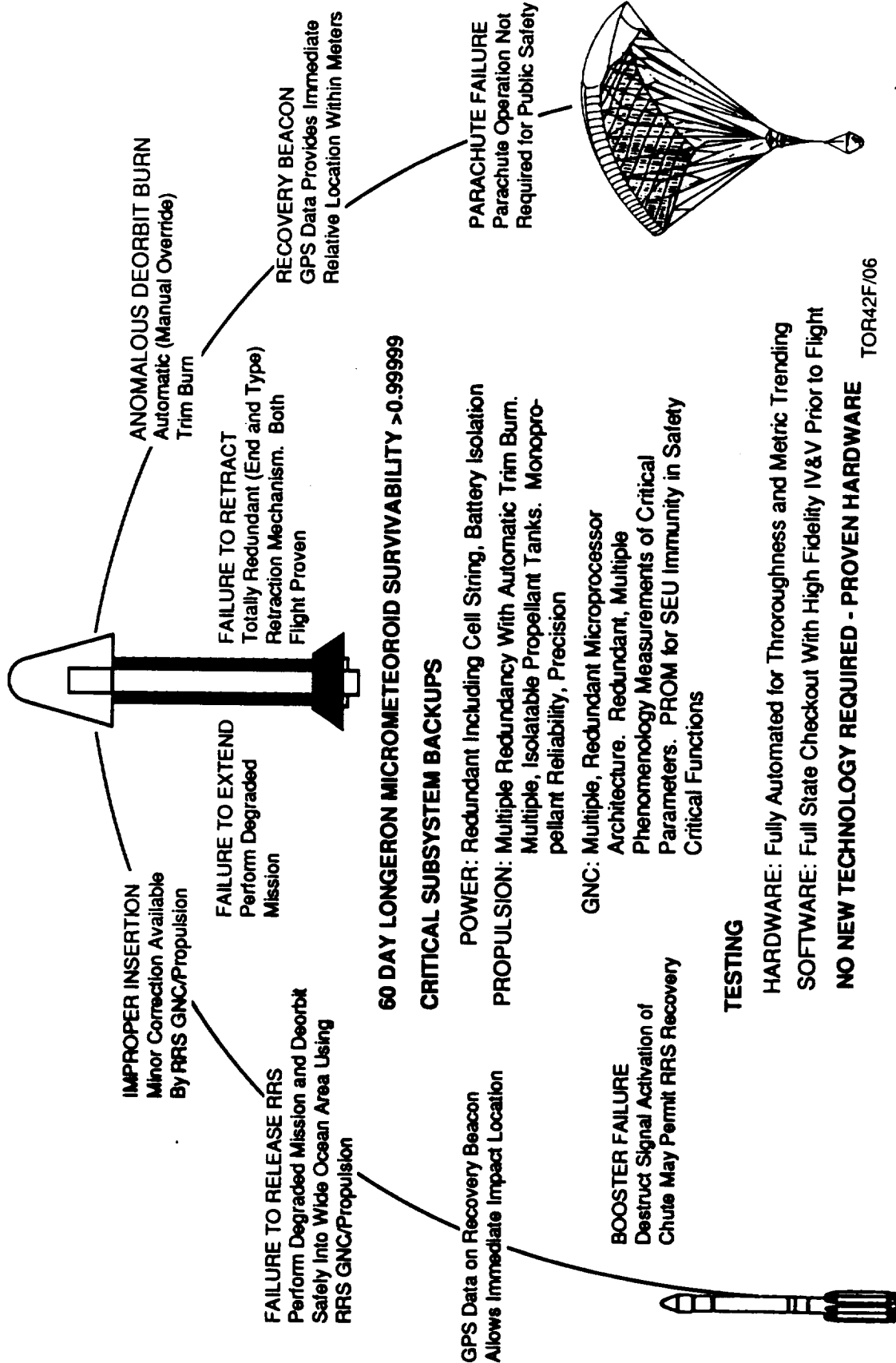


Figure 6.1-2. RRS Mission Risk Overview

- b. **Orbital Operations.** All subsystems, with the exception of the structure components, are fully redundant, and critical elements have been made multiply redundant to provide a fail operational capability. Perceptively, the greatest risk is a retraction failure of one or more of the deployable tri-masts. However, this failure mode has been mitigated through the use of retraction redundancies to the extent that the use of the mast is no longer considered to be a significant risk. The critical GNC subsystem architecture was established based upon a set of GNC design priorities (Figure 6.1-3) that resulted in a function based variable level of redundancy within the subsystem that provided the needed fail operational characteristics without causing an over redundancy for the entire subsystem.

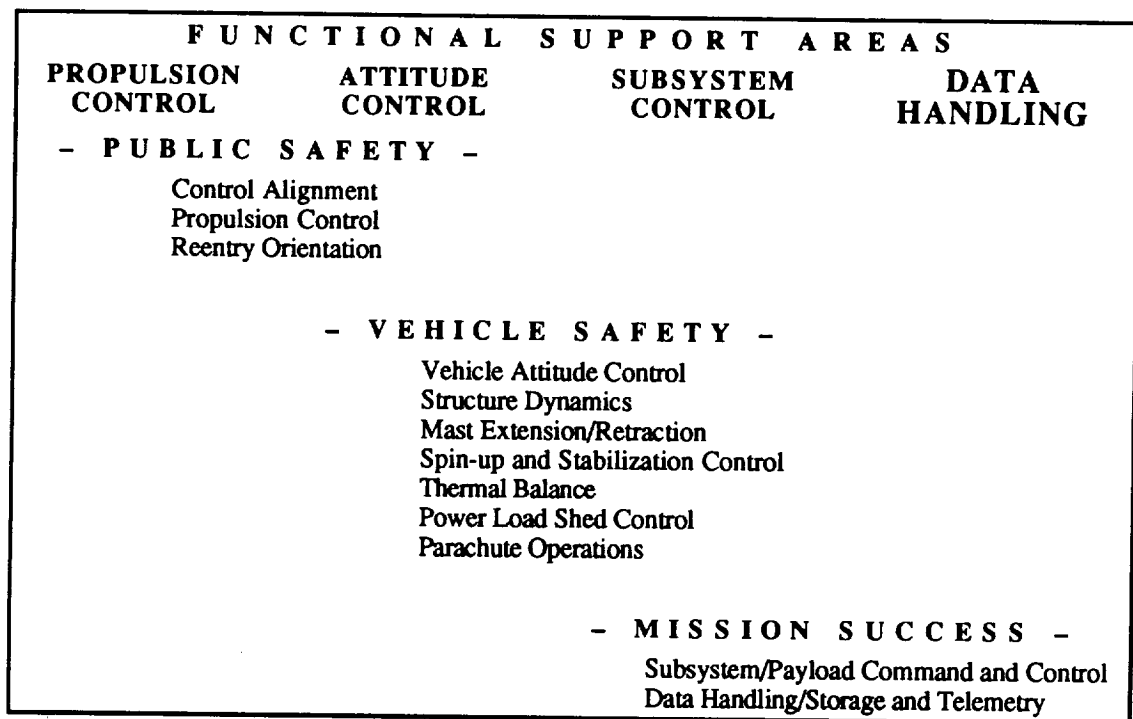


Figure 6.1-3. GNC Design Priorities

- c. **Reentry Operations.** The reentry process uses a fail operational multiple redundancy approach for both the propulsion and control functions that allows the system to automatically overcome multiple failures without degrading the landing accuracy and creating a public safety hazard. The reentry burns (main and trim) are accomplished using a "hot-redundant" triple-thruster system which is three-axis controlled by the GNC's triply redundant processor/IMU configuration. The accuracy

of this process is such that the vehicle will impact well within the required 6x30 km landing zone if there is total failure of the parachute recovery system.

- d. **Landing Operations.** A major safety consideration is the first flight concern over an unexpected failure irrespective of the magnitude and success of pre-flight analyses and test. A preliminary analysis of this concern indicates that the initial launch should be recoverable into WSMR with public safety comparable to current launch base operations. This is based upon use of the low population density corridors (Figure 6.1-4) available for access into WSMR, one of which is in the 52 to 56 degree inclination range desired for the first flight. This also assumes that the RRS would not include a destruct charge which could cause damage/injury beyond the immediate impact area. There should be no significant propellant hazard since normal RRS operations are planned to leave minimal residual fuel for quick post-landing access. However, a detailed flight path analysis must be done to firmly establish the probability of damage/injury for the specific mission.

6.1.2 Developmental Risk

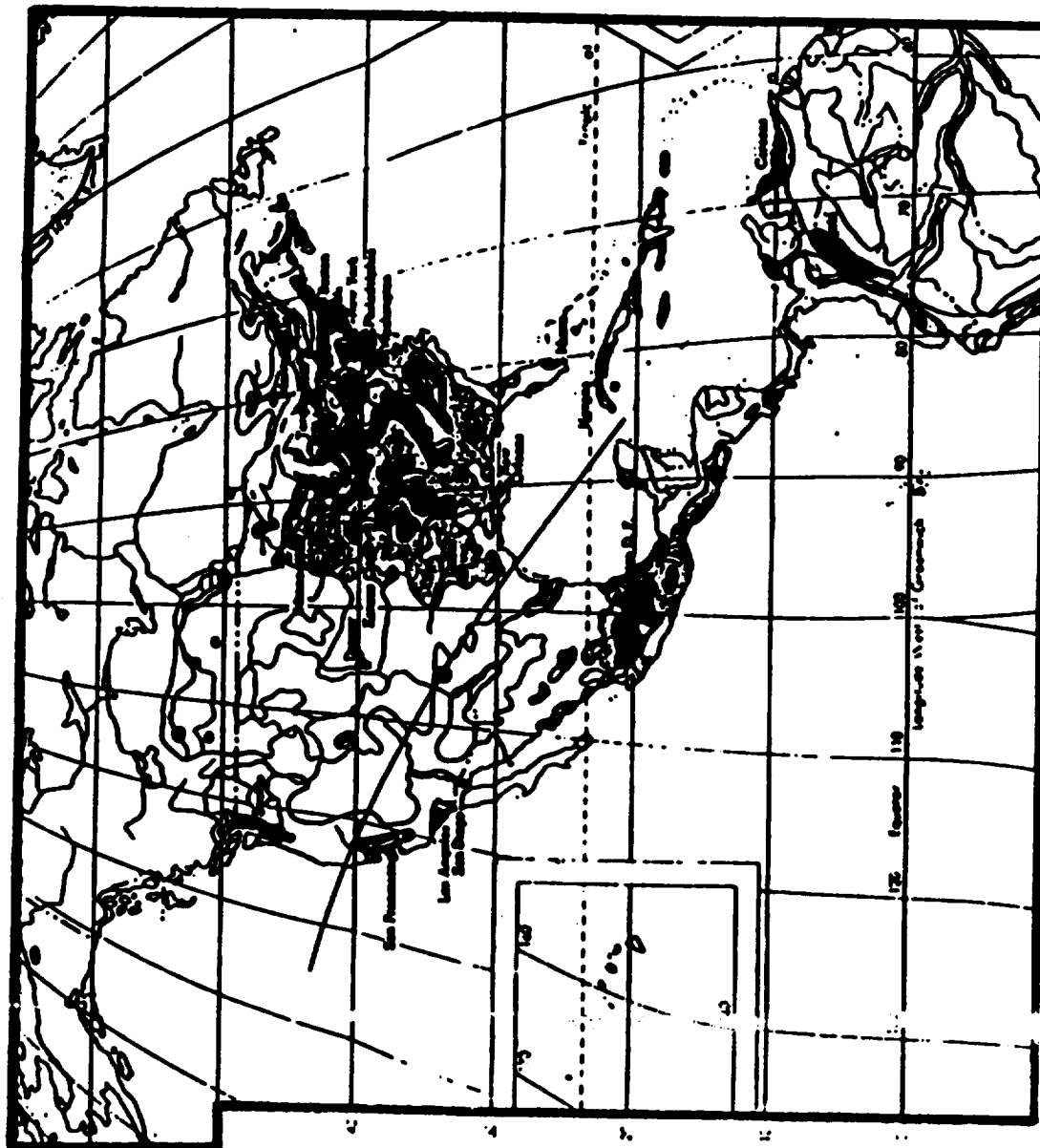
The developmental risk is a combination of technical (hardware, software, test), schedule, and cost considerations, all of which are driven by subsystem development and manufacturing considerations.

6.1.2.1 Hardware Risk. To assess the basic technical risk, a Development Risk Assessment (DRA) was performed on each subsystem to establish the relative development risk of the SAIC design. These DRAs, similar in concept to the FMECA, indicated that the vehicle development risks do not differ greatly from the NASA Phase A concept except for requirements driven variations. For example:

- a. *many subsystems are virtually identical to the subsystems needed in the Phase A concept.*

1. Recovery (parachute), TT&C and Reentry Subsystems. These subsystems are virtually identical for the two concepts, and are proven technology not requiring any special development testing.

2. Primary (non-mast) Structure and Thermal Subsystems. Although not identical to Phase A, these subsystems are very similar to the Phase A concept, and are proven technology not requiring any special development testing. The 20-degree sphere cone shape was selected partly because of the data that already exists for this configuration.



Rough Analysis Indicates Initial Flight Risk Could Be Minimized By Orbit Selection Without the Expense of a Water Recovery

Detailed Ground Track Population Analysis Needed for Accurate Probability of Injury Assessment Beyond the Scope of this Effort.

Low Population (1-10 Inhabitants Per Sq Km) White Sands Access Corridors Exist in the Western US.

For Inclinations of 52° to 56° and 102° to 107° (73° to 78°)

ASSUMING

Normal Parachute Recovery the Probability of Damage/Injury Would Be on the Order of 30×10^{-6}

TOR421/03

Figure 6.1-4. Minimal Risk CONUS Recovery Flight

b. *three subsystems which vary significantly from Phase A are an adaption of proven design/components specifically selected to meet critical operational requirements.*

1. Power Subsystem. Although different from the Phase A, the SAIC design provides greater power and eliminates mission duration constraints. The design has minimal development risk since the components are existing space technology with one exception, the tri-mast AC power transmission system. Although the AC approach, used to mitigate interaction with the earth's magnetic field, is based upon proven technology, the hardware components would have to be qualified for RRS application. The program risk is considered to be minimal since the AC approach is not required for the short deployment lengths anticipated for the initial missions.
2. Propulsion and GNC Subsystems. As discussed above, these subsystems are significantly different from the Phase A concept to provide the multi-failure tolerance needed for CONUS recovery public safety considerations. Again, the design is an integration of proven space technology/components with two exceptions, the need to space qualify the GPS receiver and the radiation hardness of the SANDAC computer.
 - (a) The GPS receiver risk is mitigated by the fact that the TI GPS receiver is a field proven design that can operate at up to synchronous altitudes without modification. Furthermore, TI is experienced at qualifying their GPS receivers for space flight applications (e.g., the Minuteman III "Fly-Two" program), and the TI receiver has been previously proposed to, and technically accepted by, GSFC for a shuttle experiment.
 - (b) The SANDAC radiation hardness is really two issues which need to be addressed separately. First, short flight durations of the RRS hold the total dose radiation environment well below that expected for most satellites and at a level that is well within the capability of the SANDAC in the RRS time-frame. Even the RRS "radiation" mission, whose objective is biological exposure to the deep space radiation spectrum, not high total dose, is not an exceptional electronics radiation environment. The second question, the single event upset caused by high energy particles, is a low probability event best considered as a probabilistic single point failure. Therefore, since we know of no evidence of any occurrence of an SEU in SNL's operational history, and the processing architecture already implemented to eliminate critical single point failures in the "fail operational" process precludes significant SEU impact, the SEU risk is minimal.

c. *other variations from the Phase A design are a unique application of proven technology/components specifically selected to meet unique, design driven requirements.*

1. Deployable Tri-mast Structure. Used to provide free space payload radiation exposure, added power capacity, and a uniform artificial gravity environment, the tri-mast is clearly a unique application of existing technology. However, the full 100-foot length is needed only for low gravity Coriolis mitigation, all components (Astromasts) are space proven, and three independent assessments of the tri-mast

structural concept have supported the initial estimates of structural integrity. Furthermore, the redundant retraction mechanism provides the space proven cable/reel capability needed for power transmission between the two vehicle modules, and as such provides the retraction redundancy at virtually no weight cost.

2. Launch Vehicle Adapter. Another major consideration was the design of a Launch Vehicle Adapter (LVA) which used proven hardware and implemented a vehicle/adapter interface which was a sufficiently simple adaption of proven technology to minimize the qualification testing and associated costs. This was achieved by adapting existing Delta interstage and fairing hardware (Figure 6.3-38) and using a simple, proven Marmon clamp interface (Section 6.3).

6.1.2.2 Software Risk. The greatest program risk in software is the lack of attention typically given to software risk in the initial program planning stages and/or the lack of emphasis on the hardware architecture and integration difficulties which almost always become the program driving aspect of software risk. Unless the code is exceptionally complex, which is not the case for the RRS, the actual generation of the code is rarely the major software risk. This rationale led SAIC to emphasize processor selection and the integrated test environment in the software risk mitigation process.

- a. **Processor Architecture.** The overriding requirement for the RRS processor is a space proven capability to operate accurately and efficiently in the real time, redundant computation environment required to ensure a "fail operational" reentry process. To minimize this risk, SAIC selected the flight proven SANDAC computer. This computer, the operating system, and the associated test tools, were developed by Sandia National Laboratories (SNL) specifically for the RRS type of environment. Furthermore, SNL's highly successful operational record in numerous reentry test flights clearly demonstrates the compatibility of the SANDAC operating system with the type of control algorithms typical of the RRS applications. The systems operational architecture, described in detail in Section 6.6, permits a "lock step" type of parallel processing that permits redundant computations to be checked virtually line-by-line when needed for "fail operational" considerations.
- b. **Test Environment.** A few "bugs" in an excellent code can be an integration catastrophe if the test tools needed to identify and eliminate the "bug" are either non-existent or sufficiently disruptive of the operational environment to preclude problem identification. The later problem is especially critical in a real-time computational process in which the problem may be timing related and the test cannot be done without altering the timing. SNL recognized this problem and devised an integrated test

approach for the SANDAC operating system and test tools that provides full, near real-time, software logic visibility without altering the operational process—a virtually unattainable capability for most processing systems.

6.1.2.3 Test Risk. If the system design is based upon proven technology, the greatest program risk is the lack of foresight in planning and executing the integration and test phase of the development. All operating modes and potential critical failures must be testable and adequately tested if operational success is to be ensured. The test risk is best minimized by levying testability and manufacturing modularity as a design requirements, and by ensuring early consideration of test requirements (e.g., the use of test specifications). To mitigate this risk, SAIC ensured that, with the exception of the deployable tri-mast, every subsystem in the SAIC design, including propulsion, is fully testable during both manufacturing and refurbishment. Even in the case of the tri-mast, test approaches have been developed to ensure full integrated ground testing of the deployment/retraction process. Only the unconstrained zero G operation must fully depend on simulation for validation and even in that case all critical simulation parameters are verifiable by test.

6.1.3 Cost/Schedule Risk

Cost and schedule risk (CSR) are intradependent with each other and with the operational and development risk discussed above. Furthermore the minimization of one element of the risk may increase the risk of a different consideration. The solid/liquid trade discussed above is a clear example of the decrease in development risk being outweighed by a much greater increase in operational risk. Similarly, while the CSR must be considered for both the initial manufacture and the refurbishment, "simple" designs that appear to have low CSR because of a lesser complexity may have an overriding integration and refurbishment CSR due to difficult maintainability—a major factor in the SAIC decision to modularize the overall design. This example also emphasizes the point that while CSR is partially driven by the above technical considerations, there are much more sensitive manufacturing/integration considerations that are system vice subsystem driven. Three key factors are involved in the assessment of these risks:

- a. **Amount of Development.** As discussed above, SAIC has minimized this risk by developing a design that primarily integrates existing components and technology into a unique architecture. Most of the hardware, other than the primary structure, is used in the existing available configuration. The deployable tri-mast is the hybridization of two current, space-qualified designs that operate independently in the existing flight-proven mode. The sole purpose of the hybrid configuration is to provide retraction

redundancy. No hardware other than the primary structure and heat shield is newly developed, and in the case of the structure/shield, the design is an application of proven technology.

- b. **Schedule Serialism.** The modular SAIC design was specifically developed to create a parallel manufacturing/refurbishment flow. This approach and the projected RRS development schedules are described in the manufacturing plans (Appendices A and B). The activity overlap characteristic of this approach both shortens the nominal schedule and mitigates the potential schedule risk of a serial schedule by minimizing contention for the limited vehicle work space and the impact of component failure. Although the acquisition of spares can also mitigate failure risk, the use of spares, unless carefully controlled, can add significant cost to the program (whereas schedule compression saves cost) and is not effective in the case of design problems. This aspect of sparing is addressed in greater detail in the System Cost Estimates Document.
- c. **Degree of Redesign.** This factor can be a major driver and is a major element in most, if not all, major program schedule slips and overruns. The critical nature of this factor is clearly demonstrated by the major role it plays in the cost and schedule estimates made by PRICE H (discussed in Section 7.0 and the System Cost Estimates Document). To mitigate this risk the SAIC/Fairchild approach assumes implementation of a Schedule Assurance Program (SAP).

6.1.4 Overall Assessment

The above discussion clearly indicates that the relative risks of the SAIC and Phase A designs are very similar with the exception three areas. However, while these areas (propulsion, the deployable tri-mast, and vehicle control (GNC)) are significant, and do represent some additional developmental risk, we believe they actually reduce overall program risk and cost.

- a. **Propulsion.** Although public safety is the driving reason for the selection of the liquid propulsion system, the flexibility of the liquid propulsion system has major performance/cost/schedule advantages over the use of solid motors (as discussed in the Propulsion Trade Study and Section 6.5) for RRS type of operations.
 - Liquid propulsion permits virtually "last minute" adjustments to compensate for payload variations (up to and including a completely different module) while the

solid performance must be specified early in the solid procurement cycle and suffer significant cost and schedule impact for late changes.

- Liquid propulsion provides the capability to make significant orbit changes during the mission while the solid approach requires an additional stage and the associated development/cost/schedule impact on the RRS and/or the booster interface.
- b. **Deployable Tri-Mast.** Although performance (radiation exposure, power, gravitational environment) is the driving factor for the tri-mast design, the resulting modularity contributes sufficiently to the overall manufacturing, test, and refurbishment savings to compensate for the added cost of the tri-mast.
- c. **Vehicle Control.** Although the complexity of the GNC is primarily driven by public safety (the IMU and use of GPS) and the control of artificial gravity operations (IMU and momentum wheels), the overall operational utility of the system should provide compensating cost advantages within the context of the total program.
1. **IMU.** Since the IMU is an essential part of the use of liquid propulsion, this aspect of the GNC contributes to the propulsion advantages discussed above.
 2. **GPS.** The availability of GPS allows a major reduction (or even elimination) in the otherwise required ground tracking and minimizes the support required for recovery operations.
 3. **Momentum Wheels.** Required by SAIC's artificial gravity concept's need to control vehicle angular momentum, this control feature will also permit compensation of the angular momentum created by any payload using a centrifuge to perform simultaneous artificial and microgravity experimentation.

6.2 Rodent Module

This section presents the preliminary SAIC design for the Rodent Module (RM), using major contributions from Allied-Signal and Krug International in the environmental and data areas, respectively. Manufacturing of the RM (Appendix B) involves parallel fabrication of key elements by qualified subcontractors/vendors under the direction of SAIC, and SAIC integration of these elements into the final product.

The design approach was intended to allow parallel development and manufacture of the RM and RRV without time-consuming combined testing prior to final integration at the launch base. This is an adaption of the GFE integration approach that has been used successfully on other programs. The success of this approach depends on strong, experienced, and active interface control and accurate documentation. Actual interface verification uses a vehicle emulator provided by the vehicle manufacturer, as described in Appendix A. Since this emulator simulates the exact 1 g mission environment (and is the basic element of the Ground Control Experiment Module), the use of the emulator should allow full testing of the RM without adding time to the RRV development schedule.

Adding to this confidence will be the RRV Engineering Test Vehicle (ETV) tests conducted by the RRV contractor. Since the shock, vibration, and thermal RRV/RM interface data obtained during ETV testing will be the initial validation of that critical design interface and the vehicle thermal/mass models, the data will be of equal and significant value to both the vehicle and payload contractors. These tests will require sufficient coordination to ensure valid simulation of the RM.

The RRS is designed to be turned around between missions within 30 days as requested in the SRD. Combined with the 60-day maximum flight time, that will allow 3 flights per year, and 30 missions over a 10-year lifetime. However, the provision of additional PMs will allow offline preparation of experiments and unique support requirements at the Principal Investigators' facilities. In that way, the fully qualified and flight ready certified PM can be delivered to the spacecraft integration facility and the flight will be paced only by spacecraft readiness and launch vehicle availability. Some advantage might have been gained by providing an integrated PM design, with reduced structural and assembly interfaces, using total vehicle packaging. However, on balance, the conclusion was that modular design offers lower life-cycle costs and will gain the operational advantages of ready changeouts and subsystem replaceability. Consequently, the PM, as well as the RRV, has been designed with modular components and system elements to facilitate a short, economical turnaround process. Modularity also enhances the ease with which systems

may be replaced as newer, better systems become available on the market, and allows more rapid reconfiguration to accommodate different experiment requirements.

Access to the PM, both on the launch pad and during post-recovery activities, was also key system design drivers. The pre-launch timeline requirement to provide access, up to 4 hours before lift-off and animal replacement up to 12 hours before lift-off, can be met. Launch vehicle imposed restraints on accessibility have been evaluated and are discussed separately in the Launch Tradeoff Study Summary Report. Post-recovery timelines were analyzed and quantified in the Recovery Tradeoff Study Summary Report.

Although the scope of this effort was limited to the design of the Rodent Module (RM), the same design, with minor modifications, would be expected to apply to any payload that can be housed in the Experiment Module (EM) volume and use the basic environmental support provided by the Support Module (SM).

6.2.1 Operation

6.2.1.1 Pre-Launch. The RM design task was structured to define the approach that would best meet the late access requirement specified in the SRD. Late access on the launch pad, as well as rapid access to the RM after touchdown, have been achieved by designing the RM as a separable module, removable as a unit, and accessible with a minimum of disassembly. Access is proposed to be through the aft end of the RRV sphere-cone after removal of the recovery parachute container (avoiding the need for penetrating the heat shield). Removal of the connections provided on the RM access cover, and then the cover, provides access to the EM/SM upper surface. Disconnecting the various lines and cables at the top of the EM and detaching the hold-down fittings will allow the EM/SM assemblies to be hoisted above the RRV aft surface until the rodent cages are exposed. Individual rodent cage doors are then accessible and experiment samples may be removed and replaced as necessary. Cage-mounted or interfacing instrumentation, as well as food dispensers, lixits, lighting fixtures, etc., may be readily changed out without further spacecraft system disturbance.

Access to the Support Module requires hoisting the EM/SM assemblies an additional 75 meters to clear the RM/RRV housing. The launch vehicle shroud design will respond to the geometry, clearances, and connections implications. The design will minimize, or prevent, damage to connections when the shroud cap is removed for access. This will simplify on-pad recheck procedures, and enhance the the desired T-4 hours late access time goal.

6.2.1.2 On-Orbit. The RRS has been designed provide the capability to subject the experiment to any required acceleration between zero and 1.5 g's, plus or minus 10%, for the duration of the flight. The specified precision of $\pm 10\%$, at a fractional gravity of 0.1 g, will require controlling the required rate of rotation of 2.44 RPM to ± 0.772 RPM (0.0808 radians/sec). The gentle rate of spinup/spindown provided by the SAIC RRS design will result in thruster firings of the order of 30 seconds or longer for this magnitude change in RPM, and presents no acceleration or precision problems.

Artificial gravity levels will be controlled through the spacecraft control logic. The procedure will be to upload a commanded acceleration to an on-board CPU. The CPU will respond by comparing the commanded acceleration to the current acceleration level. The resulting error signal will be converted to a required RPM change, and a thruster firing duration will be calculated. The response will be iterative, with the residual error causing additional thruster firings until the acceleration sensor output and commanded g's agree, within the allowable error band.

The acceleration sensor loop will remain active in order to compensate for changes in acceleration resulting from center of gravity (CG) shifts and aerodynamic drag, except when such activity can interfere with other spacecraft functions, such as in the pre-reentry phase, or during extension or retraction of the Astromasts.

6.2.1.3 Recovery. As outlined in Section 5, the current mechanical design will permit immediate access, after touchdown, to the RM. Once the RM is removed from the RRV, the modular design of the RM allows the EM to be separated and returned to the P.I.

6.2.1.4 Refurbishment. RM modularity allows a very efficient refurbishment process, because subsystems and individual elements may be either replaced immediately, refurbished, and/or reintroduced later on the same or another RRV. For example, the PM may be used as a Rodent Module housing on one flight and then support the European Botany Module on the next.

PM refurbishment will begin at the spacecraft recovery facility after the EM has been removed and delivered to the post-flight science facility. The PM will be handled as a unit and returned to an overhaul and refurbishment facility after initial cleaning of the debris filter assembly and housing, which may contain residues or animal-generated debris.

The filters will be removed and probably not cleaned for re-use, except for frames and metal parts. New filters will be installed after the PM has been thoroughly cleaned and prepared

for checkout in a clean room facility. The ECLSS will be removed and sent to a specialized facility for partial disassembly, cleaning, replacement of LiOH canisters, flushing and resealing of lines, ducts, and connections for the heat exchanger, fans, and check valves, and end-to-end check of the functionality and performance of the ECLSS elements and overall system.

All components of the PM are readily replaceable, based on condition or item life. Specific replacement criteria exists for those off-the-shelf elements, such as the ECLSS and the Instrumentation System components. Replacement criteria ensures that, except for mission-peculiar and mission-consumed elements (such as LiOH, filters, etc.), all elements of the ECLSS system will be compatible with multi-mission use.

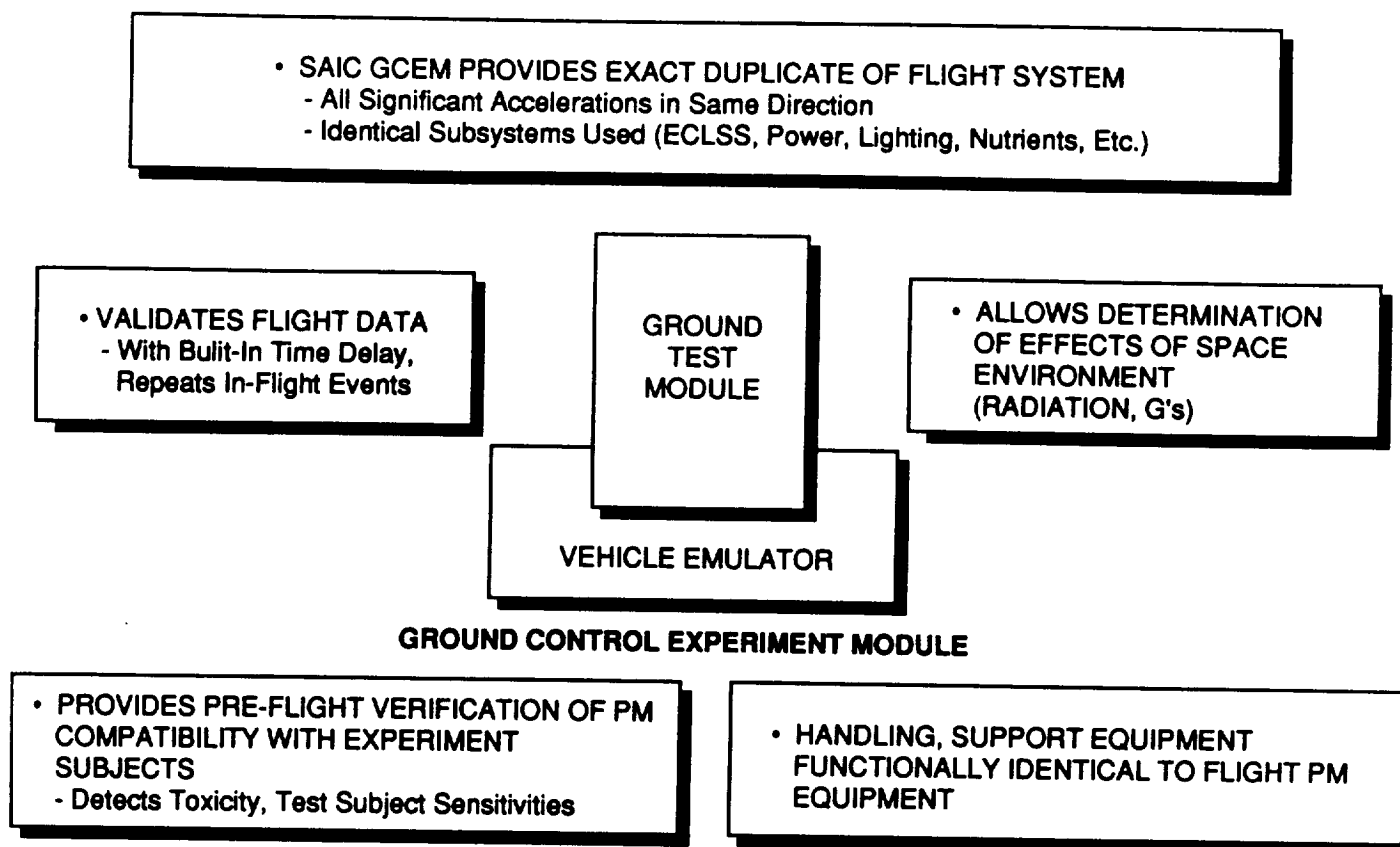
SAIC has contacted industry sources, and is in contact with NASA sources, to document specific cleaning methods and materials that meet toxicity, effectiveness, and materials compatibility requirements. The design of the RM is compatible with the use of vigorous cleaning methods because critical installed equipment, such as sensors, luxits, lighting fixtures, etc., can be removed easily for cleaning and reinstalled afterward.

After reassembly, the unit will be tested to verify complete functionality (such as heat transfer, atmosphere revitalization, and humidity control) of all components and subsystems.

The EM, which was transferred to the post-flight science facility, will be forwarded to a specialized refurbishment facility after the animals have been removed. EM equipment, including cages, instrumentation system, camera system, luxit lines, and lighting hardware will remain with the EM, and will be removed and cleaned prior to functional testing. Any specialized instrumentation belonging to a Principal Investigator (PI) will be removed and returned. The EM will be cleaned and sterilized with approved, non-toxic residue cleaning materials, and procedures such as steam, since remaining materials are metallic and tolerant of moisture and high temperatures. After checkout and replacement of failed or fatigued elements, components will be reinstalled and the assembly subjected to end-to-end continuity and functionality checks.

The ECLSS and EM will be installed in the SM housing, all connections continuity and pressure checked as appropriate, and delivered to the next user for installation and checkout of flight-peculiar equipment.

6.2.1.5 Ground Control Experiment Module (GCEM). The design of the RRS, as defined by the SAIC concept, allows the GCEM (Figure 6.2-1) to duplicate the flight vehicle-imposed environment on the experiment subjects exactly, except for variable gravity less than one Earth g. Rodents, plants, and other biological specimens will encounter the identical orientation, life support system, and instrumentation interface as those in flight. Though microgravity cannot be duplicated on earth, hyper-g can be provided by swinging the GCEM as a conical pendulum. To achieve one and one half g's, for example, the conical half angle would be arc-cosine $1/1.5$, or 0.666, which is 48.2 degrees. The angular rate of rotation required for the artificial g would be determined, as it is in space, by the radius.



TOR42E/04

Figure 6.2-1. Ground Checkout and Experimentation Control

With the exception of using nonspace-qualified elements, the GCEM, as shown in Figure 6.2-2, will be physically identical and functionally interchangeable with the flight RM. This will extend to the fabrication methods and materials used. They will be identical, in order to preclude exposure of plants or animals to unsuitable, toxic, or deleterious substances. This approach will enable the PI to duplicate all experiment specimen exposures. Tests run in the GCEM to verify the absence of such influences will constitute adequate verification of orbital systems' benign nature.

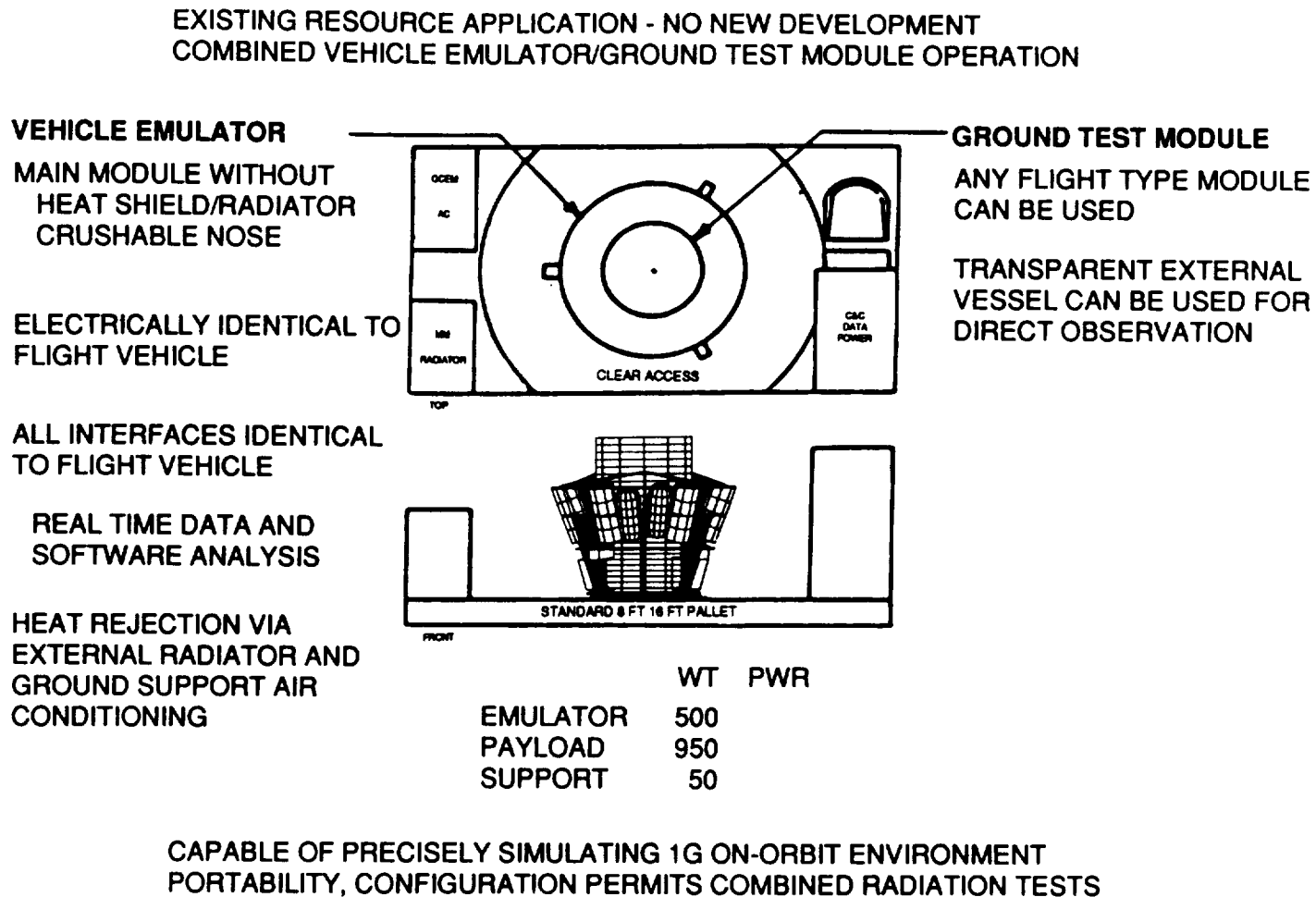


Figure 6.2-2. Ground Control Experiment Module

All expendables used by the RM, except solid food, are supplied from containers mounted in spacecraft volume outside the RM. Expendables are supplied without requiring access to the RM, when used as the GCEM. This enables the experimenters to preserve the isolation of the EM on the ground as it is isolated in orbit.

The GCEM will also support ground control tests timed for a specified time delay relative to the flight test. Flight data may be "piped" directly into the GCEM as received, or a review period incorporated. The instrumentation system in the GCEM will be functionally identical to that on board the spacecraft, and will accept and respond to downloaded command data received from the spacecraft to the extent that the ambient one g physical environment permits.

6.2.2 Requirements

The LifeSat RRS Level I Phase B Science and Technical Requirements Document (STRD), paragraph 3.0, states:

"--experiments will include a wide range of biological specimens including: cells, single cell organisms, tissues, organ cultures, small terrestrial and aquatic plants, and small terrestrial vertebrates and invertebrates."

The specific requirements of this design effort were to provide a preliminary RM design and accommodate other specified GFE payloads.

The design of the RM was driven primarily by the top-level requirement of housing 18 rodents for a maximum duration of 60 days. The RM design objective was further driven by the desire to limit abnormal and disturbing effects of high gravity gradient and Coriolis forces on the experimental animals and materials. The ability to establish a large radius of rotation when applying artificial gravity to the EM became a basic design goal and is a unique feature of the SAIC concept. Reduction, by a factor of six, in the rate of rotation necessary to achieve the maximum artificial g of 1.5 can be achieved using the SAIC concept when compared to the original Ames Research Center configuration. SAIC was well aware of information available from the Russian BioSat program that flew a small radius centrifuge, and found that results were unsatisfactory due to high Coriolis forces effects on the experimental animals.

Similarly, after considerable study of potential and planned uses of LifeSat, an internal (SAIC) design objective was established to ensure that all significant and sustained accelerations

would be applied in the same direction relative to the animal/experiment accommodations. This was desirable since it would:

- a. Create an experiment environment that could be exactly duplicated in the Ground Control Experiment Module (except for hyper-g levels).
- b. Significantly simplify design of accommodations. This results from the need for removal of debris from the same surface (consistent "floor" location), location of food and water dispensers, cameras, etc.
- c. Minimize disorientation of experimental animals by providing as normal an environment as possible in the artificial g environment.
- d. Simplify later design and accommodation of biological and botanical specimens, instrumentation, and retention systems.

The requirements used in the RM design were those defined in the RRS SRD and other NASA referenced documents such as "The Guide for the Care and Use of Laboratory Animals," U.S. Department of Health and Human Services. A list of the principal requirements is provided below:

- a. Use off-the shelf technology, whenever possible.
- b. Design for 0.99 per cent probability of safe return of the experimental animals and 0.95 per cent mission success.
- c. Provide cage space in accordance with the guidelines of U.S. Department of Health and Human Services.
- d. Provide housing that is maintained in a sanitary condition with provisions for evacuating debris, fecal matter, etc. over the duration of the flight.
- e. Limit noise level in the Experiment Module (EM) to tolerable levels, below the 85 dB limit recommended by the U.S. Department of Health and Human Services

- f. Assume that the rodents will be 600-gm sized for the duration of the flight, and consumables provisions sized accordingly. (This is a conservative assumption since the consumable supplies should be ample because somewhat smaller animals must be flown at the beginning of the flight in order to achieve an average size over the time of flight of 600 gms).
- g. Assume that rodent cages will be removed, flushed, and sterilized with an appropriate disinfectant material after each use. The design of the cages and all installed and/or attached equipment is compatible with that process.

The RM Flight Module shall be designed as a self-contained unit that provides a habitable environment to support rodents by using utility resources of the RRS vehicle. As a minimum, the RM will include rodent habitat cages; food; water; waste storage; contamination control; control of the atmosphere temperature, composition and relative humidity; mechanical, thermal, and electrical connections with the vehicle; data collection and storage; and experiment control. The RM is intended to be used to support several species of rodents, including rats, mice and hamsters.

6.2.3 Trade Study Summary

The objective of the Payload Module Trade Study was to define a RM configuration that would support 18 600-gm rodents for 60 days on orbit at selectable accelerations (artificial g) between zero and 1.5 g's. In addition, the RM needed to accommodate alternate Experiment Modules, including the General Botany Module, European Botany Module, and the multiple mid-deck lockers-sized General Biology Module. Trade studies were performed to specifically meet each of the stated RM requirements in a manner that also allows the RRS to achieve the system requirements, including safety, reliability, economy, etc.

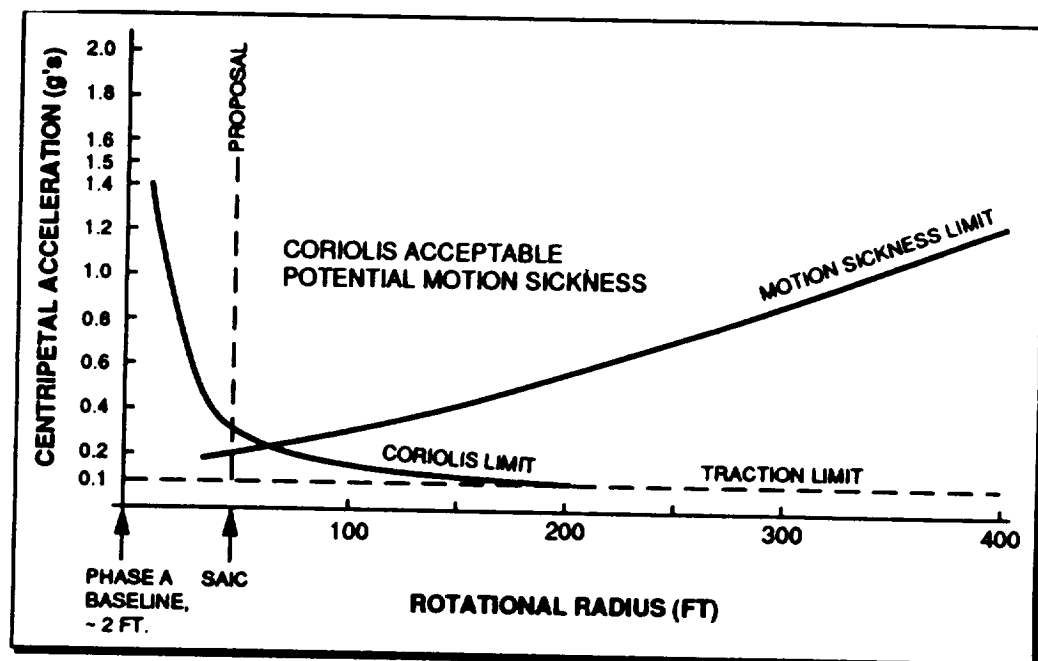
More specifically, the study paid particular attention to:

- Placement within the RRS.
- Optimal RM size, shape, center of gravity, inertial properties.
- RM mechanical mounting to facilitate assembly/access.
- Appropriate degree of vibration/shock isolation.
- Payload electrical power and thermal control requirements.
- Placement of electrical power/thermal control connections.
- Degree of thermal isolation during all phases of the mission.

- Appropriate command and data interface to the RRV.
- Appropriate RM venting interface to space vacuum.

The effectiveness of the approximately 15-meter radius achieved in the SAIC design was evaluated using data provided by Dr. Bryant Cramer in a paper entitled "Physical Considerations of Artificial Gravity" given in 1983. Although Dr Cramer's criteria indicate that an even longer radius would be desirable, radii in excess of 30 meters are not practical for a small satellite. Thus, the compromise radius of approximately 15 meters was adopted by SAIC as a design goal. At that radius, a modest motion sickness indication is predicted and the gravity gradient and Coriolis forces are hardly perceptible within the small confines of the rodent cages. Figure 6.2-3 depicts the relationships between rate of rotation, acceleration in g's, Coriolis forces, and probability of motion sickness. Only the experiments to be conducted on the RRS can determine where these curves actually lie. Nevertheless, this plot depicts the best currently known criteria for arriving at the best compromise of radius and rotation rate, and was instrumental in SAIC's design for RRS.

- Spin Radius Reduces Coriolis Effects and Motion Sickness
- Radius Chosen for Optimum Gain
- Negative Effects Increase Rapidly as Radius Decreases



DERIVED FROM: "PHYSICAL CONSIDERATIONS OF ARTIFICIAL GRAVITY"
D. B. CRAMER, "TETHER IN SPACE" WORKSHOP, JUNE 1983

TOR428/01

Figure 6.2-3. SAIC Fractional Approach

In general, the SAIC design provides all capabilities requested by the science community, and is capable of responding to a wide range of life science and other experiments. The design is especially capable of investigating the interactive effects of microgravity and/or hypergravity and radiation on any number of potential payloads, and precisely replicating any 1 g mission on the ground. Specifically, the design:

- a. Can support 18 600-gm rodents on orbit for up to 60 days at any acceleration from free drift to 1.5 Earth g's, controllable within +/- 10%, down to the required 0.1 g, or lower.
- b. Can accommodate up to 6 mid-deck lockers as requested in the RMOAD. (The original payload summary report erroneously indicated a larger vehicle would be required).
- c. Has the advantage of imposing all significant accelerations in the same direction relative to the animal cages or cuvettes through most phases of the flight.
- d. Uses modularity to allow ready removal, refurbishment, or replacement of components and subsystem elements.

Although the RM is the primary design payload used to define the RRS PM and for sizing of support systems and expendable capacities, the RRS will also accommodate other payloads. These will include the European Space Agency Microgravity Botany Facility (EBF), General Botany Module, and General Biology Module.

Geometry of the PM outer structure has been sized to accommodate any of these EMs, environmental control systems sized to satisfy all temperature/humidity requirements, and the electrical power capacity of the RRV sized to meet their needs, except for one. The European Botany Module, in the configuration which houses both free-fall and centrifuge experiment packages, will require more power for a 60-day flight than the RRV can provide. That configuration can be supported for up to 40 days.

Environmental needs of the four currently recognized EMs are compared in Table 6.2-1. It can be seen that the General Biology Module's environmental requirements do not differ significantly from those of the Rodent Module. The differences in humidity and temperature are well within the range to which environmental control systems may be adjusted.

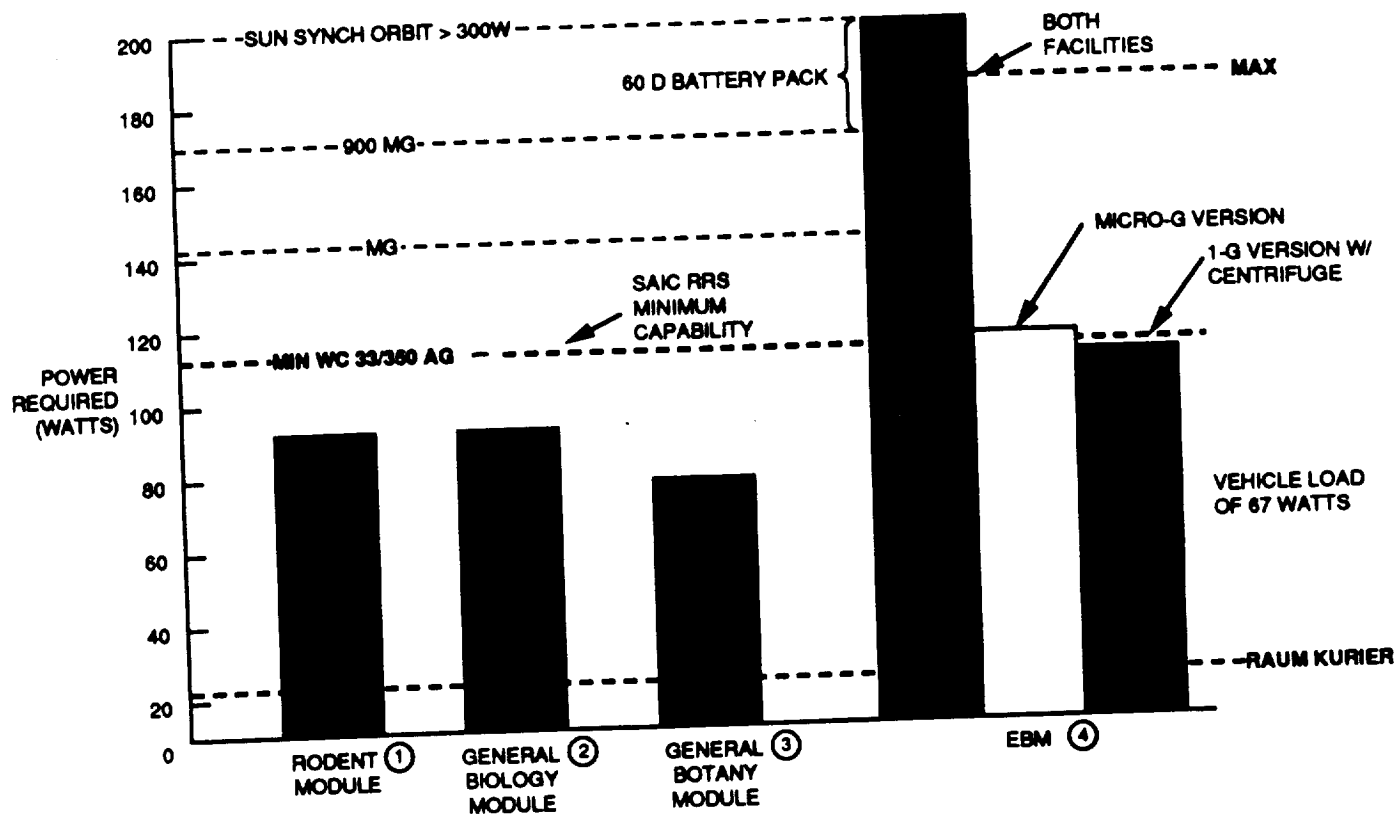
Table 6.2-1. Payload Module Environments Comparison

Parameter	Payload			
	Rodent Module	General Botany	General Biology	EBM
Temperature	18-26 °C ±2 °C	10-35 °C ±0.5 °C	20-30 °C ±3 °C	20-28 °C ±2 °C
Pressure	14.0-14.9 psia	14.7 ±1.5 psia	14.7 ±1.5 psia	1000 mbar ±100 mbar
Relative Humidity	40-70%	50-90% ±5%	50-90% ±15%	60-100%
Airflow	<240 ft/min	Continuous	Application Specific	TBD
Composition				
PPO ₂	18-22%	0-23%	Application Specific	20-24%
PPCO ₂	<1.0%	0.04-1.0%		0.1%
Lighting	40 lux ±35 lux	TBD	Application Specific	5000 lux Fluorescent

The power requirements and power available from the PM are compared graphically in Figure 6.2-4. As stated in the Reference Mission Operational Analysis Document (RMOAD) for the Life Sciences LifeSat: "...current plans are that two ... modules will be supplied by international groups; the General Biology Module by the Canadian Space Agency (CSA), and the Plant Facility Module (ESA Botany Module) by the European Space Agency (ESA)."

6.2.3.1 General Biology Module. The General Biology Module may be described as equivalent to three mid-deck locker-sized rodent RAHF stacked together. The RMOAD requirement for "4 to 6 Spacelab mid-deck lockers," is easily accommodated within the basic RRV design, as shown in Figure 6.2-5. The General Biology Module shows three Spacelab locker-equivalent sized containers fitted into the RM volume with adequate space for mounting and support provisions.

6.2.3.2 General Botany Module. The General Botany Module (referred to as the "Plant Module" in the RMOAD) is described as "designed to support the vigorous growth ... of a range of small plants as well as that of cell, tissue and organ cultures and to minimize environmental stresses." The SAIC RM will accept a General Botany Module with up to five cuvettes of 11-inch diameter (Figure 6.2-6). The power supply will allow flights of over 60 days, for two cuvettes illuminated half the time. The actual time limit for a five-cuvette system has not been determined, since power consumption is not linearly related to the number of cuvettes.



- ① BASELINE REQUIREMENT FOR 18 RODENTS
- ② FROM SATELLITE (REF. 1 - LIFE SCIENCES PAYLOAD MODULE DESIGN CONCEPT REVIEW)

- ③ TWO CUVETTES LIT 50% OF THE TIME (REF. 1)
- ④ REF. ESTEC PRESENTATION

TOR42B/03A

SOLAR ARRAY POWER ELIMINATES

Figure 6.2-4. Payload Module Comparison

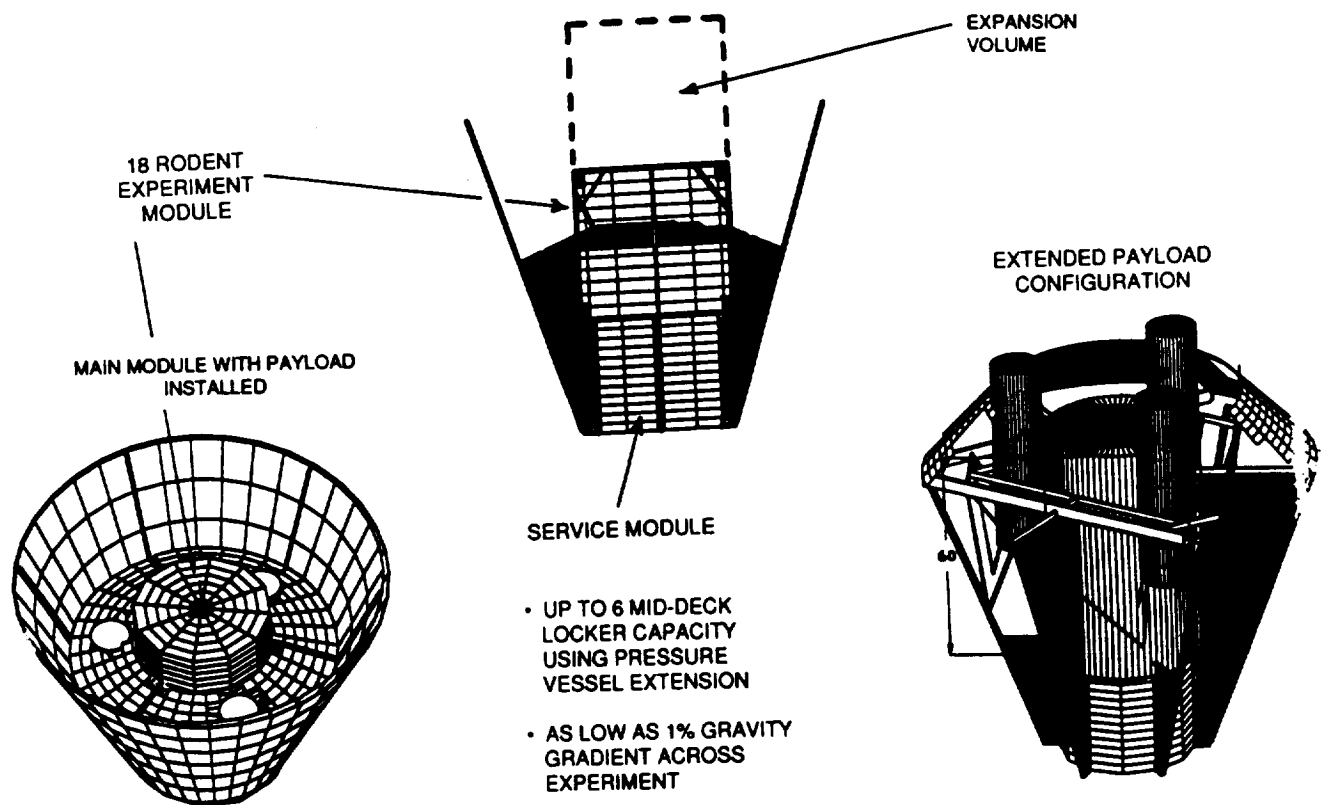


Figure 6.2-5. Variable Mid-Deck Locker Capacity

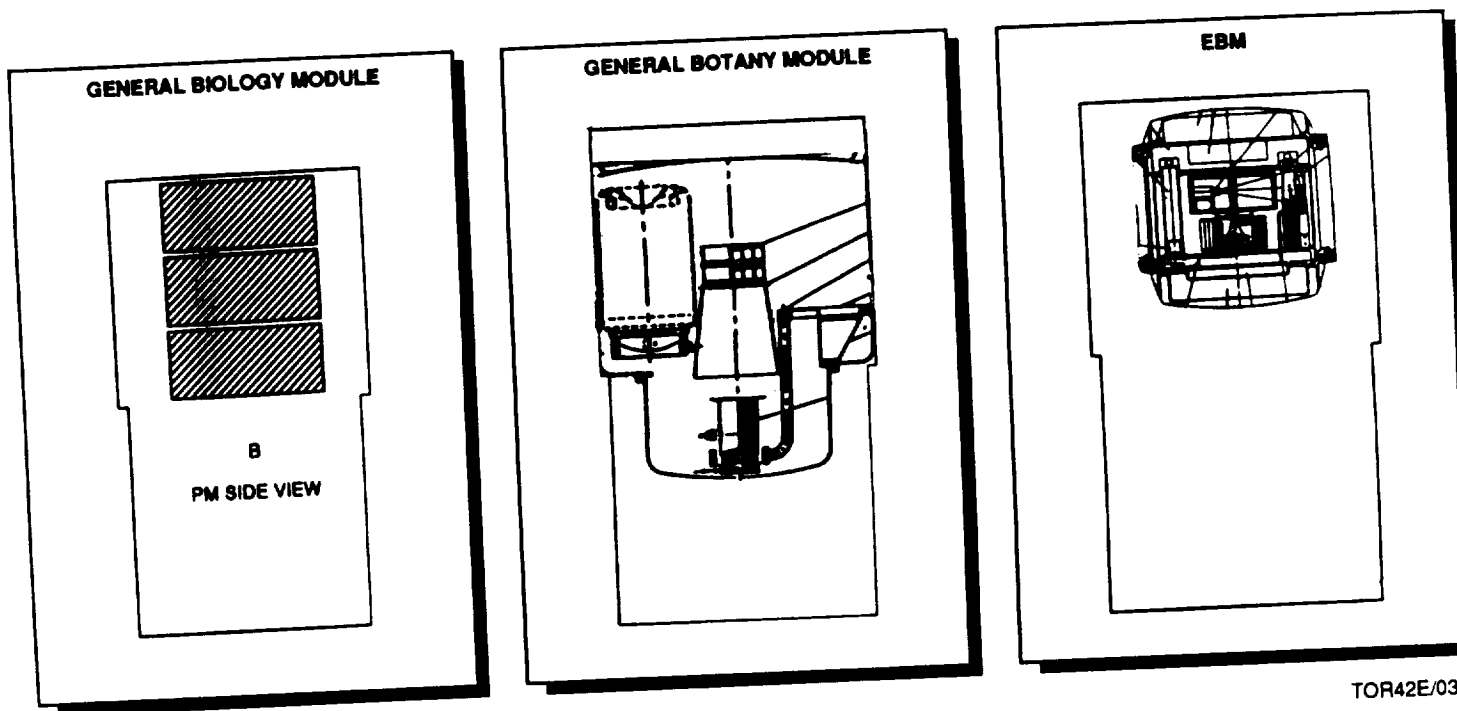


Figure 6.2-6. Payload Module Designed to Accommodate Other Science Payloads

TOR42E/03

As may be seen in the physical envelope drawing, the module contains its own environmental control system. Consequently, the volume normally occupied by the RM environmental control system will be vacant and may be used to house additional batteries. Since added mass will be required in this location to preserve the center of gravity required for stable reentry, there may be adequate power for the full 60-day flight. Detailed design of the accommodations in the PM await availability of additional information and tasking from NASA.

6.2.3.3 European Space Agency (ESA) Botany Module (EBM). Information on the EBM was obtained from ESA Botany Module on LifeSat, given as a paper at the July, 1989 LSSWG meeting. The configurations described appear in three versions: free fall only, internal centrifuge only, and a combination of free fall and on-board centrifuge. The centrifuge allows fractional gravity to be imposed on relatively small, and otherwise immobile, botanical specimens. The free fall experiment subjects are intended to be controls on the accelerated subjects, and scientists usually desire to have both control and experimental specimens exposed to exactly the same environment, except for acceleration. As may be expected, the combination version requires the highest power available which limits its flight duration. However, the SAIC RRS design allows over twice the 18-day flight duration expected for the European version. The value given for power required is 197 W and 187 kWh for a duration of 18 days, as depicted in Figure 6.2-4.

6.2.4 Baseline Design

The SAIC RM is designed to support 18 rodents for up to 60 days in conditions as close to the normal ground environment as possible, except for unique conditions applied by the Principal Investigator, such as fractional gravity forces and radiation. The cages have been sized to accommodate 600-gm rats, and provides separate specimen storage. Smaller rodent groups may be accommodated by installing revised modular cage assemblies within the current space when the specifics are known and requirements are established.

Design trades for the RM were primarily concerned with the provision of an optimum in-flight environment while remaining within reasonable power, size, mass and accessibility limits.

As shown in Figure 6.2-7, the Rodent Module consists of two separable modules. They are:

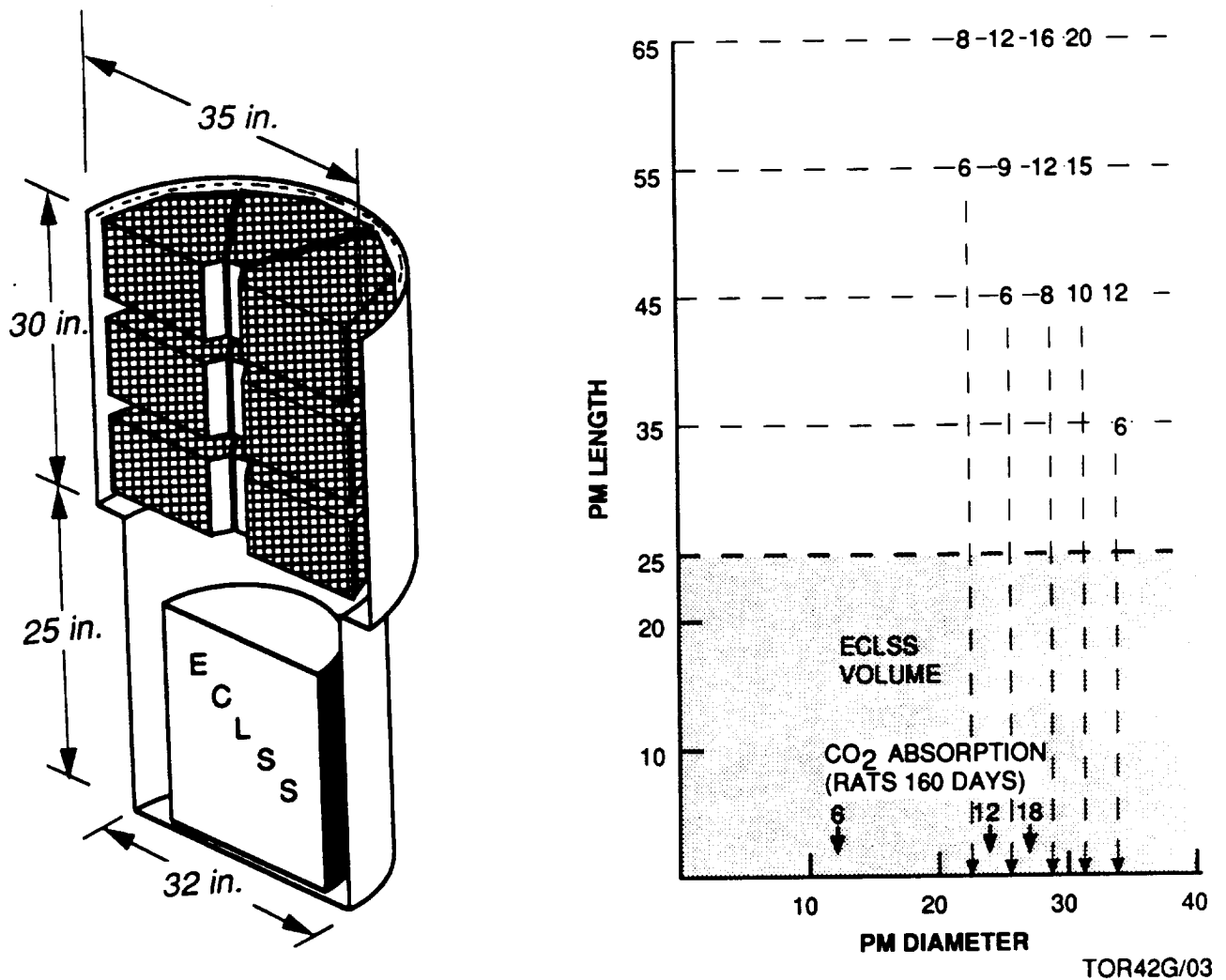


Figure 6.2-7. Payload Module Scaling

- a. **Experiment Module** - Provides experiment space and resource interfaces as defined by the experiment Principal Investigator. As described in this document, it is designed for housing 18 rodents, but has been developed to allow maximum flexibility as well as interchangeability with other payload modules.
- b. **Support Module** - Provides environment support, power source, data collection and storage capabilities, and serves as interface between the spacecraft and the EM. The SM completely isolates the EM from any anomalies induced by the spacecraft.

The RM is housed in a cylinder 60-inches long, 34 inches in diameter at the access panel end, and stepped down to 30-inch diameter at the midpoint of the RM length. These dimensions allow adequate accommodation of the Rodent Module and the miscellaneous payloads discussed in later sections of this report. The basic configuration is shown in Figure 6.2-8.

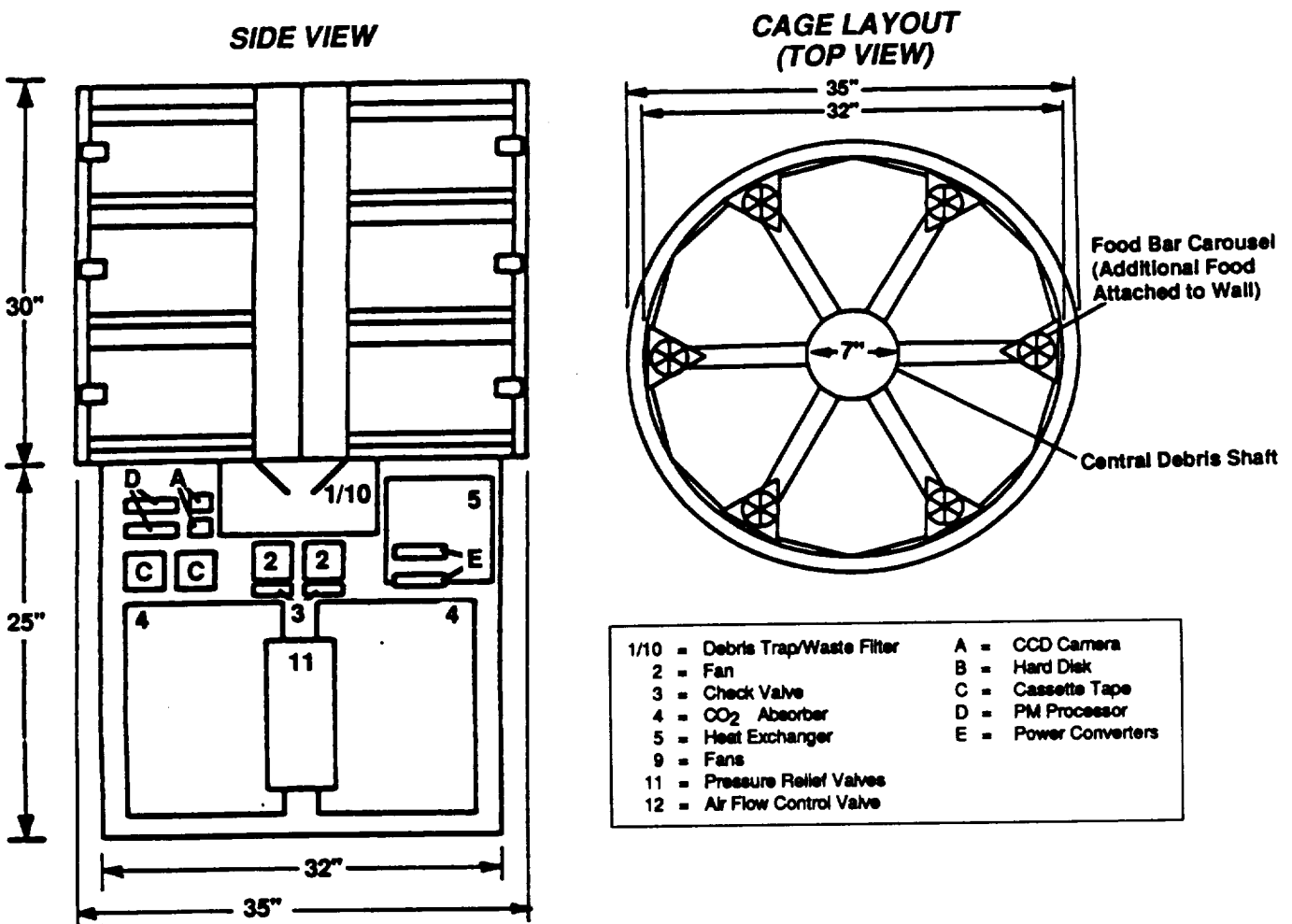
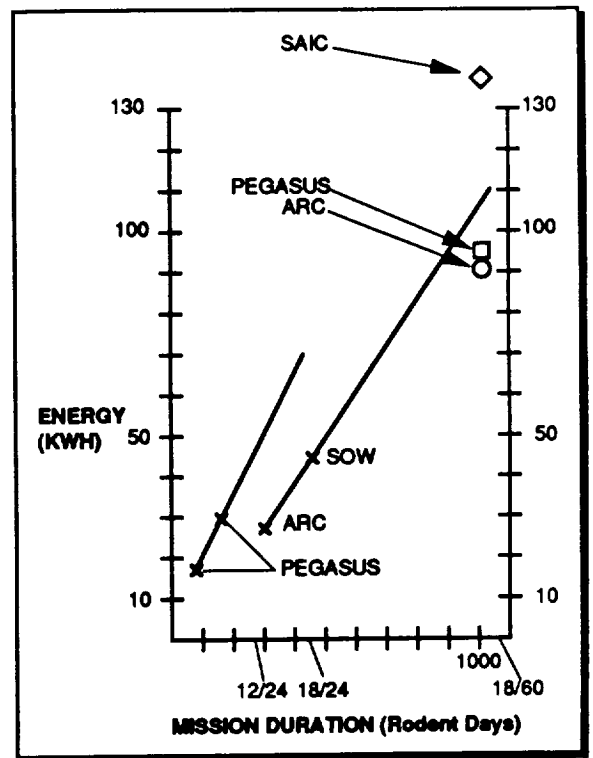


Figure 6.2-8. RM Configuration

6.2.4.1 Rodent Module Power. Ames Research Center completed a study that defined energy requirements based on the original requirement of 12 rodents for a 24-day mission. They determined that 12 rodents would require 30 Kilowatt-Hours (kWh) of energy. When coupled with 50% design margin requirement, total energy requirements for 12 rodents on a 24-day mission would be 45 kWh. With the subsequent increase to 18 rodents and a 60-day mission, a new energy baseline is established at 148 kWh. Figure 6.2-9 portrays the mission duration versus energy consumption relationship.

- SRD: RRS MUST PROVIDE AT LEAST 45 KWH
 - Mission is 18 Rodents/24 Days
- ARC STUDY: 12 RODENTS/24 DAY MISSION REQUIRES 30 KWH WITH LITTLE CONTINGENCY
- 50% INCREASE IN RODENTS (12 -18) CORRESPONDS TO 50% ENERGY INCREASE (30 - 45 KWH)
- ADDITIONAL INCREASE FROM 24 DAYS TO 60 DAYS MORE THAN DOUBLES RODENT DAYS AND THEREFORE ENERGY CONSUMPTION
- NEW BASELINE = 148 KWH
- COMPARISONS:
 - ARC Power Analysis: Increase 50% (18 Rodents) + 5% Contingency = 90 + KWH
 - Pegasus Baseline Mission Profile Provides Additional Data Points
 - Comparing Pegasus Data to ARC 12/24 to Predict 18/60 - 95 KWH



TOR42A/16

Figure 6.2-9. Baseline Energy Requirement

The electrical power requirements for the equipment selected in the above trades are listed in Table 6.2-2. This power budget was provided to the engineers performing the RRS Power System Trade Study. The RM power budget, along with the power requirements of the RRV, were used to size the overall RRS power system. Results of this analysis can be found in the RRS Power System Trade Study Summary Report.

Table 6.2-2. Power Budget for Payload Module

			130 kWhrs = Baseline 90W = Average	
Item	Power	Periodicity	Average	Peak
1. Lights – GE 400 pg. 26 28 VDC – 0.10A	54 (3 W x 18)	63% max. (15 out of 24 hrs. on)	34 W	54 W
2. Air Revitalization Fan	6 W	100%	6 W	6 W
3. Waste Removal Fans	12 W (6 W x 2)	1%	0.12 W	12 W
4. Memory	10 W	100%	10 W	10 W
5. Video Recorder	12 W	2/1440 0.14%	0.017 W	12 W
5a. Camera	4 W	1%	.04 W	4 W
6. Data Handling	5 W	100%	29.6 W	20 W
7. Sensors Thermistor – 2 Pressure – 2 Temp. – 4 Quantity – 8	5 W	100%	5 W	5 W
8. Implantable Telemetry	18 W	10%	2 W	2 W
9. Activity Monitors Lixits – 18 Food – Activity –	4 W	100%	4 W	4 W
10. EM Command and Control	5 W	100%	5 W	5 W
TOTAL POWER			95.8 W	134 W

6.2.4.2 Rodent Module Size. Beginning with the space allocation per rodent and access requirements, it was determined that the Ames Research Center Phase A study cage layout was ideally suited for RRS application. The cages used in the SAIC RM design trade study are an adaptation of the cage design used in the Phase A study. This cage arrangement uses a three tier

circular platform with each cage occupying a 60-degree sector of the platform. This type of design provides the specified interior volume, height, and floor space needed by the rodents of up to 600-gm mass. The cage is anticipated to be fabricated out of corrosion resistant steel (CRS) for durability, ease of cleaning, and resistance to wear and rodent gnawing, as well as producing no toxic residues that may be harmful to experimental animals. A schematic of the rodent cage is shown in Figure 6.2-10.

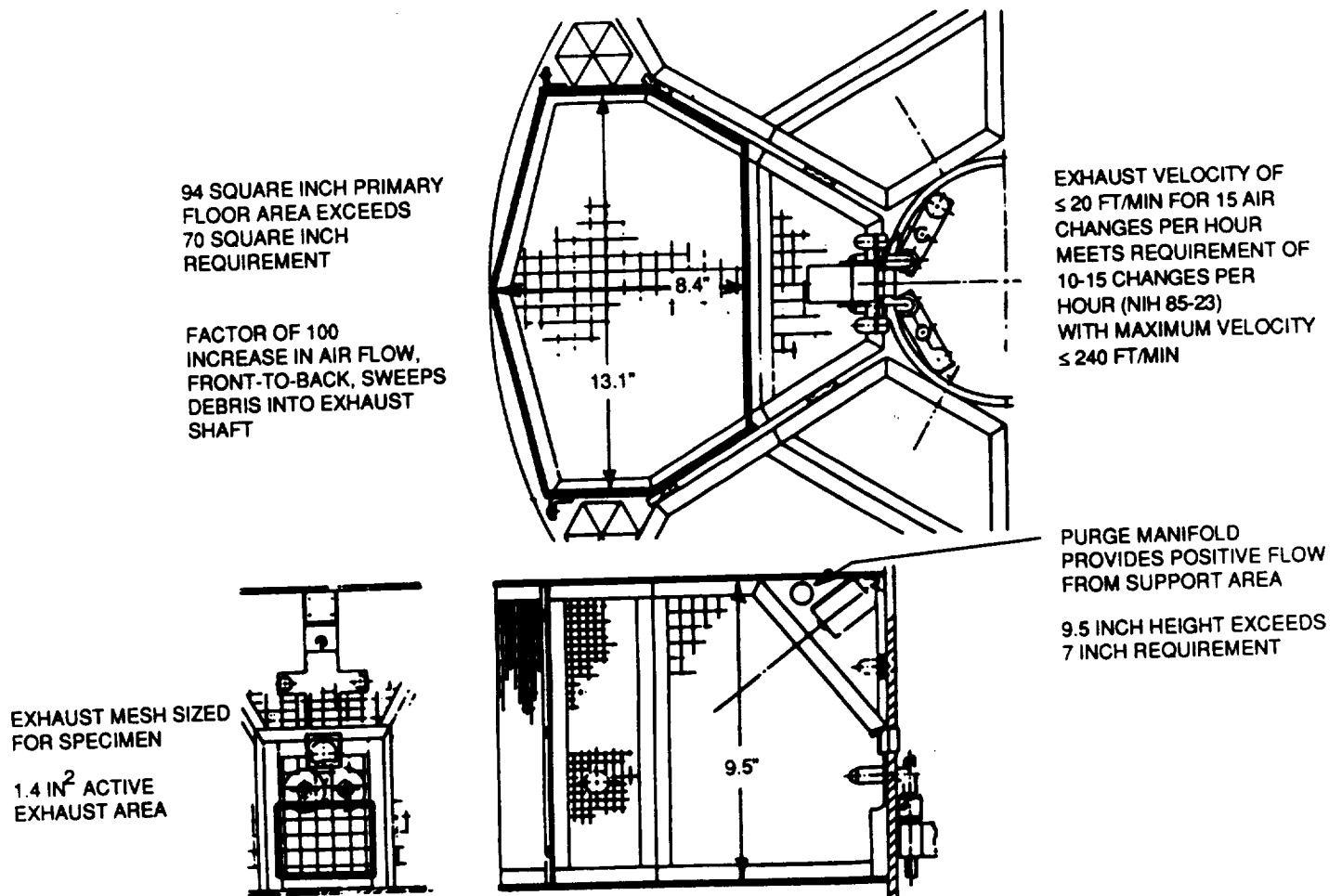


Figure 6.2-10. Cage Requirements

As shown in Figure 6.2-11, design of the cage assembly permits modification to accommodate smaller rodents in greater numbers on later flights because distribution systems for water, instrumentation, lighting, and atmosphere conditioning are readily adaptable to an increase in the number of cages and occupants. The lixit system, for example, is redundant with the two supply lines separately manifolded to 18 consumption points. Adding more lixits will only require adding the necessary lines to the manifold and routing low pressure flex lines to the lixits in the revised cage array.

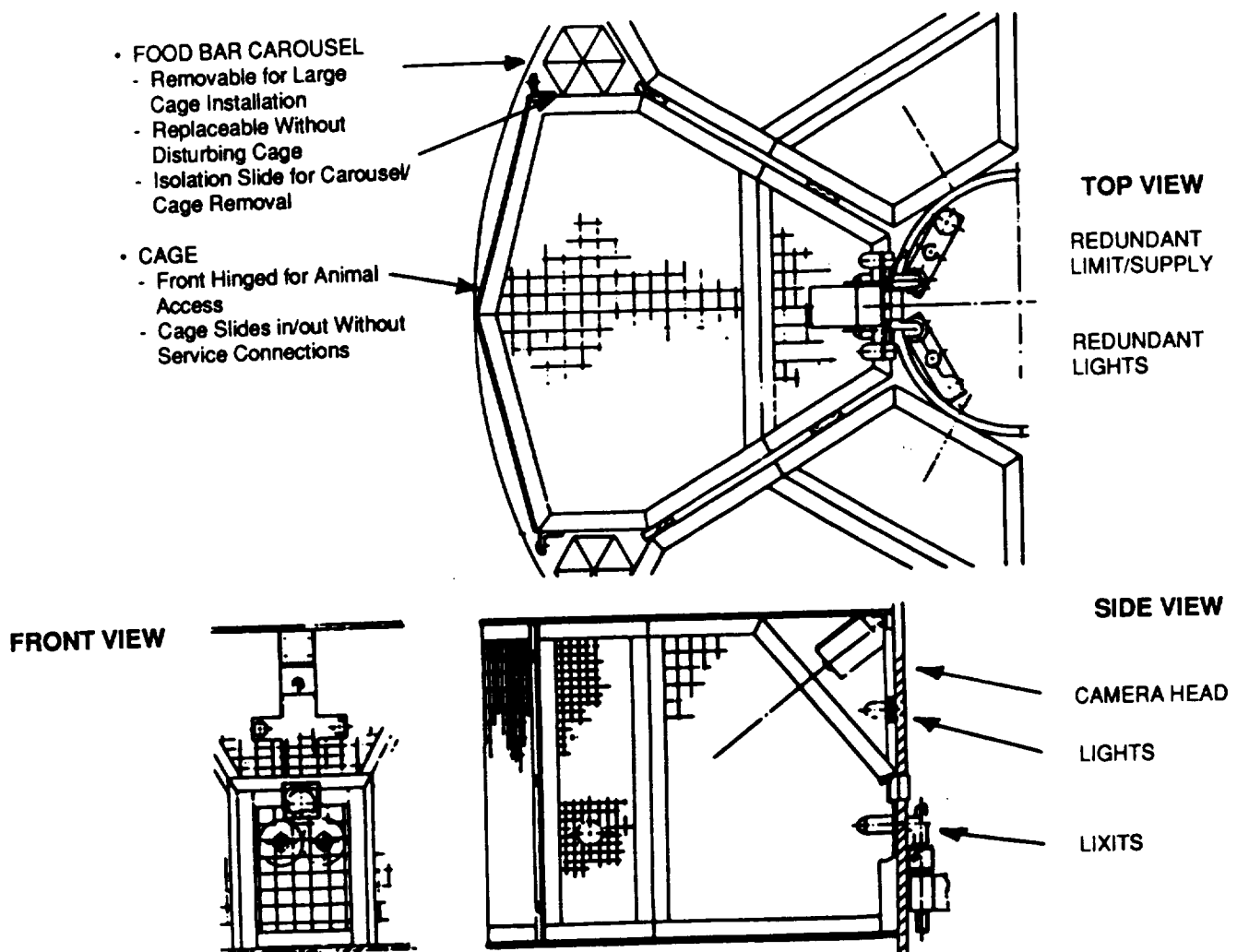


Figure 6.2-11. Cage Features

Cage design for the rodent family units contemplated for later flights will necessitate provision of special housings in the cages for rodent pups to ensure that they are accessible by the mother, but do not drift apart in reduced gravity, as the pups must remain in touch to retain body heat. Such cages will be installed in the same volume now specified for the current 18 cages, but redesigned as described for the family units. The number that may be accommodated will be determined at the time of the new cage design, and the new cages will be adapted to the currently provided "lazy susan" cage arrangement. This will allow the same ventilation, lighting, instrumentation, etc. provisions to be used with only relatively minor routing and connection revisions.

6.2.4.3 Rodent Module Mass. Consumable requirements for the RM were determined by multiplying the consumption rates for rodents, documented in the RRS SRD, by various values of rodent population and flight durations. The amounts of food, water, and gases estimated from these calculations, including 50% design margin as required by the SRD, were used to determine the types and capacities of various containers required to store these consumables. Estimates were also made of the various support requirements (ECLSS, lighting, cages, etc.) in order to arrive at set parametric curves which could be used to estimate RM mass as a function of number of rodents and mission duration.

Dry mass estimates of consumable tankage were calculated for the 18-rodent case. Thus, initial mass estimates vary only due to the increased number of rodents for the 6-, 12-, and 18-rodent cases. Figure 6.2-12 shows the parametrics obtained from these calculations. As can be seen, the mass estimate for the RM, assuming an 18-rodent payload on a 60-day mission, is approximately 950 lbs.

During design tradeoff studies accomplished during actual RM design efforts, the mass requirement was adjusted to reflect actual weight requirements. These changes resulted in mass requirements being increased to 972 pounds.

The 972-pound RM mass estimate for a full 18-rodent/60-day mission includes the mass of expendables and tanks located outside the RM, but connected to the RM by appropriate interfaces. As shown in Table 6.2-3, the Rodent Module contributes 652 pounds of mass, consisting of 276 pounds for the EM and 376 pounds for the SM. The remaining 320 pounds is allocated for support tanks and contents housed outside the RM. Specific mass breakdowns are detailed in Table 6.2-4.

- Phase A Study Established Maximum Payload Mass of 530 Lbs but Did Not Specify Mission (Rodents/Days) Accommodated
- ARC Study Required 450 Lbs for 12 Rodent/24 Day Mission
- SOW/SRD Did Not Specify Weight Limit
- Payload Mass Has Fixed Component Based on Number of Rodents and Storage Capacity and is Variable Due to Consumables
- Consumables Include Water, Oxygen, Air, Cage Mounted Food Bars and LiOH
- Weight Estimates are Based on Vendor Inputs, Allied Signal Estimates, and Scaling From Previous Studies
- Increase to Baseline 950 Lb Driven by 18 Rodent/60 Day Mission Requirement

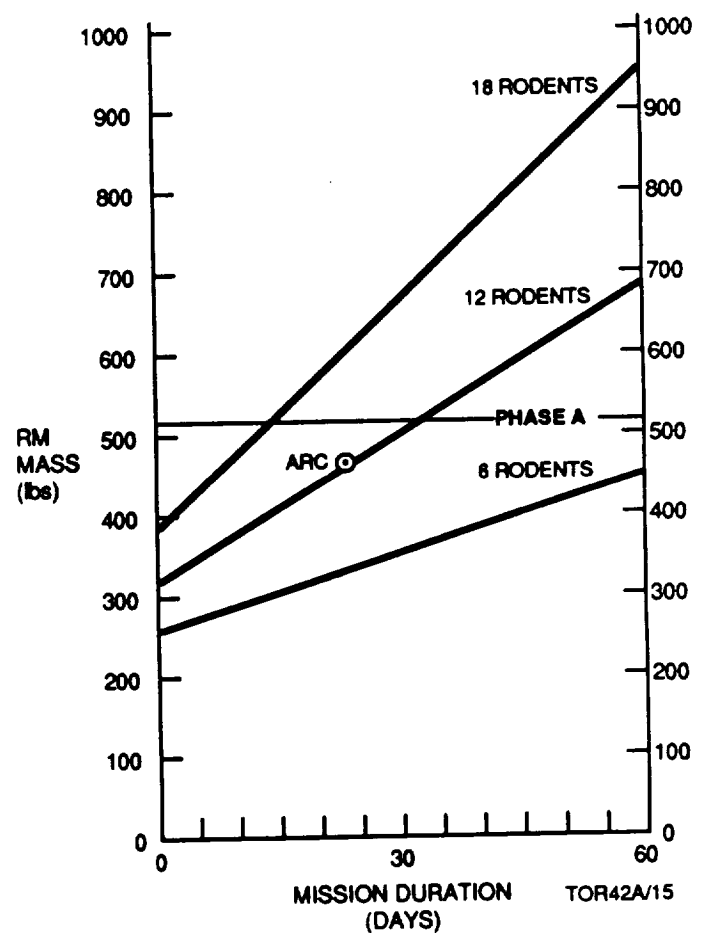


Figure 6.2-12. Impact of Consumables on Rodent Module Weight

Table 6.2-3. Payload Components - Weights

• PAYLOAD WEIGHT INCLUDES

EM	276	
SM	376	
	652	INTERNAL
EXTERNAL STORES	360	
	972	TOTAL

VEHICLE

SUBSYSTEM	WEIGHT/LBS*
EXTERNAL CONSUMABLES	
H ₂ O WITH STORAGE (H ₂ O = 130 LBS)	159
O ₂ WITH STORAGE (O ₂ = 49 LBS)	91
AIR WITH STORAGE (AIR = 24 LBS)	45
CONDENSATE STORAGE (TANK ONLY)	25
TOTAL	320 LBS

PAYLOAD MODULE

SUBSYSTEM	WEIGHT/LBS*
EM	
RODENTS (600 GRAMS EACH)	24
FOOD (7 LBS* 18 CAGE)	120
CAGES (2 LBS PER CAGE)	36
SUPPORT (2 LBS PER CAGE)	36
FOOD/WATER CONTROL (1 LB PER CAGE)	18
LIGHTING (1 LB PER CAGE)	18
SENSORS	18
OTHER	6
TOTAL	276 LBS

SUBSYSTEM	WEIGHT/LBS*
SM	
PRESSURE VESSEL	105
FILTERS	5
LiOH	134
FANS	7
HEAT EXCHANGER	21
VALVES	14
DATA MODULE	20
POWER CONTROL	20
CAMERAS	10
SUPPORT	30
OTHER	10
TOTAL	376 LBS

TOR420/37

Table 6.2-4. Payload Mass and Power

Component	Mass (lbs)		POWER	MASS VALUE (lbs)	UNCERTAINTY %	UNCERTAINTY (lbs)
RM EXTERNALS						
WATER	134.0			134.0	0	0.0
WATER TANK(50 PSI VOLUME)	25.0			25.0	20	5.0
OXYGEN	49.0			49.0	0	0.0
O ₂ TANK (6K PSI/VOLUME)	42.0			42.0	20	8.4
AIR	24.0			24.0	0	0.0
AIR TANK (6K PSI/VOLUME)	21.0			21.0	20	4.2
WASTE TANKS	25.0			25.0	20	5.0
ECLSS WEIGHT						
PRESSURE VESSEL	105.0			105.0	25	26.3
FILTERS	5.0			5.0	10	0.5
LIQH SYSTEM	134.0			134.0	5	6.7
FANS	6.6		18	6.6	5	0.3
HEAT EXCHANGERS	21.0			21.0	10	2.1
VALVES ETC	14.0		240/50MSECS	14.0	5	0.7
DATA MODULE	20.0		29	20.0	20	4.0
POWER CONTROL	20.0		25	20.0	10	2.0
CAMERAS	10.0		18	10.0	10	1.0
SUPPORTS	30.0			30.0	25	7.5
OTHER	10.0			10.0	25	2.5
EXPERIMENT MODULE						
RODENTS	24.0			24.0	0	0.0
FOOD	120.0			120.0	0	0.0
CAGES	36.0			36.0	20	7.2
SUPPORT	36.0			36.0	20	7.2
FOOD/WATER CONTROL	18.0			18.0	25	4.5
LIGHTS	18.0		54	18.0	10	1.8
CAMERAS	18.0			18.0	5	0.9
OTHER	6.0			6.0	25	1.5
PAYLOAD TOTAL (lbs)		972				
RM EXTERNALS EMPTY		113				
CONSUMABLES		207				
TOTAL		320				
TOTAL		376				
TOTAL		276			TOTAL	99

6.2.4.4 Rodent Module Accessibility. Access to the experiment (rodent cages) late in the pre-launch countdown, and as soon as possible after touchdown, is a primary scientific requirement. The RM is designed to support rapid access with a minimum of spacecraft disassembly. Access is through the aft portion of the RRV after removing the Recovery Parachute Container. The upper cover of the RM can be removed after disconnecting external power, instrumentation, and cooling lines, and releasing a single, circumferential clamp. Flexible lines inside the close-out allow it to be raised sufficiently to access the same lines internally, disconnect them from the close-out, and remove it. That will allow access to the EM hold-downs and the EM internal lines feeding the lixits, lighting, instrumentation, and cameras on individual cages. The entire EM assembly can then be lifted out of the RM, and either be removed entirely or raised sufficiently to permit access to any of the 18 individual cages.

6.2.4.5 Rodent Module Interfaces. Rodent Module interfaces are specifically defined in RRS-IFS-101.

6.2.4.6 Experiment Module. The EM (Figure 6.2-13) is designed to accommodate up to 18 600 gm rodents in individual, and/or group cages, that can be installed and removed without any service connections. It is a separable module made up structurally by the 18-rodent cages and the three-layer support structure. The cages are mounted to permit their individual removal and replacement, but contribute to the rigidity of the EM structure when assembled in place. The basic configuration, which has the cages arranged in 3 decks of 6 cages each, can be easily reconfigured for 2 or 3 cages per level (Figure 6.2-14).

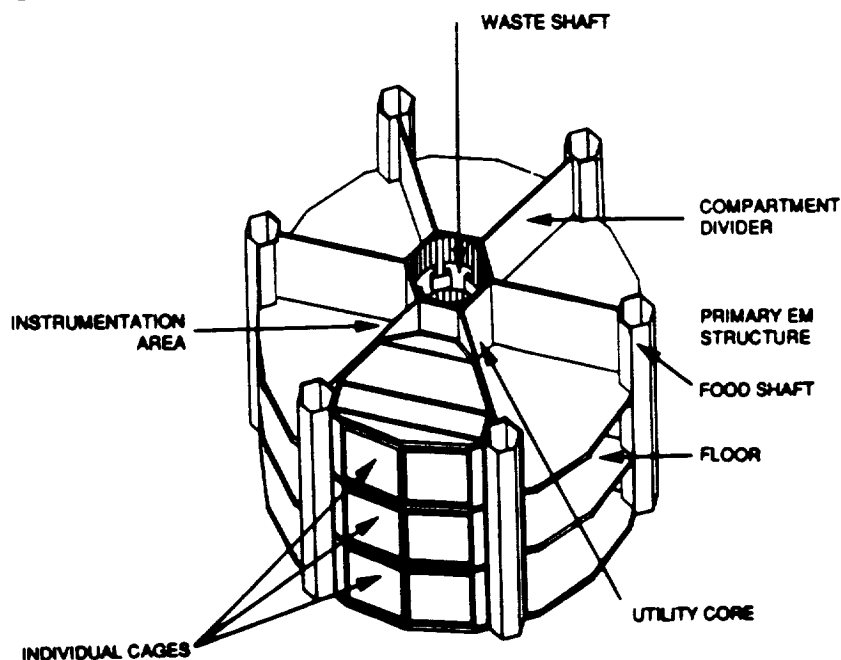
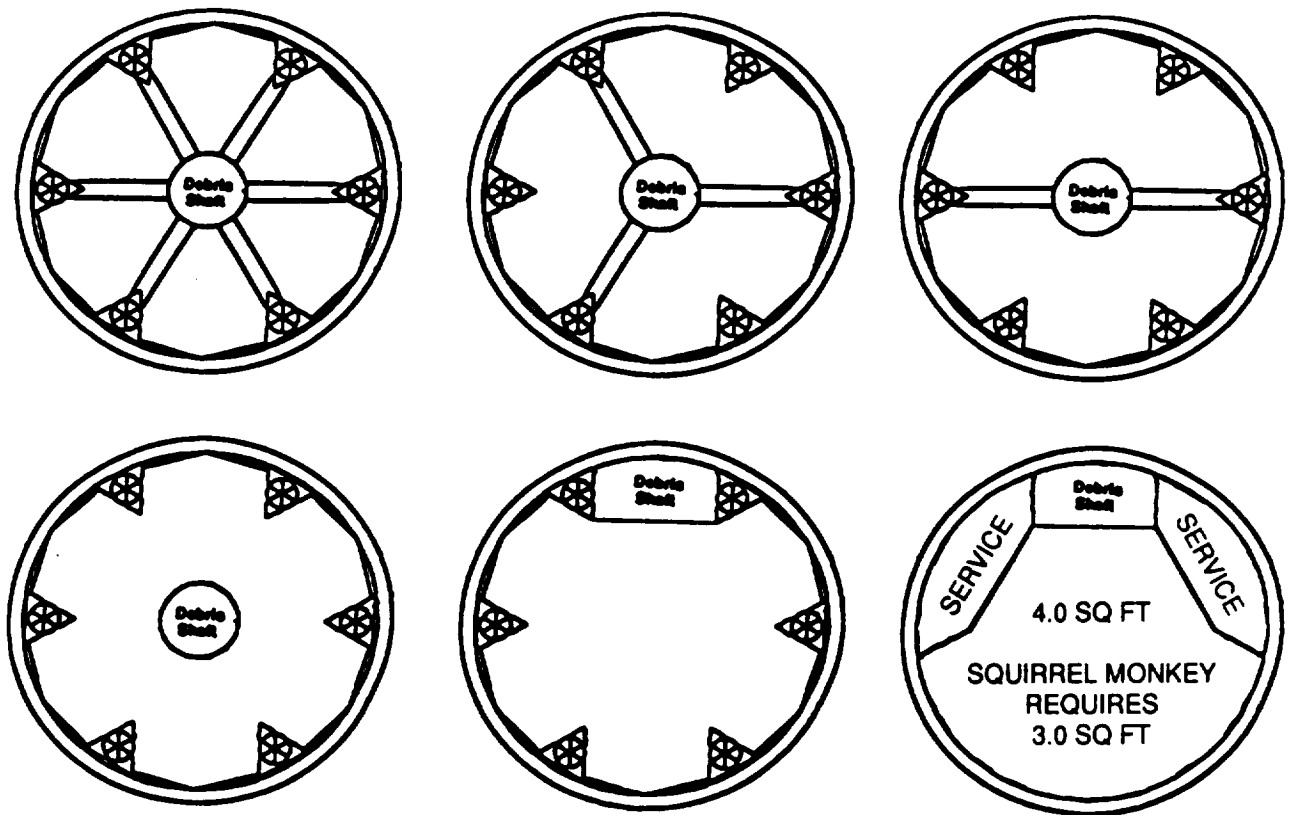


Figure 6.2-13. EM Assembly



- NO CHANGE IN SUPPORT HARDWARE
OFFSET SHAFT COMPATIBLE WITH BASIC SM CONFIGURATION
- MONKEY CAGE USES ALL 3 DECKS FOR 30" HEIGHT REQUIREMENT
GP-3 REQUIREMENT OF 4.3 SQUARE FEET CAN BE MET

Figure 6.2-14. Potential Cage Configurations

The cage support assembly consists of the central cylindrical duct (Figure 6.2-15) and three circular dividers that separate the three cage layers. The dividers provide a floor between cage layers to act as a debris catchment and ventilation duct to channel air and debris into the central column for delivery to the debris trap and filters, particularly when the spacecraft is subjected to artificial gravity or is on Earth. Space is provided for the routing of supporting equipment, including the instrumentation lines, water supplies to the lixits, camera connections, lighting power lines, and the other expendables supply lines and connections between the SM and the RRV through the access panel.

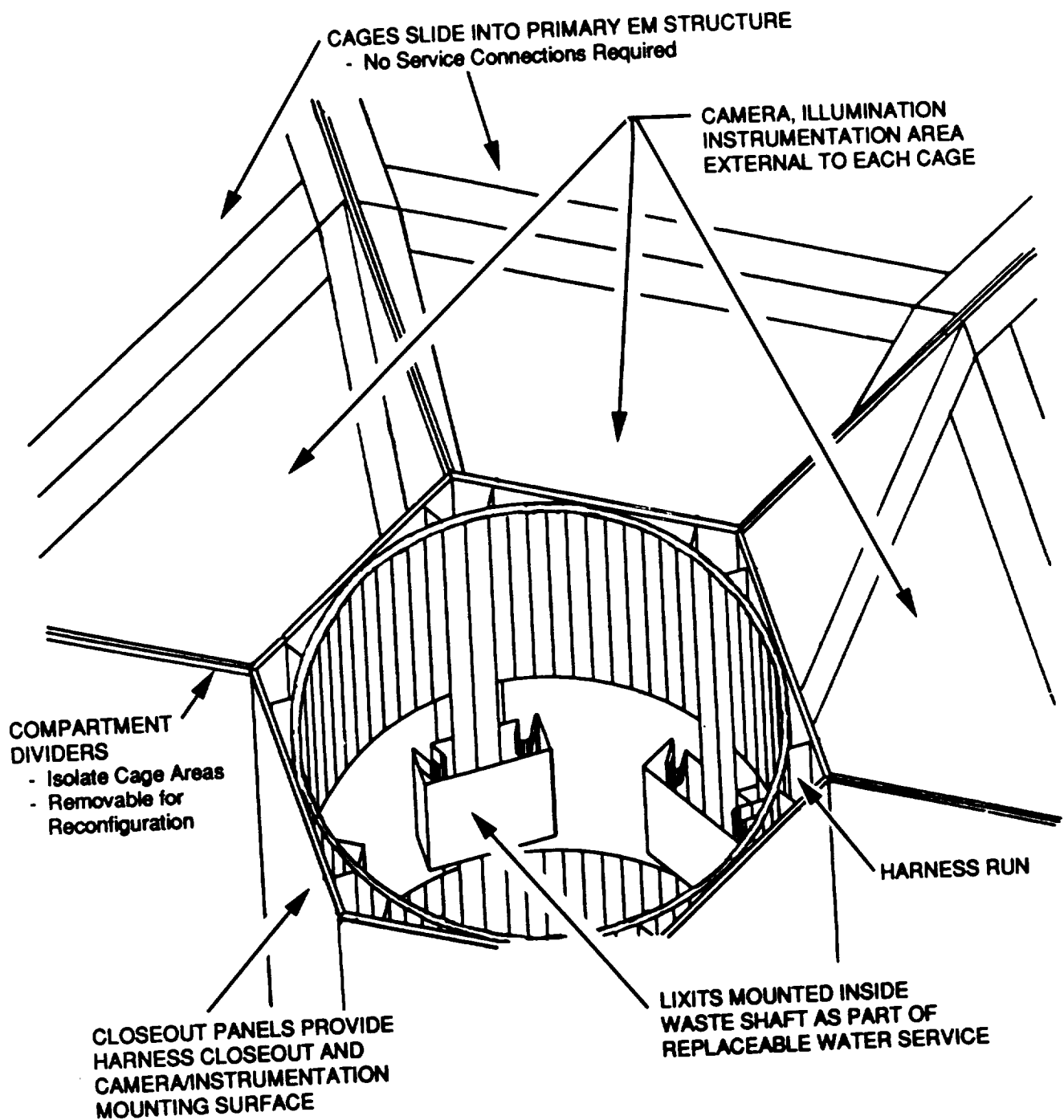


Figure 6.2-15. Utility Core Detail

Each cage has a dedicated food carousel located inside a food service shaft that permits food replacement from the top of the EM. The food service shafts are designed to be removable so that the group cages can be inserted and removed in one piece. The single cage configuration would use a dual cage design, with the walls designed to be removable after cage installation but before food shaft installation.

The offset debris shaft configuration, although compatible with the basic RM design, would require a different structural design. An alternative approach (Figure 6.2-16), also compatible with the basic RM design would be the use of 3 to 6 of the existing mid-deck locker design. In this design, a rack assembly would be used to hold the lockers within the EM volume in the SM, with an extension section added to the pressure vessel to accommodate the 4 to 6 locker configuration. No change to the RRV/RM interface is required to accommodate the RM extension.

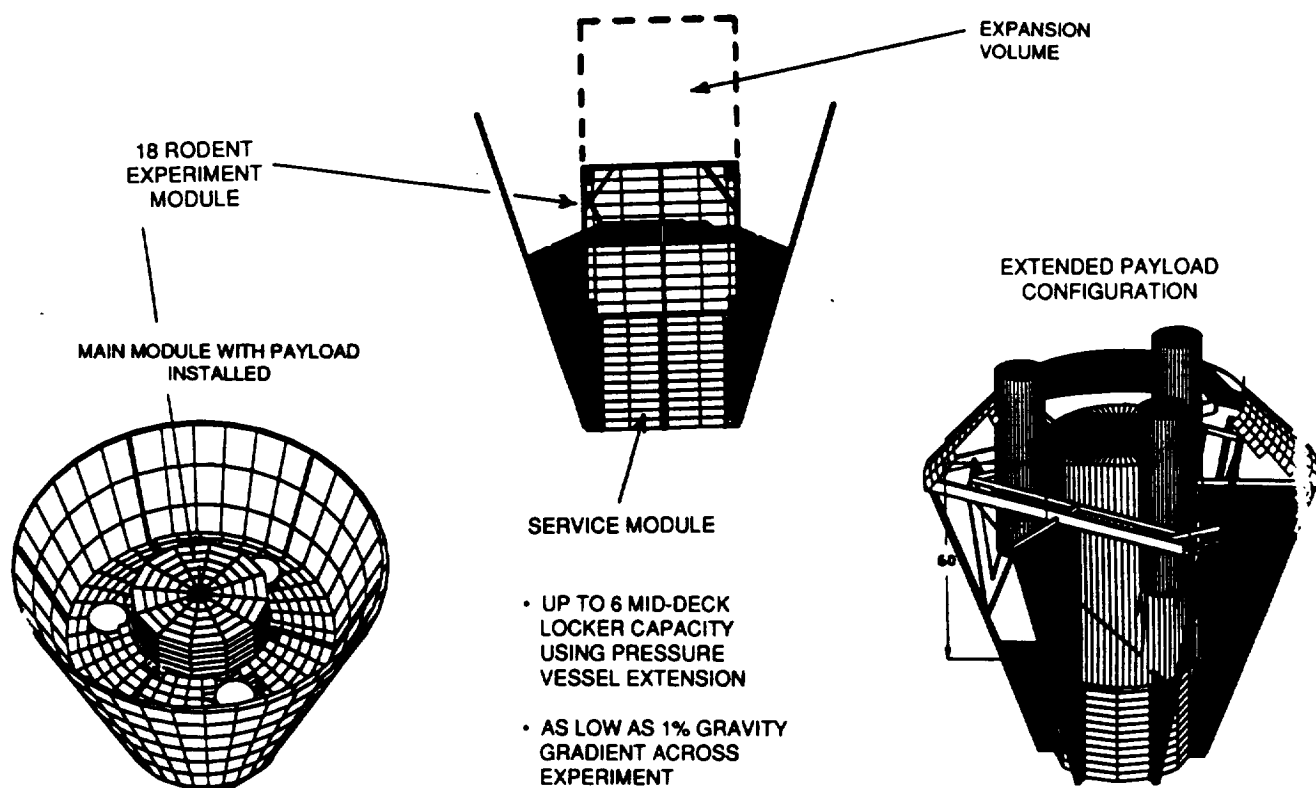


Figure 6.2-16. Variable Mid-Deck Locker Capacity

All services and instrumentation are installed on the basic structure. The water distribution service (Figure 6.2-15) is installed inside the waste shaft, and can be removed and replaced from the top of the structure. The instrumentation/power harness is mounted, external to the central shaft and behind close-out panels, to protect the harness from the potentially corrosive environment. The lighting and sensor heads (Figure 6.2-15) are mounted inside each cage compartment.

6.2.4.6.1 Waste Management. Three different systems were evaluated for ensuring removal of debris, fecal matter, and other adhesive materials from the cages. The use of intermittent scraping devices, a moving floor system, and the application of a hydrophobic coating material were examined. The mechanical complexities, and possibility of interfering with or injuring the test animals where mechanical devices were used, made use of the passive coating material the best solution. A hydrophobic agent approved for use in animal accommodations will be applied to the cages and other surfaces subject to debris and waste accumulation. Tests in the NASA KC-135 parabolic flight aircraft have shown this material to be an effective means of preventing waste adhesion to cage surfaces. The loose waste and debris will be entrained by the ventilation air and carried down the central column of the cage support structure to the waste collection filters. The filters are removed from the cage area, and debris will be retained in the collection area by constant air flow.

The RM will be designed to allow removal of all attached components (lighting fixtures, fixtures, food bar dispensers, instrumentation, etc.) so that the primary structure (cages, support structure, attach fittings) may be sterilized by steam cleaning or other suitable methods. The stainless steel cages will be coated with a hydrophobic material to prevent fecal matter, hair, or other waste and debris from attaching to the cage structure. Normal airflow, augmented by occasional added puffs, will entrain the debris, carry it to the vertical central air duct, and further to the debris trap at its SM interface. Airflow will desiccate trapped material, and carry moisture to the condensing heat exchanger where it will be absorbed by the waste water system and stored. Dry residue will be contained and desiccated in the debris trap by constant airflow.

The debris trap is designed to provide five separate traps, which will be swung into the airflow successively as the mission progresses; one in the center and four others which may be swung out, in turn, from the square side walls as they are needed. In the limit, all four will be swung back and the entire debris trap will collect debris. The debris traps have activated charcoal filters that remove trace materials, reduce odors, and ensure air freshening on each circuit through the ECLSS.

6.2.4.6.2 Food Dispensing System. Food bars will be displayed on rotary cylinders mounted vertically at one outward corner of each cage. Initial consumption food bars will be mounted on one wall of the cage, with additional bars required to provide adequate food for a 600-gm rat for 60 days, mounted on the rotary cylinders to be indexed into reach towards the end of the flight, as the need is determined or in accordance with pre-flight programming.

The use of paste food was investigated early in the study phase. Bionetics, who operate as a life science support contractor for Ames Research Center stated that, in order to achieve the required consistency, the food must contain at least 60% water. As a result, water intake from lixits would be affected and would distort dietary information and animal metabolism data. The mixture would also be very difficult to preserve and to protect from microbial, fungal, and mold infestation over a 60-day period because of its high water content. For these reasons, SAIC rejected the use of paste food for the RRS.

Pellets were found to be difficult to distribute to the cages from a central repository. The mechanisms are bulky, complex, and subject to clogging. The pellets are quite hard, which may solve the potential problem of rodent tooth growth, but can result in fragments drifting into other equipment. Ad lib delivery of pellets to the cages is also mechanically complex.

When compared to food bars, these two alternatives were considered far less satisfactory, presented complex materials handling challenges, and offered few, if any, advantages. The statement at the recent LifeSat Science Working Group (LSSWG) meeting that the food bars created a debris problem is accepted, but does not appear to be sufficient reason to eliminate possible use. Any debris created by the food bars will be carried down to the filters and immobilized.

6.2.4.6.3 Water Dispensing System. Drinking water will be provided by a lixit system based upon the system used in the Shuttle. The system will accept a range of potable water formulations, as desired for a given experiment. The water supply system is an adaptation of the system used in Space Shuttle rodent accommodations and is shown schematically in Figure 6.2-17.

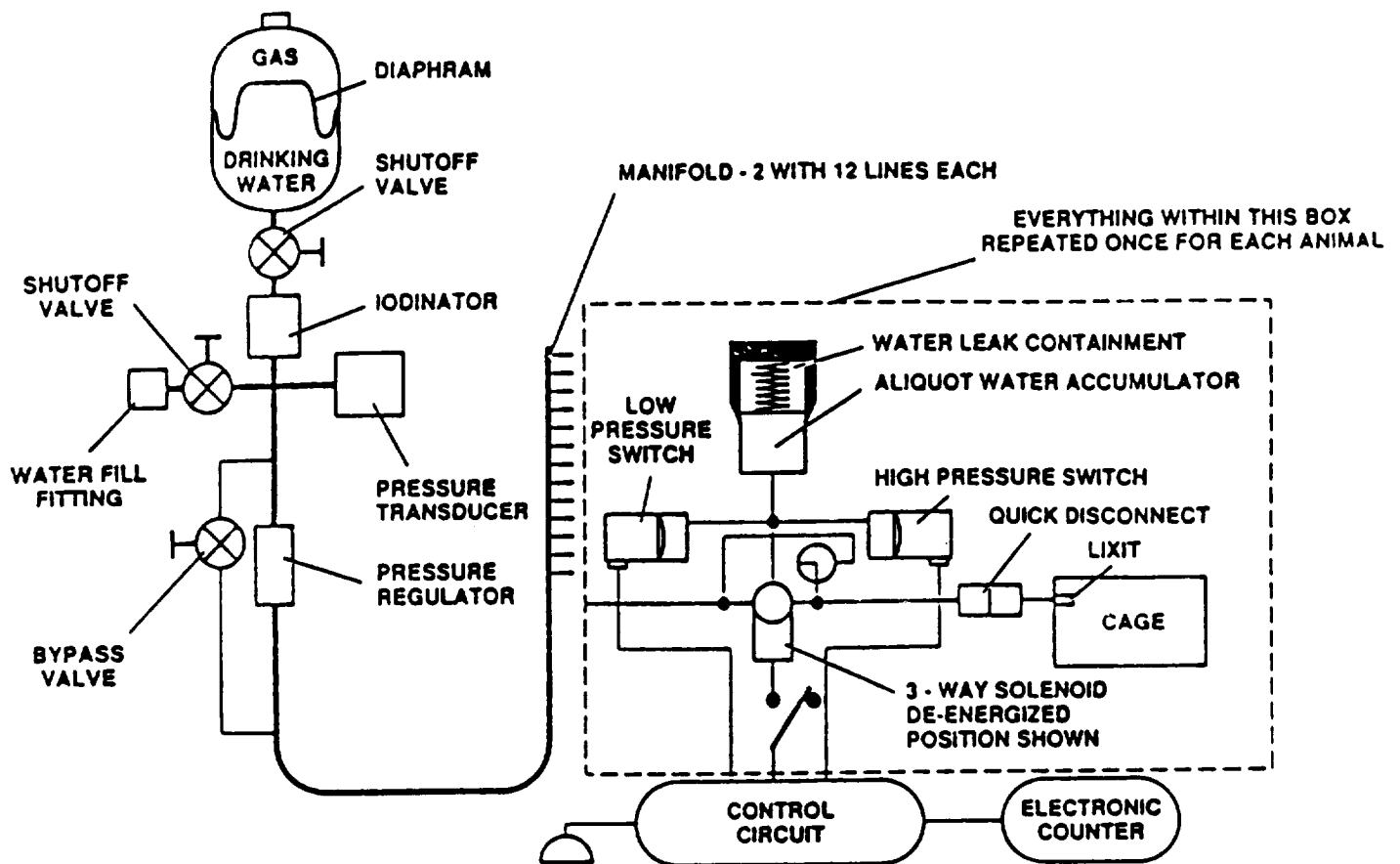


Figure 6.2-17. RAHF Drinking Water System

A reliable water supply is ensured by placing two independently supplied lixits in each cage. There will be a capability for activating and deactivating individual lixits. The supply of water is sized as required for a population of 600-gm rats for 60 days. Because the rodents will have to begin smaller in order not to exceed 600 gms before returning, sizing is conservative.

6.2.4.6.4 Mechanical

As detailed in 6.2.4, the Experiment Module is one of two separable modules. The EM interfaces with, and receives all support from, the Support Module.

6.2.4.6.5 Electrical. The cage illumination requirement in the SRD states: "During the 'light' part of every light/dark cycle, the spectrum of the illumination shall be the same as the spectrum of natural sunlight (the standard reference is sunlight at 12:00 hours at a mid-latitude on June 21st, Ref NASA Technical Memorandum 101077, Lighting Requirements in Microgravity - Rodents and Nonhuman Primates). During the "dark" part of every cycle, the spectrum of the illumination shall be TBD." Further clarification of the "natural sunlight" spectrum was found in NASA TM 101077. Table 6.2-5 contains data extracted from TM 101077, and contains comparisons of the spectra of natural sunlight, fluorescent lighting and incandescent lighting, respectively.

SAIC explored various alternatives designed to satisfy this requirement. Each alternative has inherent disadvantages, such as power consumption, size, etc. When the alternatives were presented by SAIC at the first quarterly review, we were verbally informed that the lighting spectrum was not as critical for animals as had been indicated in the RRS SRD; that the critical spectrum was for plants and will be provided by the European Botany Module.

Given this direction, SAIC investigated the use of incandescent lamps similar to the ones used in the Research Animal Holding Facility (RAHF) and the Animal Enclosure Module (AEM). These are miniature aircraft lamps just over an inch long, requiring 28V and 0.17A, with a rated average life of 1,500 hours. Two lamps can be mounted in the roof of each cage to provide redundancy.

Table 6.2-5. Lighting

REQUIREMENTS

- SAME LIGHT/DARK CYCLE AND LIGHT INTENSITY IN ALL CAGES
- PERIODICITY: "LIGHT" AND "DARK" PORTIONS SELECTABLE WITH MAXIMUM DURATION OF CYCLE EQUAL TO 30 HOURS
- "LIGHT" INTENSITY: 40 LUX \pm 35 LUX (16.4 μ W/cm²), LESS THAN \pm 10% VARIATION DURING MISSION
- "LIGHT" SPECTRUM: SPECTRUM OF NATURAL SUNLIGHT, REFERENCE 12:00 HOURS AT A MIDDLE LATITUDE ON JUNE 21
- "DARK" INTENSITY: LESS THAN 0.2 μ W/cm²

REFERENCES

- | | |
|---------------------------------------|---|
| Rodent Animal Holding Facility (RAHF) | - Uses Small Incandescent Light Sources in Each Cage |
| Animal Enclosure Module (AEM) | - Uses Small Incandescent Light Sources in Each Cage (GE 313, 1820) |
| Ames Workshop | - Specifies Natural Sunlight Spectrum and No Point Sources |

SYSTEM DESIGN

- 40 LUX (0.125 m²) CAGE AREA CONVERTS TO 200-300 LUMENS
- POWER REQUIREMENT IF CAGES ARE ALL OPEN IS LESS THAN 10W
- CAGE LAYOUT REDUCES EFFICIENCY, REQUIRES MORE SOURCES
- POSSIBLE CENTRAL LIGHT SOURCE WITH FIBER OPTIC DISTRIBUTION TO CAGES

FAVORED CONCEPT

- INDIVIDUAL INCANDESCENT LAMPS — TWO PER CAGE

Another alternative studied was halogen lamps. These lamps have a color temperature of 3200K, which corresponds to standard daylight on a slightly overcast day. However, halogen lamps generate significant heat, and require special heat dissipating fixtures. They present a thermal management problem to the spacecraft and mounting difficulties if rodent exposure to the hot fixtures is to be avoided.

As a result of these investigations, SAIC is specifying use of standard aircraft type incandescent lamps for the RRS. These light fixtures will produce diffused light at a uniform level. The wiring will be detachable to permit ready removal of the fixtures from the cages and removal of the cages themselves. The modular design will permit rapid adaptation to other payload

configurations. The recommended incandescent lights will remain within specified intensity level, $\pm 10\%$, when illuminated, for the required 60-day flight.

Two independent incandescent light fixtures will be provided for each cage. They will be mounted on the upper cage grill, with adequate space between the cage and the light housing to preclude rodent contact. The mounting will allow quick disconnect of the light fixture for replacement, cage removal, and post-flight sanitation. The lighting cycle will be regulated by on-board timing controls that respond to the experiment control software. The nominal lighting cycle will be programmed pre-launch, but may be altered in flight, if necessary.

6.2.4.7 Support Module. The SM provides environmental support and spacecraft interfaces for the Experiment Module. As shown in Figure 6.2-18, it is a totally modular system that supports all aspects of EM survival.

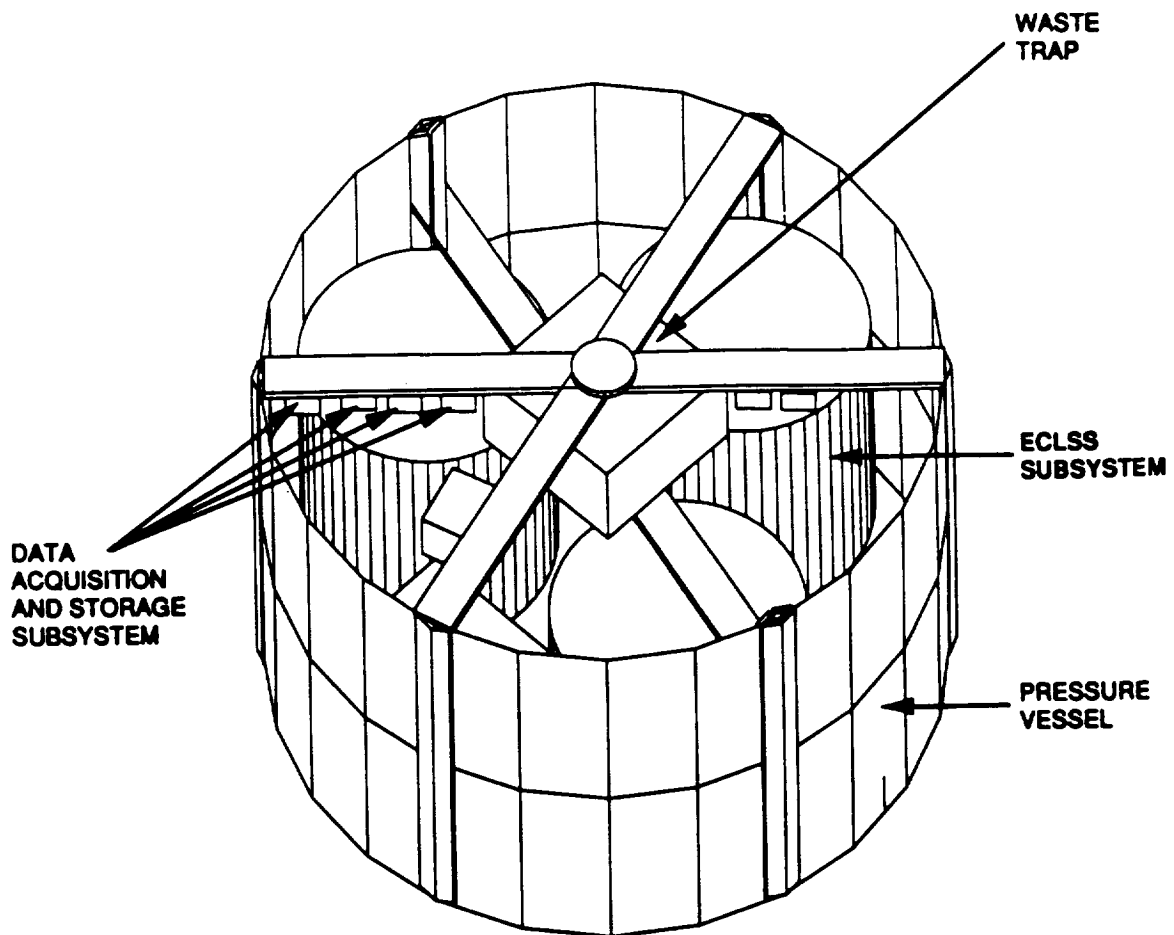


Figure 6.2-18. Fully Integrated Support Module

The RM outer structure is a pressure vessel (Figure 6.2-19) that contains the controlled atmosphere of the installed EM. Expendables are delivered to the ECLSS subsystem through lines and quick disconnects routed through the access panel at the Recovery Parachute Module end of the RM. The ECLSS is housed in the cylindrical volume nearest the nose of the reentry heat shield, and may be removed and separated from the EM after both are withdrawn from the RM. The closely packed subsystem elements of the ECLSS, ducting, supply lines, and supporting structure, form a single integrated module which is self-supporting within the RM. Its location is keyed to push-home pins in the interior of the RM and further retained at the EM/SM interface with fasteners accessible through the access panel opening in the RM.

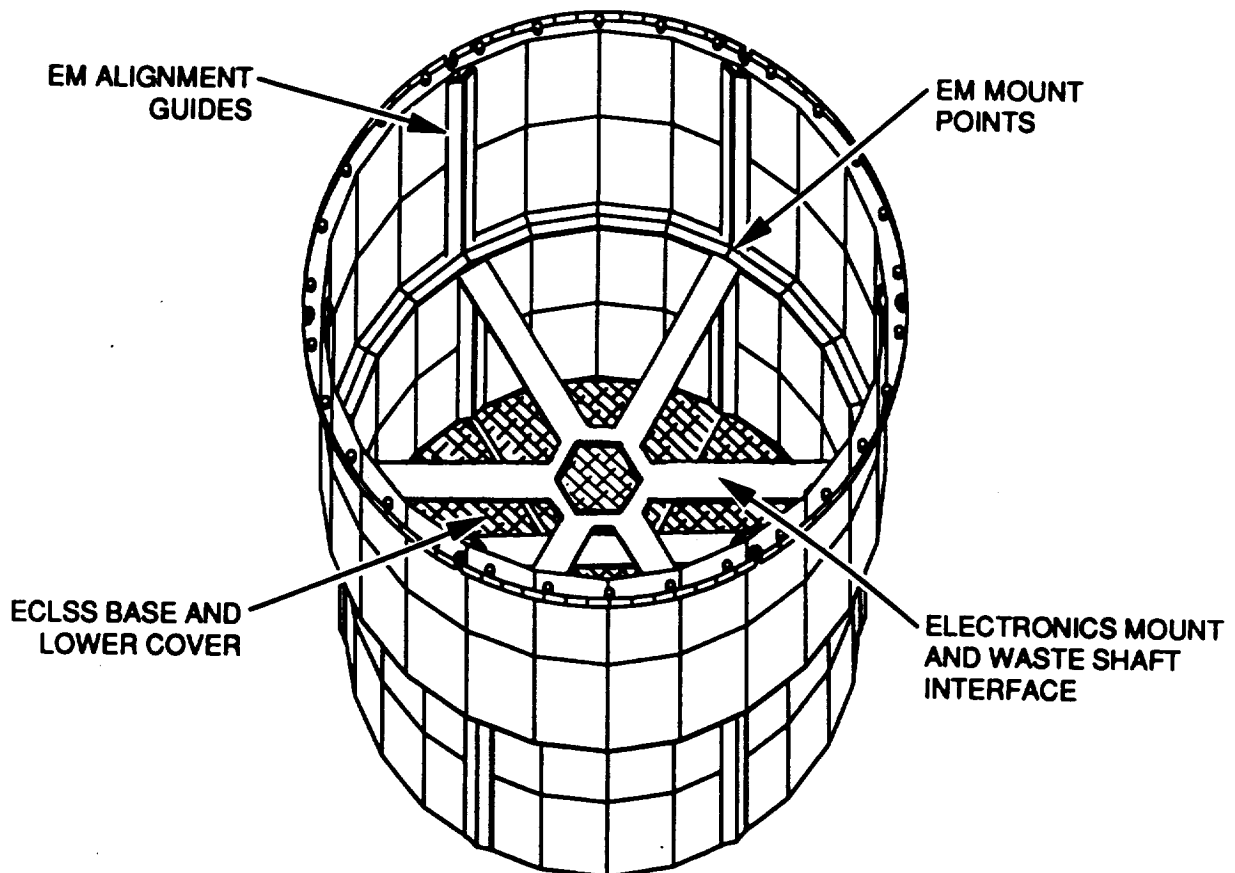


Figure 6.2-19. Pressure Vessel (With EM Access Cover Removed)

6.2.4.7.1 Electrical. The RM will receive all electrical power from the spacecraft power bus. Any unique power requirements will be satisfied via a power converter that converts spacecraft power to discrete voltages.

6.2.4.7.2 Data Management. Data management design trades applied the principle of maximum on-board autonomy in order to minimize ground support/control activities. It is our intent to maximize system self-sufficiency while providing ground control input/modification capabilities.

The full flight program will be loaded into the on-board database and initiated upon direction from the ground. On-board instrumentation will chronologically record conditions experienced by the rodents, including habitat atmospheric pressure, temperature, humidity, illumination cycle (also controlled on-board in accordance with pre-flight plans), lixit use, and specific animal instrumentation such as implants and acceleration. Video images (still pictures) will be recorded via videotape memory. A separate mass memory will record other instrumentation readings. When directed, selected images and/or data will be downloaded when the spacecraft is in range of ground tracking stations. In case of special need, the Telemetry and Data Relay Satellite System (TDRSS) can be used as a link to maintain contact anywhere in orbit.

Normally, the ground station will only transmit to the RRS if a change in flight plan is needed. However, the data management system will accept ground command transmissions to reprogram the on-board sequence, if necessary. Conditions experienced on-board will be reported to the ground station for imposition on the GCEM after a planned time interval, so that the experimental animals on the ground will act as controls on the flight animals to ensure that any differences in response of the animals can be attributed to the specific conditions peculiar to space.

Requirements for data to be obtained from the RM (and GCEM) are described in the SRD. The requirements are restated below within brackets [] as they will apply to the DASS design described by Krug. Additional information is provided as rationale.

- a. [Data is required to be "time tagged" to permit accurate reconstruction of the history of the mission. Data from each mission (launch) shall also be identified using words or bits that are unique to the RM and mission.]

Each source of data will have a unique identifier, such that each cage, instrument, camera or environmental sensor is positively identified. The DASS design will provide for time-tagging of all data.

- b. [The RM shall record module status, module environment, experiment housekeeping, and experiment status parameters and measurements at regular intervals during a flight.]

Module status and environmental data will be accessible and recorded at intervals consistent with the mission phase and module status. Alarm/warning signals will be transmitted in event of malfunction of principal life support systems.

- c. [Implanted sensor measurements will require receiving antennae and demodulation equipment for biotelemetry.]

Surgically implanted sensor/transmitters are recommended as the best method of obtaining long term physiological data from caged, but otherwise unrestrained, unattended animals.

Based on the planned mission schedule of three or more missions per year, the system must be easily reconfigurable and able to accept data from many types of biomedical (and bioscience) instrumentation, be rugged and not susceptible to "single point" failure, and be readily serviceable using commercially-available parts. Based on the planned 10-year life of the RRS vehicle, the system must be reliable and able to be updated easily to accept new developments in data transmission, storage, and display. Versatility of data acquisition and storage system equipment should permit its use in studies of space life science topics in addition to rodent studies, such as plant and single-cell organism behavior, to obtain maximum benefit from the RRS program. Even with these characteristics, a system designed to acquire and store data from space life science experiments that are as yet unidentified and unspecified requires a data acquisition and storage system that is highly modular.

The need for ground-based control of spacecraft functions as a backup to preprogrammed operation, establishes the basis for defining system housekeeping instrumentation. The RM subsystems requiring remote backup control, and consequent monitoring instrumentation, include the ECLSS, the water supply (lixits and their supply and distribution system), and power.

Monitoring will include airflow, temperature, humidity, pressure, pressure drop across the air filter system (to monitor debris build-up), heat exchanger coolant inlet temperature, quantities remaining in the consumables supply system, total RM power consumption and, possibly, discrete power consumption by selected components, such as fans, for troubleshooting. Key local temperature readings can also be useful, for example, in selected cages and fan motors. These readings will be available upon interrogation by ground control, individually or in pre-determined sets, as the need arises. The readings may or may not be recorded permanently for post-flight analysis, depending upon data storage capacity and degree of maturity of the RRS, but the data necessary for real-time RM system control will be formatted, compressed, and ready for immediate downloading on demand.

The system may be programmed to retain selected data permanently, and to purge data that has been downloaded after ground control confirms proper receipt or if not requested within a certain time frame.

Additional information generated by spacecraft systems, but affecting the RM experiments, i.e., system g's and/or attainment and maintenance of preprogrammed g level, will also be available to ground controllers and subject to explicit control, either by altering the on-board program, or by direct command intervention from the ground. In addition, preparation for changes in system operating conditions, such as a major change in g level or reconfiguration in preparation for reentry and recovery, will be implemented by preprogrammed commands monitored, in real time, from the ground, and subject to direct or program alteration override.

6.2.4.7.3 Data Acquisition and Storage System (DASS). The RRS System Requirements Document, Section 4.0, "Requirements for Rodent Module," was reviewed to derive basic concepts. The DASS design for the RM will acquire, preprocess, transmit, and store data. Capability for remote control of data acquisition and experiment protocols will also be provided. The RRS Data Handling Subsystem (DHS) will be a separate system with a data and command link to the DASS; the data handling processor will be a separate processor for satellite system and environment control.

Analyses conducted by SAIC and Krug International have defined the expected instrumentation needs of the RM, as a design condition for the EM. Experiments will be monitored using on-board biomedical instrumentation. Automated data acquisition and storage on-board is required, and is planned to be the primary experiment data record.

The instrumentation system, a direct adaptation of the system being developed for Space Station Freedom, will use hardware and software developed for the Medical Information Bus (MIB) system. The overall DASS schematic is shown in Figure 6.2-20.

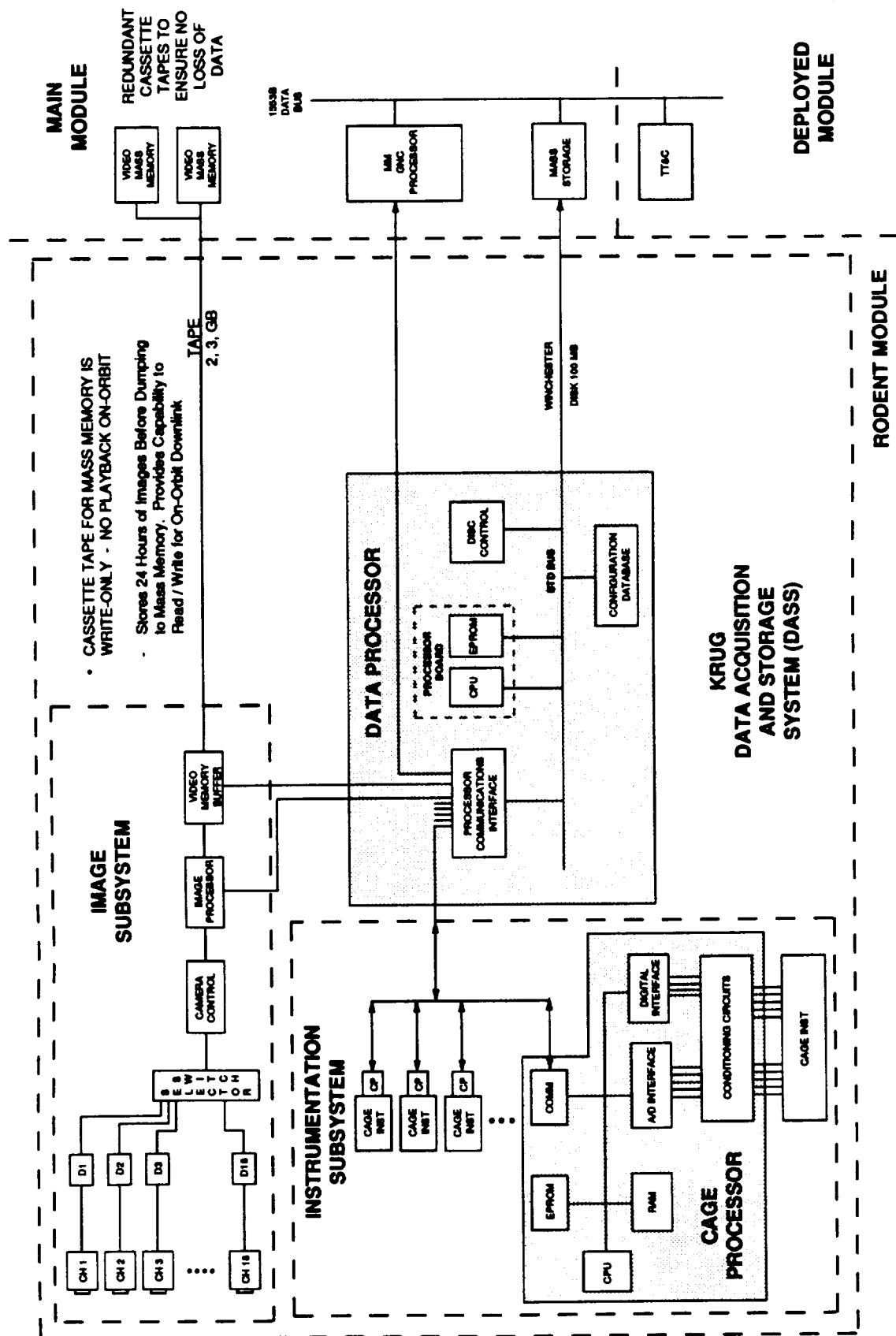
Selected data will be recorded for post-flight analysis. In addition, the bulk of the video imaging will be recorded for post-flight use. Selected video still (single frame) images may be selected and downlinked via telemetry during flight at designated times during the mission.

Because the SAIC GCEM design is identical to the equivalent flight hardware, the same instrumentation system will be installed. Control data from the GCEM will be immediately accessible for evaluation, and for comparison with flight data as it becomes available. Physiological data (temperature, heart rate, representative ECG, and blood pressure, including waveform samples) from a radio telemetry system will be sampled at 1-hour intervals. Environmental variables will be obtained from the RRS DHS and will be measured by sensors used for environmental monitoring and control.

The Data Processor (DP), the "brain" of the DASS, will function to process incoming commands, query the Cage Processor(s) (CP) for data from biomedical instrumentation, query the Image Processor (IP) for image data, and send all data to mass storage. Redundant biomedical instrumentation connections will be installed, and will access duplicate processors, with ability to switch to the backup processor in event of a failure.

Commands from a ground control station will access the Configuration Database (CD). The CD will contain preprogrammed query intervals for biomedical variables, image acquisition, and mass storage recall; the CD will also contain switch/control parameters for biomedical instrumentation. Limiting ground control station access to the CD only, will protect the DASS or biomedical instrumentation from inadvertent or unintended commands. A command from a ground control station can modify the CD in one of three ways:

- a. Modify the preprogrammed recording interval for biomedical instrumentation or image system,
- b. Modify the mass storage query interval, or
- c. Modify a biomedical instrumentation switch/control parameter.



TOR-42/11

Figure 6.2-20. Rodent Module Instrumentation

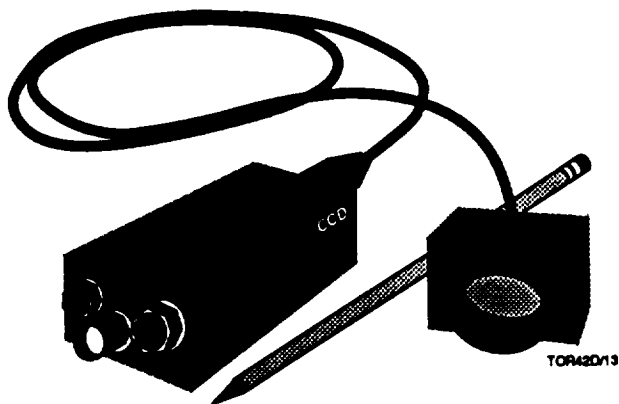
Each CP will be associated with biomedical instrumentation for a particular cage. The CP will receive data from the associated instrumentation, preprocess that data (e.g., time-tag), and store data locally in CP memory. At preprogrammed intervals, the DP will query the CP for specific biomedical data from instrumentation located at the cage. The capability to remotely switch power on or off to biomedical instrumentation will be provided.

The DP will also have the ability to query mass storage for stored biomedical data and images. After storage, the DP will have the ability to retrieve data and images for telemetry to a ground control station.

6.2.4.7.4 Video Imaging. Image acquisition will be provided from the video camera systems. An image processor will convert video images, taken at one frame per cage per hour using a 256 x 256 x 4 format, to digital format, compress image data (dependent upon final design and operational storage requirements), and transmit labeled frame data to mass storage. Recall of images from mass storage will be possible on ground or preprogrammed DP command. System design options will provide either random access from mass storage or temporary image buffer with video tape storage; the latter will preclude image recall from mass (video tape) storage.

Video images will be recorded at intervals designated before launch and controlled by the instrumentation system, with each cage being observed in sequence. Individual (still frame) images will be coded for later identification. If required, specific cages may be designated for real-time or near real-time observation and direct telemetry of images to a ground receiver. The frequency and cage sequence of imaging may also be remotely controlled.

The video camera system selected, the SONY model XC-77/DIT RH-100 remote sensor black and white camera (Figure 6.2-21), is compatible with the instrumentation system designed by Krug International, and provides the lowest volume, mass, and power consumption of the systems reviewed by SAIC. The remoting capability of the charge-coupled device imaging system allows individual placement at each rodent cage, routing the image signals to a multiplexer, and then to the single camera unit for conversion and delivery to either the mass memory device or the telemetry system for direct transmission to the ground. Simultaneous recording and transmission of designated frames will also be possible.



- DITECH DIT RH-100 REMOTE SENSOR
SOLID STATE CCD CAMERA
- 18 SELECTABLE SENSORS
- COSMICAR MODEL C20612 FIXED
FOCUS, MANUAL IRIS LENS
- 244 LINE HOR/VER RESOLUTION
- 32,774 BYTES/IMAGE
- 262 KBYTES DATA
- 5 BITS CAGE IDENTIFICATION
- 24 BITS TIME (1 SEC RESOLUTION)
- 3 BITS IMAGE REQUIREMENT SOURCE
- 16 BIT PREVIOUS ACTIVITY COUNTER

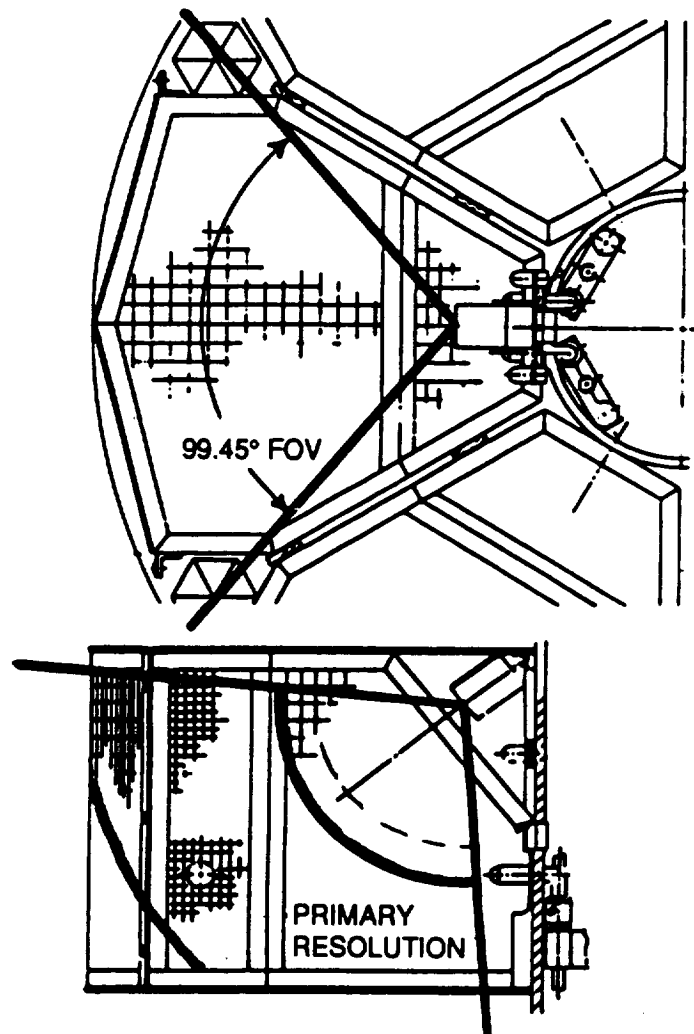


Figure 6.2-21. RRS Video Surveillance

6.2.4.7.4.1 DASS Hardware Description. The DASS design offers on-board hardware redundancy by using two mass storage units: one for biomedical data from instrumentation and one for images. The ability to switch between either mass storage device, in event of one device failure, is planned. The DASS will operate independently of the DHS, so that if the link to the DHS is disabled, the DASS will continue to function with the most recent (or default) program commands.

The preferred computer components will have STD BUS configuration. Circuit boards with STD BUS format are available from many suppliers; a variety of computer components and data acquisition modules are offered. A computer system to meet unique needs can be built from

commercial components with minimal design and development. Specific DASS hardware (Figure 6.2-20) is described below:

- a. **Data Processor (DP)** - The DP will be a processor board with general purpose Intel 16-bit processor. One such processor is the Ziatech STD DOS V50 MS-DOS (Ziatech Corporation). MS-DOS is the preferred operating system for this board, because many existing industry standard device drivers are available, e.g., optical disk drive interface. The DP processor board will be installed in a STD BUS chassis and connected to each of 18-cage processors.
- b. **Cage Processor (CP)** - The processor board for each CP will be similar to an Intel 80196 board used by Krug International for previous shuttle flight experiments. Circuits are included for cage sensor or biomedical instrumentation signal conditioning.
- c. **DP-CP Interface** - High speed communication links are planned, but design has not been finalized. Two options exist: All CPs can be installed into the same chassis with the master DP to permit data communication by Direct Memory Access (DMA), or each CP can be located at a cage with connection to the DP via synchronous communication link similar to Krug's MIB design. The first option requires no additional communications hardware, because data is transferred over the STD BUS. The second option simplifies cable requirements, but will require additional hardware. Final determination will be made during the final design effort.
- d. **Image Processor** - The IP will be used to convert standard video-to-digital data. The configuration under consideration consists of an RLC Enterprise TMS-320C25 signal processor with interface to a Computer Dynamics VIDEO STORE video digitizer. Efficient image compression will be provided, and final determination will be made during the final design effort.
- e. **DP-IP Interface** - The DP will command and access image data via the image processor. Due to the large amounts of data associated with images, the IP will be installed in the same chassis as the master DP to use high speed image transfer via Direct Memory Access (DMA).
- f. **Mass Storage** - Biomedical data from instrumentation will be stored using a Winchester disk drive. Read, write, and random access functions will provide data downlink

capability on command. Total accumulated environmental and physiological data will be approximately 200 MB. For photo images, accumulated image data will be approximately 500 MB.

- g. DP-MP Interface - The Small Computer Systems Interface (SCSI) format will be the preferred interface for the DP and MS. Winchester and optical disk drives (controllers) are available with SCSI interface format and SCSI interface cards are available for the STD BUS chassis.
- h. Video Camera -The camera selected is the SONY model XC-77/DIT RH-100 remote sensor, black and white camera, which provides a 570 line high resolution image. The camera body measures 4.4 x 2.9 x 10.7 cm, and the remote imager is approximately 3 x 2.9 x 3 cm.

6.2.4.7.4.2 DASS Software Description. Each software component of the RM, including the IP, DP, and each CP, will contain a command interpreter and command sequencer. The command interpreter resident in the DP will receive and respond to requests from the DHS to send or receive data. The command interpreter resident in each processor will be slaved to the DP. The command sequencer resident in both the CP and DP will be driven by three tables of information: event, time, and action tables. The event table will contain a list of commands and conditions required to execute them. The time table will contain programmed event schedules. The action table will contain single commands and multiple command sequences.

To communicate RM commands from the DHS (or ground control station) and to communicate with biomedical instruments, the DASS will use a Device Data Language (DDL) similar to the Medical Device Data Language. This language will permit CPs and instrumentation devices to be queried and data reported as single point values or as formatted groups. The DDL will also permit event, time, and action tables to be modified. Address capability of the language will make it sufficiently flexible to address components, system parameters, biomedical variables or image parameters within each processor. To use the DDL, the CPs and image processor will maintain a table of system and variable information, including permanent identifiers, configurable identifiers (to address definable groups), and calculated identifiers (for event triggers).

To support ground system operations, complete descriptions of biomedical instrumentation for each mission will be created. This information will be used to generate software tables and the

parameter identification code tables for the RM and GCEM. A flexible configuration system will be provided to support rapid refurbishing and reconfiguration of the RM.

6.2.4.7.5 ECLSS. The purpose of any spacecraft ECLSS subsystem is to provide an environment in which the life form (man, rodent, plant, etc.) can survive and function over the course of the mission. ECLSS requirements listed in the RRS SRD, coupled with the derived consumable requirements and waste calculations, bounded the capabilities the ECLSS needed to provide. A summary of these requirements is given in Table 6.2-6 for an 18-rodent 60-day mission.

Table 6.2-6. Environmental Control/Life Support System

- Functions: Controls Temperature, Humidity, Air Composition and Air Pressure
- Requirements:

Environmental	Materials for 60 Days
Pressure: 14.0-14.9 psia	Water Consumption: 133 lbs
Composition: 20 \pm 2% O ₂	O ₂ Consumption: 48.6 lbs
Temperature: 65-79°F \pm 3.6°F	Feces Produced: 47.6 lbs
Relative Humidity: 55 \pm 15%	Urine Produced: 52.8 lbs
CO ₂ Partial Pressure: 7.6 mmHg Max	CO ₂ Produced: 66.6 lbs

The ECLSS has been designed to meet system needs with a low risk design that is simple, reliable, and flexible in accommodating varying life science payloads, and has low initial and refurbishment costs. To accomplish these goals, the system makes extensive use of modular design and passive control, using experience and components derived from manned space programs. These features are consistent with the requirement for minimum electrical power consumption, which was a primary consideration in design of the ECLSS. Examples of system simplification through use of passive control techniques include:

- a. Passive atmosphere composition control (using pressure regulating flow control valves to replenish gas use or loss from the RM) eliminates need for an O₂ partial pressure sensor and an active control.
- b. Passive compartment temperature control using a manually adjusted heat exchanger bypass valve for trimming the cooling capacity eliminates need for an active temperature control and sensors.

- c. Passive thermal control during reentry and recovery using a fusible wax heat sink contained in the heat exchanger eliminates need for operating the cooling loop and an evaporative heat sink for this condition.
- d. Passive phase separator in the heat exchanger using capillary wicking for condensate removal eliminates need for electric motor-driven rotating water separator and its power consumption.

6.2.4.7.5.1 Atmosphere. The first ECLSS design trade was between active or passive CO₂ removal systems. Four types of systems were investigated in this trade: 1) Regenerable CO₂ removal/water dump system, 2) Regenerable CO₂ removal/water save system, 3) Electrochemical filtering system, and 4) Lithium hydroxide (LiOH) system.

The regenerable CO₂ removal/water dump system was the lowest in weight and power consumption but would require gas and water venting that would result in a contamination problem. Ice formation on the Astromasts could cause a retraction problem and affect system safety. The regenerable CO₂ removal/water save system would vent only gas, but has a relatively high power requirement. The electrochemical filtering system also has a fairly high power requirement and is unproven technology. The LiOH system uses relatively low power, but has the highest total weight of all systems. These features are briefly summarized in Table 6.2-7.

Table 6.2-7. Alternative Carbon Dioxide Removal Methods

	Advantage	Disadvantage
• Regenerable CO ₂ Removal/ Water Dump System	Lightest Weight Low Power Consumption	Requires Gas and Water Venting
• Regenerable CO ₂ Removal/ Water Save System	Vents Only Gas Modest Weight	High Power Consumption
• Electro-Chemical Filtering	Modest Weight	Unless Vented, Uses Same Power as the Regenerable System Unproven Technology
• LiOH CO ₂ Removal Recommended System	Uses Less Power	Highest Total Weight

It was determined that an LiOH system would best meet RRS unique mission needs. The design selected is based on a design by Allied Signal/AiResearch, and is derived from the system being developed for the manned Assured Crew Return Vehicle (ACRV). Use of the ACRV design

concept and components will ensure that the RM will be able to use high reliability man-rated hardware and systems. The passive control system (depicted in Figure 6.2-22) also allows significant simplification of control hardware and reduces failure modes, complexity, and cost of the system.

Initial air and oxygen supplied from consumables containers in the RRV will be free of all specified contaminants. The spacecraft atmosphere will be filtered through a two-layer filter as it cycles through the ECLSS. A particulate filter, for removal of solid matter, and an activated carbon/chemical filter, for trace contaminant control, will be utilized. Filter changes, four times during each mission, will be accomplished by rotating the frame out of the airflow path, and swinging another frame into place. Five filter frames form five sides of a cubical box placed at the exit of the central ventilation column in the EM. Each of the sides will be rotated into place in turn until airflow restriction indicates filter saturation, or 12 days of the 60-day flight have passed. Then, the filter will be swung down and the next swung into place.

The ECLSS will provide continuous airflow across the cages radially inward from the periphery to the central column, and then vertically from the first layer of cages (at the RM access panel) to the debris trap/filter assembly at the ECLSS end of the central column. Airflow continues through the filter to the fans, then to the LiOH canisters, to the heat exchanger, and then into the plenum allowing flow up the outside of the experiment module and back through the cages.

Atmospheric pressure in the EM will be maintained by a two-gas system, using oxygen and air (oxygen and nitrogen at 21%-to-79% ratio) supplied from tanks in the RRV. The ECLSS system will sense loss of metabolic oxygen as a pressure reduction and supply oxygen whenever system pressure drops below 14.7 psia +/- 0.2 psia. A flow-limiting orifice in the oxygen line will allow air to flow in to supplement oxygen flow whenever pressure drops below 14.4 +/- 0.2 psia. Replacement rate of the EM atmosphere is determined by the expected metabolic consumption rate and by a calibrated overboard dump. The overboard dump ensures replacement of the air in the experiment volume by the air and oxygen in the tanks at a rate which prevents buildup of undesirable trace gases.

6.2.4.7.5.2 Thermal Control. The thermal control subsystem of the ECLSS must be able to mitigate internal heat loads, generated by the rodent and internal electronics, and relay the heat to the RRV thermal control system for overall thermal control.

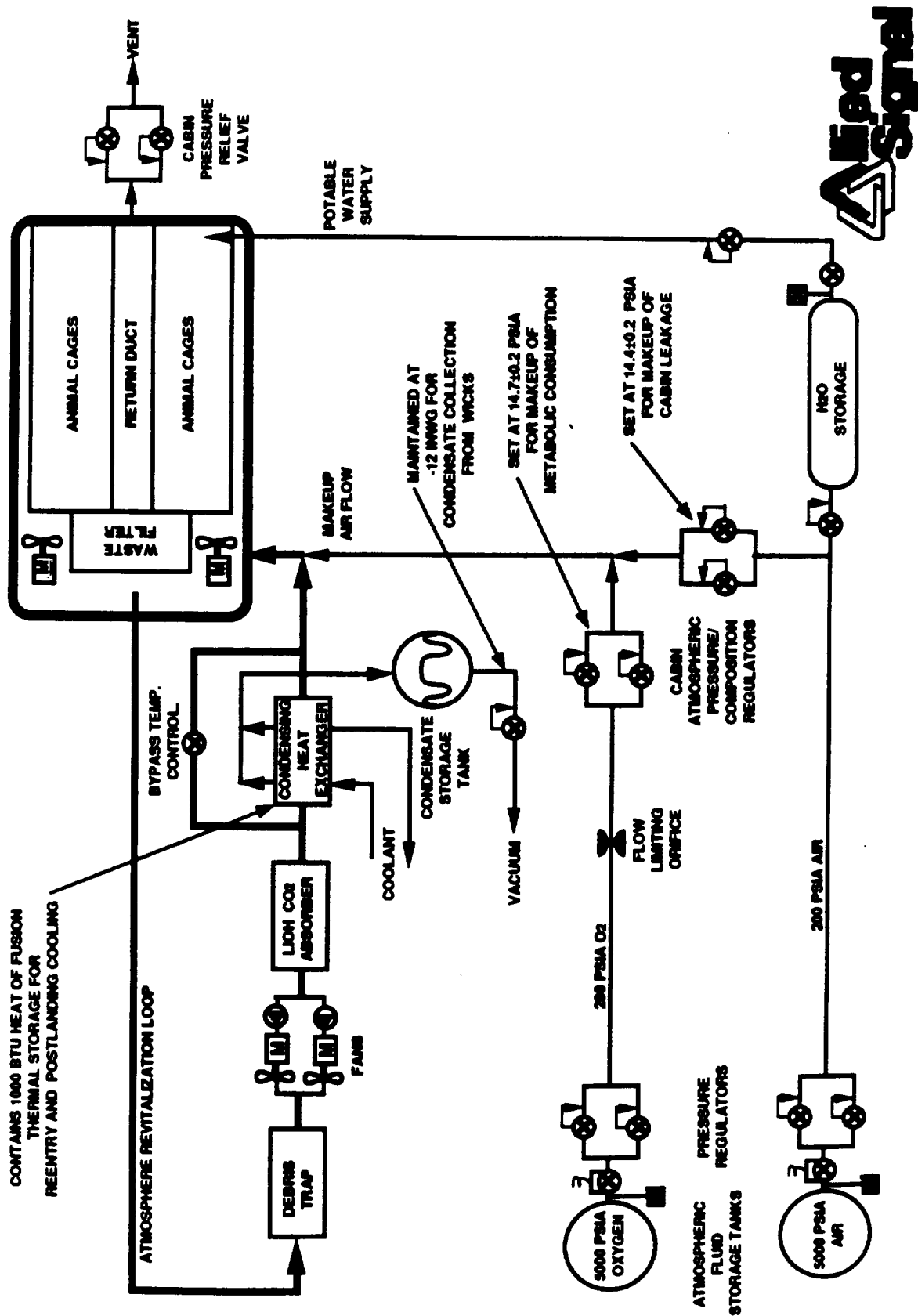


Figure 6.2-22. RRS Passive Environmental Control

Since the water evaporation provides useful cooling in the animal compartment ventilating air loop, waste dehydration appears as a latent heat load for design of the heat exchanger and a negative sensible heat load for the sensible heat balance.

The thermal control system is designed to control internal temperatures sensed by the experiment subjects in all flight regimes through use of an active condensing heat exchanger. The heat exchanger is a stainless steel air-to-liquid plate-fin design incorporating wicks between the air side fins for removal of condensate. The wicks are manifolded to a porous plate gas barrier. The condensate is conducted, at a slight (12-in water) negative pressure, to the condensate storage tank.

The heat exchanger incorporates an additional set of plate-fin sandwiches which contain a fusible wax (n-tetradecane) to serve as the heat sink for reentry and recovery of the animal pod, as well as for initial launch and orbital deployment. During normal operation, cooling will be provided by an external cooling loop using the spacecraft space radiator as the heat sink. Since the fusible wax heat sink will have a fusion temperature (41.9 degrees for the selected wax) above the normal cooling loop operating temperature (such as 35 degrees F), it will be maintained in a frozen condition. For a 3-hour reentry and recovery period, the coolant loop will not be available, and cooling will be provided by melting the thermal storage wax. During this period, the condensate collection system will not be operative, and the 0.4 pound of condensate which is formed will collect in the heat exchanger manifold.

The heat exchanger will have core dimensions of 8.0 inches by 8.0 inches by 8.0 inches, and will weigh 21 pounds, including 9 pounds of thermal material. The heat exchanger is sized to provide 50 degrees F saturated outlet air for inlet conditions of 65 degrees F, 75% relative humidity, and 10 ft³/min airflow.

After isolation on the launch pad, the cooling source for the heat exchanger will be provided through a ground support umbilical to the spacecraft thermal control system, which will then supply cooling to the ECLSS in the SM. In flight, after deployment of the spacecraft into its extended configuration, the on-board radiator will dissipate thermal buildup and deliver coolant to the ECLSS heat exchanger in the SM.

6.2.4.7.6 Mechanical

6.2.4.7.6.1 Noise. Sound levels experienced within the EM will be controlled by providing insulation, as required by launch vehicle imposed environments. The SAIC design of the RM

places the experimental animals inside a multi-layered spacecraft structure that will provide a significant degree of inherent sound insulation. In addition, all moving elements that could produce annoying noise, or mechanical vibrations, are installed in the SM, and are separated from the EM by a bulkhead. The SM contains only one set of rapidly moving parts that could be a source of significant vibration - ventilation fans. They will be very precisely balanced, and are very small and light in mass. All fluid transfer is via gas pressure and diaphragm so that the RM assembly will be inherently quiet during orbital operations.

6.2.4.7.6.2 Reliability. The design of the ECLSS system for the RRS was adapted from a design developed for manned spacecraft. Parallel redundancy has been incorporated for all dynamic components such as fans, valves, regulators etc. Valves specifically incorporate dual control elements packaged in integrated assemblies.

6.2.5 RRV Support

The RM receives command and control, electrical, mechanical, thermal and consumable storage support from the RRV.

6.2.5.1 Command and Control. The SAIC design provides the capability for pre-programming the command sequencer before launch in order to control all pre-determinable spacecraft and system functions. However, the telemetry system will include command capabilities to intervene, re-program, and/or alter spacecraft functions, as needed, either in real time or by uploading a timed sequence of events to be controlled and implemented by the command sequencer. The command sequencer will accept programming or telemetry uploads to adjust RM event sequencing and initiation to the actual spacecraft schedule. It should also be noted that because the SAIC designed GCEM is functionally identical to and oriented and operated similarly to the RM, it can respond to the same experiment-related commands as the RM.

6.2.5.2 Electrical. The RRV provides vehicle bus power, nominal +28 volts, to the RM. The RM uses a power converter to satisfy any unique discrete voltage requirements that may be levied by the EM.

6.2.5.3 Mechanical. The SM must fit within a dynamic envelope 60 inches long with upper and lower diameters of 38.0 and 32.5 inches respectively and have a dry weight not exceeding approximately 380 pounds.

6.2.5.4 Thermal. The RRV houses the active thermal control devices, and pumps cooling liquid to the RM thermal subsystem.

6.2.5.5 Consumables. The RRV provides tank storage for water, air, and oxygen consumables.

6.3 Structures Subsystem

6.3.1 Operation

The structural subsystem functional operation is divided into three major phases for an RRV flight.

6.3.1.1 Prelaunch and Launch. The structural subsystem provides support and shock isolation to the payload during the launch phase of the mission.

6.3.1.2 Orbital Flight. Once orbital flight is achieved and the RRV is separated from the launch vehicle, the commands for initial separation of the two vehicle halves (bolt operation) are given from either ground command or internal clock. Vehicle extension, as well as retraction, is computer controlled. The control function involves synchronization of the mast deployment nuts. These in synch determine the deployment rate of the deployed module. Anomalous behavior causes stoppage of maneuver and signal to ground for further instructions.

6.3.1.3 Reentry and Recovery. Final latch position check is telemetered to ground and must be verified before reentry maneuvers can be performed. Impact with the ground will be cushioned by a crushable structure in the sphere cone.

6.3.2 Requirements

The structural subsystem purpose, as outlined in Table 6.3-1, is to provide the overall vehicle configuration for the RRV. The structural design of the RRV supports the payload and RRV subsystems throughout all phases of the RRS mission. The requirements for the structural elements were broken down into the five most stressing cases, dependent on the element being sized.

- a. Prelaunch and Launch - An assumed Delta launch gave a worst case loading to the RRV of 5.5 g axial (along Z RRV axis) combined with 2.2 g in the XY vehicle plane. The vehicle mass is assumed to be 5000 pounds.
- b. Orbital - Assumes an artificial gravity mission of 1.5 g and vehicle extended to 100 foot length. The vehicle mass is assumed to be 5000 pounds.
- c. Reentry - 15 g axially deceleration forces along with maximum external aerodynamic pressure of 3000 lbs/ft². The vehicle mass is assumed to be 4400 pounds.
- d. Terminal Reentry - 6 g axially from parachute opening shock. Main module mass is assumed at 2700 pounds.
- e. Touchdown - Deceleration of 10 g axially upon earth impact with a vehicle mass of 4200 pounds.

Table 6.3-1. Structure Subsystem

PURPOSE

THE PURPOSE OF THIS SUBSYSTEM IS TO:

- PROVIDE SUPPORT AND MOUNTING FOR ALL SUBSYSTEMS
- PROVIDE PAYLOAD SHOCK ISOLATION
- PROVIDE MOUNTING POINTS FOR LAUNCH VEHICLE ADAPTOR
- PROVIDE FOR EXTENSION/RETRACTION OF TWO VEHICLE HALVES
- BE SUFFICIENTLY RIGID TO SURVIVE LAUNCH-REENTRY AND LANDING LOADS WITH MINIMAL DAMAGE
- PROVIDE QUICK ACCESS TO PAYLOAD AND/OR EXPERIMENT MODULE

The structural subsystem also provides for the vehicle separation/retraction system (Astromasts) to yield a 40 foot or greater spin radius for artificial gravity missions. Finally the structural design should be reusable to whatever extent possible.

The structural subsystem provides support and alignment for the propulsion and GNC systems and provides support for all others. In addition the structural system provides for heat paths to cool electronic components.

6.3.3 Trade Study Summary

The trade studies performed in association with the structural design involved primarily the shape of the reentry body, the placement of components within that shape, the use of the deployable tri-mast, and the scalability of the vehicle.

The only real alternative to use of the tri-mast to achieve the long spin radius is the use of a tether. This approach had been considered and rejected during the initial proposal concept trades and continued to be rejected for the lack of a credible means of control. Mast designs other than the flight Astromast type were also considered, but none could match the weight and redundancy advantages of the RRS Astromast design. Therefore, given that multiple independent analyses had indicated the Astromast approach was viable, no further work was done on other configurations.

Studies on the reentry body shape were limited to simple spherecone shapes for which reasonable experimental databases and/or extensive analyses existed to provide credibility. The

various shapes were analyzed in terms of reentry forces (related to Beta) and aerodynamic stability. The chosen 20-cone angle has a center of pressure sufficiently greater than the center of gravity (relative to the nose) to ensure aerostability while still being low enough to preclude thermal problems (which would require a heavier heat shield) and/or excessive deceleration loads.

Given the body shape and the use of the tri-mast, the question became one of proper component placement. This entailed balancing the vehicle to maintain reentry stability margin and maximize the spin radius of the main module. The basic study concluded that placing the propulsion system as far aft as possible was the most feasible, since the mass on the Deployed Module increases the spin radius. This placement is not a detriment to reentry stability because the propellant is burned off prior to atmospheric entry. The vehicle electronics were placed on the lowest possible station on the Deployed Module to minimize detrimental effect on reentry stability. The other subsystems, such as Power and ECLSS, were placed based on support of other subsystems. This basic configuration was then scaled for logical Rodent Module design points over the Taurus/Delta booster range. The resulting five configurations (Figure 6-8) are discussed in Section 6.3.4-9.

6.3.4 Baseline Design

The structural design description of the RRV is separated into the representative modules and submodules that make up the RRV design. The sections covered are:

- Deployed Module (DM) consisting of the control and propulsion submodules
- Main Module (MM) consisting of the nose, conical heat shield, and carrier submodules
- Payload module attachment fittings
- Astromasts
- Astromast analyses
- Launch vehicle to RRV attachment.

Figures 6.3-1 and 6.3-2 show the RRV in the launched or retracted configuration. The RRV has an overall length of 116 inches with a 95-inch diameter. The RRV structural design, being modular in nature, provides for easy access to all components and subsystems. This is especially important and was done intentionally to minimize manufacture/refurbish schedule time. For refurbishment, each major module can be replaced, or units on the module, once the vehicle is disassembled, with minimal impact on other subsystems. Standard refurbishment after a flight would include replacing the nose and conical heat shield submodules, inspection of all high stress

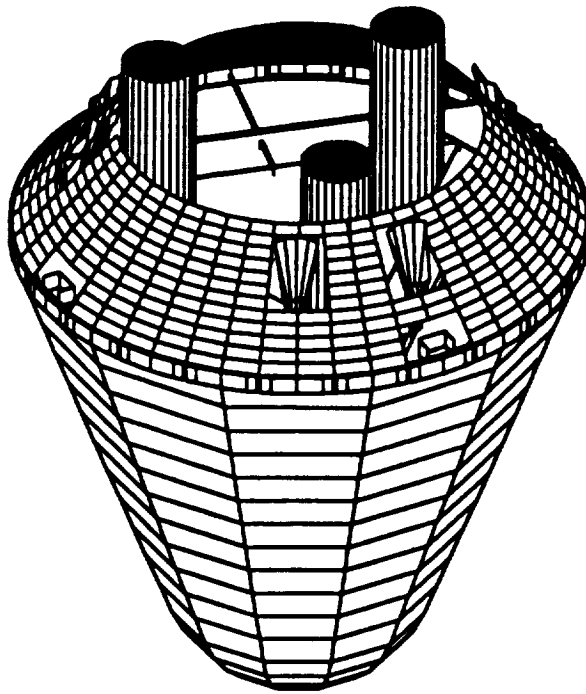


Figure 6.3-1. RRS Vehicle – Launch Configuration

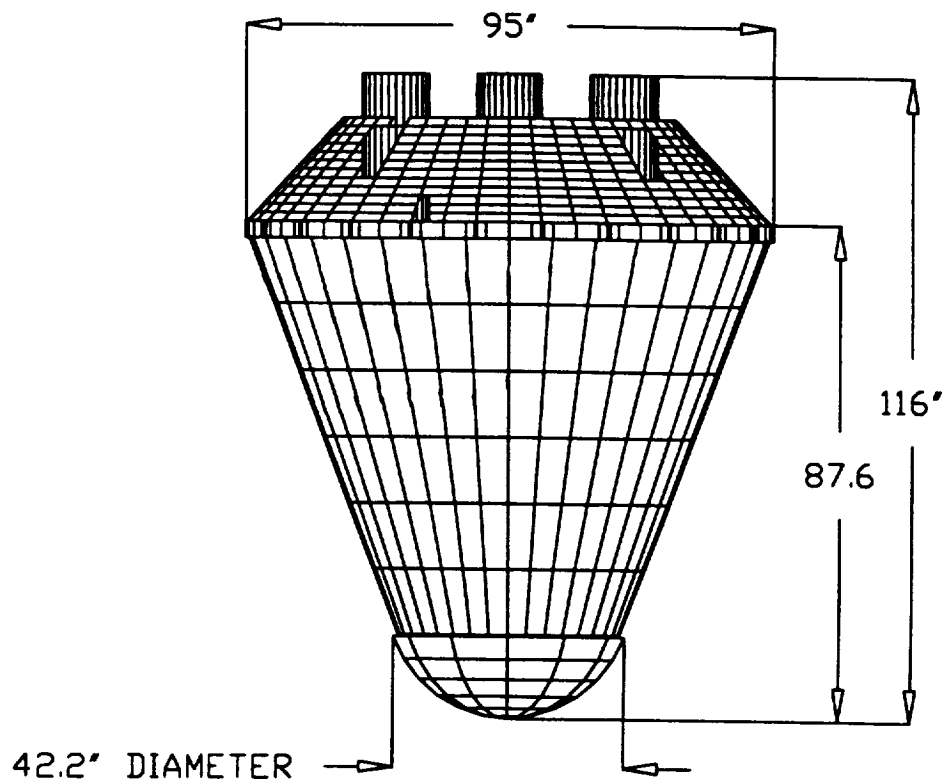


Figure 6.3-2. RRS Retracted Configuration

areas, replacement of any damaged members, and removing and replacing the Astromasts. The masts would be sent to the manufacturer for checkout, and refurbishment as required, before being approved for reflight.

Design Assumptions. The vehicle structure is constructed of 6061-T6 aluminum. The 6061 is a high strength, corrosion resistant material with good weldability and machining characteristics. Material properties are listed in Table 6.3-2.

Table 6.3-2. RRV Structural Design Assumptions

- ULTIMATE FACTOR OF SAFETY (UFS) = 1.5
- BASELINE MATERIAL IS 6061-T6 AL (HIGH STRENGTH, CORROSION RESISTANCE, WELDABILITY)
- PROPERTIES
 - Density: 0.098 lb/in³
 - Elastic Modulus: 10.9 mpsi
 - Ultimate Tensile Strength: 42 kpsi
 - Yield Strength: 36 kpsi
 - Thermal Coefficient of Expansion: $13.0 \times 10^{-6}/^{\circ}\text{F}$

The worst case loadings described above, and a 1.5:1 ultimate factor of safety (no yield) based on these loads, was assumed in the performance of the structural sizing analysis.

6.3.4.1 Deployed Module. The Deployed Module is divided into two sections: the Propulsion Submodule and the Controls Submodule.

6.3.4.1.1 Propulsion Submodule. The Propulsion Submodule shown in Figure 6.3-3 (top view) and Figure 6.3-4 (3D view) is the primary load carrying structure when in the launched configuration. It consists of three main beams, three secondary beams, three interconnect beams, three shear web caps, three launch vehicle interface blocks, and single ring support.

- a. The three primary support beams are 3-inch in diameter, 3-inch thick, 0.15-inch aluminum. The beams are sized for the worst case loads that occur when the vehicle is fully loaded during launch. Each beam weighs approximately 10.8 pounds. The beams have drilled holes with keenserts for installation of the propellant tanks, interconnection to the shear web caps and launch vehicle interface blocks. The main beams also provide connection points between the MM and the DM during launch. Additional keenserts on the top face provide for installation of the main maneuver or de-orbit thrusters.

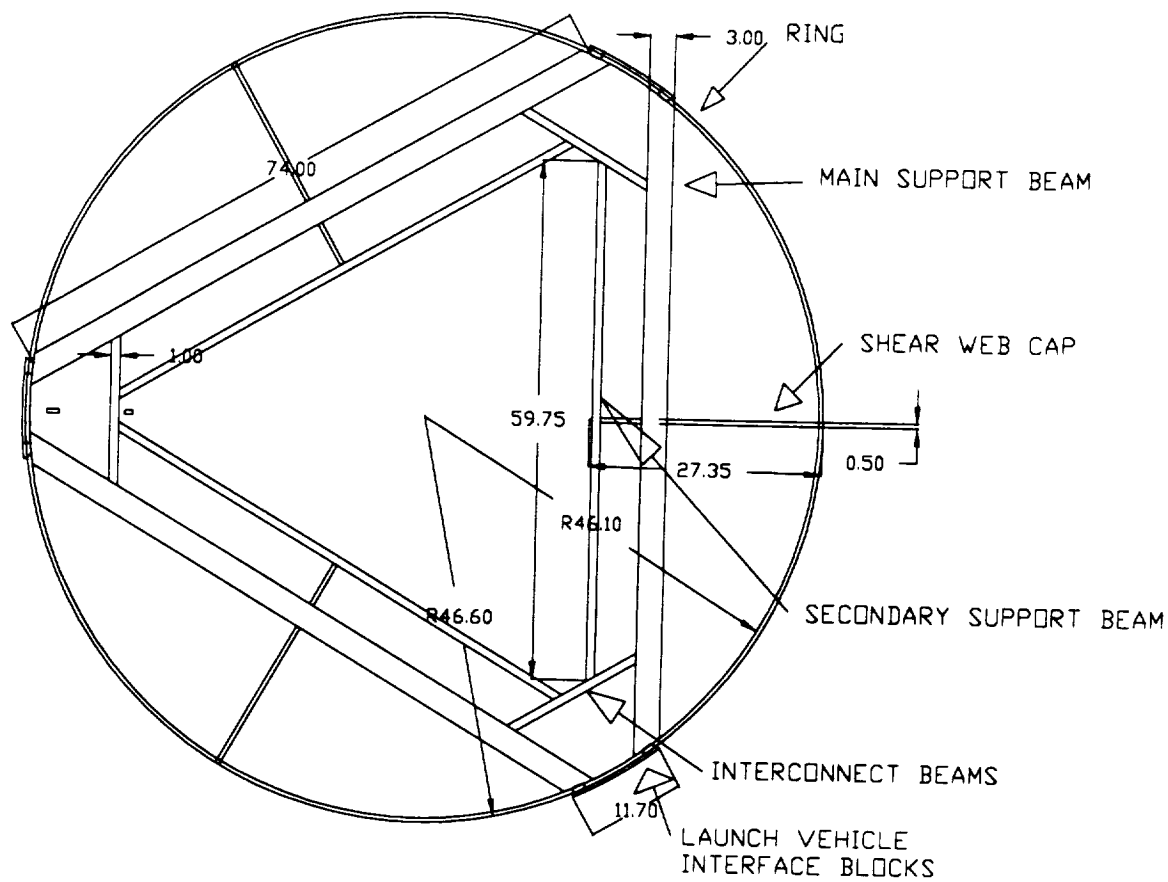


Figure 6.3-3. Propulsion Submodule Structure
Top View

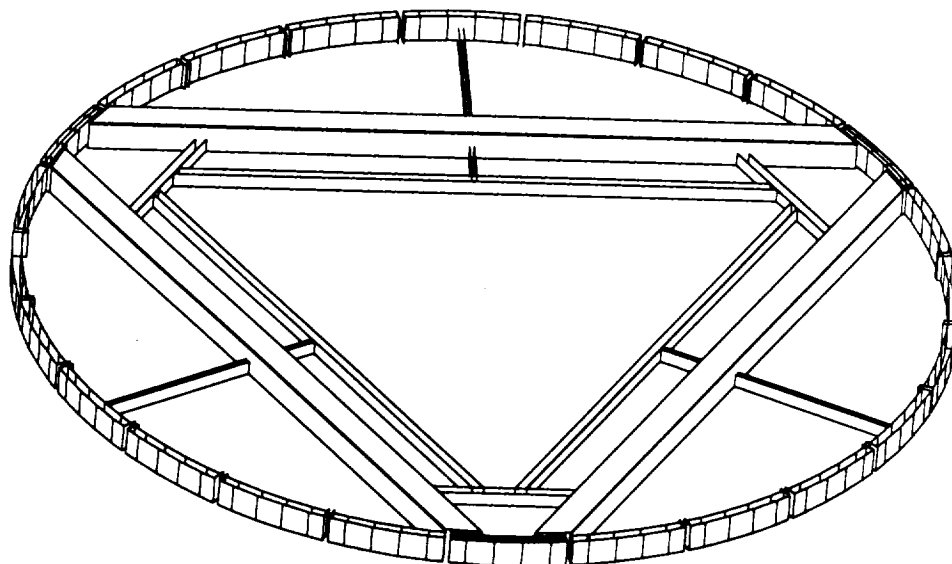


Figure 6.3-4. Propulsion Submodule (3D View)

- b. The secondary beams serve as primary mounting points for the Astromasts. The secondary beams react out the Astromasts loads when the vehicle is performing an artificial gravity mission. The beams have keenserts for installation of the Astromasts canisters and the inner cover of the deployed module as well as connection to the shear web caps. The beams are 1 inch in diameter, 1.5 inches thick made out of 0.075-inch aluminum. Each beam weighs approximately 1.6 pounds.
- c. The interconnect beams are of the same design as the secondary beams and weigh 0.5 pound each.
- d. The shear web caps provide primary interface between the Controls and Propulsion Submodules, as well as providing the reaction point for the MM-to-DM structure loads upon parachute release. The shear web caps are U-shaped beams, 0.5 inch diameter and 2 inches deep, with a 0.075-inch slot for integration with the shear webs. The shear web cap top thickness tapers from 2 inches at the main beam interface to 1 inch at the outer ring interface. The shear web caps weigh 2 pounds each.
- e. The launch vehicle (LV) interface blocks are the primary load reaction points during launch. The blocks interface with the main beams and the support ring. Attached to the outside of the block are carbon phenolic sections. Details of the sections are covered in Paragraph 6.3.4.7, LV interface. The aluminum support blocks are 11.7 inches long and 2 inches square. Each block weighs approximately 4 pounds.
- f. The outer ring provides support for the non-LV carbon phenolic sections, provides mounting for the attitude control thruster modules, and helps stabilize the vehicle during launch. In addition, the ring provides top support for the Main and Aft Solar Array panels. The worst case loads that size the ring occur during a worst case reentry. The ring is an 0.5-inch square box frame structure with 0.125-inch walls. The ring weighs approximately 6 pounds.

6.3.4.1.2 Controls Submodule. The Controls Submodule supports the electronics for the vehicle guidance, navigation and control; telemetry, tracking and command; and power subsystems. The equipment support panels consist of a conical aluminum honeycomb structure 1.0-inch thick with 0.025-inch cells. The honeycomb has 0.30-inch thick endplates. This structure provides for mounting of the electronics assemblies. This structure is sized by worst case reentry loads. Local copper straps are used to increase thermal conductivity, as required, to transmit heat away from the operating systems. The support shelf, with local doublers, stiffeners, and attach brackets, weighs approximately 16 pounds. The equipment shelf is supported by a series of support tubes and the Astromast canisters.

The support tubes are 1 inch in diameter with 0.060-inch wall. There are a total of 18 tubes. Six connect to the shear panel end caps; the other 12 are located between the Astromasts canister and the main beams. The total mass for the tubes end caps is 10.8 pounds. The configuration for the Control Submodule is shown in Figures 6.3-5 and 6.3-6.

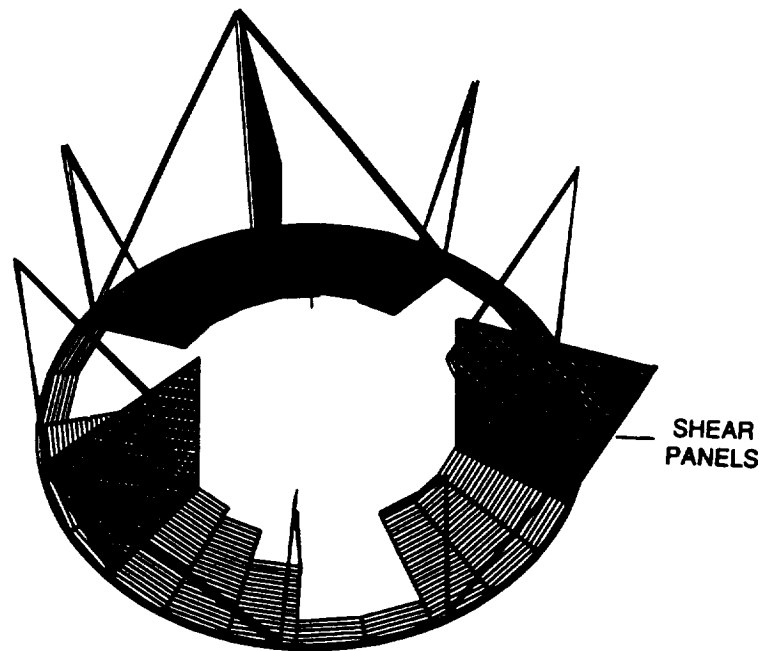


Figure 6.3-5. DM Command Submodule

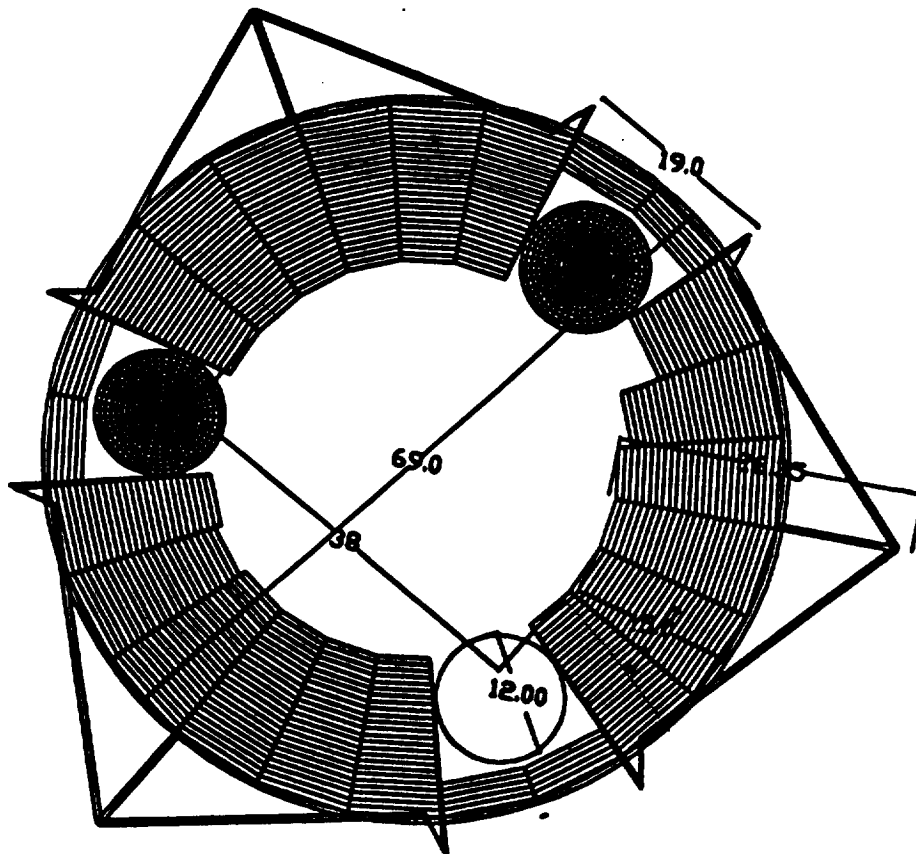


Figure 6.3-6. Command Submodule Dimensions (Inches)

The final major component of the Controls Submodule is the shear webs. The webs react out loads during launch, and provide support for the Main Solar Array. The shear panels also serve as the primary structure for latching the DM and MM together prior to reentry. The webs provide the load path for holding the MM to the DM upon chute deployment. The shear webs are 0.75-inch thick. The total mass for the shear webs, end caps, and latching system is 30 pounds.

6.3.4.1.3 Deployed Module Integration. The submodules are manufactured along parallel paths. The two submodules are first checked upon construction, and then sent to different locations for subsystem integration. The Control Submodule includes the batteries, computers, power electronics, GNC, and TT&C subsystems, as well as mounting provisions for the Astromasts. The Propulsion Submodule contains the propulsion tanks and lines installed, including the main valving. The Propulsion Submodule has its own harness, which is installed at this time. Upon completion of the subsystem integration, the submodules are integrated into a completed Deployed Module as shown in Figure 6.3-7.

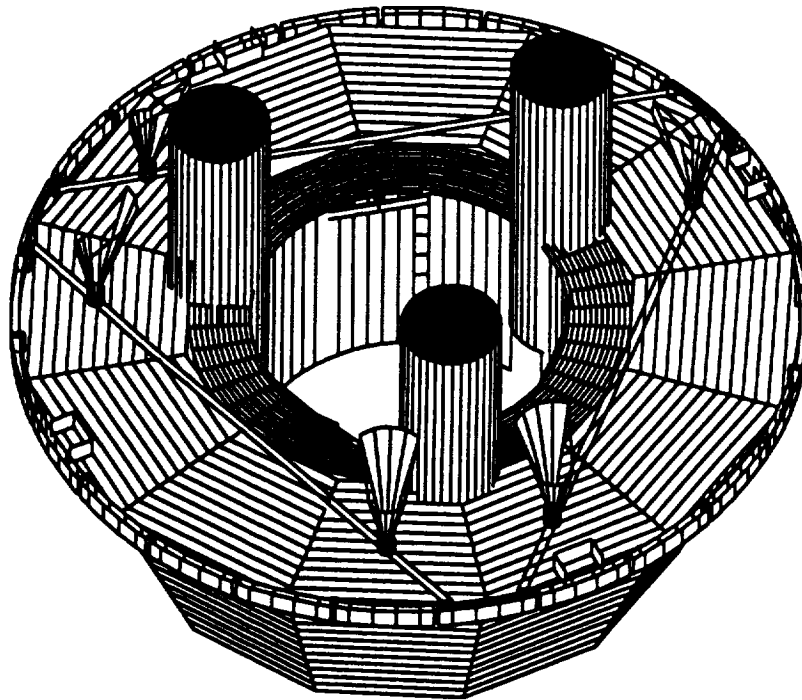


Figure 6.3-7. DM Prior to MM Mating and AFT Solar Array Installation

The Deployed Module has top closeout and inner closeout panels that seal the module and provide additional stiffness. The closeout panels are 0.5-inch thick aluminum honeycomb with 0.10-inch endplates and 0.25-inch cell size. The final view, shown in Figure 6.3-8, depicts the prelaunch configuration of the Deployed Module. The Aft Solar Array, Astromasts, and all propulsion thrusters are installed.

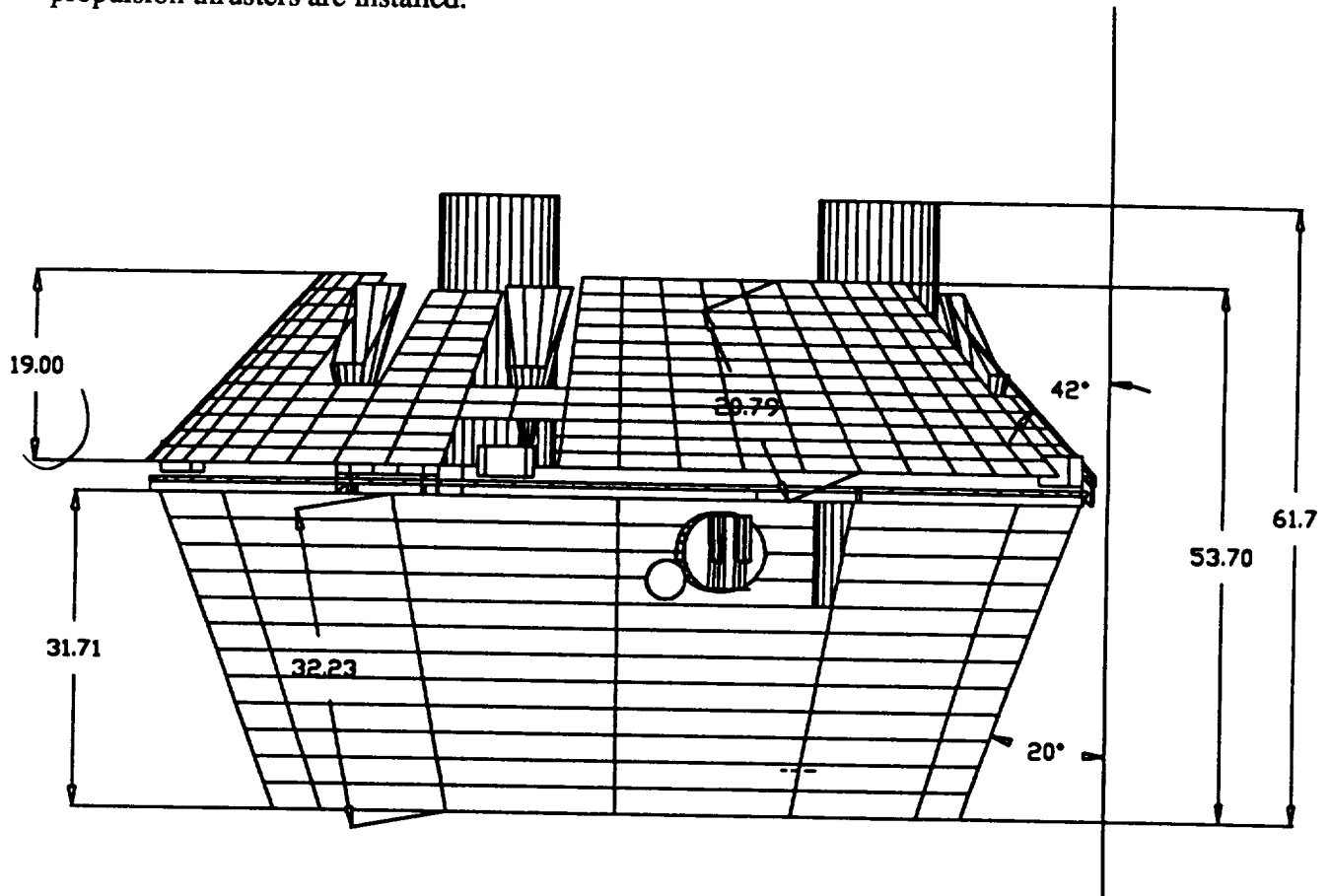


Figure 6.3-8. Deployed Module

6.3.4.2 Main Module. The Main Module is also configured such that parallel manufacturing paths exist for the submodules. There are three submodules: the nose, conical heat shield, and the carrier submodules.

6.3.4.2.1 Nose Submodule. The Nose Submodule consists of an aluminum monocoque nose. The nose structure is covered with high density ESM (50 lbs/ft³ for reentry thermal protection). The nose submodule is structurally sized based on the maximum reentry aerodynamic load of 3000 lbs/ft³. The monocoque nose is 0.050-inch thick with stiffening channels 0.25-inch thick in three places that attach to the support ring frame/longeron interface, as shown in Figure 6.3-9.

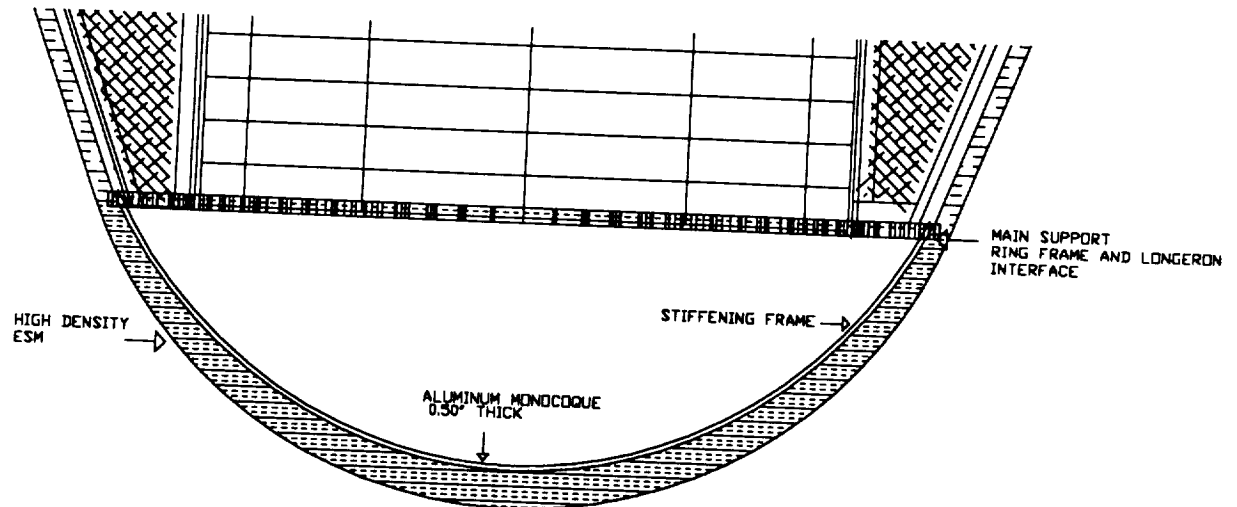


Figure 6.3-9. Nose Submodule

The nose structure weighs 13 pounds including stiffening frames.

The submodule contains one of two impact attenuation systems. For nominal missions returning to White Sands, an Impact Attenuation System is installed. This system consists of aluminum honeycomb blocks inserted with the cells parallel to the vehicle Z axis. Upon impact, the honeycomb crushes at a controlled rate, thus decelerating the vehicle from the 20 fps landing velocity to zero and delivering less than 10 g deceleration to the vehicle. The nose contains a total of 15 pounds of aluminum and phenolic honeycomb, ranging in density from 2.1 to 6.5 pounds per cubic foot. This provides deceleration from vertical, as well as side, loads caused by wind drift. The honeycomb installation is shown in Figure 6.3-10.

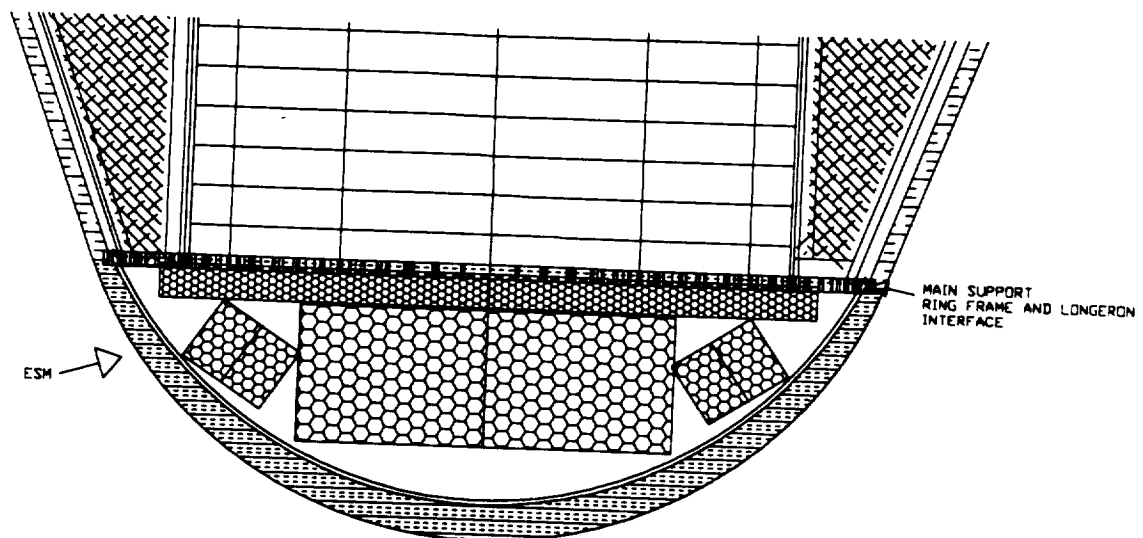


Figure 6.3-10. Impact Attenuation System Installation

The RRV is also capable of water landings. The Nose Submodule is then equipped with a flotation collar to stabilize the vehicle in the water and to cushion the landing shock. The basic configuration and operation of the inflation collar is shown in Figure 6.3-11.

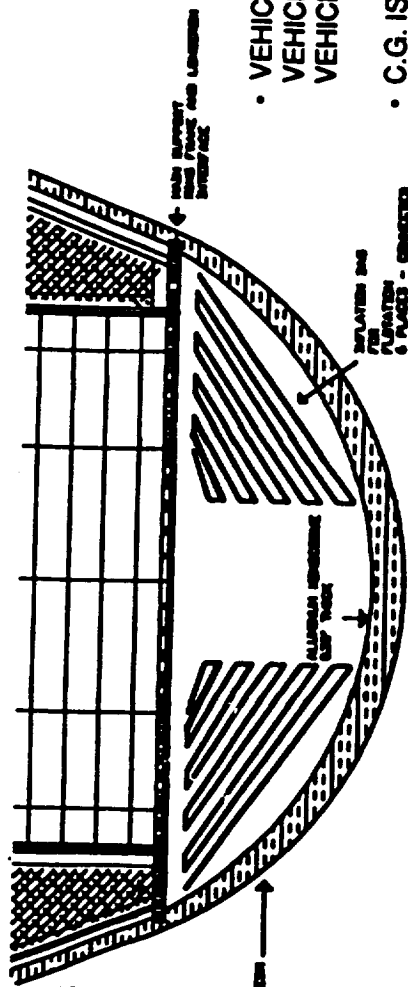
The assembly of the Nose Submodule is similar to the land version, but the mounting bolts are replaced with shear bolts that allow the submodule to fall away. This is accomplished by partial inflation of the flotation collar located in the nose cavity in place of the honeycomb. This occurs after main chute deployment. Following initial inflation, the collar rolls out of the nose cavity and continues inflating. Correct orientation of the collar is aided by the slipstream wind. Inflation gas is provided by the air tanks located on the RRV. The inflation bag contains vent panels for controlled gas release upon water impact. This cushions impact shock to an estimated 6 g. The inflated collar, along with the vehicle center of gravity in the water, is shown in Figure 6.3-12, with the 3D view shown in Figure 6.3-13.

6.3.4.2.2 Conical Heat Shield Submodule. The conical heat shield consists of an aluminum honeycomb substructure and a 1-inch low density (36 lbs/ft³) ESM coating for reentry thermal protection. The aluminum honeycomb structure is manufactured in triangular sections (gores), and the ESM is sprayed on prior to bolting or riveting together. The joints between the ESM and aluminum sections are filled with RTV adhesive. Two gore sections joined together are shown in Figure 6.3-14.

The heat shield substrate is sized by the worst case aerodynamic loads of 3000 lbs/ft³. The honeycomb structure consists of 0.25-inch cells with 0.030-inch thick face sheets. Interface with the carrier module is performed in high density areas of honeycomb as shown in Figure 6.3-15. The aluminum honeycomb substrate provides a stiff insulative support structure for the ESM heat shield material, and weighs 93.3 pounds.

Located under the ESM are coolant tubes for the MM thermal control radiator. The honeycomb dimensions are shown in Figure 6.3-16, and the three-dimensional view is shown in Figure 6.3-17.

6.3.4.2.3 Carrier Submodule. The Carrier Submodule is the primary structure for the RRV MM. This structure provides support for the payload, conical heat shield, and nose submodules, power and data handling systems for the MM, and interfaces for the Astromasts and DM. The Carrier Submodule structure consists of six longerons and shear panels, along with a series of stiffening frames and crossconnects. The longerons are 2-inch wide, 1-inch deep rectangular



- VEHICLE VOLUME COULD DISPLACE 10800 POUNDS
VEHICLE WEIGHT < 4000 POUNDS
VEHICLE WILL FLOAT
- C.G. IS 10" ABOVE CP. WHEN UPPICAT
VEHICLE WILL ORIENT ON SIDE
- INFLATED FLOTATION COLLAR WILL
ASSURE PROPER ORIENTATION
- 8.5 CuFt FOR INFLATION COLLAR IN
NOSE (REPLACE ALUMINUM)
- USE AIR TANKS FROM BAYLOAN TO INFLATE

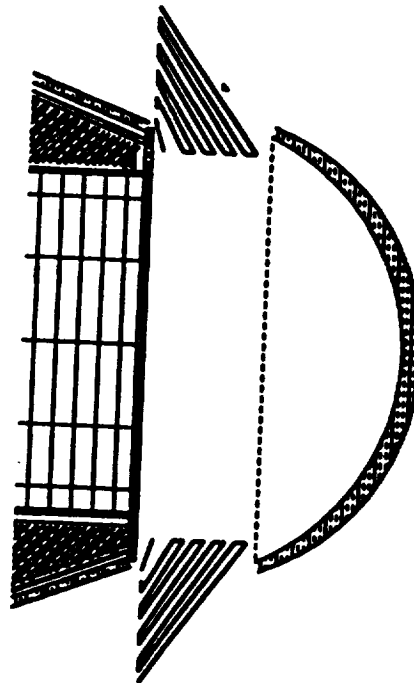


Figure 6.3-11. Water Landing Option

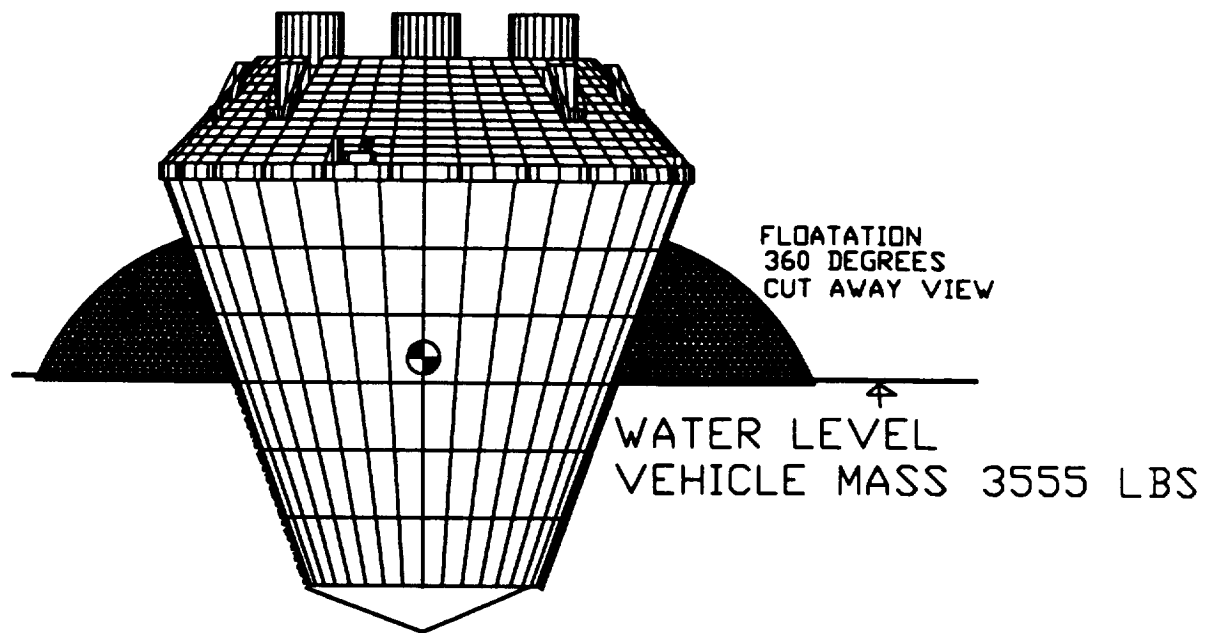


Figure 6.3-12. Water Landing Flotation Collar

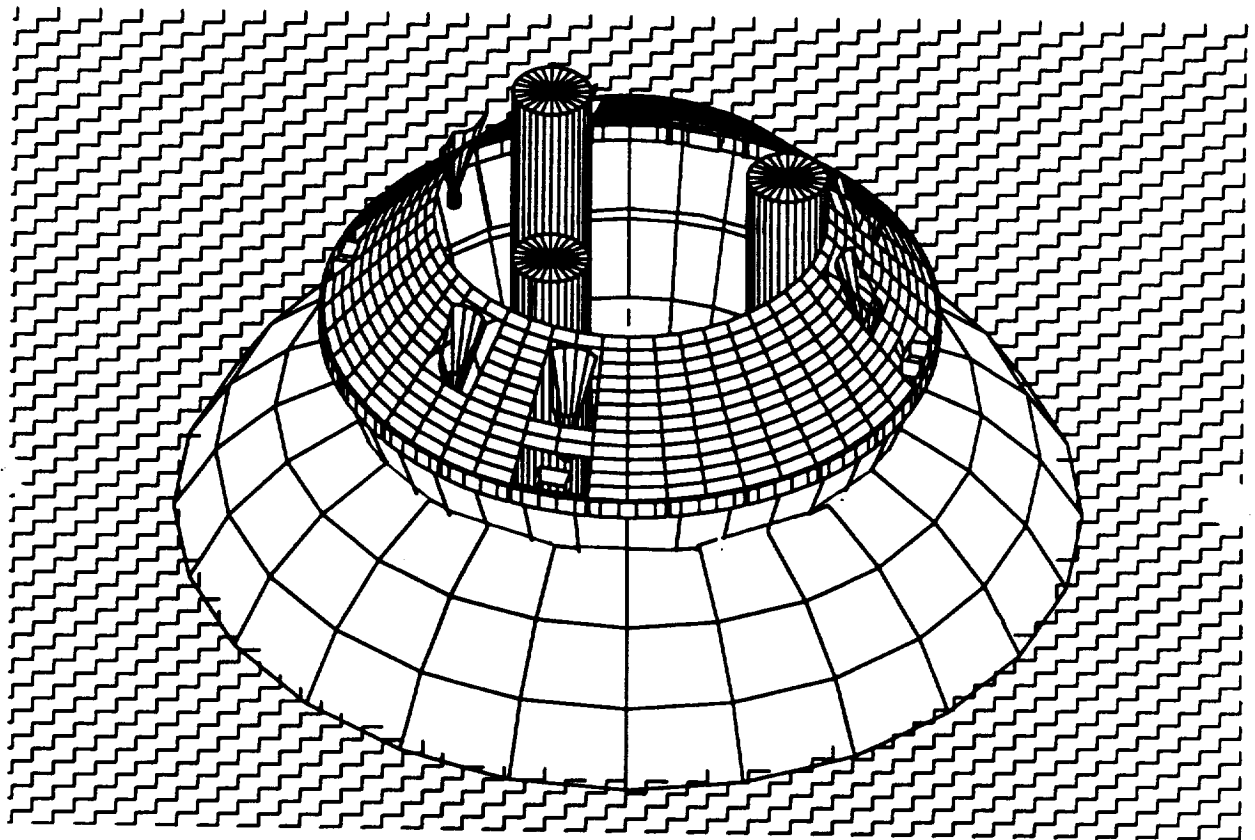


Figure 6.3-13. RRV - Water Landing Flotation Collar Inflated

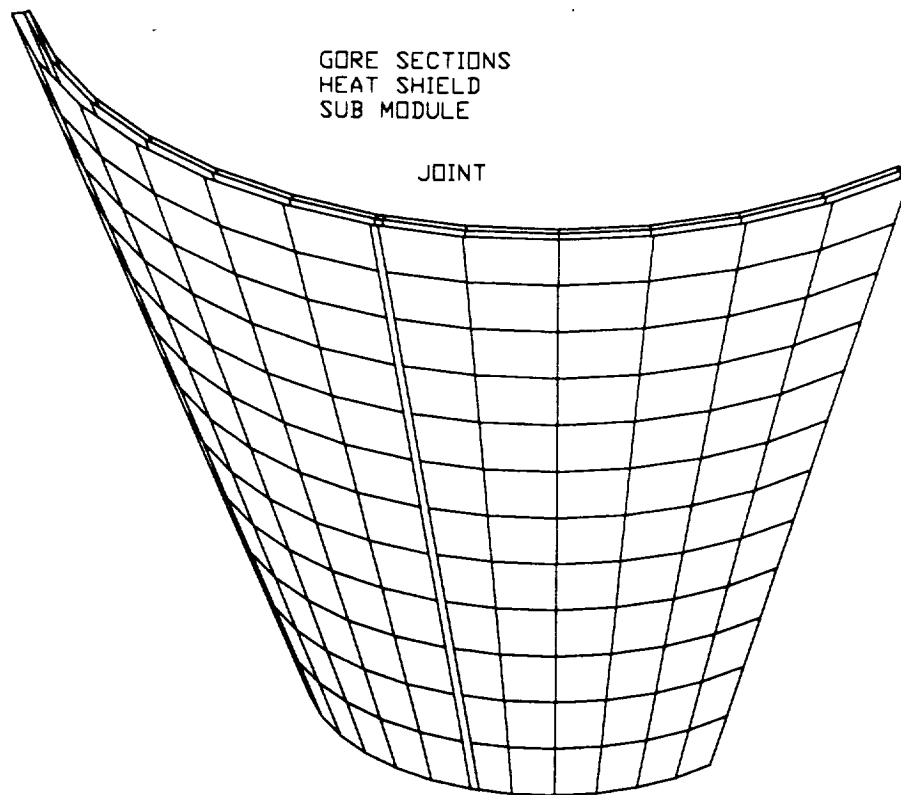


Figure 6.3-14. Gore Section Heat Shield Submodule

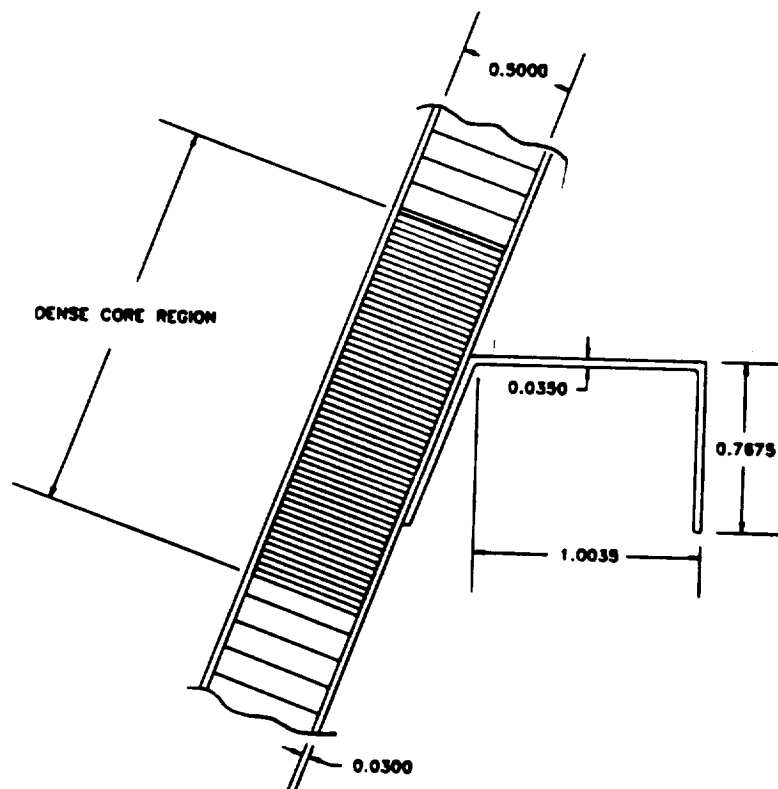


Figure 6.3-15. Typical Intermediate Frame Cross-Section

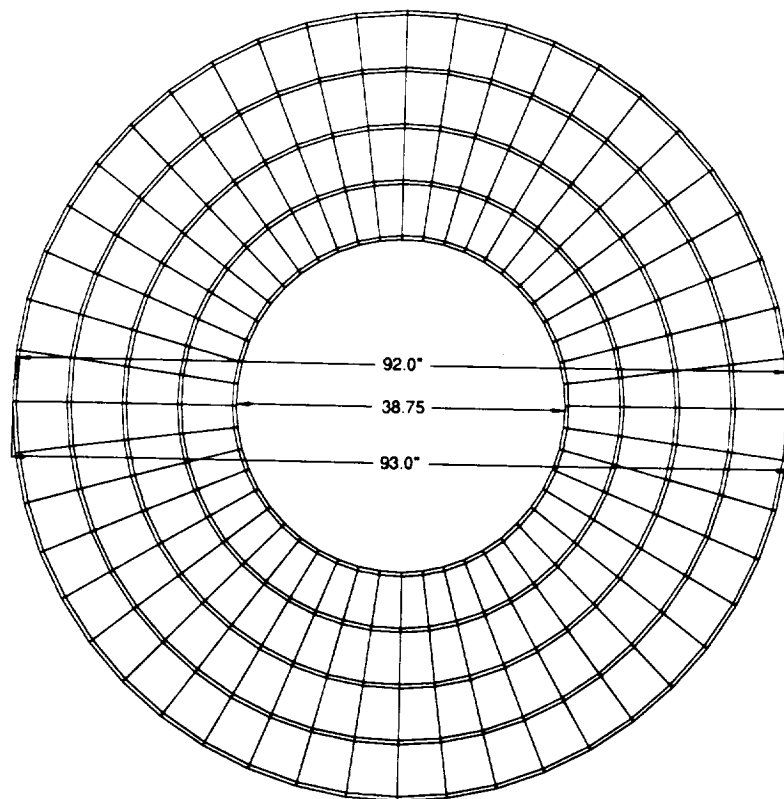


Figure 6.3-16. Honeycomb Heat Shield Substrate Dimensions

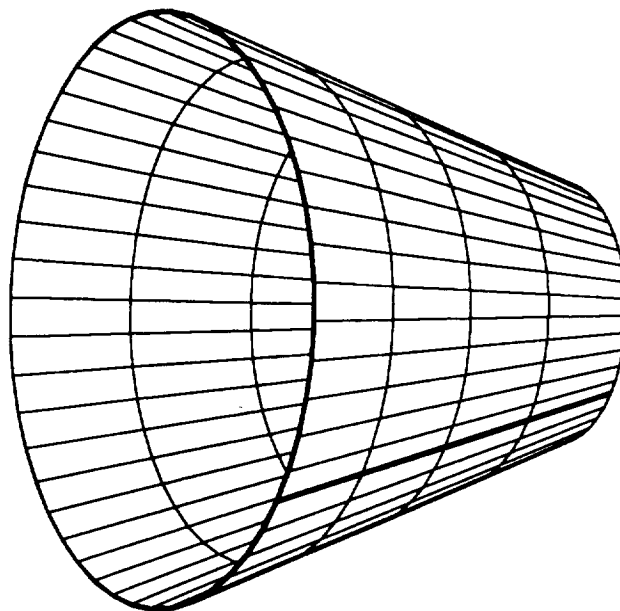


Figure 6.3-17. Substrate 3D View

sections, 0.20-inch thick. The longerons are sized for buckling loads generated by landing deceleration of 10 g. In addition, the longerons have provisions to accept the explosive bolts that hold the vehicle together during ground operations and launch loads. The longerons interface with the stiffening frames and shear panels. The longerons weigh a total of 47.9 pounds. The longerons interface on the lower half with six shear panels and end cap assemblies. Figure 6.3-18 shows the longeron and shear panels, and Figure 6.3-19 gives the shear panel dimensions.

The two smaller shear panels are the MM interface for the Astromasts. These are sized for reacting out the MM vehicle loads when spun up to 1.5 g. They are 0.020-inch thick. The larger shear panel reacts out the parachute opening loads to the Deployed Module of ~ 6 g. These panels are 0.80" thick and contain provisions along the top to accept the DM latching mechanism. The combined shear panels and cap assembly weighs 20 pounds.

The shear panel longeron assemblies are tied together by a series of stiffening frames and longeron crossconnects. The frames are nominally 0.5-inch square with 0.10-inch walls. One frame designed differently is the top frame, which is solid. The final elements in the carrier construction are the interconnect frames located at the bottom of the assembly. These serve as braces for the honeycomb shock absorption system and also tie the longeron assemblies together. The interconnect frames are 2-inch wide by 0.5-inch hollow block construction with 0.1-inch thick walls. The assembled carrier module structure is shown in Figure 6.3-20 with the dimensions from top and side views shown in Figures 6.3-21 and 6.3-22 respectively.

6.3.4.3 Main Module Integration. Figure 6.3-23 shows the carrier structure fit-checked with the conical Heat Shield Submodule. This is done prior to installation of the ESM material on the heat shield, and prior to installation of the electronics and harness on the carrier module.

Figures 6.3-24 and 6.3-25 show installation of the electronic components and ECLSS tankage respectively. Two sets of 16 cell nickel/hydrogen batteries are located around the outside diameter of the Payload Module support area. They are mounted to two sets of support rings. Power control electronics, Astromast cables (alternate retraction system) reel and motor, Payload data handling, and the MM IMU are located on brackets attached to either side of the shear panels.

The final components installed after tank integration are the ECLSS controls and forward cover. The cover is shown installed in Figure 6.3-26, along with the conical heat shield assembly. The cover serves as a mounting plate for the air and oxygen valves and regulators, and also stiffens the shear web assemblies for torsional loads. The cover also works to seal the vehicle from water

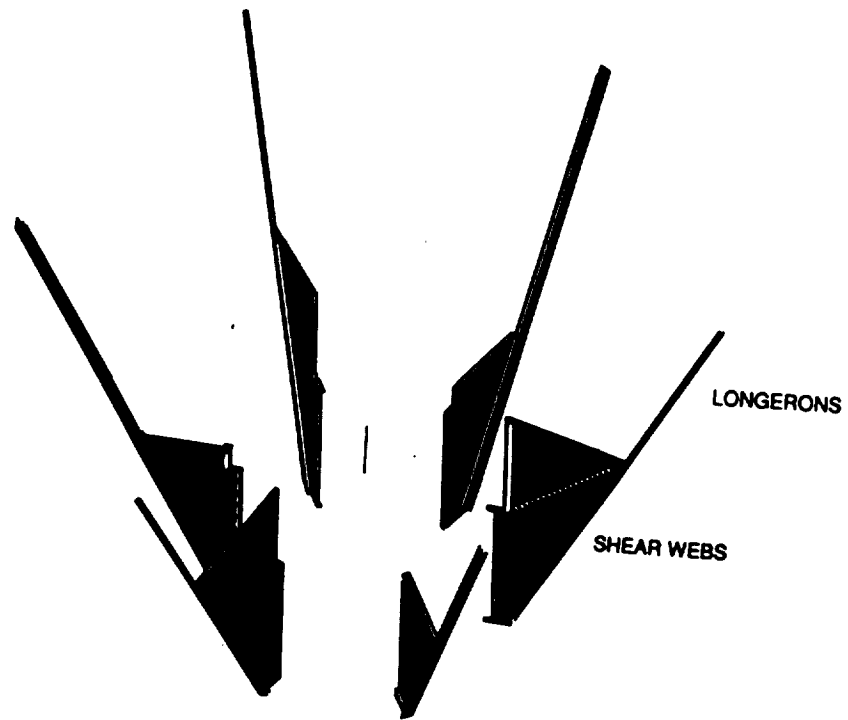


Figure 6.3-18. Main Module Basic Structure

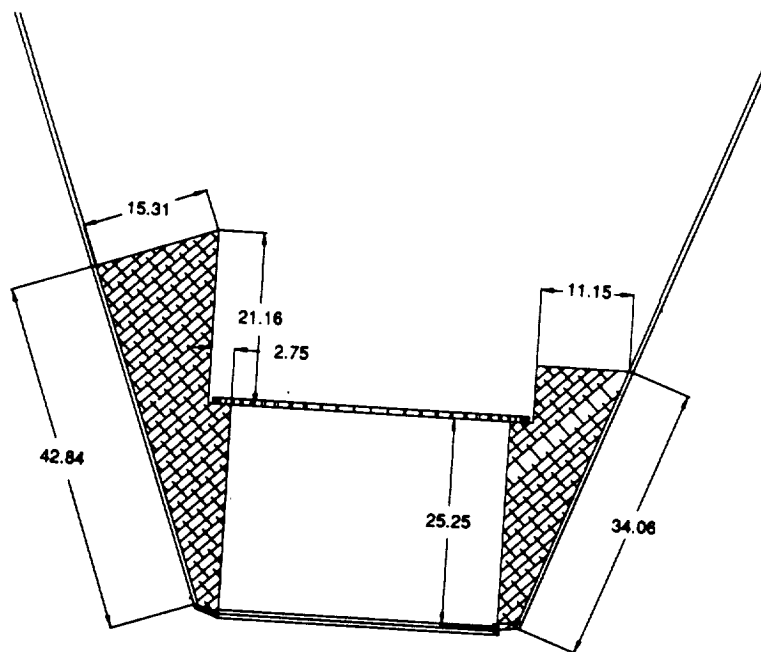


Figure 6.3-19. Shear Panel Dimensions

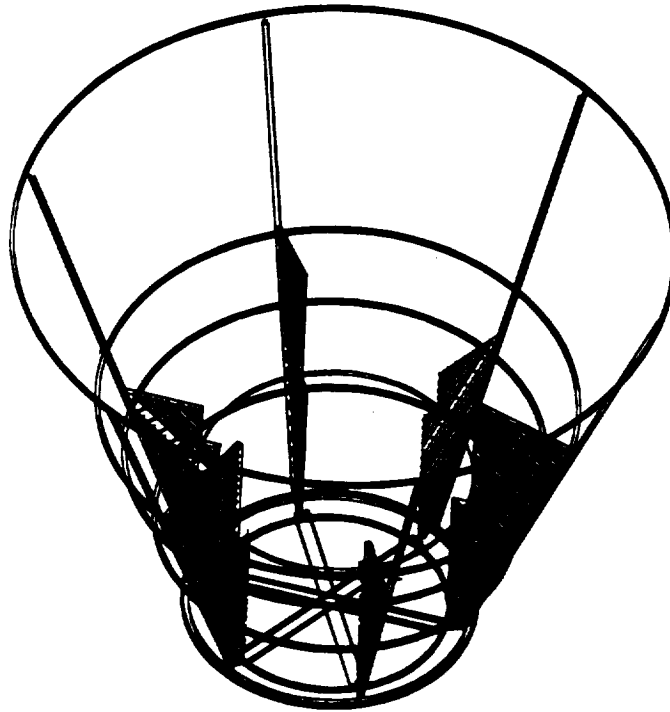


Figure 6.3-20. Carrier Module Structure

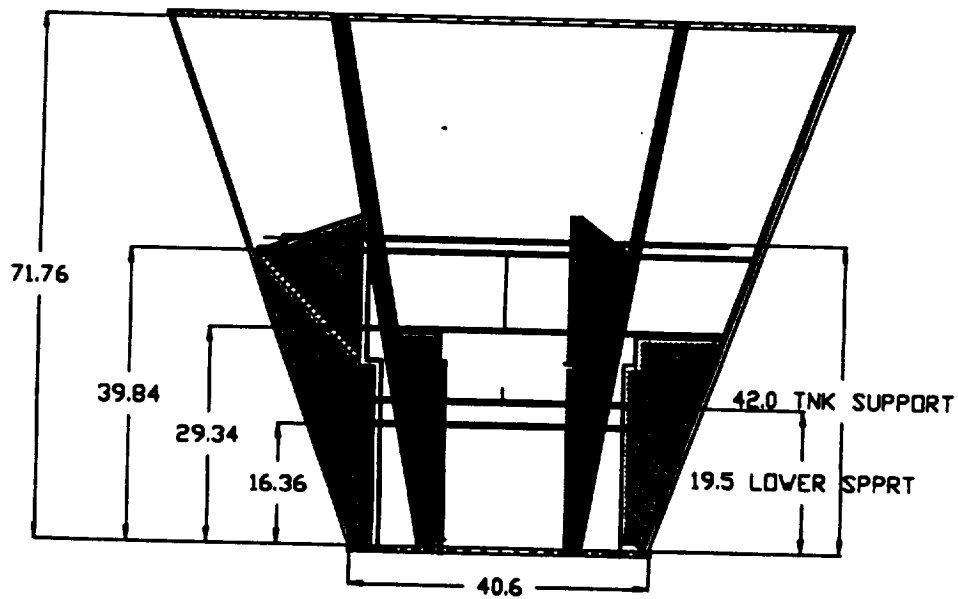


Figure 6.3-21. Main Module Side View

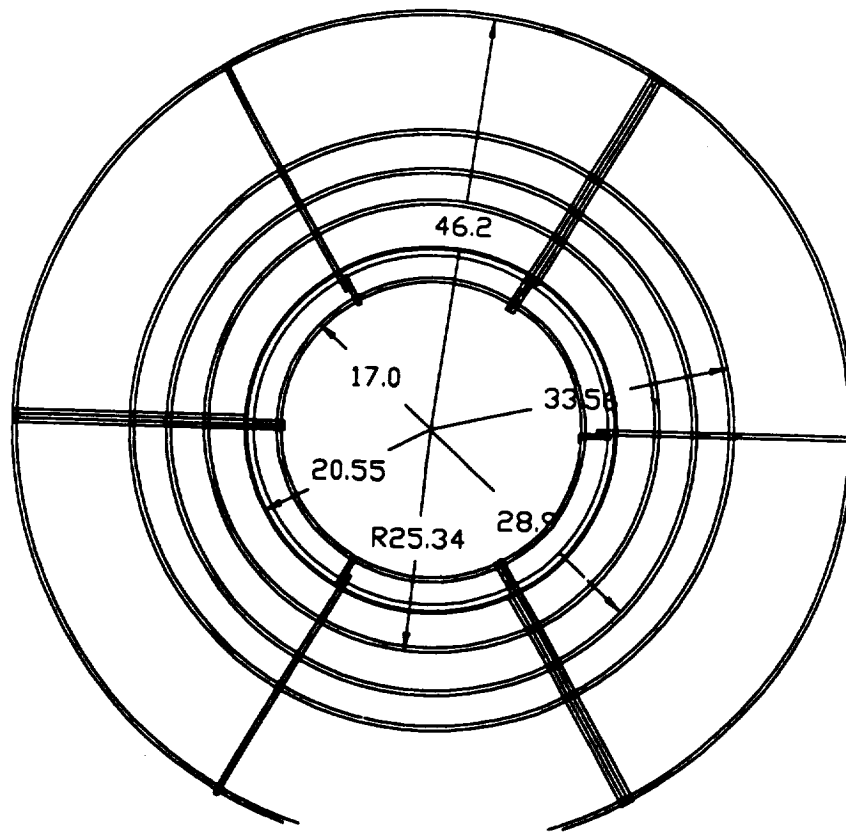


Figure 6.3-22. Main Module Top View

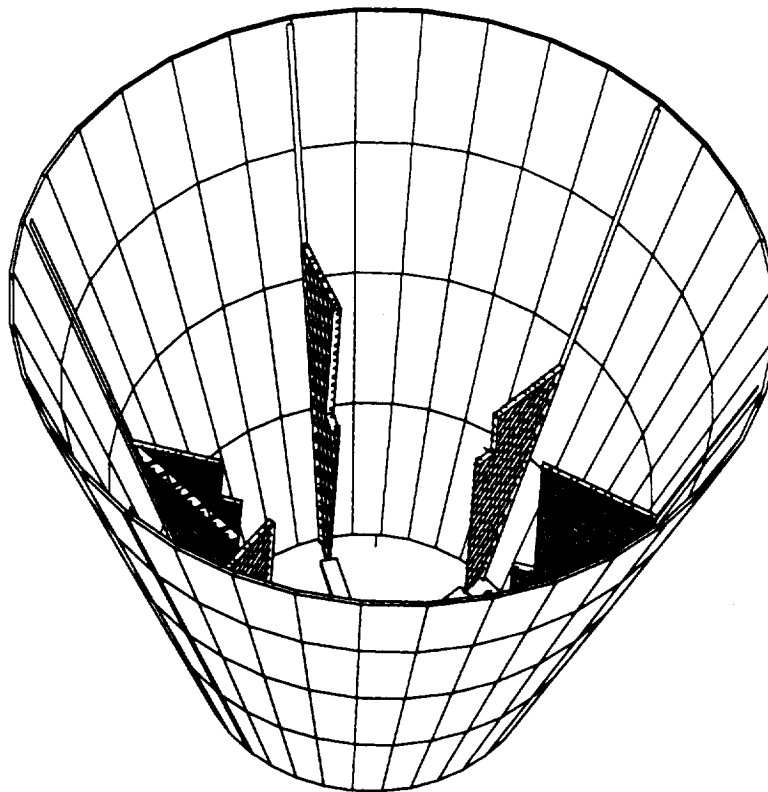


Figure 6.3-23. Carrier Structure With Heat Shield

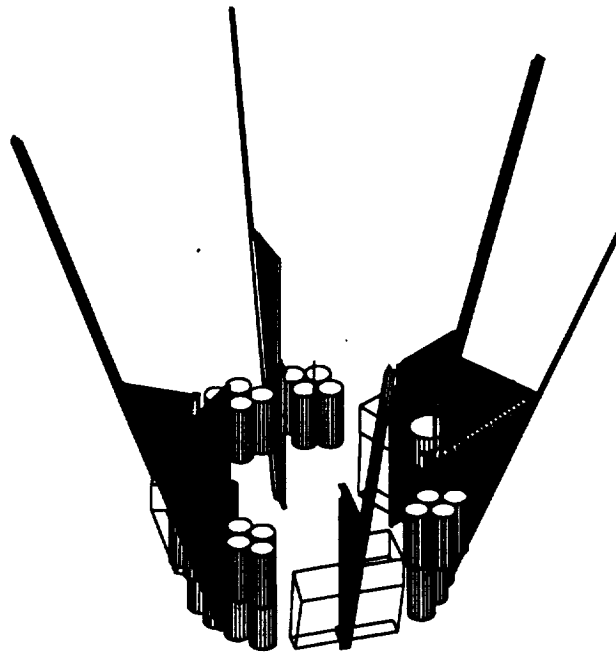


Figure 6.3-24. Electronics and ECLSS Tank Installation

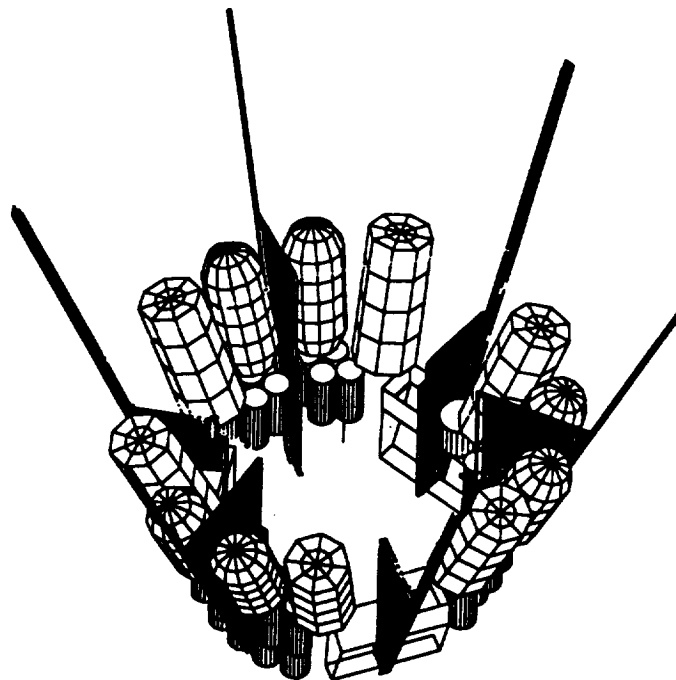


Figure 6.3-25. Main Module With ECLSS Tanks Installed (Support Rings and Frames Removed for Clarity)

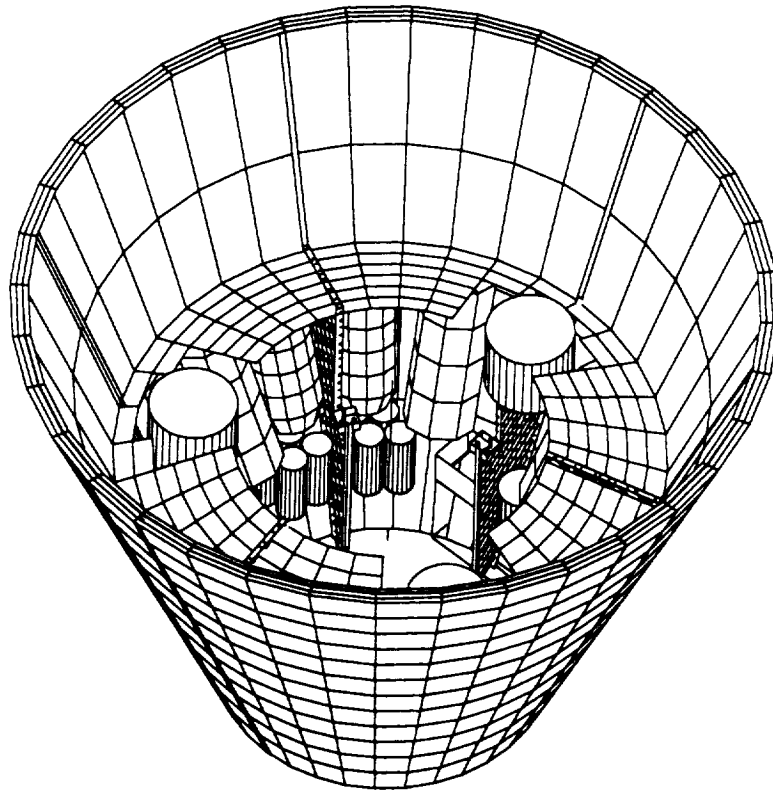


Figure 6.3-26. Main Module With Cover Installed

or other abusive environment factors after landing. The cover is a honeycomb structure 0.5-inch thick with 0.25-inch cells. It contains three raised sections, 10.25 inches in diameter and 4 inches tall, that fit into holes in the Deployed Module. The holes provide for the Astromasts to connect from the DM to the MM.

Final Integration of the MM consists of installation of the completed heat shield assemblies onto the carrier structure.

6.3.4.4 Astromasts. The Astromasts are incorporated into the SAIC RRV design to provide a large spin radius for the payload during artificial gravity missions. The Astromast characteristics are listed in Table 6.3-3.

Table 6.3-3. Astromast Characteristics

• TYPE:	CONTINUOUS LONGERON COILABLE LATTICE STRUCTURE
• MATERIAL:	LONGERON AND BATTEN — FIBERGLASS
• DIAMETER:	10 INCHES
• DEPLOYMENT MECHANISM:	INTERNAL NUT CANISTER — FULL DEPLOYED OUTSIDE CANISTER
• DEPLOYMENT RATE:	0.3 TO 8.0 INCHES/SEC
• STRUCTURAL:	
- Bending Stiffness	7.1×10^6 lb-in ²
- Torsional Stiffness	9.3×10^4 lb-in ² /RAD
- Shear Stiffness	7.4×10^3 lb
- Bending Moment	63 ft-lb
- Tension	2280 lb (760 lb per longeron)
- Compression	290.1 lb (96.7 lb per longeron)
• LENGTH STOWED:	48"
• LENGTH DEPLOYED:	1200"

The masts provide a maximum extension of 1200 inches. Astromasts have been used on a variety of space programs. However, they have never been used for separating and retracting two large masses.

The large spin radius is an integral part of the SAIC design. Incorporation of the Astromasts in this manner has been perceived as the high risk element of the RRV. Therefore, the following analyses have been performed to clarify issues associated with implementing the masts in the RRV design.

- Determine feasibility of concept
- Determine maximum propulsive loading for spin up.
- Determine relative displacement of the masts when spin up force is applied.
- Design of masts to eliminate all single point failures that prevent successful retraction.

Items a-c were performed early in the study with the results summarized in Table 6.3-4.

Table 6.3-4. Astromast Loads Summary

- DEPLOYED ASTROMAST CONFIGURATION CAN BE SAFELY SPUNUP/DESPUN
- COMPRESSION LOADING
 - 37 lb/lb of Spinup Thrust
 - 96.7 lb Allowable
- BENDING LOADING
 - 256 in-lb/lb of Spinup Thrust
 - 760 in-lb Allowable
- SPINUP THRUSTER SIZES UP TO 1.35 LB MAINTAIN A FACTOR OF 2 MARGIN OF SAFETY
 - Negligible Side Loading on Experiment from Spinup (<0.1 g)

The analyses were performed independently by Astro Aerospace and SAIC to verify the results. The results are shown in Figures 6.3-27 and 6.3-28.

The analyses showed that, with a 1 lbf square wave pulse, the relative deformation would be less than 10 inches. In addition, the structure would have a fundamental frequency of 0.4 Hz, and would damp out in approximately 1 hour. These analyses were made with the assumption that one end (the MM) of the vehicle is fixed. This does not represent a flight configuration. However, it is conservative.

Dynamic analyses were performed on the given deployed RRV in order to predict on-orbit maneuvering loads in the Astromasts. A finite element model was constructed assuming two point masses for the main and deployed modules connected by flexible elements that represent the Astromasts. The three Astromasts were modeled individually and tied to the modules fixed in all six degrees of freedom. Each mast was modeled with 12 interstitial nodes. The model mass properties, stiffness properties, and geometry are given in Table 6.3-3.

The finite element analyses included a normal modes run with and without the geometric stiffness effect of the 1.5 g centrifugal force due to the spin maneuver, startup/impulse static loads cases both cantilever from the main module (worst case) and free-free using inertial relief methods, control thruster sine, and transient analyses.

The normal modes analysis shows that the first mode is torsional at 0.087 Hz, with the first bending mode at 0.77 Hz and the first axial mode at 3.54 Hz with densely populated higher order bending modes. The effect of geometric stiffening increased the torsion mode by 49.4% to 0.13 Hz and the first bending mode by 20.8% to 0.93 Hz.

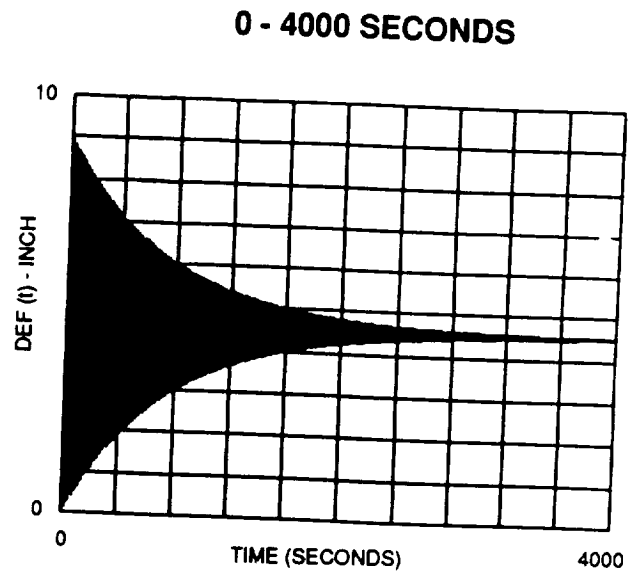
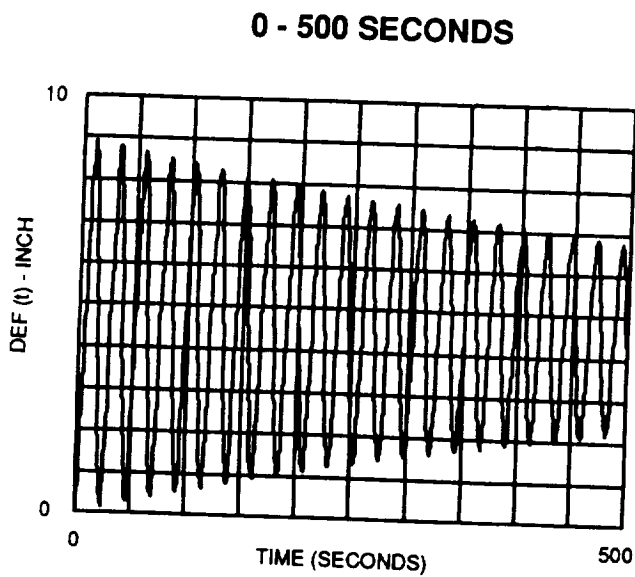


Figure 6.3-27. Relative Structural Deformation Results

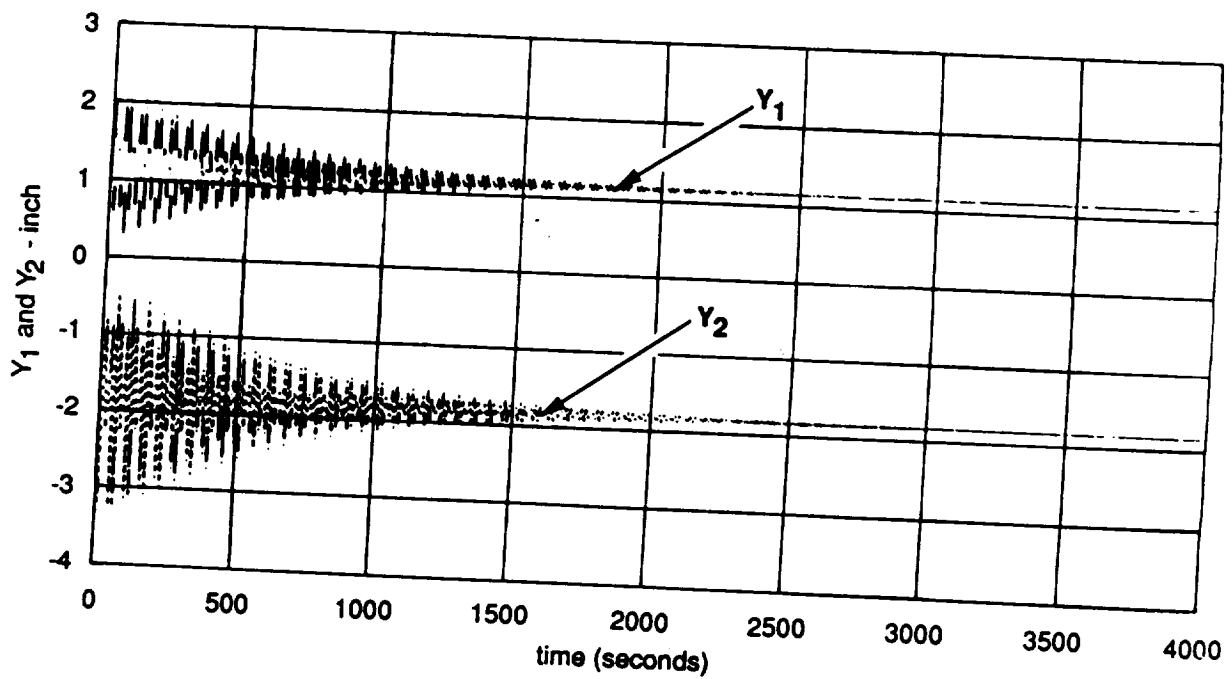


Figure 6.3-28. Structural Deformation Results

Static analyses were run in order to calculate the Astromast loads due to the thruster firings for both the spinup and rotisserie conditions. A maximum dynamic magnification factor of 2 is included in all loads to account for initial overshoot. The spinup and rotisserie maneuvers were analyzed for various combinations of thruster configurations with both cantilevered and inertial relief methods. The cantilevered analysis is overly conservative and implies that all thruster force is transmitted into strain energy. The cantilevered results show positive margin (relative to given loads capabilities) for spinup with two 0.5-pound thrusters and rotisserie with two or four 0.5-pound thrusters or a spin rotisserie combination with two 0.5-pound thrusters. The maximum relative deflection is 15 inches and the maximum relative twist angle is 14 degrees.

The inertial relief analysis is the actual loading environment where the thruster force is transmitted to accelerating the structure as well as strain energy. Results show high margins for all cases analyzed. The maximum relative deflection and thrust angle are 0.15 inches and eight degrees respectively. These results indicate that growth exists for the spinup thrusters from 0.5 to 5 pounds, but due to large twist angles the rotisserie thrusters should remain at 0.5 pound.

A sine analysis was performed to analyze the effect of a single 0.5-pound tangential control thruster. The sine analysis was run applying a 0.5-pound peak sine force from 0.05 to 40 Hz using a given damping value of 0.2% critical damping. The results show high loads (negative margins) at the fundamental vehicle torsional mode (0.087 - 0.13 Hz). However, above this frequency range the loads drop considerably and the minimum margin is greater than 6.3 for a firing frequency above 8 Hz.

A transient control thruster analysis was run assuming one thruster with a 0.5-pound tangential peak force. An ideal square wave shape was assumed with an 8 Hz frequency. The critical damping used was 0.2% and the duration of the analysis was 10 seconds which is nearly twice the half cycle (time of peak loads) of the lowest mode. All loads and relative displacements were small.

Another transient analysis simulating the spinup maneuver was performed assuming two 5-pound tangential spinup thrusters. The impulse was applied at $t=1$ second. The pulse duration was 610 seconds and the total analysis duration was 630 seconds, again 0.2% critical damping was assumed. All loads and relative displacements were small. The axial load due to centrifugal force must be added to the mast internal loading. The spinup time is estimated to be 560 seconds to achieve 1.5 g.

Equally important as the determination of the Astromast's feasibility was looking at design changes to the standard masts that would eliminate any single point failure in the retraction system. In addition, the SAIC concept requires power and data transmission between the two vehicle halves. These two requirements provided answers to each other. The RRV mast configuration changes are depicted in Table 6.3-5.

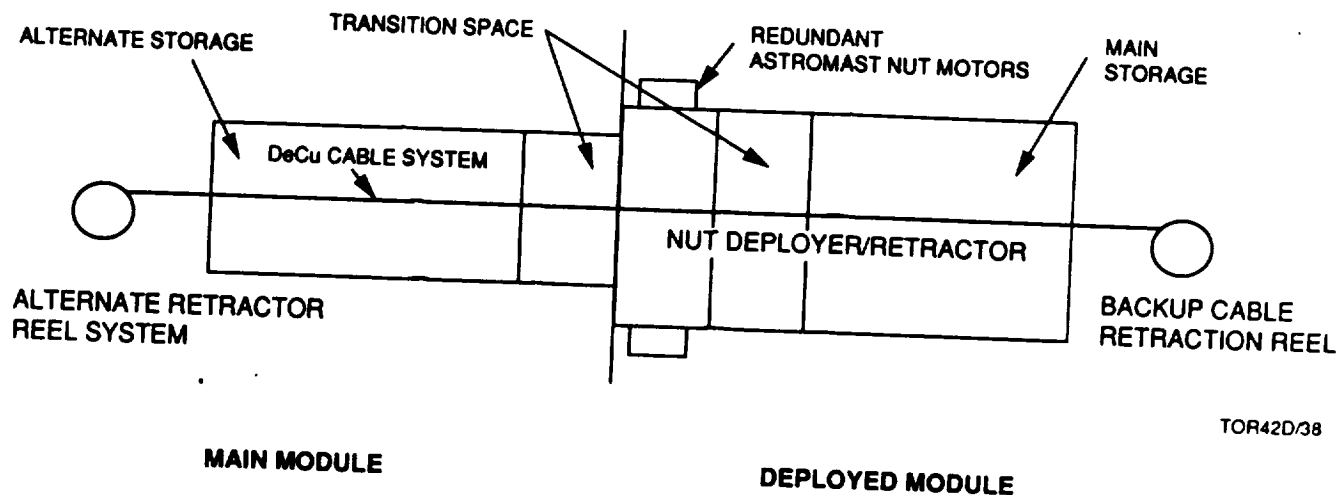
Table 6.3-5. Astromast Design

<p>BASIC</p> <ul style="list-style-type: none"> • NUT DEPLOYED ASTROMAST 10" DIAMETER • DUAL BRUSHLESS DC MOTOR DRIVES NUT <p>CHANGES/ADDITIONS</p> <ul style="list-style-type: none"> • CABLE RETRACTION MECHANISM IN MAIN MODULE • CABLE SYSTEM IN DEPLOYED MODULE • DUAL BEARING ASSEMBLIES ON NUT AND CANISTER • DUAL STRUNG NUTS ON MAST • CARBON FIBER HOUSING • MOTOR SYNCHRONIZING SYSTEM (6 MOTORS)
--

The basic Astromast design used by the RRV is the nut deployed 10-inch mast. This design has the masts rigid upon extension from the nut. This allows for any length masts to be deployed, thus giving the experimenter increased flexibility. The current design incorporates dual brushless DC motors to drive the extension/retraction nut. To ensure that a nut or canister failure would not affect the mission, dual bearing assemblies on these two critical items are specified. The major change to the existing nut deployer is the incorporation of a lanyard system in the Main Module, as shown in Figure 6.3-29.

The lanyard system provides two functions. First, the BeCu cable is used for 3-phase 20 kHz power transmission between the two modules. In addition, in the event of a nut deployer failure to retract a mast, the cable reel is capable of acting as a cable mast retractor, retracting the masts into the cavity between the MM shear web and the top of the mast canister in the Deployed Module.

6.3.4.5 RRV Integration. RRV integration joins the MM and DM with the Astromasts and then with the explosive bolt connectors. This gives the vehicle the configuration shown in Figures 6.3-1 and 6.3-2. For prelaunch activities and integration of the Payload Module, the Aft Solar Array and main propulsion thrusters thrust chambers would be removed for easy access and to prevent damage. These would be reinstalled just prior to launch after installation of the Payload Module.



TOR42D/38

Figure 6.3-29. Astromast Schematic

6.3.4.6 Rodent or Payload Module Interface. The Rodent Module interfaces are defined by the structure of the Rodent Module and the requirements of the science experimenters. Figure 6.3-30 is an exploded view of the Rodent Module (RM) canister and the main module longeron and shear webs.

In terms of structural integration, the RM consists of three basic pieces. The pressure vessel, or payload module in Figure 6.3-30, the top cover, and the payload support brackets. The pressure vessel is a cylindrical sectioned device. The lower portion contains the payload ECLSS and data handling subsystems for the RM. The upper half contains the experimental subjects and, on the external surface, has connections for power, data, water, oxygen, air and thermal control fluid. The top of the vessel has a dual O-ring inside the bolt pattern to ensure positive sealing. The pressure vessel integrates into the MM structure via six teflon V-guides that correspond to six V-guide protrusions from the side of the pressure vessel wall. These protrusions are located on the lower segment of the pressure vessel. The payload support bracket location is shown in Figures 6.3-31 and 6.3-32 from top and side views respectively. The top view shows the location of the alignment holes. The Payload Module has a matching set of studs to fit the holes.

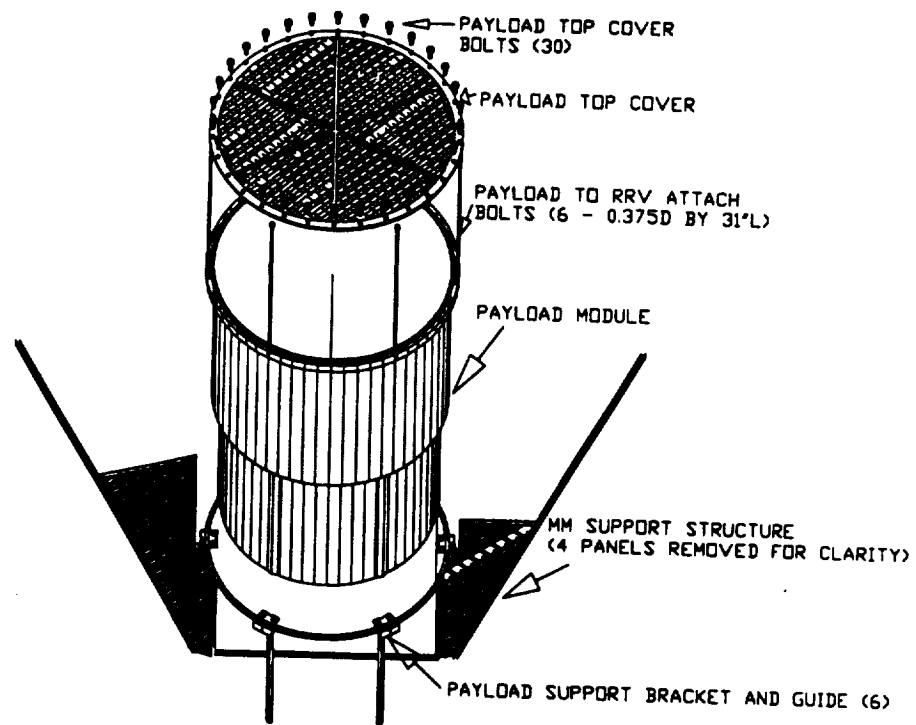


Figure 6.3-30. RM Installation - Exploded View

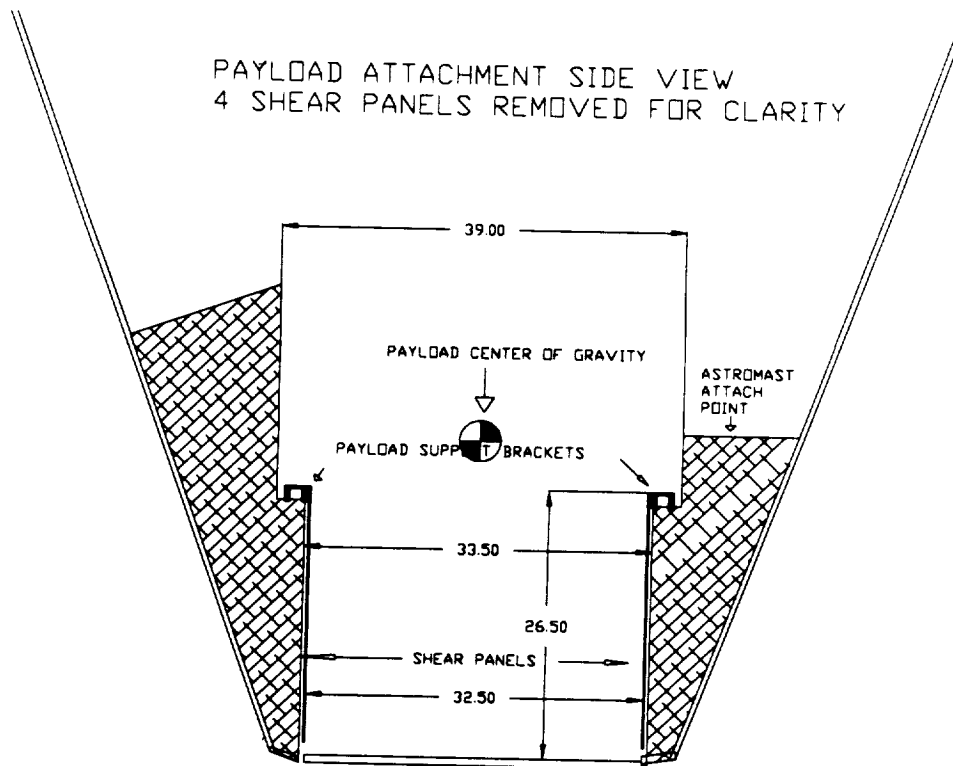


Figure 6.3-31. Payload Attachment

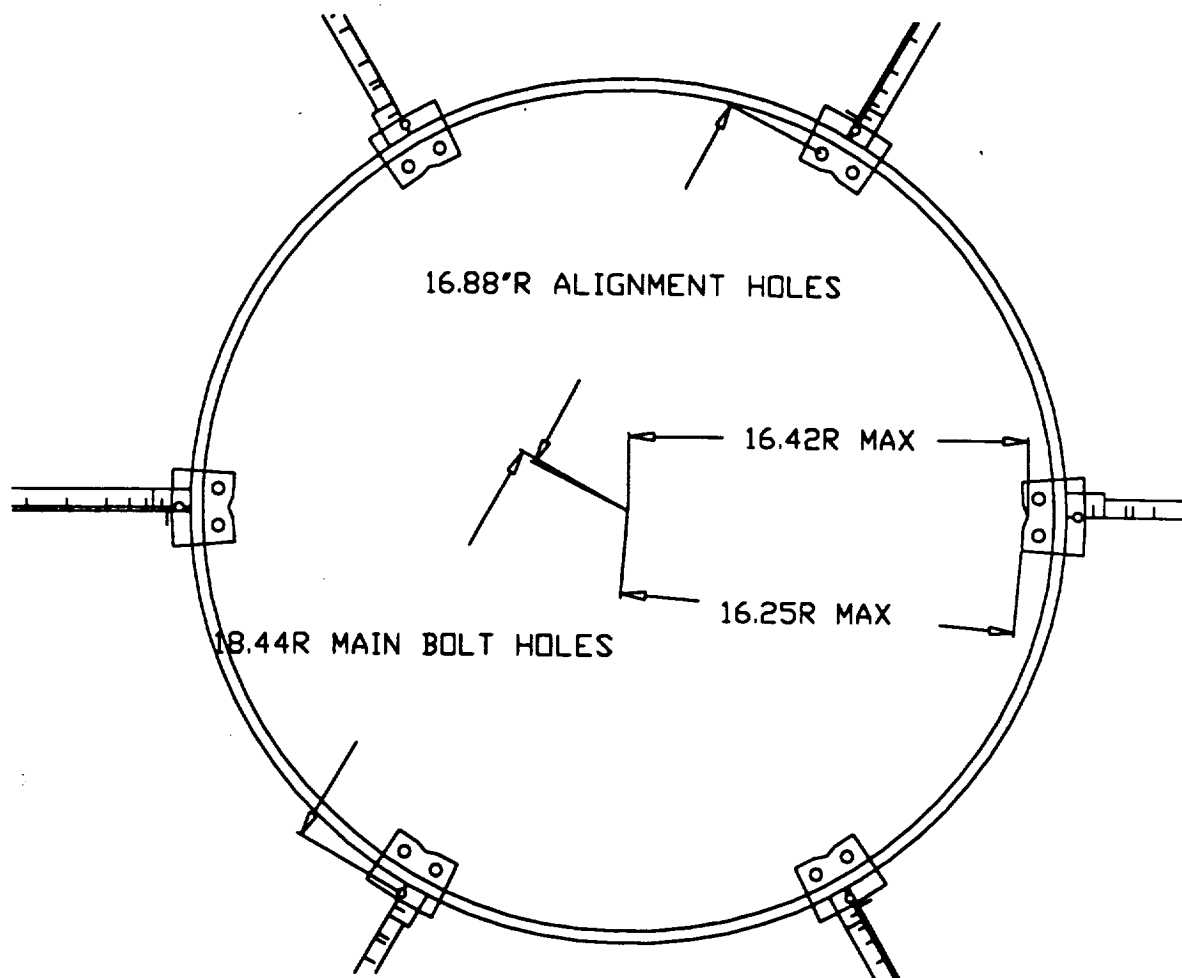


Figure 6.3-32. Payload ICD Mechanical Top View

The Payload attach fittings are shown in Figure 6.3-33.

The fittings incorporate a "floating" construction, where the payload interfaces on one side and the vehicle on the other of an elastomer compound. The elastomer compound provides shock and vibration isolation to the payload. The bolts that secure the Payload Module attach from the top flange of the module, as shown in Figure 6.3-30, to the support fittings. After installation of the Payload Module, the top hat can be installed. An alternate design, instead of using the 30 bolts, is to use a single marmon clamp installation. This would lower the time required to get into the payload, but at the cost of sealing effectiveness. The final installation operations are the connection of the fluid and power connections as shown in Figures 6.3-34, 6.3-35 and 6.3-36.

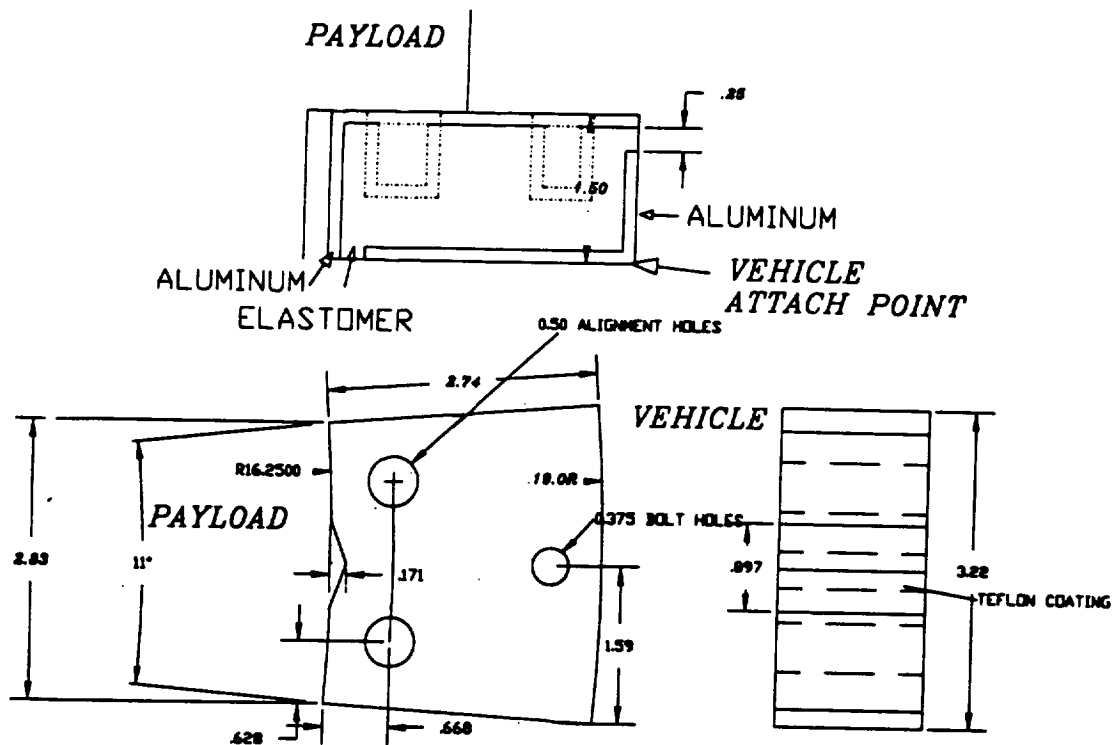


Figure 6.3-33. Lower Payload Support Bracket

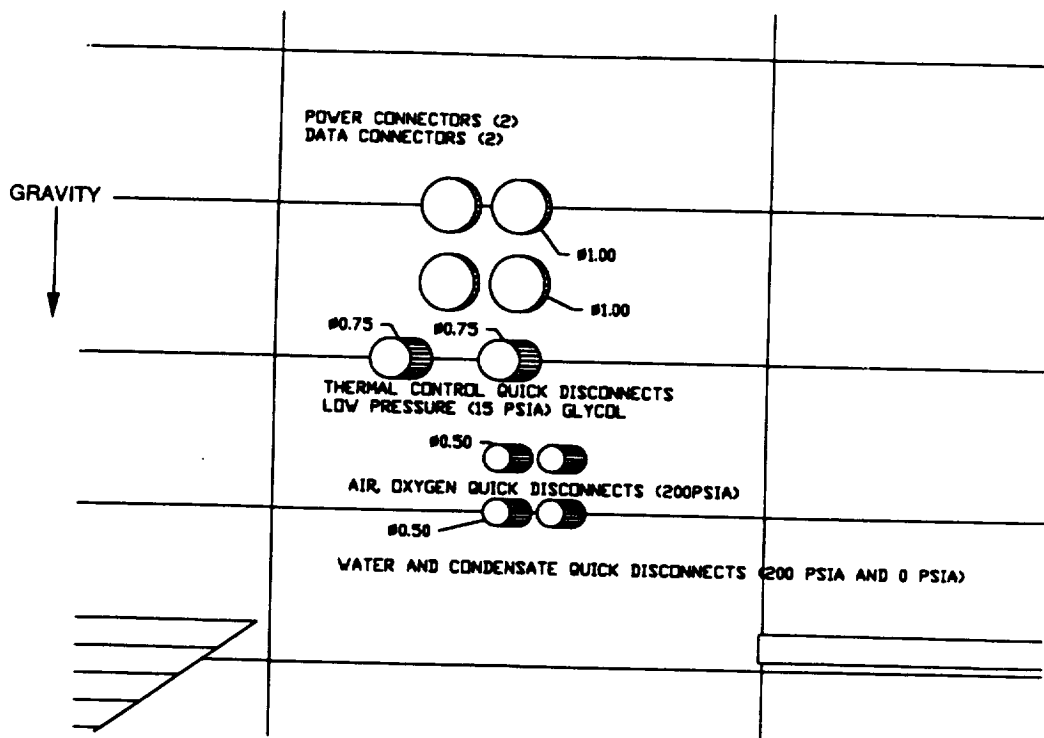


Figure 6.3-34. Detailed Fluid and Power Connections

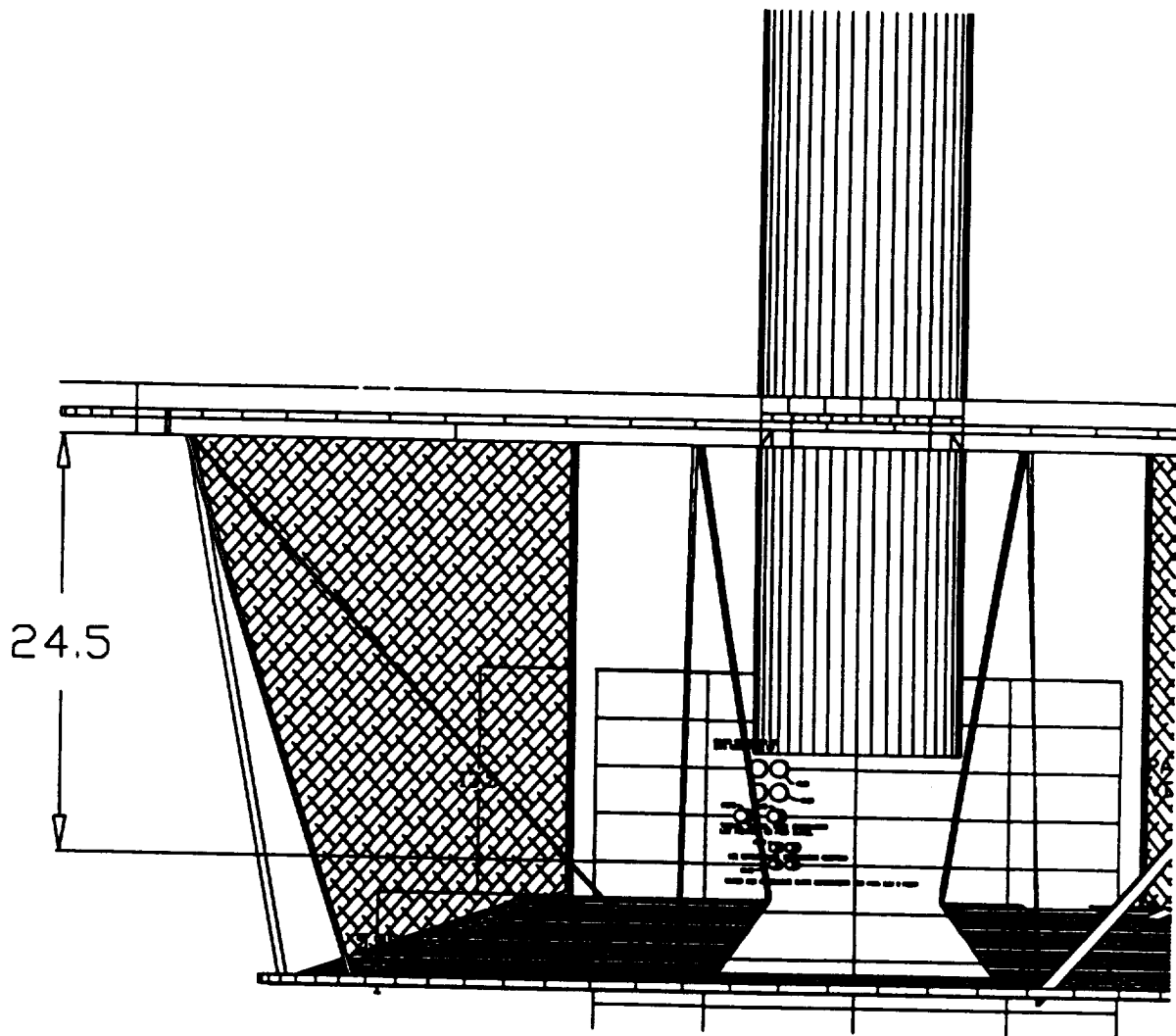


Figure 6.3-35. Fluid and Power Connection Location

Liquid fluid connections are MOOG quick disconnects. These offer multiple seals to prevent leakage, and have the lowest spillage of any disconnect available. The power and data plugs use standard pin type connectors. The gas connections are dual soft seal flanged type.

6.3.4.7 Launch Vehicle Interface. The launch vehicle interface was designed to work within the overall RRS concept. This entailed being able to access the payload at T-4 hours before launch, and launching with the nose down such that the floor of the experiment was the same for all major phases of the mission.

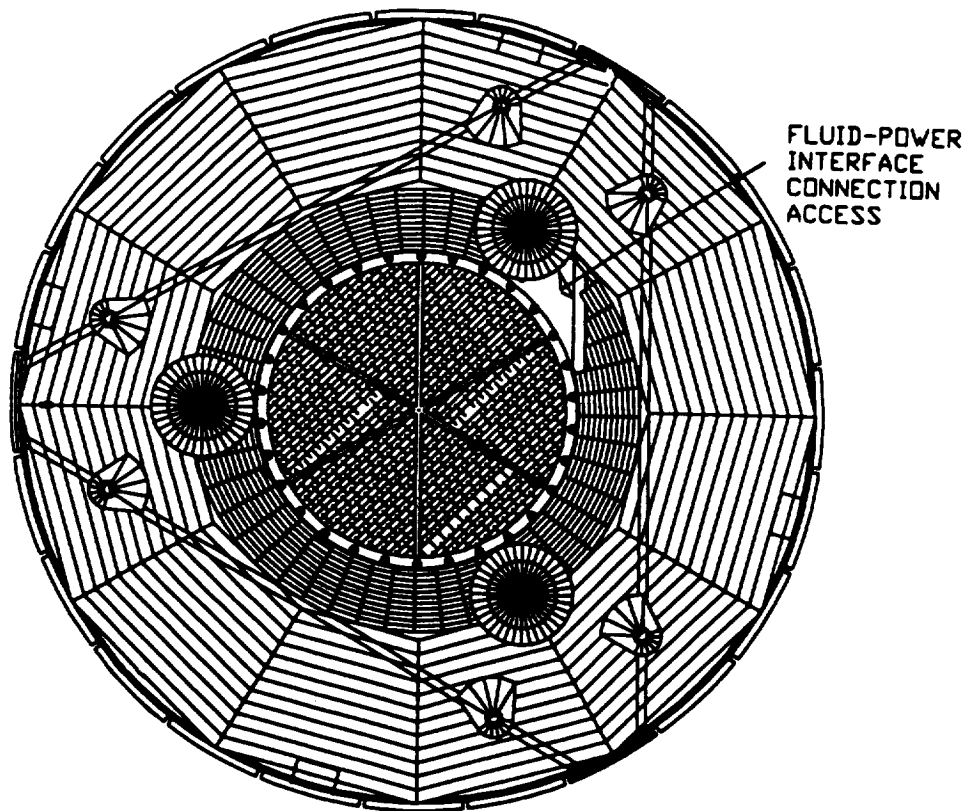


Figure 6.3-36. Fluid and Power Connection Access Top View

Two concepts were reviewed for integrating with the Delta launch vehicle. The first was incorporating the Arianespace Spelda. The spelda is a carbon filament wound tube and aluminum structure that supports two payloads. The spelda has provisions for mounting two vehicles on standard interface rings. The upper spelda would be used to "hang" an RRV from this position. The lower spelda platform would not be used. This concept uses flight proven hardware, but would not fit, with sufficient rattle space, in the Delta 10 foot fairing. This concept is an option for the Atlas vehicle, however, which has up to a 14-foot fairing diameter. For launch of two RRVs, two speldas would be mated together so that each RRV would hang from the upper satellite support fitting.

The integration concept chosen for the Delta incorporates a second interstage structure. The present Delta interstage is an aluminum monocoque structure 15.5 feet long and 95.4 inches in diameter. It weighs 1035 pounds, including the separation system. The interstage separates the Delta first and second stages during flight. The integration concept entails using an 11 foot section of the interstage attached to the second stage at the bottom, and to the RRV spacecraft attach fitting at the top. This is depicted in Figure 6.3-37.

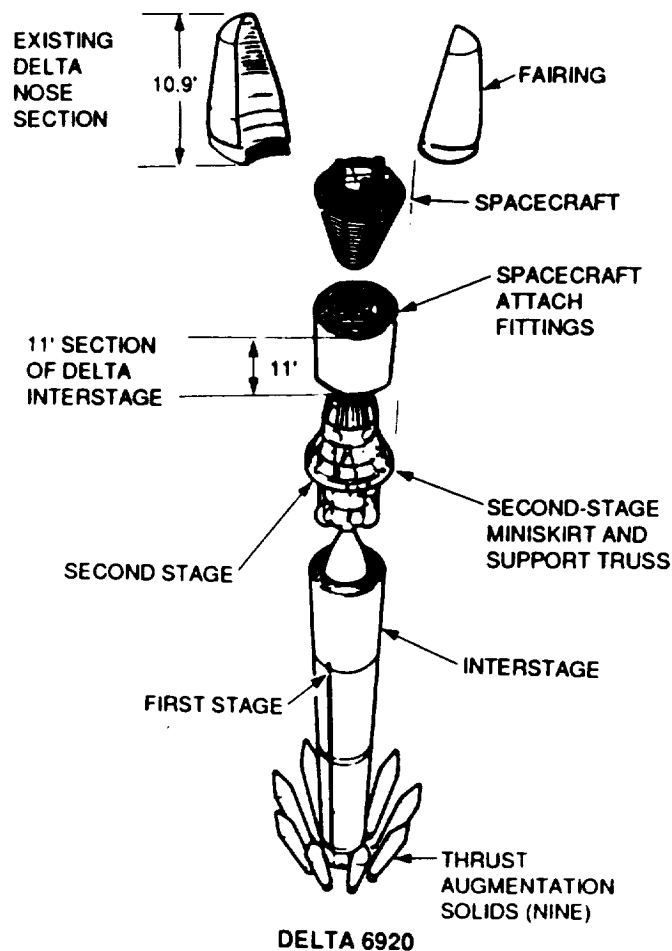


Figure 6.3-37. Launch Vehicle Installation Single Spacecraft

Figure 6.3-38 shows the spacecraft attach fitting, along with the primary interfaces with the RRV. The interface structure is an aluminum stiffening ring at the bottom, with three tube truss members that extend to the vehicle interface, and an interface ring. The stack-up of the pieces is shown in cross section in Figure 6.3-38

The nose fairing is a standard 9.5-foot Delta fairing with the cylindrical sections removed. The fairing interfaces into the new interstage section in the same manner as the standard Delta. This concept has the Launch Vehicle Adaptor (LVA) fitting as the only new piece. The vehicle position in the Delta allows for easy access to the Payload Module with the Delta nose removed. Details of the vehicle, LVA, interstage, and fairing interface are shown in Figure 6.3-39.

The RRV sits on three point connections as shown in Figure 6.3-40 and 6.3-41.

Figure 6.3-40 provides detail of the RRV's interface area. The launch vehicle attach ring is made up of carbon phenolic sections. These sections are integrated into the main support beams described earlier. The 0.375-inch lip provides approximately 13 square inches of surface. This, coupled with the carbon phenolic compressive strength of 5000 psi, supports the RRV during

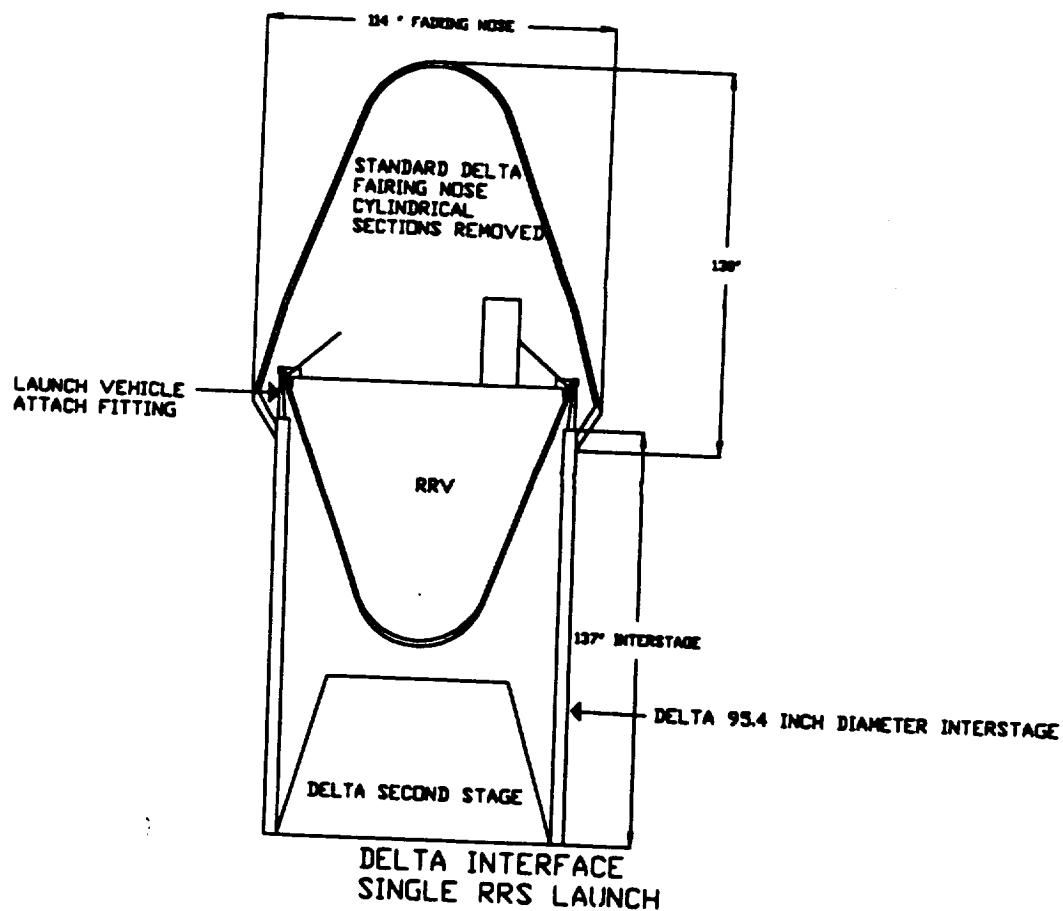


Figure 6.3-38. Delta Interface Single RRS Launch

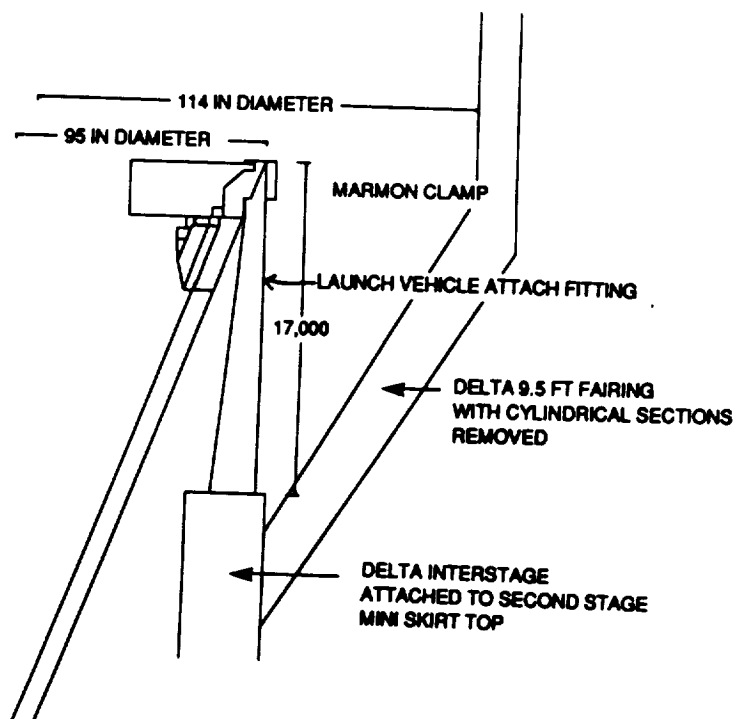


Figure 6.3-39. Delta Launch Vehicle Mechanical Interface Single RRS Launch

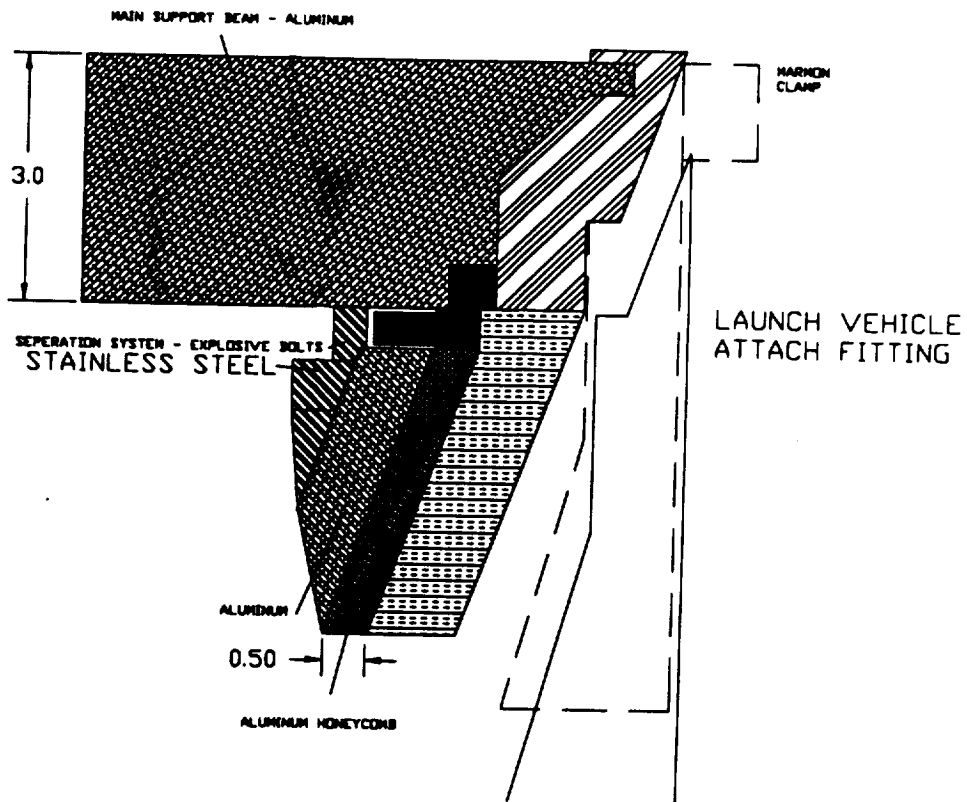


Figure 6.3-40. Launch Vehicle Interface (RVV)

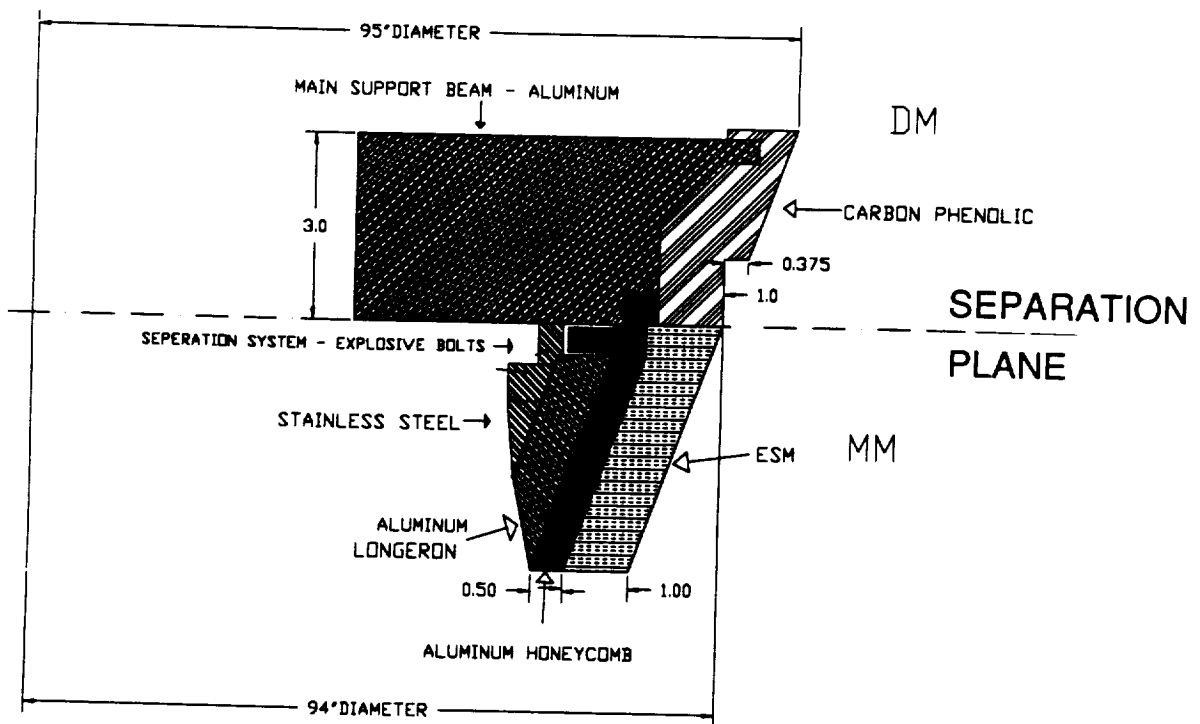


Figure 6.3-41. Detail View RRV Launch Vehicle Interface Area

launch with greater than 2:1 safety factor. This view also shows the explosive bolt location for separation of the MM and DM after launch vehicle separation. Launch vehicle separation is performed by releasing a marmon clamp that holds the three interface areas against the RRV. After release, a gas bag is inflated in the base of the Delta second stage, as shown in Figure 6.3-42, to gently push the RRV away from the Delta.

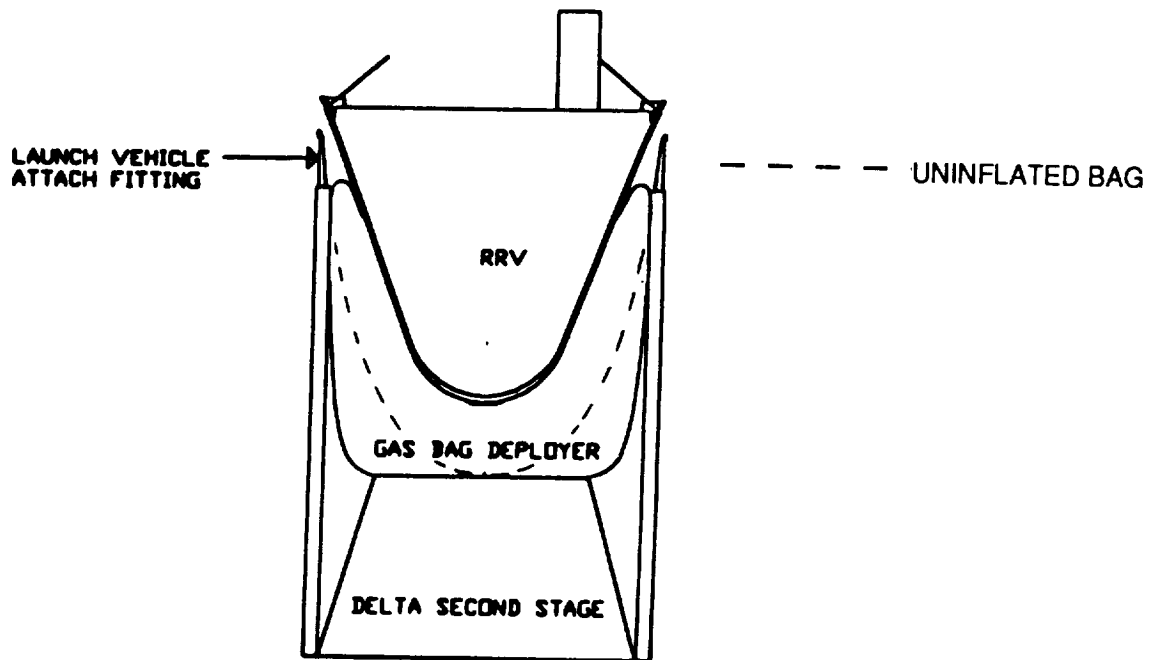


Figure 6.3-42. RRV Deployment From Delta Launch Vehicle

This deployment process is also conceptually useful as part of an Emergency Recovery Process (ERP). The ERP, conceived as a means of de-weighting the less than 0.99 probability of booster flight success sufficiently to achieve the required (SRD) 0.99 probability of safe specimen recovery, would be initiated by the thrust termination signal. The signal would initiate both the RRS/LVA separation process (Marmon clamp release, deployment bag inflation) and the RRV ERP. Although the gas bag force would be insufficient to eject the RRS from the LVA, the inflated bag would provide a cushion around the vehicle that would assist freeing the RRS following the destruct signal initiated segmenting of the LVA (and nose cone fairing if not previously released). The GNC would then, following a short delay for debris separation, use IMU data to initiate recovery by appropriately deploying the drogue chute.

The Launch Vehicle Adaptor design is also capable of handling a dual launch as shown in Figure 6.3-43.

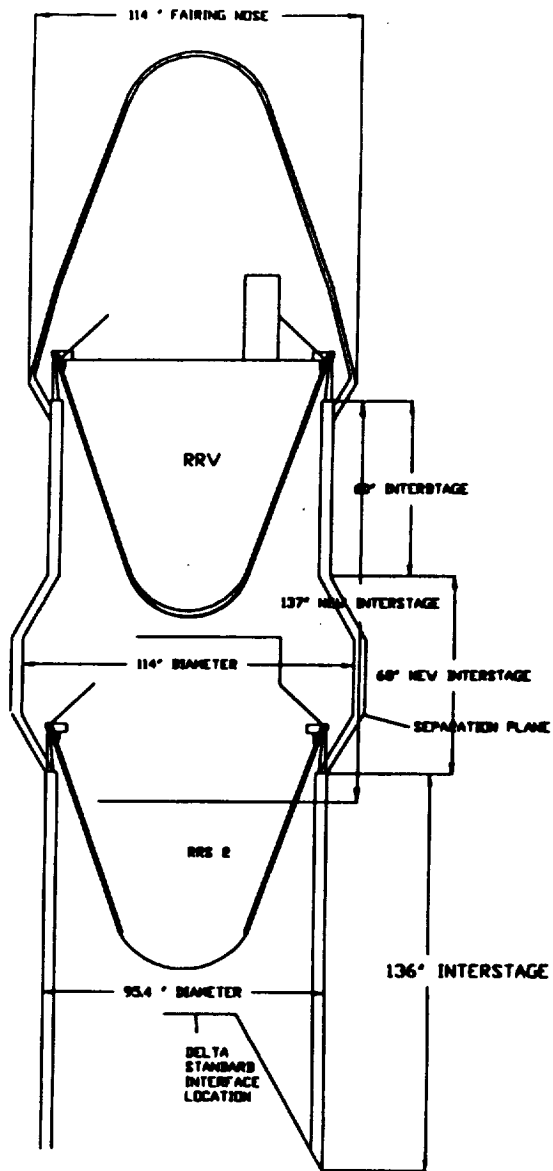


Figure 6.3-43. Dual-Launch System

The dual launch requires development of a 65-inch new long interstage section. This section flares out to 114 inches in diameter and then flares back to the standard interstage 95.4-inch diameter. The new interstage can be built using existing Delta fairing tooling. The new interstage design uses the same diameter and angled sections as the 9.5 foot fairing. The rest of the launched concept is the same as the single RRV launch.

6.3.4.8 Vehicle Mass Properties

- The integrated vehicle mass properties are given in Table 6.3-6. The margins shown are determined on a unit level and are passed on to the total vehicle. This table also calculates the empty center of gravity for determination of reentry stability. The presently designed RRV, with the RM, has greater than 10% stability through $M=2.5$, at which time the supersonic drogue chute deploys.
- Table 6.3-7 depicts the extended vehicle mass properties. The mass assumes approximately 40 pounds of propellant have been consumed in orbit trim and orientation maneuvers.
- The combination of these two tables was used to determine the vehicle mass properties and to compute the propulsion consumption. These tables were also used in calculating a range of CG and payload mass the RRV design could support. The present design has the CG of the payload below the center of pressure of the vehicle. Thus, heavier payloads, up to 1730 pounds (gives a 5000-pound RRV) help the CG balance for reentry. Lighter payloads, however, than the standard RM ballast will be required to achieve the necessary stability margin for reentry. For example, a 600-pound payload with a CG 60 inches from the nose would require 175 pounds of ballast. This hypothetical payload would achieve a 48.8-foot spin radius as seen at the payload CG.

Table 6.3-6. Mass Properties Launch Configuration

TOTALS (LBS AND INCHES)					MASS MARGIN CALCULATION		
Component	Mass	X	Y	Z	MASS VALUE	PERCENT MARGIN	LBS MARGIN
MAIN SUPPORT STRUCTURE	417.1	0.0	0.0	52.0	417	24	102.1
ASTROMAST	152.7	0.0	0.0	91.6	153	4	5.7
PAYLOAD	971.6	0.0	0.0	43.7	972	10	99.3
POWER SYSTEM EXTENDED	240.0	-28.0	-15.0	59.7	240	8	19.7
POWER SYSTEM MAIN	212.0	0.0	0.0	21.3	212	9	19.7
PROPULSION SYSTEM	157.3	0.0	0.0	82.6	157	12	18.2
PROPELLANT	400.0	0.0	0.0	77.0	400	0	0.0
THERMAL EXTENDED MODULE	10.0	0.0	0.0	84.0	10	20	2.0
THERMAL MAIN MODULE	50.4	2.0	3.0	34.4	50	24	12.1
TERMINAL RECOVERY SYSTEM	193	0.0	0.0	89.0	193	6	12.5
REENTRY THERMAL PROT.	421.0	0.0	0.0	47.8	421	5	21.1
TT&C	45.6	28.0	22.0	60.1	46	3	1.3
GN&C	204.0	22.0	7.0	67.4	204	9	19.3
COMPUTER	20.0	25.0	35.0	58.0	20	20	4.0
HARNESS	85.0	0.0	0.0	55.0	85	20	17.0
BALLAST	35.0	1.0	0.0	40.0			
MARGIN	353.9	0.0	0.0	55.6			
	0.0	0.0	0.0	0.0			

C.G. COORDINATES		
X	Y	Z
-0.1	-0.1	56.5
EMPTY		54.1

MOMENTS OF INERTIA		
Ix	Iy	Iz
1310902	1310902	2152672

C.P./C.G. MARGIN CALCULATION	
VEHICLE LENGTH	87.6
C.P. @ M=3 FACTOR	0.74
C.P. @ M=3	64.8
C.P.-C.G. > 10% VEHICLE LENGTH	
C.P.-C.G.	10.67717
10% Vz	8.76
YES	

TOTAL		353.9
-------	--	-------

Table 6.3-7. Extended Vehicle Mass Properties

Component	Mass
MAIN SUPPORT STRUCTURE	268.6
MAIN SUPPORT STRUCTURE	148.5
ASTROMAST	65.0
PAYLOAD	971.6
POWER EXTENDED	240.0
POWER MAIN	212.0
PROPULSION SYSTEM	157.3
PROPELLANT	379.0
THERMAL EXTENDED	10.0
THERMAL MAIN	50.4
TERMINAL RECOVERY	193.0
REENTRY THERMAL	421.0
TT&C	45.6
GN&C	204.0
COMPUTER	20.0
HARNESS MAIN	42.5
HARNESS EXTENDED	42.5
BALLAST	35.0
ASTROMAST	85.0
MARGIN	177.0
MARGIN	177.0

**TOTAL
MASS
3945**

C.G VEHICLE EXTENDED
X Y Z
-0.08 -0.08 579.3

PAYLOAD OBSERVED SPIN RADIUS
43.3

MOMENTS OF INERTIA
Ix Iy Iz
1.438E+09 1.439E+09 2.153E+06

SHADED VALUES ARE VARIABLE

6.3.4.9 Vehicle Scaling

The payload design study contemplated alternate payload module sizes for fewer total rodent days. This smaller payload capacity was then applied to the vehicle design as well. The rationale for a smaller vehicle would be to achieve a lighter launched mass and possibly ride on a less expensive vehicle (Taurus). The problems with downsizing, however, are that the same vehicle functions must be supported regardless of vehicle size. Specifically, the GNC system must perform with the same level of accuracy as in the baseline design to allow for a Conus White Sands recovery. The vehicle's power production capability was based on a zero gravity DRM-1 mission. Four smaller versions of the RRV were examined. The first design was capable of holding a 32-inch diameter Payload Module. This module contains 15 rodents. This vehicle is depicted in cross section in Figure 6.3-44.

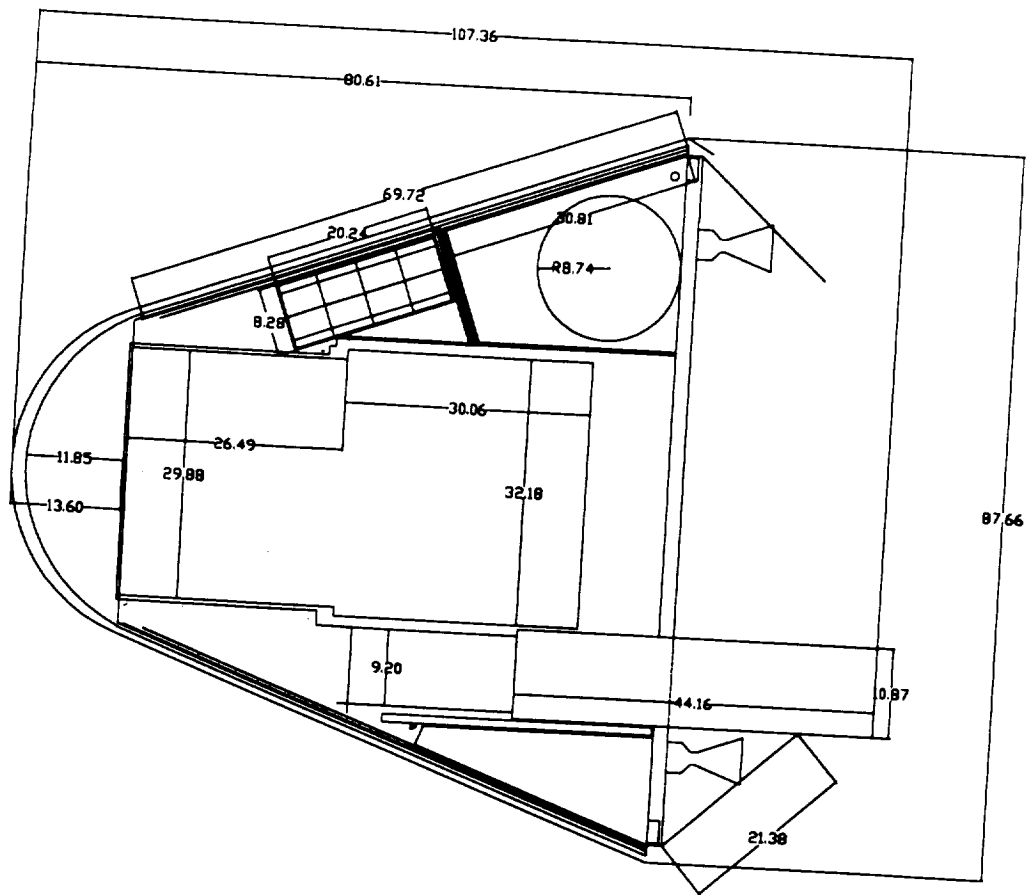


Figure 6.3-44. 15-Rodent Module

The 15-rodent vehicle would be capable of supporting a 204 watt payload and would weigh at launch approximately 3650 pounds fully loaded. A breakdown of the vehicle mass is given in Table 6.3-8.

This vehicle would use 9-inch Astromasts. The vehicle would use the same components in the GNC and TT&C as the standard 18-rodent RRV. The structure, and all other subsystems, scale linearly with the downsizing. The exception to this is the Reentry Heat Shield. This downsize would not be capable of flight on a Taurus or other small launch vehicle. In addition, this vehicle would not support the EBM or the five plant Cuvettes payload.

Table 6.3-8. 15-Rodent Mass and Power

Component	Mass 18 RAT	FACTOR	NEW MASS
MAIN SUPPORT STRUCTURE	417.0	0.85	354.45
ASTROMAST	144.0	0.85	122.40
PAYLOAD	972.0	0.85	826.20
POWER SYSTEM EXTENDED	240.0	0.85	204.00
POWER SYSTEM MAIN	212.0	0.85	180.20
PROPULSION SYSTEM	157.0	0.85	133.45
PROPELLANT	600.0	0.85	510.00
THERMAL EXTENDED MODULE	10.0	0.85	8.50
THERMAL MAIN MODULE	50.0	0.85	42.50
TERMINAL RECOVERY SYSTEM	150	0.85	127.50
REENTRY THERMAL PROT.	421.0	0.90	378.90
TT&C	58.0	1.00	58.00
GN&C	205.0	1.00	205.00
COMPUTER	20.0	1.00	20.00
HARNESS	85.0	0.85	72.25
BALLAST	35.0	0.85	29.75
MARGIN	328.8		328.77
	0.0		

TOTALS
(LBS AND INCHES)

MASS
3802

POWER
204 WATTS

MASS MARGIN
CALCULATION

MASS VALUE	PERCENT MARGIN	LBS MARGIN
354	29	102.1
122	4	5.3
826	12	99.3
204	8	16.3
180	9	16.2
133	14	18.2
510	0	0.0
9	20	1.7
43	29	12.1
128	8	10.3
379	5	18.9
58	3	1.9
205	4	8.0
20	20	4.0
72	20	14.5

TOTAL 328.8

Scaling down further to a 12-rodent configuration gave a vehicle with dimensions and mass properties as shown in Figure 6.3-45 and Table 6.3-9.

This vehicle design would have a power load capability of 156 watts, and would weigh 3036 pounds. This design has less flexibility in that it is marginally able to support the required satellite functions and still supply sufficient power to the payload for 12 rodents. This design incorporates Nickel Cadmium batteries replacing the nickel hydrogen from the baseline design. This design also requires the development of an 8-inch Astromast. Without performing detailed analyses, it appears that this design would be imposed with launch window restrictions to ensure sufficient power production through all mission phases.

Figure 6.3-46 depicts a 9-rodent configuration with Table 6.3-10 showing the mass and power.

This vehicle design cuts in half the level of redundancy the previous designs had in order to save power. This would make the design questionable for a White Sands landing. In addition, the consumables go down linearly with the number of rats. The volume for storage, however,

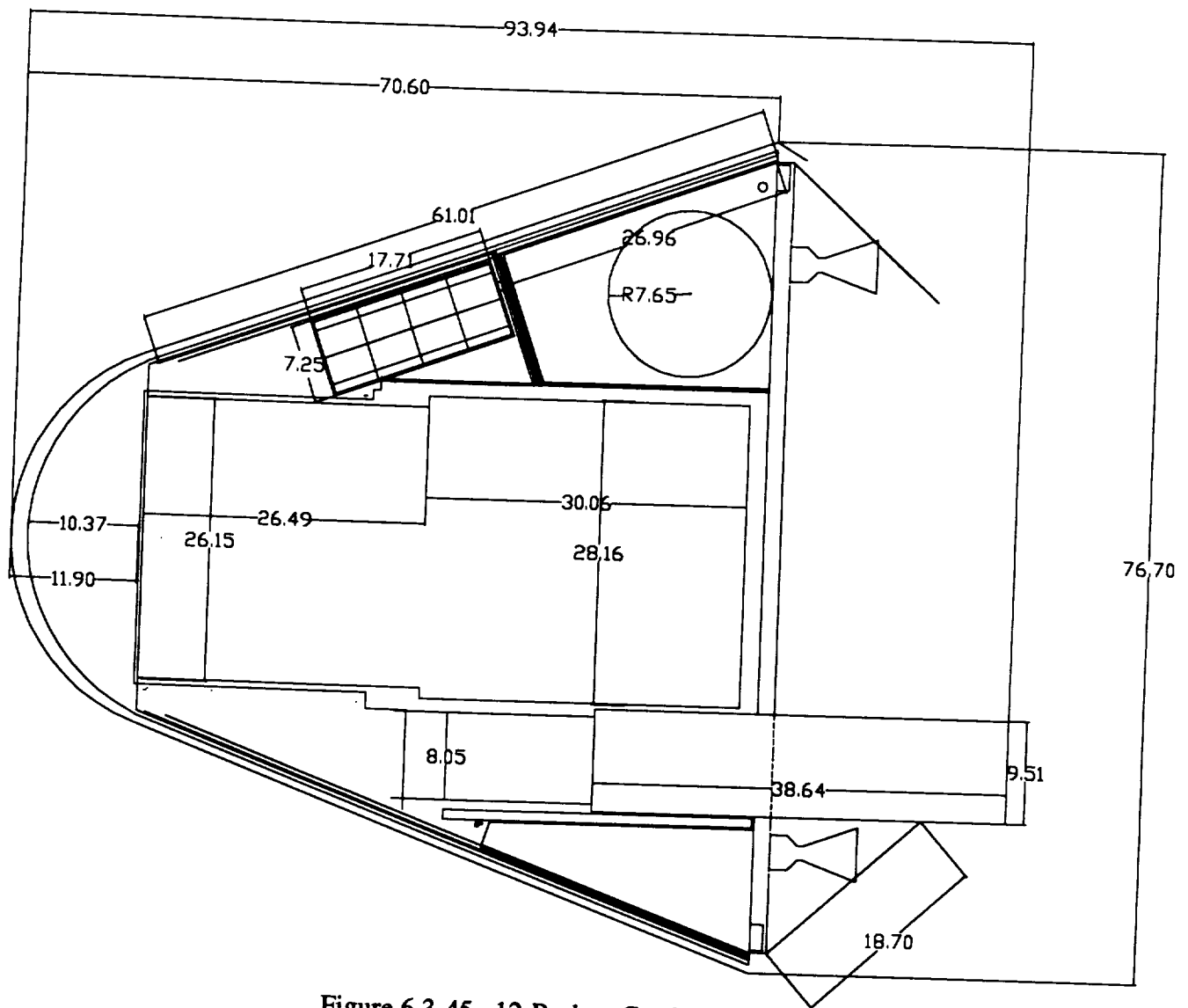


Figure 6.3-45. 12-Rodent Configuration

Table 6.3-9. 12-Rodent Mass and Power

Component	TOTALS (LBS AND INCHES)			MASS MARGIN CALCULATION		
	Mass 18 RAT	SCALING FACTOR	NEW MASS	MASS VALUE	PERCENT MARGIN	LBS MARGIN
MAIN SUPPORT STRUCTURE	417.0	0.70	291.90	292	35	102.1
ASTROMAST	144.0	0.65	93.60	94	6	5.3
PAYLOAD	972.0	0.70	680.40	680	15	99.3
POWER SYSTEM EXTENDED	240.0	0.70	168.00	168	15	25.2
POWER SYSTEM MAIN	212.0	0.70	148.40	148	15	22.3
PROPULSION SYSTEM	157.0	0.65	102.05	102	18	18.2
PROPELLANT	600.0	0.65	390.00	390	0	0.0
THERMAL EXTENDED MODULE	10.0	0.65	6.50	7	20	1.3
THERMAL MAIN MODULE	50.0	0.65	32.50	33	37	12.1
TERMINAL RECOVERY SYSTEM	150	0.65	97.50	98	11	10.3
REENTRY THERMAL PROT.	421.0	0.80	336.80	337	5	16.8
TT&C	58.0	1.00	58.00	58	3	1.9
GN&C	205.0	1.00	205.00	205	4	8.0
COMPUTER	20.0	1.00	20.00	20	20	4.0
HARNESS	85.0	0.65	55.25	55	20	11.1
BALLAST	35.0	0.65	22.75			
MARGIN	337.8		337.79			
	0.0					

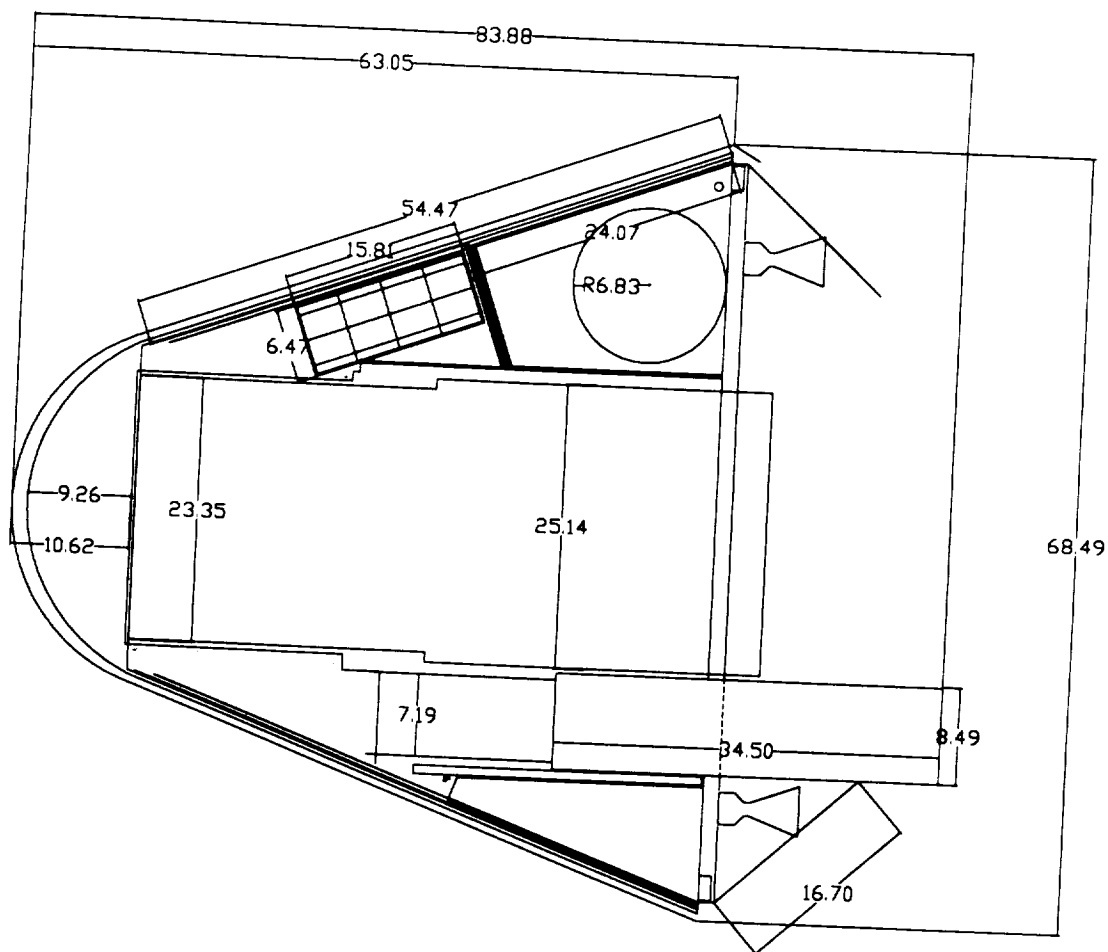


Figure 6.3-46. 9-Rodent Module Configuration

Table 6.3-10. 9-Rodent Mass and Power

Component	Mass 18 RAT	SCALING FACTOR	NEW MASS
MAIN SUPPORT STRUCTURE	417.0	0.60	250.20
ASTROMAST	144.0	0.55	79.20
PAYLOAD	972.0	0.58	563.76
POWER SYSTEM EXTENDED	240.0	0.55	132.00
POWER SYSTEM MAIN	212.0	0.55	116.60
PROPULSION SYSTEM	157.0	0.52	81.64
PROPELLANT	600.0	0.52	312.00
THERMAL EXTENDED MODULE	10.0	0.52	5.20
THERMAL MAIN MODULE	50.0	0.52	26.00
TERMINAL RECOVERY SYSTEM	150	0.52	78.00
REENTRY THERMAL PROT.	421.0	0.70	294.70
TT&C	58.0	0.50	29.00
GN&C	205.0	0.60	123.00
COMPUTER	20.0	0.60	12.00
HARNESS	85.0	0.60	51.00
BALLAST	35.0	0.52	18.20
MARGIN	322.8		322.81
	0.0		

TOTALS
(LBS AND INCHES)

MASS
2488

POWER
125 WATTS

MASS MARGIN
CALCULATION

MASS VALUE	PERCENT MARGIN	LBS MARGIN
250	41	102.1
79	7	5.3
564	18	99.3
132	15	19.8
117	15	17.5
82	22	18.2
312	0	0.0
5	20	1.0
26	47	12.1
78	13	10.3
295	5	14.7
29	6	1.9
123	7	8.0
12	20	2.4
51	20	10.2

TOTAL 322.8

decreases with the cube of the vehicle radius. Thus, a 60 day mission would be difficult to support without going to higher storage pressures on the gases. This vehicle could fit on an enlarged fairing (70-inch) Taurus. However, it would probably require launching in a nose-up attitude, thus, negating late payload access and single direction g loading on the payload.

The final downsizing to a 6-rodent configuration is shown in Figure 6.3-47 and Table 6.3-11.

This design would easily fit on small (Taurus) launch vehicles. However its 6-rodent capacity is below the minimum scientific sample size of 7 rodents. In addition, the less than 100 watts power production capability severely limits the operational flexibility and power available to the payload.

The scaling design exercise indicated that a smaller RRV does not offer the flexibility to handle the different payloads presently manifested to be flown. In addition, the principal rationale for downsizing (flying on a smaller booster) requires a major downsize, and would not meet the science desirements or be as reliable as the baseline design. The lower reliability, in part caused by the decrease in the redundancy levels, would make a White Sands landing difficult, given range safety restrictions. In addition, the cost savings from the cheaper booster can be offset by flying two RRVs on a single Delta, as discussed earlier.

6.3.5 Control, Command and Telemetry

The control functions for the structural subsystem apply to operation of the Astromasts, separation bolts, and attachment system engagement prior to reentry. The primary control for these functions is the GNC. The latch operation and Astromast functional status are telemetered to ground before initiation of final reentry maneuvers.

6.3.6 Structure Test

The structure subsystem requires special testing for the astromasts, and pre-reentry attachment system. The astromasts shall be tested at the vendor for proper deployment and retraction in both normal and failure mode conditions. Operation of all cable reel systems and slip ring assemblies (for power and data transmission) shall be checked as well. The pre-reentry attachment system shall be tested to ensure capture between the two modules in both nominal and

misaligned cases. The test shall be performed for each of the six actuators using a vehicle simulator.

6.3.7 Conclusions

The RRV structural design, being modular in nature, provides for easy access to all components and subsystems. This is especially important when operating a reusable vehicle. The structure is also easily repaired in sections, so that any landing damage can be quickly replaced and the structure readied for another flight. For refurbishment, each major module can be replaced, or units on the module, once the vehicle is disassembled, with minimal impact on other subsystems. Standard refurbishment after a flight would include replacing the nose and conical heat shield submodules, inspection of all high stress areas, replacement of any damaged members, and removing and replacing the Astromasts. The masts would be sent to the manufacturer for checkout, and refurbishment as required, before being approved for reflight.

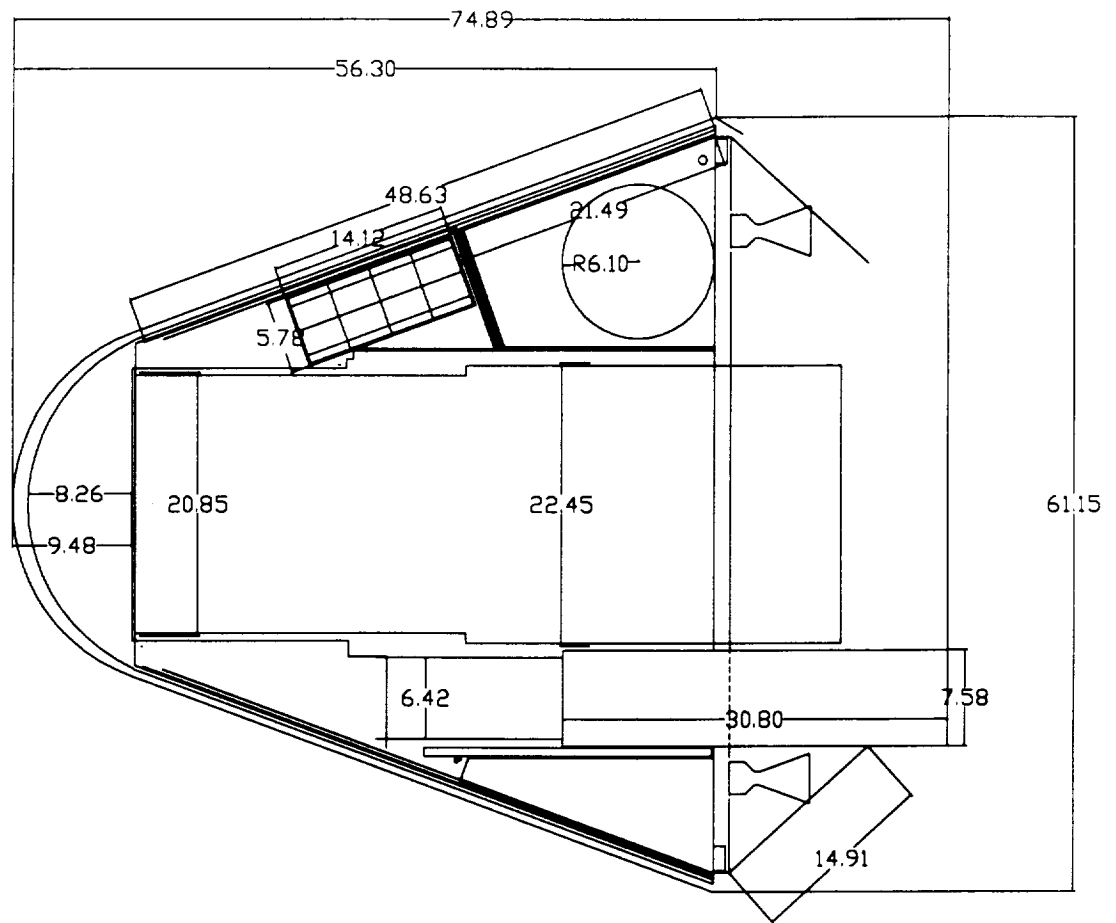


Figure 6.3-47. 6-Rodent Module Configuration

Table 6.3-11. 6-Rodent Mass and Power

TOTALS (LBS AND INCHES)				MASS MARGIN CALCULATION		
Component	Mass 18 RAT	SCALING FACTOR	NEW MASS	MASS VALUE	PERCENT MARGIN	LBS MARGIN
MAIN SUPPORT STRUCTURE	417.0	0.50	208.50	209	49	102.1
ASTROMAST	144.0	0.50	72.00	72	7	5.3
PAYLOAD	972.0	0.46	447.12	447	22	99.3
POWER SYSTEM EXTENDED	240.0	0.45	108.00	108	15	16.2
POWER SYSTEM MAIN	212.0	0.45	95.40	95	15	14.3
PROPULSION SYSTEM	157.0	0.45	70.65	71	26	18.2
PROPELLANT	600.0	0.41	246.00	246	0	0.0
THERMAL EXTENDED MODULE	10.0	0.41	4.10	4	20	0.8
THERMAL MAIN MODULE	50.0	0.41	20.50	21	59	12.1
TERMINAL RECOVERY SYSTEM	150	0.45	67.50	68	15	10.3
REENTRY THERMAL PROT.	421.0	0.60	252.60	253	5	12.6
TT&C	58.0	0.50	29.00	29	6	1.9
GN&C	205.0	0.60	123.00	123	7	8.0
COMPUTER	20.0	0.60	12.00	12	20	2.4
HARNESS	85.0	0.60	51.00	51	20	10.2
BALLAST	35.0	0.41	14.35			
MARGIN	313.7		313.70			
	0.0					

MASS
2138

POWER
98.4 WATTS

TOTAL 313.7

6.4 Reentry Thermal Protection Subsystem

6.4.1 Introduction

A primary motivation in pursuing the Reusable Reentry Satellite concept is the vehicle's ability to de-orbit and reenter the atmosphere for consequent recovery and refurbishment. During atmospheric reentry, the vehicle's aeroshell will experience an aeroheating environment with maximum rates on the order of 60 to 80 W/cm². Such an environment necessitates the use of a reentry thermal protection material capable of withstanding these heat loads while effectively insulating the vehicle's substructure and internals. This section describes the assessment performed to determine the reentry thermal protection subsystem requirements for the SAIC RRS design.

6.4.2 Modeling Tool

To assess the performance of the RRS reentry thermal protection subsystem, a modeling tool capable of predicting the pyrolytic, charring, and ablative response of prospective aeroshell materials was required. Since the assessment would involve response analyses at representative vehicle axial stations over numerous descent trajectories, a modeling tool which was user friendly and fast running was preferred. A tool which fits these requirements is the SAIC-developed System-Level Ablation Penetration Erosion Model (SLAPEM) computer code (Ref. 1). SLAPEM computes the response of reentry body nose cones and heat shields to severe aerothermal and particle laden environments. The model includes aeroheating, transient indepth heat conduction, charring, and thermochemical ablation.

6.4.3 Model

The RRS aeroshell model development for the assessment is presented in Figure 6.4-1. The reentry thermal protection system consists of a layer of heat shield material of varying thickness over a substrate of aluminum. The aeroshell itself is a sphere/cone configuration. For the assessment, five analysis locations were chosen as indicated in the figure. The locations consisted of the nosetip, 40° away from the nosetip, the sphere/cone transition point at 70°, and at the midpoint and extreme aft locations on the conic portion of the aeroshell. The aluminum substructure was modeled as aluminum, 0.145 cm in thickness, which is of a mass representative of the proposed vehicle substrate of aluminum honeycomb. The backface of the substructure was treated as a perfectly adiabatic boundary.

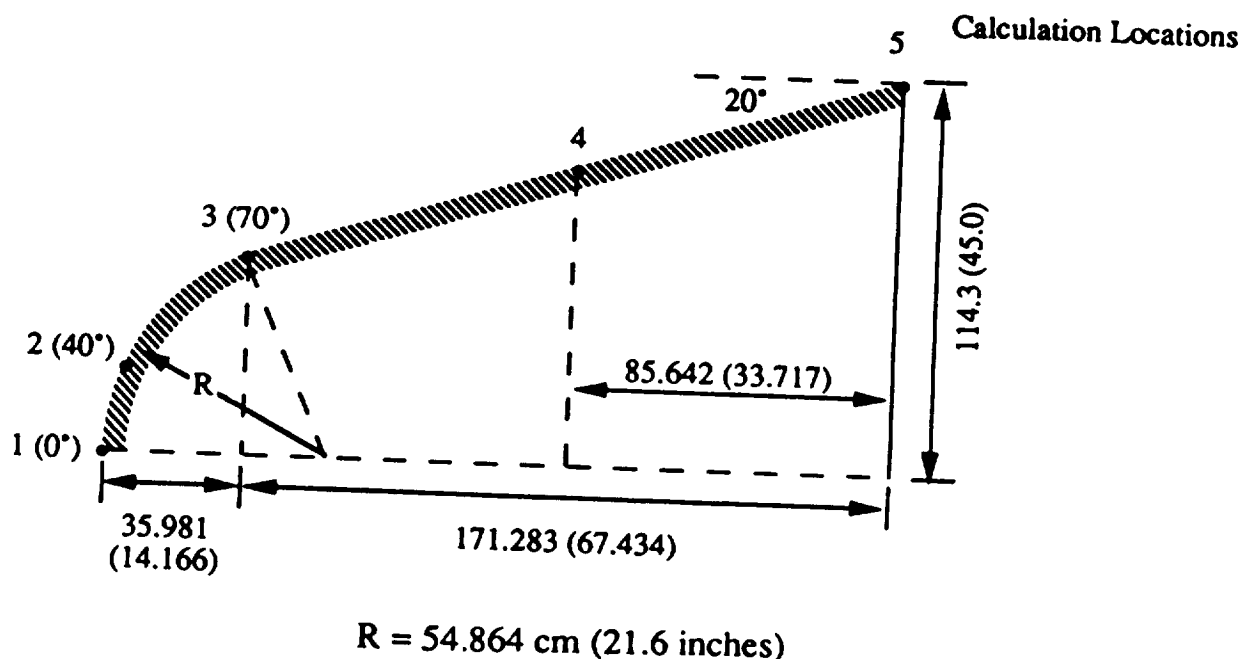


Figure 6.4-1. RRS Aeroshell Model

The heat shield material modeled in the assessment was a cured foam silicon elastomer developed by General Electric designated ESM 1004 AP (Elastomeric Shield Material). This blend of ESM provides a low weight thermal protection system with well characterized thermal physical properties which has been successfully flight tested (Ref. 2). The thermophysical properties of ESM 1004 AP are described in Table 6.4-1. These properties were incorporated into the SLAPEM material response routines.

The reentry trajectories considered in the analysis are presented in Figures 6.4-2 and 6.4-3. These trajectories span the full spectrum of anticipated RRS reentry scenarios.

6.4.4 Assumptions

The primary assumption in the response analysis was that the backface of the aluminum substrate was treated as an adiabatic boundary. The heat shield sizing philosophy applied in this analysis, however, dictated that an acceptable aeroshell thickness had been arrived at when for a prescribed trajectory, the aeroshell backface experienced a temperature rise of no greater than 20°K. Therefore, heat transfer across the backface boundary was small and the adiabatic assumption reasonable.

Table 6.4-1. ESM 1004 AP Thermophysical Properties

T (K)	0.0	255.6	422.2	533.3	811.1	1088.9	1366.7	1644.4	1922.2	2777.8
k (W/m K)	0.21	0.16	0.14	0.13	0.13	0.16	0.19	0.23	0.27	0.46
C _p (J/kg K)	4.2	984.0	1256.0	1800.0	1842.0	1842.0	2261.0	2973.0	3643.0	3643.0
C _{p,g} (J/kg K)	Specific Heat (pyrolysis gas)									
H _d (kJ/kg)	Heat of Decomposition									
H _v (kJ/kg)	Heat of Vaporization (estimated)									
ρ (kg/m ³)	Density (virgin ESM)									
ρ _c (kg/m ³)	Density (char)									
MW _g	Molecular Weight (pyrolysis gas)									
C _t	C _{p,g} /C _{p,air}									
C ₁	1 - k _{char} / k									
ε	Emittance									

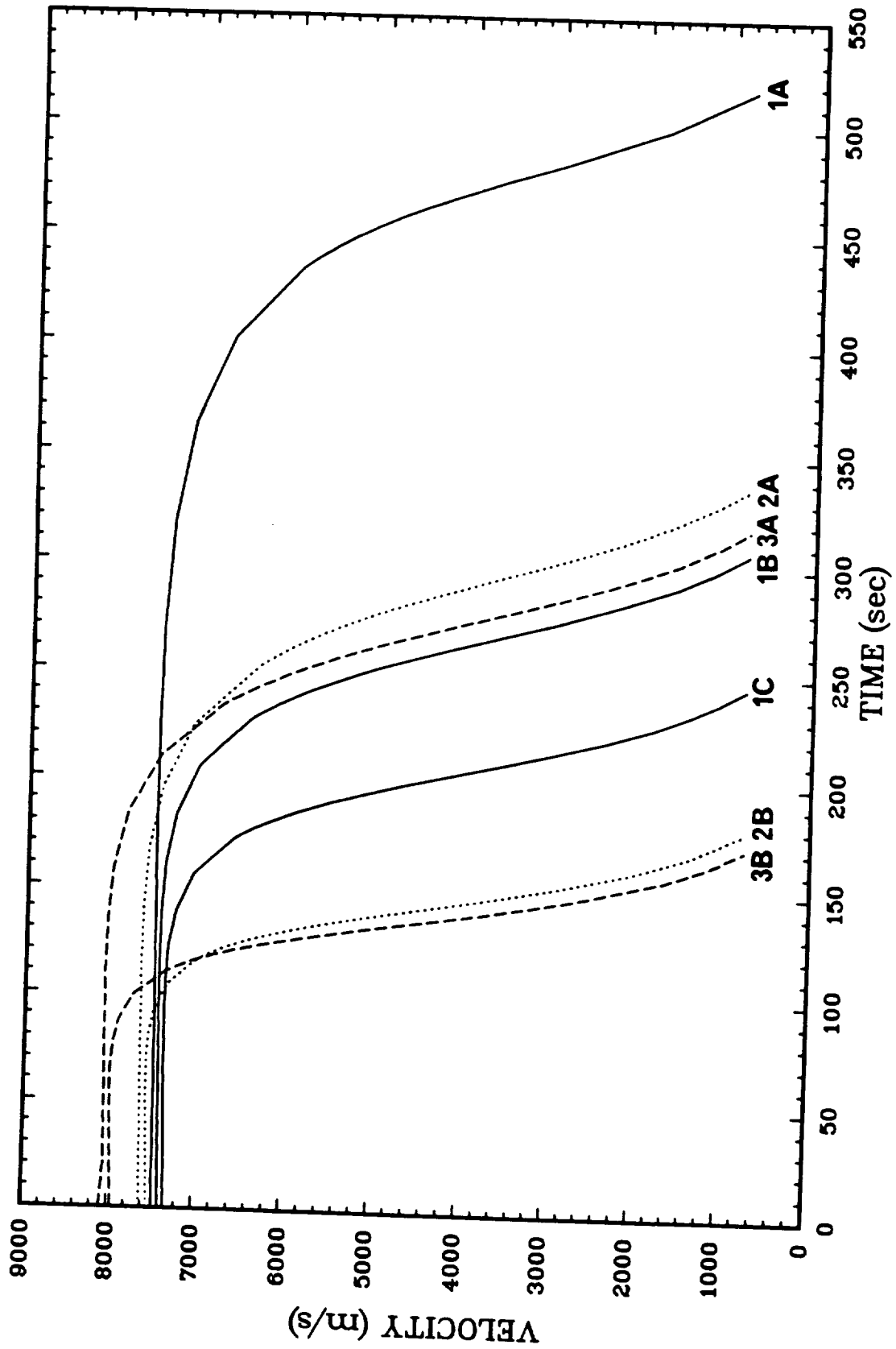


Figure 6.4-2. Reentry Model Trajectories-A

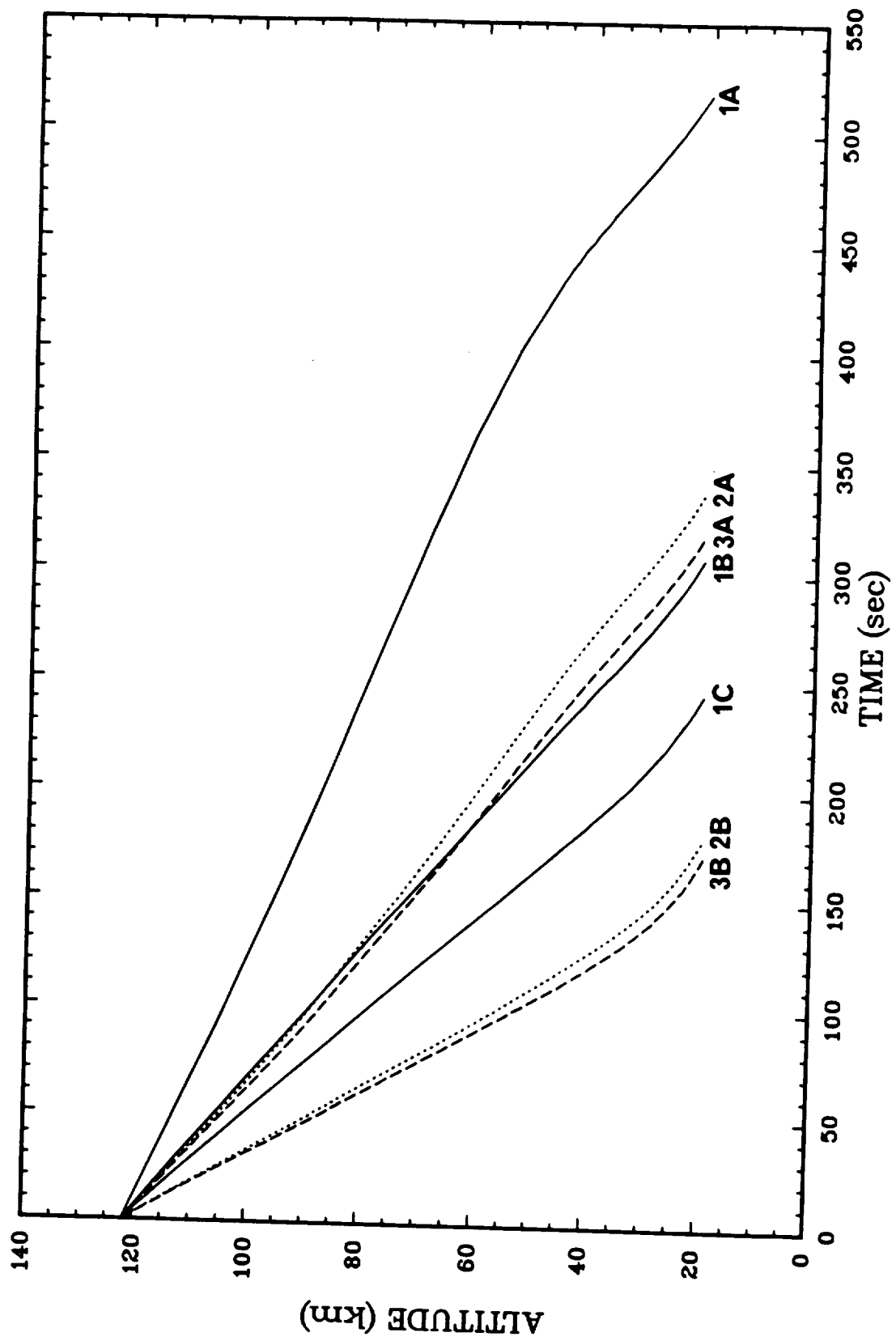


Figure 6.4-3. Reentry Model Trajectories-B

6.4.5 Results

The reentry heating rates predicted by SLAPEM for descent trajectories 1A, 2A, and 3A at the vehicle nosetip are presented in Figure 6.4-4. As is evident from this result, for the nosetip, trajectory 3A is the most severe. The heat sizing approach consisted of making consecutive runs of SLAPEM at each station, gradually thickening the ESM until the substrate temperature remained below the mandated 450°K. This was performed at each of the five stations for seven trajectories. A compendium of the results is presented in Table 6.4-2. Trajectory 3A results in the highest recession for the spherical portion of the aeroshell. Along the conic section, this trajectory also results in the thickest heat shield requirements. Figure 6.4-5 presents the thickness requirements, predicted recession, and char depths for this trajectory. These thicknesses result in a total heat shield weight of 389 kg.

6.4.6 Conclusions

Reentry trajectories 1A, 2A, and 3A subject the vehicle aeroshell to the most severe aero-heating and ablative environments. Highest material loss is predicted for reentry trajectory 3A and, therefore, this trajectory drives the heat shield thickness requirements. The resulting thicknesses maintain the heat shield bondline with the substructure well below the 450°K requirement.

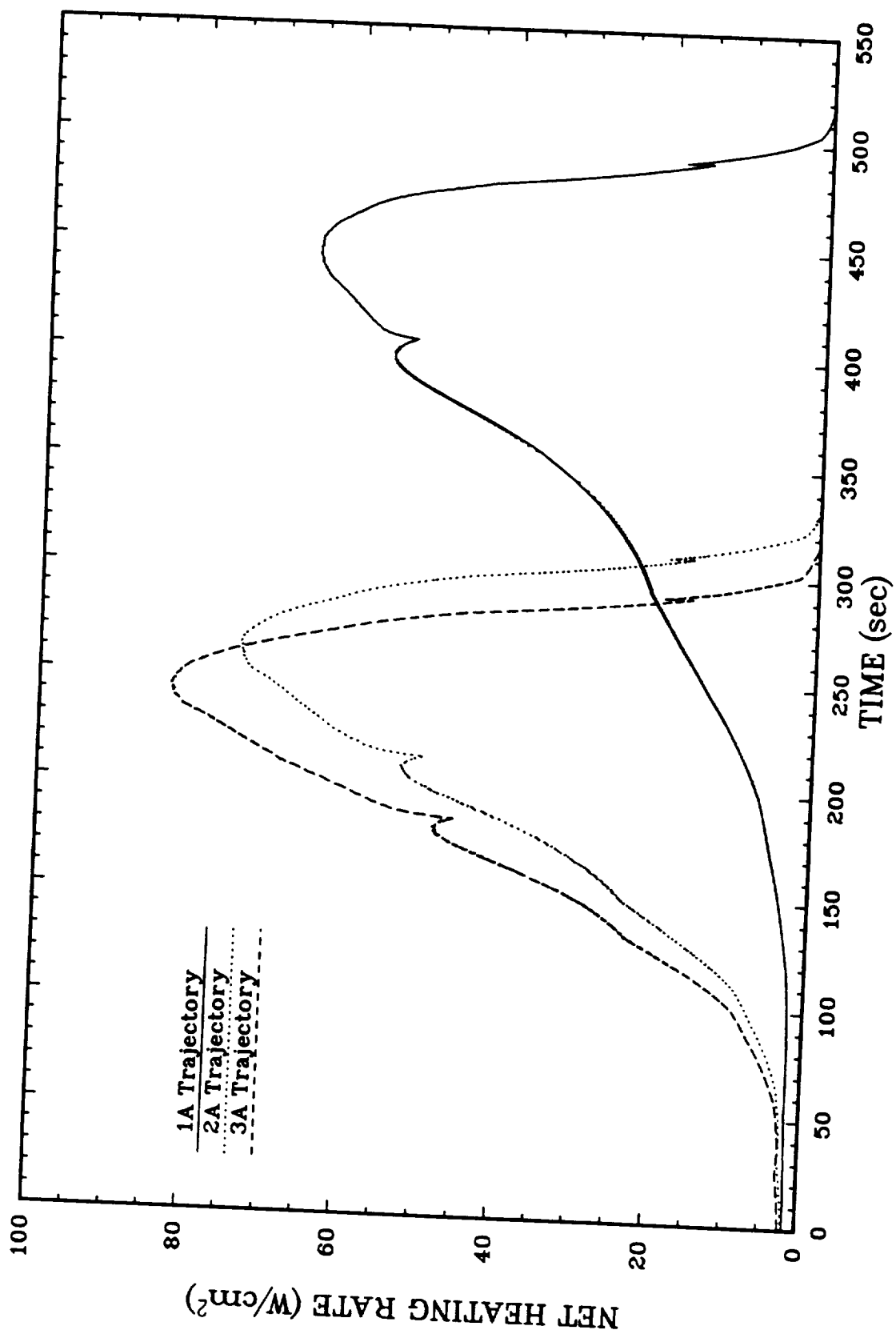
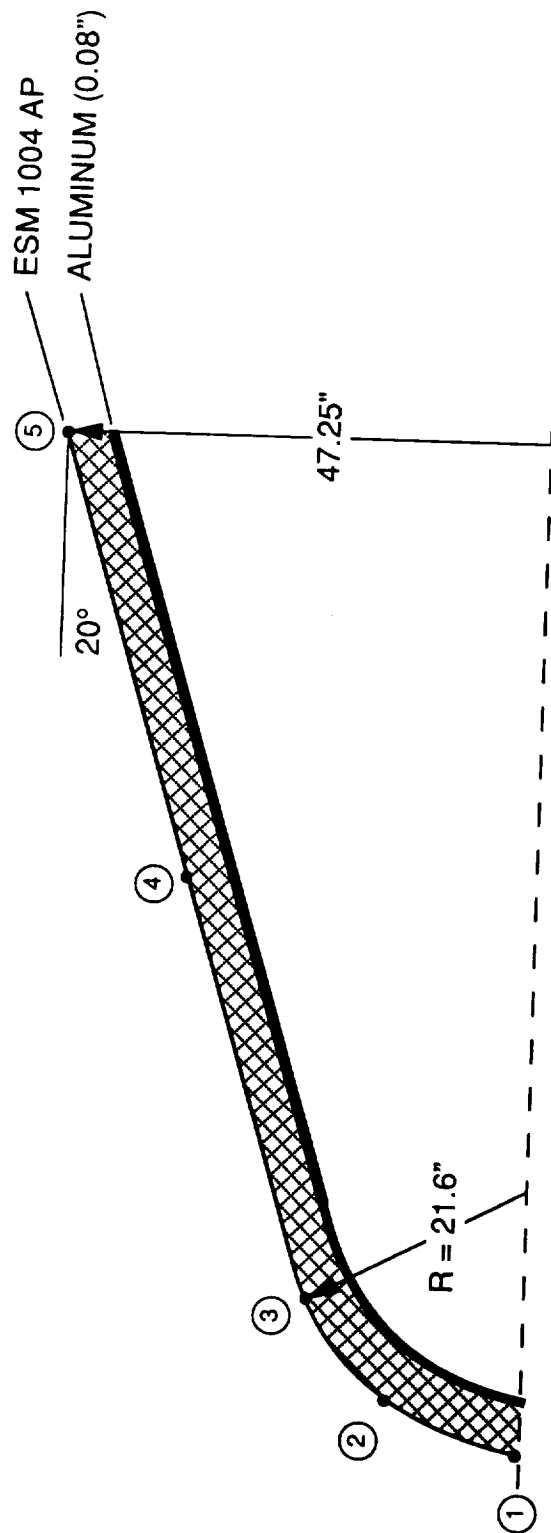


Figure 6.4-4. Net Heating Rates Trajectories 1A, 2A, and 3A - Vehicle Nostrip

Table 6.4-2. ESM Thickness Requirements and Total Predicted Recession

Trajectory	Analysis Locations					
	ESM Thickness (Inches)	1	2	3	4	5
1A		1.6 / 1.24	1.1 / 0.47	0.9 / 0.0	0.9 / 0.0	0.9 / 0.0
1B		1.6 / 1.21	1.0 / 0.58	0.9 / 0.02	0.9 / 0.0	0.9 / 0.0
1C		1.6 / 1.12	1.0 / 0.60	0.9 / 0.02	0.9 / 0.0	0.9 / 0.0
2A		1.8 / 1.42	1.1 / 0.69	0.8 / 0.0	0.8 / 0.0	0.8 / 0.0
2B		1.6 / 1.20	1.1 / 0.77	0.9 / 0.0	0.9 / 0.02	0.9 / 0.0
3A		2.2 / 1.82	1.4 / 0.95	1.0 / 0.04	1.0 / 0.0	1.0 / 0.0
3B		1.8 / 1.47	1.0 / 1.00	0.8 / 0.16	0.8 / 0.07	0.8 / 0.03



STATION #	ESM THICKNESS (INCHES)	PREDICTED RECESSION (INCHES)	PREDICTED CHAR DEPTH - INTO REMAINING MATERIAL (INCHES)
1	2.2	1.82	0.03
2	1.4	0.95	0.04
3	1.0	0.04	0.16
4	1.0	0.00	0.15
5	1.0	0.00	0.13

TOR42B/12

Figure 6.4-5. Results - Heat Shield Thickness Requirements

6.5 Propulsion

6.5.1 Functional Operation

The propulsion subsystem provides the following functions during the various mission phases.

6.5.1.1 Prelaunch. Propulsion subsystem loading is performed using existing ground support equipment. Loading procedures follow standard range safety rules and procedures. Loading helium pressurant is accomplished first, followed by pressure loading the hydrazine. The propellant is isolated from leakage by three valve seats at the completion of the loading procedure.

6.5.1.2 Orbital Flight. After launch vehicle separation, the valve drivers are initiated (electrical inhibit 1), valve driver units are armed (electrical inhibit 2), and latch valves are opened (electrical inhibit 3) for priming the propellant to the thrusters. The propulsion subsystem is now ready for operation.

During the mission, the propulsion subsystem is used to maintain or change spin speeds. For this case, 1 rpm of spin speed adjustment and 10 feet per second of drag makeup are required. After completion of mission, the vehicle is spun down and reoriented for Astromast retraction.

6.5.1.3 De-Orbit. After retraction, the ground track is aligned for the de-orbit maneuver. The de-orbit maneuver is performed in two parts, a main burn and trim burns as required. Finally, the vehicle is oriented for atmospheric reentry and spun at 2 rpm to balance out any asymmetric heating caused by center of gravity offsets.

6.5.1.4 Reentry-Recovery. The mission sequence is completed after atmospheric entry when the propulsion subsystem safes for recovery. This entails closing the latch valves and opening the thruster valves to purge propellant from the thruster manifold. Final safing is completed by shutting down in reverse order of the sequence after launch vehicle separation. This ensures that the RRV propulsion subsystem has three electrical and mechanical inhibits preventing propellant leaks.

A maneuver history and propellant budget example for a DRM-1 mission are given in Table 6.5-1. This budget assumes that a 25 feet per second trim burn is required after separation from the launch vehicle. The vehicle is then re-oriented for optimal thermal conditions and minimal

Table 6.5-1. Propellant Budget DRM-1 - Blowdown

CANDIDATE ENGINE PERFORMANCE VALUES									
THRUST lbs	TOTAL #	# USED main	# USED OTHER	BLOWDOWN PSI	ISP @ 300 PSID	SCARFED NOZZLES			
ACS ENGINES	12.0	4.0	8.0	350-75	225				
MAIN ENGINES	6.0	6.0		350-75	220				
POTENTIAL ENGINE MANUFACTURES									
TRW, HAMILTON STANDARD									
ROCKET RESEARCH, HAMILTON STANDARD									

PROPELLANT BUDGET									
MANUEVER MAGNITUDE FT/SEC, RPM, DEGREES	MANUEVER TYPE NOTE	ISP (SEC)	TIME (SEC)	FUEL USED (lb)	VEHICLE MASS (LBS)	POWER (WATTS)	COMMENTS		
SEPARATED MASS				382.5	3955.0		NOTE: SS= STEADY STATE, OP = OFF PULSE P= ON PULSE		
orient	P	140	184.8	1.3	3953.7	42.0	NULL LAUNCH VEHICLE TIP OFF ERRORS		
spin up z-z	SS	225		0.0	3953.7		OPTION IF NO THRUST PULSE MODULATION		
circularize	SS	220		13.9	3939.8	336.0	REMOVAL OF LAUNCH INJECTION ERRORS		
ANC	P	200		0.0	3939.8		USED IF SPUN - PREVENT FLAT SPIN		
spin down	SS	225		0.0	3939.8		ORIENT FOR MAST EXTENSION		
orient	P	140	320.0	2.3	3937.5	42.0	SPIN UP TO 1.5 G		
spin up x-x	SS/P	225	4160.2	18.5	3919.0	84.0	SPIN AND ORBIT CONTROL		
out gassing	P	140		0.0	3919.0		DUE TO DRAG AND OTHER FORCES		
spin maint.	P	140	668.6	4.8	3914.2	42.0	FOR THERMAL AND OR POWER CONTROL		
attitude maint.	P	140		0.0	3914.2		FACTOR OF SURFACE AREA AND ALTITUDE		
drag makeup	SS/P	140		8.7	3905.6	42.0	SPIN DOWN		
despin	SS/P	225	4160.2	18.5	3887.1	42.0	NULL RATES ORIENT FOR MAST RETRACTION		
orient	P	140	30.6	0.2	3886.9	84.0	ALIGN ORBIT FOR REENTRY		
orbit maint.	SS	220		5.5	3881.4	336.0	IF SPUN DE ORBIT BURN		
ANC	P	140		0.0	3881.4	42.0	SET UP FOR ATMOSPHERIC ENTRY		
deorbit	SS/OP	215		308.8	3572.5	672.0	SPIN UP FOR DE ORBIT BALANCE		
orient and hold	P	140	337.3	2.4	3570.1	42.0			
spin up	SS	215	325.9	1.5	3568.6	42.0			
EMPTY MASS					3568.6				

disturbance torques prior to Astromast operation. After Astromast extension, the spinup maneuver to 10 rpm (1.5 g artificial gravity mission) is performed.

6.5.2 Requirements

6.5.2.1 Top Level Requirements. The RRV propulsion subsystem provides velocity increments to the vehicle after separation from the launch vehicle. These include attitude control, spin speed control, minor orbital adjustment, and most importantly, the de-orbit maneuver. The design has to provide highly accurate, controllable total impulse in order to meet the landing dispersion requirements.

Since the propulsion subsystem is one of the critical subsystems involved in the de-orbit maneuver, it is, therefore, directly linked to public safety. For this reason, it has been designed with a fail operational/fail operational capability for the de-orbit maneuver. For other mission phases, it was designed as fail operational/fail safe. This design configuration ensures that no combination of failures other than tank or line burst or major leak is capable of creating a safety hazard, and that no single failure would prevent successful completion of the mission.

The design also needs to be flexible in order to handle a variety of RRV payloads and possible orbits. The initial list of Design Reference Missions (DRMs) used to perform the design trade studies is included in Table 6.5-2.

It was also deemed necessary to maximize the use of space qualified hardware, whenever feasible, and to ensure maximum reusability in order to lower life cycle costs.

6.5.2.2 Science Requirements. Science payloads have two operational modes, artificial gravity and zero gravity. The artificial gravity requirement levied on the propulsion subsystem is that the gravity level be selectable at any value between 0.1g and 1.5 g and be maintained to within $\pm 10\%$.

The SAIC design incorporates Astromasts to increase the vehicle spin radius for artificial gravity missions. When fully extended, the masts are ~100 feet long. The structural strength limitations of the deployed masts imposed a derived requirement on the propulsion subsystem. The analyses performed by Astro Aerospace, the mast's manufacturer, determined that the maximum thrust of the spinup thrusters could not exceed 1.3 lbs total in order to maintain a 2:1 structural safety factor.

Table 6.5-2. RRS Design Reference Missions

- FIVE DRMs REVIEWED FOR RRS APPLICATIONS:

DRM #	Character	Inclination	Altitude km (nm)	Orbit Type	Launch Site	Recovery Site
1	Land Recovery	33.83°	350 (189)	Circ	ETR	WSMR
2	High Altitude	33.83°	900 (486)	Circ	ETR	WSMR
3	High Inclination	98	897 (484)	Circ, Int	WTR	WSMR
4	Integer Orbit	35.65°	479 (259)	Circ, Int	ETR	WSMR
5	Water Recovery	28.5°	350 (189)	Circ	ETR	Water (ETR, WTR, Gulf)

- DRM 1, 2, & 3 SELECTED FOR USE IN STUDY

Abbreviations:

DRM	Design Reference Mission
Circ	Circular
Int	Integer
ETR	Eastern Test Range
WTR	Western Test Range
WSMR	White Sands Missile Range
Gulf	Gulf of Mexico

The zero gravity mission imposed a not-to-exceed acceleration level of 1×10^{-5} g for 95% of the mission and less than 1×10^{-3} g during the remainder. The 1×10^{-3} g requirements imposed a maximum thrust level of 0.6 lb each for the attitude control thrusters.

The final design requirement levied by the science payload was to minimize the thrust level of the de-orbit burn. Since this is the only time, other than launch, when an acceleration greater than 10^{-3} g is applied to the vehicle in a direction that changes the "floor" of the experiment, the de-orbit maneuver thrust must be less than 0.25 g.

6.5.2.3 Total Impulse Requirement. Analysis of the five DRMs, and the corresponding de-orbit burns, was used to derive the total impulse requirement for the vehicle. The reentry trade analyses studied de-orbit burns ranging from 328 to 1174 feet per second. The 1174 feet per second burn, combined with an artificial gravity mission at 1.5 g, corresponded to worst case for

propulsion system sizing analyses. For this mission, the de-orbit burn constitutes more than 80% of the total propellant required.

Since the impulse requirement is related to the vehicle mass properties, a propellant budget based on the latest vehicle design data was calculated and compared to the simulations performed for the propulsion subsystem trade study. From the updated mass properties and reentry analyses, a total impulse requirement of 130,000 lbf seconds was baselined.

6.5.3 Trade Study Summary

The propulsion trade study looked at weight, cost, performance, complexity, power consumption and hardware availability to determine the optimal propulsion subsystem for the RRV. The study considerations and analyses performed are outlined in Table 6.5-3. The first cut trades are documented in Table 6.5-4.

The all-liquid subsystem was selected because it had lower life cycle costs, provided a low g de-orbit burn capability, was restartable, delivered accurate impulse, and was inherently flexible to accommodate various orbits, orbit changes, spin speed changes, and de-orbit profiles. The results of the liquid subsystems investigated are presented in Table 6.5-5.

Table 6.5-3. Propulsion Study Considerations

- REQUIREMENTS — SUPPLY Δ VELOCITY FOR:
 - Orbit Adjustments (Minor)
 - Spinup/Spindown
 - Attitude Control/G-Level Control
 - Deorbit Maneuvers
- FUEL OPTIONS CONSIDERED
 - Monopropellant - N_2H_4
 - Bipropellant
 - $N_2H_4 + N_2O_4$
 - $N_2H_3CH_3 + N_2O_4$
 - Solid (Deorbit Only)
 - $GO_2 + GH_2$
- PRESSURANT OPTIONS CONSIDERED
 - Pressure Regulator
 - Blowdown
- WEIGHT BUDGETS
 - Mass Properties
 - Deorbit ΔV s for DRM-3 Mission Used for Sizing Tankage
 - Margin/Residuals Calculated

Table 6.5-4. First Cut Propulsion System Trades

Item	Pros	Cons	Comments
Solid Motor for De-Orbit Burn With Liquid Attitude Control System	Simple-Low Cost	Requires High Spin Rate for Thrust Averaging (20-50 rpm) Impulse/Velocity Error of 0.5% High g Burn Not Flexible	Nonreusable Science Desires Not Met Major Contributor to Landing Inaccuracy - Can Perform Trim Burn With Liquid System Science Desires Not Met Changes of Motor Propellant Load Difficult to Perform in Timely Manner
All Liquid System	Flexible System Highly Accurate Impulse Delivery Reusable Low g Deorbit	Higher Nonrecurring Cost	Minimize Landing Dispersion Errors Trim Burn Capability

BASELINED ALL LIQUID SYSTEM

Table 6.5-5. Liquid/Propellant Trades

	Pros	Cons
Monopropellant (Baseline)	<ul style="list-style-type: none"> Simplest – Lowest Initial Cost Helps Spin Balance Lowest Refurbishment Cost Thruster Tolerance to Temperature is High 	<ul style="list-style-type: none"> Lowest Performance High Propellant Freezing Temperature
Dual Mode Bipropellant	<ul style="list-style-type: none"> Existing Hardware Higher (314 sec.) Isp vs. 235 sec for Monopropellants for Major Burns Lower Propellant Mass 	<ul style="list-style-type: none"> Complexity
Bipropellant	<ul style="list-style-type: none"> High Isp 	<ul style="list-style-type: none"> No Existing Engines Less Than 2.2 lbs Thrust Rules Out System
GOX/GH ₂	<ul style="list-style-type: none"> Highest Engine Performance 	<ul style="list-style-type: none"> Heavy/High Volume Tankage Rules Out System

The baselined monopropellant subsystem has the lowest hardware cost (half the number of lines and valve seats as a bipropellant subsystem). This also lowers refurbishment time and cost. In addition, monopropellant subsystems are tolerant of high and low propellant temperatures, thus simplifying the vehicle thermal design.

Another unique advantage of the monopropellant subsystem is that it requires more propellant than a comparable bipropellant subsystem. At first glance, this would be deemed a disadvantage. However, the SAIC design has the two opposing vehicle halves separated by 100 foot Astromasts. The intent of this design technique is to increase the radius that the payload "sees" when the vehicle is spun. The more mass in the Deployed Module, the greater the spin radius. Thus, a lower performance propulsion subsystem assists in achieving a greater spin radius for the payload by increasing mass in the Deployed Module.

The trade study observed that the higher performance propulsion subsystems weight savings were not enough to allow the use of lower cost launch vehicles. Thus, the added propellant weight required by the monopropellant was not deemed a negative factor. Finally, the monopropellant subsystem makes the greatest use of existing, qualified, flight proven hardware.

6.5.4 Baseline Design

6.5.4.1 Mechanical. The propulsion subsystem is a monopropellant system that uses hydrazine (N_2H_4). The design is composed of 18 thrusters, and performs two distinct functions. Six 100 pound thrusters are used for major maneuvers and de-orbit burn, and twelve 0.5 lbf thrusters are used for attitude control (AC). The major maneuver thrusters are operated in two groups of three, and the AC thrusters are configured in two groups of six. The AC thrusters are further arranged in modules of three thrusters 180° apart on the backface of the vehicle. The thruster groups are isolatable by bistable latching valves.

As depicted in Figure 6.5-1, the propellant tanks are configured in two sets of three, isolated by bistable latching valves. The two sets of propellant tanks are connected via a line and another latch valve. The tanks are 19-inch diameter spheres with internal rubber bladders for zero gravity propellant expulsion and propellant management. The subsystem uses helium as a pressurant gas and operates in blowdown mode such that the initial pressure is 350 psia and the minimum end of life pressure is approximately 75 psia. Each tank has a capacity of 100 lbs of hydrazine.

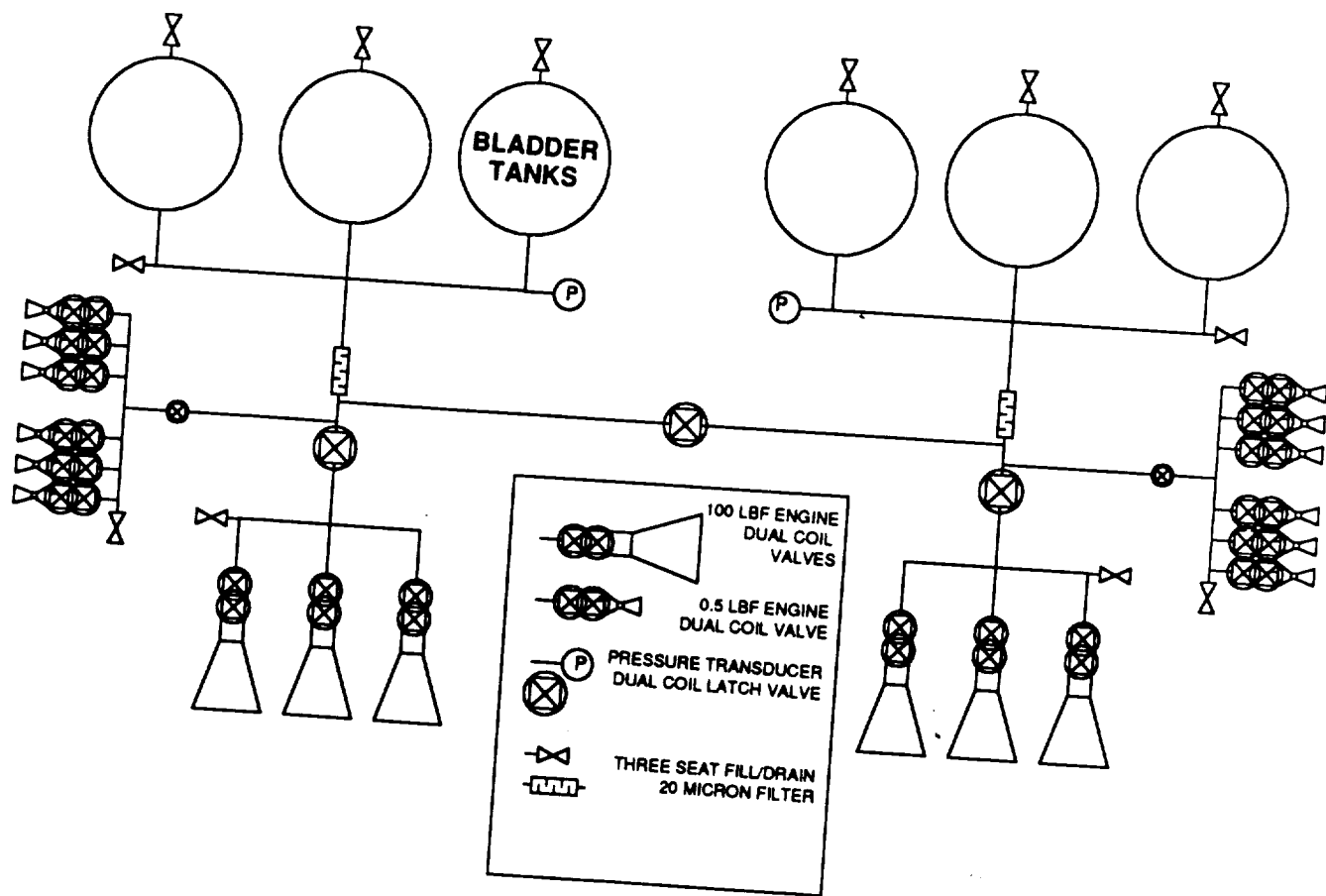


Figure 6.5-1. RRS Propulsion Schematic

Each set of three propellant tanks incorporates an etched disk filter element downstream in the tank manifolding and a pressure transducer to measure the propellant line pressure. In addition, all valve assemblies have a built-in filter. Each set of three tanks has a single 3/8 inch fill and drain valve, with each tank having a single helium 1/4 inch fill and drain valve. Additional fill and drain valves are located on the thruster banks to allow for leak test and flush/purge operations as required.

6.5.4.2 Propulsion Electrical Design. The propulsion subsystem receives all electrical commands from the GNC subsystem. The GNC subsystem delivers hard-wired commands to three redundant Valve Driver Units (VDU) pairs.

Each VDU has 11 output channels. VDUs are configured in groups of two, thus providing 22 output channels. Each thruster valve has a dual coil configuration, with a separate VDU connected to each coil. Thus, either VDU can operate the valve by activating its coil.

As shown in Figure 6.5-2, VDU 1 (two valve driver units, providing 22 outputs) serves as the primary valve driver unit for a group of six AC thrusters, and is also connected to the other six AC thrusters as a backup activator. In addition, VDU 1 is connected to three de-orbit thrusters. These de-orbit thrusters are connected in parallel, thus enabling a single VDU to operate the de-orbit thruster set.

Similarly, VDU 3 serves as the primary driver for the other group of six AC thrusters, and is configured to act as backup activator for the valves for which VDU 1 is the primary driver. Additionally, VDU 3 is connected to the remaining three de-orbit thrusters.

The remaining six drivers of each VDU operate the primary (VDU 1) and secondary (VDU 3) coils on the main thruster isolation latch valves. These valves are double action valves, requiring one command for valve open and a separate command for valve close.

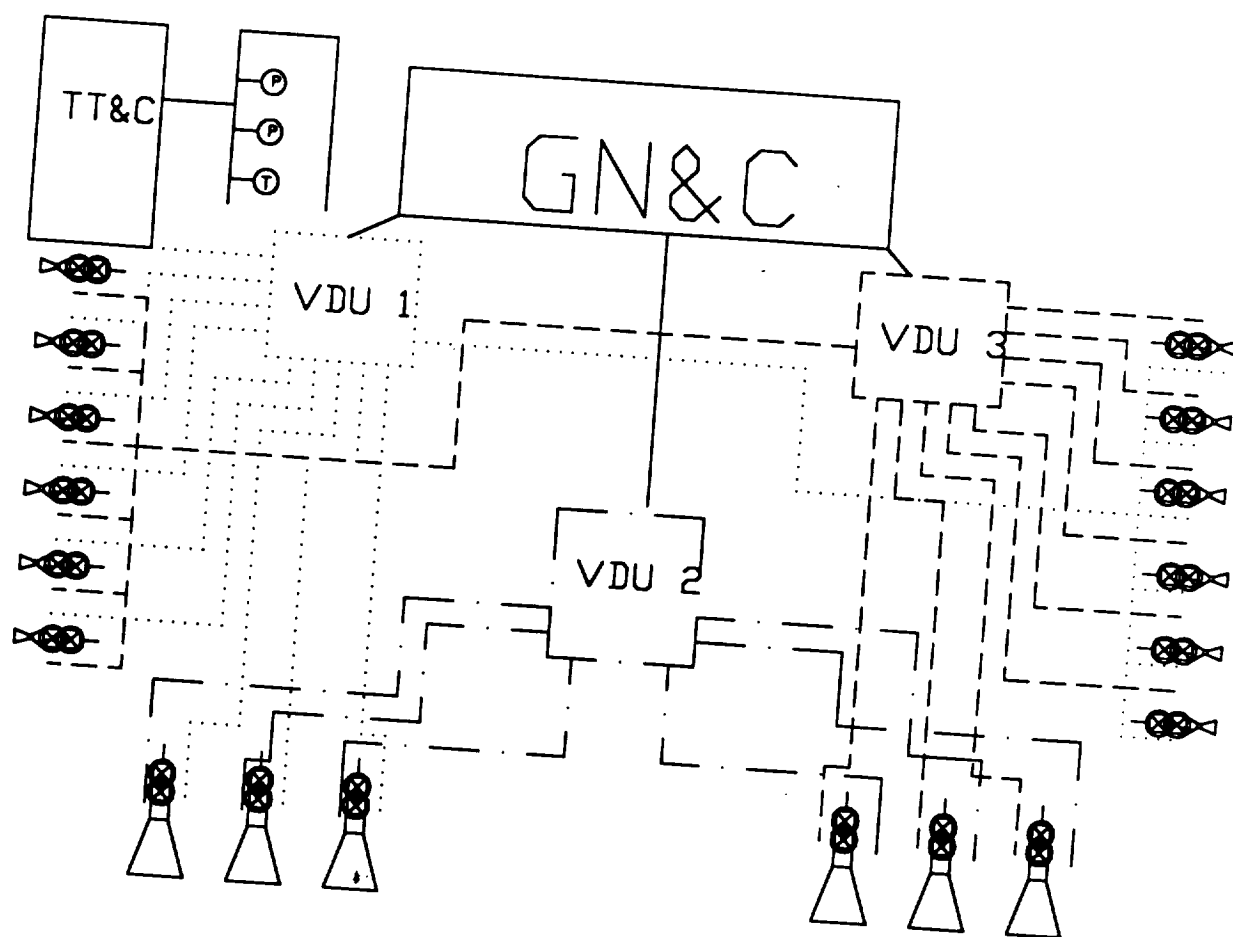


Figure 6.5-2. Propulsion Electrical Schematic

VDU 2's primary function is to operate the de-orbit thrusters, and to serve as a redundant control of the thruster isolation latch valves and tank interconnect latch valves.

6.5.4.3 Components

6.5.4.3.1 Tanks. The propulsion tanks are 19.1-inch spherical titanium tanks with internal bladders made of AFE-332 rubber. The tank has a nominal operating pressure (initial loaded pressure) of 377 psia. It has a minimum 2:1 safety factor of operating pressure to burst. The tank is flight proven and has a qualified propellant volume capacity of 2748 in³. This gives a nominal propellant capacity of 100 lbs per tank. The propellant capacity is presently limited by the diaphragm design. A delta qualification can be performed to achieve a propellant load of 110 lbs, using a 3021 in³ propellant capacity diaphragm. This would give an end of life pressure of 70 psia assuming a 377 psia initial load. As currently configured, the tank incorporates a four-bolt polar mounting scheme with a 1/4-inch propellant and gas port on each boss. Again a delta qualification may be required to increase the port diameter to 3/8-inch to limit pressure drop during main thruster burns.

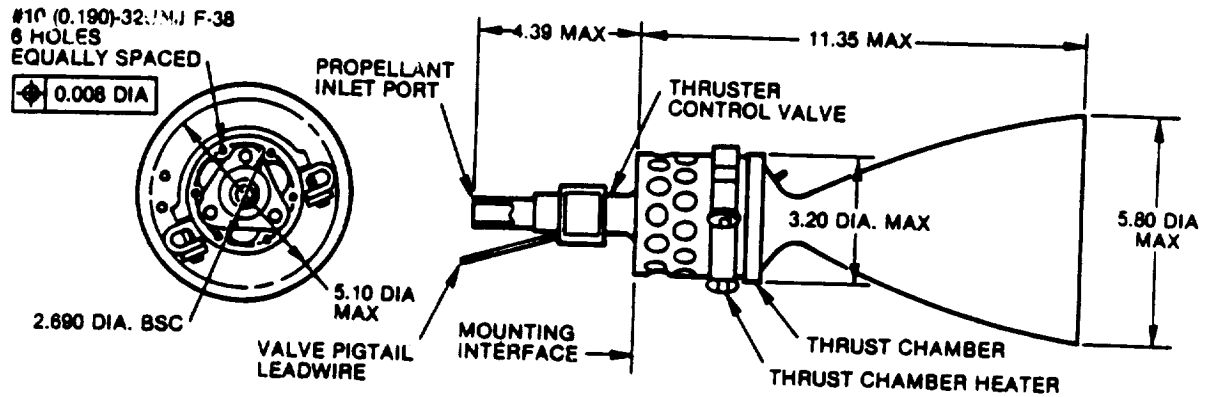
Each tank, as presently configured, weighs 13.3 lbs.

6.5.4.3.2 Main Thrusters. The main maneuver thrusters are Hamilton Standard REA 20's (Figure 6.5-3).

This thruster has flown on the MARK II vehicle and will fly on the Gamma Ray Observatory. The thruster incorporates a catalytic thrust chamber assembly using Shell 405 catalyst. The thruster nominally has a 40:1 expansion ratio bell nozzle. The RRS will require the design of a scarfed nozzle having a minimum 30:1 expansion ratio. The present configuration thruster incorporates a single coil single seat valve assembly. A delta qualification will be performed to provide a dual coil, dual seat configuration for the RRV. The new configuration thruster will weigh 5.5 lbs compared to the original 3.43 lbs. The weight increase is attributable to the additional valve assembly.

6.5.4.3.3 AC Thruster. The attitude control thruster is a Hamilton Standard REA 17-7 0.5 lbf thruster (Figure 6.5-4).

IDENTIFY



REA 20 THRUSTER

COMPONENT	WEIGHT (LB _M)	
	MARK II THRUSTER	GRO THRUSTER
THRUST CHAMBER ASSEMBLY	2.20	2.20
PROPELLANT CONTROL VALVE	1.50	0.96
THRUST CHAMBER HEATER	0.21	0.21
CHAMBER TEMPERATURE SENSOR	0.06	0.06
PROPELLANT VALVE HEATER	0.02	0.02
TOTAL	3.78	3.43

156-31A

REA 20 THRUSTER WEIGHTS

Figure 6.5-3. Hamilton Standard Main Maneuver Thruster

Over 232 thrusters have been built and flown on a DoD program. The configuration has a dual seat Wright propellant valve. The thruster has a 135:1 expansion ratio bell nozzle. The thruster valve would require modification and a delta qualification for the RRV dual coil valve configuration. The thrusters are grouped in series of three to allow common heater and heatshield use. This will save power and overall subsystem weight. The REA17-7 estimated weight is 1.0 lb with the dual coil, dual seat valve.

6.5.4.3.4 Latching Valves. The latching valves are bistable dual coil/single seat units manufactured by Vacco Industries. The Vacco valves are flight qualified and will fly on the Aussat B and UHF follow-on satellites. The valves incorporate an all-titanium construction and have teflon soft seats. The current valve has a 3/8 inch inlet/exit port. The RRV configuration may require increasing the seat and inlet/exit port diameter to 1/2 inch to limit pressure drops during the de-orbit burns.

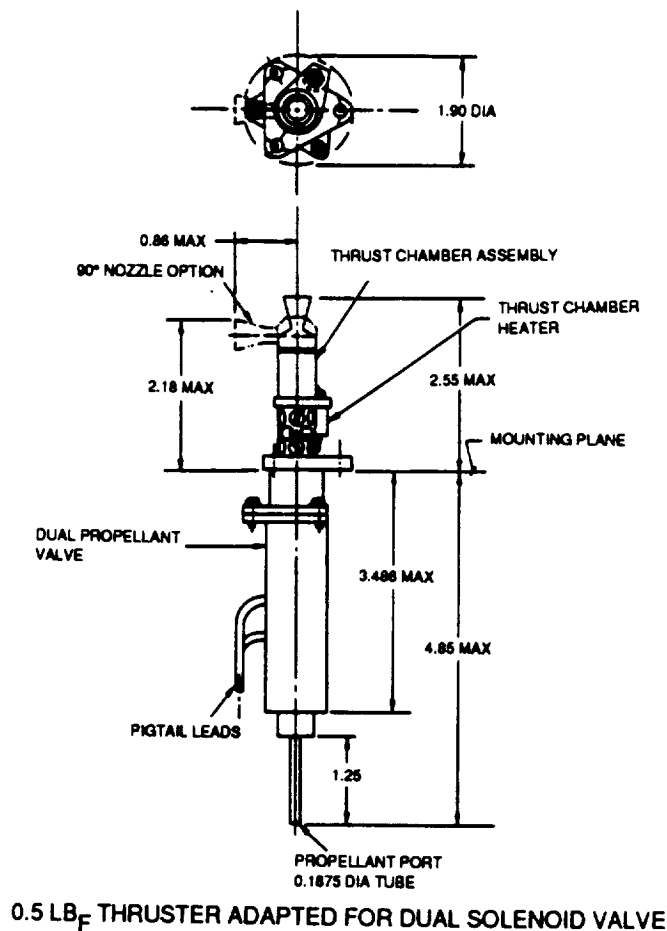


Figure 6.5-4. Hamilton Standard ACS Thruster

6.5.4.3.5 Filters. The main filters are an etched disk titanium element in a titanium body. They are manufactured by Vacco industries and have 1/2 inch inlet and exit ports. The filters weigh 0.5 lb each.

6.5.4.3.6 Fill/Drain Valves. The fill and drain valves are all titanium designs incorporating a hard seat. The valves are manufactured by Vacco industries, and have been successfully flown on numerous long life space vehicles. The valves incorporate a triple redundant sealing scheme to ensure no helium or propellant loss during a mission.

6.5.4.3.7 Pressure Transducer. The pressure transducer is a Gulton Industries piezo-electric sensor. The unit has a pressure range of 500 to 0 psia and an accuracy of ± 5 psia. It has flown on all Hughes HS-376 class satellites.

6.5.4.4 Interface Support. The primary electrical interface for propulsion is the GNC subsystem. This supplies all commands for system operation and thruster firings. The only commands not controlled by the GNC are the line and tank heaters that are controlled by switches independent of other systems. Table 6.5-6 details the other subsystem interface support for the propulsion subsystem.

Table 6.5-6. Propulsion Subsystem Interface Support

- | |
|---|
| <ul style="list-style-type: none">• Payload: No Requirement• GNC: Controls Valve Operations• TT&C: Telemetry State of Health Safe and Arm of System• Power: Provide Heater Power, Valve Power Through GNC System• Reentry: Supply Rotation Prior to Reentry• Thermal: Prevent Freezing or Overheat During Reentry Soak• Structure: Support and Alignment for Thrusters, Supports for Tanks• LV Adaptor: No Requirement |
|---|

6.5.5 Command and Control

Propulsion subsystem control is provided by the GNC subsystem with a ground override capability through the TT&C subsystem. Nominally, all burns are performed in a 3-axis thrust pulse modulation control scheme. This entails turning on or off at sufficiently high rates (on or off pulsing at 1 to 400 Hz) to align the thrust vector or offset to the CG of the vehicle. The rate is selectable by the GNC subsystem such that fundamental modes of the structure are not excited. Though CG alignments of the thrust vector produce pure translational motion, offset alignments produce combination translation and rotation. Thrusting perpendicular to the CG produces pure rotational motion. Nominal operation requires that all AC thruster operation be performed with pairs or thruster couples. The de-orbit maneuver uses all six main thrusters operating on a single set of coils. This ensures that any failure occurring during the burn does not necessarily require termination of the burn. Telemetry for the propulsion subsystem entails tank pressures and thruster temperatures for prefire condition. Other data includes tank and line temperatures and latch valve position switches.

6.5.6 Test

The thrusters are acceptance tested, hot fired with slave valves, while the flight valves are installed on the vehicle. This lowers the cost and delays associated with hot firing the thrusters using the flight valves. The propulsion subsystem testing performed at the contractor includes leak test of all valves and the entire subsystem, as well as proof pressure testing to 1.5 times maximum operating pressure.

6.5.7 Manufacturing

The RRV propulsion subsystem is installed on the Deployed Module main structure by the propulsion subsystem integrator. The tanks, latch valves, and thruster valves are all installed during the RRV manufacturing/integration process. The thrust chamber assemblies are installed during final vehicle assembly before subsystem test. The design goal is to employ a fully welded subsystem. This minimizes leak checks before and after flight. The detriment to an all welded subsystem is that component replacement is more difficult.

6.5.8 Refurbishment

Propulsion subsystem refurbishment is accomplished by purging the subsystem of remaining hydrazine, cleaning the subsystem with isopropyl alcohol, and drying and testing of all valves. Valve testing will consist of electrical, functional, and leak tests. The purge and dry operation can be performed by applying a vacuum to the subsystem as the tanks are rated for vacuum (-14.7 psid). The thrusters are removed from the valves and hot fired to determine their reusability. The total propellant usage of each thruster is estimated and a thruster is ineligible for reflight if it has come within 75% of the estimated lifetime propellant throughput.

6.5.9 Conclusions

The RRV propulsion subsystem implements flexible, highly reliable, and reusable design techniques. The high accuracy impulse delivery, along with the high total impulse capability, gives a mission flexibility not possible with other designs. The system also has built-in growth capability by using larger tanks or going to a dual mode system or both. The RRV can easily accommodate 23-inch tanks, giving a 77% increase in propellant capacity with only ~30 lbs additional dry mass. The dual mode system provides for 30% higher specific impulse and, coupled with larger tanks, can provide 2.3 times the presently designed impulse capability.

6.6 Guidance, Navigation and Control (GNC)

The purpose of the Guidance, Navigation and Control (GNC) subsystem is to provide overall command and control of the vehicle from umbilical ejection through post-flight securing. Functions to be performed include:

- Vehicle Health Assessment and Safing
- Vehicle Attitude Determination
- Vehicle Attitude Control
- Precision Orbit Determination
- Precision Reentry Control
 - Pre-Burn IMU Alignment
 - Thrust Vector and Burn Duration Control
- Precision Location Determination

6.6.1 Operations Timeline Support

Since the RRS cannot operate as an integrated vehicle without the GNC, operations concerning the GNC subsystem occur during all phases of the RRS operations. The following discussion presents an integrated view of GNC operations/requirements commensurate with the operations timeline discussed in Section 5.0.

6.6.1.1 Pre-Launch Phase. The pre-launch phase begins with mission initiation and consists of payload selection, mission planning, experiment verification, biocompatibility testing, vehicle integration, and launch site activities. The following GNC requirements apply during this phase:

- a. Identify any mission-unique GNC requirements and develop/test any software modifications.
- b. Perform GPS/IMU launch pad alignment checks.

6.6.1.2 Vehicle Operations. The GNC subsystem must perform the following functions during RRS operations. Those requirements identified with an asterisk (*) are specified by the NASA SRD. All others have been derived in the development of preliminary vehicle design.

6.6.1.2.1 General. The following requirements apply to all phases of vehicle operations:

- (*) a. Perform attitude determination, stabilization, and control functions at any orientation as required throughout all phases of the mission.

- b. Provide on-orbit calibration of inertial (IMU) reference.
- (*) c. Perform relative and actual three axis position/velocity determination.
- d. Provide telemetry data necessary for precision orbit determination.
- e. Provide position, velocity, acceleration (impact), and attitude data for tracking beacon telemetry and recovery operations.
- (*) f. Control all propulsion subsystem operations.
- g. Provide correct thrust vector application for attitude, orbit adjust, and de-orbit maneuvers.
- h. Provide for closed and extended mode de-orbit operations.
- i. Execute real-time/stored commands to create/maintain proper vehicle configuration.
- j. Accept and validate ground reprogramming of GNC/propulsion and payload onboard programs.
- k. Monitor power use, and perform load sheds, as necessary, to ensure vehicle and payload safety, in that order of precedence.
- l. Provide State-of-Health and payload data control and storage.
- (*) m. Payload mass storage devices shall be removed and delivery to the PI consistent with post-landing payload access requirements.

6.6.1.2.2 Launch Phase. The launch phase begins with liftoff (first motion), and continues to to RRV/LVA separation. The following requirements apply:

- a. Provide for parachute deployment in the event of catastrophic launch failure. (Assumes destruct command initiated faring/payload release.)
- b. Determine injection location and attitude in any orientation.
- c. Provide attitude control and de-orbit operations in the event of payload release failure.
- (*) d. Adjust orbital parameters to correct launch errors.

6.6.1.2.3 Orbital Flight. The orbital flight phase begins upon insertion (RRS separation), and concludes with first de-orbit command. The following requirements apply:

6.6.1.2.3.1 Pre-Mission Checkout

- a. Adjust vehicle to proper power/thermal attitude for safe extended operations in preparation for vehicle checkout.

- b. Provide controlled, common rate extension of tri-mast assembly.
- c. Monitor nut-deployment mechanism (NDM) for proper operation.
- d. Activate/control all three lanyard retraction mechanisms in event of any NDM failure.

6.6.1.2.3.2 Mission Operations

- (*) a. Control attitude rates to provide a uniform gravity environment for the entire payload during selected portions of flight.
- (*) b. Microgravity (Figure 6.6-1)
- (*) 1. Control gravity levels to $\leq 10^{-3}$ during the entire Orbital Flight Phase, and $\leq 10^{-5}$ during 95% of the phase.
2. Payload magnetic field levels shall be minimized during the entire Orbital Flight Phase.

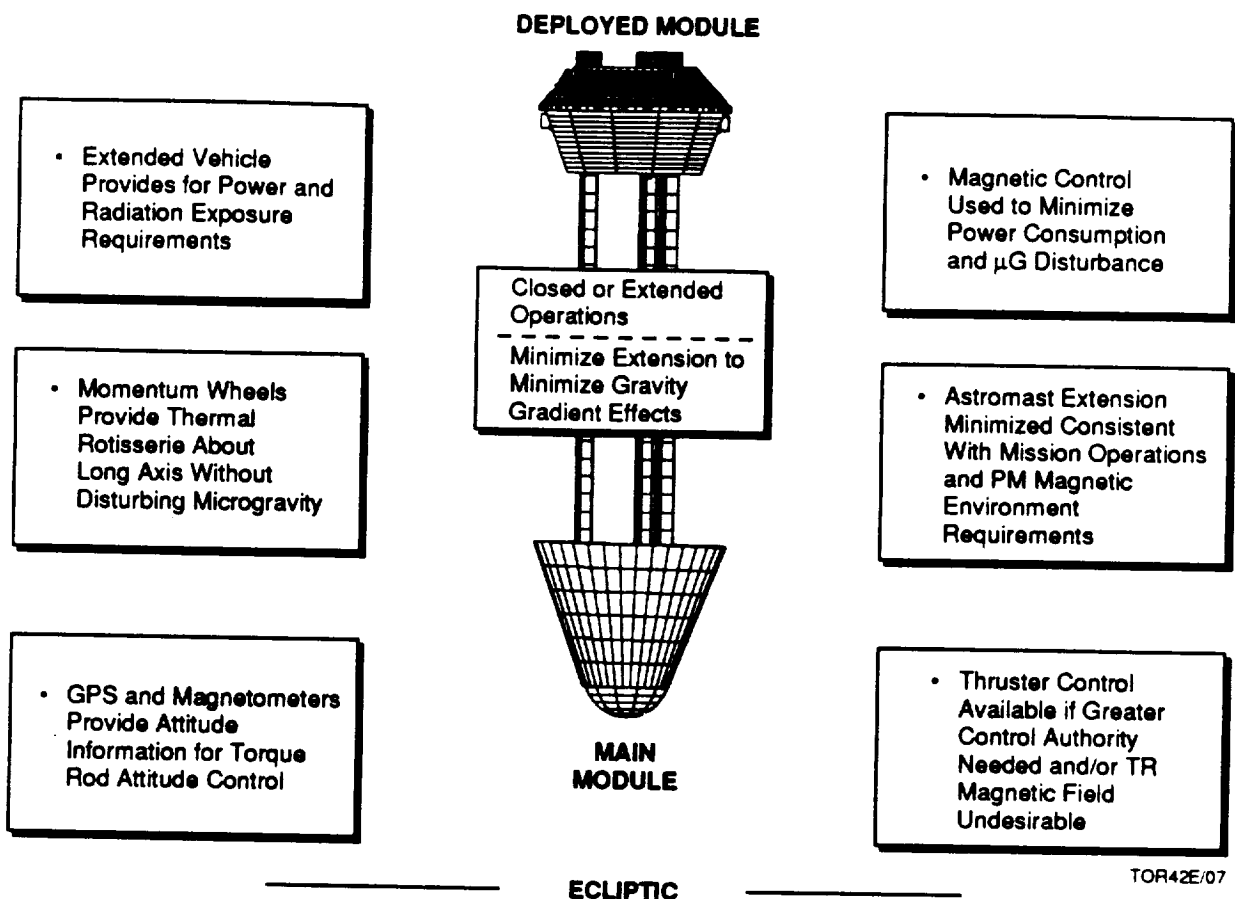


Figure 6.6-1. GNC Orbital Flight – Extended μ G

- (*) c. Fractional gravity (Figure 6.6-2)
- (*)
 1. Spin up to, and maintain steady within $\pm 10\%$, artificial gravity acceleration at any selected value between 0.1 and 1.5 g.
 2. Provide inertial stiffening for the axis perpendicular to the spin plane to establish a preferential spin plane.
 3. Provide inertial monitoring/control and independent reference assessment of vehicle dynamics throughout the full 360 degrees of rotation.
 4. Provide monitoring/correction of the structural dynamics/stresses to ensure vehicle safety.
- (*)
 5. Provide the capability to de-spin for microgravity levels in the same flight.

6.6.1.2.4 Recovery Phase. The recovery phase consists of the following three phases: De-orbit, Reentry and Terminal. The primary requirement for these phases is that all performance-critical functions shall be fail operational (i.e., no single failure shall preclude required performance and/or jeopardize public safety).

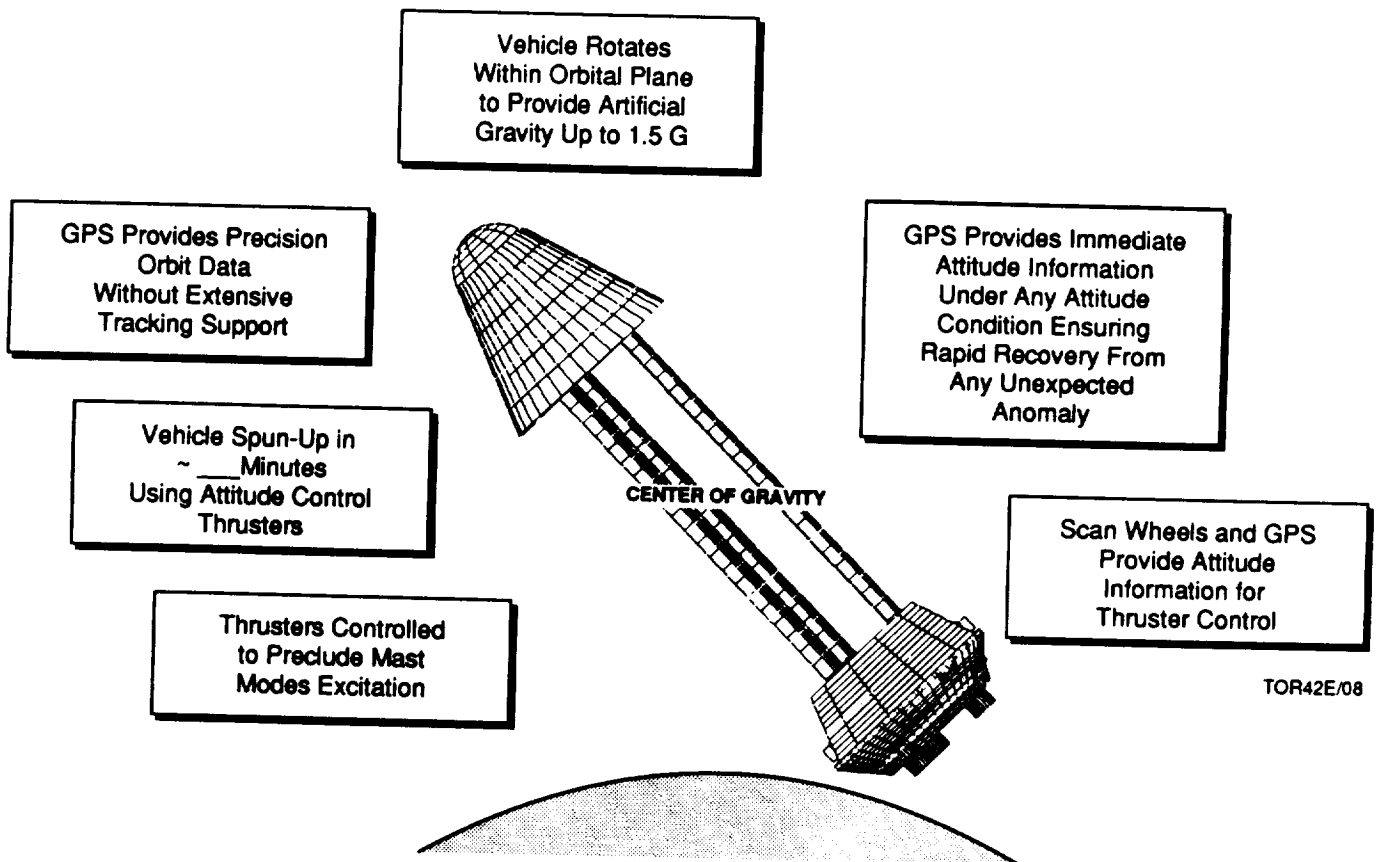


Figure 6.6-2. Extended Vehicle – Artificial Gravity

6.6.1.2.4.1 De-orbit Phase. The de-orbit phase begins with the first de-orbit command, and continues until the vehicle is aerodynamically reoriented for reentry. The following requirements (Figure 6.6-3) apply:

- a. Prepare for de-orbit.
- (*) b. Adjust orbital parameters for compatibility with recovery site requirements.
- c. Provide pre-burn on-orbit calibration of inertial reference system.
- (*) d. Provide necessary velocity changes for de-orbit maneuvers.
- e. Perform a main burn with a 3-sigma performance that does not exceed the required ΔV .
- f. Perform a trim burn to attain the required ΔV within 1-sigma.
- g. Prepare for reentry.
- h. Provide re-orientation for minimum dispersion aerodynamic reentry.
- (*) i. Spin up sufficiently (1 to 2 rpm) to ensure uniform ablation during reentry.

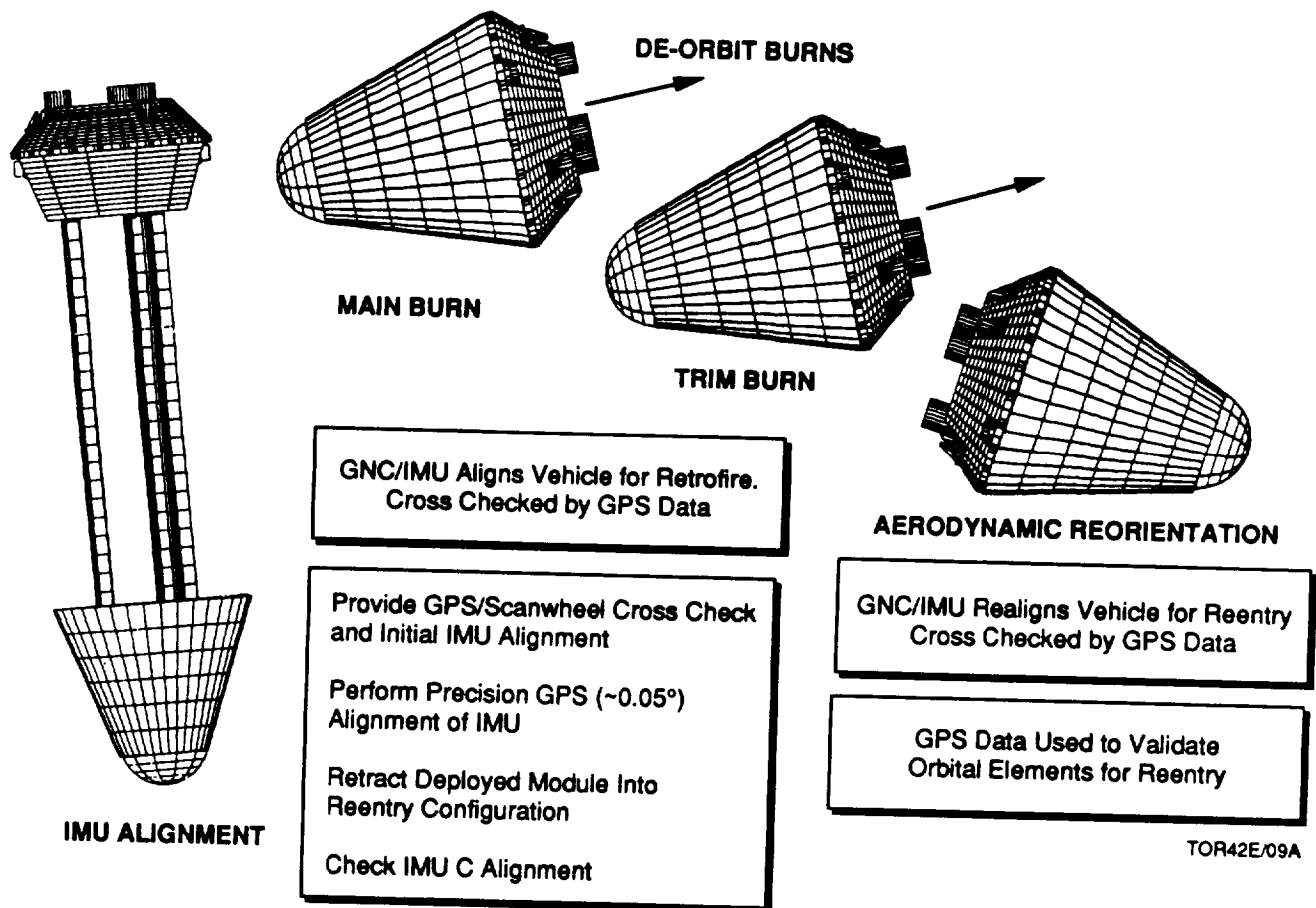


Figure 6.6-3. GNC Recovery – De-Orbit

6.6.1.2.4.2 Reentry Phase. The reentry phase begins when the vehicle is oriented for reentry, and continues until the pilot parachute is deployed. The following requirements apply:

- a. Activate homing beacon, and transmit Global Positioning System (GPS) position data at mission-determined altitude.
- b. Command pilot parachute release based upon mission-determined IMU/GPS/barometric altitude (timer backup).

6.6.1.2.4.3 Terminal Phase. The terminal phase begins with pilot chute deployment, and continues until landing. The following requirements apply:

- a. Provide IMU/GPS guidance for gliding parachute.
- b. Provide Differential GPS (DGPS) altitude determination for landing.

6.6.1.2.5 Post-Recovery Phase. The post-recovery phase begins with landing and continues until: 1) the experiment/data is delivered to the Principal Investigator (PI) and, 2) any ground control experiments completed. The following requirements apply:

- a. Power down vehicle to conserve power and minimize thermal load.
- b. Maintain homing beacon/telemetry with vehicle location, attitude, acceleration, power and thermal data.
- c. Maintain command/control capability, including ability to power down the TT&C subsystem and GNC data handling capability.

6.6.1.3 Ground Control Experiment Tests. These experiments are used to: 1) verify experiment design, 2) verify the hardware biocompatibility and performance, and 3) serve as controls for the flight experiments.

6.6.2 Design Requirements

The GNC attitude determination and vehicle control requirements encompass all operational phases from launch to landing. The operation of the RRS GNC Subsystem is critical to the successful completion of an RRS mission.

6.6.3 Trade Studies

Although there were no tradeoff studies specifically required by the Statement of Work, a study was performed to determine the configuration of the GNC subsystem. The results of this

study, presented in Section 6.6.4.1, Subsystem Architecture, represent a standard application of space-proven technology with one exception, the unique use of the GPS for attitude determination. The use of GPS receivers to determine satellite position has been successfully demonstrated (e.g., LandSat) during the GPS R&D (Block I) operations.

The GPS, currently deployed into a 6-plane, 24-satellite operational constellation, provides worldwide two-dimensional positioning service. The system is scheduled to achieve full three-dimensional capability well before the initial launch of the RRS, and will provide excellent capability. Although the system's location (positioning) performance (Figure 6.6-4) varies, due to the dynamics of the constellation geometry (Dilution of Precision (DOP)), the available system performance for a 21-satellite system (allowing for 3 random failures) is generally a factor of 2 to 3 better than the nominally stated performance (DOP of 6).

- 21 Satellite Constellation, 12 Hour Plot
- Receivers at 800Km Altitude
- GPS Advertised Accuracies are for DOP = 6

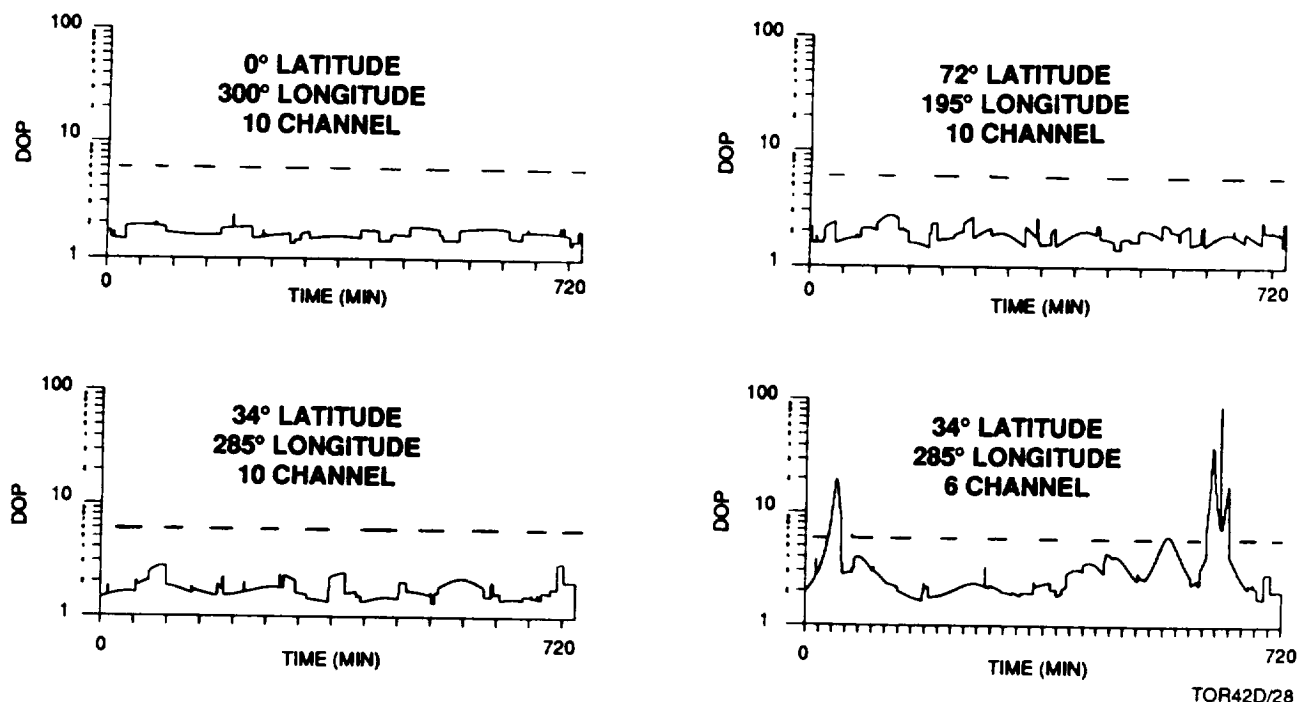


Figure 6.6-4. Typical GPS Performance

The potential cost savings achieved by using GPS just for the position determination functions (Table 6.6-1) justifies the use of GPS as a basic part of the RRS GNC. Since the further use of the GPS receivers for attitude determination does not add any additional hardware to the basic fail operational configuration, and use of GPS to determine direction (a vector, and any two vectors will provide vehicle attitude) is a proven surveying technique, the attitude determination function is available at minimal additional cost.

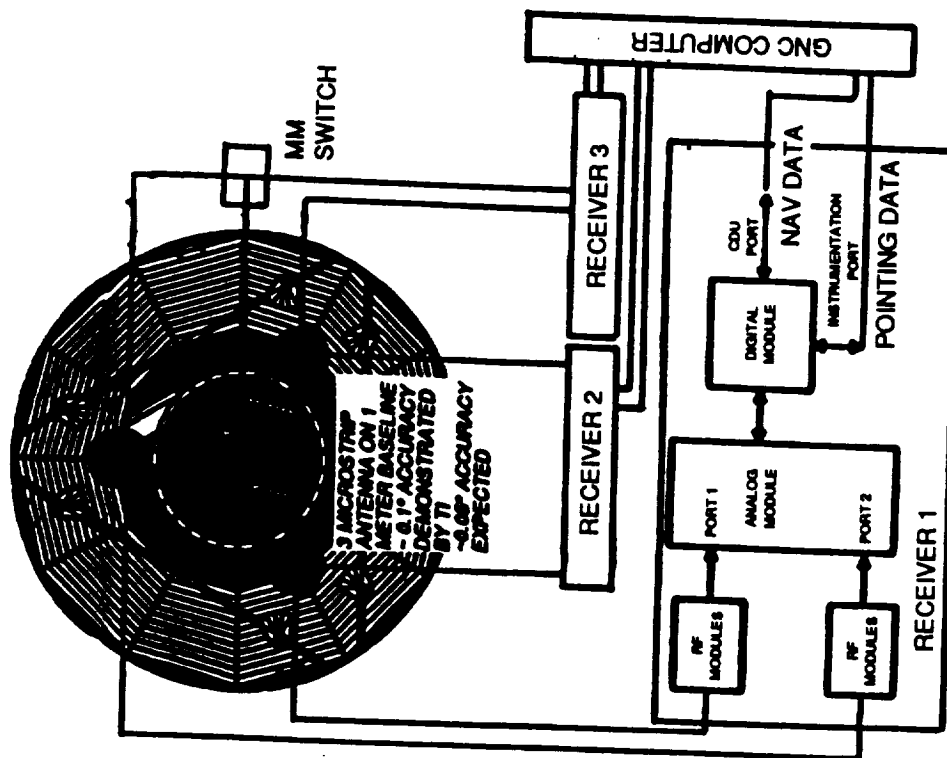
Table 6.6-1. RRS Unique GPS Applications – Safety and Cost Driven

• LOCATION	
-	Recovery Force Support
-	Relative RRS/RF Location (<1 m) Reduces Force Cost and Recovery Time
-	Precision Parafoil Landing Without Predeployed Recovery Force Support
-	Orbit Determination
-	Precision Capability Without Ground Tracking Reduces Operations Cost
-	JPL Has Demonstrated GPS/SA Independence
-	Main Burn Assessment
-	Triple Redundant Independent Public Safety Impact Assessment
• ATTITUDE	
-	IMU On-Orbit Calibration Corrects Gyro Drift
-	Minimized Deorbit Burn Thrust Vector Alignment Error
-	Vehicle Independent Anomaly Correction
-	Orientation Independent Attitude Determination
-	Immediate Data for Ground Corrective Action
-	No Sun/Earth Search Procedure Required
-	Immediate Auto-Reorientation for Power/Thermal Safety
-	Vehicle Independent Anomaly Correction
-	Deorbit Burn and Reentry Alignment Check

Using GPS to determine a pointing vector is the least known of the three modes of GPS user operations (Table 6.6-2). NASA/JPL demonstrated this basic GPS capability with the Rogue/DC-8 experiment in 1988, and several organizations are investigating the use of the technique for vehicle attitude determination. The use of the technique for surveying has been successfully demonstrated and widely reported by several companies. The key to high precision vector determination is elimination of common system errors.

The Texas Instrument (TI) AN/PSN-9 receiver (Figure 6.6-5) was chosen for the RRS task because of the unique dual port subchip sampling design that allows virtual elimination of critical common system errors. Furthermore, the receiver software does not have the low altitude limit typical of most other GPS receiver designs. This has allowed TI to propose, and NASA/GSFC accepted in principle, the use of the AN/PSN-9 for an STS attitude determination experiment. The TI 1 meter baseline surveying field test data, which fortuitously simulates the 1 meter RRS application, clearly demonstrated an acceptable performance for the RRS application (Figures 6.6-6 and 6.6-7) when a microstrip/choke-ring antenna installation was used.

- TRIPLE BASELINE CONFIGURATION
 - Any Two Provide Vehicle Attitude
 - Dual Port (or Dual) Antenna
- TI UNIQUE TWO-PORT-PER-CHANNEL RECEIVER
 - Precisely Simultaneous Phase Measurement
 - Analog Module: Digital Differential (Ref/Slave) Phase Signals
 - Digital Module: Navigation; Single Difference Phase Data
- STRUCTURE DYNAMICS ASSESSMENT
 - AN/PSN Has 100 Foot Antenna Remote Capability
 - 3D Differential DM/MM Measurement Available



6.6-9

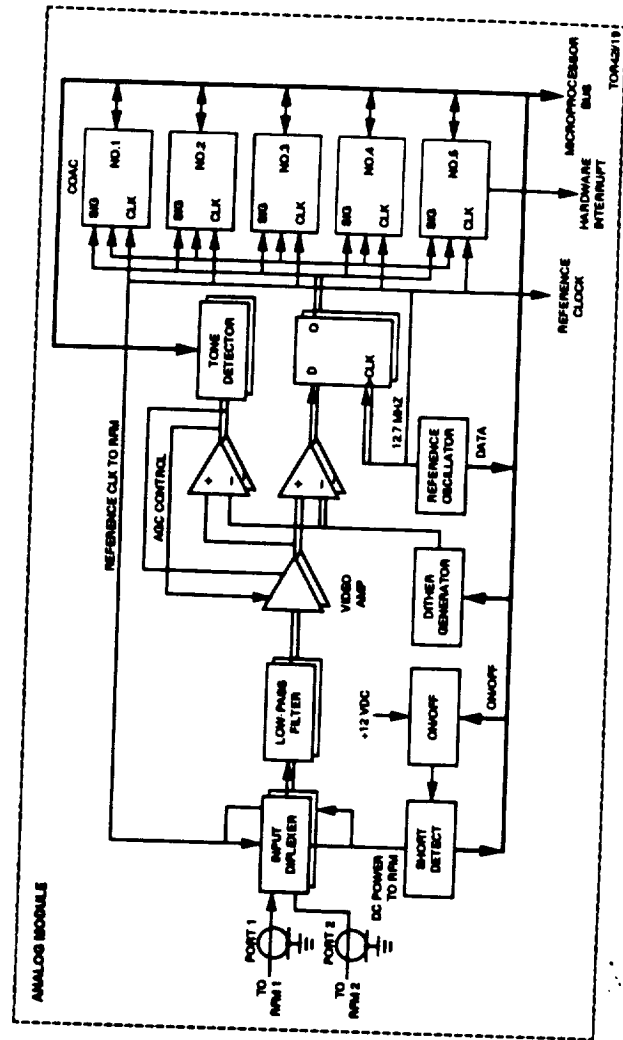
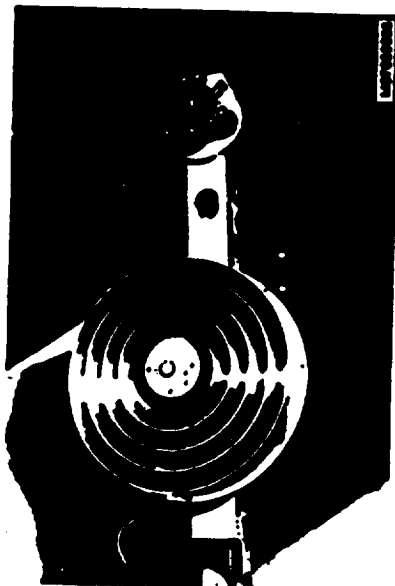
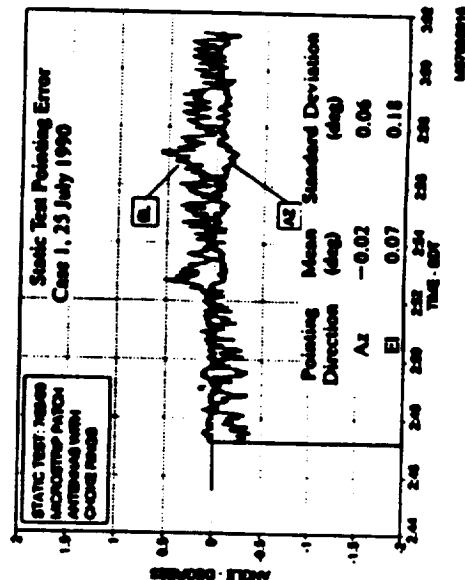


Figure 6.6-5. TI AN/PSN-9 RRS Configuration – A Space Capable Precision Pointing GPS Receiver



Microstrip Patch Antenna with Choke Ring Ground Plane

- GPS "DILUTION-OF-PRECISION" (DOP)
 - Constellation Geometry Effects Observable, Proportional to DOP
 - - Operational Constellation Has Better Geometric Availability
 - - Orbiting Systems Have Better Satellite Availability and Geometry
 - SV Selection Should Be Optimized for Performance
- MULTIPATH
 - SV 13 Had High Noise Attributable to Multipath Interference
 - Consistently Observed for Low Elevation Angles
 - RRV Configuration Has No Comparable Low Angle Obstructions



Example of AZ and EI Pointing Error During Static Test

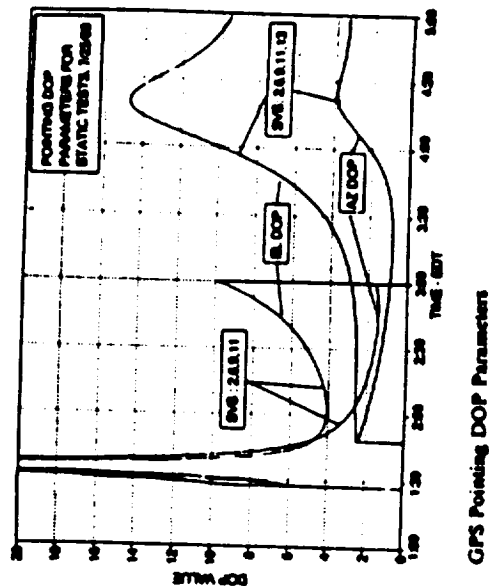
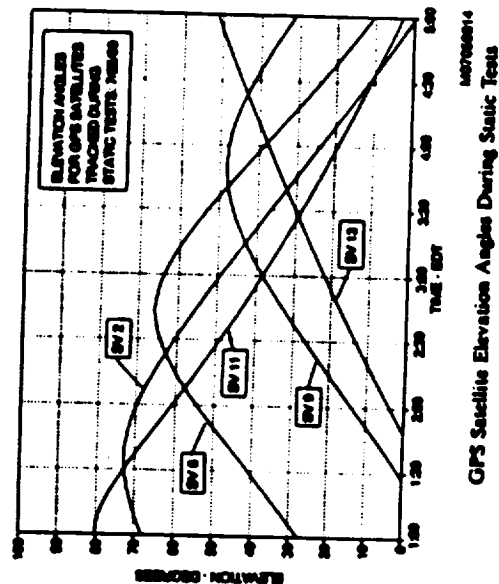


Figure 6.6-6. TI AN/PSN-9 Field Test Data - Geometry (DOP) and Multipath Effects

- EARLY TEST SHOWED SIGNIFICANT DEGRADATION FOR <1M ANTENNA BASELINE

- MULTIPLE ANTENNA AND GROUND PLANE CONFIGURATIONS TESTED WITH 1M BASELINE

- Microstrip Patch: Sensor Systems Model S67-1575-2 Airborne L1 GPS

- Drooped Turnstile: Dome and Margolin DM C146-Series L1 GPS

- No Ground Plane, 2 Ft Diameter Flat Plate, JPL Choke Ring Assembly

- MICROSTRIP PATCH WITH CHOKE RING ASSEMBLY PERFORMED BEST

- Mean Error Under 0.1 Degrees, Azimuth and Elevation

- Instrumentation Port Phase Data Processed by External Computer

Table 5. Summary of November 1989 Test Results

Antenna Separation (M)	Az Error (deg) Mean	EI Error (deg) Mean	Number of Tests
0.25	-3.35	-5.00	1
0.50	-9.85	3.00	1
0.75	2.15	-3.00	1
1.00	-0.11	0.72	15
2.00	0.03	-0.63	2
3.00	0.09	0.42	3

Table 3. Static Test Results, 25 July 1990

Case	Azimuth (deg)		Elevation (deg)		Time Local	Number of Samples	Double Difference (mm)	
	Mean	Standard Deviation	Mean	Standard Deviation	Start	End	Standard Deviation	
1	-0.02	0.06	0.07	0.18	2:45	3:01	849	1.7
2	-0.08	0.09	-0.24	0.21	3:05	3:20	838	2.8
3	-0.04	0.11	-0.67	0.34	4:03	4:19	479	6.2
4	0.05	0.14	0.07	0.24	1:57	2:14	925	2.2
5	-0.17	0.13	-0.39	0.16	2:20	2:36	744	4.3
6	0.06	0.18	-0.58	0.52	3:41	3:58	844	3.6

Table 4. Static Test Results, 26 July 1990

Case	Azimuth (deg)		Elevation (deg)		Time Local	Number of Samples	Double Difference (mm)	
	Mean	Standard Deviation	Mean	Standard Deviation	Start	End	Standard Deviation	
1	-0.04	0.08	-0.05	0.23	2:37	2:54	947	2.2
2	-0.15	0.07	0.39	0.17	2:57	3:16	1080	2.4
3	0.12	0.13	-0.50	0.29	3:59	4:15	880	5.8
4	-0.06	0.10	0.10	0.23	1:49	2:08	639	2.0
5	-0.28	0.08	0.27	0.21	2:14	2:30	560	4.8
6	0.10	0.19	-0.67	0.88	2:29	2:54	890	3.8

Table 1. Antenna Configuration Tested

Case	Description
1	Microstrip Patch Antenna and Choke Ring Assembly
2	Microstrip Patch Antenna and Flat Plate Ground Plane
3	Microstrip Patch Antenna With No Ground Plane Structure
4	Drooped Turnstile Antenna and Choke Ring Assembly
5	Drooped Turnstile Antenna and Flat Plate Ground Plane
6	Drooped Turnstile Antenna With No Ground Plane Structure

Figure 6.6-7. TI AN/PSN-9 Field Test Data - Multiple Antenna Configurations



Table 6.6-2. GPS Attitude Determination – Adaptation of Ground Proven Technology

<ul style="list-style-type: none"> • GPS MODES OF OPERATION <ul style="list-style-type: none"> - Time/Position - Normal Operations <ul style="list-style-type: none"> - Single Receiver and Antenna - Least Accurate; Location Within GPS Frame of Reference - Relative Position - Differential Navigation <ul style="list-style-type: none"> - Among Multiple Single Receiver/Antenna Observations/Sets - All Receivers With Common System Error Base - Pointing - Carrier Phase Surveying ("Interferometer") <ul style="list-style-type: none"> - Single Receiver With Dual Antenna - Common System and Receiver Error • APPLICABLE FIELD TEST EFFORTS <ul style="list-style-type: none"> - NASA JPL - 1988 - DC-8 Aircraft Azimuth/Pitch Measurements <ul style="list-style-type: none"> - 23M Antenna Baseline with Dual, Common Clock JPL/Rogue Receivers - Texas Instruments - 1989 - Land Survey Azimuth/Elevation Measurements <ul style="list-style-type: none"> - 1M Antenna Baseline With Single, <u>Dual Port</u>, TI AN/PSN-9 Receiver - Magnavox - 1990 - Land Survey Azimuth/Elevation Measurements <ul style="list-style-type: none"> - 1M Antenna Baseline With Dual, Common Clock Magnavox Receivers - Adroit Systems, Inc. - 1990 - Land Survey Azimuth/Elevation Measurements <ul style="list-style-type: none"> - 1M Antenna Baseline With Single Ashtec XII (Modified) Receiver • PRIMARY ERROR SOURCES <ul style="list-style-type: none"> - Antenna Electronic Phase Center - Multipath
--

6.6.4 GNC Baseline Design

The unique RRS vehicle architecture requires precise control of the vehicle rotational rate while maintaining stability. To ensure vehicle safety in the event of anomalous attitude control operations, the GNC needs to be able to determine vehicle attitude in any random orientation. Similar "any attitude" performance is needed during deorbit operations, and to ensure precision terminal landing control. Confidence in the landing accuracy is necessary to ensure public safety, and is a major obstacle to overcome during the process of achieving eventual project approval by Congress.

6.6.4.1 Subsystem Architecture. There are a multitude of design drivers that have led to the current RRS GNC design concept. These drivers can be grouped into three categories: 1) system functional requirements; 2) capabilities currently available technology will support; and 3) limitations placed upon the system due to the unique requirements of the RRS mission.

The RRS GNC design has been influenced by the system functional requirements. Since the RRS has random orientation during mission operations, there are field-of-view restrictions on

the sensors used for attitude determination. During the reentry operations, there can be RF and optical interference due to retrofire burn, thus limiting the use of GPS or an optical device such as a star tracker, during this critical timeframe when a delta velocity error could cause landing outside of the required location. During landing maneuvers, the navigation and attitude references must be operational in order to ensure that range safety requirements are met. Since the RRS is operating autonomously during the majority of its mission profile, the GNC must have the capability to perform failure and upset re-initialization without intervention. Finally, the system reliability requirement of a 0.99 probability of recovering the experiment in a healthy condition has a considerable impact on the entire RRS system design, particularly for the GNC subsystem.

The use of available technology is a primary requirement for the RRS. For navigation and attitude control, the system components available include inertial measurement units (IMUs), sensors (stellar, earth and sun), magnetic detectors, and GPS receiver sets.

Limitations placed on the RRS by its various functional requirements drive the selection of GNC subsystem components. The requirement to operate in any random orientation requires attitude and navigation determination components to be either an IMU, magnetic, or GPS, eliminating the use of stellar, Earth, and Sun sensors as navigation sources. During reentry operations, the only system types that are capable of providing support are the inertial type during retrofire, and reentry with GPS available during reentry. During landing operations, the IMU, GPS receiver set, and landing aids can all be used to provide required landing accuracy. Since the RRS GNC must be available throughout the mission, random orientation causes component selection to be redundant, utilizing a combination of either stellar, magnetic, or GPS to perform navigation and attitude determination.

Because of functional requirements, available technology, and mission limitations, the RRS GNC subsystem must be a synergistic and redundant system made up of a variety of components that can provide the availability and random orientation performance in order to fulfill the RRS system requirements.

The RRS GNC design accommodates all phases and modes of operation. Following launch and insertion operations (Figure 6.6-8), the use of basic GPS position determination capability enables immediate determination of position and velocity. Since the GPS receivers will be operated during launch, this information could also be provided to the launch vehicle, if desired. Another advantage of having GPS operation during launch is the ability to immediately determine

vehicle attitude in any random orientation. This also allows rapid insertion error correction and orientation of the RRS to a preferable thermal condition.

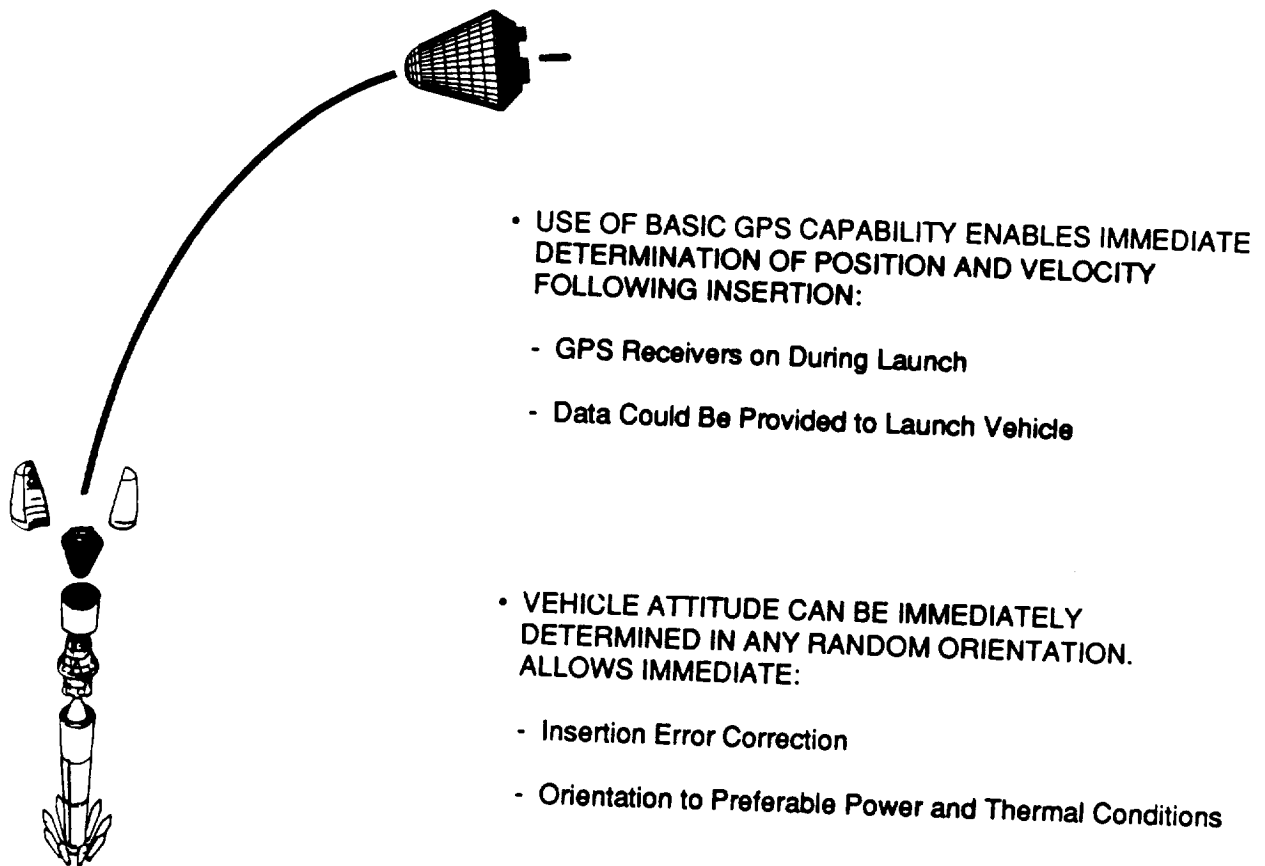


Figure 6.6-8. GNC Launch Phase

The RRS GNC provides support for all modes of required on-orbit operations (Table 6.6-3). Support provided by the GNC during tri-mast extension operations will consist of a GPS alignment, followed by extension under control of the IMU. Vehicle spin-up will be controlled by the IMU, and will be performed using thrusters. Although normal operations will be under IMU control, the GPS receiver set will provide a performance check and emergency backup. In addition, GPS will provide an inertial update, de-spin alignment, and orbit determination for recovery planning. Spin down operations will also be under IMU control using the thrusters. Tri-mast retraction will be performed with attitude control provided by the IMU. A final precision inertial alignment will be performed with GPS prior to reentry operations. Finally, orbital adjustments will be made under IMU control with GPS utilized for orbital determination.

Table 6.6-3. GNC On-Orbit Operations

- | |
|--|
| <ul style="list-style-type: none">• EXTENSION OPERATIONS<ul style="list-style-type: none">- GPS Alignment; IMU Control• VEHICLE SPIN UP<ul style="list-style-type: none">- IMU Control Using Thrusters• NORMAL OPERATIONS<ul style="list-style-type: none">- IMU Control- GPS Provides<ul style="list-style-type: none">– Performance Check and Emergency Backup– Inertial Update and Pre-Despin Alignment– Orbit Determination for Recovery Planning• SPIN DOWN<ul style="list-style-type: none">- IMU Control• CONTRACTION<ul style="list-style-type: none">- Final Precision Inertial Alignment With GPS- IMU Control• ORBITAL ADJUST<ul style="list-style-type: none">- IMU Control- GPS Orbit Determination |
|--|

Although the use of GPS during reentry and recovery operations provides multiple advantages, its implementation is constrained by potential interference of the retrofire with the GPS RF signal. This prevents use of GPS during this burn, even though it is more accurate than the IMU for the long burns needed for low G reentries. The solution to this dichotomy is to first align the IMU using GPS prior to retrofiring. Then, the IMU will be used for positive control during the retrofire burn. After the retrofire burn, GPS will be used to determine position and velocity information, while the IMU will control any corrections that may be required. During the landing phase, the basic 16-meter Spherical Error Probable (SEP) GPS accuracies can provide autonomous control to ensure adequate safety margins at any location on earth. DGPS operations will provide submeter precision landing capability at a GPS-surveyed position.

The GNC is central to the overall RRS architecture (Figure 6.6-9). The dual computers, one in each module, provide for independent operation of each module and the level of redundancy required for a fail operational system. All external communication is via the Deployed Module GNC computer. All communication within the RRS is via data bus within and between modules. The GNC design is priority driven (Figure 6.6-10) with safety being the most critical consideration. The attitude control configuration (Figure 6.6-11) is composed of an array of components, each with its own unique contribution (Table 6.6-4) to the overall mission. Conceptually and functionally, the control system consists of three parts:

- a. Attitude determination.
- b. Attitude control.
- c. Reentry control.

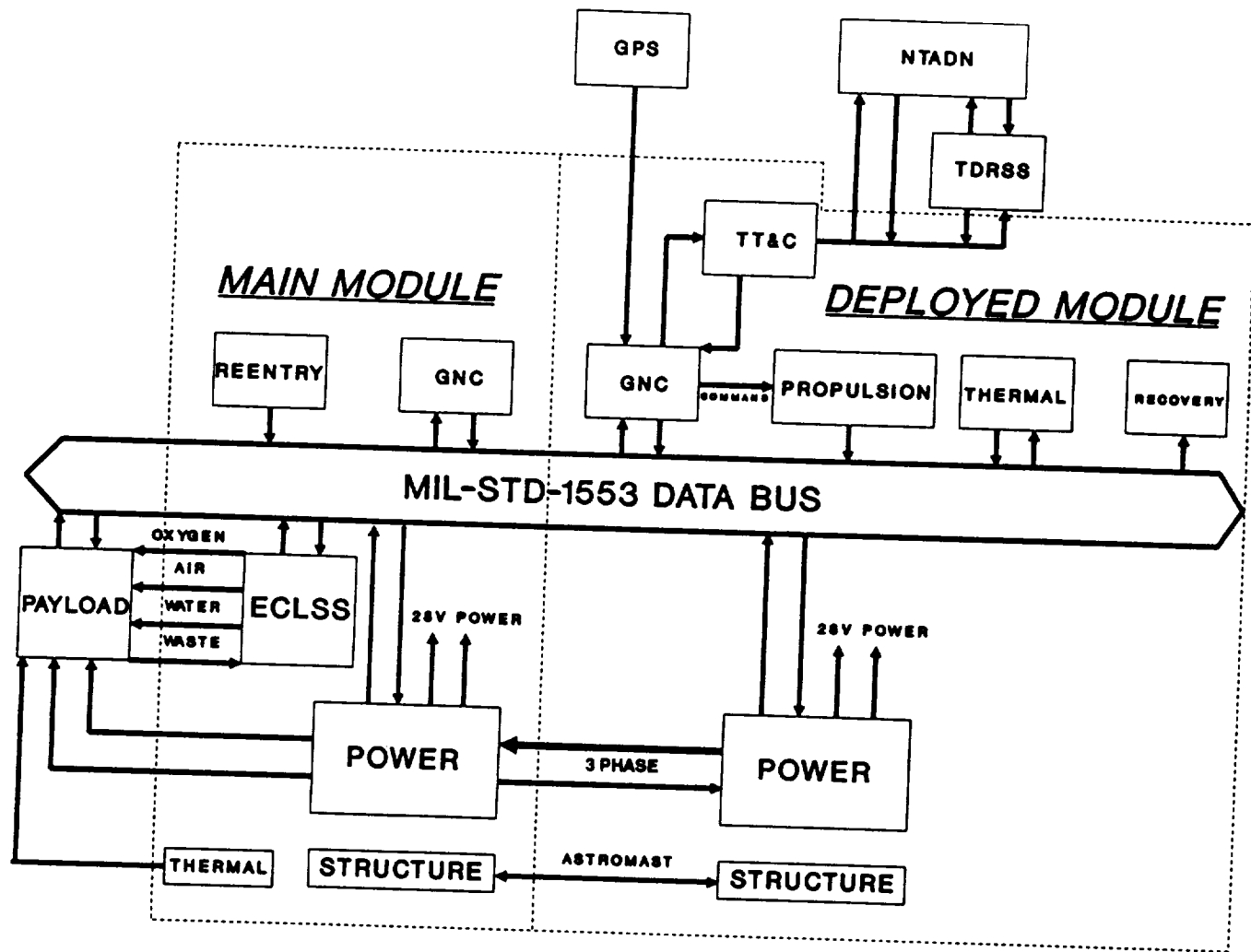


Figure 6.6-9. Architecture

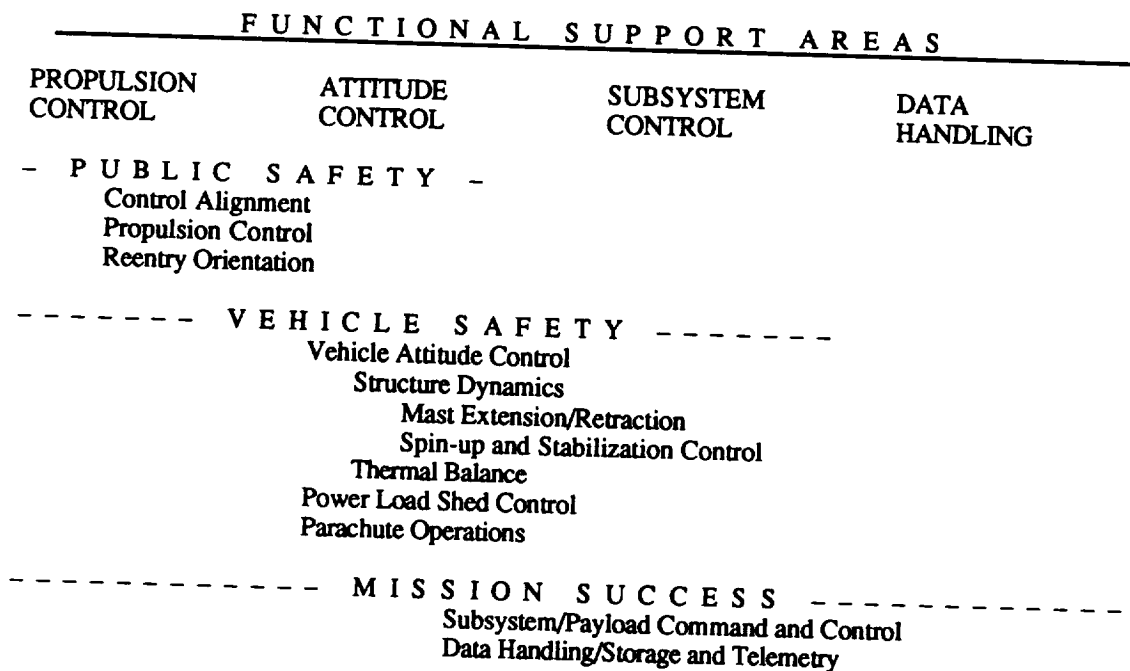


Figure 6.6-10. GNC Design Priorities

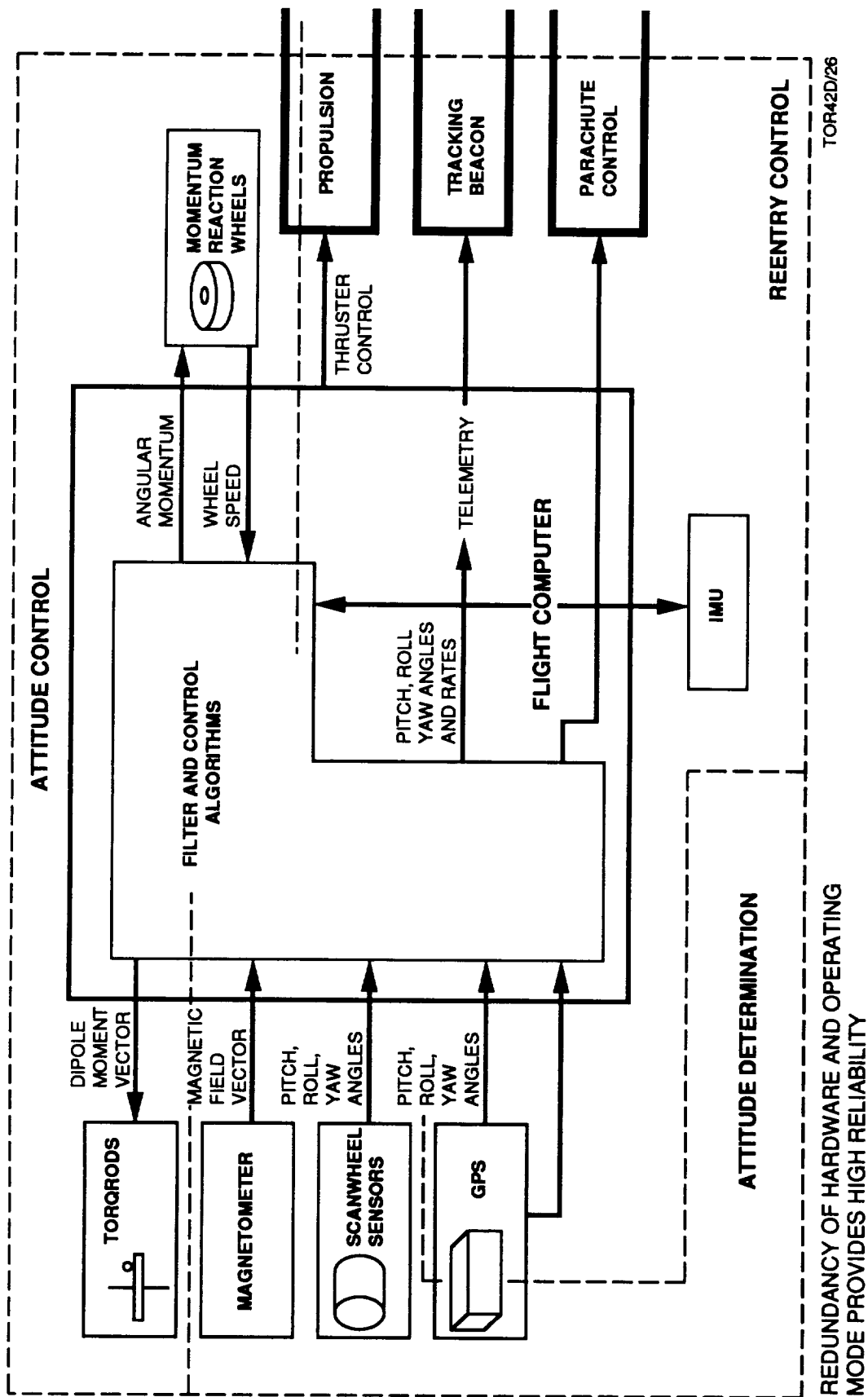


Figure 6.6-11. Attitude Control Configuration

Table 6.6-4. GNC Functional Allocation

EACH COMPONENT OF THE GNC HAS A UNIQUE APPLICATION			
<u>Component</u>	<u>Unique Use</u>	<u>Attitude Control</u>	<u>Other Use</u>
IMU	Deorbit Burn Control	AG Control	Launch, Structure and P/L Environment TLM
GPS	3D Location IMU Onorbit Calib. Main Burn Assessment	Orientation Independent Attitude Determination. Closed Mode Operations	Launch and Structure Telemetry
Magnetometer	Low Power Attitude Determination	Low Power Attitude Determination	Location Assessment
Torquerods	μ g Attitude Control	μ G Attitude Control	
Scanwheels	AG Axial Inertia	Rotating Attitude Determination	
Attitude Thrusters	Control Authority (Deorbit Burn; AG)	AG Vehicle Control	

6.6.4.1.1 Attitude Determination. The attitude determination portion of the RRS GNC contains three elements: magnetometers, scanwheel horizon crossing sensors, and GPS receiver.

The magnetometer is a two-axis flux gate instrument that provides magnetic field measurements for two spacecraft axes over the range of ± 1 gauss. These magnetometers provide the magnetic field vector to the flight computer, which then compares this to a stored reference magnetic field vector database to determine position of the vehicle. This process is fairly slow, and takes several orbits to accomplish.

The Scanwheel is a momentum/reaction wheel with an integral high accuracy Horizon Crossing Indicator (HCI). The wheel provides angular momentum, while the HCI obtains precise attitude information. These scanwheels provide Yaw, Pitch and Roll Angles to the flight computer in order to determine vehicle orientation. This process results in accuracies in the order of 0.5 degrees, and is subject to restrictions of vehicle orientation.

The GPS receiver set also provides Yaw, Pitch and Roll Angles, and accurate navigation information to the flight computer. The accuracy obtainable from the use of GPS is significantly better than that available from the other GNC components.

6.6.4.1.2 Attitude Control. GNC attitude control is maintained by the Kalman Filter and control algorithms that reside in the RRS Vehicle Computer. Attitude determination information obtained by the magnetometers, scanwheels, and GPS receiver is coordinated with the Kalman Filter and used to update the bias factors of the IMU. Vehicle attitude is then controlled by use of a combination of TORQRODs, momentum reaction wheels, and thrusters contained in the RRS propulsion system.

The TORQROD is an electromagnet consisting of a magnetic core and two coils, each of which provides a dipole moment of 350 Am^2 . Current flowing through the coil generates a dipole moment capable of interacting with an external magnetic field to produce a torque.

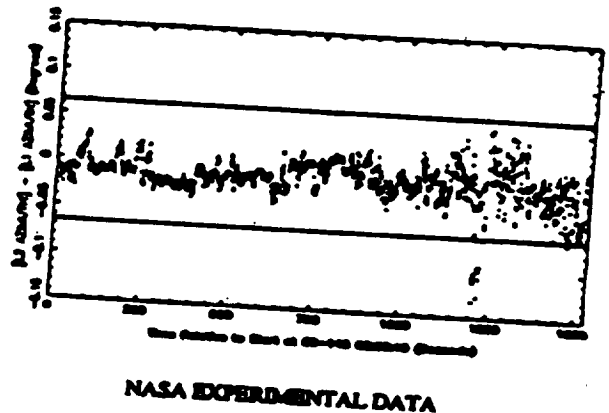
The basic approach of using GPS to provide attitude control is technically justified. Basic location information is obtained from the GPS code information. This technique of determining on-orbit position has been flight proven on LANDSAT. The precision location will be obtained by tracking the GPS carrier phase. The feasibility of performing this technique has been demonstrated on an aircraft (Figure 6.6-12). This experimental data was obtained from a recently completed NASA study program where precise aircraft azimuth (yaw) determination via GPS carrier phase measurements was demonstrated through post-flight analysis of experimental data. The results of this study clearly indicate that the pointing accuracies required for RRS (the horizontal lines), are achievable via the carrier phase technique. The two key issues that must be resolved for successful satellite use, how to perform on-orbit initialization and how to handle the potential cycle slips, have several possible solutions that are currently being investigated by several studies including an SAIC internal IR&D program.

The development of a process for initialization and phase cycle slips identification was initiated, in parallel with the analyses, to ensure consistency between subsystem requirements and current technology performance, and is being followed by the development of the initialization/identification process. The primary difficulty is that, unlike the standard GPS operation in which the pseudo-random code lock ensures knowledge of position within the modulation stream, the carrier phase contains no unique identifying features that allow discrimination among phase cycles.

Since the incident RF carrier from a given satellite will arrive at the RRS antennas at different times, the relation among the observed cycles must be established. Initialization (the process of determining which received cycles from a particular carrier correspond to each other) is performed by knowing the geometry of the satellite/space vehicle/antennas, and being able to calculate the time it takes for the incident wave to travel from one antenna to another.

TECHNICALLY JUSTIFIED

- BASIC LOCATION OBTAINED FROM GPS CODE INFORMATION
 - GPS On-Orbit Position Determination Has Been Flight Proven (LANDSAT)
- PRECISION LOCATION OBTAINED BY TRACKING CARRIER PHASE
 - Precise Aircraft Yaw Determination Has Been Demonstrated by Analysis of Aircraft Data



On-Orbit Process for Initialization and Cycle Slip Identification

Figure 6.6-12. GPS-Based Attitude Control Feasibility

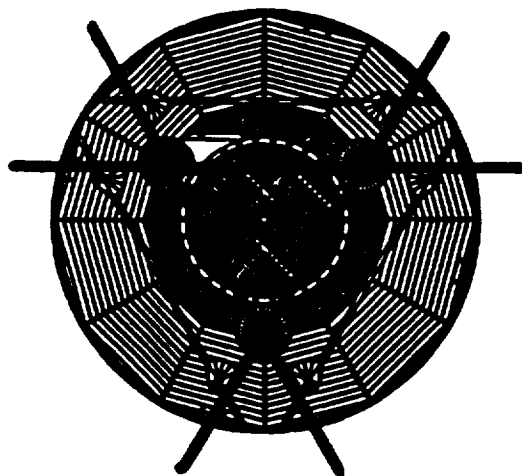
Cycle slips, which occur when phase lock on the carrier is lost, create two problems. First, they must be immediately identified to preclude performance degradation, and second, the magnitude of the slip must be determined for re-initialization. The reacquisition time following a cycle slip is a function of the processing capability and the phase lock-loop quality.

Another goal of the SAIC IR&D is to develop the RRS subsystem model and digital simulation required to assess the performance of the proposed techniques. The SAIC algorithm performance will then be evaluated using the simulated RRS subsystem to determine the probable system performance under random orientation conditions. The simulator development will be specifically targeted to enable integration with actual hardware to facilitate field testing.

6.6.4.1.3 Reentry Control. Reentry control (Figures 6.6-13 and 6.6-14) is maintained by the Vehicle Computer, which uses GPS receivers to align the RRS and re-initialize the IMU prior to retrofiring. Active control is provided via the IMU/Vehicle Computer during the retrofire process. Following retrorocket firing, the IMU is again aligned using the GPS receiver. If a second correcting retrofire is necessary, it will then occur. Redundancy of the hardware and operating modes is prevalent throughout the GNC design. In the event of a GPS receiver failure, the magnetometers can provide a similar, albeit degraded, capability. GPS receivers and

PREBURN INS CALIBRATION AND DE-ORBIT BURN ASSESSMENT

- CALIBRATION CAN BE DONE IN EXTENDED OR CLOSED CONFIGURATION
 - Full 3 Receiver GPS Operation
 - Uses 3 DM/GPS Antenna Baseline
 - Internal GPS Redundant Axis Check
 - Scanwheel Consistency Check
 - Structure Telemetry Data Adds Confidence if Extended
 - Upload Burn Time and Duration
- GPS ORBIT DETERMINATION (SA GROUND COMPUTATION CORRECTION)
 - Final Atmospheric (Wind/Density) Correction
 - Upload Burn Initiation Time and Duration



DE-ORBIT BURNS

- IMU THREE AXIS VECTOR AND DURATION CONTROL
 - Triple IMU/GPS/Computer Redundancy
- MAIN BURN - INCONSISTENCY ABORTS TO NO-BURN
 - Within Landing Zone at/Beyond Planned Impact
 - Clock Initiated Burn
 - Within GPS Time Window
 - Manual Override
- TRIM BURN - ERROR AUTOMATICALLY CORRECTED
 - Minimum Dispersion Correction
 - Triple GPS Location/Velocity Correction
 - Individual Satellite Data Sets
 - Assessment Telemetered to Ground
 - Limited Override Correction Window

TOR42D/26j

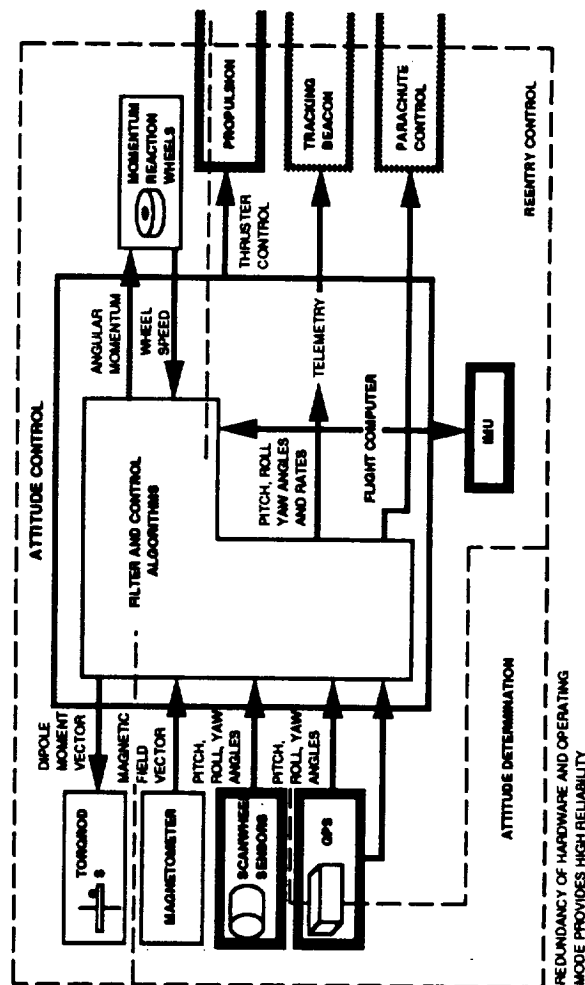


Figure 6.6-13. GNC Operating Configuration – Recovery Phase - De-Orbit

FAIL OPERATIONAL "THREE VOTE" ARCHITECTURE REQUIRED

- The Question of Failure is Not "If," But "When"
- Any Single Failure Must Not Affect Performance
- Anomalous Engine Performance Must Be Corrected
 - Abort, Main Burn Correction, Trim Burn

FUNCTIONAL REQUIREMENT

MEASUREMENT	INERTIAL AND ACCELERATION MEASUREMENTS Three IMUs Provide Three Independent Sets of 3-Axis Gyroscopic and Accelerometer Measurements
ASSESSMENT	3 AXIS INERTIAL, ACCELERATION AND ΔV DETERMINATION Each IMU Paired With an Independent Processor for Independent Vehicle Dynamics Assessment IMU Data Not Averaged Nor Shared to Preclude Error Propagation. Pre-Use Correlation Adds Complexity and Failure Modes
DIRECTION	PROPULSION CONTROL Three Independent Determinations of <ul style="list-style-type: none">- Attitude Assessment Consistency- Required Propulsion Activity<ul style="list-style-type: none">- Engine Selection and Burn Duration- Engine Performance- Current, Temperature, Acceleration
EXECUTION	VALVE CONTROL 2 Sets of 3 Engines, Each Engine Redundantly Controlled Real-Time Anomalous Performance Control

Figure 6.6-14. De-Orbit Propulsion Control

scanwheels are also similarly redundant in attitude determination capabilities. Tridundant units are also provided for the Vehicle Computer, IMU, Momentum Wheels, and GPS receiver equipment. This redundancy of equipment and operating modes will ensure an RRS GNC subsystem with very high reliability.

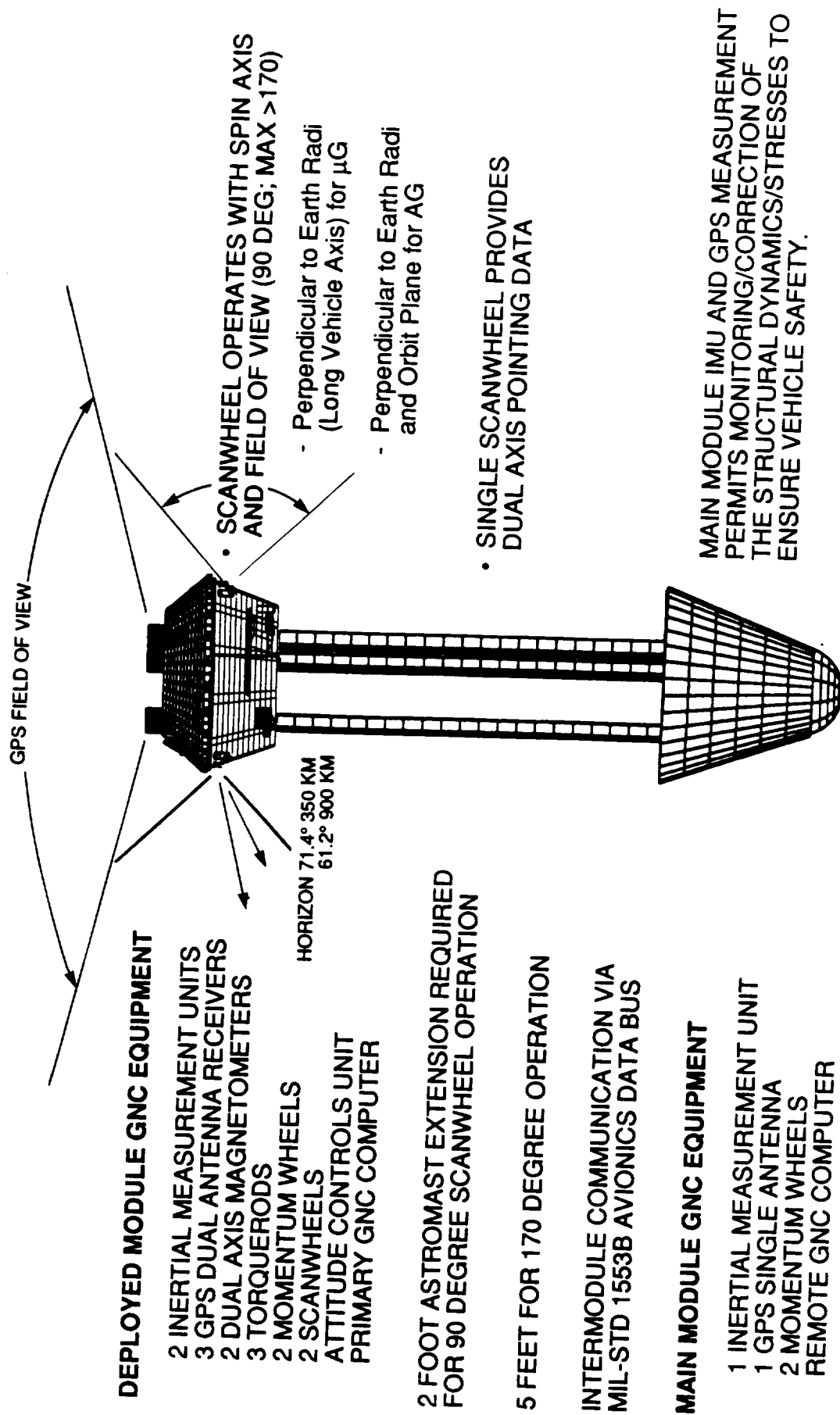
The sensor geometry of the RRS GNC is shown in Figure 6.6-15. The two principal sensor systems are the GPS receiver antennas and the scanwheels. In the microgravity mode, the magnetometer will provide primary control with the GPS set performing initialization and backup. The key consideration in the use of the scanwheels is that the tri-mast needs to be extended only about 5 feet to allow for use of the maximum possible scanwheel field of view.

In the artificial gravity mode, the scanwheels will provide the primary attitude determination data with GPS initialization and all orientation backup.

During the reentry and recovery operations, GPS will also be available to provide the precise field of view necessary to obtain very accurate attitude and navigation information.

A performance summary of the RRS GNC subsystem is contained in Table 6.6-5. The redundant nature of the RRS GNC architecture is clearly demonstrated in the attitude knowledge category. The MADs provides a reasonable amount of accuracy while GPS provides precision accuracy capability.

6.6.4.1.4 Precision Location and Attitude Information. The specific technique that will be used to provide precision location and attitude information is the use of differential GPS. Basic location information will be obtained using the GPS code information, and precision location will be obtained by tracking the carrier phase using advanced GPS receiver technology. Attitude determination will be performed using 3 5-channel receivers connected to 2 sets of antenna. These microstrip antennas will be mounted on the Deployed Module and have a one meter baseline between each leg. Recent testing by Texas Instruments (Figure 6.6-7) of their advanced GPS receivers has demonstrated a 0.1° accuracy, and TI expects this performance to increase to 0.05° when used with a matched antenna. The specific attitude determination technique to be used involves measuring the differences in phase caused by a change in attitude of the host platform. The phase shift induced by vehicle motion allows the new baseline coordinates to be solved and instantaneous attitude to be computed. The principal difficulty that must be handled with this approach is the detection of cycle slips and the method of re-initialization of the phase lock accuracy following such a cycle slip.



TOR42D/29

Figure 6.6-15. Attitude Control Sensor Geometry

Table 6.6-5. GNC Performance Summary

Case	Attitude Knowledge++					Attitude Control		
	MADS			GPS**		MADS		
	Roll (deg)	Pitch (deg)	Yaw (deg)	All Axes	Extended Pitch/Yaw	Roll (deg)	Pitch (deg)	Yaw (deg)
GG Stable	0.4	0.9	1.0*			0.1	0.1 (0.3)+	0.5 (1.2)+
Yaw Spin	0.4	0.9	1.0*	0.05	0.01	0.2	0.2	–
Spin Stable	0.2	0.2	0.5			0.1	0.1	0.3

* Improved MADS 3-sigma accuracy

** Absolute knowledge of control ordinates

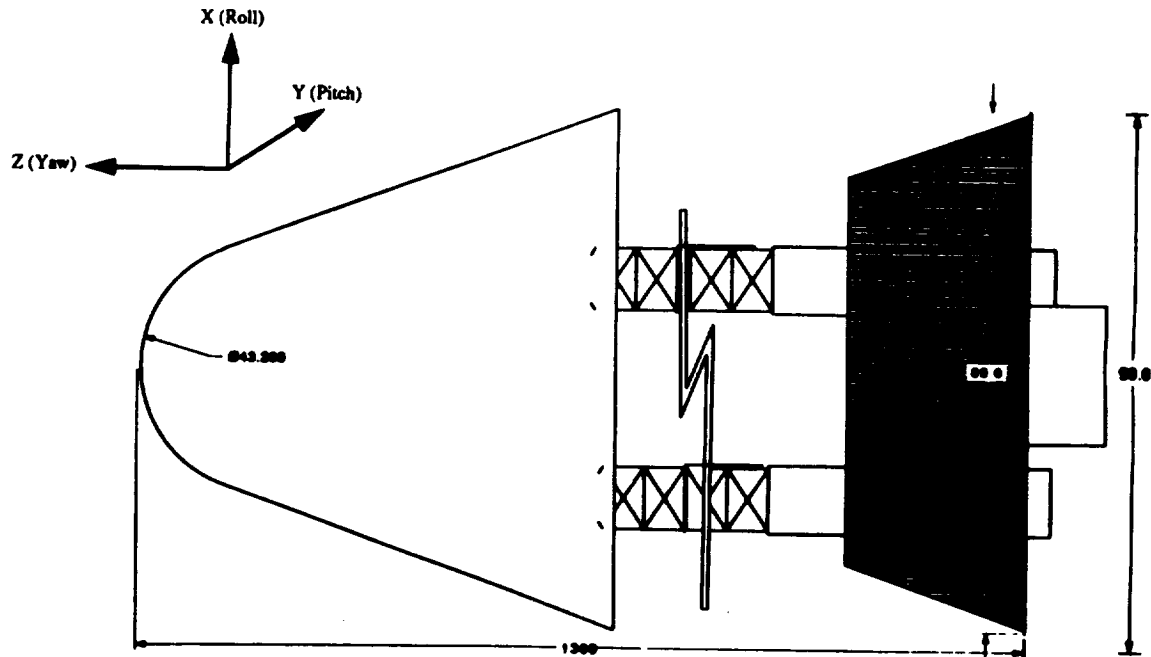
+ Attitude bias (drag and solar pressure) of control ordinates

++ Currently demonstrated to be ~0.1 with 1 meter baseline

A graphical representation of the typical performance of the GPS system for an RRS mission is presented in Figure 6.6-4. These four plots depict DOP versus time for several latitude/longitude combinations. The DOP value is an indication of location potential for a given set of geometries as a function of time for specific conditions. The advertised GPS accuracies are based on a DOP = 6, so actual performance of the RRS will be substantially better than the advertised 15m SEP as the $DOP \leq 2$ for these examples. Even the example for the 6-channel receiver consistently has a DOP of less than 6 despite brief periods where it blows up to 10 or more.

The spin-stabilized mode will be achieved through use of the propulsion subsystem thrusters controlled by the IMU. First, the spin axis will be oriented using magnetometers and TORQRODs. Then, spin-up and subsequent de-spin will be achieved using the thrusters. Reentry support will consist of vehicle alignment using GPS, scanwheels, and TORQRODs prior to retrofiring.

ITHACO, Inc. has performed analyses (Appendix E) of the performance of the RRS GNC subsystem during all operational modes. The satellite configuration used in these analyses is shown in Figure 6.6-16. Worst-case disturbance torques induced on the extended RRS configuration by solar pressure and atmospheric drag are presented in Figure 6.6-17. This worst case environment is for a 350 km, 33.83° inclination, circular orbit that has the largest atmospheric and smallest magnetic performance of all of the RRS design reference missions. The following analysis results represent these worst case environmental conditions.



Contracted: $I_x = 3340 \text{ Kg-m}^2$
 $I_y = 3340 \text{ Kg-m}^2$
 $I_z = 790 \text{ Kg-m}^2$

Extended: $I_x = 384916 \text{ Kg-m}^2$
 $I_y = 384916 \text{ Kg-m}^2$
 $I_z = 469 \text{ Kg-m}^2$

ITHACO

Figure 6.6-16. Satellite Configuration

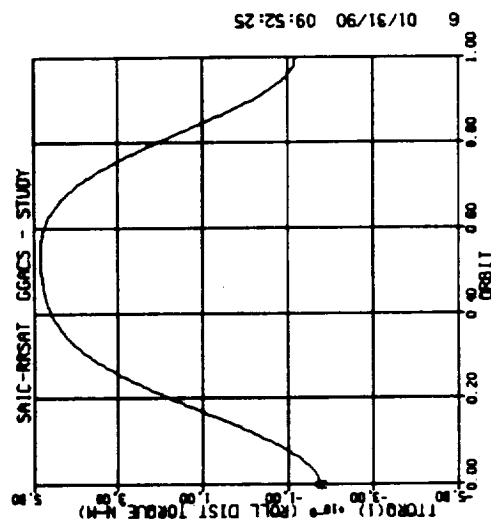
The RRS GNC configuration, in the microgravity mode, is presented in Figure 6.6-18. In the three-axis gravity gradient stabilized mode, attitude data is provided via Kalman filtering of GPS and three-axis magnetometer data. Active attitude control is provided by the three TORQRODs.

The RRS GNC configuration in the microgravity mode, with a thermal balance rotation, is presented in Figure 6.6-19. As in the three-axis gravity-gradient stabilized mode, attitude data is provided via Kalman filtering of GPS and three-axis magnetometer data, and active attitude control is provided by the three TORQRODs. The additional Yaw rotation is provided by the momentum wheel.

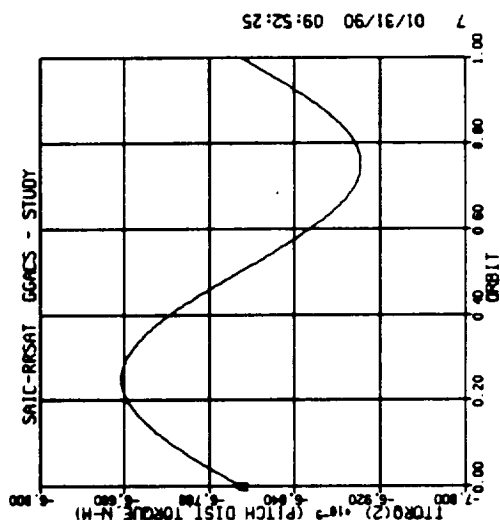
The RRS GNC configuration in the artificial gravity mode is presented in Figure 6.6-20. Roll and pitch attitude data is provided via processing of GPS and Earth horizon crossing data. This is necessary because the magnetometer is insufficiently responsive to support this mode.

- Worst Case Disturbance Torque Profiles For Extended Configuration
 - Circular Orbit
 - Orbit Altitude 350 Kilometers (atmospheric drag)
 - Orbit Inclination 33.83 Degrees (magnetics performance)

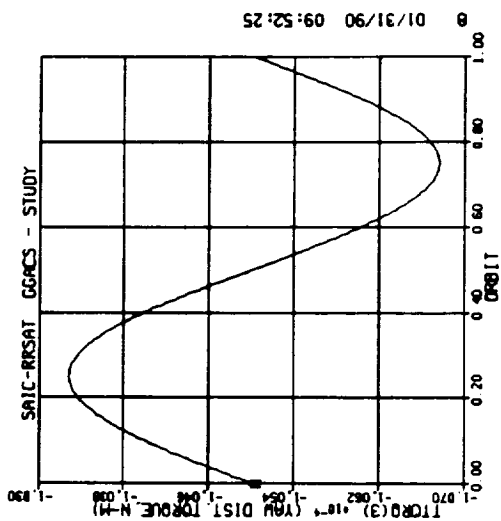
ROLL



PITCH



YAW



ITHACO

Figure 6.6-17. Disturbance Environment

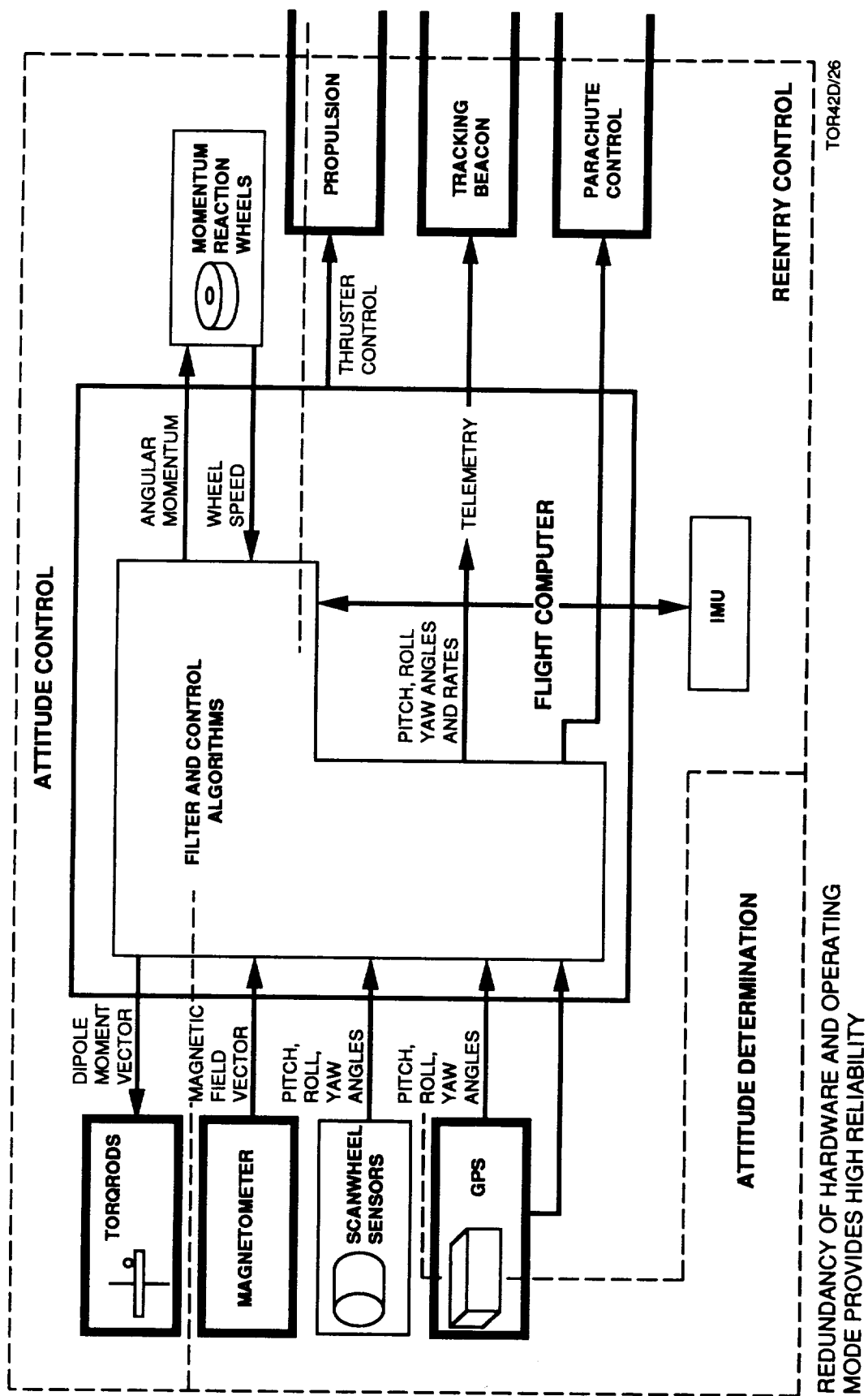


Figure 6.6-18. RRS GNC Configuration Microgravity Mode

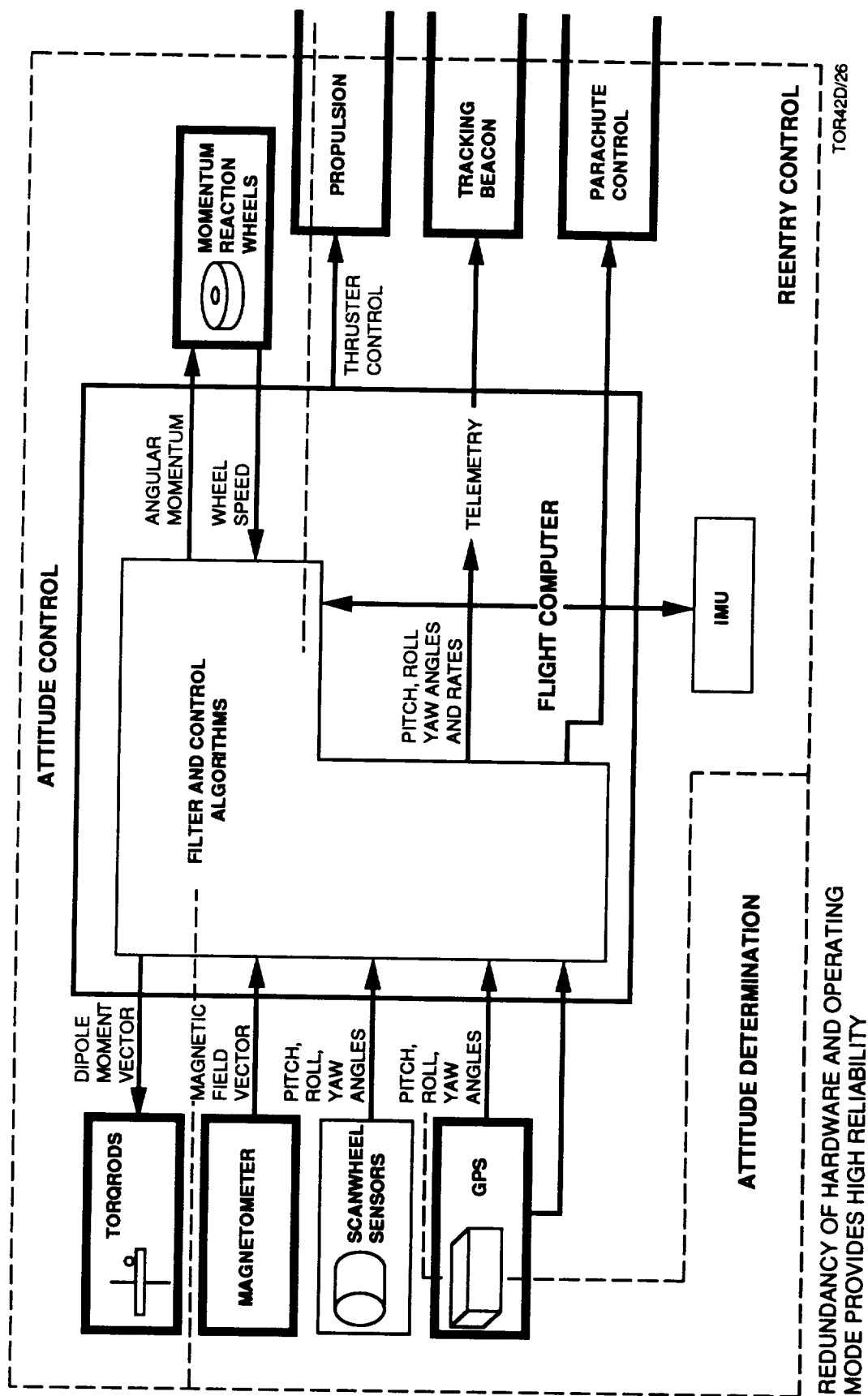


Figure 6.6-19. RRS GNC Configuration Microgravity With Thermal Roll

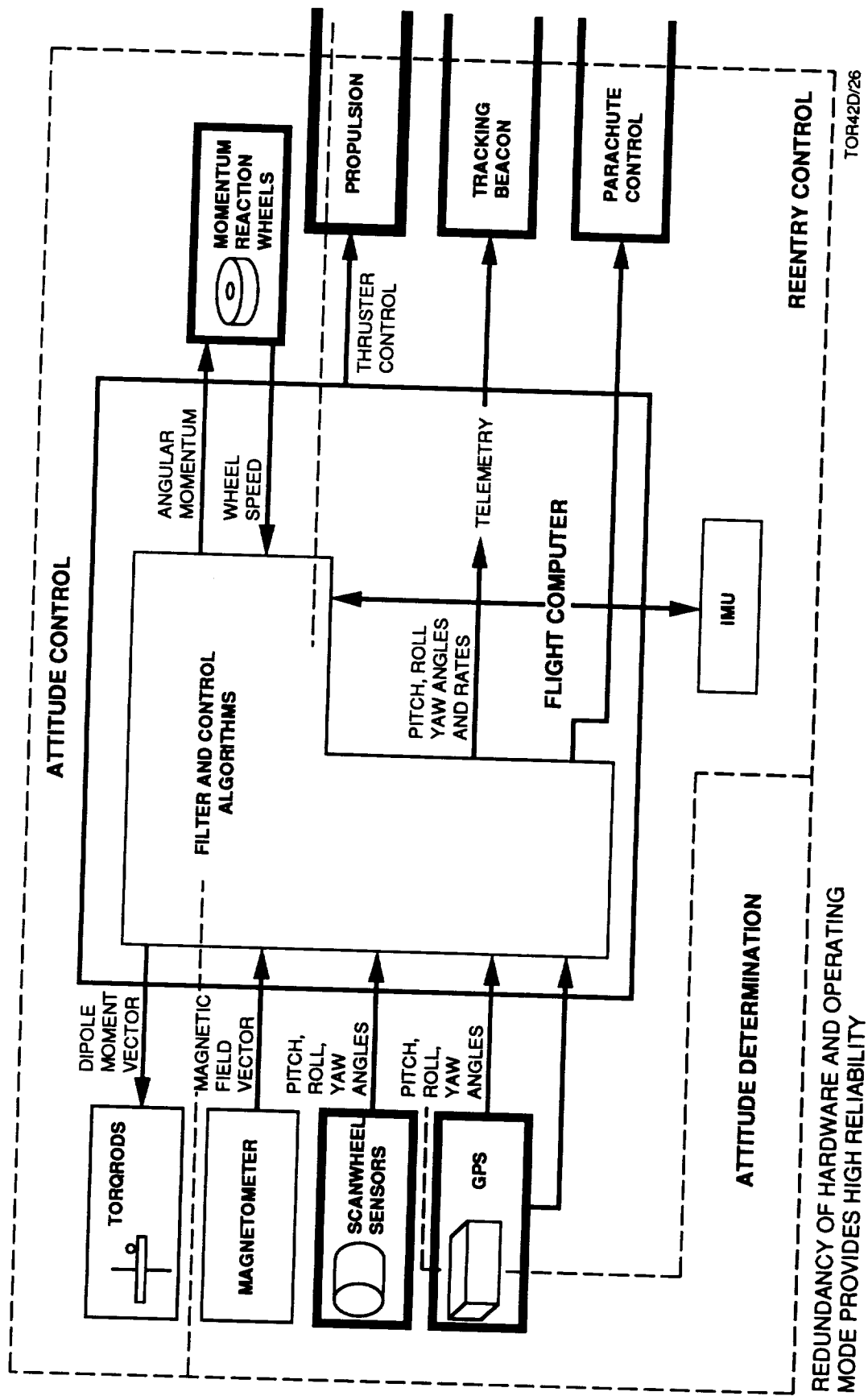


Figure 6.6-20. RRS GNC Configuration Artificial Gravity Mode

Spin-up and de-spin operations will be performed via thrusters. In addition, the thrusters will provide the active control required during the spin operations.

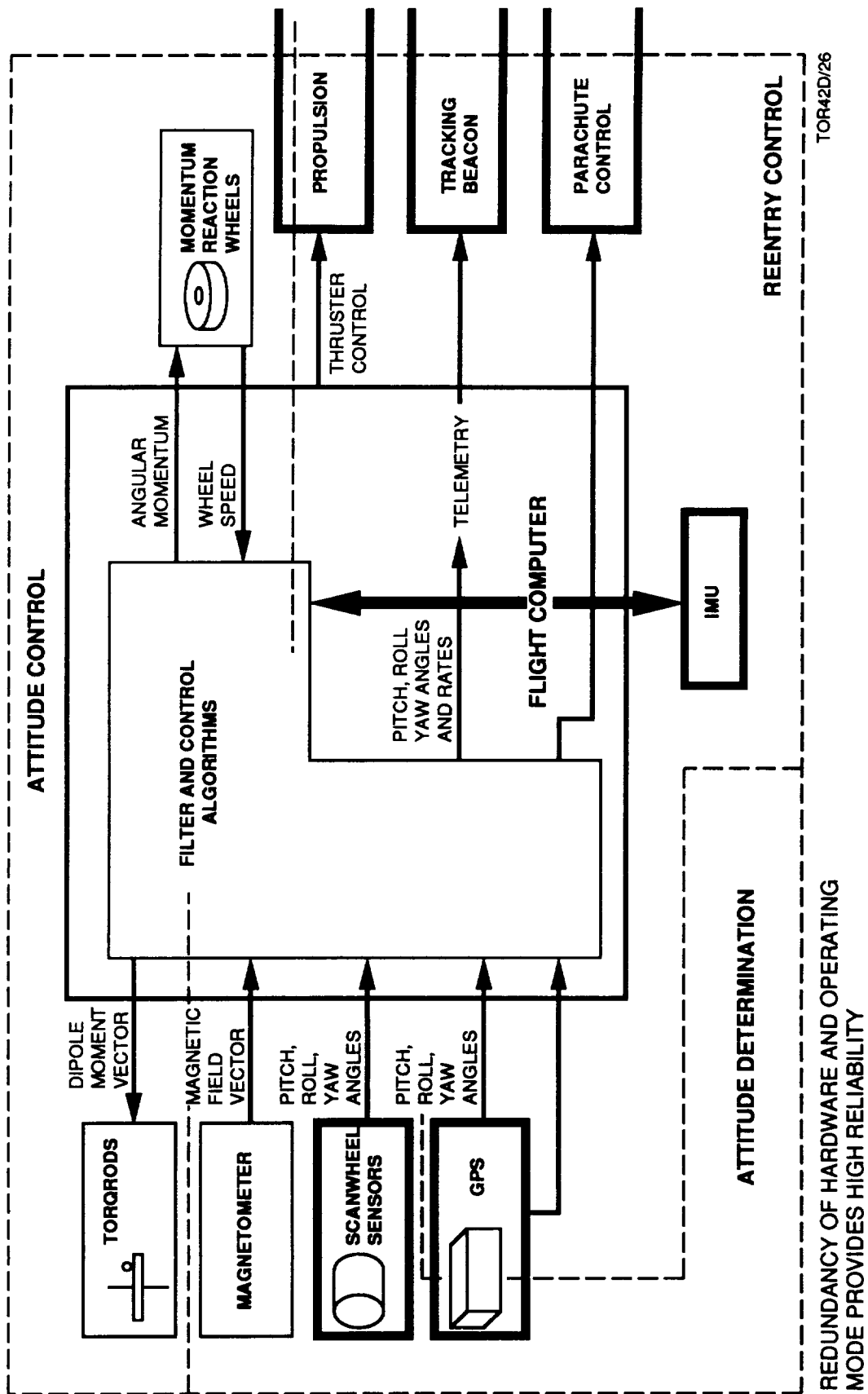
The RRS GNC will be responsible for performing all vehicle major maneuvers including spin-up for artificial gravity, de-orbit burn, and orbital adjustment. Prior to maneuvering, an IMU alignment (Figure 6.6-21) will be performed using GPS and scanwheels. Once aligned, the IMU, in conjunction with the pulse modulated thrusters (Figure 6.6-22), will control vehicle attitude and velocity vector. The performance required during these major maneuver operations are an angular accuracy of $\geq 0.1^\circ$, an acceleration of $\geq 0.10 \mu\text{G}$, and a velocity error $< 0.25 \text{ FPS}$ for a 250 second burn.

The results of the ITHACO analysis are shown graphically in Figures 6.6-23 through 6.6-26. Figure 6.6-23 depicts typical system performance in the gravity gradient stabilized mode with a yaw rotation. The 1.5 g spin stabilized mode, shown in Figure 6.6-24, has a steady state pitch rate of -1 rad/sec within one orbit. The three-axis gravity gradient stabilized mode is shown in Figures 6.6-25 and 6.6-26. These figures are for an initial tip-off condition of $6^\circ/\text{axis}$ with zero rate. Figure 6.6-26 clearly shows that the steady state pitch and yaw values each have an offset value associated with them. The pitch offset is due to an atmospheric drag bias, while the yaw offset is due to a solar pressure bias.

In summary, the RRS GNC design concept is composed of proven techniques and utilizes existing hardware. The design accommodates all phases and modes of operation from launch through recovery. Advanced GPS receiver technology will be utilized to provide precision attitude determination. SAIC is currently developing these techniques through an internally funded IR&D effort. The performance of the RRS GNC subsystem has been thoroughly modelled, and all required operational modes and requirements are achievable with our current design concept.

6.6.4.2 Equipment Summary

6.6.4.2.1 Scanwheels. The "Scanwheel" (Figure 6.6-27) is an ITHACO integration of two space-proven components, the momentum wheel and the IR horizon sensor. This sensor configuration was picked because of its unique dual function applicability to the RRS artificial gravity operation. The two functions are: 1) the establishment of the RRS orbit plane as the vehicle's preferential spin plane and 2) the ability to provide earth scan data throughout the 360 degrees of RRS rotation. These objectives are achieved by mounting the dual Scanwheels with their spin axis perpendicular to the long (extended) axis of the RRS (Figure 6.6-15). The Scanwheel momentum,



TOR42D/26

Figure 6.6-21. RRS GNC Configuration IMU Alignment

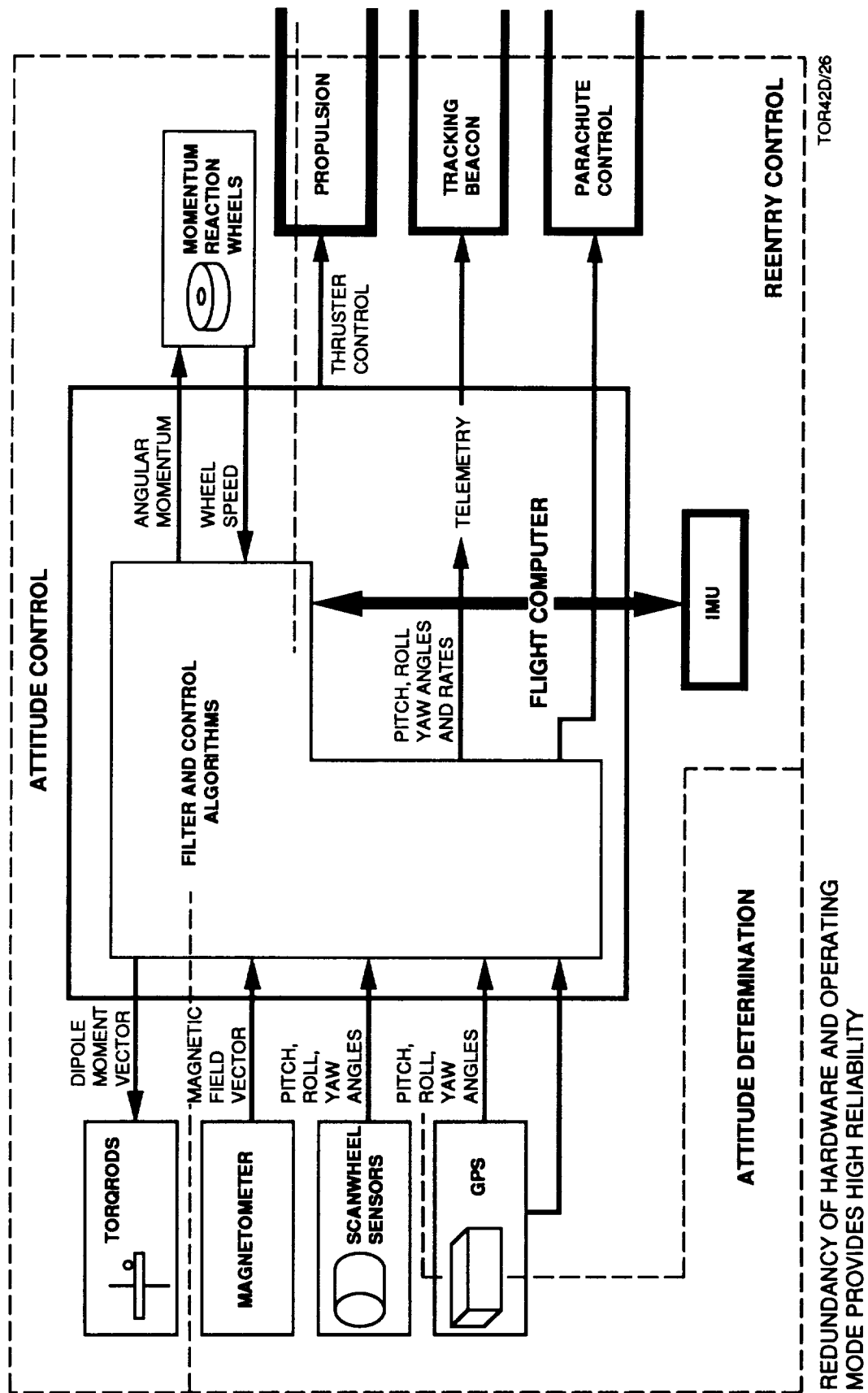
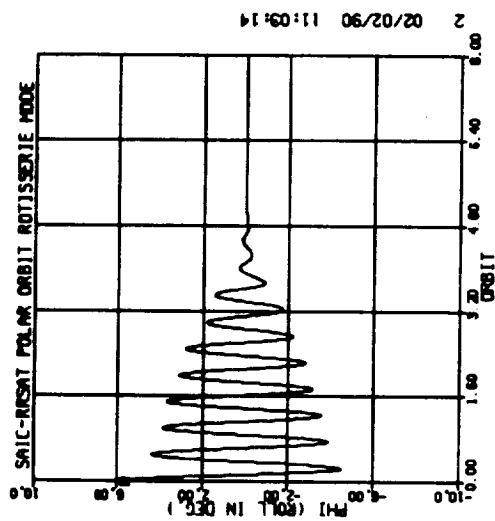


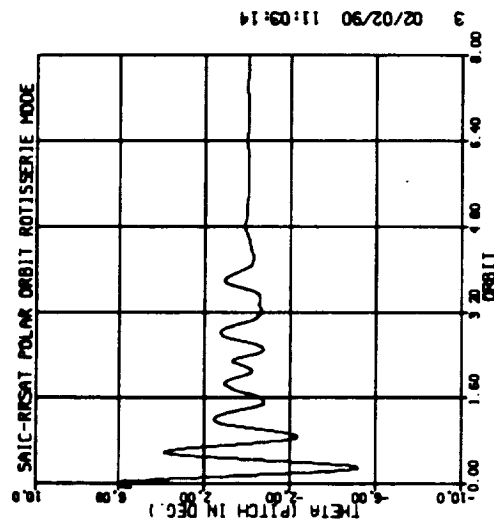
Figure 6.6-22. RRS GNC Configuration Major Maneuvers

TYPICAL PERFORMANCE

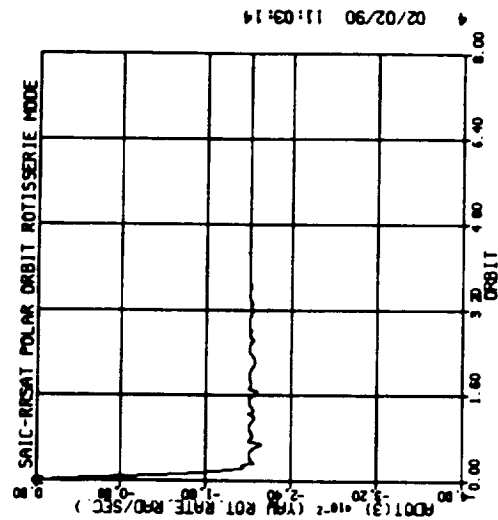
ROLL



PITCH



YAW



ITHACO

Figure 6.6-23. Gravity Gradient Stabilized Mode With Yaw Rotation

TYPICAL SPIN UP PERFORMANCE (Without Active Thruster Control)

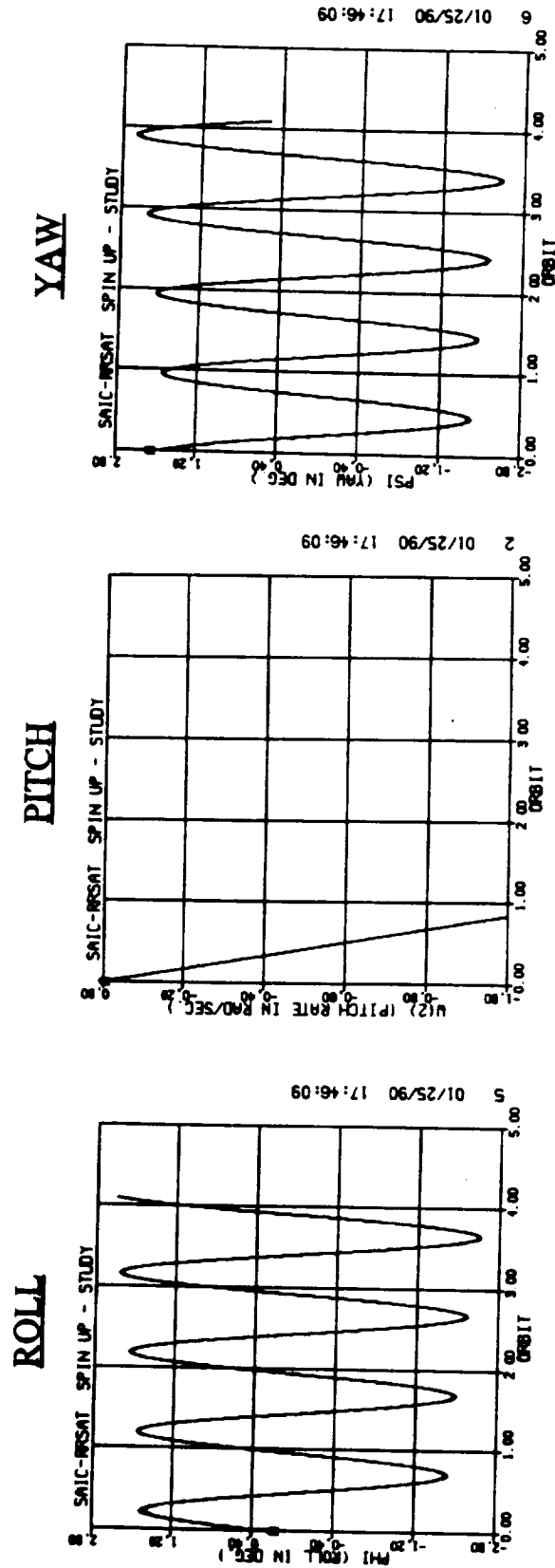
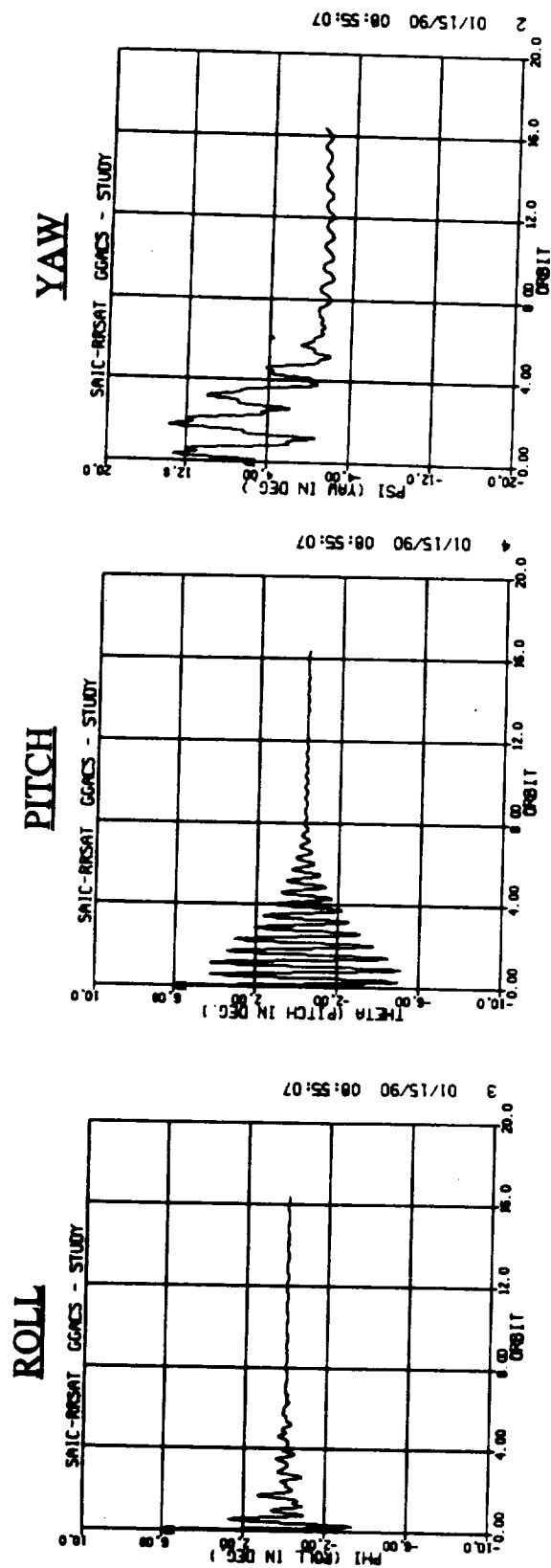


Figure 6.6-24. Spin Stabilized Mode – 1.5 G

TYPICAL CAPTURE PERFORMANCE

(Initial Conditions = 6°/axis with zero rate)

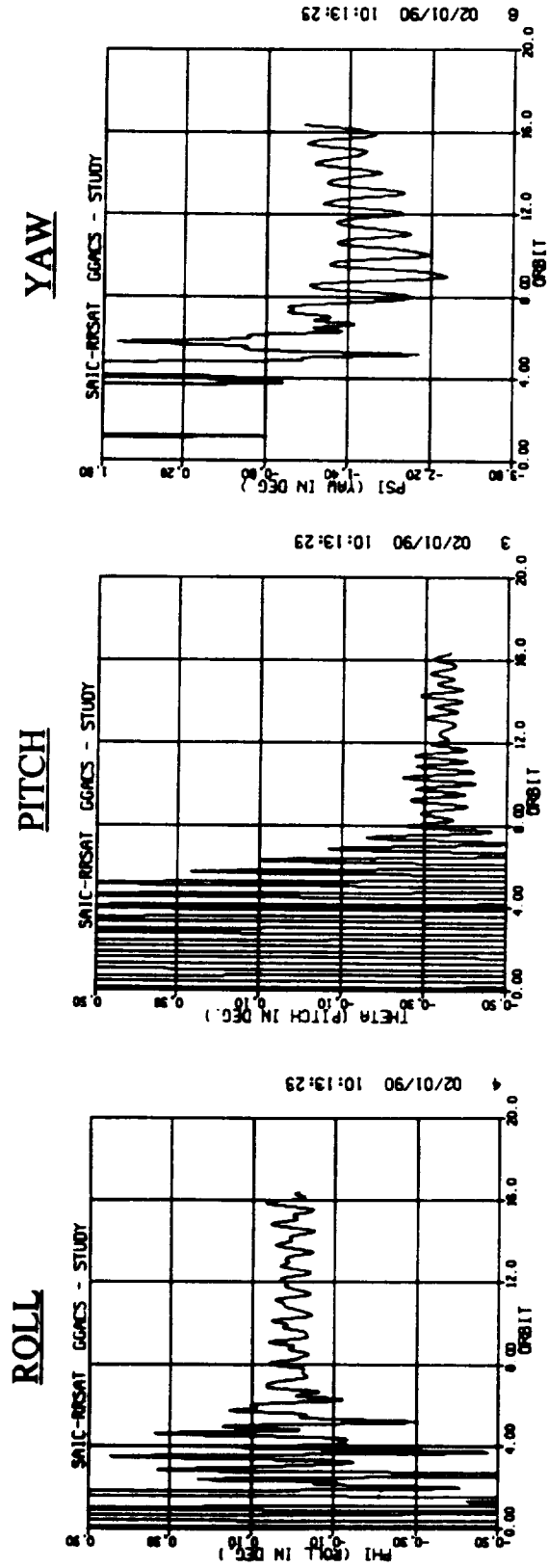


ITHACO

Figure 6.6-25. Three-Axis Gravity Gradient Stabilized – Typical Capture Performance

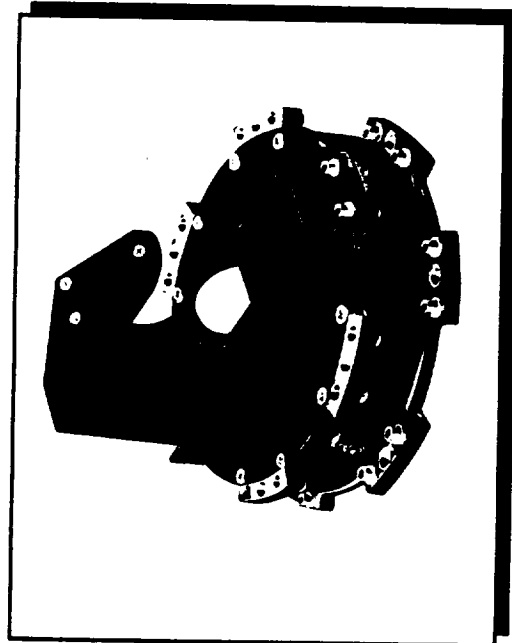
TYPICAL STEADY-STATE PERFORMANCE

(Expanded Capture Sequence to Show Steady State)

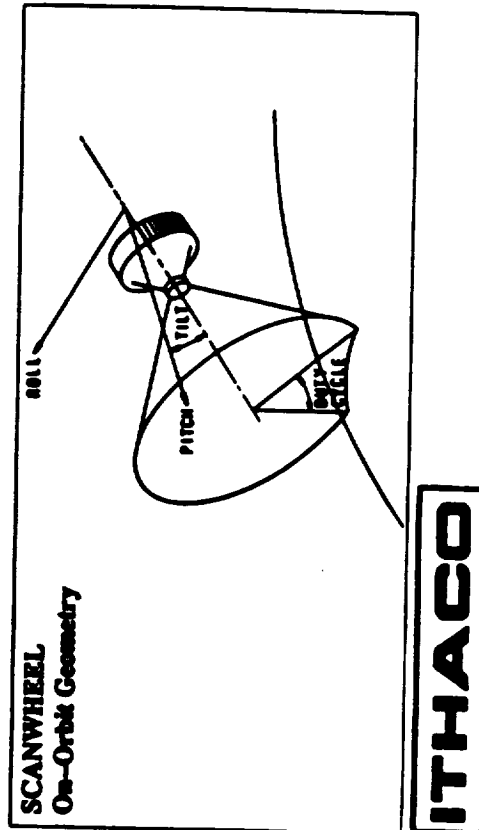
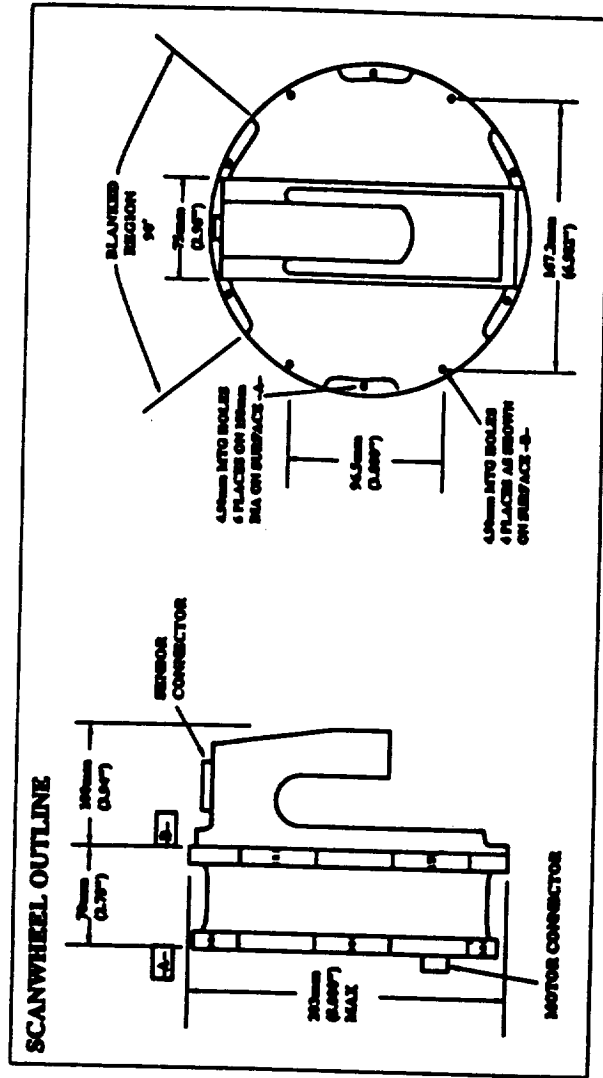


ITHACO

Figure 6.6-26. Three-Axis Gravity Gradient Stabilized – Typical Steady-State Performance



**COMBINATION MOMENTUM WHEEL
AND HORIZON SENSOR**



- 45 – 85 DEGREE SCAN CONE HALF APEX ANGLE
- 14 – 16 MICRON OPTICAL PASSBAND (FULL DISK)
- PHASE (CHORD CENTER) PROVIDES ROLL MEASUREMENT
- CHORD DURATION PROVIDES PITCH MEASUREMENT
- ± 0.05 DEGREE (3-SIGMA) MEASUREMENT ACCURACY

TOR421i/15

Figure 6.6-27. GNC Artificial Gravity Control – Ithaco Scanwheels

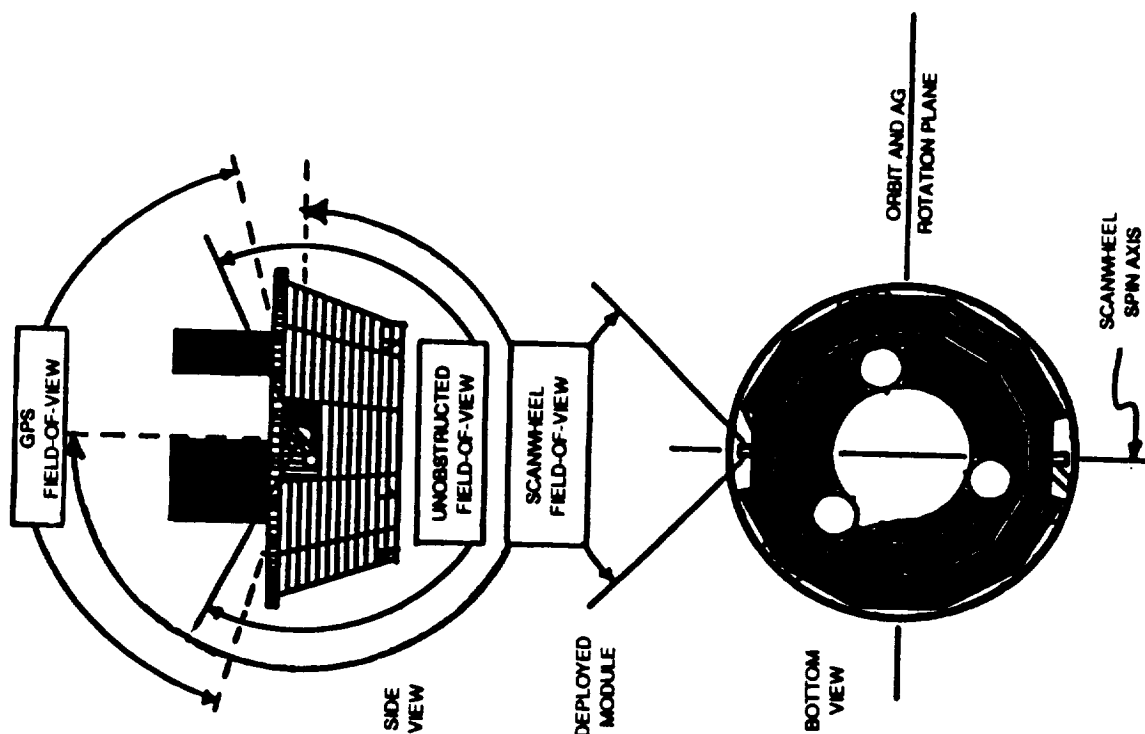
combined with the inertial properties of the extended RRS, then results in a preferential spin plane that contains the RRS's extended axis and is perpendicular to the Scanwheel spin axis. This places the Scanwheel's field-of-view perpendicular to the RRS spin plane (Figure 6.6-28), allowing earth crossing data to be obtained through the entire 360 degrees of sensor and vehicle rotation. This provides continuous orientation of the RRS spin plane relative to the earth and the position of the earth within the Scanwheel scan provides rotational data (position and rate) on the RRS operations. The 360-degree Scanwheel coverage is achieved by clocking the Scanwheel installation so that the "blanked regions" of the "hot redundant" wheels do not overlap. The "hot redundancy" approach is taken to ensure vehicle control is maintained even with a single failure.

6.6.4.2.2 GPS Antennas/Receivers. The proposed GPS antenna configuration is based upon the performance achieved by TI (Figures 6.6-6 and 6.6-7) using a microstrip/choking antenna and a more detailed analysis of a similar choke ring configuration (Figures 6.6-29 and 6.6-30) done by the Ball Communications Systems Division. The current RRS configuration has a total of six microstrip antenna, two mounted (stacked) on top of each tri-mast storage container, that have a reflection free field of view, limiting any performance degradation to multipath from the vehicle structure. Furthermore, since the vehicle structure lays in the antenna null, vehicle reflections should not cause problems. However, a mockup test should be done early in the vehicle development cycle to validate the multipath conditions. A single antenna with a power splitter may be a better option and further performance/reliability analysis is required to complete this tradeoff consideration.

The TI AN/PSN-9 dual-port configuration (Figure 6.6-5) is uniquely applicable to the RRS application. In this configuration, each receiver has two antenna, one for each port. Each pair of antenna establishes a vector, allowing any two of the three receiver/antenna sets to provide vehicle attitude. The result is a single GPS configuration that is redundant for attitude determination and tridundant for fail operational use. The AN/PSN-9's 100-foot remote antenna capability allows the GNC to determine the relative Main/Deployed module position by using a remote antenna on the Main Module. This provides an independent assessment of the tri-mast performance for performance analysis without any significant increase in cost/complexity. More specifically, the GPS application involves:

a. Orbit Control.

1. There are three factors associated with orbit control—position, attitude, and time. It is widely known that GPS provides extremely accurate determinations of position and time, but GPS can also assist with attitude control. Using the method of carrier tracking, GPS can provide data accuracy, in centimeters, at a frequency



SCANWHEEL BLANKING OFFSET 90 DEGREES TO PROVIDE MEASUREMENT THROUGHOUT THE FULL ROTATION.

OPPOSING GPS/SCANWHEEL FOV PERMITS PRECISION ON-ORBIT CROSS CALIBRATION.

180 DEGREE COMMON FOV PERMITS SCANWHEEL PERFORMANCE CROSSCHECK.

GPS USED TO RESOLVE ERROR AMBIGUITY

170 DEGREE SCANWHEEL FOV WOULD

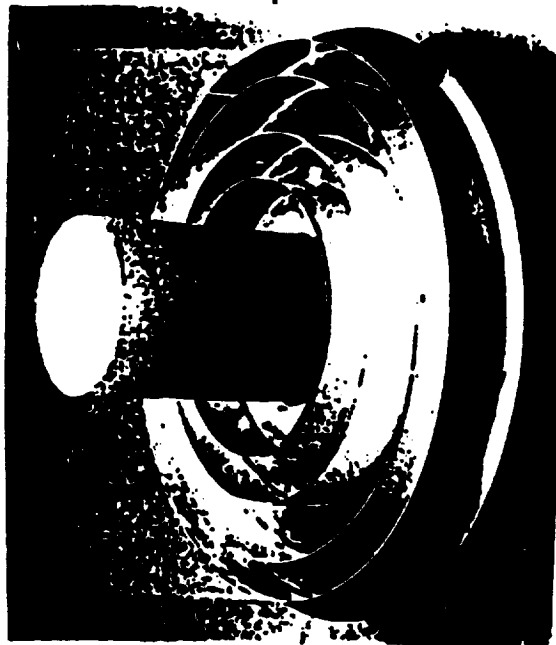
PERMIT OPERATIONS UP TO 30,000 KM

BE OBSTRUCTED, PERMITTING ON-ORBIT STRUCTURAL ALIGNMENT CHECK

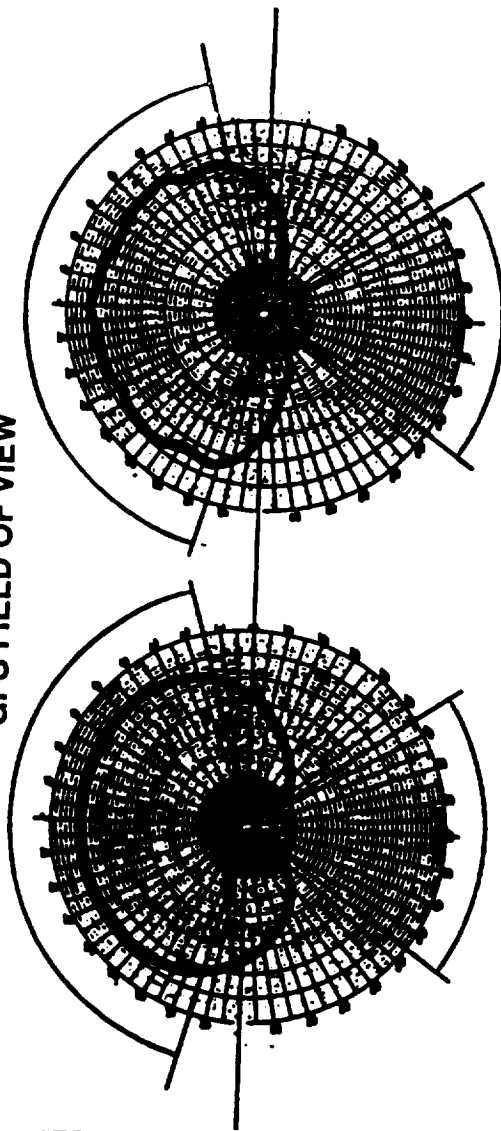
SCANWHEEL AXIS, PERPENDICULAR TO THE SPIN PLANE, PROVIDES THE INERTIAL STIFFENING NECESSARY TO ESTABLISH A PREFERENTIAL SPIN PLANE.

TOR42i/20

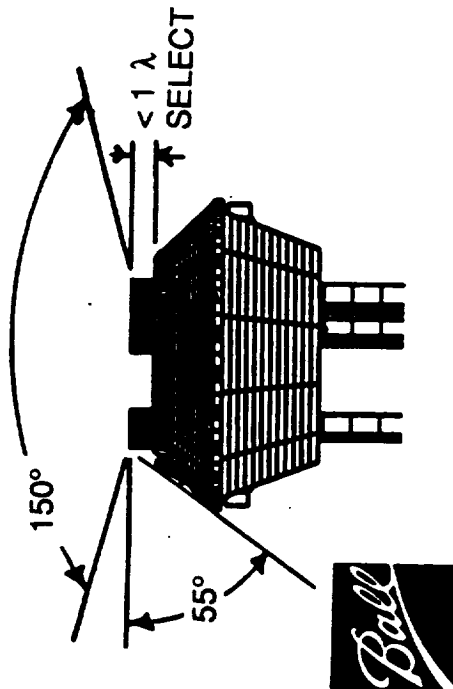
Figure 6.6-28. GPS/Scanwheel Sensor Geometry



GPS FIELD OF VIEW



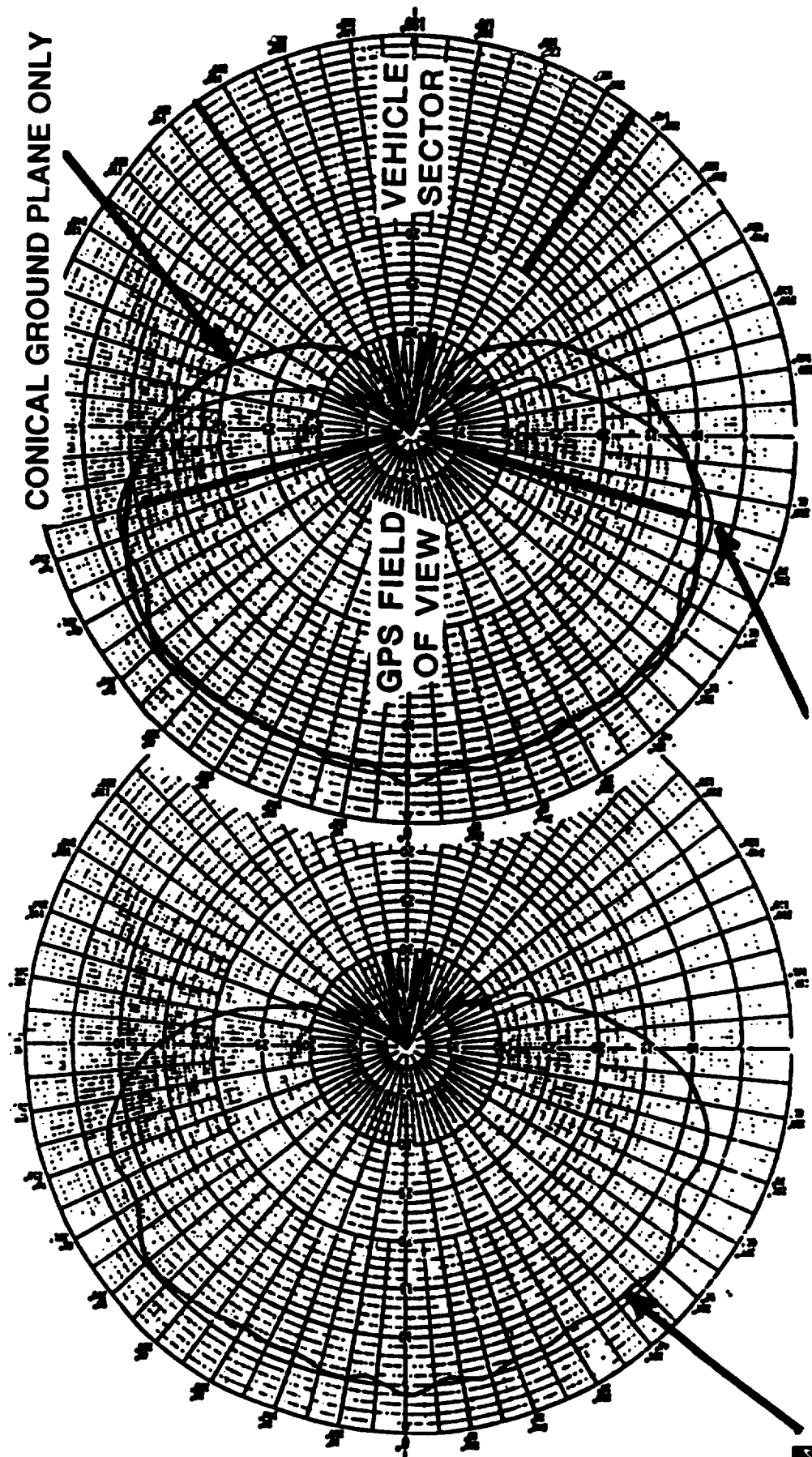
VEHICLE SECTOR



- 2267 MHZ BIFILAR HELIX DATA
 - 12" Diameter, 12 Degree Conical Choke Ring Ground Plane
 - Without (Left)/With(Right) Mounting on Metallic Surface
 - Similar to TI Receiver Test Configuration
- EXTENDED GROUND PLANE
 - Ripples; Decreased Reward Pattern
 - Backlobing in Vehicle Sector
- RRS ANTENNA CONFIGURATION MUST BE TESTED
 - RRS Uses GPS L1 (1567 MHZ); 10" Diameter Mount

Figure 6.6-29. Anticipated GPS Antenna Performance -- Ball Communications Systems Division Antenna

PLANNED GPS FOV AND VEHICLE SECTOR FOR RRS ARE INDICATED
TEST DID NOT INCLUDE RRS CONFIGURATION AT 1575 MHZ (GPS L1)



WITH EXTENDED METALLIC SURFACE MOUNTING

Figure 6.6-30. Ball 2267 MHz Bifilar Helix Data – 12" Diameter, 12 Degree Conical Ground Plane



of 1.5 GHz. This is much more desirable than C/A-and P-code tracking at 1 MHz and 10 MHz (respectively) with accuracies of 16-100 meters.

2. One problem with this type of control is that of cycle slips—changes in carrier phase ambiguity by an integer number of cycles. The difficulty with cycle slips is in detecting them and determining the number of cycles slipped to reestablish the baseline. If the cycle slip is not detected, the position data computed after the epoch of the cycle slip are incorrect. There are two ways to decrease the percentages of cycle slip occurrence. If GPS receivers are placed on the RRS vehicle (RRV) at a separation of less than the carrier phase wavelength of 19 cm, the chances of cycle slip are greatly reduced. The second method is by redundant receivers—one receiver can instantaneously reestablish the baseline if the other detects a slip.
3. Two of three GPS receivers can be placed on the RRV service module and the payload module to provide this orbit control. Receivers on both modules will provide reliability and precise attitude control during operations when the Astronauts are extended. GPS information received during extended operations can assist in controlling the rotation, since exact locations of both ends of the RRV can be monitored.

b. Reentry Control.

1. The second type of control is reentry control. There are three requirements for reentry control - thrust vector, time of firing, and change in velocity (or final velocity). Redundant systems are required for control and propulsion (multiple thrusters). With GPS, the time of firing requirement becomes one of position. Using GPS data, firing can be executed at a precise location rather than at a predetermined time. In addition, the effective thrust vector can be known at any time, and if one thruster fails, corrections can be made within minutes for the next firing. Similar adjustments can be made for velocity. Intermediate velocities can be obtained to compute new changes in velocity (or final velocity) to correct for the next firing.
2. There are three areas of error in reentry control - the de-orbit phase, reentry, and terminal landing. Errors in the de-orbit phase due to propulsion can be effectively eliminated using information received from GPS. Reentry errors caused by atmospheric effects cannot be addressed, but the wind effects during terminal landing can be controlled with GPS.

c. Landing Control.

1. The RRV will utilize parasails for landing control. With GPS information, wind effects can be determined and corrective measures taken. The relative wind velocity can be continuously computed during descent by comparing the parasail controls needed with those baselined for the case of still air. Again, corrections can be made at any time based on the information received.
2. Another landing issue is that of recovery. With a GPS receiver on board, the RRV can broadcast its exact location to the GPS satellites - a location that can then be received by any recovery vehicle. That rescue vehicle can then target to the RRV's precise location for recovery. This also eliminates the need for any ground support at the landing site, which reduces the number of required personnel, and allows for changing the landing site at any time for emergency situations.

6.6.4.2.3 Inertial Measurements Unit. The Inertial Measurements Unit (IMU) proposed for use in the RRS is the Honeywell GG1320 ring laser gyro assembly (RLGA) (Figures 6.6-31, 6.6-32 and 6.6-33). This RLGA was specifically designed for use with the S5 SANDAC computer which was chosen for the RRS.

6.6.4.2.4 Magnetic Control. The stringent 10^{-5} g microgravity specification requires essentially a free flyer mode. However, to ensure the vehicle stays in the thermal preferable orientation, a means of low-level long-duration control forces, unachievable with the low-level thrusters, must be provided. Therefore, the GNC includes the space-proven ITHACO magnetometer/TORQUEROD combination (Figure 6.6-34) for microgravity operations. The currently analog design is expected to be available in digital form for RRS use, allowing full electronic integration with the other elements of the GNC. However, the system can use the current system "as is," minimizing any risk from the completion of the development of the digital version. Since the thermal control for many orbits is best achieved with a slight rotation about the RRS's extended axis, a momentum wheel has been included to cancel the angular momentum of the overall vehicle. Furthermore, since these wheels are mounted at right angles to the Scanwheels, the combined wheels have the ability to cancel the angular momentum that may be caused by rotating assemblies internal to the Payload Module.

6.6.4.2.5 Flight Processor. The core element of the GNC subsystem is the flight computer. Unlike most satellites, the RRV has GNC and propulsion computational requirements involving continuous critical timing constraints that influence both vehicle and public safety. This requires a computer system that can function in what is known as a "hard real-time" environment. Furthermore, a fast, multi-tasking operating system (OS) and the ability for "real-time" debugging are required for efficient operation and low risk software development in such an environment.

The wide range of computers considered varied from the "space qualified" version of the VAX to proprietary advanced processor concepts scheduled for space qualification in time for RRV use. However, the need for a real-time multi-processing environment which could handle both multiple tasking and multi-parallel processing of a single task (for failure identification) eliminated most of the processors considered. Ultimately, the choice became one of proven hardware/OS vice a "probable" new system, and program risk dictated use of a proven system - the SANDAC V. Furthermore, the SANDAC is tailored for executing strap-down navigation/control algorithms very similar to those needed for the RRV, and has been successfully used for inertial navigation and attitude reference control on numerous reentry vehicle flights. The following discussion is a

Honeywell

RLGA

*Ring Laser Gyro
Assembly
Inertial Measurement
Unit
GG1320
Ring Laser Gyro*



Specifications

Size	161 in ³
Weight	<13 lb
Power	14W
Operating Temperatures	-10° to +160°F
Accel	1 ppm/gauss

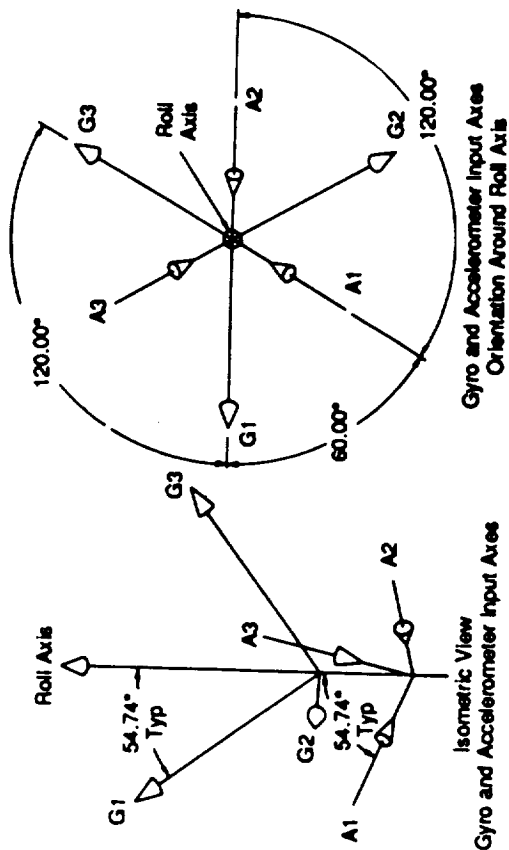
Features

- Inertial or strapdown sensing of angular rate and acceleration
- Built in test capability
- Compensated $\Delta\Theta$, ΔV output with processor
- May utilize S-5 or alternative processors (GVSC, TMS320, etc.)
- Isolation Mount available
- Bell XI or Sundstrand Accelerometer

SUBJECT TO EXPORT CONTROL LAWS

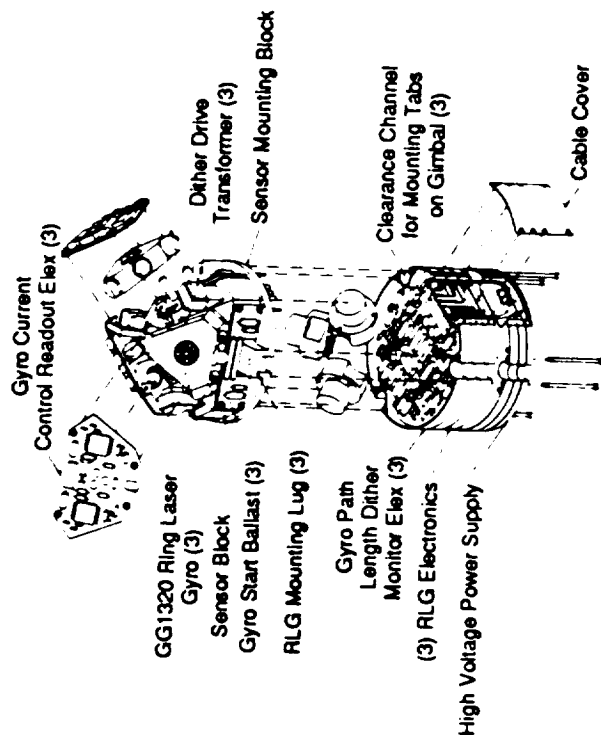
This document may contain information covered by the International Traffic in Arms Regulation (ITAR). Export of such information contained herein, or released to foreign nationals, as defined in ITAR, without first obtaining an export license is a violation of the ITAR and subject to criminal penalties.

Figure 6.6-31. Honeywell Ring Laser Gyro Assembly (RLGA)



Honeywell Ring Laser Gyros have proven performance across multiple environments:

- Temperature — High vibration
- High g — Radiation hardenable
- Instant on, no calibrations required over time.



Unique RLGA configuration maximizes capabilities with minimum volume.

SUBJECT TO EXPORT CONTROL LAWS

This document may contain information covered by the International Traffic in Arms Regulation (ITAR). Export of such information contained herein, or released to foreign nationals, as defined in ITAR, without first obtaining an export license is a violation of the ITAR and subject to criminal penalties.

Honeywell

Figure 6.6-32. RLGA Sensor Configuration

• Size:	161 in ³
• Weight:	<13 lb
• Performance	
Gyro	
Random Walk:	0.002 deg - 0.008 deg/√hr
Bias:	0.005 deg/hr
Scale Factor:	<1 ppm
Frequency Response:	Sample Rate Determined
Alignment:	<1 arc-sec
Input Rate:	>1000 deg/sec
Accelerometers	
Bias:	10-15 ppm
Scale Factor:	10-15 ppm
Alignment:	<10 μradf
• Life:	>100,000 Operating Hr

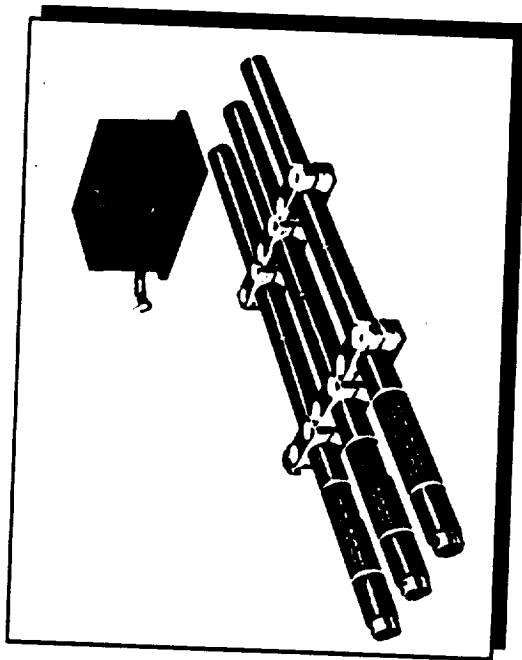
Figure 6.6-33. RLGA Performance

summary of the key information in the SANDAC V Hardware Reference Manual (SAND87-2618) and Software Development Guide (SAND87 26-16)

The Sandia Airborne Computer (SANDAC) V, developed by Sandia National Laboratories as a hard real-time embedded computer which can respond to external events and update variables in real time, includes a operating system (OS) that allows applications software to be developed to take advantage of the multi-processor, multi-tasking environment. This OS also provides a unique ability to debug the applications software in real-time on the host processor - a major risk limiting feature for the RRV development.

Another risk consideration is the difficulty in replacing firmware to change an application given the small size of the computer and the limited access inside of the flight vehicle enclosure. Therefore, the SANDAC V powerup code is stored in ROM; the application code and data in battery-backed RAM. The application code is downloaded into the SANDAC V via a serial channel from a nearby portable computer (the "Gateway") prior to initiating a mission.

Basically, the SANDAC is a smart way of configuring / packaging available parts to provide state-of-the-art capability for throughput and memory capacity with minimal impact on weight, power, and sizing demands. Although the SANDAC V is not throughput-limited for RRS, the increased capability of the 68040 processor module of the enhanced SANDAC V (also called the ES5) provides a reserve capability in case of unforeseen problems or user needs. This added capability adds other benefits and comes at little added expense and risk. The designers-



MAGNETICS APPROACH

LOW PERTURBING FORCES
LOW POWER CONSUMPTION

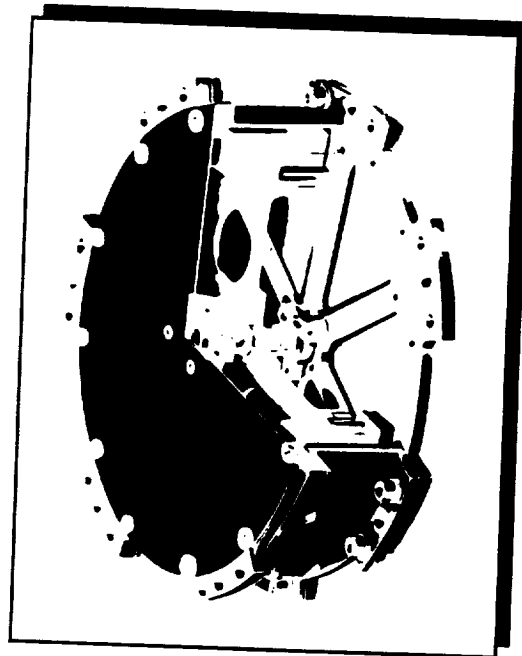
ATTITUDE CONTROL

DETERMINATION:

DUAL TWO-AXIS FLUX GATE
MAGNETOMETERS DESIGNED FOR
DARPA'S SCSC SATELLITES

CONTROL:

THREE 350 AM2 DIPOLE
TORQUERODS SAME MOMENT AS
SATCOM/KU APPLICATION



THERMAL ROTISSERIE

10 N-M-S MOMENTUM WHEEL
PROVIDES SLOW (≤ 0.2 RPM) SPIN CONTROL
CANCELS ANGULAR MOMENTUM

NON-REDUNDANT – GPS/THRUSTER BACKUP

TOR421U/16

Figure 6.6-34. GNC Microgravity Control – Magnetometer, Torquerods and Momentum Wheels

developers of the SANDAC have techniques for ensuring hardness in the RRS space and descent environment. Basically, natural radiation hazards can be circumvented by 1) providing for shielding (such as by wrapping in quarter-inch aluminum or tantalum layers, since the whole computer is so small and lightweight, 2) epi-taxial layering of the associated chips (available now for the S5 and likely within two years for the ES5 drop-in replacement processor), and 3) other proprietary. The SANDAC computer, for both the S5 and experimental ES5 parts, has been flown successfully in space as well as aboard controlling boosters and reentry vehicles.

Although the RRS processing considerations largely involve memory and hardness as opposed to throughput, SAIC is considering using the ES5 configuration of the SANDAC instead of the S5. Although both are 32-bit processors (using, respectively, the 68040 and 68020 chips by Motorola), there are a few other key features worth considering. For example, the ES5 has optional 10- or 28-volt power supply provisions and ability to be powered off to save energy. When powered off, the 68040 is "awakened" by the companion 68020 processor module that is used to control the data traffic of the I/O module.

6.6.4.2.5.1 System Architecture. The SANDAC V uses a modular architecture that is expandable in processors, I/O ports, and the amount of memory, to provide for flexibility. The availability of multiple processors permits an application to be divided into logically independent activities that can be distributed among the processors. This division of activities creates potential execution overlaps that improve performance and help meet critical timing constraints.

As an embedded computer, SANDAC V typically performs without direct human interaction through keyboards and display devices. However, terminal access to SANDAC V is required for software development. This access is provided by the "Gateway", a portable computer that operates under MS-DOS and has terminal-emulation capabilities. The Gateway also provides the means for transfer of the application code from the host to the target system and provides a console for debug and test operations. The debug operations are supported by the GATAR and Hawkeye software packages developed specifically for the SANDAC V system. Both packages are loaded and run on the Gateway. GATAR loads, activates, and monitors programs and controls the target system for machine-level debugging. Hawkeye monitors and controls the Hawk operating system while an application code is running.

The target system, during software checkout, is a SANDAC V with the same hardware configuration required for the actual application. This permits real-time testing of application

programs. During software development, a user's chassis provides power and isolates and buffers the serial channel between the Gateway and the target.

6.6.4.2.5.2 Hardware Configuration. A typical SANDAC V system configuration is illustrated in Figure 6.6-35. Signal propagation delays limit the SANDAC V to a maximum of 20 global (Utility, Processor, and Global Memory) and local (Expansion Memory, System I/O, or MIL-STD-1553B) bus modules.

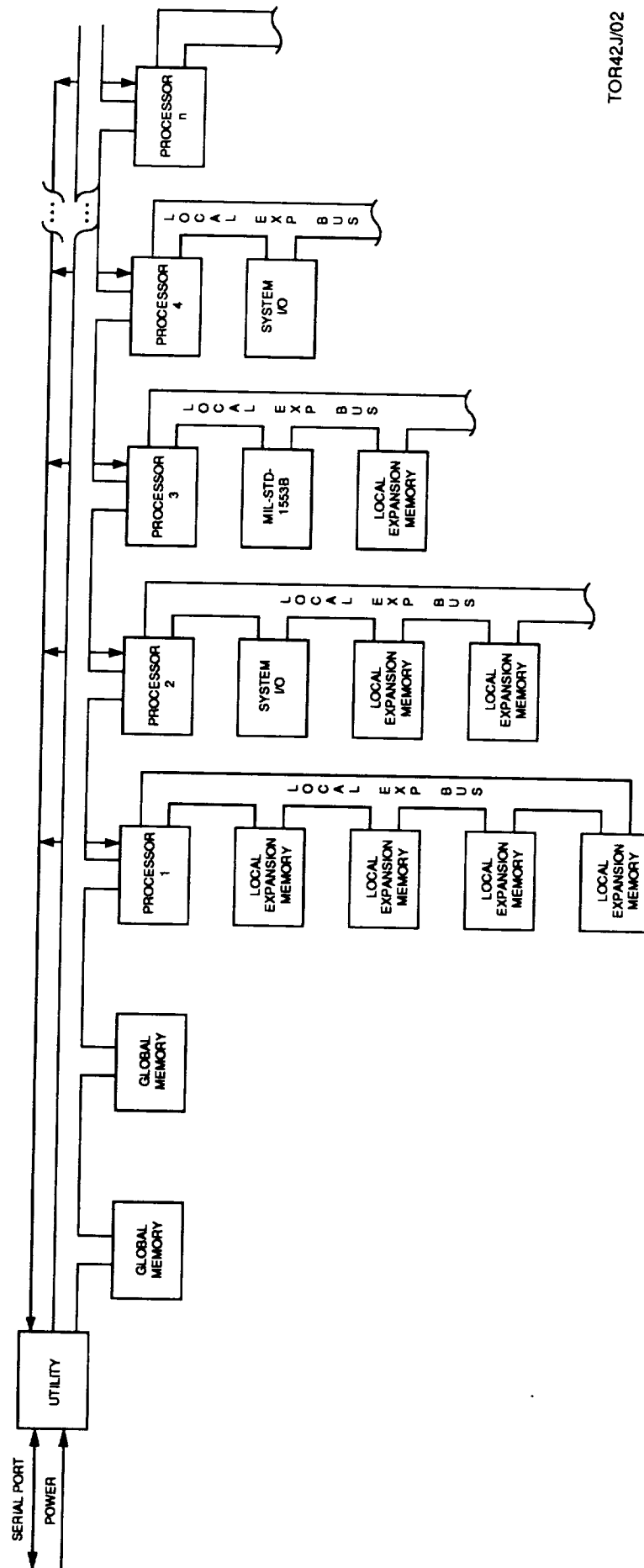
A local bus is a parallel bus with 32 data lines, associated with a given Processor Module, that provides the module's Motorola MC68020 microprocessing unit (MPU) with access to dedicated memory and I/O resources. The Gateway communicates with SANDAC V via a third bus (the global serial bus) that connects all Processor Modules to an external port on the Utility Module. The considerations in Table 6.7-6 restrict the architecture for any given system configuration.

Each SANDAC V module is a printed circuit board framed with aluminum rails keyed so that only one orientation is possible when interconnecting the modules. Groups of modules are interconnected by rows of pins and sockets on the circuit boards. Rows of pins and sockets on two outer edges of the modules provide the global bus between all system modules. A second set of pins and sockets on the processor and expansion modules provides the local expansion bus.

Although the expansion modules must be mated to the component side of the host Processor Module, the expansion modules can be placed in any order on the expansion bus, and a Processor Module and its associated expansion modules can be placed anywhere in a SANDAC V stack. For electrical continuity, expansion modules pass the global bus signals through, but do not connect to, any of these signals. Once a set of modules is interconnected, the set is assembled between two end plates. An assembled SANDAC V, and the physical arrangement and interconnection scheme, is shown in Figure 6.7-36.

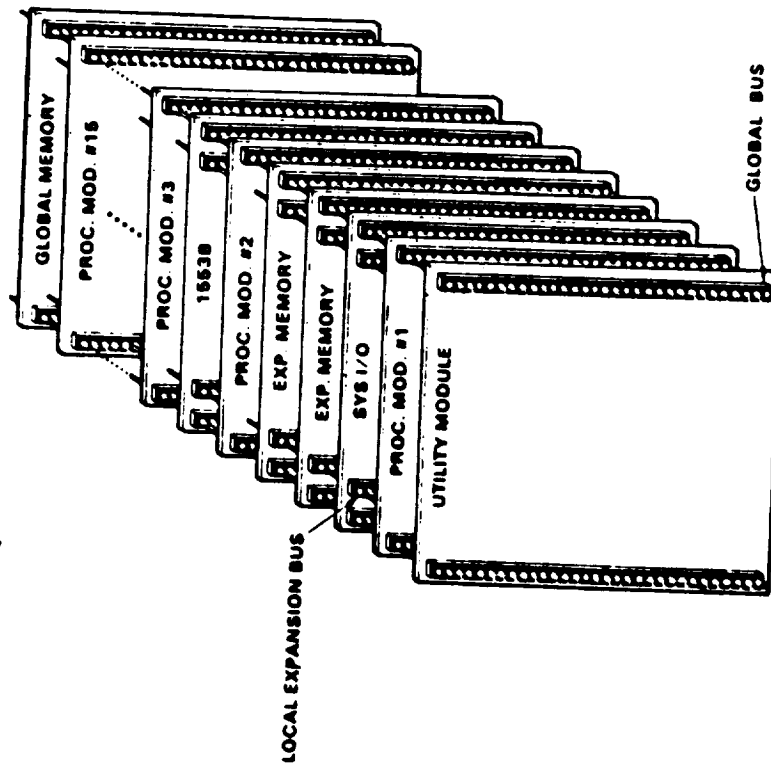
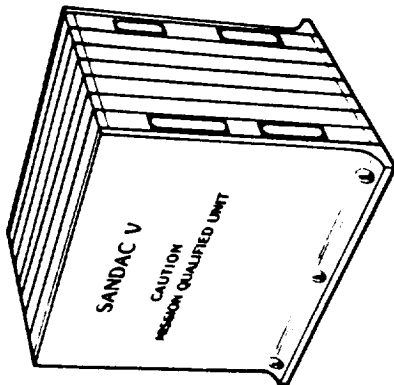
The Gateway may be an IBM PC, XT, or AT, or any completely IBM-compatible computer. This computer must have at least one 360K-byte or 1.2M-byte floppy-disk drive, 256K bytes of memory, and a serial communications port configured as port 1 [COM1:]. MS-DOS/PC-DOS, versions 2.1 through 3.2, must be installed. Hawkeye functions with either a monochrome or a color monitor; the color monitor requires a color graphics monitor controller.

Typically, SANDAC V applications must respond in real time to external events and handle a number of operations concurrently. In developing an application that meets these requirements, a

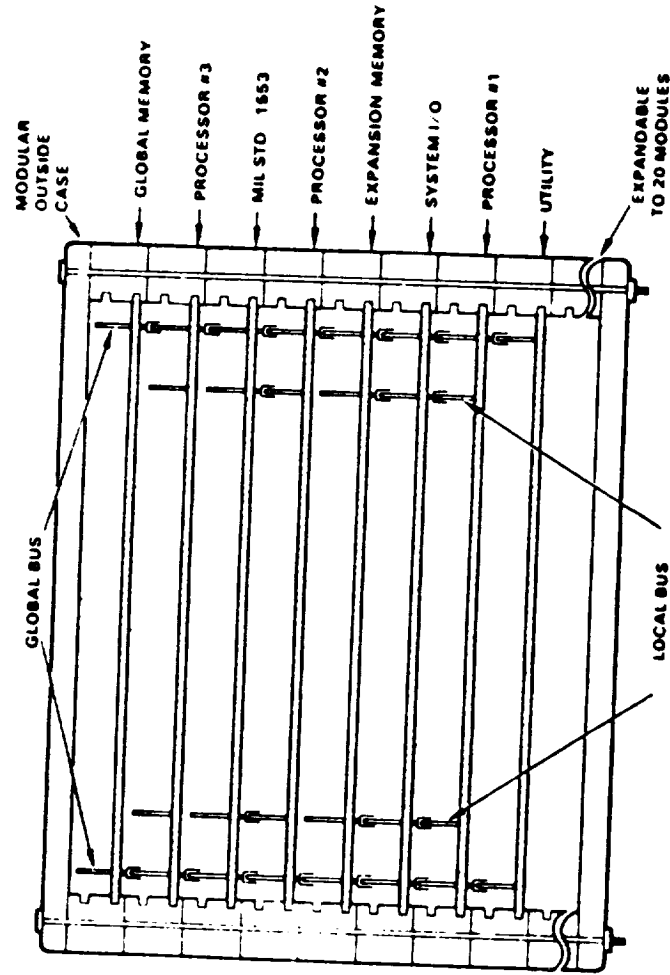


TOR42J/02

Figure 6.6-35. SANDAC V Architecture



PHYSICAL MODULE ARRANGEMENT



INTERCONNECTION SCHEME

Figure 6.6-36. SANDAC V Mechanical Design

Table 6.6-6. System Configuration Considerations

- One Utility Module, per system, providing:
 - Power
 - Clocks
 - Global Serial Bus Interface
 - Global Resources
 - 256K Bytes of EPROM
 - 128K Bytes of RAM
 - 32-bit Timer
 - Status Register
- A maximum of 15 Processor Modules, each with a Motorola MC68020 MPU and Motorola MC68881 Floating-Point Coprocessor, accessing global resources through the global interface bus arbitration logic and supported with a variety of local resources by:
 - 128K Bytes of RAM
 - 1 VSLI Gate Array
 - 1 512-Byte First-In-First-Out (FIFO) Buffer
 - 1 Motorola MC68901 Multi-Function Peripheral
- A Processor Module supports a maximum of four local bus expansion modules in the quantity indicated:
 - 1 System I/O Module
 - As many as 4 Expansion Memory Modules
 - As many as 4 MIL-STD-15553B Modules

multitasking approach may be necessary. For SANDAC V, several options are available when considering a multitasking solution:

- Assigning one task to a single Processor Module
- Assigning multiple tasks to a single Processor Module
- Assigning multiple tasks to multiple Processor Modules

Whatever the division, each task of an application should be associated with one SANDAC V Processor Module and its corresponding local memory (RAM).

For SANDAC V applications, support for true multitasking and multiprocessor solutions is provided by the Hawk operating system.

In the software development environment, the target system consists of a SANDAC V and a user's chassis. The target SANDAC V may be the hardware set used in the final mission or it may be duplicate dedicated to laboratory use. The user's chassis supplies power for SANDAC V and also provides optical isolation for the Gateway-target serial communication channel.

The specific hardware configuration of the target system SANDAC V varies, depending on the application. Specific characteristics of the SANDAC V processor are provided in Table 6.6-7.

Table 6.6-7. SANDAC V Features

<ul style="list-style-type: none">• 128K of global ROM containing firmware for:<ul style="list-style-type: none">- SANDAC V initialization routine- SANDAC V portion of the GATAR debugger- Hawk operating system kernel- Hawkeye support features• 128K (minimum) of global RAM<ul style="list-style-type: none">- Stores data available to all Processor Modules in the system. Used by the initialization routine to store configuration information.• 128K (minimum) of RAM local to each Processor Module<ul style="list-style-type: none">- Stores the code to be executed by that particular Processor Module.• Size (per module): 6.25 H x 7.0 W x 0.57 D in.• Weight (per module): 1 lb (typical)• Power Dissipation (per module): 5 W (maximum)• Modules per System: 2 to 20• Shock (flight-qualified system): Minuteman and Polaris A3 Payload• Vibration (flight-qualified system) 18 g rms random from 20 Hz to 2 kHz• Operating Temperature: -20°C to +70°C (case temperature)• External Power Requirement: 8 to 12 Vdc
--

When power is applied to the target system, all Processor Modules begin initialization from global ROM and compare IDs, with the highest ID becoming the "master processor" and continuing with the initialization activities. The master processor then checks to see if a Gateway running GATAR or Hawkeye is connected, and if so, execution is started. If neither is detected, the master processor begins executing the application code, loaded by a previous GATAR session, from the system's default start address. A flowchart illustrating the general operation of the target system at power-up is shown in Figure 6.6-37.

6.6.4.2.5.3 Host-Target Interface. The single Gateway used as the host interface requires only a single serial port and VTERM terminal emulation software. The Gateways interfacing with the target systems also require only a single serial port as well as GATAR, HAWKEYE, and, optionally, a printer to support debugger logging functions. Figure 6.6-38 illustrates a typical Gateway configuration.

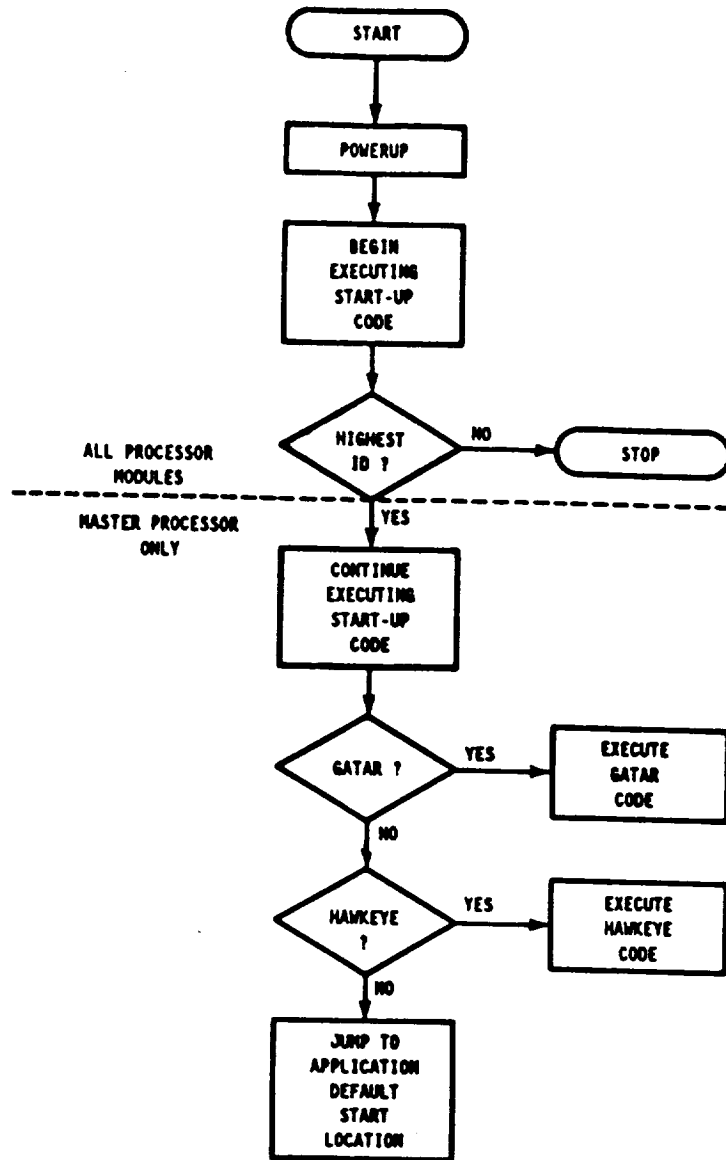


Figure 6.6-37. Target System General Operation Sequence

The Gateway is a portable computer of the IBM PC, or compatible, type that operates under MS-DOS to communicate with the Host and/or Target computer. To communicate with the host, the Gateway uses VTERM terminal emulation software to emulate a VT-100 display terminal. To communicate with the target system, the Gateway uses either the GATAR debugger or the Hawkeye debugger. The configuration (Table 6.6-8) of the Gateway depends upon the specific software development system.

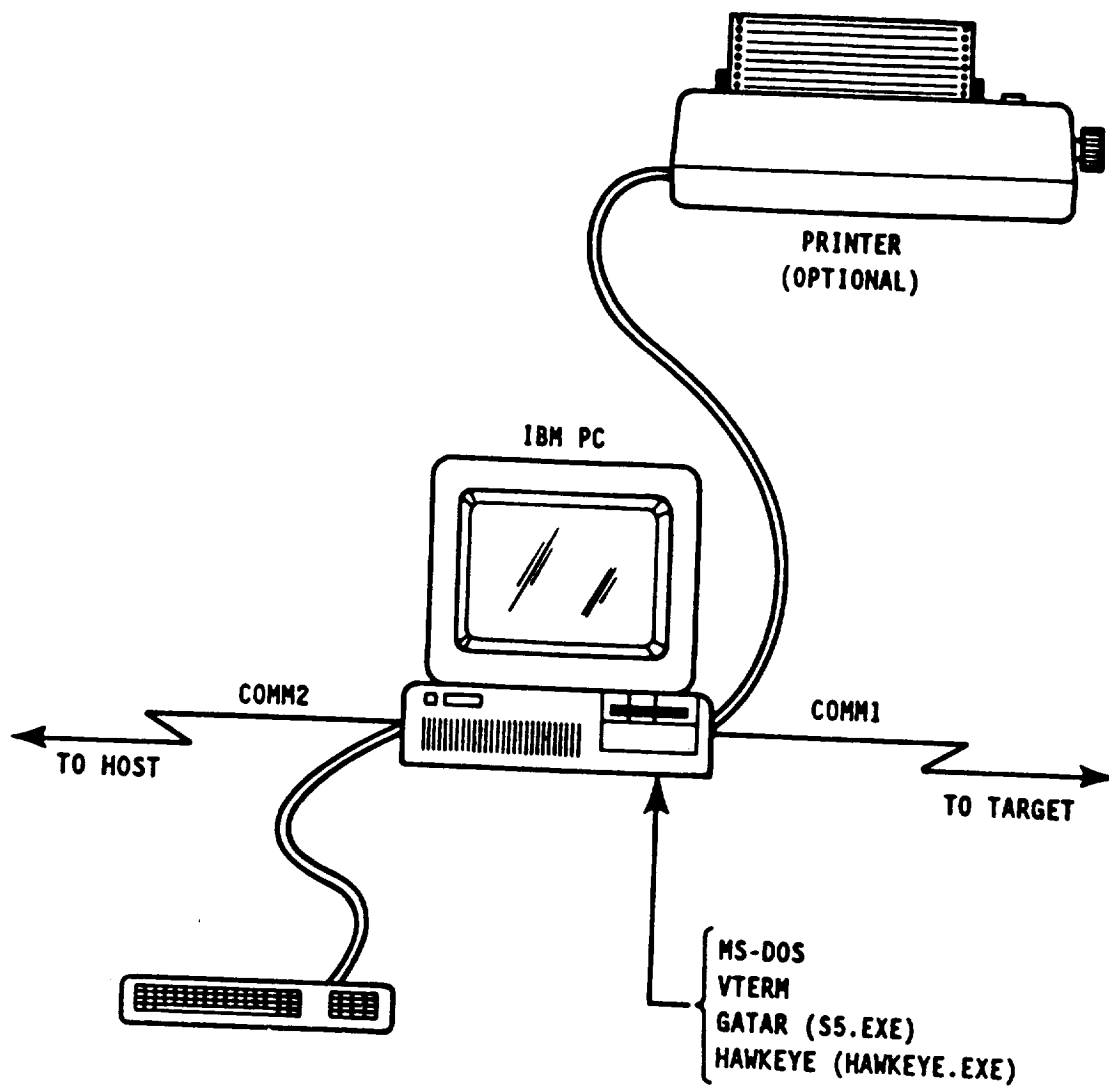


Figure 6.6-38. Typical Gateway Configuration

Table 6.6-8. GATEWAY Host-Target Interface

The Gateway is typically used as follows:

- Communication with the host is established, and files containing executable application code are generated with the software development tools and then transferred to the Gateway.
- After transferring application code files from the host, communication with the target system is established, and the files are downloaded into the target SANDAC V.
- After downloading the target system, the Gateway monitors and controls the application.

A single Gateway can serve as the host interface and while additional Gateways are interfacing with several evolving systems. In the basic system consisting of a host, a single Gateway, and a target system, the following features are required:

- Hard disk
- Floppy disk drive or network link
- RS-232 serial interface for the host (MS-DOS COMM2)
- RS-232 serial interface for the target (MS-DOS COMM1)
- Terminal emulation software package (VTERM for a VAX host)
- SANDAC V GATAR debugger (MS-DOS file S5.EXE)
- SANDAC V Hawkeye debugger (MS-DOS file HAWKEYE.EXE)
- Printer (optional)

When running:

- GATAR, the target is connected via an RS-232 serial channel to the SANDAC V Utility Module external connector.
- Hawkeye, the RS-232 channel is connected to the System I/O Module's serial channel A.
- Within the development system environment, these connections are through the user's chassis, which provides optical isolation and buffering for all communication signals and provides power for the target system.

6.6.4.3 GNC Processing. The RRS GNC Flight Computer will process the signals and data relative to the RRS for the operations that entail:

- Monitoring the satellite operating environment/conditions
- Executing the procedures for the satellite functions of
 - Guidance, Navigation & Control (GNC)
 - Telemetry, Tracking & Control (TT&C)
 - Habitat / Experiment Data Handling (HEDH)

The RRS Processing hardware and software resides aboard the RRS, as described herein, but there are also provisions for ground interface, controlling and emulation.

6.6.4.3.1 Mission

6.6.4.3.1.1 Design Scenarios. There are five basic design scenarios to be used. The parking orbits vary in altitude between 350 and 900 kilometers with inclinations between 28.5 and 98 degrees. Launches are to be made from ETR or WTR pads (latter for 98°) with selected WSMR or "coastal" water recoveries (in ETR, WTR or Gulf regions for 28.5°) either by soft-landing or air-pickup. The space habitat will be extensively varied between 0 and 1.5 g's (see Attachment A for details). A reentry angle of roughly 3.5 to 4 degrees is planned for the RRS descent, depending upon the DRM used in accordance with the g-load (<15) and heating constraints. The RRS recovery dispersion is constrained to be $<\pm 6$ and 30 kilometers for crossrange and downrange errors respectively. The RRS system is designed to be reusable within 60 days of turnaround time for as many as 3 flights per year over 10 years of total refurbished system lifetime.

6.6.4.3.1.2 Design Requirements. In addition to the main and secondary design requirements that are specifically imposed by the customer. There are certain software requirements relating to the development/documentation/review, as well as design pads (arbitrarily assumed 50% for the sizing and timing estimation) for uncertainty/growth provisions which must be considered. However, there is not a mandated real-time language, and neither is fault tolerance directly demanded. Tentatively, SAIC has decided on using the "C" languages for implemented code. In addition, certain provisions will be made for fault tolerance to enhance mission performance.

The C language will be supplemented with assembly language routines as necessary. The SANDAC operating system is written in C, as is much of the systems level software and applications software to date. Ada has been considered since an Ada cross-compiler has been up and running for over 2 years. However, because of the importance of life-cycle costs and the time-criticality of operating latencies, C is the better choice for both signal and data processing applications. The use of C gives the programmers access at a low enough level to produce efficient code that is required for hard real-time applications, and yet, still be free of the details that are an inherent part of assembly language programming.

The provisions for fault tolerance will include spotting/averting SEU susceptibility (by voting the results of redundant processors or by using memory checksums for bit drop), yet other forms of diagnostics, checking buffers, and statistical estimation filters for overload and impending in-observability respectively, bus/processor/memory redundancy, alternative logic paths, equipment cooling, occasional memory refreshing from more reliable storage facilities to avoid fault buildup, etc., will be implemented.

6.6.4.3.2 Processing Overview

6.6.4.3.2.1 Basic RRS Design Considerations. The RRS spacecraft is comprised of two modules that are separated while in orbit in order to achieve the RRS scientific objectives. The Main Module contains the Payload Module, the GNC equipment/logic, an IMU, and is encased in a nose cone with a passive heat shield. The Deployed Module contains the propulsion elements, most of the TT&C elements, and passive provisions for thermal control, and an IMU and GPS receiver(s) / antennas used for both navigation and primary attitude determination. The variation in artificial gravity (centripetal acceleration) is achieved by spacecraft rotation at 0 to 10 rpm about its center of mass. The RRS configuration is axially symmetric with the moment of inertias approximately a factor of 4.23 larger about the two X and Y axes (associated with roll and pitch respectively) than that for the longitudinal Z axis (yaw) of the spacecraft when the masts are contracted, whereas the factor is approximately 821 when the masts are extended. The masts are contracted before the attitude-critical de-orbit maneuver is made. Relevant spacecraft dynamic and environmental considerations are provided in Table 6.6-9.

RRS software development/performance issues that must be considered include:

- Spacecraft flex effect on attitude estimation and control
- GPS attitude determination accuracy and filter convergence time
- De-orbit targeting of atmospheric disturbances

RRS software development guidelines include:

- Integrated GPS approach / rationale (navigation and attitude)
- Pseudo-targeting concepts for de-orbit simplicity / effectiveness
- De-orbit maneuver that controls impact position and reentry flight path angle
- Closed-form solutions of Euler Equations of 6DOF motion amenable if symmetrical torqued body (constants, per certain general axial circumstances)
- Closed-form circular orbit partials also amenable for perturbing accelerations that are constant or even vary quadratic in time
- Artificial gravity
- Technology freeze date
- RRS system users

The key assumptions made in the software analyses done for this study include:

- Rigid body dynamics
- Idealized point-mass motion along conics with smart compensation for realistic modeling

Table 6.6-9. Satellite Dynamic/Environmental Considerations

<ul style="list-style-type: none"> • Environment <ul style="list-style-type: none"> - gravitational oblateness - aerodynamics (drag, climatology, winds) - solar radiation pressure • Dynamics <ul style="list-style-type: none"> - 3DOF for guidance, navigation, attitude determination - 6DOF for attitude control (concern of rigid body adequacy versus flexible body motion / ramifications) • Sensors (associated concerns) <ul style="list-style-type: none"> - clock (master identity, accuracy) - GPS receiver (number & type) - GPS (number & type) & com antennas - interferometer (need?) - magnetometer - altimeter - beacon • Measurements <ul style="list-style-type: none"> - time - altitude - TOA of RF signal - DTOA - LOS - magnetic flux • Controls <ul style="list-style-type: none"> - main propulsive engine of booster - de-orbit / retro engine - vernier / attitude control thrusters - torque rods - reaction wheel - heat shield - chutes - s/w pseudo controls
--

6.6.4.3.2.2 Processing Functions. The software design problem can be considered a multi-faceted process. The associated functions, in the modularized multi-processor context, includes the distinct operations of:

- GNC
- TT&C
- HEDH

6.6.4.3.2.3 Computers. The GNC process will be an entirely onboard processing operation (except for nav messages being refreshed), with total ground emulation and simulation capability in compatible ground computers.

The software development, debug and execution environment is comprised of three separate computers—target, host and gateway. SAIC anticipates that the software development will be done in a VAX-11/780 computer running the VMS operating system (the so-called "host" machine). Since the embedded computer ("target" processor) chosen for onboard processing does not have provisions for user peripherals such as snazzy human-oriented displays and printout, the "gateway" computer to do these things is envisioned to be an IBM PC or a compatible version running on MS-DOS. Interaction between the the host and gateway computers is via a serial communications link. Code is written, compiled and linked on the host. The executable object code is downloaded to the gateway and stored there on a disk file. A second gateway (serially connected to the target) is then used to download the executable code into the target.

6.6.4.3.2.4 Algorithms. This section describes the baseline algorithmic schemes for RRS GNC, as well as other variants also under consideration.

An integrated GPS approach has been adopted for both the conventional solution of the navigation problem and for the unconventional solution to the attitude determination problem. Other considerations such as systematic noise rejection by using DTOAs, pre-filtering of random noise wild points, and an extremely simplified alternative to statistical filtering such as weighted averaging of correlated "bi-planar" estimates of body-coordinates for the LOS with *a priori* or adaptive weights can be applied.

Other algorithm considerations and design features are noteworthy. One is that for any choice of an RRS parking orbit, the time-averaged variations in the semi-major axis (a) and eccentricity (e) over an orbital period are zero to first order in the first zonal harmonic term (J_2) of the Earth's gravitational potential. Moreover, these are two orbital elements that uniquely represent the dominant terms (radial velocity \dot{r} and tangential position θ) in the buildup of circular orbit errors / uncertainties. Another consideration / feature is that similarly analytical expressions can be readily formulated for the perturbing influence of atmospheric drag and solar radiation pressure can also be used for the nearly constant orbital perturbation of gravitational oblateness as well as perturbations due to other influences. This is germane, for example, when the satellite is not sunlit (occurring roughly one-third of the time) or when its frontal area to mass ratio varies significantly such as during lengthy orientation maneuvers, or even if there are unequal aero and solar loads

because of flexible body dynamics. A third consideration/feature is that station-keeping which is conventionally done via corrective strategy such as

- changing i with a small impulse at nodal crossing
- changing a and e with a tangential impulse at apsis (Hohmann transfer)
- changing ℓ with an assumably small impulse 90 degrees from node

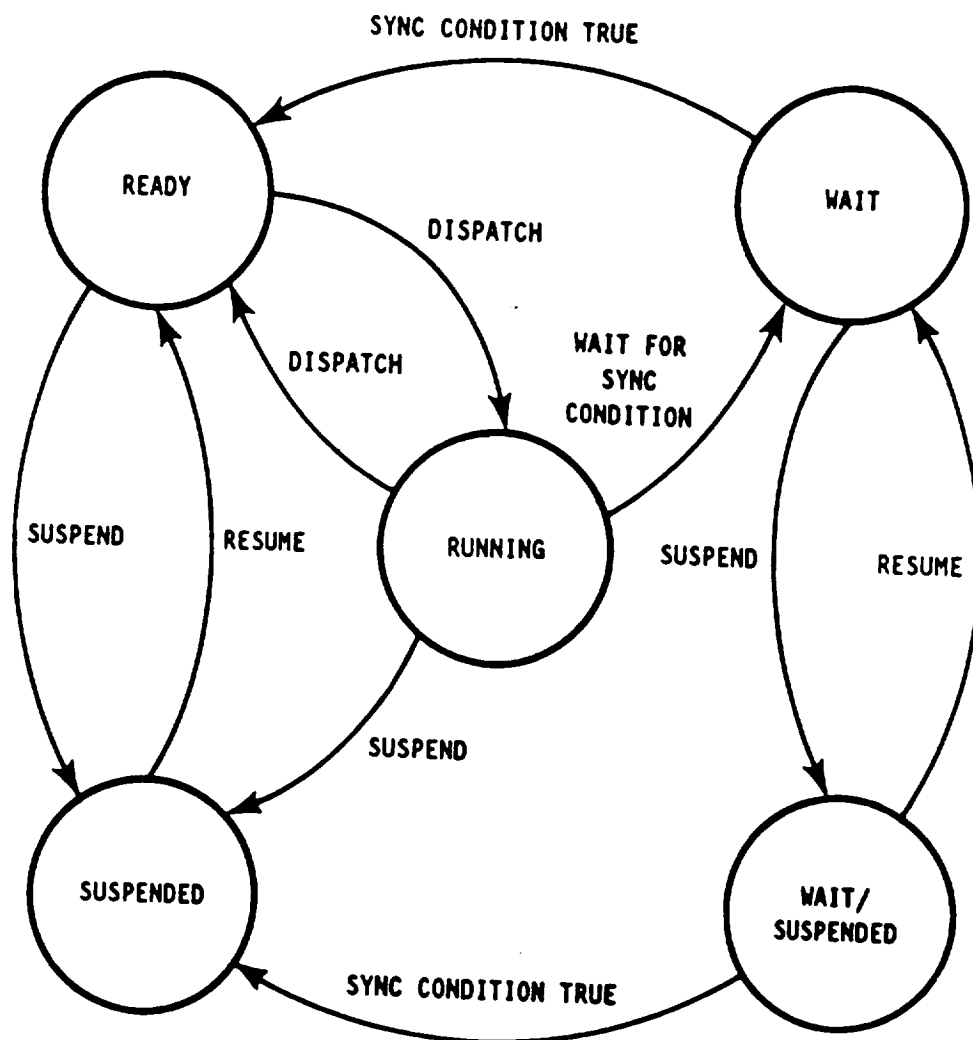
can be alternatively performed by simply interrelating the variations in the orbital elements to the Frenet coordinate variations (RTN frame) or even directly performed solely on the basis of the Frenet variables. The last consideration / feature is that the orbits of the RRS DRMs have bounds on certain orbital elements (a and i) that are specified by NASA and by range safety considerations for ETR and WTR launches. In addition, there are other constraints, due to public safety concern and interface with other satellite constellations, that further restrict the choices of i and even somewhat ℓ . The former entails reentry / approach flight corridors say to WSMR that put a minimal population at risk in case of malfunction. The latter entails using GPS or TDRSS for navigation / attitude functions and user / controller effectiveness respectively.

6.6.4.3.3 Operating System. The SANDAC V has an operating system kernel, known as Hawk, that provides an extremely fast set of primitives, or services to support the multitasking solutions needed for applications software that can take advantage of the unique real-time environment. Hawk also provides transparency to system details and supports performance measurement and debugging. Optimally, application programs are written using the C programming language, and requests for Hawk services are specified as C-language procedure calls.

Hawk resides in global ROM, and at power-up, is replicated in each Processor Module's local RAM. Calls for Hawk services (Table 6.6-10) by a given Processor Module are handled Hawk copy resident in local memory. If the service call involves another Processor Module, the processing is done locally, and upon completion, the other module is notified via a hardware mechanism.

With Hawk-supported multitasking, each task is assigned an initial priority. A dispatcher mechanism, which can be disabled if required, is used to schedule tasks using a highest-priority-first mechanism. Only tasks associated with a particular Processor Module are scheduled by its copy of Hawk. Hawk task states are shown in Figure 6.6-39.

- Task control
 - Tasking
 - Task Creation
 - Task Priority/Scheduling
 - Task Control Block
 - Task States
 - Ready
 - Running
 - Wait
 - Suspended
 - Wait/Suspend
- Intertask communication
- Timer control
- Memory allocation
- Interrupt control
- Window functions for the Hawkeye Debugger



6.6-63

When enabled, the scheduling activities of the dispatcher make Hawk an active component of the task over which the application has no control. When an application requires stringent control of the sequencing of an operation, the dispatcher can be disabled.

The basic logical unit controlled by Hawk is the task. An application may consist of a single task or may be partitioned into multiple tasks. Multiple tasks can run on the same SANDAC V Processor Module or on separate modules. An application may be a single task or partitioned into multiple tasks which in turn may be run on a single or multiple Processor Modules. Multiple tasks run on a single module appear to execute concurrently since they are executed in an interleaved fashion by distributing processing time on a task priority basis. The task ID, established when the task is created, allows Hawk to ready tasks or to block them in a Wait state on a selective basis. The ID also lets tasks suspend other tasks or themselves. A dispatcher in the Processor Module's copy of Hawk automatically schedules tasks with the highest priority first and then executes the highest priority task. Tasks with the same priority are dispatched in a serial, rotating fashion. The dispatcher schedules only tasks associated with the local Processor Module; no global scheduling is provided.

Hawk provides the ability to disable the automatic dispatcher since real-time situations may require a task to have complete control over the sequencing of operations. The ability to disable the dispatcher allows task-level control whereby a running task actually controls the sequencing of task execution.

Since multiple tasks must be able to intercommunicate, the Hawk allows a message to be passed between tasks operating on the same Processor Module, between those operating on different Processor Modules, or across a communication channel to the Gateway or another SANDAC V. The destination for any communication involving separated tasks is referred to as a remote message queue, and a sender need know only the name of the queue to establish a link to it. A receiving task may interact with its queue in either a synchronous or an asynchronous manner. However, a receiving task must always take an active role in polling for receipt of messages since there is no way for a task to be interrupted asynchronously upon receipt of a message. Since "Real-time" applications require a precise way of determining the elapsed time of an operation as well as a predictable mechanism for the synchronization of tasks to absolute time, the Hawk services provide for elapsed time and for delay functions.

6.6.4.3.4 Applications Development. SANDAC V application programs are developed, coded, and tested with an integrated software development system consisting of a host computer, a

Gateway, and a target SANDAC V. The GATAR (Table 6.6-11) debug program serves as a "front panel" to SANDAC V, and is used for downloading executable files into SANDAC V memory and controlling all hardware features in addition to hardware/software debugging. GATAR also provides a simple interface between software and the programmer for operating and debugging applications that do not use the Hawk operating system. GATAR is functionally self-contained—the SANDAC V may be turned on and exercised with no additional software.

Table 6.6-11. Summary of GATAR Functions

File Handling	<ul style="list-style-type: none"> • Load binary data from Gateway files to target system memory • Save binary data from target system memory to Gateway file • Verify the contents of target system memory with a Gateway file
Operator Interface	<ul style="list-style-type: none"> • Enter and display parameters in hex, decimal, floating-point, and text formats in all sizes supported by the hardware • Handle application code input and output via simulated <i>stdin</i> and <i>stdout</i> • Access MS-DOS without exiting GATAR • Execute all functions either manually via the keyboard or in batch mode • Log all transactions to a disk file or printer • Enter and display parameters by symbolic name • Extend the command set through operator-defined keyboard macros • Display contents of target memory locations in an operator-specified screen format
Execution Control	<ul style="list-style-type: none"> • Reset a target system processor • Execute application code beginning at a given instruction address and stopping at a given address or previously installed breakpoint • Execute the current machine instruction and stop • Install, remove, or modify up to eight instruction breakpoints • Break the execution of a process immediately • Display target system memory, registers, and execution status • Change the contents of individual target memory locations or registers • Fill a block of target system memory with a specified data pattern • Assemble and disassemble 68020 and 68881 instructions in target system memory

A user interacts with GATAR by entering commands on the Gateway keyboard. Optionally, this command input may be redirected to come from a prepared text file on disk in an auto-execution mode. From the keyboard commands, the Gateway constructs request packets that are transmitted to the SANDAC V, triggering the interrupts that are serviced by the GATAR firmware. The processor completes the action required by the command and transmits a response packet back to the Gateway, if necessary. The Gateway then processes the response packet and formats a display on the Gateway screen.

The SANDAC V hardware and applications software interact with GATAR by means of traps. A few of the processor's software traps are dedicated to GATAR functions, such as simulation of console input and output. The rest, including processor exceptions, are handled by

default exception handlers in the GATAR firmware, but they may be reassigned to user-supplied exception handlers.

The relationship between the Gateway and target portions of the GATAR software is such that user commands and responses have minimal impact on application software running on SANDAC V. When SANDAC V services a command interrupt, the state of the target is saved so that it can be examined or modified and restored after execution of the command. Since GATAR is a software-based debugger, it necessarily disturbs the SANDAC V slightly to observe its state. However, the SANDAC V processor time to service a command has been minimized to avoid problems when troubleshooting time-critical application software. When the GATAR terminal is not active on the global serial bus and no exceptions are being handled, the GATAR firmware has no effect on the execution of application software.

GATAR can process console I/O from any of the 15 possible processors in a SANDAC V, even though the Gateway is functionally attached to only one processor at a time. The SANDAC V resident GATAR code maintains separate input and output queues for each processor, and the processor using the global serial bus manages all input and output queuing to and from the Gateway for all the processors. In the Gateway, one buffer is reserved for each SANDAC V processor to collect messages to and from that processor.

The software development system (Figure 6.6-40) provides interaction between the host and the Gateway via a serial communications link. The executable object code is downloaded from the host to the Gateway and stored in a disk file on the Gateway. A second Gateway, with a serial connection to the target machine, is then used to download the executable code into the SANDAC V. The host computer is a mainframe (i.e., a VAX-11/780) equipped with a set of software development tools (Tables 6.6-12 and 6.6-13) targeted for the SANDAC V 68020 processor/68881 coprocessor environment.

During the host computer applications software creation, C-language or assembly language source code is written using the resident editor (VAX EDT or LSE for a VAX-11/780) and stored within the host file system. Software development tools then convert the source code into executable machine code. Figure 6.6-41 is a flow diagram illustrating the software creation process.

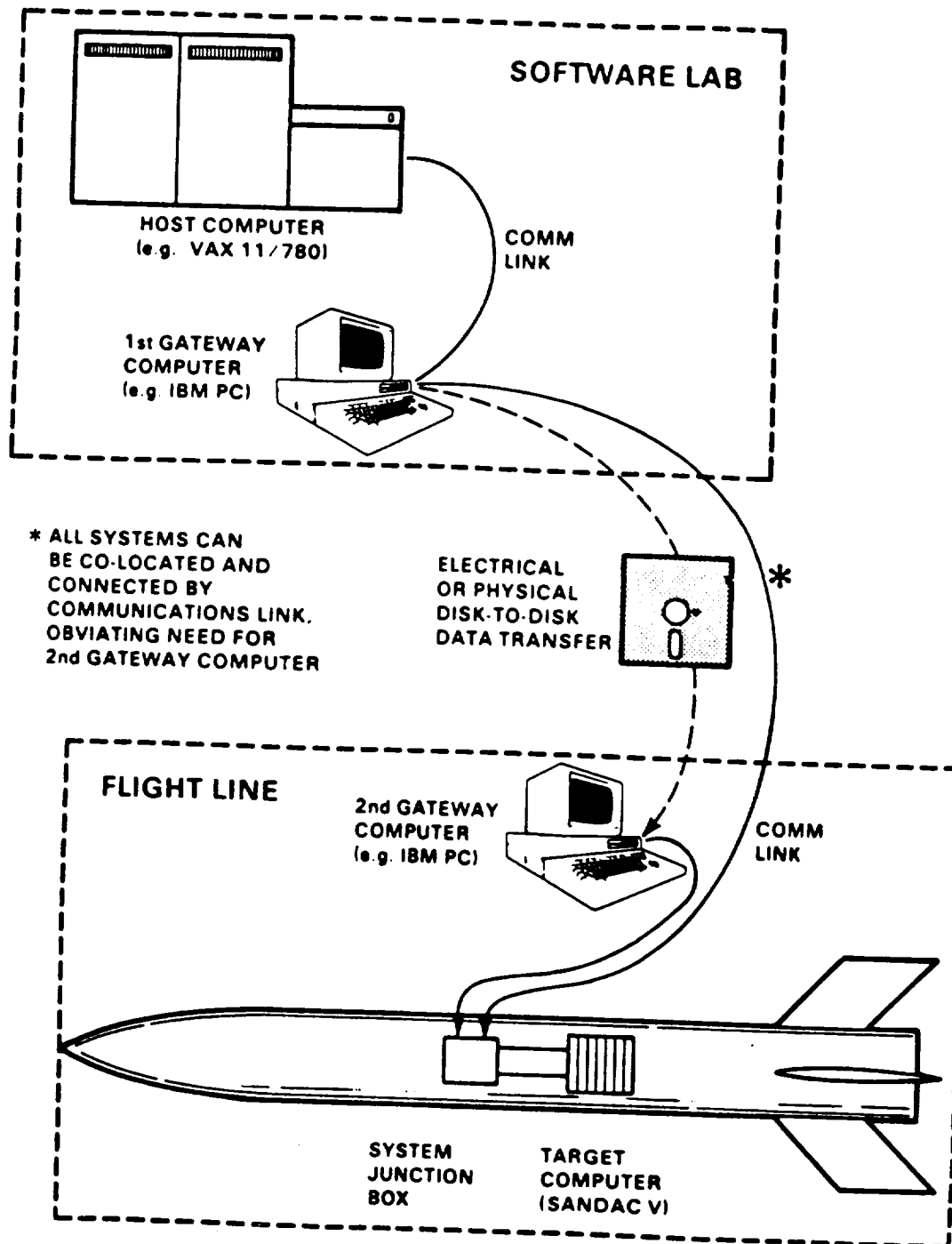


Figure 6.6-40. SANDAC V Software Development System

Table 6.6-12. Standard SANDAC V Tool Set

- C-Language Compiler

Kernighan/Ritchie implementation of the C programming language and the extensions implemented in AT&T and Berkeley UNIX. Takes as input one or more files containing C-language source code and produces a single output file containing 68020 assembly language source code.

- OASYS CMERGE Utility

Generates assembly language listings that contain, as comments, the lines of C-language source code that produced the assembly language code.

- Quelo Assembler Package (Table 6.6-13)

- SANDAC V Object Format Conversion Utilities

- Libraries Supporting

- C Programming Language

Math functions (e.g., sin(x), etc.) are grouped separately since the C compiler can generate 68881 floating-point coprocessor instructions for mathematical operations.

- Hawk Operating System

- GATAR/Hawkeye Debug Programs.

Table 6.6-13. The Assembler Package

The Quelo 68020 Assembler Package, which includes the following components:

M68K Macro Preprocessor. Takes a source file of macro definitions and calls and produces an assembly language output file of macro expansions; the original definitions and calls are retained as comments.

A68K 68020 Assembler. Takes one or more files of 68020 assembly language source code as input and outputs a single file of relocatable object code.

QLINK Linker/Locator. Brings together separately assembled modules of object code into one large program. During the link operation, the code is relocated to executable memory addresses, and references between modules are resolved.

QLIB Object Librarian. Collects in a single file separately assembled modules of object code.

OSYM Symbol Report Generator. Interprets assembler, linker, and librarian file symbol information to produce module revisions, symbol table, cross-reference, and memory map reports.

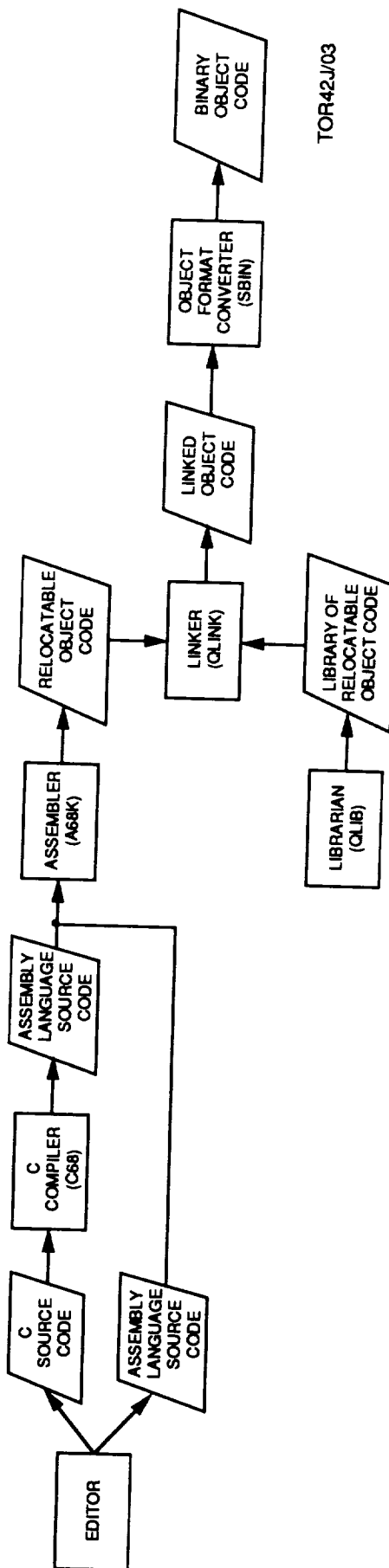
OHEX Hex File Utility. Converts object files in Motorola S-record format to Motorola S1, S2, or S3, Intel hex, or Tekhex record formats for ROM programming.

LTXDUMP Linker Text Dump Utility. Displays the contents of binary object files in readable form.

The tool sets for conversion of the SANDAC V object code to a binary format before being loaded into a target system includes:

BIN Utility. Converts object files in Motorola S-record, UNIX a.out, or a binary image to the SANDAC V binary load format.

SBIN Utility. Converts object files in Motorola S-record format to the SANDAC V binary load format.



TOR42J/03

Figure 6.6-41. SANDAC V Software Creation Process

6.6.4.3.5 Debug Operations. GATAR, a self-contained monitor/debugger developed specifically for the SANDAC V, consists of two cooperating programs, one running on the Gateway under MS-DOS (S5.EXE) and one running on the target system (GATAR ROM, also referred to as the GATAR firmware). The programs, communicating over a bidirectional data link (Figure 6.6-42) using an efficient binary protocol, load and activate other software and control the target system for machine-level debugging. The target system's portion of GATAR is resident in SANDAC V firmware. Commands entered via the Gateway keyboard are interpreted by the Gateway's portion of GATAR, which interrupts the target and sends a command packet. When the target's portion of GATAR receives the command, the application is interrupted, and either the command is executed or an information packet is created and returned to the Gateway, or both. All appropriate information is displayed at the Gateway. Functions available through GATAR are summarized in Tables 6.6-14 and 6.6-15.

The Gateway portion of GATAR, manages all interaction with the user, formats data into and from user-readable form, and provides mass-storage facilities. The Gateway assumes much of the time-consuming, text-processing workload to avoid overloading the SANDAC V and minimize the effort required to make cosmetic changes in the operation of the system. Most of the Gateway program is coded in C-language to facilitate maintenance.

The SANDAC V portion of GATAR (GATAR ROM) extracts/alters data and controls the SANDAC as commanded by the Gateway. The GATAR ROM, consisting entirely of trap- and interrupt-driven code written in assembler language for maximum speed, resides in the SANDAC V's Utility Module ROM and is available whenever system power is applied.

Hawkeye, a task-level debugger developed specifically for the SANDAC V system consists of the MS-DOS Hawkeye program in the Gateway and Hawk kernel services that monitor/control the Hawk operating system while an application is running under Hawk control. The program:

- Provides an interactive user interface to the application code that executes under the Hawk OS in the SANDAC V,
- Enables a user to monitor and debug tasks executing in the multi-processor, multi-tasking environment of a SANDAC V.
- Manages all user Gateway/Hawk interaction including access to the Hawk-kernal debugger (Cbug)
- Monitors and controls applications running under the control of the Hawk operating system

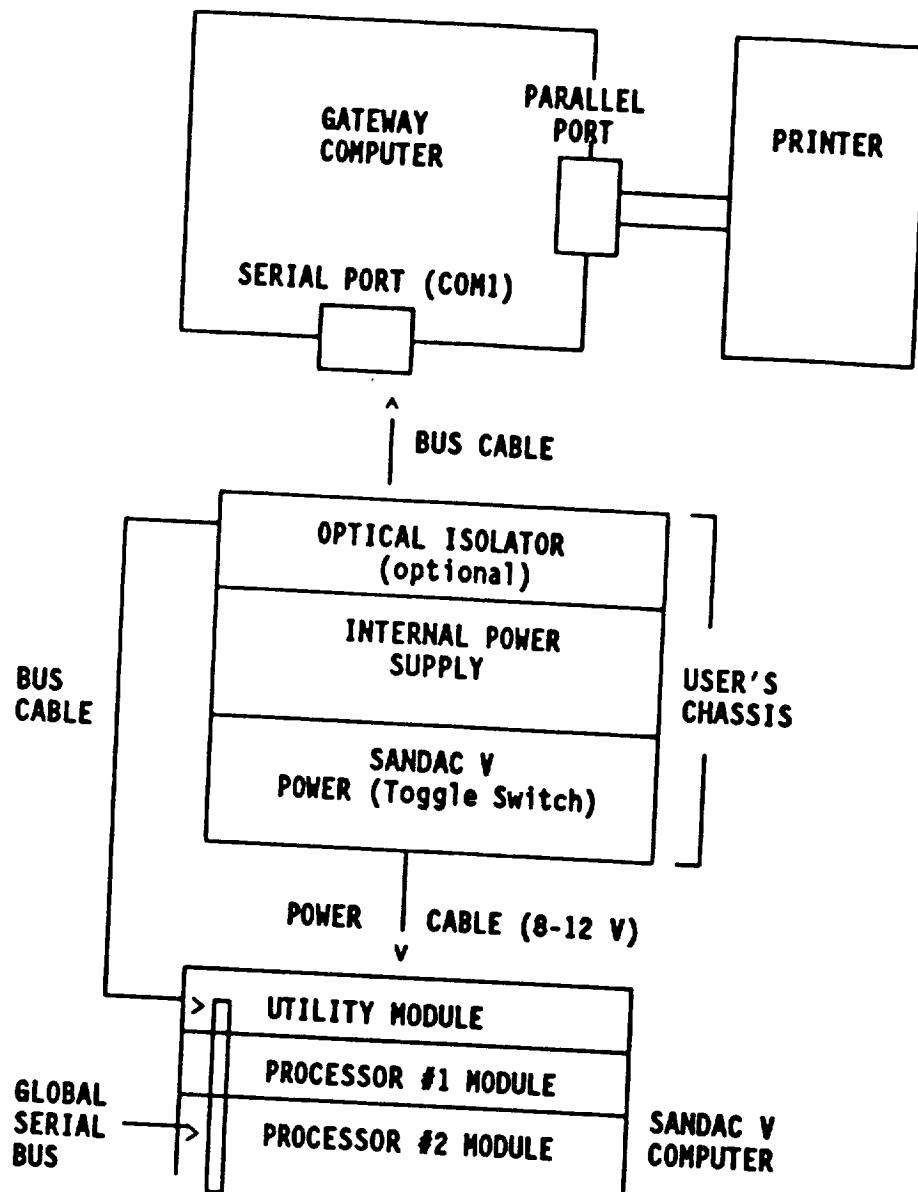


Figure 6.6-42. Debugging Equipment Configuration

Table 6.6-14. GATAR Capabilities

- Load code from Gateway disk file to SANDAC V memory,
- Save code from SANDAC V memory to a file on the Gateway,
- Verify the contents of SANDAC V memory with saved file,
- Reset a processor,
- Execute code from a given point to a given point,
- Execute a single machine instruction,
- Set, remove, or change instruction breakpoints,
- Terminate a process immediately,
- Display contents
 - memory, registers
 - current execution status,
- Change contents of individual memory locations, registers
- Fill a block of memory with a given data pattern,
- Assemble and disassemble 68020 and 68881 instructions,
- Enter and display parameters in
 - hexadecimal, decimal, floating-point, textual formats—all sizes supported by the hardware,
- Handle input/output via simulated standard I/O functions,
- Access MS-DOS commands without leaving GATAR,
- Start all functions
 - manually from the keyboard,
 - batch mode via a text file,
- Log all transactions to a disk file or to a printer,
- Enter and display parameters by symbolic name;
- Support symbol tables
 - built by compilers, assemblers, and user commands,
- Display contents of memory locations
 - user-defined screen format
 - continuous updating.

Table 6.6-15. GATAR Symbolic Debugging

- The symbol table can hold about 2000 symbols, depending on the average length of the symbol names and the memory available in the Gateway.
- Each symbol has a name, an associated data type, and an integer value.
- In general, the name corresponds to a global variable name, a function name, or a public label name from the application program.
- The data type corresponds to the storage format of the named data, i.e., the format in which the data will be displayed or modified by a GATAR command. For example, the symbol "sqrt" would be an INST data type if sqrt() is a function in the application program. Or the symbol "alt" would be a FLOAT64 data type if "alt" is a variable declared "double" in a C program.
- The value of the symbol generally corresponds to the absolute address of a data element, as assigned by the linker.

User input can be invoked at the keyboard or from a command file (auto-execution mode). The user, by making a few calls to the Hawk run-time library, can open display buffers in Hawkeye, send output to them, request input from them, read and write disk files on the Gateway, and a log data to disk files or a printer.

Hawkeye kernel services can be embedded in an application for diagnostic purposes. When the services are called during program execution, they work with the Hawkeye program to create display windows on the Gateway, to output messages to the windows, or to accept inputs entered in the windows.

The Hawkeye software resides on the Gateway. However, for Hawkeye to communicate with the Hawk operating system, Hawk creates a special window-server task. This server task, which is less than 1K bytes, is linked with the application code to be loaded into the SANDAC V. Hawkeye then communicates with the server task over a bidirectional data link, using variable length datagrams.

Cbug resides in the SANDAC V PROM at all times and is capable of displaying all of Hawk's internal data structures in an easily readable text format. Cbug also provides more traditional debugging features such as setting breakpoints, displaying/modifying memory, and assembling and disassembling instructions.

6.6.4.4 Computer Sizing Details. The formal methodology for processor selection ideally begins with prototype software being in-hand for RRS application. An "algorithm data flow analysis" is then performed and related throughput and memory analyses are made. The memory analysis consists of an apportionment of the nonvolatile memory (for storing data and code of the programs) and the local addressable memory (per program function sizing). The throughput analysis consists of transforming the measured throughput from the mix of operations in the developmental code to the mix of instructions that is typically the standard of comparison for candidate s/c processors (such as the DAIS mix conventionally used for 16-bit machines). The separate processing throughputs for each software function, or at least for the "driving functions," enter into play as do also whether the functions can be done in parallel. This transformation entails a mapping from the throughput currency of Mops, used for the developmental code, to Mips as candidate processors are rated, and is machine and somewhat language dependent. In addition, a mapping is needed for the ramification of single to double or extended precision (which is usually considered x 2 for a VAX but seemingly much closer to 1 if a 1750A / Ada is used). Finally the ramification of using the desired real-time language as opposed to the language of the

developmental code enters into the mapping (with effect and capability somewhat nebulous, but still one can make certain quantitative statements such as Ada requiring 20 to 50% more code than Fortran or C). The actual precision and mix figures are modified in accordance with rules of thumb such as an extra bit being needed whenever a power or multiply is encountered in the coding. Taking into account needs such as re-starting to save power, the processor recommendation is made by blending the three analyses to make a comparison between the throughput rating and memory capacity of the candidates. The final recommendation is in the form of the desired word length, memory (addressable / primary), and operating system.

6.6.4.4.1 Software Sizing and Timing. Ideally sizing and timing analysis and the methodology for selecting a processor for real-time space processing are linked together. However, since prototype software was not available for the preliminary RRS design, a mixed suite of state-of-the-art techniques supplemented by certain potentially simplifying enhancements to routines that are commonplace for RRS GNC functions were used to estimate the software resources that are needed.

Although we have considered certain nominal TT&C operations in the estimation of needed computer resources, the HEDH functions have not been factored into the analysis since they are considered a relatively minor contributor to the budgeting.

The resultant sizing and timing analysis is succinctly treated in Table 6.6-16.

The main premises of our software sizing and timing analysis have been the following: 1) use of the C real-time language, 2) a pad of 50% for accounting for design uncertainties and future growth considerations, and 3) provision generally for doubly redundant software manipulations that are even triply so for decisions entailing "controlled reentry" (tantamount to safety and eventual man-rated considerations for events starting with the de-orbit maneuver in the descent timeline of events). In addition, we have further padded the sizing and timing estimates by an added 50% factor for un-sized (but preliminarily formulated) functions starting with the de-orbit maneuver logic.

6.6.4.4.2 Memory Sizing Requirements. We have estimated that the memory requirements for applications software as 0.50 and 0.51 Mbytes needed for data and code, respectively. For the generalized operating system (of OS / I-O / test / utilities functions), the corresponding estimates are 0.10 and 0.12 Mbytes respectively. These numbers were obtained by presuming that 48-bit words of extended precision are relevant for the "raw" sizing estimates that are documented

for a 1750A machine of 16-bit words. In addition, there is the slight wrinkle of enlarging the data storage by 0.04 Mbytes to account for GPS navigation messages of presumed two-weeks duration/validity. The memory breakdown by function is 0.36 Mb of data for "conventional ephemerides," deterministic orbit / attitude solutions, Kalman filter, and attitude control system. For code, it is 0.54 for executive and s/w control and the latter three aforementioned entities. Also, 0.07 and 0.05 Mb of data and programs storage respectively is needed for fault detection monitoring and correction logic. Software for power and thermal management / control functions and command / telemetry processing necessitate 0.07 and 0.04 Mb respectively.

Table 6.6-16. Software Sizing and Timing

<ul style="list-style-type: none"> Resources Needed for all Non-HEDH Functions of GN&C and TT&C Operations Estimated on Basis of <ul style="list-style-type: none"> Similarity to Generic Functions of Pre-Sized Needs Preliminary Definition of Baseline Algorithms Blending Independent Estimates of Needed Resources Premised on <ul style="list-style-type: none"> C Language Usage 50% Pad for Design Uncertainty and Growth General Double Redundancy Except Triple for Decisions Affecting Events in Timeline Starting With De-Orbit Need (Disregarding Pad and Added 50% for Roughly-Sized Functions Starting With De-Orbit) <ul style="list-style-type: none"> Memory <ul style="list-style-type: none"> 0.50 and 0.51 Mb for Data and Code Respectively of Applications Software 0.10 and 0.12 Mb Respectively for OS/Test/IO/Utilities Throughput <ul style="list-style-type: none"> 1.44 Mips (DAIS Mix) If Data IO and Fault Correction Logic Not Swingers (Nominal Provisions Accorded) SANDAC Requirements for RRS <ul style="list-style-type: none"> Multi-Processor Computer of 11 Modules (of Commercially Available Parts Arranged in Parallel) <ul style="list-style-type: none"> 2, 2, 2, 2, 1, and 2 for System IO, Utility, 1553B, 68020 Processors, 68040 and Local memory Respectively Providing Capability of 1 (-UM) + 1 (-20 PM) + 2 (-40 PM) + 4 (-LMM) = 8 Mb and 2 (1.3) + 1 (14) = 16.6 Mips DAIS Which Suffices for $2.46 \times 3 = 7.38$ Mb for Code and Data and $2.88 \times 3 = 8.64$ Mips Per Double/Triple Redundancy as and When Needed Corresponding Subsystem Requirements of <ul style="list-style-type: none"> Power of $10 \times 5 + 1 \times 6 = 56$ watts* Weight of $10 \times 1 + 1 \times 1.2 = 11.2$ pounds** Size of $10 \times 26 + 1 \times 26 = 286$ cubic inches** 	
	<ul style="list-style-type: none"> * 10 or 28 volts DC ** Plus Shielding/Cooling Needs

6.6.4.4.3 Throughput Requirements. RRS throughput was estimated as 1.44 Mips for a DAIS mix. The brunt of this amount is due to 1.3 Mips needed for the navigation and attitude software. Approximately 0.11 Mips is required for fault tolerance, and 0.25 Mips is needed for power and thermal management/control as well as command/telemetry processing. Only a nominal amount of task scheduling and message traffic was assumed in the timing analysis.

Adding up the memory demands gives $0.5 + 0.51 + 0.12 + 0.1 = 1.23$ Mb times two factors of 2 and 3 respectively for the effect of the design pad and un-sized functions and for the mandated triple / double redundancy. Thus, 7.38 Mb is required for local memory.

Similarly, the throughput demand is $1.44 \times 2 \times 3 = 8.64$ Mips DAIS.

6.6.4.4.4 Computer Resources Summary. These software resources can be achieved with 11 SANDAC modules. Accordingly, the local memory capability is 8 Mb of which 1 Mb comes from the utility module (so-called UM), 1 Mb from two 68020 processor modules (20PM, that is also needed for managing the system I/O data traffic interface), 2 Mb from the single 68040 processor module (40PM), and 4 Mb from two local memory modules (LMM). The throughput capability accorded is $2 (1.3) + 1 (14) = 16.6$ Mips DAIS, which had an added reserve of 92% in case extra message traffic and task scheduling is needed.

The corresponding s/c loads for these 11 SANDAC computer modules are as follows:

- Power = 56 watts
- Weight = 11.2 pounds
- Size = 286 cubic inches

6.6.4.4.5 Other Underlying Considerations. There are certain underlying considerations that are important to software development for the GNC portion of RRS project, such as:

- Paramount requirements analyses
 - Error analyses
 - Sizings/accuracies needed/driving considerations
 - Orbit choice
 - Station-keeping (total delta-v, schedule & strategy)
 - Attitude stabilization modes used / reason / regimes
 - Attitude accuracy for de-orbit (vs artificial g)
 - De-orbit delta-v, burn time, predicted impact velocity
 - Retrofire delta-v per impact velocity
 - Chute delta-v handled, redundancy, winds effect / model
 - Details of event timeline
 - Range / public safety (constraints, provisions)
 - SEUs from Van Allen belt

- Integrated hi-fi simulator & associated building blocks
 - Software tools available, needed, mapped out / overview ,.....
 - Mission analyses of import similarly
- Orbit choice
 - Basic notions / variables at play (why circular orbit, why certain inclinations and altitudes used,)
 - Effect on thermal loading, station-keeping, etc
- Treatment of jointly optimized G&C or attitude problems

6.6.4.5 Interface Support. The GNC has functional interface requirements associated with all vehicle subsystems (Table 6.6-17).

Table 6.6-17. GNC Interface Support

• PAYLOAD:	PROVIDE ARTIFICIAL GRAVITY CONTROL <ul style="list-style-type: none"> - Comply With Magnetic Field Limitations - Provide Command and Data Interface - Cancel Angular Momentum
• PROPULSION:	PROVIDE ATTITUDE THRUSTER CONTROL <ul style="list-style-type: none"> - Provide Retrofire Thrust Alignment - Control Retrofire and Trimburn Thrust Duration
• TT&C:	RECEIVE COMMANDS <ul style="list-style-type: none"> - Provide Telemetry Measurements for: <ul style="list-style-type: none"> - Attitude Determination and Control - Structural Dynamic Alignment - Reentry/Recovery Performance - Provide Location/Attitude/Impact Data for Tracking Beacon
• POWER:	CONTROL SUBSYSTEM CONFIGURATION AND REDUNDANCY SWITCHING CONTROL LOADSHED
• REENTRY:	PROVIDE VEHICLE STABILIZATION DURING RETROFIRE AND TRIMBURN <ul style="list-style-type: none"> - Compute Trimburn Required for Precision Landing - Reorient for Correct Aerodynamic Reentry
• THERMAL:	CONTROL THERMAL ROTISSERIE AND CANCEL ANGULAR MOMENTUM
• STRUCTURE:	MONITOR STRUCTURAL ALIGNMENT

6.6.4.6 Weight/Power. Tables 6.6-18 and 6.6-19 provide the weight and power summary for the preliminary GNC design.

Table 6.6-18. GNC Mass and Power Summary

Component (watts)	Function	Mass (lb) Ave.	Power Peak	
MICROGRAVITY MODE				
GPS - Receivers(*) (3)	Navigation/Orientation	30.0	18.0	27.0
IMU - RLGA	Inertial Reference (2)	13.0	17.0	34.0
MADS - Magnetometers (2)	GG Attitude Determination	0.4	0.06	0.06
- TORQRODS (3)	GG Attitude Control	27.3	2.7	34.2
- Momentum Wheel (2)	Yaw Momentum Control	26.4	2.0	32.0
- Electronics	Pwr Supply (1) (80%)	1.4	15.64	15.64
	Subsystem Interface (1)	1.4		
	TQR Controller (1)	1.4		
	Motor Drivers (2)	2.8		
	Microprocessors(*)(*):			
	MADS (1)	1.4		
	Thruster (1)	1.4		
	GPS/RLGA (1)	1.4		
	Control Law (1)	1.4		
	Subtotal	109.7	55.4	142.9
ARTIFICIAL GRAVITY MODE - Additional Equipment				
MADS - SCANWHEELS (2)	Attitude Determination/Cont	30.8	2.2	32.2
- Electronics	Additional Power (80%)	—	8.75	8.75
	Motor Drivers (2)	2.8		
	Microprocessors(*)(*):			
	Sensor Sig (2)	2.8		
	Attitude (2)	2.8		
	Subtotal	39.2	10.95	40.95
GNC SYSTEMS TOTAL		148.9	66.35	183.85

(*) One 5 Channel C/A Rcvr with Dual Antenna provides single vector determination.
(*)(*) Microprocessor total is 14.0 lb, 22.5 watts

6.6.5 Control Requirements

Although the GNC subsystem has been configured to not require TDRSS coverage, TDRSS coverage for the de-orbit burn and other similar critical functions will probably be viewed as desirable by operations personnel.

6.6.6 Special Testing

Both the fail operational nature of critical functions (e.g., propulsion control) and the precision of the GPS attitude determination capability require special test consideration. Of these

Table 6.6-19. Guidance and Control Mass and Power

Component	Mass (lbs)	Power (Watts)	TOTAL MASS		
			MM	DM	MM
MAGNETOMETER A	0.2	0.03	215		
MAGNETOMETER B	0.2	0.03	24		
TORQUE ROD 1	9	0.9 AVG/11.4 PEAK			
TORQUE ROD 2	9	0.9 AVG/11.4 PEAK			
TORQUE ROD 3	9	0.9 AVG/11.4 PEAK			
DUAL WHEEL AND SENSOR	28	2 AVG/16 PEAK			
DUAL MOMENTUM WHEEL 2	26	2 AVG/16 PEAK			
WHEEL AND SENSOR	14	1 AVG./16 PEAK			
MOMENTUM WHEEL 4	13	1 AVG./16 PEAK			
ACS ELECTRONICS	20	10.00			
INERTIAL PLATFORM 1	13	14.00			
INERTIAL PLATFORM 2	13	14.00			
INERTIAL PLATFORM 3	13	14.00			
GPS RECEIVER 1	10	3.33			
GPS RECEIVER 2	10	3.33			
GPS RECEIVER 3	10	3.33			
GPS RECEIVER 4	10	3.33			
GPS ANTENNA 1-6	6	0.00			
GPS ANTENNA 7	1	0.00			
TOTAL			215	24	191

MASS VALUE (lbs)	UNCERTAINTY %	UNCERTAINTY (lbs)
0.2	2	0.0
0.2	2	0.0
9.1	2	0.2
9.1	2	0.18
9.1	2	0.2
28.0	2	0.6
26.0	2	0.5
14.0	2	0.3
13.0	2	0.3
20.3	2	0.4
13.0	2	0.3
13.0	2	0.3
10.0	5	0.5
10.0	5	0.5
10.0	5	0.5
6.0	2	0.1
1.0	2	0.0
TOTAL		

the fail operational aspect of the GNC operation is the most critical and the most difficult to test. Although the test will not require extensive special test equipment, the test will require a failure insertion capability and will require testing over a wide range of potential, not just anticipated, operating conditions. The GPS test will, on the other hand, be primarily an antenna test to demonstrate that multipath conditions do not exist that will significantly affect the subsystem performance. Although the propulsion/GPS/IMU/Scanwheels need to be appropriately interaligned, any misalignment error will simply become part of the total propulsion and GNC performance error corrected during de-orbit operations.

6.6.7 Manufacturing

The GNC subsystem is not expected to require any unusual manufacturing requirements.

6.6.8 Refurbishment

With the possible exception of the GPS antenna which will receive some aft end reentry heating, no equipment replacement is anticipated for the GNC subsystem. There is a significant chance that the choke ring assembly used to minimize ground plane effects will be sufficiently warped by heating to impact the attitude determination (but not position determination) accuracy.

6.7 Telemetry, Tracking, and Command (TT&C) Subsystem

The TT&C subsystem provides for command and control of the vehicle and the means to telemeter vehicle and payload data from the vehicle to ground controllers. In the case of the RRS, the downlinked data is primarily the status data required to ensure the vehicle and payload are performing in an acceptable manner. Payload data, including pertinent vehicle status data, is stored by the vehicle for playback at a later time. TT&C operations include:

- Acquiring, receiving, transforming and decoding discrete and quantitative command information from ground controllers for execution or storing for later execution.
- Output commands received from the ground and stored sequences of commands initiated by ground command and/or timer to the payload and other vehicle subsystems
- Interface with the payload and other spacecraft subsystems to format, convert, and encode data for downlink transmission
- Radiate telemetry signals with adequate signal strength and coverage to ensure communications with downlink telemetry stations during the orbital and recovery phase
- Communicating via TDRSS relay satellites to enhance coverage performance for certain RRS orbital missions and path segments

Implementation of these operations must satisfy the RRS mission objectives for design/operating constraints on ground station spatial/temporal coverage, data link capacity, off-the-shelf technology, frequency interference, and possibly redundancy of key components. The recommended TT&C configuration consists of:

- Antennae and selection switches
- TDRSS transponder
- Telemetry data system
- Power dividers

6.7.1 Operations Timeline Support

DRMs 1, 2 and 3 (Table 6.7-1) were used to analyze and design the RRS TT&C subsystem. Contact opportunities were calculated for NASA Ground Stations, the AFSCN, and TDRSS.

6.7.2 Design Requirements

6.7.2.1 Guidelines. The general groundrules and assumptions used in the TT&C trade study included: 1) a single TT&C design should be capable of meeting all mission needs; 2) proven

hardware and software should be used in the design; 3) ground-based support must be sufficient; and 4) a minimum of two contacts per day is desired.

Table 6.7-1. RRS Design Reference Mission Set Definition

DRM #	Character	Inclination	Altitude km (nm)	Orbit Type	Launch Site	Recovery Site
1	Land Recovery	33.83°	350 (189)	Circ	ETR	WSMR
2	High Altitude	33.83°	900 (486)	Circ	ETR	WSMR
3	High Inclination	98.0°	897 (484)	Circ, Int	WTR	WSMR
4	Integer Orbit	36.65°	479 (259)	Circ, Int	ETR	WSMR
5	Water Recovery	28.5°	350 (189)	Circ	ETR	Water (ETR, WTR, Gulf)

NOTE: Circ and Int denote circular and integer orbits.
ETR and WTR denote Eastern and Western Test Ranges.

The features listed in Table 6.7-2 are desirable. Note that the normal requirement is to telemeter down payload status, not the detailed scientific data on the experiments. The requirement is for the onboard data handling subsystem to collect the primary experiment data in bulk memory for post mission analysis. However, the design allows selected data to be telemetered to the ground station in lieu of normal status telemetry when commanded by ground controllers.

Table 6.7-2. TT&C Design Requirements

• Single TT&C Design for All Missions
• Minimum 2 Contacts Per Day – 8 to 12 Hours Separation
• Minimum 10 Minutes Each Contact
• Uplink – Maximum – 2 Kbps
• Downlink – Satellite 16 Kbps
Payloads <u>16 Kbps</u>
Total 32 Kbps
• Redundancy of Key Systems
• Omnidirectional Coverage

6.7.2.2 Requirements Analysis. The RRS communications subsystem is required to provide a capability for spacecraft and experiment operators to interface with the vehicle and experiments during all phases of the mission. NASA's initial studies resulted in requirements to uplink vehicle and payload commands, and downlink orbital tracking and vehicle/payload telemetry, at least twice a day. System design goals are to utilize equipment that is simple, available, reliable, and affordable. Concepts that were considered to meet these goals include: use of off-the-shelf

technology, generous margins of capability, high reliability, easy maintenance, operational cost effectiveness, and compatibility to existing communications support networks.

The first part of this section is a summary of the coverage study performed with the goal of identifying the best combination of onboard and ground support systems for the RRS application. It addressed both NASA and non-NASA (i.e., Department of Defense) ground stations that have the required support capability and will be available over the RRS 10-year operational lifetime, i.e., 1994 - 2004. The second part examined the impact that orbital parameters have on the RRS TT&C subsystems, and combined with the output of Part 1, determined which communication stations/systems could provide, as a minimum, two contacts per day. The remainder addresses which subsystems best supported the RRS mission. This latter part evaluated power utilization, cost, and risk of the TT&C options as they affected or constrained the interfaces between the RRS and the payload subsystems.

The overall TT&C system requirements were postulated for telemetry, command, and tracking functions necessary to support operations in the post-1993 time period. NASA ground stations, Air Force Satellite Control Network ground stations, and TDRSS capabilities that are planned to be available by then were determined. NASA and DoD engineers, vendors, and other sources were contacted to develop guidelines and requirements to provide initial TT&C definition data necessary to complete the studies.

6.7.2.2.1 NASA & Non-NASA Ground Support Sites. This analysis collected data on Space Tracking and Data Network organization at Goddard Space Flight Center (GSFC), the Deep Space Network organization from Jet Propulsion Laboratory, and the Air Force Space Network Division from the Air Force Space Test Center. In addition, the GSFC Space Network User Guide and the AF Space Test Range Handbook were used as references. From these discussions and inferences, the following information and results were developed.

The NASA Space Tracking and Data Network (STDN) consists of a Ground Network (GN) and a Space Network (SN). The GN is being phased down, and, by 1994, will consist of the Merritt Island Launch Area (MILA), Ponce de Leon (PDL), and Bermuda Tracking and Communication Sites (BDA). These sites will provide pre-launch, launch, and landing/recovery communications support for spacecraft and launch vehicles during the RRS operations era. Depending on schedules, these sites could provide some limited support to RRS, but could not be considered as prime orbital support sites on a continuous basis. The SN consists of the space segment and the ground segment. The space segment consists of two operational Tracking and

Data Relay Satellites (TDRS) and a spare TDRS in geostationary orbit. Each TDRS provides functionally identical communications capability. Figure 6.7-1 shows the basic TDRS configuration available in 1990.

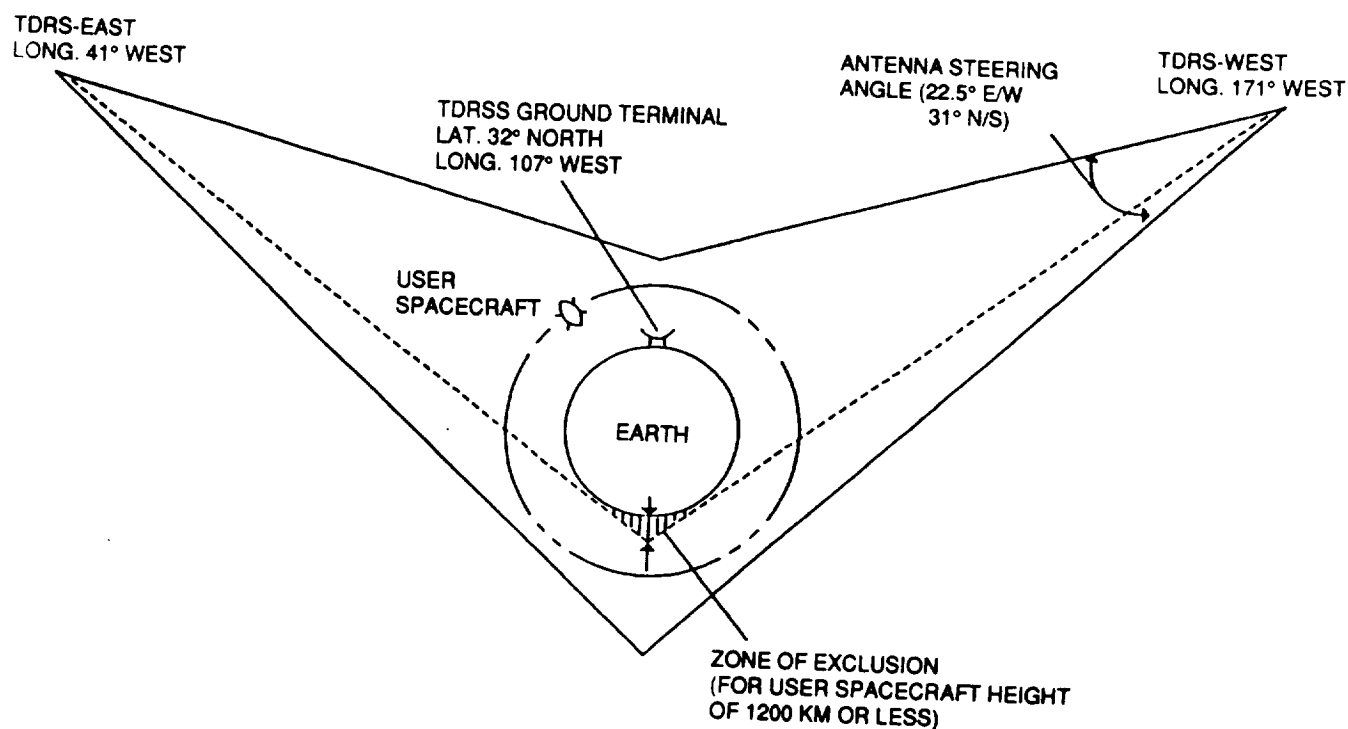


Figure 6.7-1. TDRSS/User Spacecraft Configuration

The ground segment consists of: White Sands, New Mexico, which provides the communications capability for data transfer via the TDRS as well as operations control for the TDRS itself; the NASA Ground Terminal (NGT) which provides the operational interface between TDRSS and NASCOM common carrier circuits; the MILA and Vandenberg Air Force Base (VAFB) TDRSS relays, which provide a prelaunch, launch, and bonding support for the Space Transportation System and spacecraft payloads of various users. Based on the above discussion, the only NASA STDN service available in 1994 and beyond would be TDRSS.

The Deep Space Network (DSN) consists of the Goldstone, California; Madrid, Spain; and the Canberra, Australia deep space communication sites. Controlled by the Jet Propulsion Laboratory (JPL), these are dual sites, i.e., one site portion (or side) provides only deep space support; the second side is comprised of the old STDN sites which were turned over to JPL with the phase down of STDN. These sites provide telecommunications and tracking support during an Inertial Upper Stage (IUS)/TDRS deployment for the NSTS as well as transfer and on-orbit operations during initial checkout and verification phases of the TDRS mission. In addition, the Orbital Space Network (OSN) provides backup support to the DSN until TDRSS becomes fully

operational. Figure 6.7-2 depicts the NASA Space Network for 1994 and beyond. The old STDN sites which are now part of the JPL Deep Space Network (DSN) would also be available for limited support during the 1994 to 2004 timeframe. However, they should not be considered for full time (60 days at a time) support to the operational RRS.

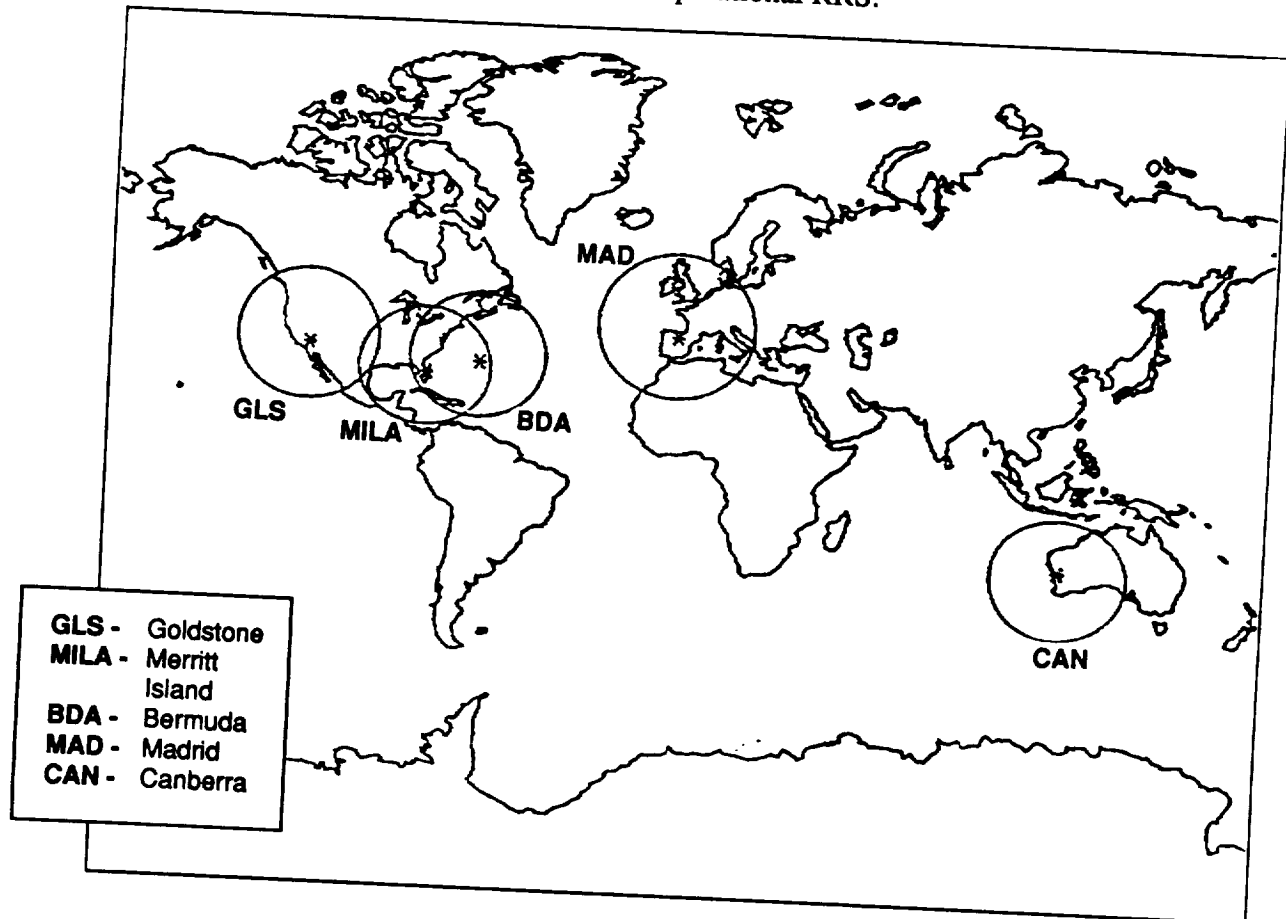


Figure 6.7-2. NASA Space Network (1992)

The ASFCN is a set of common user resources and facilities that collectively are used to provide telemetry, command, and tracking support for the DoD spacecraft plus limited NASA and foreign government space programs. An overview of the current AFSCN is shown in Figure 6.7-3. The ASFCN will consist of nine (9) sites in the 1994 and beyond timeframe. Six of the sites are dual sites and three are single sites. The dual sites have two antennae and associated equipment to allow multi-vehicle support at the site. These sites are located around the world and consist of the Vandenberg Tracking Station, New Hampshire Tracking Station, Thule Tracking Station, Guam Tracking Station, Hawaii Tracking Station, and the Telemetry and Command Station at Oakhanger, England. The single sites are the Indian Ocean Tracking Station, Colorado Tracking Station, and the Diego Garcia Tracking Station. Figure 6.7-3 depicts the AFSCN from its current state to its projected state in year 2004. In addition to the remote tracking sites, the

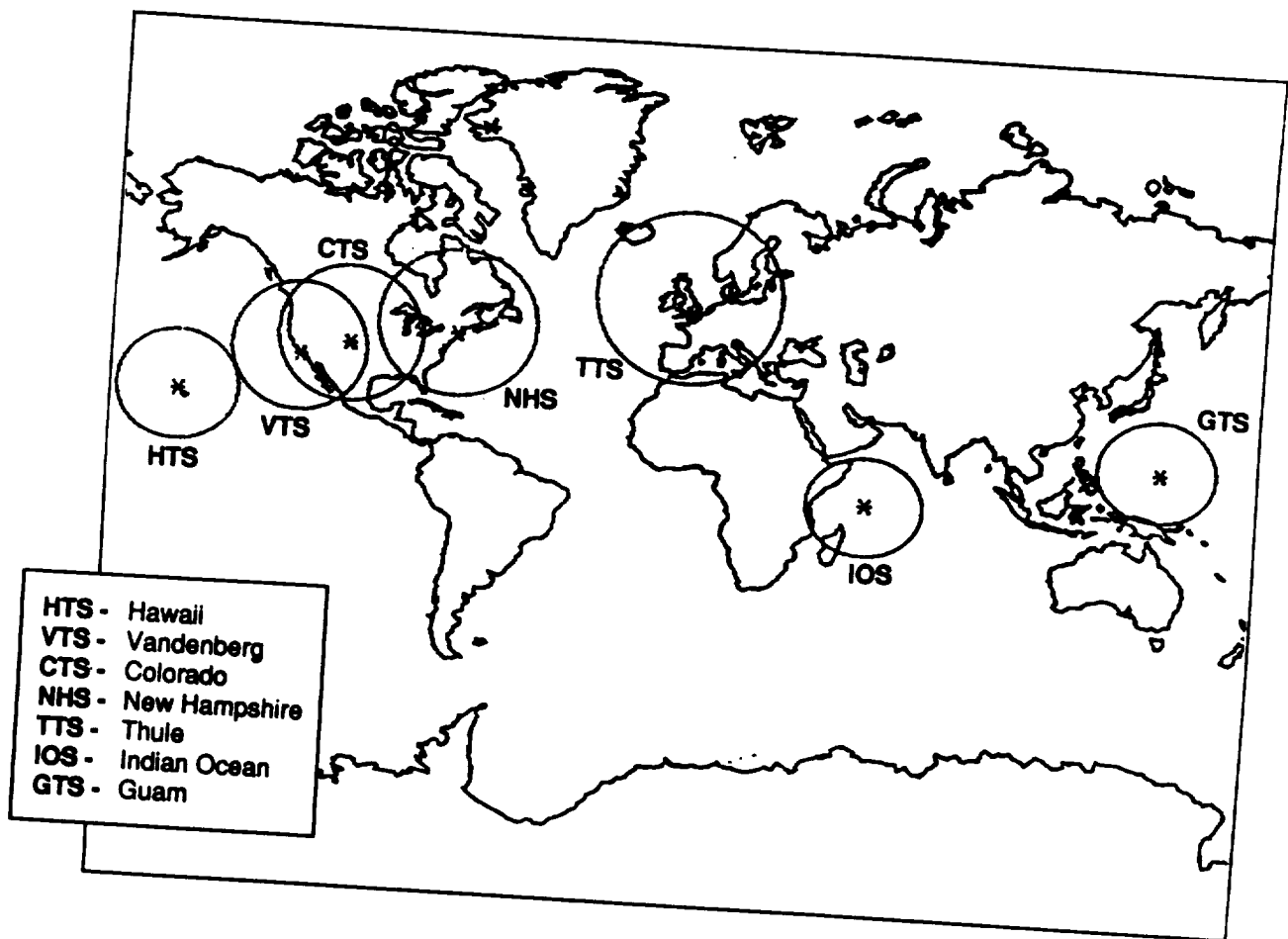
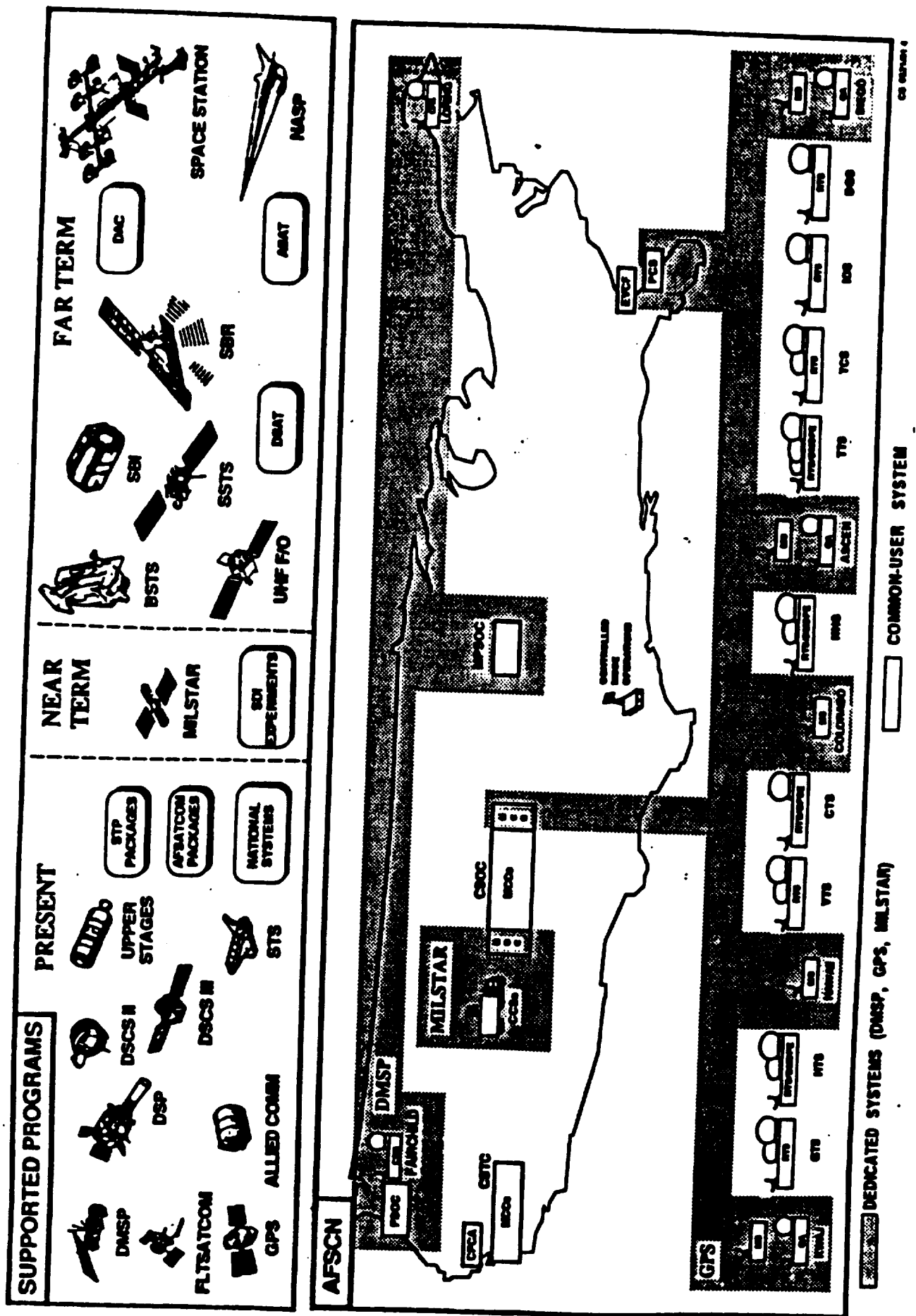


Figure 6.7-3. Air Force Space Network (1992)

AFSCN has two control centers, the Satellite Test Center at Sunnyvale, California, and the Consolidated Space Operations Center at Colorado Springs, Colorado. The AFSCN "landscape" is shown in Figure 6.7-4.

The AFSCN can provide RRS-to-ground interface for TT&C. However, its prime function is support to the DoD satellite programs. The Air Force could provide limited/backup coverage, but it would not be available for full time (60 days at a time) support for an operational RRS.

6.7.2.2.2 Impact of Orbital Parameters. To determine orbital parameters for the RRS, orbital characteristics for the three Design Reference Missions were plotted for the NASA Space Network, the TDRSS, and the AFSCN. Figure 6.7-5 shows the ground trace for DRM-1, which is characterized by a 350 km circular orbit altitude and 33.83 degrees inclination relative to the Equator. As shown, the NASA network limits its coverage to the northern hemisphere. At this altitude and inclination, there are two contacts per day. However, the contacts are less than 10 minutes each and occur within 2 to 3 hours of each other. Figure 6.7-6 displays the DRM-2 configuration, characterized by 900 km altitude and 33.83 degrees inclination. This gives



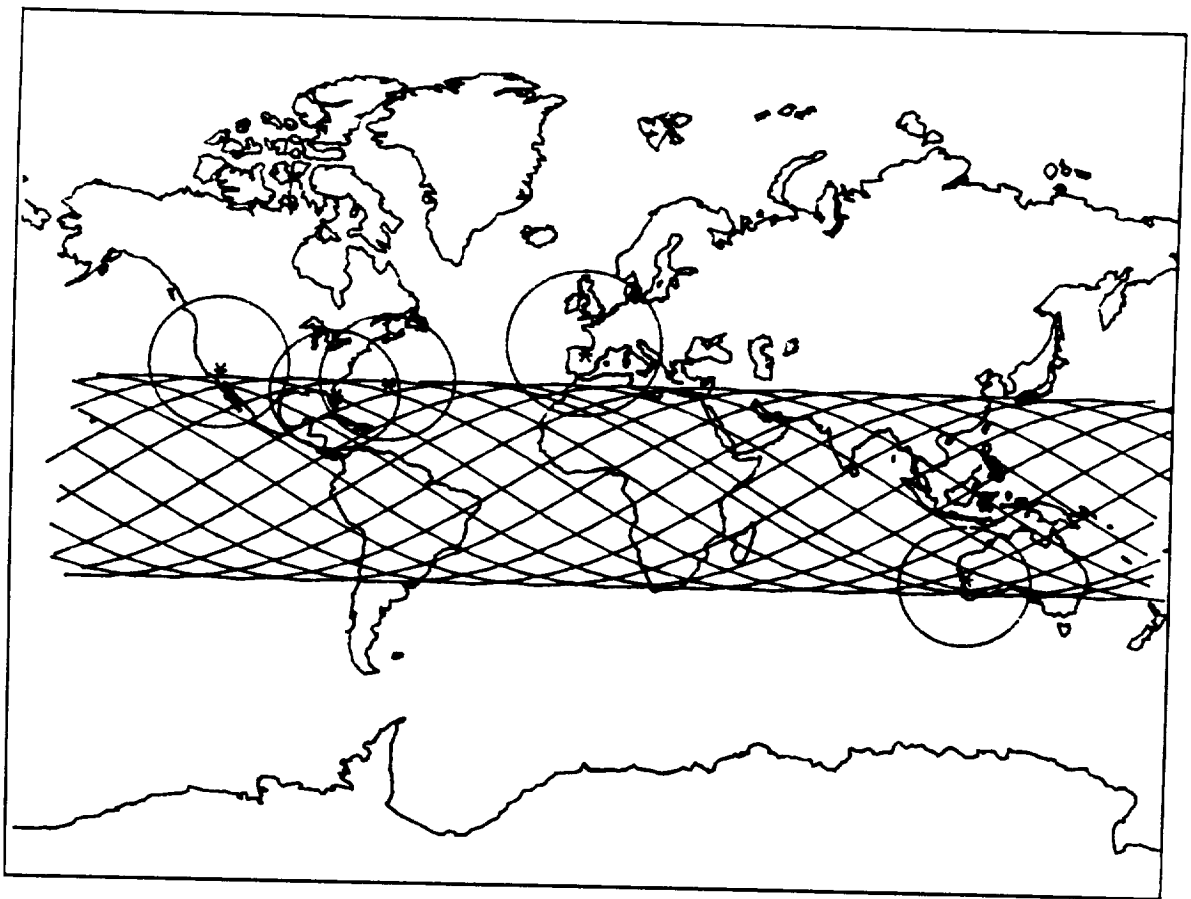


Figure 6.7-5. DRM-1 Ground Trace – NASA Space Network

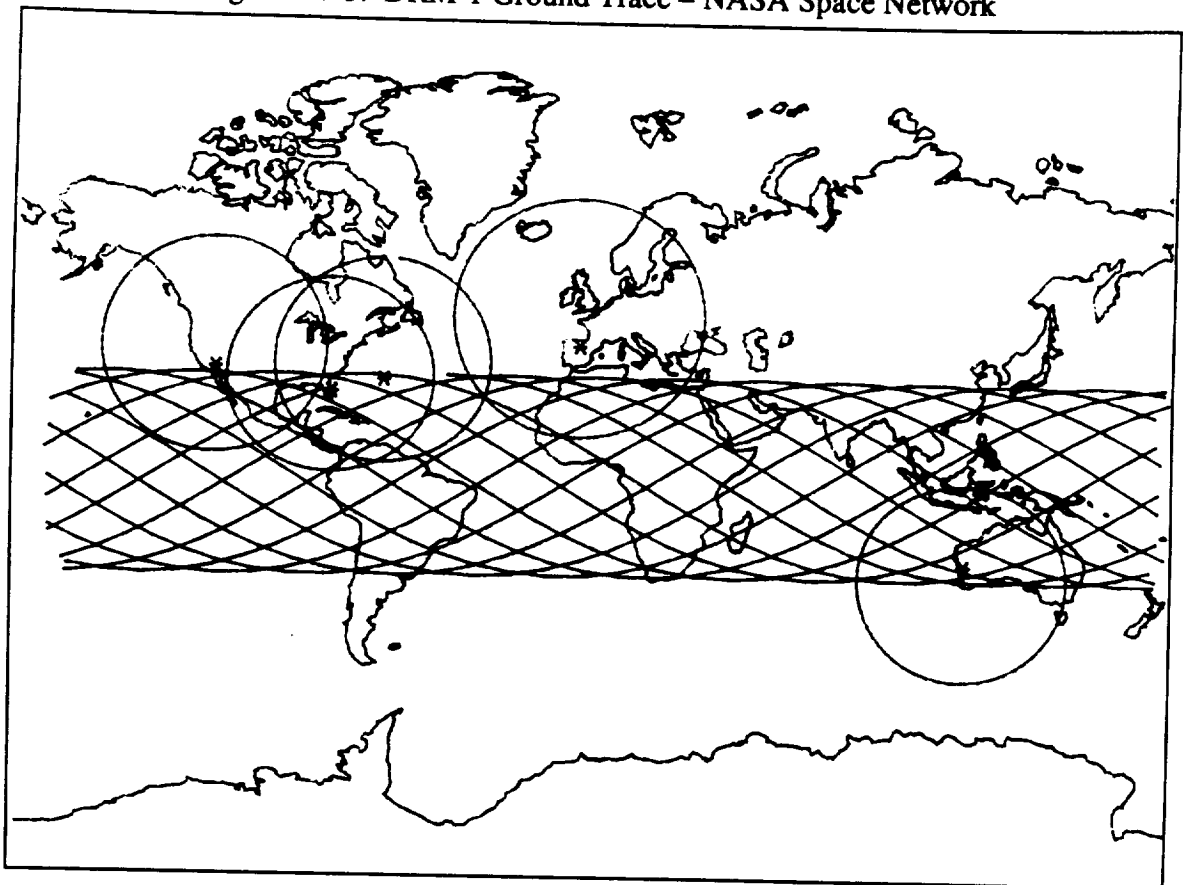


Figure 6.7-6. DRM-2 Ground Trace – NASA Space Network

basically the same coverage as for DRM-1; contact time does increase to about 10 minutes each. Figure 6.7-7 shows the ground track for DRM-3, characterized by 897 km altitude at 98 degrees inclination. At this altitude and inclination, the NASA network can meet all of the communications requirements, except continental U.S. coverage, i.e., two contacts per day each of 10 minutes coverage; and there are 10 to 12 hours separation of data collecting (between contacts). However, in order to get the needed separation, the Canberra tracking station would have to be utilized. The detailed contact histories for DRMs 1, 2 and 3, using the NASA Tracking Network, appear in the TT&C Coverage Summary Report.

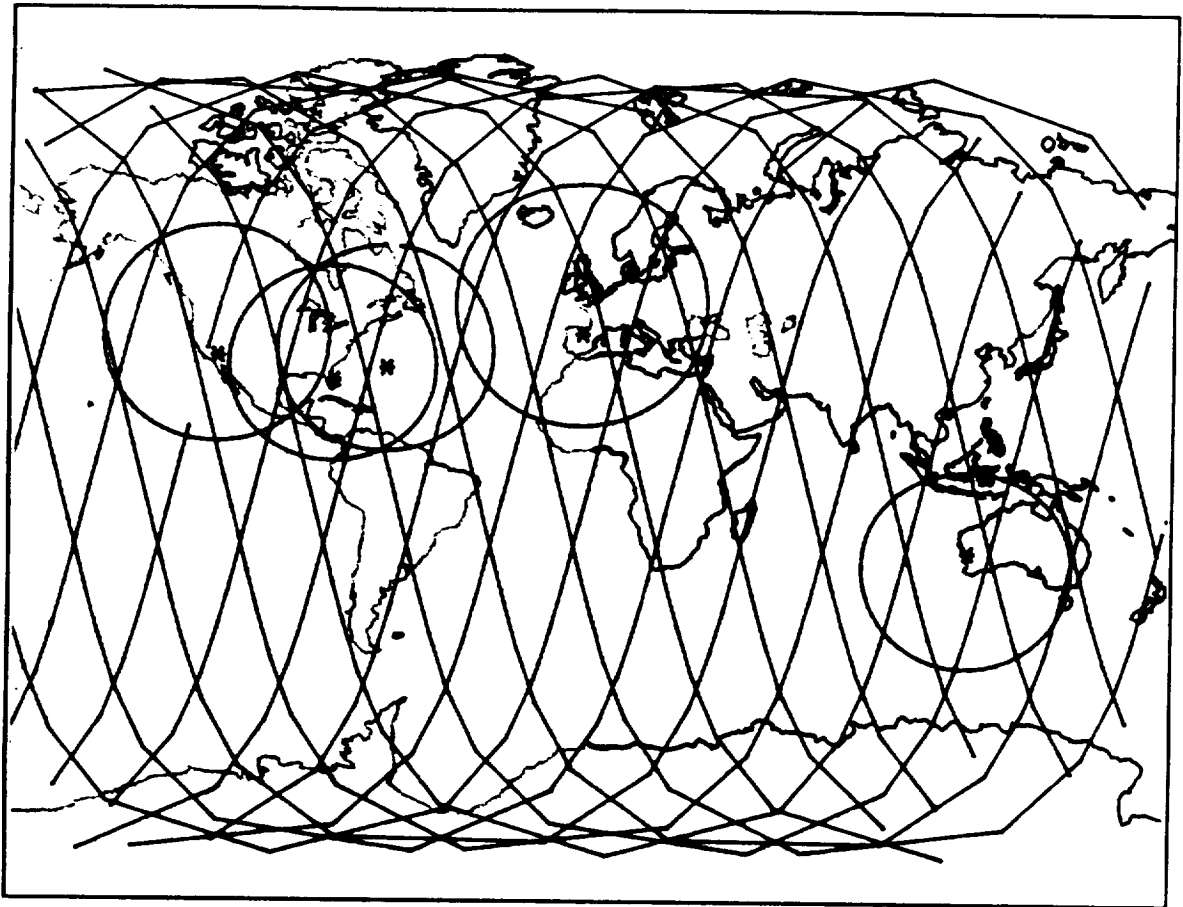


Figure 6.7-7. DRM-3 Ground Trace – NASA Space Network

AFSCN orbital traces are depicted in Figures 6.7-8 through 6.7-10. These figures depict coverage for each of the design reference missions DRM-1, DRM-2, and DRM-3, respectively. In DRM-1, the coverage approximates the NASA network's coverage for DRM-1. However, 10 to 12 hour separation can be attained utilizing foreign sites. DRM-2 will allow coverage for over 10 minutes, but foreign sites must be used for the separation. DRM-3 allows coverage as required and, with judicious planning, could provide continental U.S. site coverage. Detailed

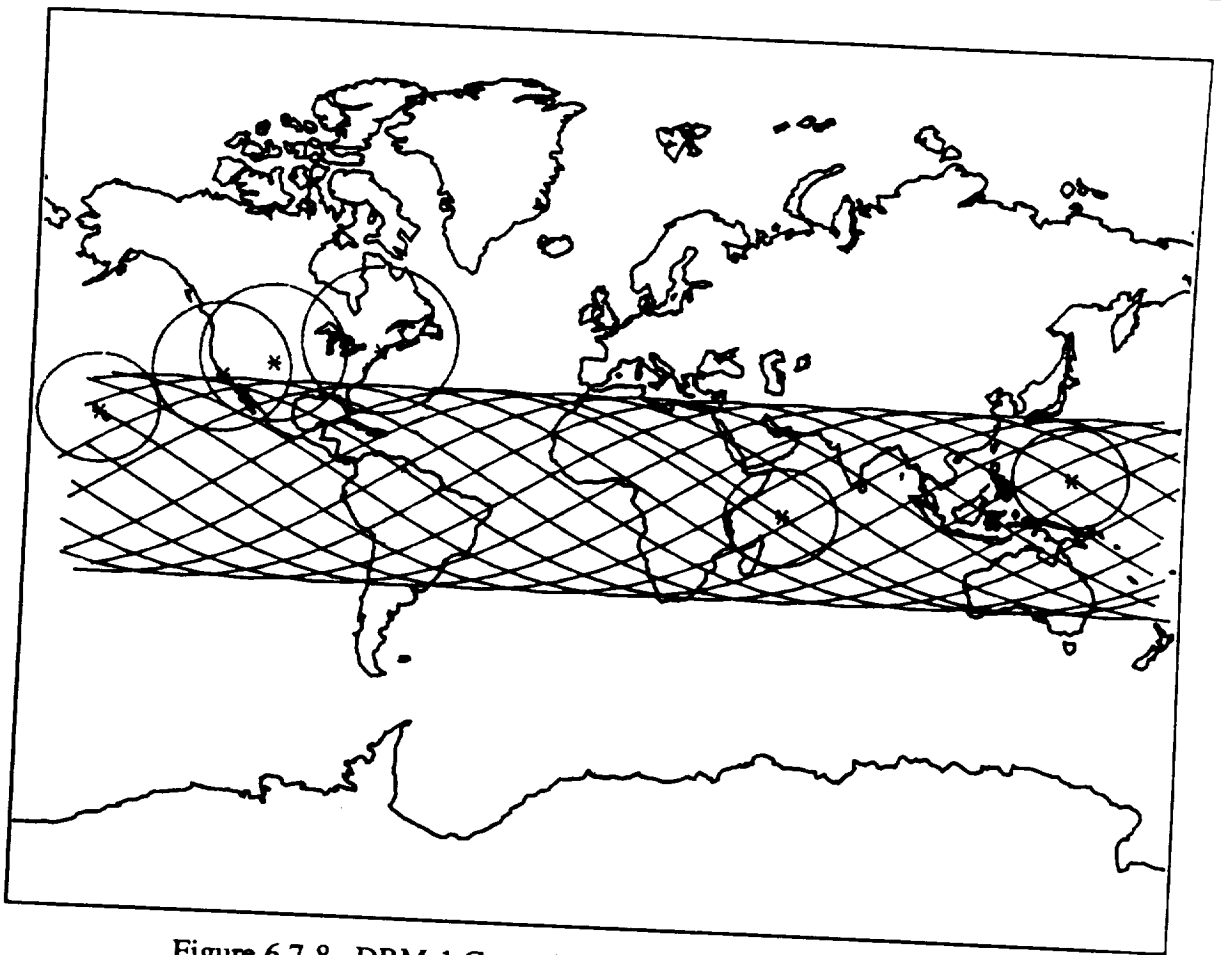


Figure 6.7-8. DRM-1 Ground Trace – Air Force Space Network

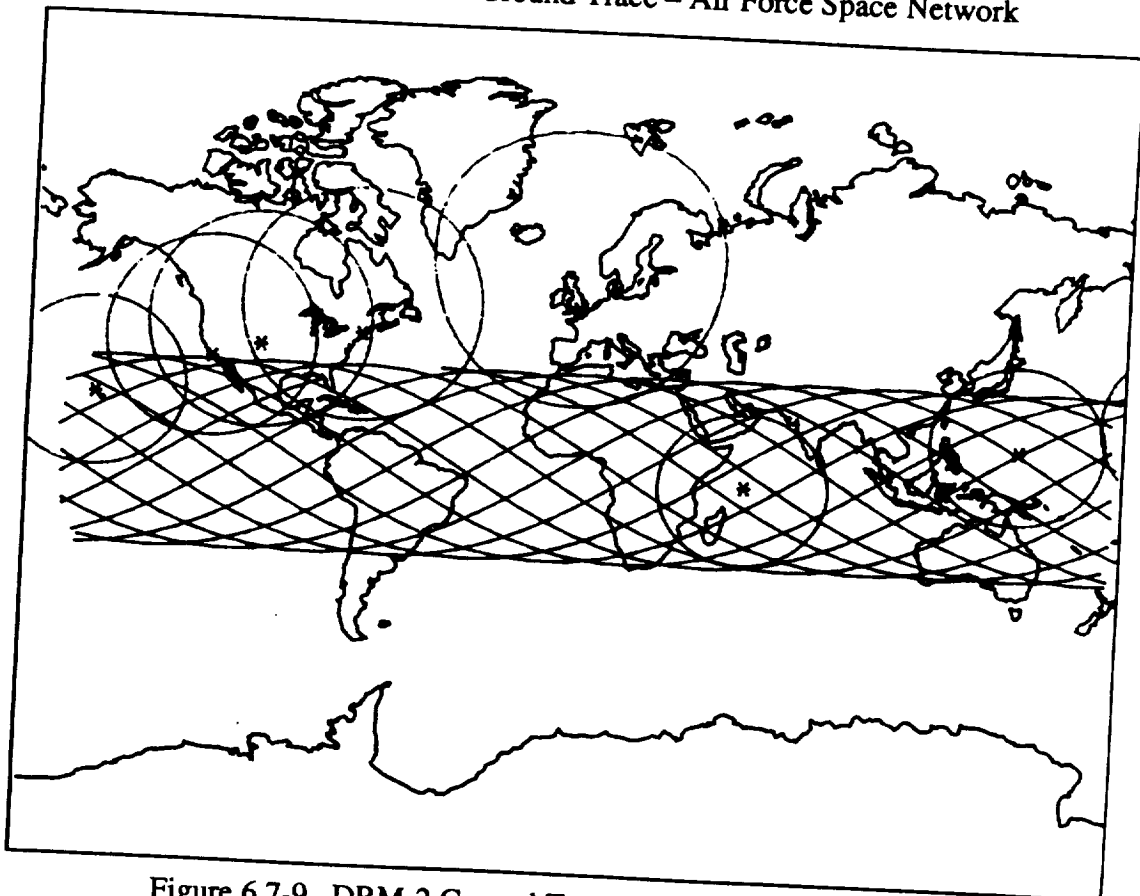


Figure 6.7-9. DRM-2 Ground Trace – Air Force Space Network

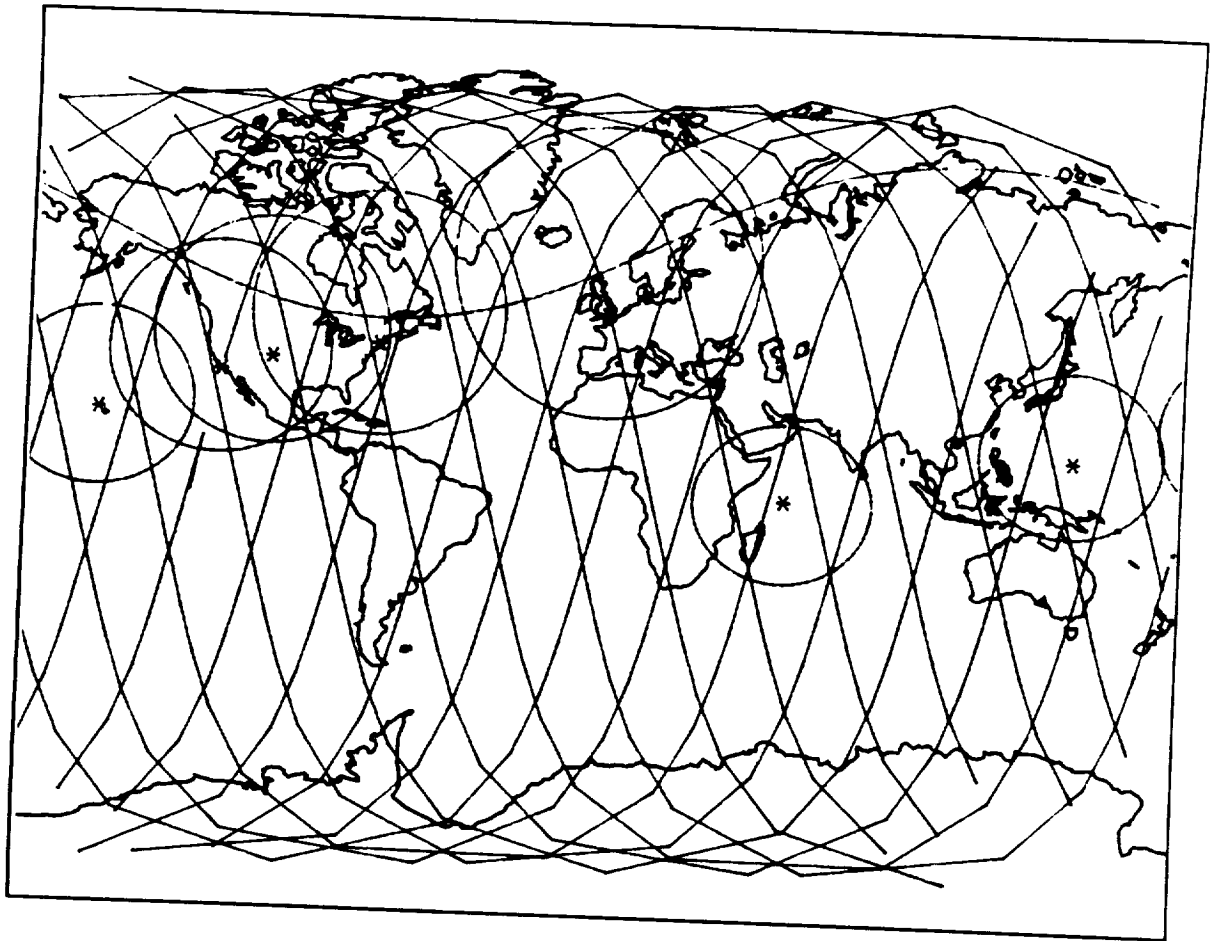


Figure 6.7-10. DRM-3 Ground Trace – Air Force Space Network

contact histories for DRMs 1, 2 and 3 using the Air Force Satellite Control Network appear in the TT&C Coverage Summary Report.

TDRSS geometric coverage is summarized for DRMs 1, 2 and 3 in Figure 6.7-11. As shown, each of the Design Reference Missions would have all requirements met, and even in cases where additional real-time support might be dictated, support could be scheduled. The detailed contact histories for DRMs 1, 2 and 3 using TDRSS appear in the TT&C Coverage Summary Report.

Table 6.7-3 summarizes the contact histories for each of the networks discussed above. Based on the coverage tabulation and the ground traces, the best solution for RRS TT&C appears to be the use of TDRSS to support the 10-year life span of the RRS.

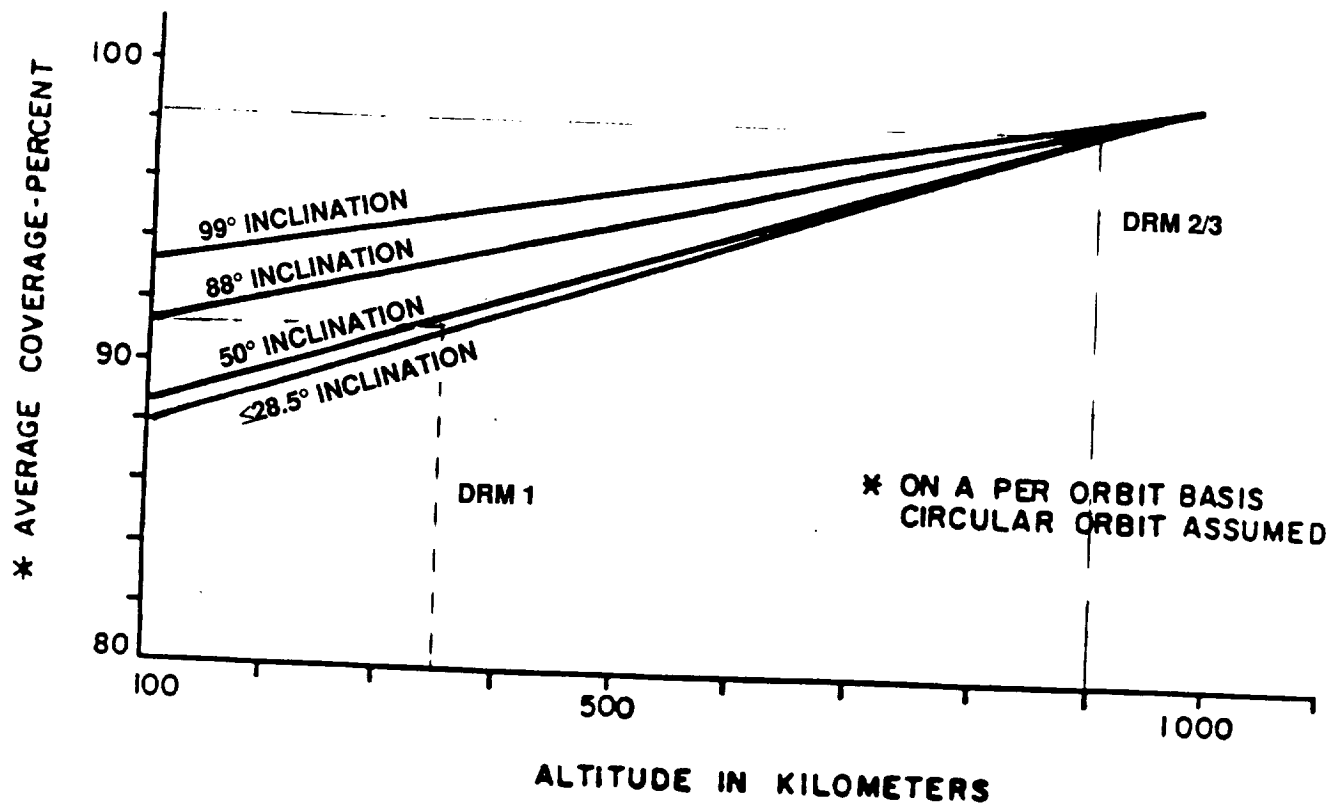


Figure 6.7-11. TDRSS Coverage Versus Altitude and Inclination

Table 6.7-3. Contact History Summary

	NASA Space Network - 1992	AF Satellite Control Network	TDRSS
DRM-1 (350 km - 33°)	<ul style="list-style-type: none"> • Can Get 2 Contacts Per Day • Minimum 8 Minutes Each Coverage • Cannot Get Coverage of 8-12 Hours Separation (Get 2-3 Instead) • Coverage of Northern Hemisphere Only 	<ul style="list-style-type: none"> • Can Get 2 Contacts Per Day • Maximum Coverage 8 Minutes • Can Schedule to Get Coverage - 10-12 Hours Separation for Foreign Sites Only • Northern Hemisphere Coverage Only 	<ul style="list-style-type: none"> • Allows Coverage at Any Time Needed • Data Received in USA • Only Limitation Is Scheduling • Greater Than 80% Coverage Available Each Day • 10 Minutes Contact Minimum • Minimum 8-10 Hours Between Contacts
DRM-2 (900 km 33°)	<ul style="list-style-type: none"> • Same as for 350 km, Except Each Contact of 10 Minutes Minimum 	<ul style="list-style-type: none"> • Can Get 2 Contacts Per Day • Maximum Coverage 12-14 Minutes • Can Schedule Coverage - 10-12 Hours Separation for Foreign Sites 	<ul style="list-style-type: none"> • Same as 350 km • Greater Than 95% Coverage Available Each Day
DRM-3 (897 km 98°)	<ul style="list-style-type: none"> • Can Get 2 Contacts Per Day • Can Get 10 Minute Coverage • Can Get Coverage - 10-12 Hours Separation if Canberra Used • No CONUS Coverage 	<ul style="list-style-type: none"> • Same as 33° Inclination • Possible U.S. Site Coverage if Scheduled Wisely 	<ul style="list-style-type: none"> • Same as 900 km, 33° Inclination

6.7.3 RRS TT&C Subsystems

The telemetry data system is a modularized processor that encompasses functions of timer, power supply, formatter, programmer, sample and hold, and analog-to-digital converter. The transponder downlink is a multiple of the uplink frequency. Two separate sets of hardware are located in the Main Module and Deployed Module that have a "master and slave" relationship within the telemetry data system. The recommended TT&C subsystem configuration (Figure 6.7-12) is summarized in Table 6.7-4 with the associated power and weight summary provided in Table 6.7-5.

6.7.3.1 Frequency Selection. Although other frequencies were considered, S-Band frequencies were chosen as the preferred space-ground communication link for numerous reasons. S-Band frequency provides the best propagation through space at all inclinations and is compatible with both NASA and USAF services. Using S-Band also enables use of TDRSS for critical operation

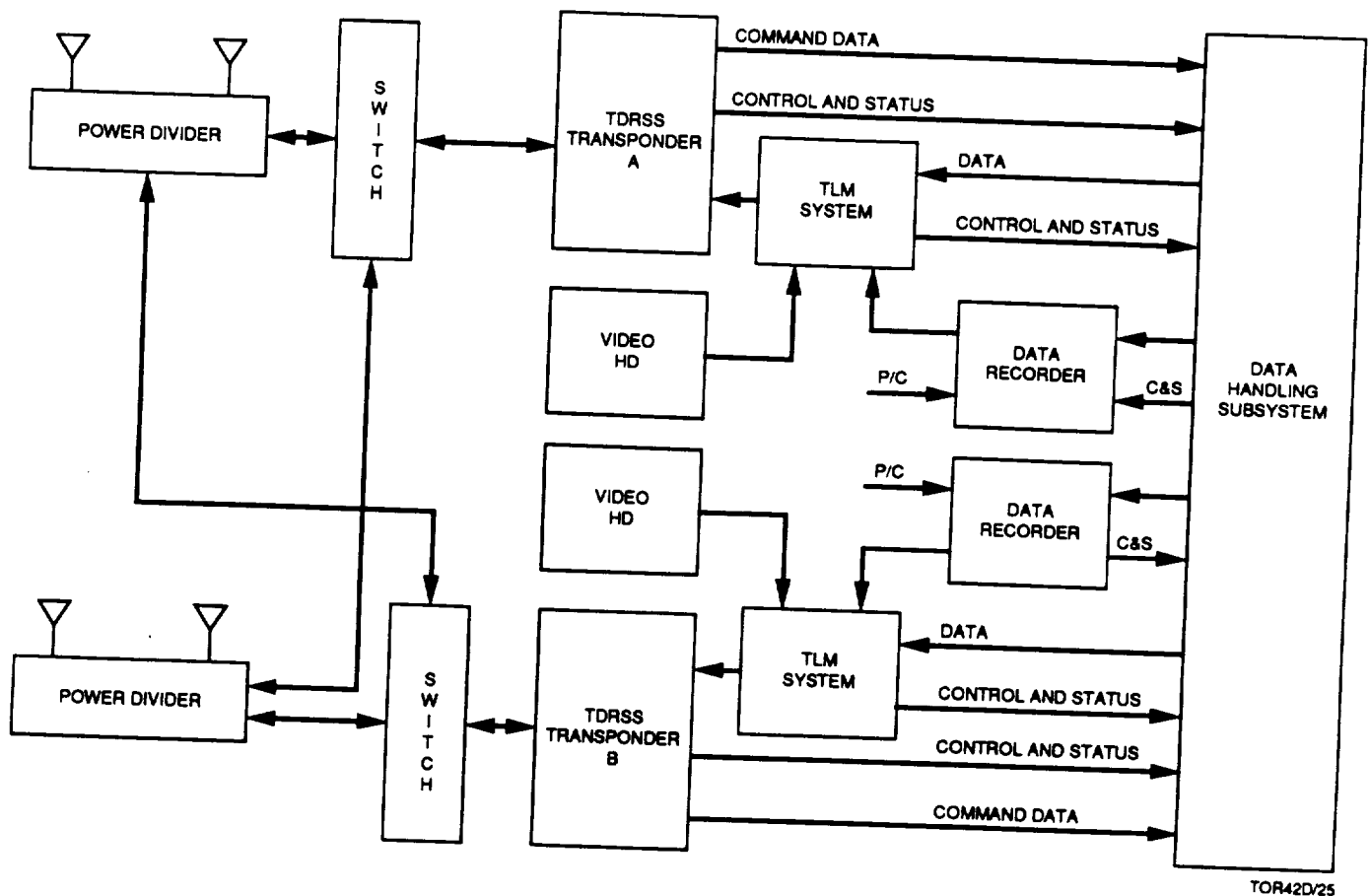


Figure 6.7-12. RRS Communications Subsystem

Table 6.7-4. Recommended TT&C Configuration Summary

Use S-Band Frequency	
• Both multi-access and single access on TDRSS available at both NASA and Air Force sites by 1994.	
• Best coverage at all inclinations and altitudes available for reentry/recovery at WSMR.	
Use TDRSS Transponder	
• Allows communication mode to remaining NASA sites by 1994.	
• Allows communication mode to Air Force sites.	
• Readily available.	
• Space-qualified on numerous space vehicles.	
Use Command System Integral to TDRSS Transponder	
• No additional equipment required.	
• Allows commands direct to payload or via data handling system.	
• Status and control integral to transponder status and control system.	
Use Programmable Telemetry System	
• User programmable - easily changed if needed between missions	
• Up to 10-bit accuracy	
• Hardware modularity	
• Bit rates between 1 Kbps to 500 Kbps	
• Optional 1.024 Mbps	
• Allows data recorder dump	
• Allows video hard disk interface	

Table 6.7-5. TT&C Weight and Power Budget

Antennae	
20 oz overall	
S-Band cavity backed helix antenna (8 required, could reduce to 6)	
Antenna Selector	
6 oz each	
100 MA each	
20 to 32 V dc	
2 Required	
Transponder	
15.15 lbs each	
36 or 45 W max power consumption in transmit mode total for receive & transmit per 2.5 or 5 W power amplifier respectively (17.5 if receiver mode used)	
28 \pm 7 V dc voltage source	
Standard TDRSS User Transponder (2 required)	
Telemetry System	
6 oz each	
500 MA each	
28 \pm 4 V dc	
Miniature programmable telemetry system (2 required)	
Power Divider	
0.3 lbs each	
TBS	
TBS	
4 required	

coverage. Use of the L-Band frequency is not recommended because of potential interference with use of GPS onboard the RRS and the limited support available at NASA ground network sites. Space-ground links at S-Band were examined on other programs including Shuttle Orbiter, Land Sat, Space Lab, Space Telescope, Pioneer, and Galileo—and this evaluation provided confidence in application of S-Band to the RRS.

6.7.3.2 Subsystem Selection. A series of investigations were performed of candidate equipment possibilities, utilizing NASA program documents, manufacturers' brochures, and past experience in order to derive a TT&C configuration that would be supportable by off-the-shelf equipment. Although, TV downlink is not clearly required, 10 W S-Band FM transmitters are available if this becomes a requirement. Possibilities for upgrading the S-Band communications were investigated and include: 1) providing some attitude control to RRS, 2) using a directive antenna with medium gain, and 3) providing a power amplifier and low-noise amplifier (LNA) to the transmitter and receiver of the S-Band transponder interfaces.

Discussions were initiated with companies making products in the S-Band frequencies, including transponders, telemetry, command, antennas, antenna selectors, and power dividers. Johnson Space Center (JSC) engineers, having expertise in S-Band communications and on GSTDN and TDRSS operational performance, were contacted and provided technical information on the overall communication system used to TT&C on JSC projects. Investigation of the equipment candidates resulted in the following proposed configuration for the RRS TT&C.

6.7.3.3 Command and Control. The NASA Second Generation S-Band User Transponder is recommended since the equipment can communicate via the TDRSS Satellite Multi-Access system (Figures 6.7-13 and 6.7-14) as well as directly with the GSTDN and USAF ground stations. Although the TDRSS omni-directional data rate capacity is only 125 bps, this is sufficient to provide worldwide visibility for critical operations. Since the current power output of 5.0 W is being used successfully via omni-antenna over the operational altitude envelope of the RRS missions, the system should have no difficulty closing the link over any of the three potential communication routes.

The command system is comprised of a separate receiver/decoder. The NASA Second Generation S-Band User Transponder (Figure 6.7-15), which is compatible with both TDRSS and ground stations, provides the receiver function. The uplink command capacity is 2 and 1 Kbps maximum for the STDN and TDRS modes respectively. The command decoding function is performed within the GNC computer.

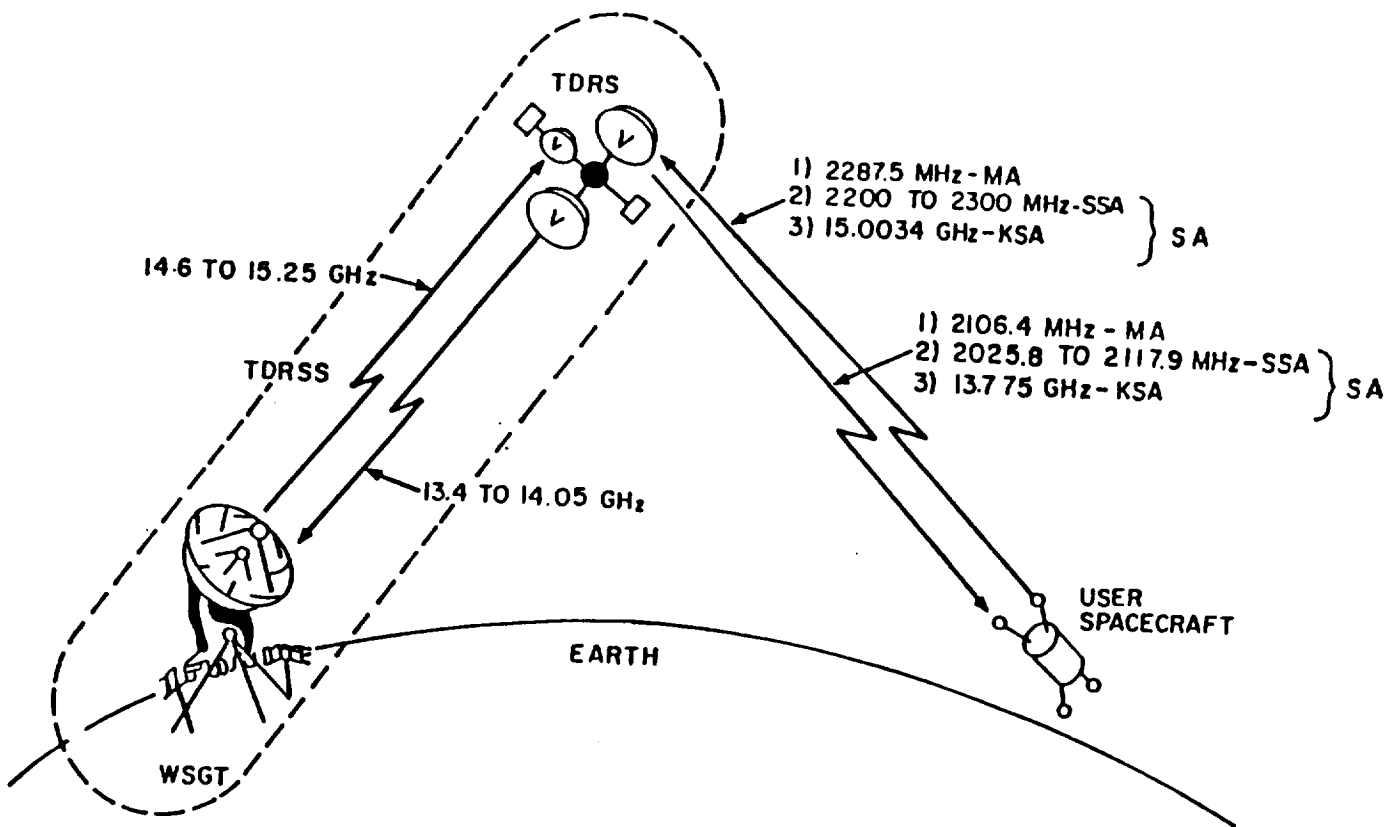


Figure 6.7-13. TDRSS Forward and Return Service Frequency Plan

One approach to achieving the required omni-directional antenna coverage is the use of S-Band cavity-backed spirals. These are broadband antennas for both command and telemetry frequencies. A typical radiation pattern for one antenna element is plotted in Figure 6.7-16. The antenna would consist of multiple installations of 8 or maybe 6 antenna elements, using power dividers and mounted on the exterior surface of the Deployed Module. Antenna orientation for the multiple antenna elements is illustrated in Figure 6.7-17. Use of an antenna selector switch gives the best radiation pattern coverage for omni-directivity. An alternate approach that would use a cross dipole system, also mounted on the DM, and would appear to provide better performance, is still being evaluated.

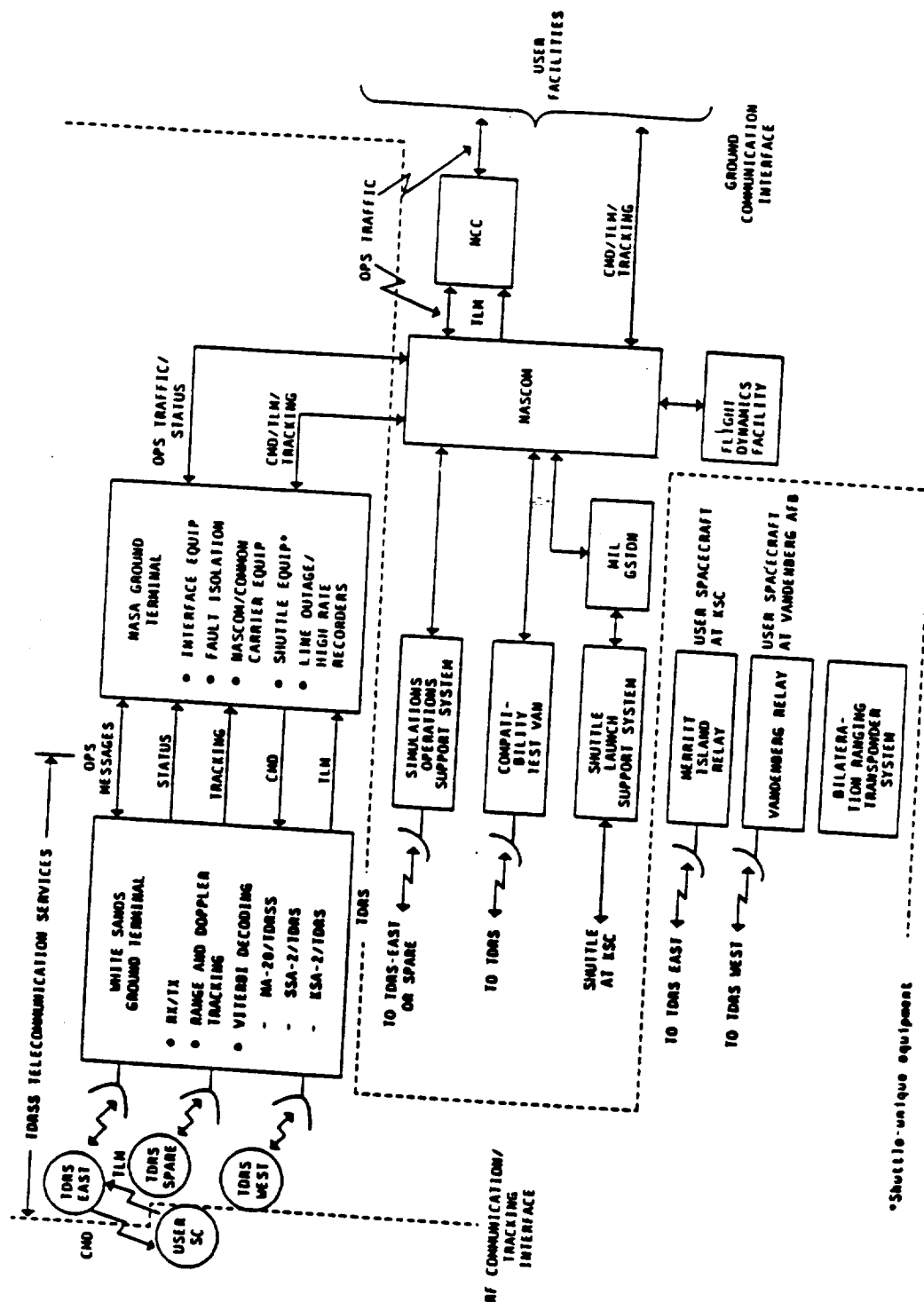


Figure 6.7-14. Space Network Elements and Interfaces

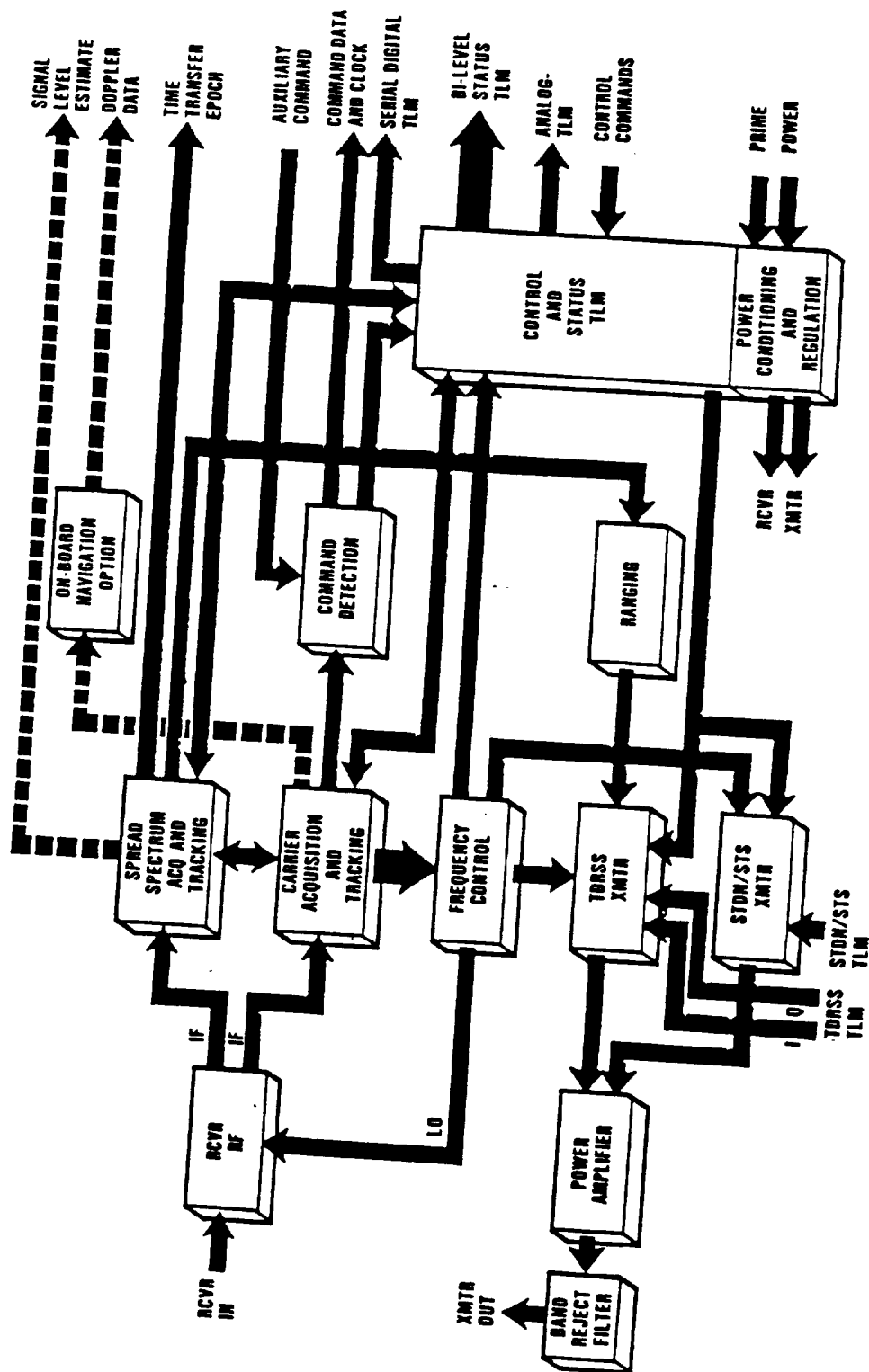
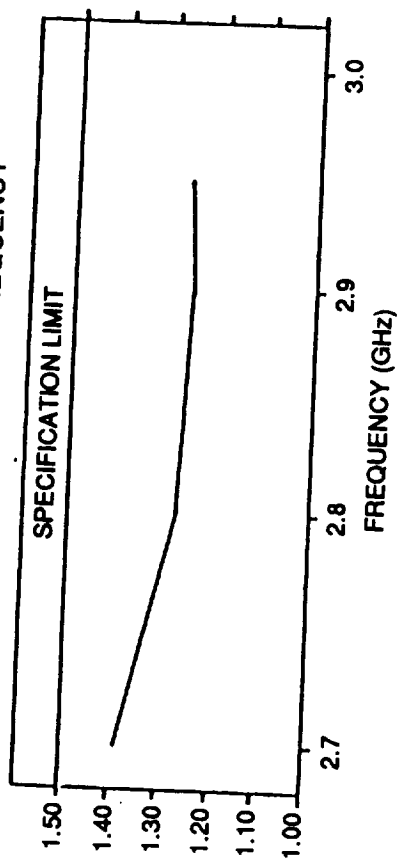
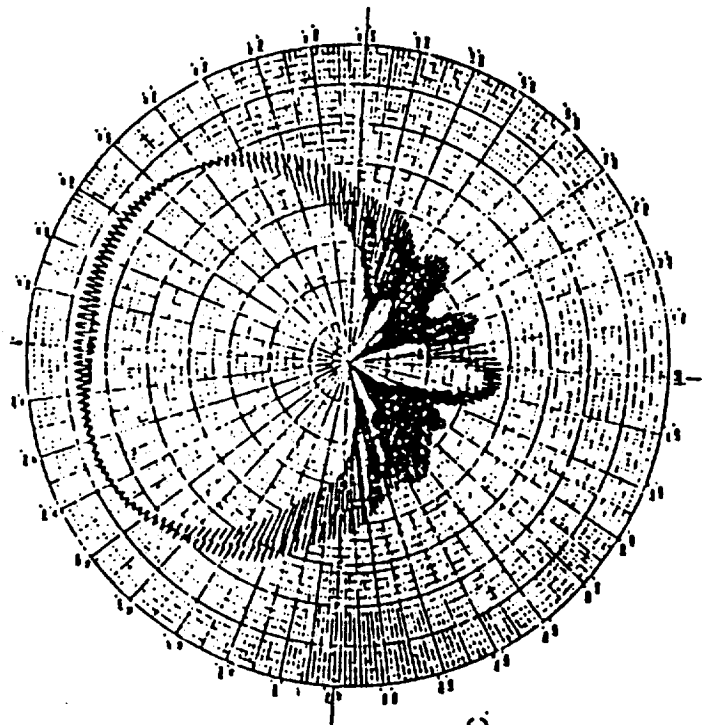


Figure 6.7-15. NASA Standard TDRSS User Transponder Functional Block Diagram

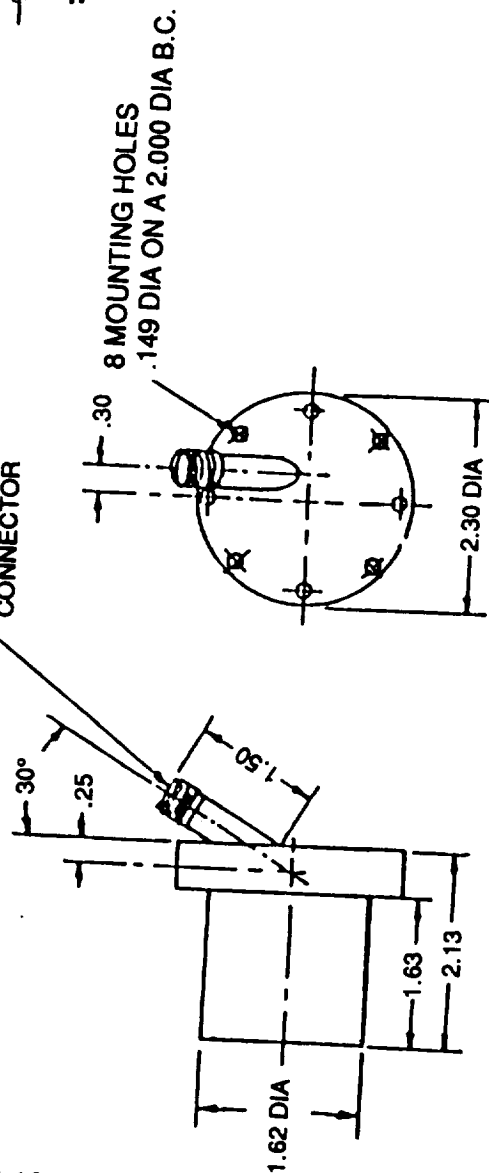
TYPICAL VSWR VS FREQUENCY



TYPICAL RADIATION PATTERN



TYPE TNC FEMALE CONNECTOR



OUTLINE DIMENSIONS (INCHES)

Figure 6.7-16. TT&C Antenna

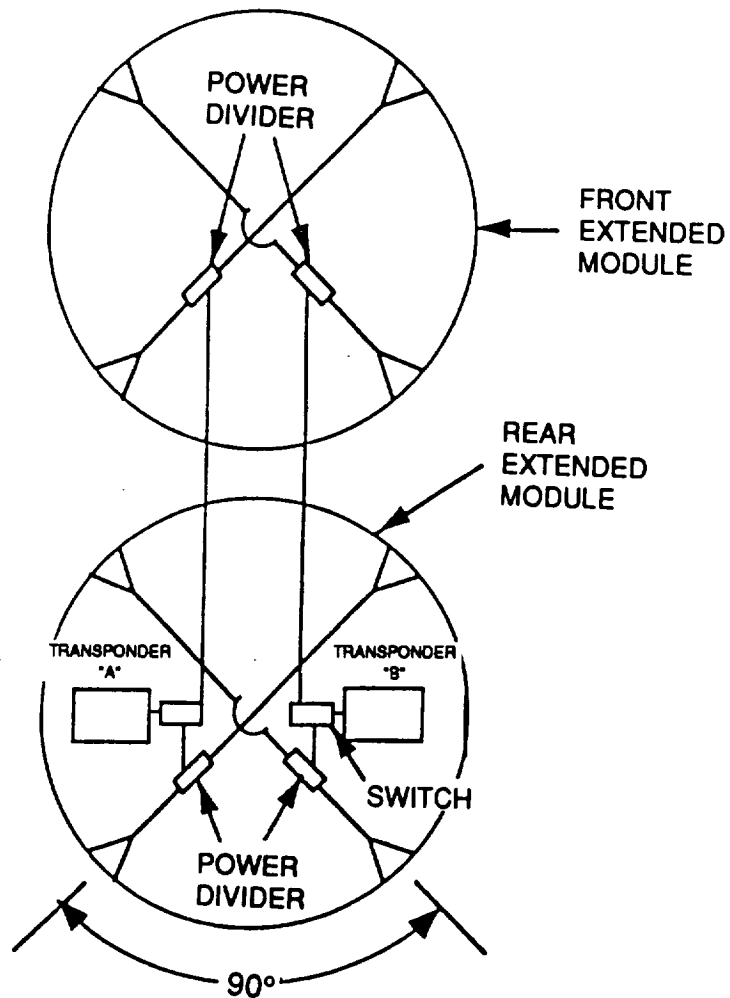


Figure 6.7-17. Antenna Orientation

6.7.3.4 Telemetry. The type of telemetry (Figure 6.7-18) likely to be needed by the vehicle was investigated by analyzing the Rodent Module requirements (Tables 6.7-6 through 6.7-10, for example). Since this resulted in a clear need for flexibility, a miniature, programmable data system manufactured by Ayden Vector was selected. This modularized system is designed for high performance data acquisition and operation in severe environmental applications where size, performance, and reliability are primary requirements. The system combines data multiplexing and conditioning with user programmable gain, offset, and format selection. A 10-bit high speed analog-to-digital converter and programmable gain amplifier provide digitization of a wide range of analog inputs.

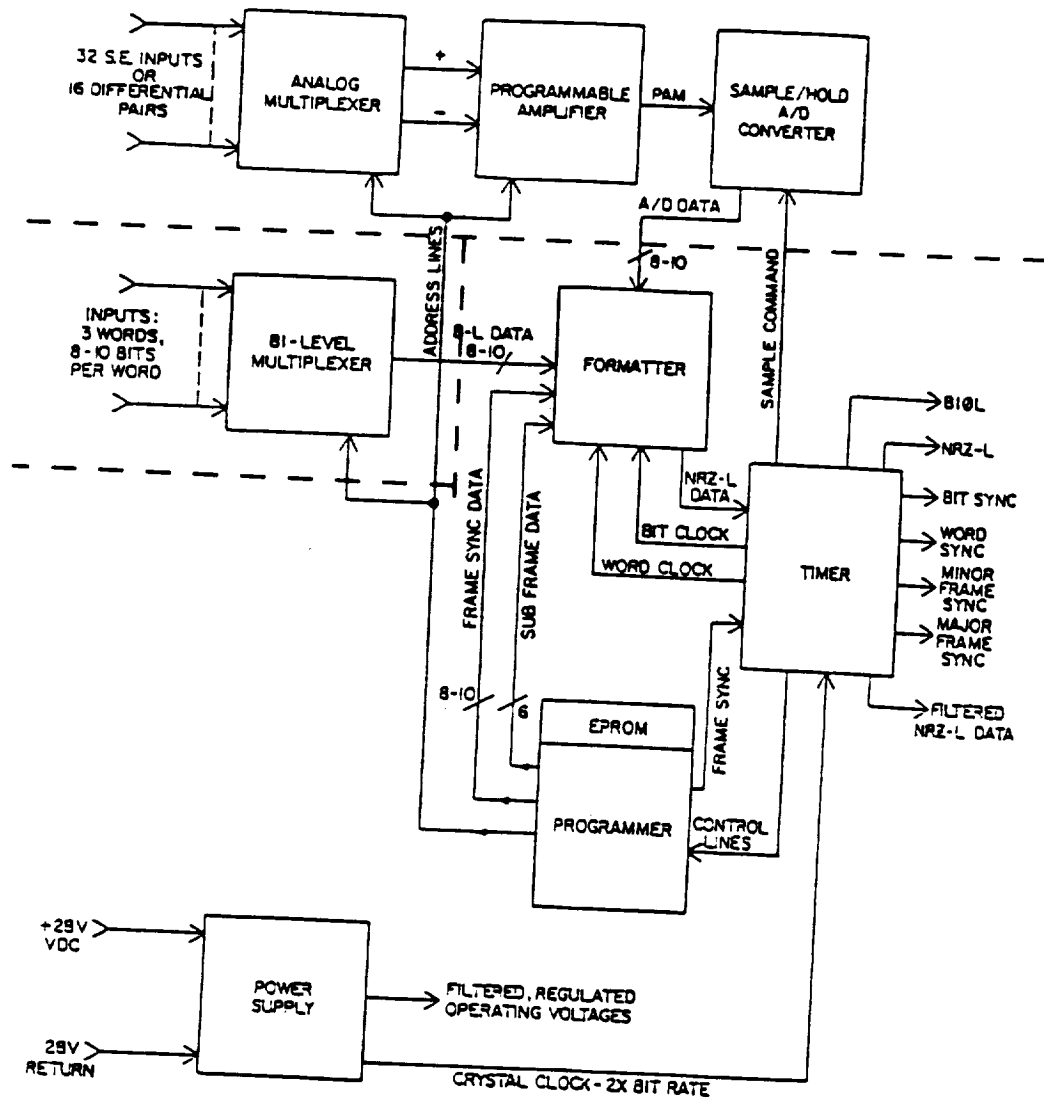


Figure 6.7-18. Telemetry System

Each module is fully ruggedized so the user can remove any module, add additional modules, and then reconfigure the software Electronically Programmable Read-Only Memory (EPROM) to accept a new measurement list. The system can be assembled in various configurations sized to handle 32 analog or 30 bi-level channels (i.e. words). Modules are defined at the vendor facility and can be assembled in various configurations (Tables 6.7-11 and 6.7-12, for example). A remote "slave" module can even be incorporated and positioned as far as 300 feet away from its "master" unit, but there is roughly a 50% penalty in power consumption for the slave.

The system will accept digital or analog data from guidance computers and 1553B data buses, and is reprogrammable in the field without removal from the vehicle. The programmable features are based on Complementary Metal Oxide Semiconductor (CMOS) EPROM technology and provide up to 64 gains and offsets from one programmable module. A preliminary architecture for the RRS configuration is presented in Table 6.7-13.

Table 6.7-6. Vehicle Event Correlation

EVENT SIGNALS			
LAUNCH VEHICLE SEPARATION			40 b
ATTITUDE CONTROL			40 b
MODE CHANGES	64 states	6 b	
FREE DRIFT	acceleration	10 b	
FRACTIONAL G RATE CONTROL	(8 meets requirement)	10 b	
ATTITUDE (operating, DE-ORBIT)		24 b	
COMMANDS	ID/time		56 b
REAL TIME PROGRAMMED			

Table 6.7-7. Module Monitoring

AT REGULAR INTERVALS			
MODULE			
STATUS	CLOCK		
	EQUIPMENT STATUS	fine/medium	40 b
ENVIRONMENT	OPERATING MODE	65K state capacity	16 b
		256 state capacity	8 b
LIGHT/DARK	STATUS	18 Discrete, 2 each. O/O	8 b
INTENSITY	18 Analog/SE, 5/75 lux; 10%; 8 b	144 b	
ACCEL (LOR)	15 MIN RES, $\pm 2\%$	3 Bridge	8 b
ATMOSPHERE COMPOSITION			
BR-963 CJC-900, TC-953	Total PRESSURE	2 Analog/SE; ID/2048	24 b
	O ₂ CONCENTRATION	2 Analog/SE	24 b
	CO ₂ CONCENTRATION	2 Analog/SE	24 b
	Air Reg Diff	1 Analog/DE	16 b
	O ₂ Reg Diff	1 Analog/DE	16 b
	HUMIDITY	2 Bridge	24 b
	TEMPERATURE	16 Thermocpl	128 b
	Air Flow - pres	32 Analog/SE	256 b
		18 cage	
		4 supply fans	
Condensate pres		6 supply plenum	
		4 exhaust plenum	
		2 Analog/SE	24

Table 6.7-8. Experiment Monitoring

<u>AT REGULAR INTERVALS</u>				
SUPPORT				
STORAGE	AIR	feed pr	2 Analog SE	
		regul	2 Analog DE	24 b
	OXYGEN	feed pr	2 Analog SE	24 b
		regul	2 Analog DE	24 b
	WATER	supply pr	2 Analog SE	24 b
STATUS				
			65K state capacity	16 b
MEASUREMENTS/ANIMAL				
	Mass - floor strain guage	18 Bridge	10 b each	<u>180 b</u>
				1052 b
BIOTELEMETRY ANTENNA/DEMODULATION - 18 single channel receivers				576 b
temperature	102.6 degree dyn range	0.1 deg		10 b
heart rate	260-600 bps	beats		10 b
blood pres	systolic/diastolic	128 units		7 b
ECG waveform				
identification	32			<u>5 b</u>
				32 b

Table 6.7-9. Activity Monitoring (per cage)

ACTIVITY			
Array of IR beams emitted from source assemble (18 cages)			432 b
cage ID		5 b	
beam ID		4 b	
counter	most/least beam, 7sec/15min res	14 b	
source on		1 b	
		24 b	
USE RATE (18 cages)			540 b
WATER -	Lixit activity counters	10 b	
FOOD -	food bar counters	10 b	
	general purpose counters	10 b	

Table 6.7-10. Image Recording

AT SCHEDULED TIMES			
INTERNAL CAGE IMAGES			
512x512x8 optimal	2.097 Mb		
256x256x4 acceptable	262 Kb		
f8 bits, f4 res, f16 contrast			32,768 KB/image
1/cage/hour for 30 days = 424.67 MB			
SELECTED RECORDS/IMAGES SHALL BE TELEMETERED DURING FLIGHT			

Table 6.7-11. MMP-900 PCM Encoder Configuration for the PM

I/O	SYS 1	SYS 2	FUNCTION
	#####	#####	End Plate and EPROM access cover.
	PR-914E	PR-914E	Programmer - Sync/address/cntl/cntr, entire system
TLM OUT	TM-915A	TM-915A	Timer - Generates bit/word clock and sample pulse for sys timing. Transforms formatter output into PCM input (NRZ-L/M/S, Bi-0-M/S/L, DD-M, RNRZ-L) with bit/word and minor/major frame synch. All TTL compatible.
DATA IN	MP-901		Analog Multiplexer/Amp - Accepts 32 analog sensor inputs, conditions for single or differential, forwards to amp, which provides sampled pulse amplitude modulation level, per prog sequence.
DATA IN	MP-901		Analog Multiplexer/Amp - 32 sensors Analog Multiplexer/Amp - 4 sensors, 28 spares
DATA IN	MP-901		
	LA-975A		Analog Multiplexer/Amp - Accepts 24 (8 bpw) inputs and forwards data directly to formatter. Digital inputs of more than one type, including MIL-STD-1553B, can be formatted within the same encoder.
			Level Amplification - Converts full scale single range from 5-10 volts to user selectable 1-20 volts SE, 10 mv to 1 volt DE. (200ma)
		BR-963	Bridge Conditioner - 8 bridges
		BR-963	Bridge Conditioner - 8 bridges
		BR-963	Bridge Conditioner - 4 bridges, 4 spares
		TA-953	Thermocouple conditioners - 8 sensors
		TA-953	Thermocouple conditioners - 8 sensors
		CJC-900	Cold Junction Compensator - 16 TC pairs
		FM-918	FM-918 Formatter
		AD-906	AD-906 Sample/Hold A/D Converter - Holds sample, converts to 8, 9, or 10 bit, and forwards to formatter.
		CI-942	CI-942 Computer Interface - coarse/medium time tag (5B)
		CI-922	CI-922 Counter/Accumulator - SV clock, 20 bits (12 day)
PWR IN	PX-984	PX-984	Power Supply - Includes crystal clock. Accepts external clock input for synchronized operations.
28V		14.0 W	11.2 W (assumes 33.3ma/slice other than LA-975A0)

Table 6.7-12. Aydin Vector MMP-900 Micro PCM Encoder

I/O	SYSTEM A	SYSTEM B	FUNCTION
	#####	#####	End Plate and EPROM access cover.
	PR-914	PR-914	Programmer - Sync/address/control/counter for entire system
TLM OUT	TM-915	TM-915	Timer - Generates bit/word clock and sample pulse for sys timing. Transforms formatter output into PCM input (NRZ-L/M/S, Bi-0-M/S/L, DD-M, RNRZ-L) with bit/word and minor/major frame synch. All TTL compatible.
DATA IN	MP-901	MP-901	Multiplexer/Amp - <u>Either</u> analog or digital. Accepts 32 analog sensor inputs, conditions for single or differential, forwards to amp, which provides sampled pulse amplitude modulation level, per prog sequence. Or accepts up to 30 digital (24-8bpw, 27-9bpw, 30-10bpw) inputs and forwards data directly to formatter. Digital inputs of more than one type, including MIL-STD-1553B, can be formatted within the same encoder.
	LA-926	—	Level Amplification - Converts full scale single range from basic, user selectable 5-10 volts to user selectable 1-20 volts single, 10 mv to 1 volt differential.
	FM-918	FM-918	Formatter
	AD-906	AD-906	Sample/Hold A/D Converter - Holds sample, converts to 8, 9, or 10 bit, and forwards to formatter.
PWR IN	PX-928	PS-907	Power Supply - Includes crystal clock. Accepts external clock input for synchronized operations.
28V Power	14.0W	8.4W	Added power for LA-926 amplifier

NOTE: Interface modules using CMOS OR TTL line driver/receiver devices can allow remote devices to be used hundreds of feet from and under control of the master unit. The master unit provides addresses and control lines. The output can be from either unit.

Table 6.7-13. RRS MMP-900 Micro-Modular PCM Architecture

	MODULE	FUNCTION	PL1	PL2	DM1	DM2	DM3	MM1	MM2
	#####	End Plate	1	1	1	1	1	1	1
	PR-914E	Programmer	1	1	1	1	1	1	1
TLM OUT	TM-915A	Timer	1	1	1	1	1	1	1
DATA IN	MP-901	Multiplexer	4	-	4	-	1	3	1
	AD-906	S&H A/D Conv	1	1	1	1	1	1	1
	LA-975A	Level Amp	1	1	1	1	1	1	1
	FM-918	Formatter	1	1	1	1	1	1	1
PWR IN	PX-984	Power Supply	1	1	1	1	1	1	1
DATA IN	MP[-902	Bi-lev Multi	-	-	-	-	3	2	-
DATA IN	SD-924	Serial Data	-	-	1	-	1	1	-
DATA IN	BR-973	Bridge Cond	-	2	1	-	-	-	1
DATA IN	TA-958	Thermocouple	-	1	-	4	-	-	2
	CJC-900	Cold Junction	-	1	-	4	-	-	2
	PD-929	Comp Interface	1	1	1	1	1	1	1
	CI-922	Counter/Accum	1	1	1	1	1	1	1
Modules			12	12	14	14	15	14	14
Power (watts)			7.7	11.3	9.5	11.1	9.4	8.3	11.2
Weight (pounds)			0.8	0.8	0.9	0.9	0.9	0.9	0.9

6.8 Power

6.8.1 Operations

Power is a critical support subsystem for the payload and must be available for payload operations from PM installation through removal.

6.8.1.1 Prelaunch. Prelaunch power normally will be provided from a ground source via the service tower umbilical to the power subsystem for distribution to the remainder of the vehicle. The GSE power/thermal pack, normally used for post-recovery operations, may be used as necessary to maintain continuous power during launch pad anomalies and/or transport. Battery power is used to ensure continuous power whenever the payload is installed within the vehicle.

6.8.1.2 Launch. The vehicle operates on internal power from just prior to umbilical ejection until the fairing (nose cone) is separated during powered flight. The launch phase power budget is limited to ensure sufficient battery power is available to: 1) maintain safe vehicle/internal operations for at least 2 hours after umbilical ejection, 2) execute a first opportunity emergency recovery of the vehicle in the event of a total array failure, and 3) safely recover the vehicle and payload if the aft solar array is operable. Although ground commanding will normally be used to control the power load under emergency conditions, autonomous load shedding will occur as necessary to save the vehicle.

6.8.1.3 On-Orbit. The vehicle normally operates under solar array power with battery supplement for low array power or high load conditions. Although the vehicle is capable of operating in the closed configuration, a minimum deployment of the DM that allows full power operation is considered the normal operating mode. Each module acts as an independently powered vehicle with full bus control and battery operations. External control (e.g., automatic load shed) is exercised by a processor in the GNC computer in each module. The primary power sources are the solar array for the DM and the DM for the MM. Redundant battery systems provide full battery backup at all times.

6.8.1.4 De-Orbit. Sufficient battery power must be available prior to the initiation of de-orbit to maintain the required vehicle and payload operations up to at least 2 hours after landing. Vehicle operations should be organized to permit trickle charge from the aft array up until the main burn is initiated.

6.8.1.5 Reentry. The vehicle and payload will operate on internal battery power throughout reentry.

6.8.1.6 Recovery. There must be sufficient battery power available at landing to operate the vehicle/payload up to 2 hours until GSE power can be provided.

6.8.2 Requirements

The key RRS power requirements levied in Paragraph 3.3.2 of the RRS SRD are summarized below. However, other than the implication that greater power may be required by the PM, neither these nor the more detailed requirements in the SRD significantly drive the design. The real drivers are the power required by the PM (Table 6.8-1) and the power subsystem reliability required to meet the public safety and animal welfare (SRD 4.2.3.2, 99% probability of healthy recovery) requirements.

Table 6.8-1. Power Trade Summary

System	Weight (lbs)	Savings (lbs)	Volume (ft ³)	Pros	Cons
Li/(CF)x Battery	817		11.6	<ul style="list-style-type: none">• Easy Spin Balance	<ul style="list-style-type: none">• Replacement Costs• Thermal Impact
Fuel Cell With Cables	508	309 (rodents) 189 (other)	24	<ul style="list-style-type: none">• Weight Savings	<ul style="list-style-type: none">• Thermal Impact• Volume for Consumables• Water Storage Tank Mass
Solar System	460	351 (battery) 48 (fuel cell)	5	<ul style="list-style-type: none">• Lowest Volume• Weight Savings• Reliability• Low Development Cost	<ul style="list-style-type: none">• Spin Balance

The SRD specifies no basic architecture for the RRV power subsystem other than there must be an internal power source available "for some prelaunch, launch, flight, recovery and post-recovery operations." The RRV is required to provide 45 kWh of 28 Vdc power to the PM from prelaunch through post-recovery, with the PM responsible for any power conditioning beyond the basic bus. However, the SRD cautions that "These power requirements are a lower limit and higher power levels should be studied."

The following derived requirements were equally critical in determining the preliminary design:

- The allocated reliability for the 99% probability of safe recovery requires no single point failure opportunity and an autonomous load shed capability.
- The DM to MM power transmission should not magnetically interact with the earth's magnetic field sufficiently to create a disturbing force which would exceed the 10^{-5} g microgravity and/or require compensating attitude control activity under any other conditions.

6.8.3 Trade Study Summary

The most critical trade study for the power subsystem was not the power study itself, but the analysis of the PM required power. These studies indicated that in actuality, the RM requirement for a 60-day mission (See Section 6.2) is almost a factor of 2.5 higher than the required 45 kWh, the EBM payload would be over a factor of 3.5 higher, and materials processing probably even higher, making the use of consumable energy sources (batteries or fuel cells) virtually impossible.

The power subsystem trade studies did, however, investigate the use of batteries (rechargeable and single use), fuel cells, and solar arrays as the primary power source. The solar array assessment included the use of a 12 degree-of-freedom simulation that modeled both the vehicle geometry/dynamics and the thermal effects on solar cell performance. Since the SAIC vehicle configuration has extensive areas available for body mounted solar cells, the solar array based system was the obvious design choice (Table 6.8-1) in terms of weight, reliability, and power availability for just the biological payload requirements.

The final design has evolved well beyond the initial trade study, and the use of the solar array clearly eliminates a major mission limitation. With the addition of the aft array, the minimum RRS capability for fractional gravity operations provides sufficient margin for the basic biological/botanical payloads (Table 6.8-2), 30 to 50 percent (orbit dependent) margins for the worst case microgravity missions, and greater than 65% margin for Sun-synchronous microgravity operations. This represents approximately an order of magnitude greater power availability than the basic SRD requirement without major design impact without optimizing the arrays for maximum output or projecting the use of advance cell technology that could increase output by another 30 to 100 percent.

Table 6.8-2. Power Subsystem Interface Support

SUBSYSTEM	VOLTAGE, V	AVE MSN PWR, W	PEAK PWR, W	60 DAY BUDGET, kW HRS
Payload	28	11.1	174.98	160.0
Propulsion	28	0.5	626	0.7
GNC	28	25.9	626	66.6
TT&C	28	42.1	67	60.7
Power (N/A)	—	—	—	—
Reentry (N/A)	—	—	—	—
Thermal	(Must Be Kept Within Temperature Bands)			
Structure				
	+28 to Astromast	0	90	0
Total	—	79.6	—	288.0

TOR42F/32

The other major power design trade considered several means of DM-MM power transmission, with emphasis on the full 100 foot tri-mast extension. At this length, and at the potentially high payload power levels, a fail operational approach with some means of magnetic field interaction mitigation should be employed. After consideration of high voltage direct current (HVDC), shielding, the use of twisted-pair cabling and other options, the use of the high frequency three-phase approach described in this section was chosen. However, a normal 28 Vdc transmission bus should be adequate for all microgravity and most 1 g artificial gravity missions, the initial missions currently included in the RMOAD.

6.8.4 Baseline Description

The RRS power system is configured to derive its prime source of energy from solar panels, which will be mounted on the Deployed Module (DM), as illustrated in Figure 6.8-1. These panels have sufficient capability to provide all power necessary for operating the RRV and Payload, and to fully charge the batteries during sunlit portions of the worst-case orbit. Power required for operation during ascent, eclipse, reentry, and recovery is provided by nickel/hydrogen batteries, capable of supplying 2 kilowatt hours of energy, with 2 kilowatt hours of energy as redundant backup. The power subsystem is consists of:

- Solar Panel Interface (Bus Voltage Limiter).
- Primary and Backup Battery Discharge Controller.
- Primary and Backup Battery Charge Controller.
- Power Distribution Unit.
- 28 V DC to 3-Phase 220 V - 20 kHz Converter.
- 3-Phase 220V - 20 kHz to 28 V DC Converter.
- Ground Support Equipment (GSE) Interface.
- Computer I/O Interface.

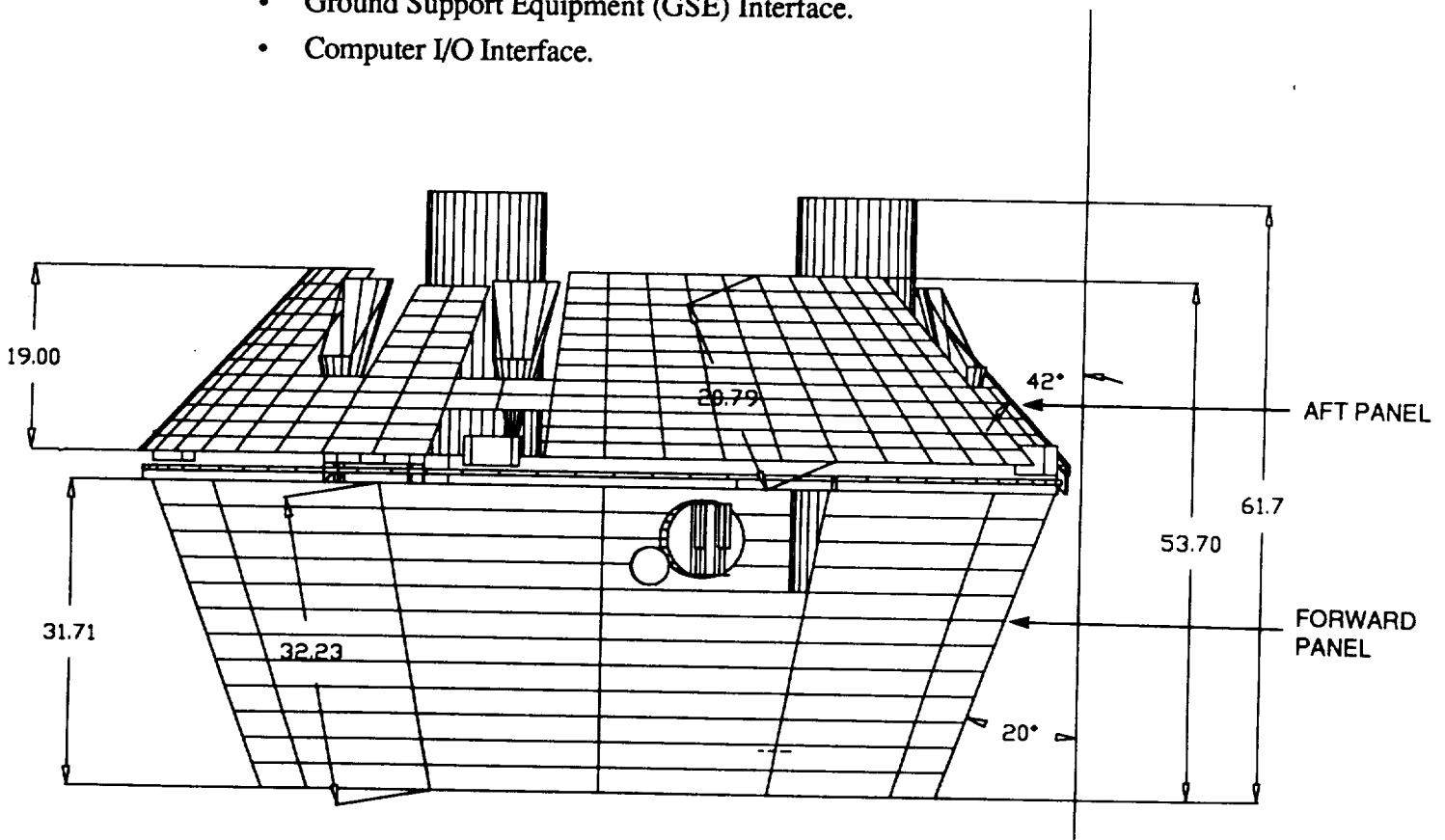


Figure 6.8-1. Deployed Module With AFT Array Dimensions (Inches)

Four 16-cell, 52 amp-hour, 24-volt nickel/hydrogen batteries are located in the RRS. One battery in each module serves as the main battery supply for that module, and a second battery is provided as a backup in the event of a malfunction. Each battery is capable of storing 1 kWh of energy. The batteries selected are manufactured by Hughes, and will fly on the A11 spacecraft. Triple redundancy is achieved by allowing power transfer between the MM and DM via the Astromast so that a battery on either module can support the RRS during a fault condition. These

batteries are sized to power the RRS during launch, reentry, and eclipse, and are capable of accommodating three orbits and descent under emergency conditions.

Two sets of solar panels are mounted on the DM. The forward array consists of approximately 51.5 square feet of GaAs cells, and the aft panel is approximately 25 square feet, (Figure 6.8-1). Because the aft panel is subject to reentry aeroheating backface loads, this aft panel may require replacement after each mission.

Cabling in the three Astromasts serves to provide power, ground, and MIL-STD-1553 Avionics Bus interconnections between the MM and DM. The copper beryllium retraction ribbon contained in each of the Astromasts serves to transfer power between the MM and DM. The Astromast will contain the necessary sliprings at both ends of the beryllium copper cable to transfer the 3-phase power between the MM and DM.

A functional block diagram of the RRS power system is shown in Figure 6.8-2. The Deployed Module power subsystem contains two nickel/hydrogen batteries, two solar arrays, battery discharge controllers, battery charge controllers, and nine bus voltage limiters. The MM also contains two nickel/hydrogen batteries, battery charge controllers, and battery discharge controllers. The controllers and batteries in the MM are identical to those used in the DM. Three Astromasts cables serve as both a backup mast retraction capability and as the means for electrical connection. All electronics are fully redundant flight-tested hardware, with the exception of the 3-phase electrical connection between the DM and MM. The 3-phase circuits are considered to be current nonchallenging technology and are implicitly fail safe.

6.8.4.1 Load Characteristics

Table 6.8-3 lists the Main Module and Deployed Module power requirements. Mission average power (Artificial Gravity) is 199.6 watts divided almost equally between the MM and DM. The requirement to supply a 200 watt average power to the bus for three orbits under a fault condition would require (200 watts by 96 min/orbit by hour/60 min by 3 orbits) 960 watt-hours. Thus, selection of a battery with a 1 kWh rating will ensure power availability. Sufficient circuitry has been provided to allow for computer control of the loads. Load control will include power switching to shed individual loads. Monitoring will include both load current and load voltage.

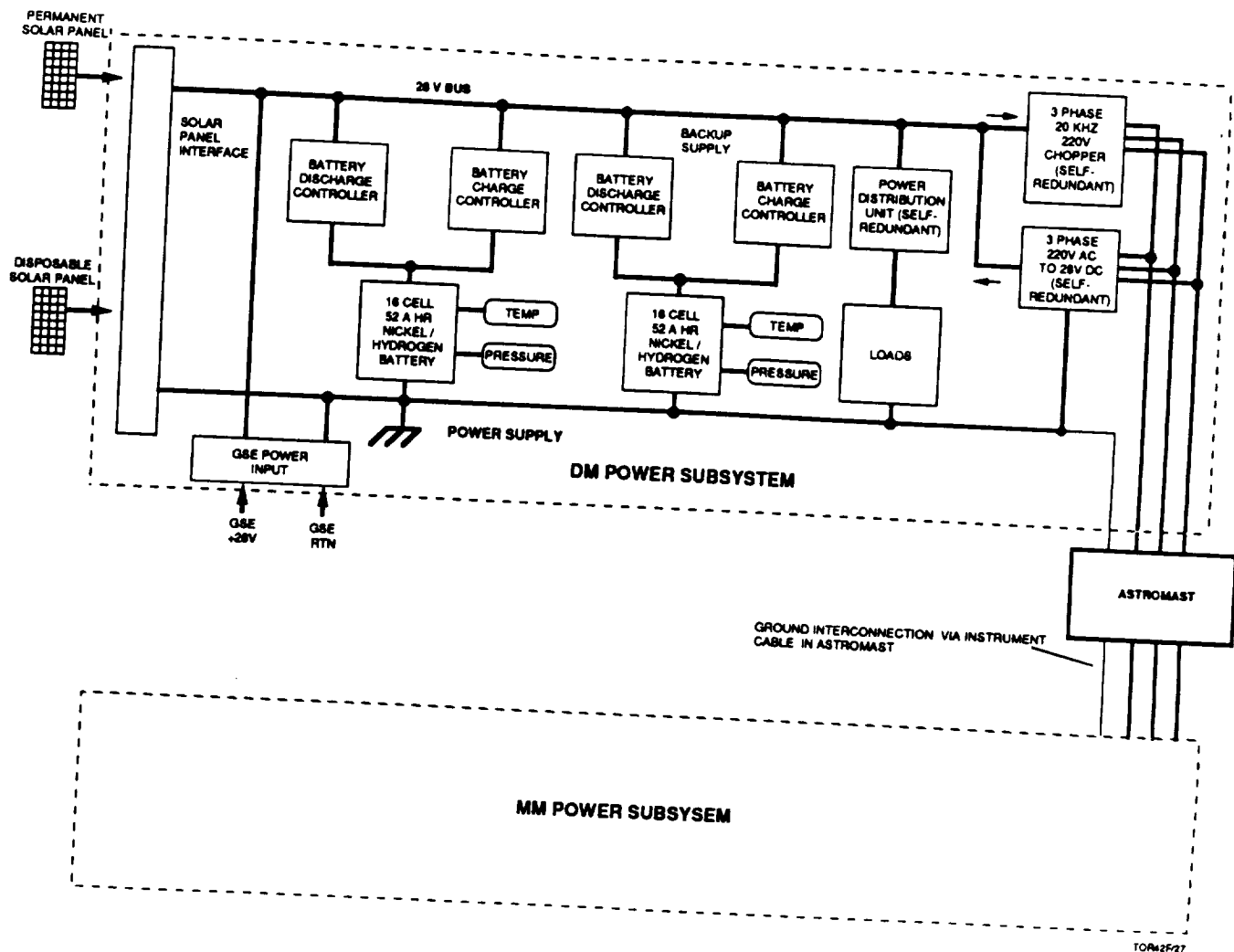


Figure 6.8-2. Power System Schematics

Table 6.8-3. Main Module and Deployed Module Power Budgets

UNIT	POWER (WATTS)	ARTIFICIAL GRAVITY			ZERO GRAVITY		
		DUTY CYCLE	MISSION AVERAGE POWER (WATTS)	60 DAY BUDGET (KWHRS)	DUTY CYCLE	MISSION AVERAGE POWER (WATTS)	60 DAY BUDGET (KWHRS)
MAIN MODULE							
PAYLOAD							
LIGHTS	54.0	0.630	34.0	49.0	0.63	34.0	49.0
FANS	6.0	1.000	6.0	8.6	1.00	6.0	8.6
WASTE FANS	12.0	1E-01	1.2	1.7	1E-02	1.2	1.7
VIDEO	16.0	4E-03	0.1	0.1	4E-03	0.1	0.1
DATA HANDLING	20.0	1.000	20.0	28.8	1.00	20.0	28.8
SENSORS	30.0	0.250	7.5	10.8	1.00	7.5	10.8
IMPLANTS	18.0	0.250	4.5	6.5	0.10	4.5	6.5
ACTIVITY MONITORS	10.0	0.250	2.5	3.6	1.00	2.5	3.6
PAYLOAD SUB TOTAL			<u>75.8</u>	<u>109.1</u>		<u>75.8</u>	<u>109.1</u>
THERMAL PUMP	7.0	1.000	7.0	10.1	1.00	7.0	10.1
IMU 1	14.0	1E-02	0.1	0.2	5E-03	0.1	0.2
COMMAND CONTROLLER	5.0	1.000	5.0	7.2	1.00	5.0	7.2
SUB TOTAL			<u>87.9</u>	<u>126.6</u>		<u>87.9</u>	<u>126.6</u>
TRANSMISSION LOSSES	10.00%		8.8	12.7		8.8	12.7
DEPLOYED MODULE							
PROPULSION							
COMPONENT HEATERS	10.00	0.000	0.0	0.0	0.00	0.0	0.0
MAIN VALVES	252.00	4.05E-05	1E-02	1E-02	4.05E-05	1E-02	1.5E-02
ACS VALVES	112.00	2E-03	2E-01	3E-01	9.65E-05	1E-02	1.6E-02
MAST AND CABLE MOTORS	105.00	2.89E-04	3.0E-02	4.4E-02	1.2E-04	3E-02	4.4E-02
MAIN COMPUTER	25.00	1.000	25.0	36.0	1.00	25.0	36.0
MEMORY BOARD	10.0	1.000	10.0	14.4	1.00	10.0	14.4
TT&C DATA MODULES	68.50	0.100	6.9	9.9	0.100	6.9	9.9
TRANSMITTER	30.50	4E-02	1.2	1.8	4E-02	1.2	1.8
RECEIVER	17.50	1.000	17.5	25.2	1.00	17.5	25.2
TORQUE RODS	2.70	0.000	0.0	0.0	1.00	2.7	3.9
MOMENTUM WHEELS	4.40	1.000	4.4	6.3	0.00	0.0	0.0
GPS RECEIVERS	10.00	1.000	10.0	14.4	1.00	9.0	13.0
ELECTRONICS	10.00	1.000	10.0	14.4	1.00	10.0	14.4
IMU 2,3	28.00	1E-02	0.3	0.4	5E-03	0.3	0.4
SUBTOTAL			<u>85.5</u>	<u>123.1</u>		<u>82.6</u>	<u>118.9</u>
TOTAL			<u>182.2</u>	<u>262.4</u>		<u>179.3</u>	<u>258.2</u>
MARGIN 10%			17.3	25.0		17.1	24.6
GRAND TOTAL			<u>199.6</u>	<u>287.4</u>		<u>196.4</u>	<u>282.8</u>

SAIC has performed a detailed analysis of the power generated by the solar panels, as a function of solar irradiance, and solar panel temperature over the anticipated orbital missions. Figure 6.8-3 shows the maximum sustainable continuous power load that the solar power system can handle in the microgravity mode when the spacecraft attitude is perpendicular to the plane of the ecliptic.

The power generated in the worst case artificial gravity mission, (a 350 kilometer circular orbit) is more than adequate (over 10% margin) to supply the Payload Module and all RRV systems as shown in Figure 6.8-4. In the Artificial Gravity mode, the spacecraft is spinning about its center of gravity with the spin axis perpendicular to the orbital plane. The "worst case," in this instance, specifies a transient 0 degree ascending node orbit during vernal equinox. This orbit describes the worst geometry for power production due to the incidence angle of the solar radiation on the solar array. The 900-kilometer orbit has a greater power capacity than the 350-km orbit due to the shorter Earth occultation.

The Sun-synchronous orbit, while having a constant 90-degree angle between the ascending node and the Earth-Sun vector, is included here to illustrate the power system performance during the worst case thermal environment. This orbit describes the case in which the solar array receives the most heating, and thus a corresponding drop in solar cell electrical production. It is clear that the improved solar incidence geometry of the Sun-synchronous orbit outweighs the performance penalty of the increased thermal heating.

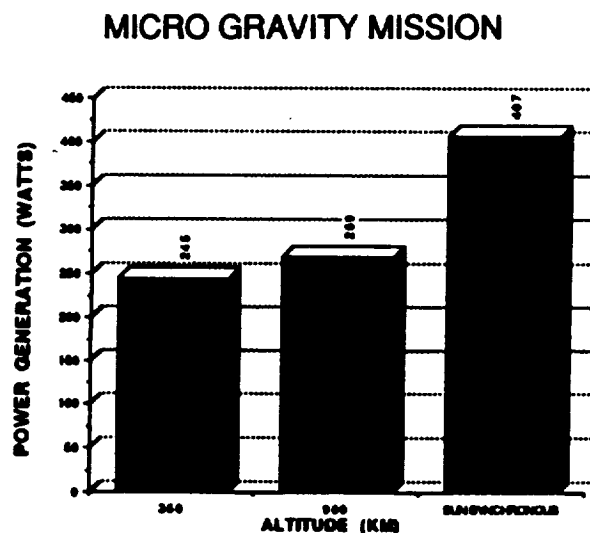


Figure 6.8-3. Power Generation Capability for a Gravity Gradient Mission

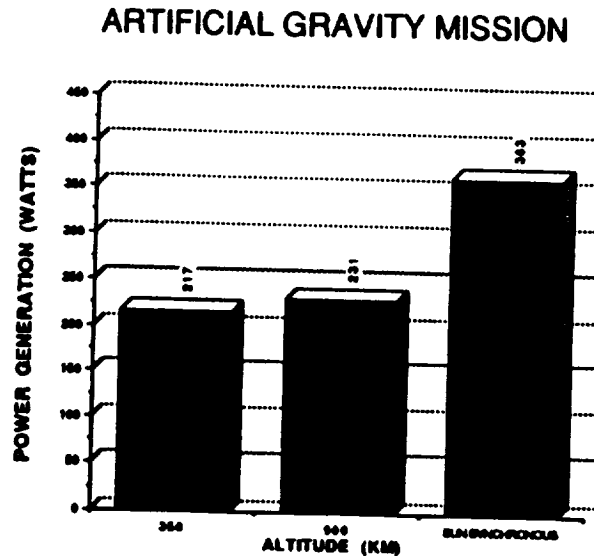


Figure 6.8-4. Power Generation Capability for an Artificial Gravity Mission

The microgravity thermal roll is a 0.14 rpm rotisserie-type rotation around the long axis. In the artificial gravity mode, there is no thermal roll to prevent stabilization problems. The artificial gravity rotation itself provides a certain amount of thermal cooling because all sections of the array are able to give off some deep space re-radiance and no sections are continuously staring at the Sun. The exception to this is the Sun-synchronous orbit which experiences higher operating temperatures.

Artificial gravity maximum power load, Figure 6.8-4, is the same format as the microgravity chart, except for the spinning artificial gravity flight mode and the lack of thermal roll. The artificial gravity spin mode is a 7.0 rpm rotation around an axis through the midpoint of the Astromasts and colinear with the cross product of the position and velocity vectors. The lower performance of the artificial gravity case versus the microgravity case is due primarily to the worse incidence angle of the solar radiation on the array. The Sun-synchronous orbit, while thermally hotter, still has a high maximum power load capability.

Array performance, Figure 6.8-5, charts the array electrical production during a single artificial gravity spin in a 350-km orbit at the worst case ascending node transient. The heavier line at top is the total array performance, the sum of the forward and aft arrays' performance as shown. The straight, horizontal line is the 215 watt continuous power load supplied to the spacecraft. The large margin between the array output and the load is necessary so that sufficient power may be stored in the batteries to power the spacecraft during the passage through Earth shadow.

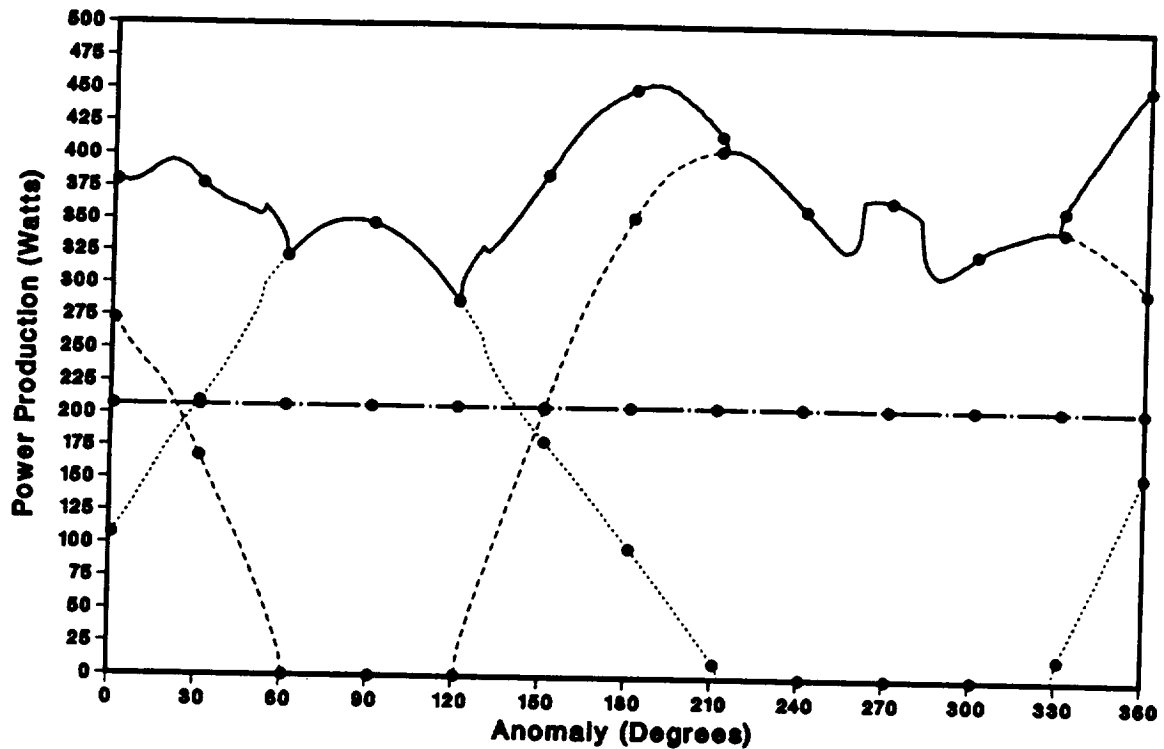


Figure 6.8-5. Array Performance Profile Per Rotation Artificial Gravity/Worst Case Orbit

Battery performance - For the same mission as the array performance chart, Figure 6.8-6 profiles the drain/charge characteristics for the entire orbit starting with the beginning of occultation.

6.8.4.2 System Components

6.8.4.2.1 Solar Panels. The solar arrays mounted on the DM consist of approximately 51.5 square feet of GaAs cells mounted to the skin of the DM, and approximately 25 square feet of GaAs cells mounted on the aft structure. This provides a minimum of 225 watts of sustainable power at 28 volts available for Artificial Gravity missions. The cells used in the solar panels will be GaAs cells, 4 cm x 4 cm. Panel interconnections consist of 45 cells in series ~32V. Sufficient circuitry will be provided to allow for computer monitoring of the solar panel parameters. Monitoring will include:

- Monitoring of each panel segment current.
- Monitoring of each panel voltage.

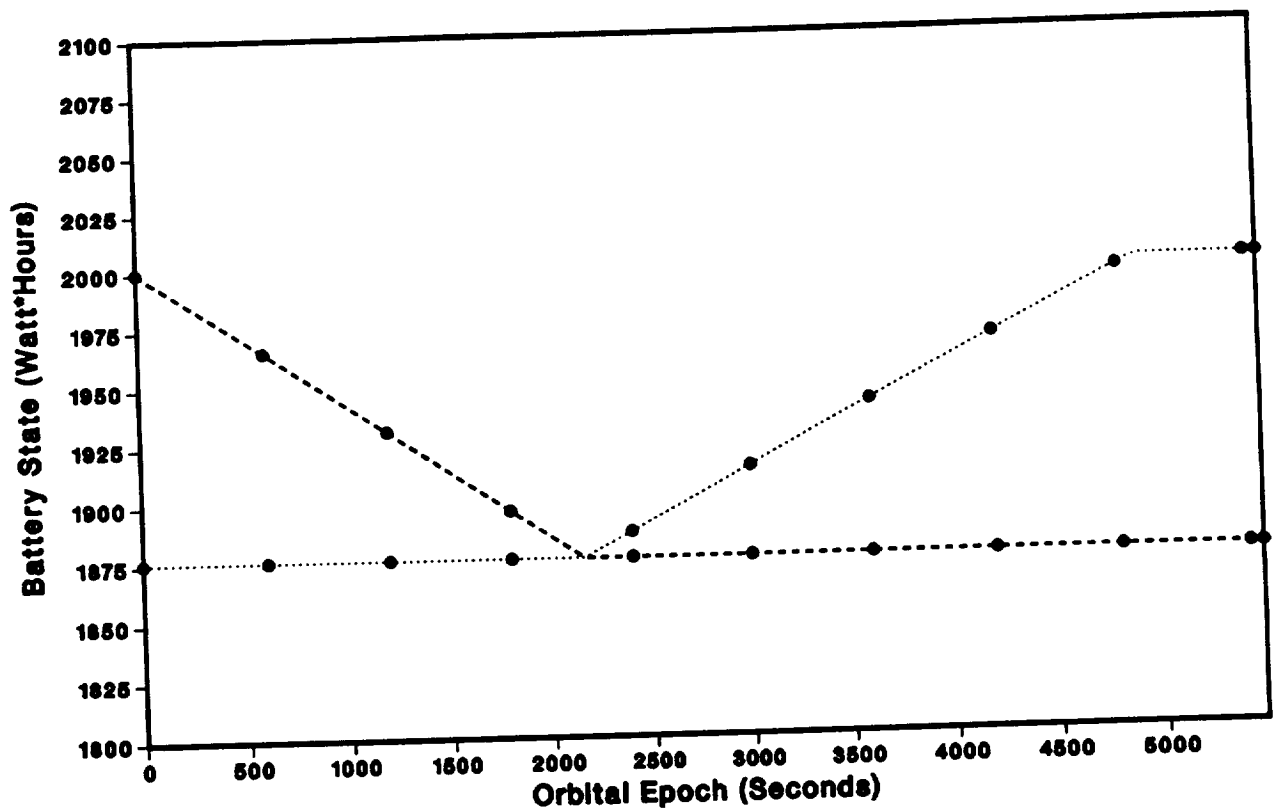


Figure 6.8-6. Battery Cycling Profile Artificial Gravity/Worst Case Orbit

Bus voltage limiters will be capable of shunting solar panel strings to ensure maximum bus potential is held to less than 31 volts. Suitable electronic power switching capability will be provided to shed individual solar panel segments in order to support +28V bus regulation, and will serve as an aid to fault isolation and management.

6.8.4.2.2 Batteries. Four 24-volt batteries (Figure 6.8-7) are located in the RRS, two in the DM and two in the MM. One battery in each module serves as the main battery supply for that module, and a second battery is provided as a backup. Each battery is capable of storing 1 kWh of energy. Rechargeable 1 kWh nickel/hydrogen batteries were selected to accommodate the operational mission of launch, deployment, eclipses, and recovery. The selected batteries are 24-volt nickel/hydrogen batteries, comprised of 16 3-1/2 inch cells, manufactured by Hughes. The nickel hydrogen cells selected for the RRV have energy capacity which is relatively insensitive to thermal variations. Measured data on four cells over a temperature range of -12°C to 29.4°C is presented graphically in Figure 6.8-8. Over this range, cell capacity decreases at less than 0.02 percent per degree C.

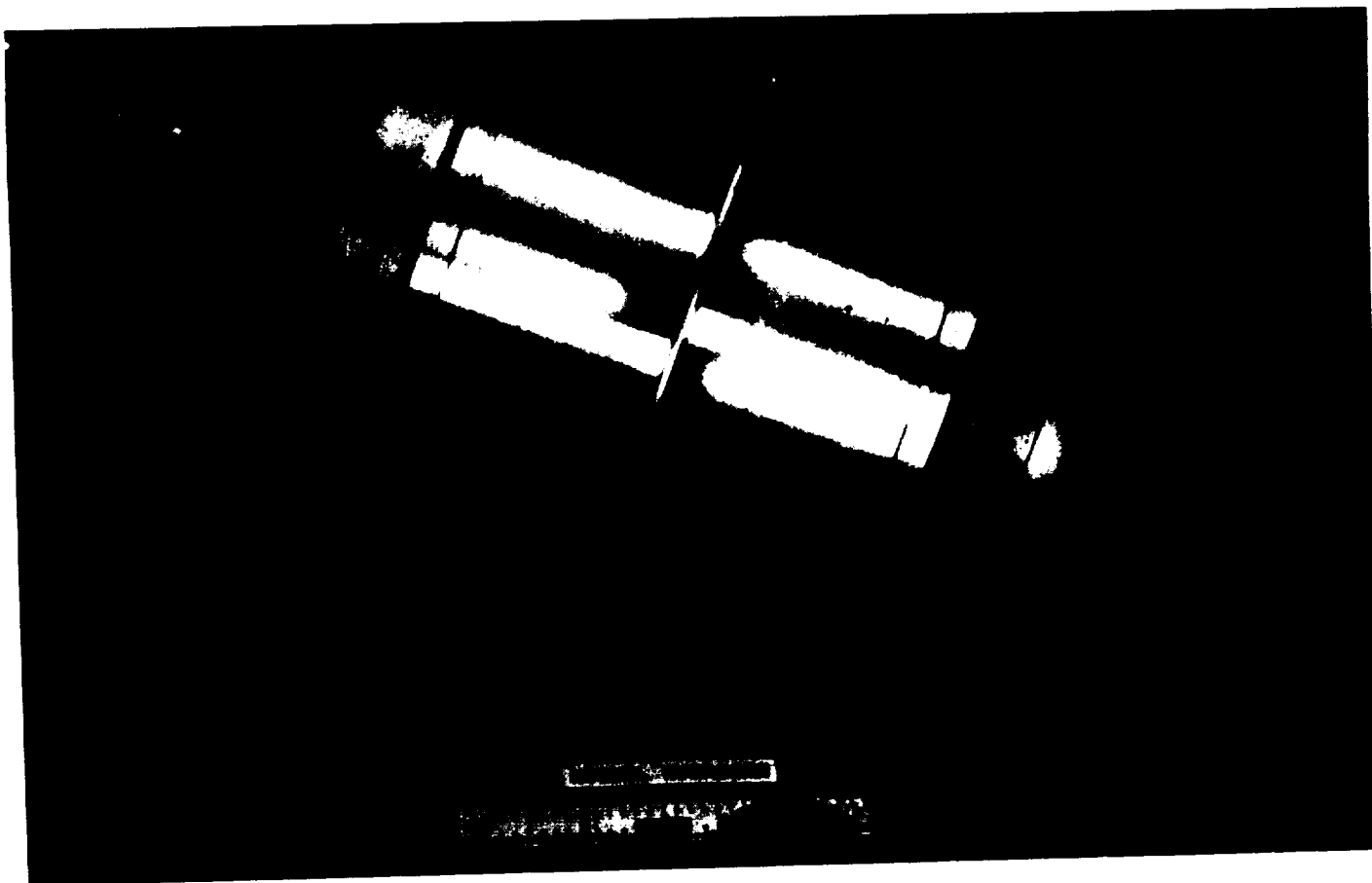


Figure 6.8-7. Nickel Hydrogen Battery Cell

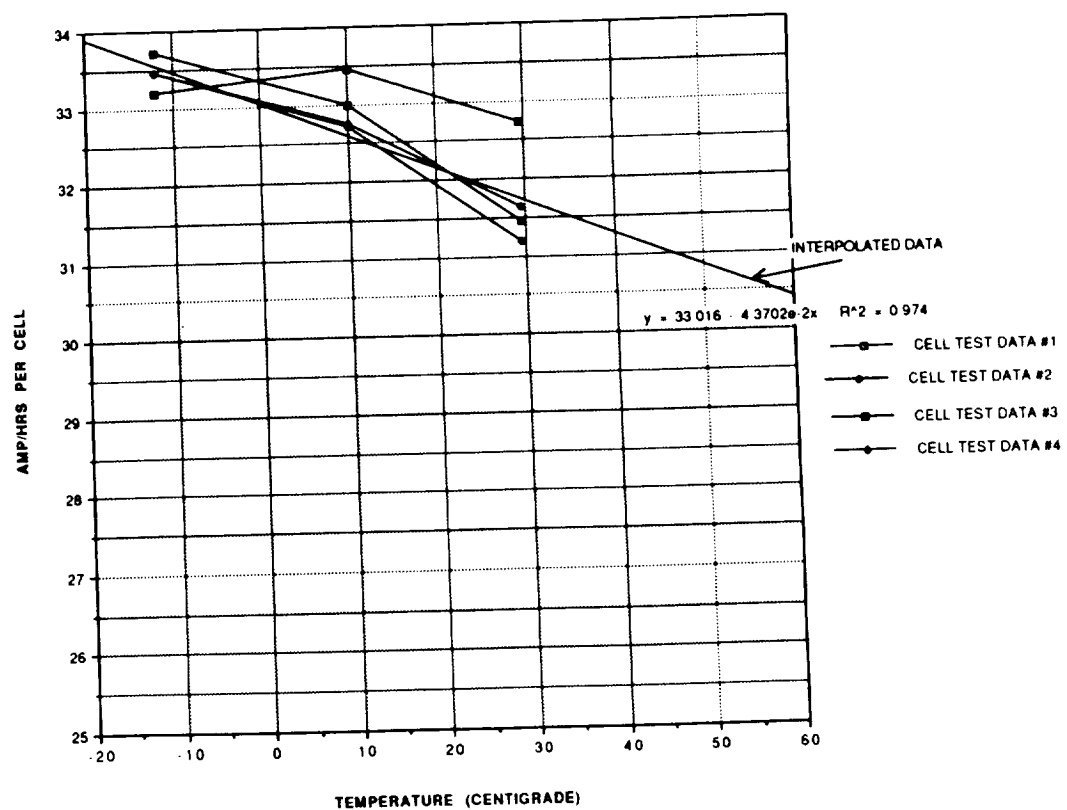


Figure 6.8-8. Cell Energy Capacity Versus Temperature

6.8.4.2.3 Battery Charge Controller (BCC). Four sets of BCCs are located in the RRS, two in the DM and two in the MM. One BCC (Figure 6.8-9) in each module serves as the primary unit, and a second is provided as a backup in the event of a malfunction. The BCC design will allow software to control the operating modes of each of the four units. One of the units in each module will be defined as the primary and the other as the backup unit. Software will be designed to prioritize the charge on the various batteries within the RRS. The following tradeoffs should be considered in the preparation of the Charge Control software:

- The backup batteries will be constantly maintained at 100% charge during nonfault conditions.
- The battery in the DM will have charge priority over that in the MM under nonfault conditions.
- Appropriate control algorithms will be developed to handle all fault conditions.

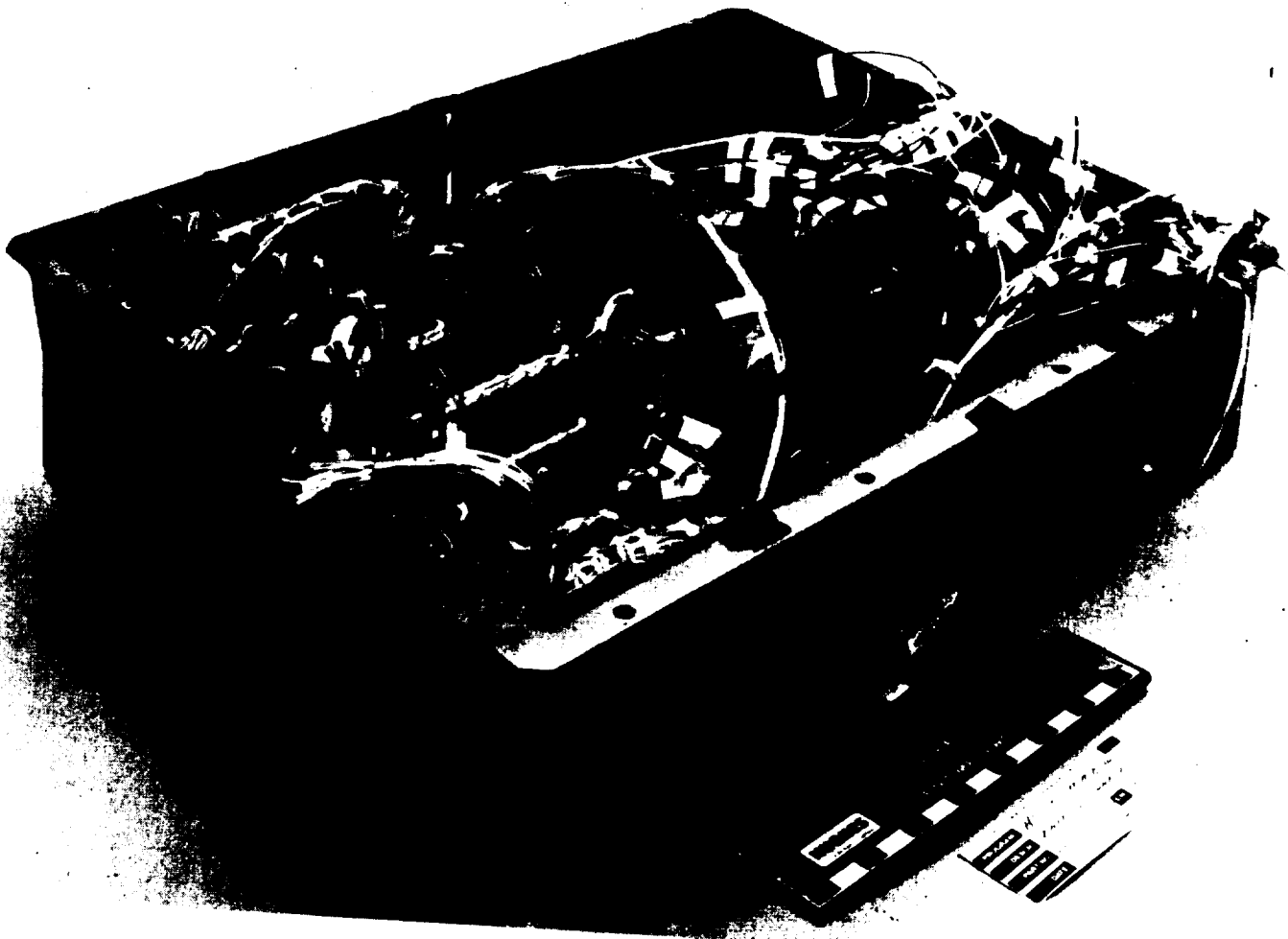


Figure 6.8-9. Battery Charge Controller

The BCC will have the following operating modes:

- a. **Eclipse Mode.** During eclipse, the BCC operates in standby mode. Battery charge current will be zero and the total BCC standby power losses will be less than 2 watts.
- b. **Automatic Charge Control Mode.**
 1. **Hi-rate Charge** - Upon exiting eclipse, the BCC operates in Hi-rate charge mode. Hi-rate charge current is defined as the combination of the hi-rate charge solar array current and trickle charge solar array current, about 9.6 amperes maximum. Hi-rate charge mode will be terminated when battery cell pressure exceeds the preselected pressure setpoint, as defined in Table 6.8-4.
 2. **Trickle Charge** - When battery cell pressure reaches the preselected pressure setpoint, hi-rate charge will be terminated. Only trickle charge panel current will then be supplied to the battery to maintain a full state of charge.
- c. **Manual Charge Control Mode.** Automatic charge control can be overridden and hi-rate charge or trickle charge can be selected by ground commands.

Table 6.8-4. Selectable Battery Cell End-of-Charge Pressure Levels

Level	Address	Battery Cell	Pressure (psi)
0	0000	375	±3
1	0001	398	±3
2	0010	421	±3
3	0011	444	±3
4	0100	467	±3
5	0101	490	±3
6	0110	513	±3
7	0111	536	±3
8	1000	559	±3
9	1001	582	±3
10	1010	605	±3
11	1011	628	±3
12	1100	651	±3
13	1101	674	±3
14	1110	697	±3
15	1111	720	±3

The two BCCs (primary and redundant) in each module are packaged together to form one unit. As shown in Figure 6.8-10 the primary BCC is identical to the redundant BCC. Charge current flows from the solar boost array to the battery through relays and a current shunt resistor. There are two modes of charging: high rate charging and trickle charging. During high rate charging, the main charge relay, high rate charge relay, and trickle charge relay are closed,

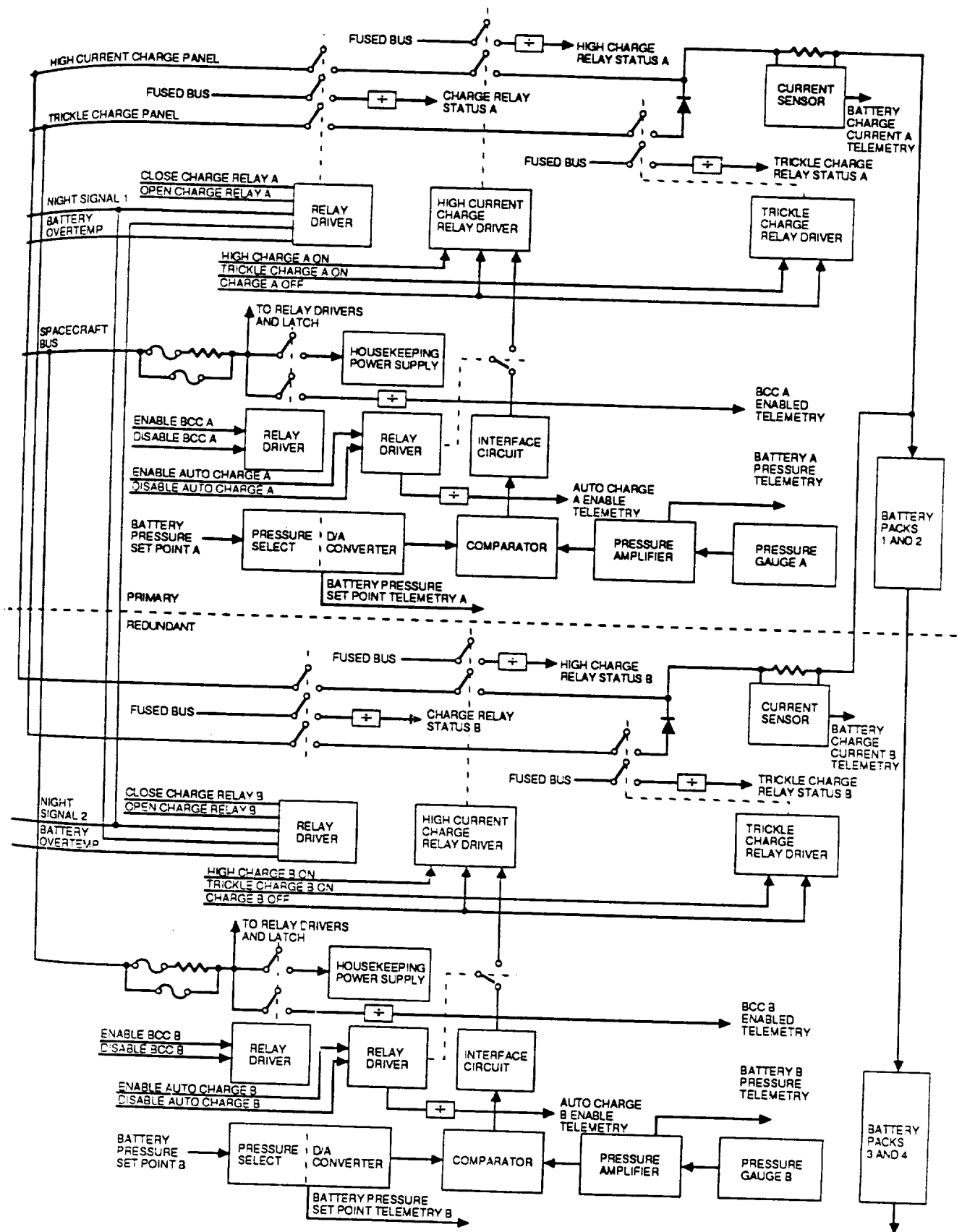


Figure 6.8-10. Battery Charge Controller Block Diagram

allowing current from the high rate charge solar cell groups and the trickle charge solar cell groups to charge the battery. During trickle charging, the high rate charge relay is open while the trickle charge relay is closed, allowing current from only the trickle charge solar cell groups to maintain battery capacity. The main charge relay is normally closed and will open on an overtemperature signal from the battery, but close again on a night signal from the day/night current sensors, these relays can also be controlled by ground commands. A diode in series with the trickle charge relay is used to block current flowing from the battery. A current sensor across the current shunt resistor monitors the charge current.

The charge control electronics consist of a housekeeping power supply, D/A converter, pressure amplifier, comparator, and interface circuit. The battery pressure is sensed by a pressure gage in the battery pack. This signal is amplified in the pressure amplifier. The pressure level to determine termination of charge is preselected by ground command in the form of a digital signal. This digital signal is converted to an analog signal by the D/A converter. The amplified pressure signal is then compared to the analog signal in the comparator. The bilevel output of the comparator is converted into command pulses by the interface circuit, thus controlling the position of the high rate charge relay accordingly. However, this automatic charge scheme can be overridden by ground command by opening the autocharge relay.

The circuits in each BCC include.

- a. **Housekeeping Power Supply.** The housekeeping power supply shown in Figure 6.8-11 is a 100 kHz flyback converter with multiple outputs, ± 12 and ± 10 volts. The converter consists of a SG1524B PWM driving a bipolar transistor which modules the primary of the flyback transformer. Feedback for the pulse width modulation is obtained from the +12 volt output. The -12 volt output and the ± 10 volt output regulation are dependent upon transformer coupling. The ± 12 volt supplies are used for housekeeping functions and the floating ± 10 volt supplies power to the current sensor. The +12 volt supply is also used to generate an accurate +10.00 volt reference for the strain gage and battery pressure monitor circuitry. Current limiting, undervoltage lockout, and soft start features are also provided.
- b. **+10.00 Volts Regulator.** An accurate +10.00 volt reference is required for the strain gage and the battery pressure monitor circuitry. A linear regulator regulates the housekeeping supplies +12 volt output to +10.00 volts.
- c. **Strain Gage Amplifier.** The strain gage amplifier shown in Figure 6.8-12 provides battery pressure information for telemetry purposes and for an input to the battery pressure monitor circuit to determine when to terminate or resume battery charge. The battery pressure is measured by a strain gage with a gain of 10 mV/1000 psi which is sensed differentially by the strain gage amplifier. The gain of the amplifier is trimmed by an SIT resistor such that full scale telemetry voltage represents full battery pressure range.

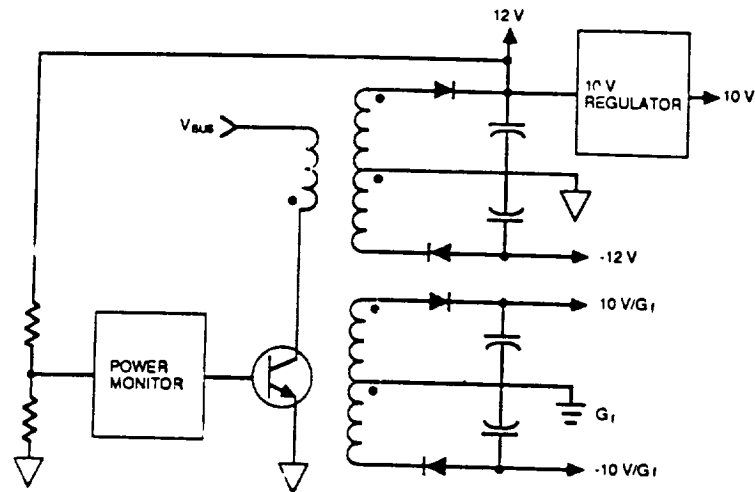


Figure 6.8-11. Housekeeping Power Supply

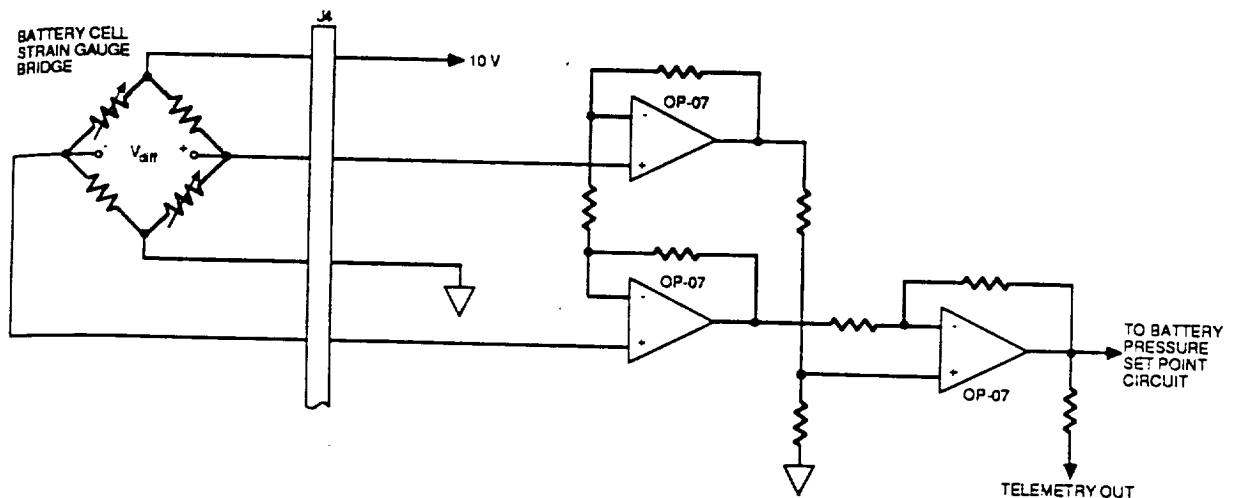


Figure 6.8-12. Strain Gage Amplifier

- d. **Battery Pressure Monitor Circuit.** The circuit shown in Figure 6.8-13 allows 16 different battery pressure set points to be selected by ground commands via a digital to analog converter. When information from the strain gage amplifier indicates that the battery pressure has reached a preselected level, a comparator trips which terminates high rate charge to the battery. DC hysteresis is provided which allows the battery pressure to fall $15 \pm$ psi before high rate charge is resumed.
- e. **Current Sensor.** The current sensor shown in Figure 6.8-14 is a current to voltage transducer which provides battery charge current telemetry information. Charge current through a shunt resistor is measured by a differential amplifier. The gain of the amplifier is such that a 0 to 5 volt telemetry output represents 0 to 15 amperes of charge current.

- f. **Battery Overtemperature Signal.** When battery temperature has reached a level which indicates battery overcharge, an overtemperature telemetry signal is sent to the BCC which terminates both high rate and trickle charges. A ground command may also perform this function. Battery charge is resumed by either receipt of a ground command or a night signal.

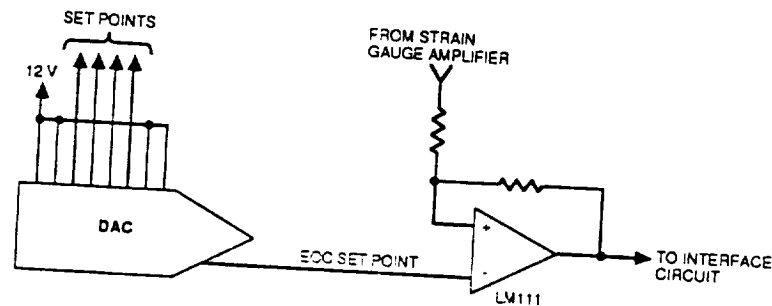


Figure 6.8-13. Battery Pressure Monitor Circuit

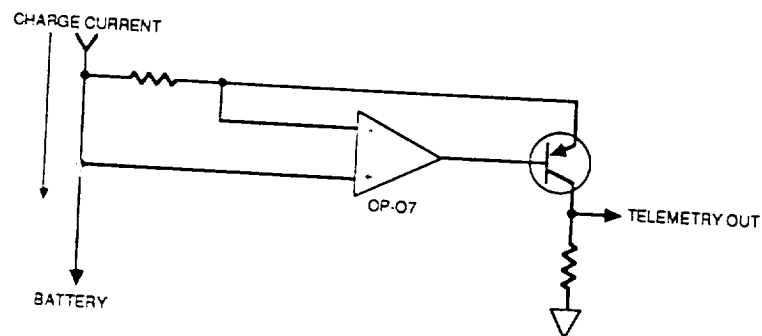


Figure 6.8-14. Current Sensor

- g. **Night Signal.** Upon entry into eclipse, a night telemetry signal is sent to the BCC which closes the main charge relay. This readies the BCC for high rate charge once the charge array returns to sunlight.
- h. **Interface Circuit.** As the telemetry inputs and the output of the battery pressure monitor circuit are bilevel signals, an interface circuit is needed to convert the bilevel signal to the negative pulse command required by the relay driver hybrid.
- i. **Auto Charge Enable/Disable.** A ground command can enable or disable automatic charge control by the battery pressure monitor circuit. Ground commands can then assume control of the high rate charge relay.
- j. **Enable/Disable BCC.** Either side of the BCC may be enabled or disabled by a ground command which closes or opens a relay contact closure in series with the

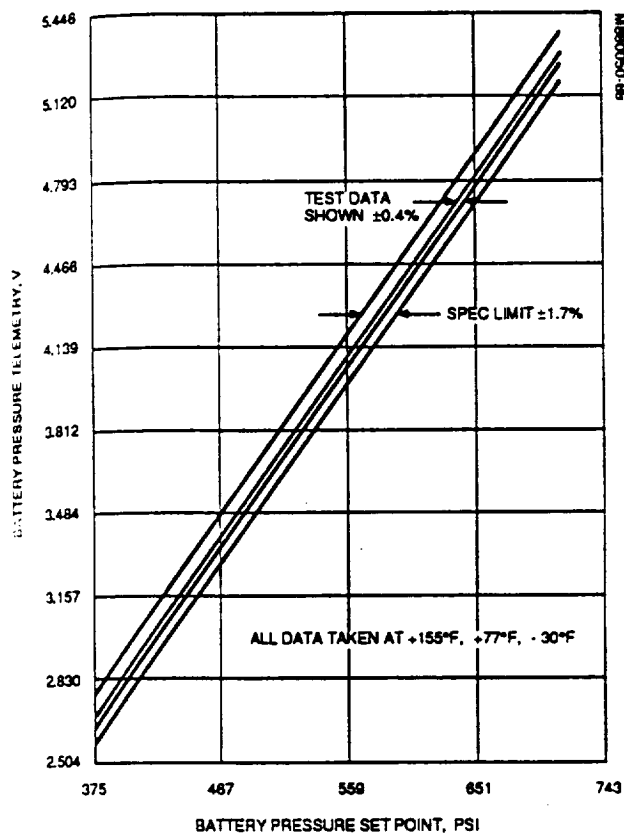
The battery charge controller has 22 subassemblies that are existing designs. The hardware is packaged in a nickel plated aluminum housing measuring 2.640Hx10Wx15.200L, including a 1/2 inch mounting flange down the length of both sides. Four circular connectors (1E02 and 1E06 type), one each for charge array input, battery output, telemetry and command, and strain gages, are located on one 2.64x10 end. Walls and webs in the unit are 60 mil thick to provide EMI and radiation shielding. All circuitry on PWBs and on the chassis are conformally coated and, prior to final acceptance testing, the unit will be encapsulated with polyurethane foam to provide stiffness and vibration damping. Fuses are easily accessible for rework.

The BCC dissipates approximately 6 watts, mainly in chassis mounted components. These parts and the printed wiring subassemblies are located and mounted to minimize thermal paths to the spacecraft shelf. Walls and webs are selectively thickened to improve heat conduction, and the unit will be painted with high emissivity black paint to improve radiative heat transfer to spacecraft sinks (i.e., the inside of the solar panel). The breadboard is tested at the survival temperature range of -30° to +155°F. The breadboard test results are shown in Figure 6.8-15.

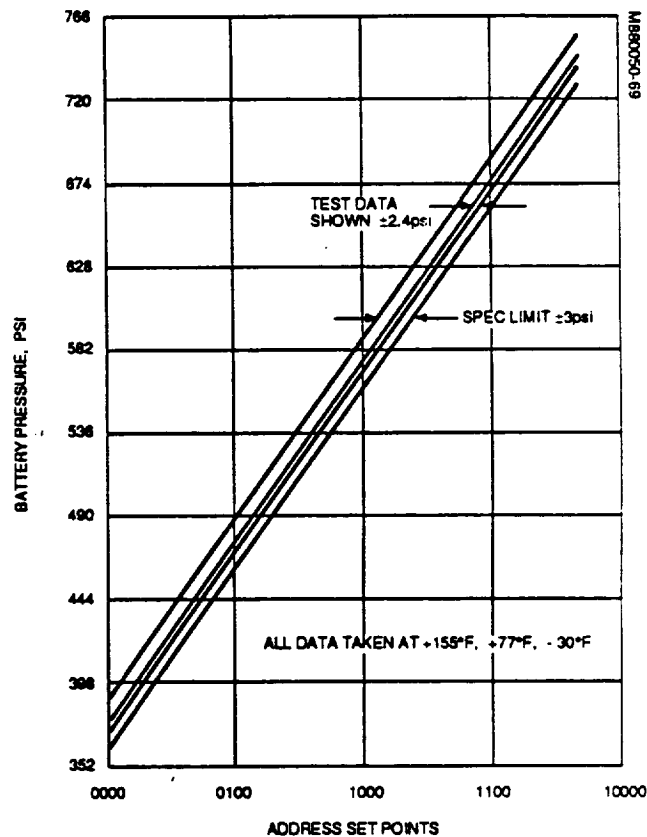
There are four major reasons why an absolute pressure termination method was chosen: 1) This is a proven design that is already being used on other programs and was quite easy to adapt to RRS; 2) it is less expensive than the ampere-hour integrator, which is the termination scheme on three earlier spacecraft; 3) improvement in the strain gage installation process as a result of increased experience; 4) minimizes over-charge better than the other methods, hence resulting in longer battery life. A summary of the candidate charge termination methods is shown in Table 6.8-5.

Table 6.8-5. Battery Charge Termination Options

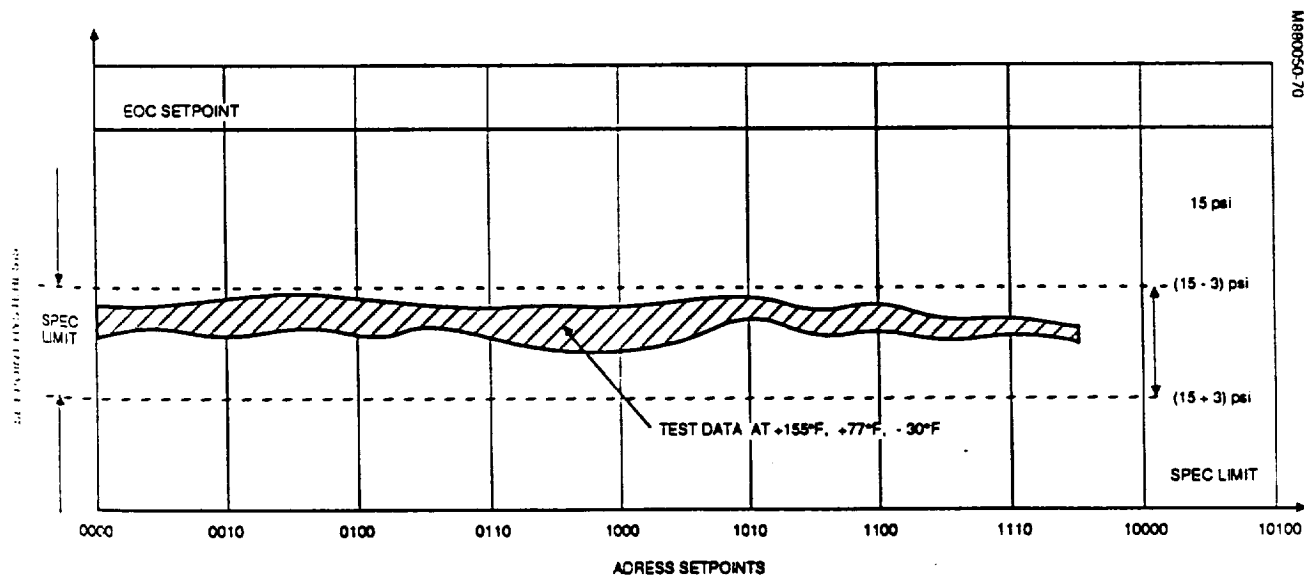
Charge Termination Method	Advantages	Disadvantages	Scheme Proven
Ampere-hour integrator	Proven design Overcharge is controllable	Require precise control at low temperature High degree of temperature sensitivity Complex electronics needed	Yes
Absolute voltage level	Temperature sensors inexpensive, reliable, and proven Stable on-off control Inexpensive electronics	Requires tight temperature range (-10° to +10°C)	No
Temperature-compensated controlled voltage	None	Laboratory experience <ul style="list-style-type: none"> • Works at cold temperature only • Difficult to establish set point • Unstable Complex electronics needed	No



a) BATTERY PRESURE TELEMETRY ACCURACY



b) PRESSURE SETPOINT ACCURACY



c) HYSTERESIS ACCURACY

Figure 6.8-15. BBC Telemetry Accuracy Over Temperature

6.8.4.2.4 Battery Discharge Controller (BDC). The BDC maintains the 28V Bus at $+28V \pm 4V$ with a load of 38 amps maximum. Four sets of BDCs (Figure 6.8-16) are located in the RRS, two in the DM and two in the MM. One BDC in each module serves as the primary unit for that module, and the second is provided as a backup in the event of a malfunction. The BDC design allows software to control the operating modes of each of the four units. One of the units in the MM is defined as the backup and the other as the primary unit. Similarly the DM has one of the Discharge Controllers defined as a primary and the other as a backup unit. The battery discharge controller's main function is to support the bus during eclipse, or when the spacecraft load exceeds the solar array output current. There is a dead band of 0.45 volt between the BDC (BDC) maximum (26.75 volts) and the Bus Voltage Limiter (BVL) minimum (27.20 volts) setpoints. This dead band ensures that these units will not operate simultaneously. To ensure a consistent separation between the BDC and the BVLs, remote sensing is provided from the BDC capacitor bank to each BVL sense control through 1-ampere fuses. Software will be designed to select between the primary and backup controllers.

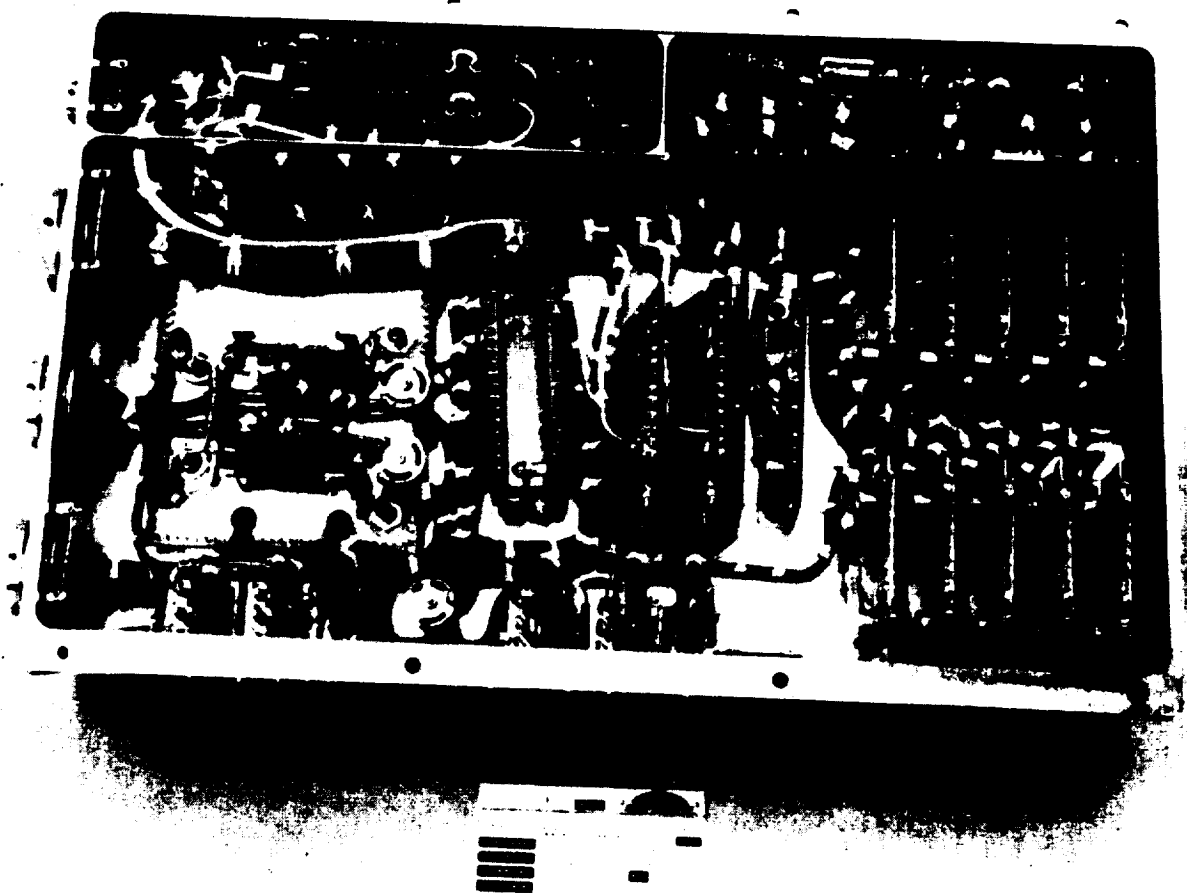


Figure 6.8-16. Battery Discharge Controller

Packaged within each chassis are two completely functioning independent BDCs with a single battery at the input and the two BDC outputs connected at the bus. Either string A or B may be disabled/disconnected from the bus due to anomalies or tests. A single string is capable of supporting the bus with a 26.5 volt output regulation at zero to 38 amperes load. Since there is no forced current-sharing between the A and B active strings, there is a possible chassis thermal dissipation of 100 watts at 38 amperes.

Each string (Figure 6.8-17) consists of a power stage, modulator, housekeeping power supply, overvoltage protect, current limit, overcurrent protect, output diode fault detect, and battery discharge current monitor circuits. Each circuit is described in detail below:

- a. **Housekeeping Power Supply Circuit** (see Figure 6.8-18). The house-keeping power supply is a fixed frequency (40 kHz) flyback converter with multiple outputs. One output ± 13 volts winding is controlling the regulation for all other isolated outputs. There are two DC isolated ± 13 volt outputs that are regulated by virtue of transformer coupling. This supply uses an SG1524J pulse width modulator driving a discrete bipolar transistor switch. Current limiting is provided, as are undervoltage lock out and soft start.

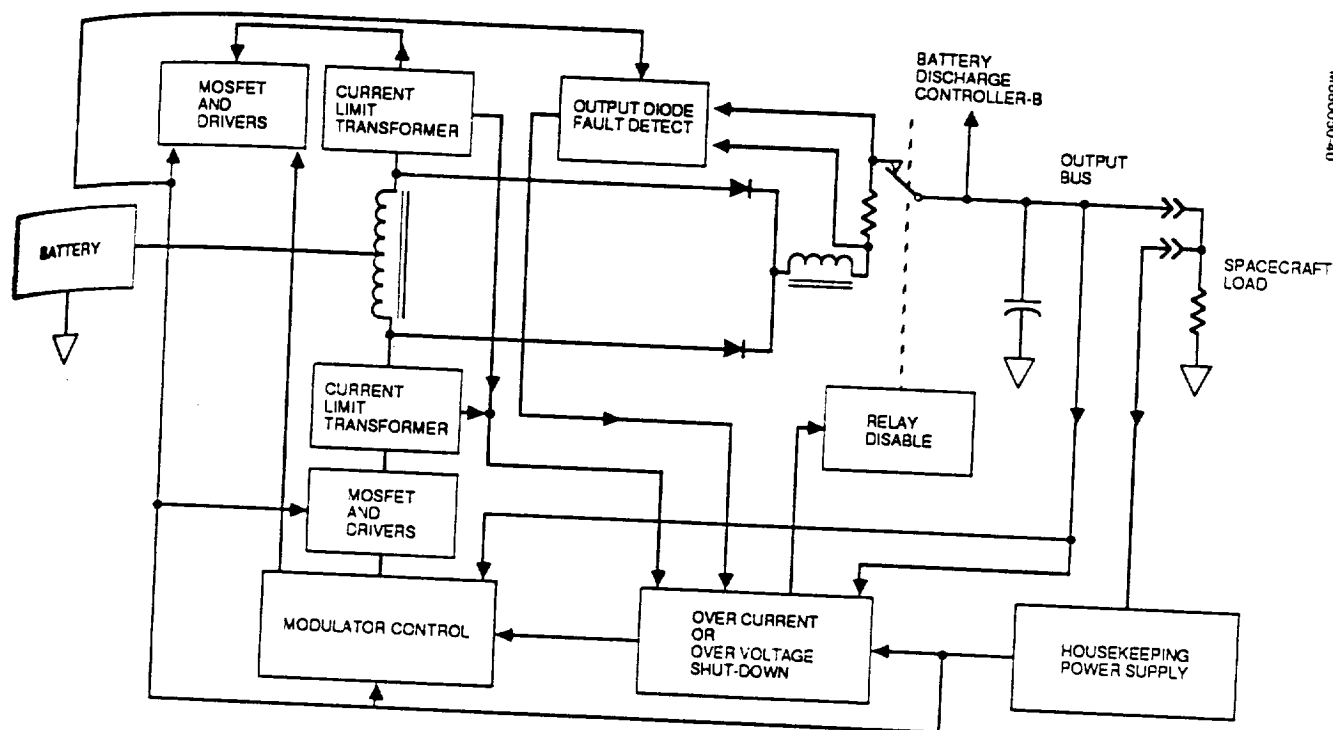


Figure 6.8-17. Single Battery Discharge Controller String Functional Block Diagram

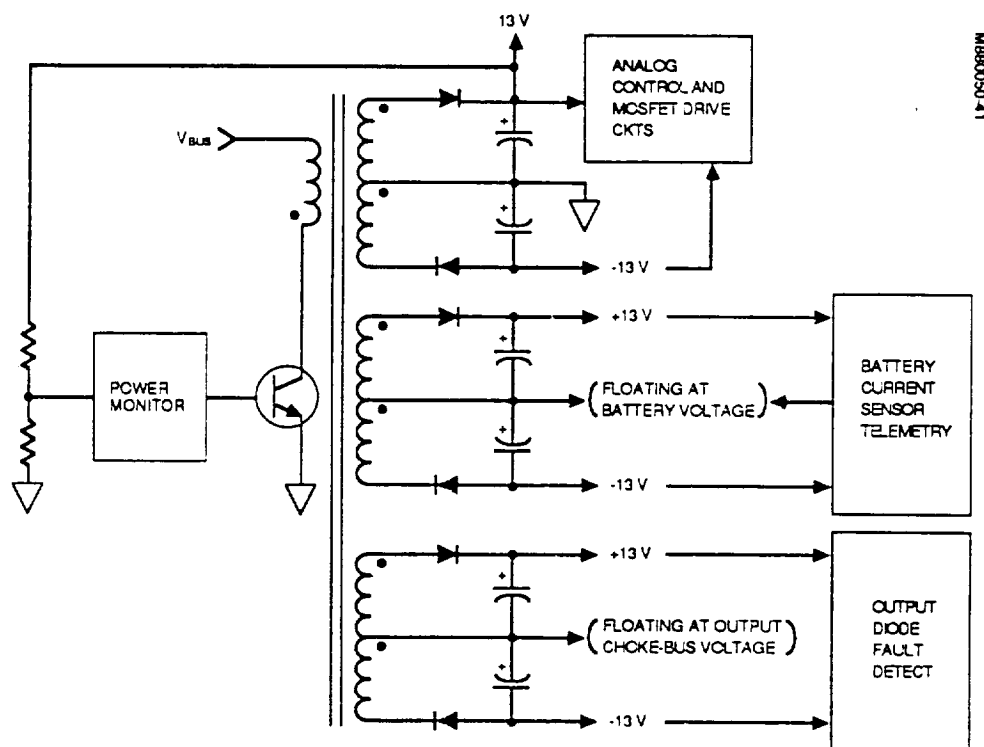


Figure 6.8-18. Housekeeping Power Supply

- b. **Startup (Soft Start) Circuit** (see Figure 6.8-19). When either string is commanded on (enable), two magnetic latching relays will close. If the bus was zero at the moment the unit was enabled, one of the magnetic latching relays connects the battery directly to the bus. When the bus voltage reaches 14 volts, the housekeeping power supply will provide power to the regulator control. The regulator control will slowly allow the pulse width modulator SG1526J to phase up. When the SG1526J phases up, it is allowing the very narrow pulse to slowly get wider, until the output reaches its regulation set point. At 26.5 volts bus the SG1526J will then maintain the appropriate pulse width to sustain regulation.

The soft start is occurring as C1 charges through R1, allowing pin 4 of the SG1526J to slowly rise. This permits the SG1526J to phase up until output regulation is achieved.

- c. **Steady State Operation of Power Output Stage.** The power stage is a boost-add converter. With the power output magnetic latching relay closed, there is a direct connection from battery to output bus through the output boost transformer utilizing Schottky output diodes. At both ends of the boost transformer are four parallel IRH150 MOSFETs that function in a push and pull action prompted by the SG1526J pulse width modulator (PWM). An error amplifier initiates a chain action to the PWM that drives a (totem pole) bipolar transistor which charges the four MOSFET gates in parallel. With the MOSFETS turned on, the auto transformer action boosts the battery voltage to twice its voltage. The boosting action charges the output capacitor bank through one diode and the output choke, until the output reaches the regulation setpoint sensed by the error amplifier. The PWM sensing the output voltage in regulation will

turn off the four MOSFETS concluding one-half of the pushing transformer action. When the output starts to fall, the error amplifier will then detect the droop initiating the pulling transformer action repeating the circuit action described previously but for the pulling circuit.

With the completion of one cycle, the error amplifier will continue to regulate the output with any variations to input battery and output load as in unit specifications. The BDC uses current mode control to provide a wide bandwidth, with a stable output voltage control loop.

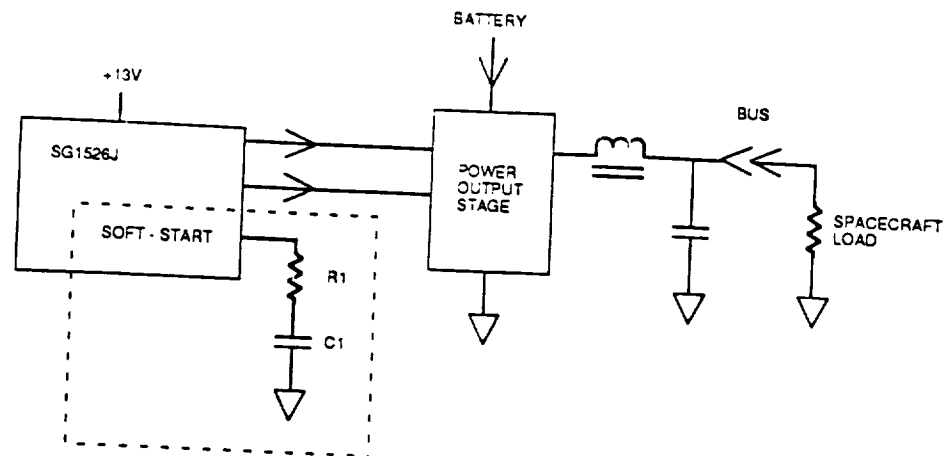


Figure 6.8-19. Soft Start Circuit

The regulation control and gate drive circuit (Figures 6.8-20 through 6.8-22) are of particular interest. As mentioned in the soft start description, the SG1526J PWM chip maintains the output regulation. The PWM senses the bus voltage from a network of wire wound resistors. This resistor divider network is attached to the error amplifier which compares this voltage to the reference. To maintain a regulated output the SG1526J will alternate the push and pull action at pins 11 and 14. Each push and pull signal from the PWM is attached to a gate drive transistor that turns the MOSFETS on. To turn the MOSFETS off, the drive signal is removed causing a PNP bipolar to rapidly remove the charge from all four gates. The off signal pulse will occur at the falling edge of the SG1526J at pins 13 and 16. More specifically:

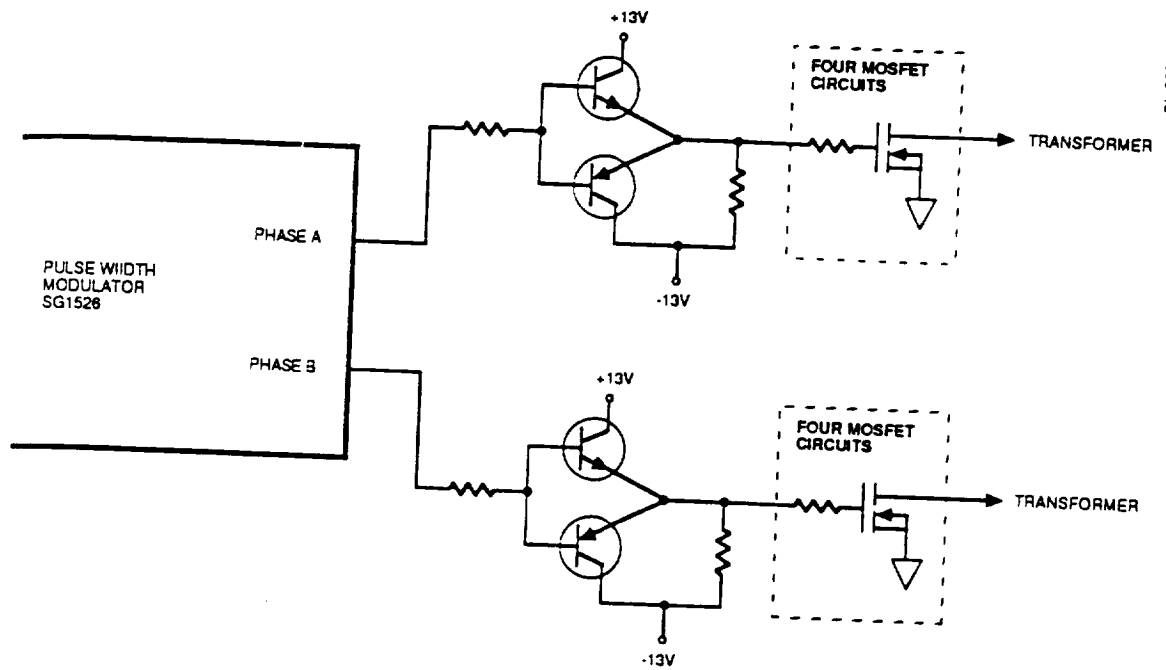


Figure 6.8-20. Gate Drive Circuit

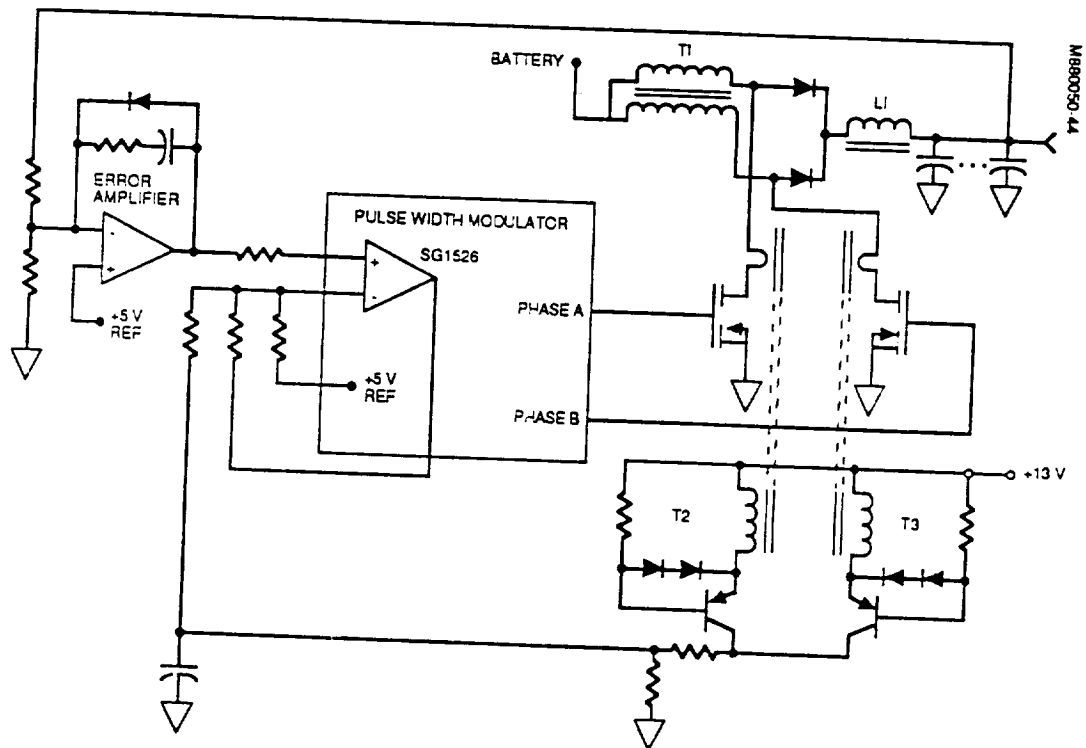


Figure 6.8-21. Regulation Control Circuit



Figure 6.8-22. Timing Diagram

- a. **Current Limit Circuit.** The current limit circuit is activated to prevent serious damage or stress to BDC components if for any reason the spacecraft load should be exceeded. The manner in which the current limit is achieved is by the primary current transforming action. This current transformer is center tapped to power return which generates to the secondary winding that is rectified by turning on a transistor, producing a voltage proportional to the primary winding current across a sense resistor. The two primary halves of the transformer are attached to each group of MOSFET common drain connection providing the push and pull reset action of the primary. Each half-cycle of the primary winding has the total current that passes through the MOSFETS. The secondary voltage setpoint is selected to a safe operating current level of 50 amperes for the MOSFETS in parallel. When a high current level is reached, the rectified voltage at the secondary will shut down the SG1526J (PWM) each half-cycle that the output bus load is in excess. To provide some noise immunity, the current setpoint threshold was elevated to +5.2 volts. When the BDC is in current limit mode, the output voltages will collapse as the load is increased. The output voltage will slowly decrease from the regulation setpoint to the input battery voltage as the load is varied.

If there is a hard short on the bus requiring current to be in excess of 75 amperes for >1 μsec , the BDC will no longer control every half-cycle. After detecting this high current, the PWM will shut down for 6 to 10 seconds, allowing the battery to clear the short. Following this, the BDC will soft start again (assuming the fault was cleared).

- b. **Output Diode Fault Detect Circuit (see Figure 6.8-23).** The fault current shutdown circuit detects currents that can be excessively high due to an output Schottky diode short. This abnormally high current will also produce a signal across a shunt resistor, opening the output and housekeeping relays, turning the BDC off.
- c. **Overvoltage Protect (see Figure 6.8-24).** The overvoltage protect detects when the output voltage is above the unit specification, not to exceed 35 volts. Because the BDC is always turned on and attached to the bus, the only time a BDC will shut down is when it produces the high voltage on the bus.

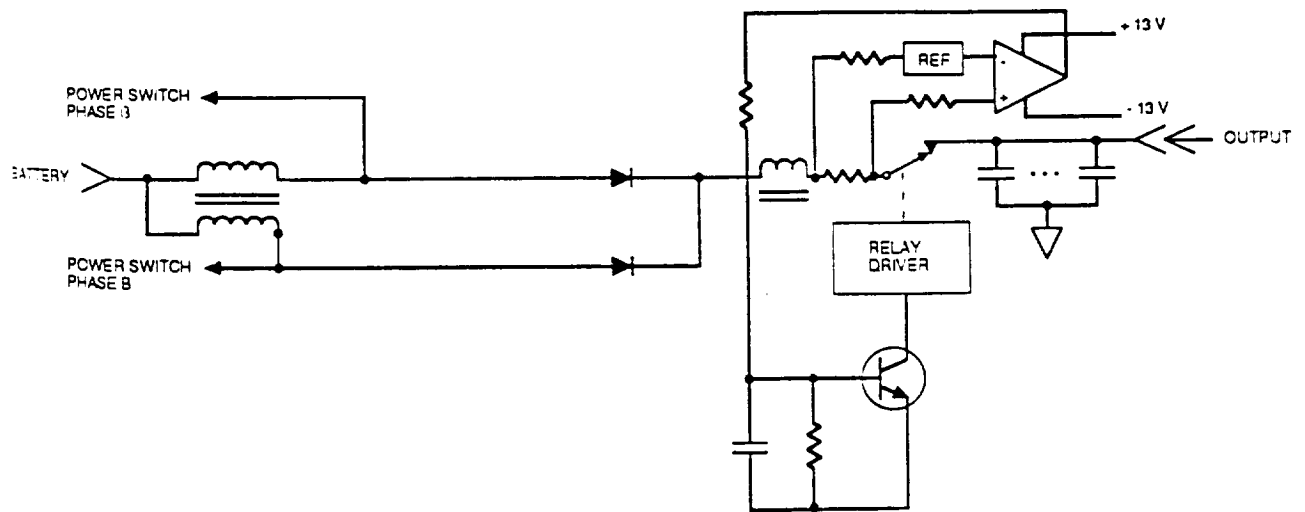


Figure 6.8-23. Output Power Diode Fault Detect Circuit

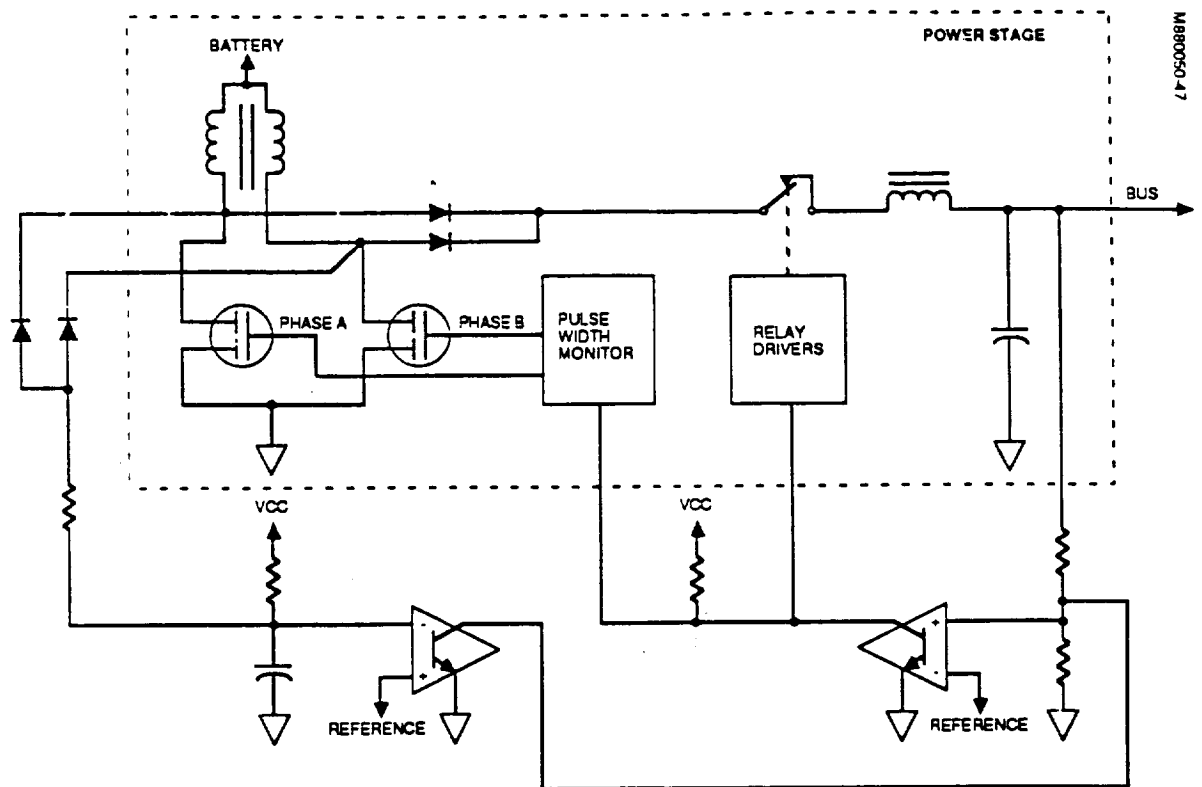


Figure 6.8-24. BDC Overvoltage Protect Circuit

This circuit has two comparators with their outputs connected. If both comparators are high, the output relay will open turning the BDC off. One comparator detects whether the output voltage is excessively high and the other comparator detects whether the push and pull power MOSFETS are functioning. The reason for two detectors is that because there are two BDC strings functional at all times, the string that is generating the high output voltage is the one to disconnect from the bus. If an external source should cause the bus to rise above the BDC set point, then neither string would respond and disconnect from the bus. Both would remain in standby mode for either eclipse or a transient load.

- d. **Relay Contact Protection.** Each power output relay has two contact snubbers: one is connected in reverse parallel of the other to accommodate either of two failure modes. One snubber network functions when the BDC source is greater than the bus as described during overvoltage shutdown. The other snubber network functions when the bus is greater than the BDC source described during the output diode fault shutdown.
- e. **Battery Reconditioning Resistor Circuit.** The battery reconditioning resistor circuit is a resistor network that can be attached across the battery on command through the telemetry and command link.

The 14.0 ohm load is a series parallel combination that can be connected to the positive terminal of the battery through two relays. K1 and K2 are wired to be connected if both relays are either in the upstairs or downstairs position. Each relay can be commanded separately providing redundancy; should one relay fail to respond, then the operational relay can enable to disable the load resistor.

The load is a network of 14.0 ohms for each resistor with four parallel strings with four series resistors in each string. This network provides minimum variation in the discharge current in the event of a single failure of one resistor opening or shorting, with a minimum amount of components.

To enable reconditioning load resistors, both the BATT RECOND A STATUS and BATT RECOND B STATUS must be of the same digital logic, either 0 or 1.

- f. **Telemetry Circuit.** Each BDC string has telemetry outputs to indicate the status of the housekeeping power supply, power bus relay, reconditioning load, spin bus voltage with battery voltage and current.

The battery voltage and spin bus voltage will have two separate resistor networks, each with a single output for redundant analog telemetry monitoring.

BDC A and BDC B each has a current sensor with a single analog output for monitoring each, if both BDC sections are enabled.

- g. **Battery Current Sharing Circuit (see Figure 6.8-25).** The purpose of the battery current sharing circuit is that if two separate BDCs are to regulate a common bus, each BDC will maintain equal battery discharge current. Each BDC compares its discharge current with the other BDC, varying their output voltages slightly within the voltage regulation limits to equalize the battery currents.

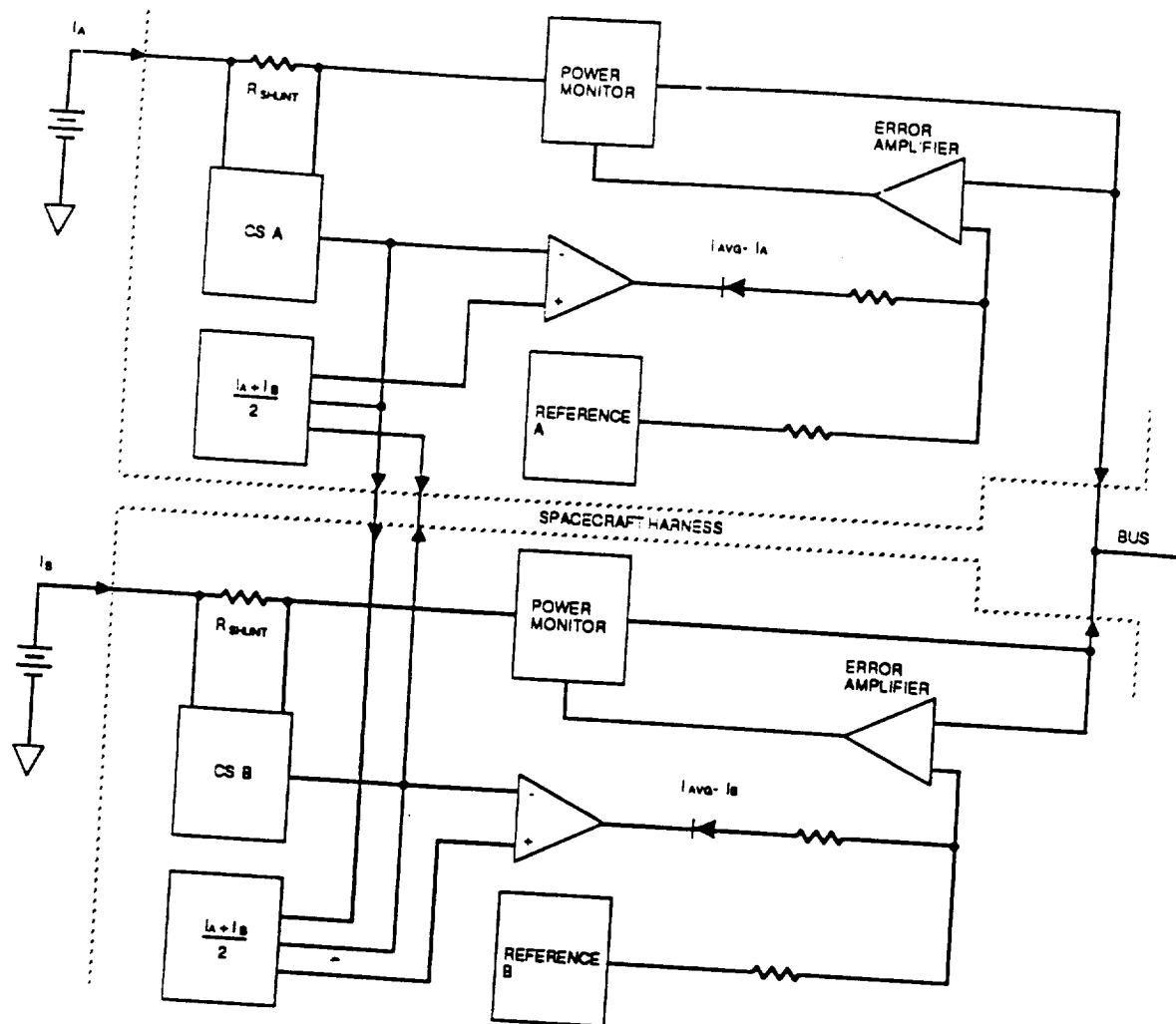


Figure 6.8-25. Battery Current Sharing Circuit

Basically in each BDC there are two amplifiers. One monitors both battery currents which provides an average signal. The second amplifier compares the average signal with its own battery current which provides the differential output signal. With the differential signal having sufficient gain and a very slow slew rate, the BDC's reference voltage is adjusted varying its output regulation voltage and consequently, changing the battery current.

If current sharing is not required, then it will be essential to provide an artificial signal to the averaging amplifier through the spacecraft harness. This signal will be provided so the main control loop can maintain the required regulation.

- h. **Redundancy.** There are two BDCs in one chassis. Each string can meet all requirements to support the bus loads or both can function in parallel.

There is redundant circuitry to provide the above except there are three components that are used equally between the two strings. They are:

- Individually fused capacitors in the input capacitor bank.
- Individually fused capacitors in the output capacitor bank.
- The battery discharge current shunt is common to the input of both strings. Because of the unique construction of the shunt, it is believed it will never fail short. Ten elements in parallel represent the desired resistance. If any one shunt fails open, the resulting resistance is adequate to meet the unit requirements.

6.8.4.2.5 Bus Voltage Limiter. Nine bus voltage limiters, packaged three limiters per assembly, regulate the output voltage of the solar panel. Each limiter is connected to regulate 21 or 22 parallel strings of solar cells that are equally spaced around the circumference of the solar panel. Each limiter acts as a shunt load on 27 of the 45 series cells in the solar cell strings. They will shunt their respective strings current capability between 0 and maximum (i.e., short circuit current) as a function of load and solar panel temperature conditions. The limiters are designed with staggered setpoints so that they will operate in steps and thus reduce power dissipation. This overlap also reduces perturbation on the regulation curve caused by the failure of one limiter (without the overlap, the regulation curve would follow the shape of the unregulated solar panel during a failure). Initial limiter action begins at 29 volts, thereby ensuring full panel capability at the nominal 27 volt operation point. Each tap regulates another 95 mV as the solar panel potential increases, with the final setpoint being 30.615 volts. This ensures that the maximum bus potential is held to less than 31 volts (during natural environments). Each limiter has redundant fuses which are connected in series with the solar panel tap to protect against excessive tap current due to a shorted diode on the solar panel.

Three limiter circuits are packaged together to form a bus voltage limiter unit. The setpoints are staggered so that no two limiter circuits in the same unit will be in the active region at the same time. As a result, the thermal design of the unit is simplified, since the maximum power dissipation will be limited to the maximum power of a single circuit in the active region plus the power of two circuits fully saturated. Each limiter consists of an error amplifier, a driver, and a Darlington output stage. The three parallel npn transistors have 0.2 ohm emitter resistors to force current sharing. These resistors also form part of a current feedback network. The purpose of this current feedback loop is to make the transadmittance of the limiter less dependent on the gain of active devices and, therefore, more predictable at BOL and more stable with age. In addition, as a minor loop, it simplifies the stability problem for the major loop.

Figure 6.8-26 shows a detailed schematic of the limiter circuit. The error amplifier function is performed by Q4A and Q4B. A fraction of the bus voltage obtained from the divider chain R24, R25, and R26 is compared with the voltage of the temperature-compensated reference diode VR2. When the bus voltage rises above the setpoint for this limiter, Q4A turns on. This turns on the Darlington pnp pair Q2 and Q3, which turns on the npn driver transistor Q4, which turns on the Darlington connected shunt translators (the three 2N3599 transistors mounted on the chassis). Regulation is achieved as follows:

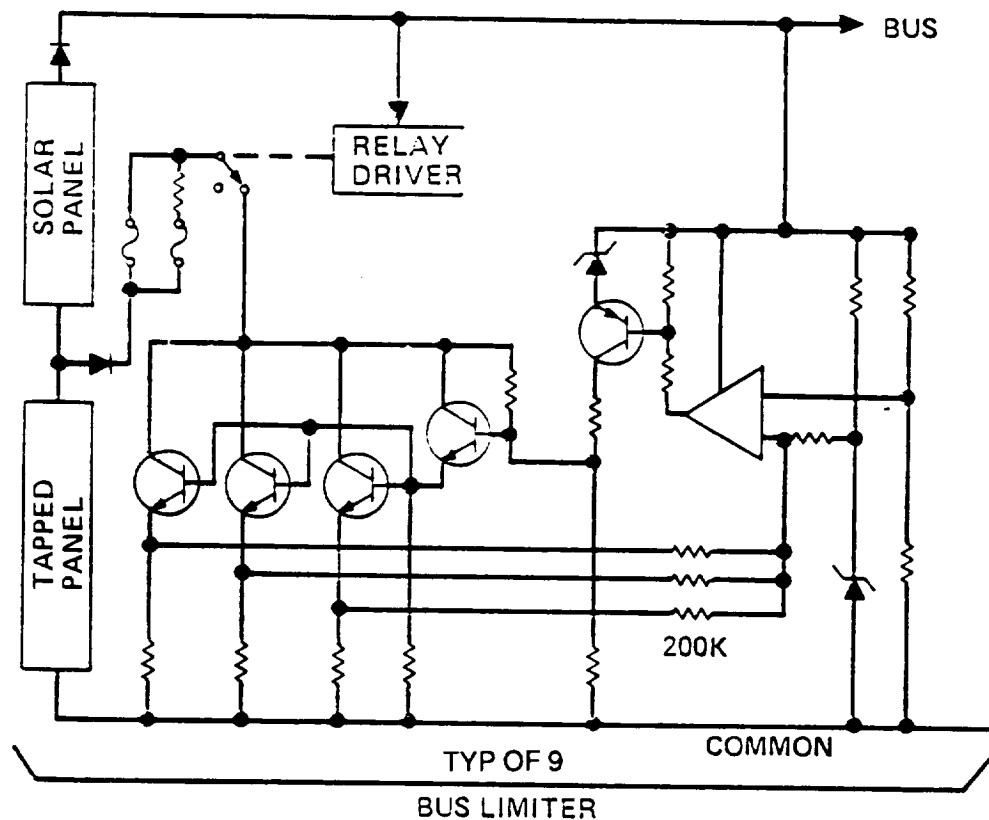


Figure 6.8-26. Bus Voltage Limiter Block Diagram

Chassis-mounted resistors (R7, R8, and R9) in the emitters of the shunt transistors develop a voltage across them proportional to the current being shunted out of the solar panel tap. This current feedback then controls the overall gain of the error amplifier via resistors R3, R4, R5, R12, and R17. If the shunt current becomes too large, then transistor Q1 turns on which shunts drive away from Q4, and turns off the shunt transistors. Telemetry is developed across the divider R1 and R2, clamped to 8.2 volt maximum by VR2 and filtered by C1. The rest of the circuitry is used for biasing and filtering of signals.

The bus voltage limiter package is identical to that used in F-5 (see Figure 6.8-27). It consists of six printed wiring boards (three identical bus limiter circuit boards and three identical relay driver boards). The current sharing resistors, drive transistors, relays and power shunt transistors are mounted on the chassis, which serves as an adequate heat sink for these components (the fuses and some bus filter capacitors are also mounted on the chassis). Two 37 contact Microdot push-pull lock and bayonet coupling connectors with different keying will be mounted as shown in Figure 6.8-27. J1 is used for power interconnections, and J2 contains commands, telemetry, and test points. Both the top and the bottom of the chassis will be open allowing maximum access for assembly, inspection, and repair.

After assembly and initial checkout, the unit will be conformal coated, after which in-process testing will be completed. The unit will then be injected with low-density polyurethane foam, which is easily removed for repairs if necessary. The top cover is bonded onto the unit with silver-filled bonding material to minimize EMI effects. After the foaming process the unit will then undergo acceptance testing.

6.8.4.2.6 Power Distribution Unit. The Power Distribution Unit provides the necessary EMI filters, fusing, and software controlled power switches needed to distribute the 28V bus power in each module (MM and DM) to their respective loads. Two identical sets are located in the RRS, two in the DM and two in the MM. Figure 6.8-28 details the block diagram for the MM, Figure 6.8-29 for the DM. Figure 6.8-30 details a concept for the fusing and software controlled power switching.

The Power Distribution Unit will contain power conditioning circuitry to filter, switch, and fuse 15 branch circuits. The design of the Power Distribution Unit will be self redundant such that a single point failure will not cause a system failure. Table 6.8-4 details the switch, current and software controlled switch requirements for the MM Power Distribution Unit. Table 6.8-5 details this same information for the DM Power Distribution Unit.

Each branch circuit will contain an EMI filter capable of handling the currents specified in the peak current columns of Tables 6.8-6 and 6.8-7. In addition, the filter will be designed to meet the requirements to withstand the 30A clearing current needed to blow the safety fusing. A total of 15 EMI filters will be required.

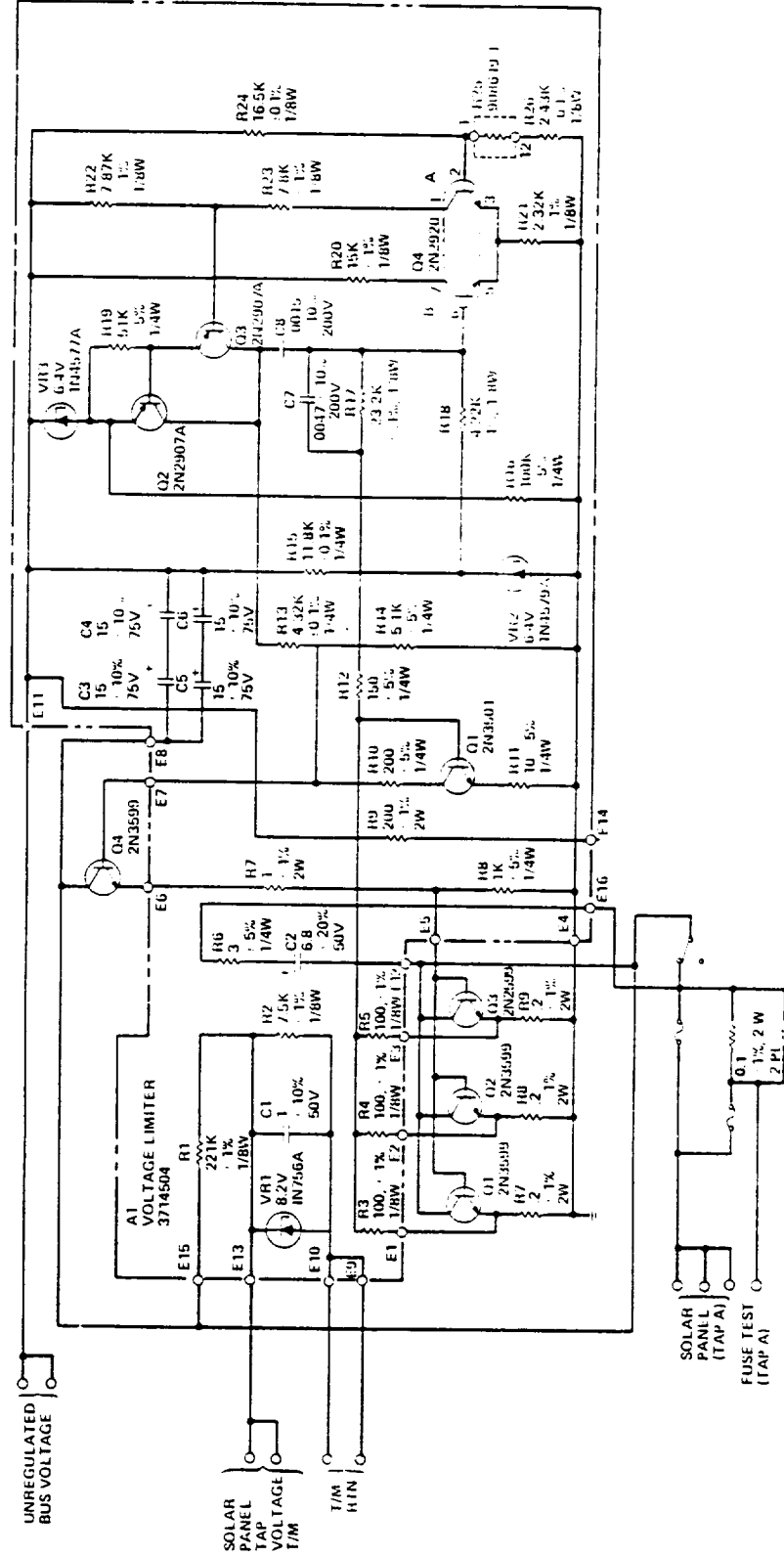
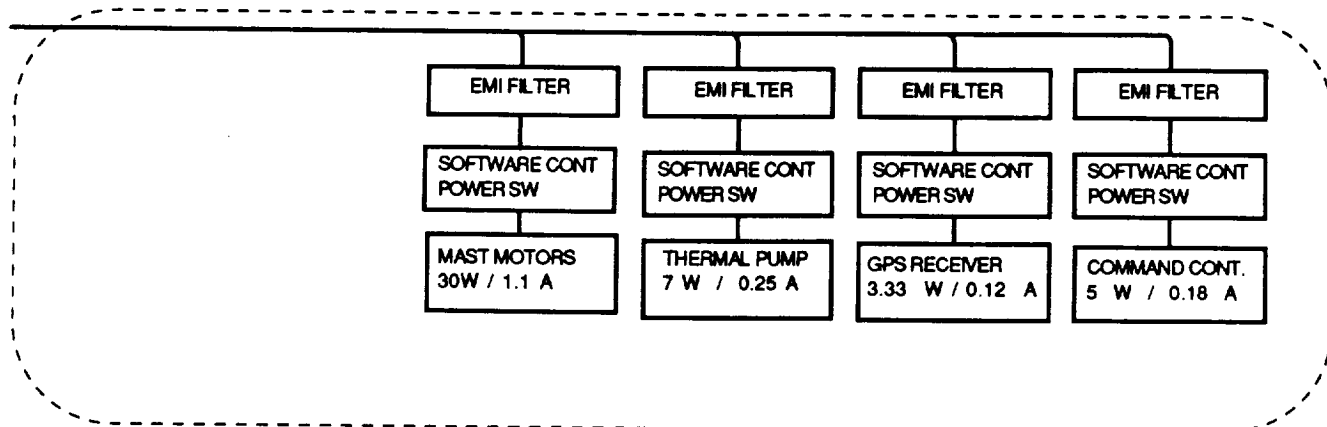


Figure 6.8-27. Detailed Schematic, Bus Voltage Limiter Circuit



MM POWER DISTRIBUTION UNIT

Figure 6.8-28. MM Power Distribution Unit

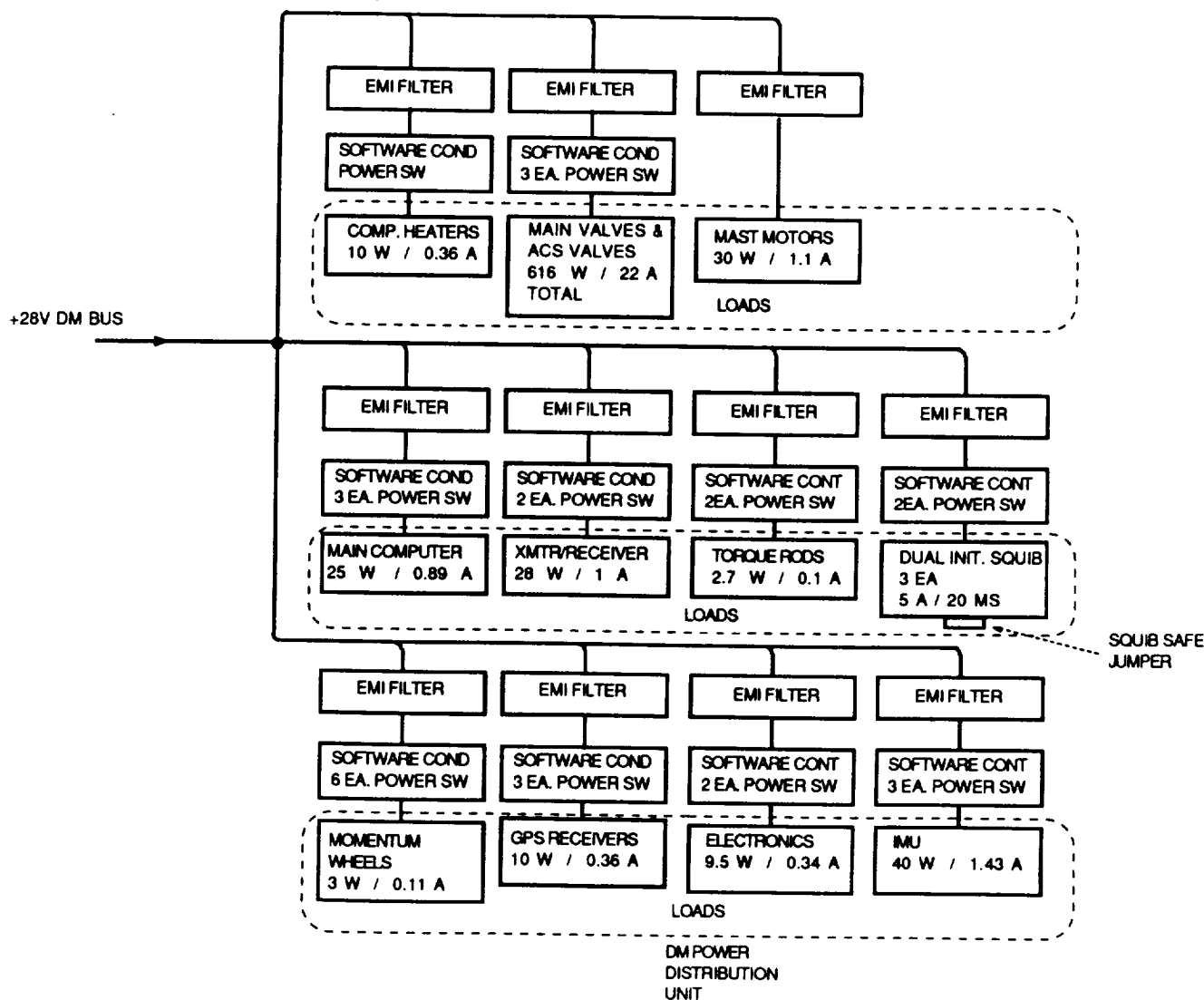


Figure 6.8-29. DM Power Distribution Unit

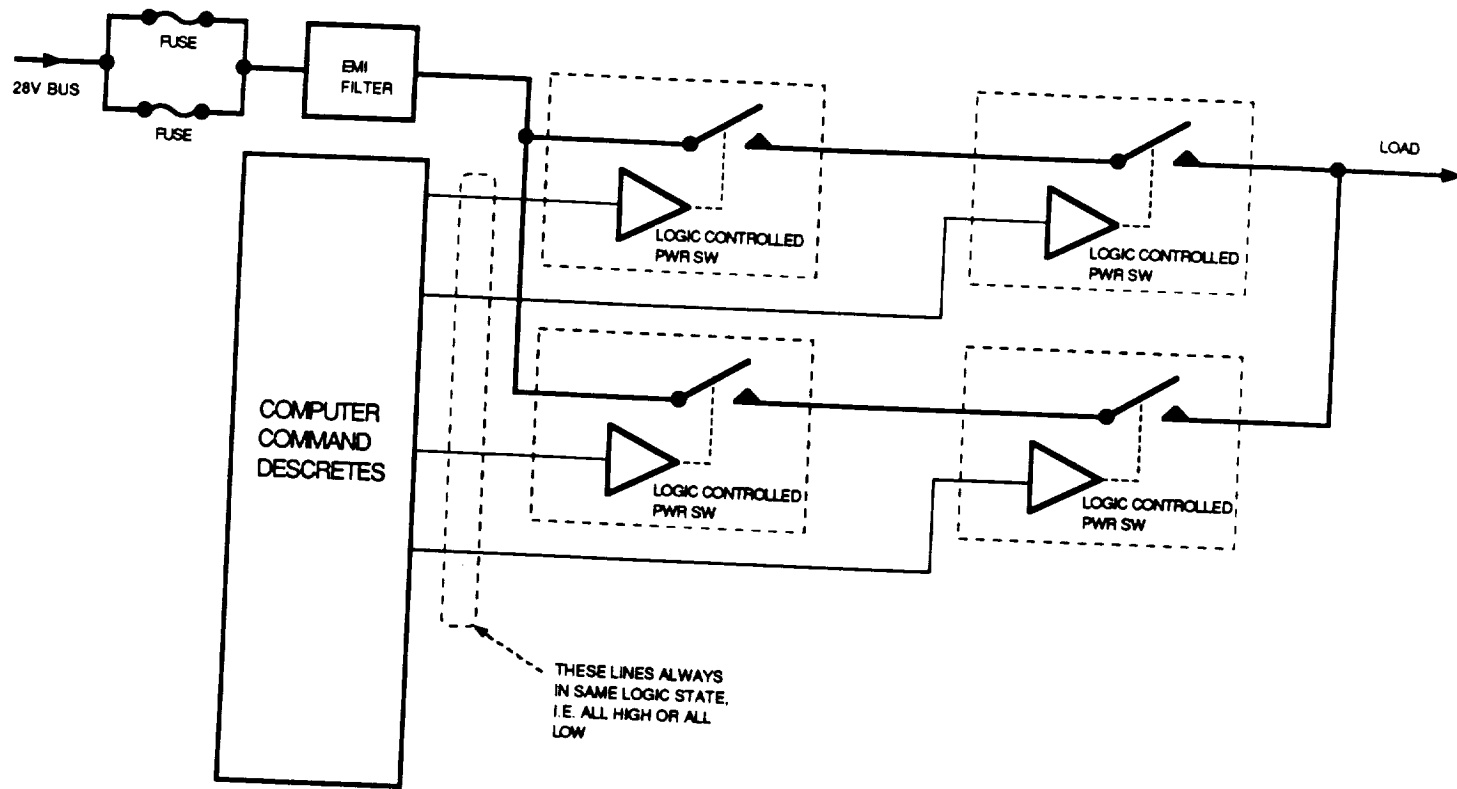


Figure 6.8-30. Concept for Software Controlled Switch

Table 6.8-6. Main Module Power Distribution Switch Requirements

	No. of Switches	Peak Wattage	Peak Current	Peak Current Per SW
S/C Command Cont	1	5	0.18	0.18
S/C GPS Receiver	1	3.33	0.12	0.12
S/C Dual Init Squibs	2	N/A	10	10
S/C Motor Mast	0	45	1.61	0.00
S/C Total No. of Switches	4			

Table 6.8-7. Deployed Module Power Distribution Switch Requirements

	No. of Switches	Peak Wattage	Peak Current	Peak Current Per SW
DM Component Heaters	1	10	0.36	0.36
DM ACS Valves	3	616	22.00	7.33
DM Mast Motors	0	45	1.61	0.00
DM Main Computer	3	25	0.89	0.30
DM XMTR/Receiver	2	28	1.00	0.50
DM Torque Roads	2	2.7	0.10	0.05
DM Momentum WHL	6	3	0.11	0.02
DM GPS Receivers	3	10	0.36	0.12
DM Electronics	2	9.5	0.34	0.16
DM IMU	3	40	1.43	0.48
DM Pyro	2	N/A	10	5
DM Total Number of Switches	27			

Figure 6.8-28 illustrates the power distribution of the MM Power Distribution Unit. Figure 6.8-29 depicts the power distribution of the DM Power Distribution Unit. The 28 V bus is connected to each channel via a redundant set of safety fuses that are sized to allow for clearing in the event of a short, i.e., sized just small enough to allow the battery to clear the fuse in the event of a short. The fuse output is then fed through a self-redundant EMI filter used to prevent interference between power loads to a self-redundant power switch. The current rating for the EMI filter shall be sufficient to allow for the transient flow of a fuse clearing current as well as the load current called out in Tables 6.8-6 and 6.8-7. A self-redundant computer controlled switch is provided. The design of this switch is such that a single short or open will not interfere with proper circuit operation. The circuit actuation is to be provided from four redundant discrete output lines from the computer.

6.8.4.2.7 Tri-Mast Power Transfer Unit. The three Astromasts will provide power, ground and MIL-STD-1553 Avionics Bus interconnection between the MM and DM. The existing copper beryllium retraction ribbons will transfer power between the MM and DM. This allows the solar cells in the Deployed Module to charge the Main Module's batteries, the transfer of GSE power to reach the MM, and creates a triple redundant battery system. The use of 3-phase 220 V - 20 kHz power transmission was chosen to meet the following objectives:

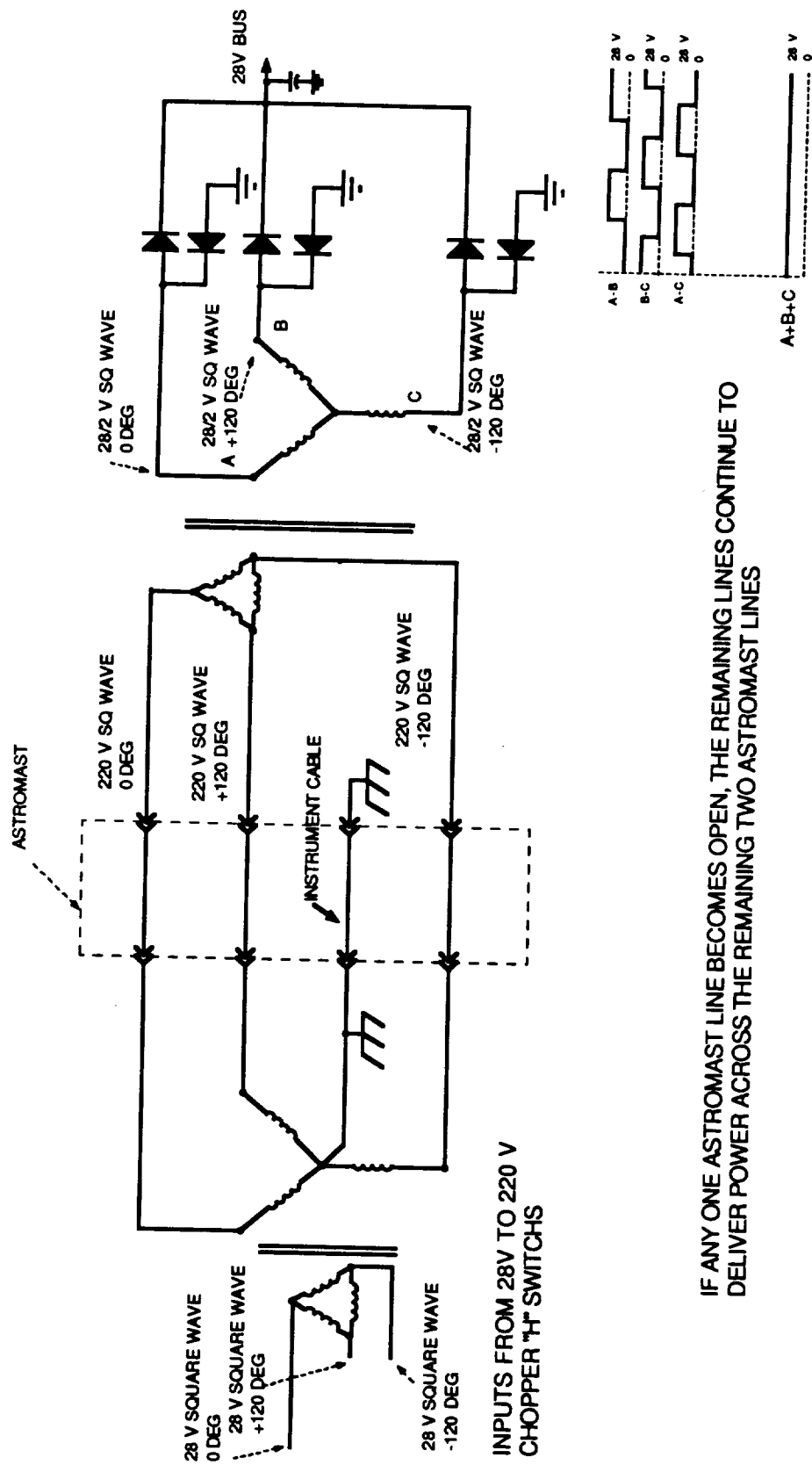
- a. AC transmission prevents interaction between the Earth's magnetic field and cable current from producing any force on the RRS.

- b. Three-phase transmission provides fault protection in the event of a electrical break in any of the Astromast power paths. In addition, it reduces the size of the filtering components needed to convert AC to +28 V DC.
- c. A 220 V transmission voltage was chosen to ensure that the worst case current flow through the Astromast cables will be less than 1 ampere. This will ease the voltage drop due to cable resistance and cable currents through the Astromast. In addition, this will allow downsizing of the Astromast sliprings.
- d. The 20 kHz frequency was chosen to keep component size down. Smaller core sizes and smaller filter capacitors will be required.

Redundant software controlled 28 V to 3-phase 220 V - 20 kHz choppers provide a means of transferring power via the Astromasts. The chopper circuit shall be actuated by four discrete lines from the computer. In the enabled state the output on each of the 3-phase output lines will be a 20 kHz square wave having a peak voltage of 220 V. In the disabled state, the output will be in an open state. The chopper circuit will be capable of supplying a 3-phase AC output having a 200 V ± 4 V square wave output at a maximum output current of ± 2.1 A. The rise and fall time for the square wave output shall be 5 microseconds ± 1 microsecond. The MM output shall be connected in the "Y" configuration, and the DM connected in the delta configuration with the common line connected via instrumentation cable ground return.

The design of the chopper output circuit will be such that a failure of any one device shall not cause the failure of the chopper. A TTL logic low on any of three of the four discrete input lines will cause the chopper to be in the actuated mode, i.e., provides 3-phase 200 V at 20 kHz. A TTL logic high on any three of the four input discrete input lines will cause the chopper to be in the third state, high impedance mode. In this mode, the output impedance will be at least 100 K ohms.

Figure 6.8-31 illustrates how the use of 3-phase power provides circuit protection in the event of an opening on one of the three Astromast cables. Under nonfault conditions, the chopper output generates 3-phase 28 V peak square wave drive for the "delta" to "Y" step-up transformer at the left side of this figure. This transformer steps the 28 V peak drive to a 220 V peak square wave which is passed through the Astromast sliprings and cables. At the right side of this figure, the voltage is applied to the "delta" to "Y" step-down transformer where the voltage is stepped down to 3-phase 28 V peak square waves. The peak-to-peak voltage at each tap of the right hand transformer will be 28 V.



IF ANY ONE ASTROMAST LINE BECOMES OPEN, THE REMAINING LINES CONTINUE TO DELIVER POWER ACROSS THE REMAINING TWO ASTROMAST LINES

Figure 6.8-31. Schematic Diagram of Astromast Power Transmission

Redundant software controlled 3-phase 220 V - 20 kHz to 28 V DC converters provide a means of transferring power from the Astromasts to the 28 V bus in the MM or the DM. The 3-phase 220 V 20 kHz to 28 V DC converters will be actuated by quad discrete lines from the command computer. In the enabled state, the output on each of the 3-phase output lines will be converted from the 20 kHz square wave having a peak voltage of 200 V to 28 V and delivered to the 28 V bus. In the disabled state, the output of the 3-phase AC to 28 V DC converter will be in an open state.

The 3-phase to 28 V Converter circuit will be capable of supplying 28 V DC at 30 amps to the 28 V bus and will be designed such that a failure of any one device will not cause the failure of the chopper. A TTL logic low on any of three input of the four discrete input lines will cause the chopper to be in the actuated mode, i.e., convert the 3-phase 200 V/20 kHz power to 28 V power bus. A TTL logic high on any three of the four input discrete input lines will cause the chopper to be in the third state, high impedance mode. In this mode, the 3-phase to 28 V bus power output impedance will be at least 100 K ohms.

6.8.5 Command and Control

The external control for the power subsystem process will be provided by redundant processors housed in the GNC computer in each module. The external controls include both manual configuration/process control via ground command and automatic load shed operations. Although the load shed priority is vehicle first and payload second, the independent module power operations allow the DM to operate in a vehicle safe mode with the MM performing internal load shed operations to preserve payload integrity on battery operation. The GNC computers provide full visibility into the load shed operation and full ground override capability.

6.8.6 Test

Special testing is required for the power transmission system between the deployed and main modules of the vehicle. Verification of operation and determining efficiency in normal and failure modes is required.

6.8.7 Manufacture

The power system shall be manufactured from off-the-shelf components. Assembly of the power subsystem consists of installation of the components (batteries, electronics, and solar array

panels), wiring the components into the harness, and then performing continuity and performance checks and testing. No special manufacturing processes are required.

6.8.8 Refurbishment

Refurbishment of the power system is performed after separation of the two halves of the deployed module. Battery inspection and recharge, performance check of all charge and discharge controllers, inspection of the solar cell strings, and a full functional test will be performed. Inspection procedures shall include internal (for electronic boxes) and external (for batteries and boxes). Replacement of faulty assemblies and solar array panels shall be performed if faulty. Repair would be performed offline at the vendor facility.

6.9 Thermal Control Subsystem (TCS)

6.9.1 Operations

6.9.1.1 Prelaunch. The only cooling will be from the pad air conditioning flow around the vehicle inside of the launch vehicle adaptor. The thermal subsystem must maintain the payload module within operational thermal limits for an undefined time using the pad air conditioning flow around the heat shield for thermal rejection.

6.9.1.2 Orbital Flight. The thermal subsystem must operate on internal capacity from loss of pad air conditioning just prior to lift-off until the vehicle is separated from the launch vehicle adaptor. During fractional gravity operations, no rotation can be used for thermal balance other than that provided by the gravitational rotation. Rotation may be used during microgravity operations, but cannot cause forces beyond the overall microgravity requirements.

6.9.1.3 De-Orbit and Reentry. The thermal subsystem must be isolated from reentry heating and operate on internal capacity from just prior to the initial de-orbit thruster firings until one hour after landing.

6.9.1.4 Recovery. The thermal subsystem must be able to operate indefinitely in the presence of heat shield and local environmental heat soak for an indefinite period of time when connected to external coolant support.

6.9.2 Requirements

The overall requirements of the RRS TCS are summarized in Table 6.9-1. These requirements and the Design Reference Missions (DRMs) defined early in the study, and shown in Table 6.9-2, were the only top-level groundrules and assumptions used in the thermal trade system studies.

6.9.3 Trade Study Summary

The purpose of the RRS Thermal Control Trade Study was to assess the design of the TCSs necessary to maintain the temperatures of applicable RRS hardware within prescribed limits during on-orbit operations. Specifically, the report describes the efforts to define and verify TCS designs for maintaining the satellite's PM environmental control system heat exchanger, propellant, and water supply within required temperature limits.

Table 6.9-1. Thermal Subsystem Requirements

• ORBITAL FLIGHT
- Initial
- Dissipate 207 Watts in Stowed Position
- Microgravity:
- Dissipate
• MM 131 Watts
• EM 74 Watts
- Artificial Gravity:
- Dissipate
• MM 131 Watts
• EM 74 Watts
• Keep Propellant Tanks Above 275° K Is Stressing Case
• S/C in Deployed Configuration in Flat Spin at 7 RPM in Plane of Orbit at Summer Solstice
• RECOVERY
- De-Orbit Phase:
- Same as Initial
- Reentry Phase:
- 168 Watts in Stowed Configuration With Thermal Soak in From Skin
- Heat of Fusion Thermal Storage
- Terminal and Post Recovery
- Same as Reentry

Table 6.9-2. RRS Design Reference Missions

Definition Parameter	Design Reference Mission Set				
	DRM-1	DRM-2	DRM-3	DRM-4	DRM-5
Character	Land Recovery	High Altitude	High Inclination	Integer Orbits	Water Recovery
Inclination	33.83°	33.83°	98°	35.65°	28.5°
Orbit Type	Circular	Circular	Circular, Near-Integer	Circular, Integer	Circular
Orbit Altitude	350 km (189 nm)	900 km (486 nm)	897 km (484 nm)	479 km (259 nm)	350 km (189 nm)
Launch Site	Eastern Test Range (ETR)	ETR	WTR	ETR	ETR
Recovery Site	White Sands Missile Range (WSMR)	WSMR	WSMR	WSMR	Water (ETR, Gulf of Mexico, WTR)

A review of the Ames RRS design study and a preliminary evaluation of the SAIC RRS configuration indicated that a liquid coolant loop, in conjunction with a space radiator, was a viable thermal control concept for the ECLSS heat exchanger. Ethylene glycol was identified as an appropriate coolant, and the vehicle aeroshell was determined to have sufficient radiative capacity for dissipating the anticipated PM heat load.

A thermal-fluid response assessment of the fluid network and radiator was performed considering the proposed RRS orbits and vehicle orientations that subjected the aeroshell to the most thermally stressing environments. The analysis indicated that eight, 0.889 diameter coolant tubes, in conjunction with a coating of low absorptivity, high emissivity white paint on the aeroshell's surface, were adequate space radiator design measures for effectively cooling the ECLSS heat exchanger. The estimated power requirement for the subsystem is a continuous 7.4 watts and the projected mass is 38.4 lbs (17.4 kg).

A conservative assessment of the on-orbit thermal response of the RRS Extended Module indicated that the propellant housed within its interior should remain between 280 and 295 K for all anticipated RRS missions. Shielding the propellant tanks from direct extraterrestrial exposure and coating the exterior surfaces of the module's forward and aft covers with a high absorptivity black paint will maintain the propellant above its minimum allowable of 273 K. The thermal assessment of the Extended Module also indicated that an 0.14 rps vehicle axial rotation is necessary to alleviate excessive cell temperatures experienced by the module's exterior solar array. The rotation induces accelerations below the maximum allowable of 10^{-5} g.

The PM water supply tanks will experience radiant exchange primarily with the inner surface of the aeroshell substructure and the external surface of the PM cannister. Since the temperatures of these surfaces will fall between 281 and 291 K, which is above the 273 K minimum allowable, it was concluded that no active heating of the water will be necessary.

6.9.4 Baseline Design

This section documents the design and assessment work performed in defining the on-orbit TCS requirements for the RRS. Specifically, it describes the hardware and design measures necessary for maintaining the PM Environmental Control Life Support System (ECLSS) heat exchanger, the hydrazine propellant, and PM water supply within their required temperature limits.

6.9.4.1 Payload Module ECLSS Heat Exchanger Thermal Control Subsystem

6.9.4.1.1 Introduction. The RRV contains a complete ECLSS capable of providing the required atmosphere for sustaining 18 rodents, and a suite of related electronics and hardware, for up to 60 days. Within the PM, the air supply's humidity, chemical content, and temperature are monitored and adjusted continually. The humidity and content are controlled by subsystems completely internal to the PM. The temperature is maintained by regulating the flow of air through the ECLSS heat exchanger.

During satellite launch, ascent, reentry, and recovery periods, the heat exchanger functions autonomously to cool the PM airflow through the incorporation of a fusible wax within its construction. The wax in the PM undergoes a solid/liquid phase transition at 278.8 K and the quantity contained the heat exchanger has been sized to provide 1055 kilojoules of thermal storage. This translates into approximately 3 hours of independent cooling capability. A complete description of the ECLSS heat exchanger design is provided in the SAIC RRS Payload Module Trade Study. While the satellite is in orbit, however, heat removal and consequent dissipation must be provided by a TCS coupled to the heat exchanger, but external to the PM.

The heat generated within the PM is attributable to the rodents and electronics/hardware which produce, on average, 45 and 75 watts, respectively. The external TCS must, therefore, be capable of transporting and dissipating approximately 120 W of heat. In addition, the minimum anticipated PM air temperature is 291 K, which requires the TCS to maintain the PM ECLSS heat exchanger at or below this temperature.

The Ames Reusable Reentry Satellite Design Study, confronted with a similar set of capability requirements, went a long way in identifying the character of a potential TCS. Two preliminary observations were instrumental in shaping the basic concept and defining the final TCS design. First, the RRS concept places maximum emphasis on the reusability of onboard subsystems and, therefore, an expendable TCS was not permissible. Secondly, the satellite's geometry, in conjunction with the transient nature of the PM heat loads, did not bode well for passive TCSs. Therefore, it was concluded that an integrated, active TCS, consisting of a fluid network coupled with a space radiator, was the most efficient alternative. The SAIC RRS configuration is no exception to the above considerations, and this study addressed the design and corresponding assessment of a fluid network/space radiator TCS concept.

The concept for the heat ECLSS exchanger was developed based on the aeroshell as a space radiator.

An assessment of the Extended Module's on-orbit thermal response indicated that a vehicle axial rotation rate of 0.14 rpm was necessary during the microgravity mode of operation. This requirement was imposed to alleviate the excessive temperatures experienced by the sun-facing portion of the module's solar array that resulted in a significant degradation in cell power production efficiency. Polar orbits, such as DRM-3, in conjunction with the microgravity vehicle orientation (no rotation in the orbital plane), resulted in the most severe temperature excursions. An axial rotation rate of 0.14 rpm was found to effectively smooth the highly nonuniform heating about the module's circumference, consequently lowering the bulk temperature of the power producing portion of the solar array.

This axial rotation rate was found to induce an acceleration of 0.8×10^{-5} g at a radius of 35.6 cm, which is the maximum radius of the PM rodent cages. This acceleration falls below the maximum allowable level of 10^{-5} g set forth in the RRS System Design Study Statement of Work, Section 4.2.5.2 and is therefore acceptable.

The resulting subsystem is presented in Figure 6.9-1. Coolant is pumped through the ECLSS heat exchanger and then distributed into one of two sets of cooling tubes, each spanning 180° sections of opposing aeroshell circumference. The cooling tubes are integrated directly into aeroshell's aluminum substructure. During transit, heat is transferred from the coolant to the aeroshell backface and then conducted to the aeroshell surface where it is radiated to the environment. The cooled fluid streams are then merged and pass through a reservoir before returning to the heat exchanger.

A schematic of the complete ECLSS heat exchanger TCS is presented in Figure 6.9-2. Valves are incorporated to permit the network to interface with a ground support cooling system during the RRS prelaunch period. Additional valves are included to permit the coolant loop to bypass the ECLSS heat exchanger and/or space radiator and thereby provide some degree of coolant temperature control. An auxiliary pump serves as a backup in the event of primary pump dysfunction or failure. A thermal control unit interfaces with the various valves providing fluid network flow control as dictated by the environmental control unit processor.

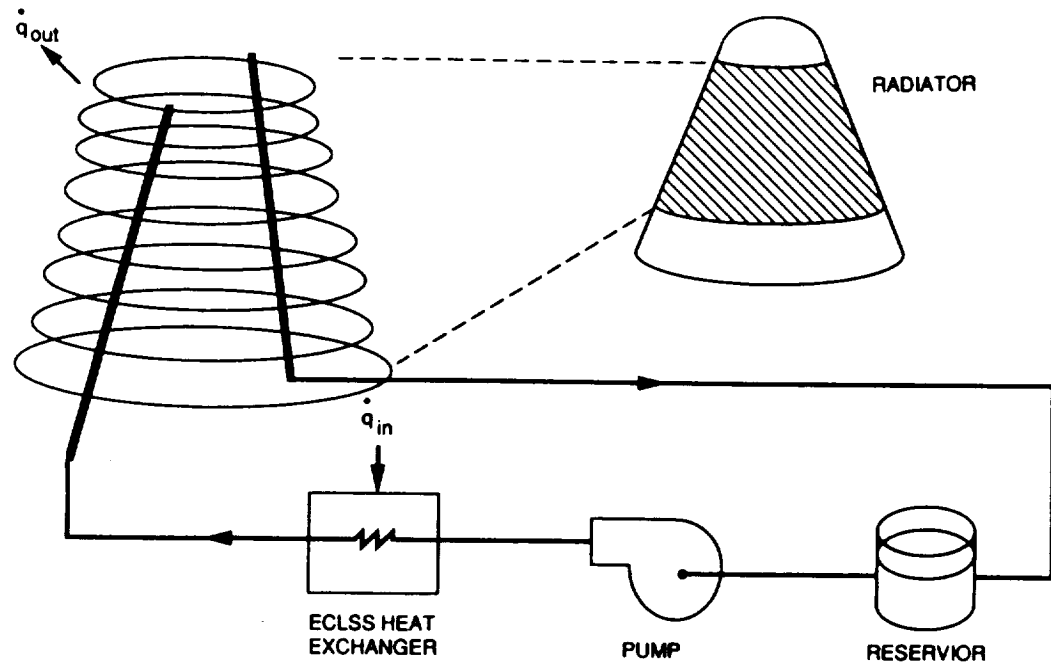


Figure 6.9-1. Payload Module ECLSS Heat Exchanger TCS Coolant Loop and Space Radiator Concept

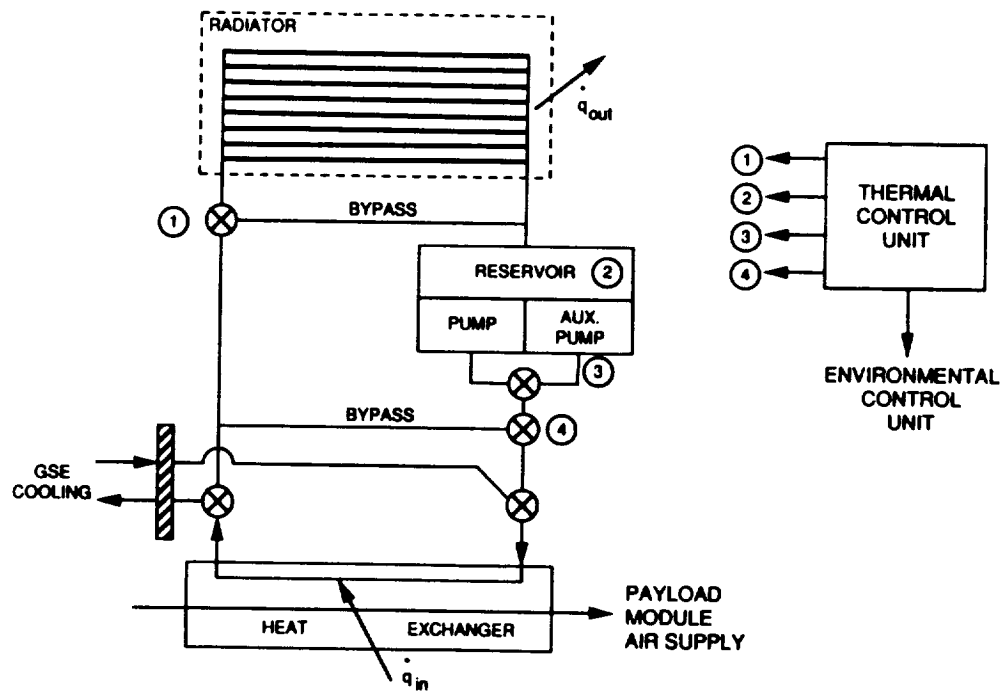


Figure 6.9-2. Payload Module ECLSS Heat Exchanger Thermal Control Subsystem

Having arrived at a general TCS concept, the design issue of identifying the appropriate coolant was addressed. For this concept, it was decided that a low system operating pressure of somewhere between 10 to 20 psia would provide a good balance of safety, cost, complexity, thermal efficiency, power requirements, and weight. At these pressures and anticipated ECLSS heat exchanger temperatures ranging between 270 to 300 K, a single-phase system using a liquid coolant such as ethylene glycol appeared appropriate. One inherent disadvantage, however, with using this coolant is that its viscosity displays a strong dependence on temperature. As a result, the viscosity becomes restrictively high as the temperature approaches its freezing point of 258 K. Therefore, in addition to a maximum allowable coolant temperature of 291 K imposed by the PM payload, a minimum allowable coolant temperature of 273 K was artificially imposed to prevent the viscosity of the glycol from becoming unacceptably large.

6.9.4.1.2 Modeling Tool. To assess the performance of the proposed TCS concept, a modeling tool capable of handling in depth thermal response of multi-material structures, coupled with the thermal-fluid response of a coolant network, was required. Such a capability is achieved in the SAIC-developed Hypersonic-Vehicle Structural, Thermal, and Acoustic Management (HYSTAM) computer code. HYSTAM was originally developed to assess the performance of candidate cooling concepts for hypersonic vehicles. The code consists of three coupled modules that predict aeroheating and acoustics loads, structure thermal response, and cooling network thermal-fluid response. For the application at hand, the aeroheating and acoustics module was replaced by a module that predicted the solar insolation, Earth-reflected solar insolation, and Earth IR flux on an arbitrarily oriented surface in Earth orbit. Included within the routine were algorithms that tracked the orientation of each radiator panel as a function of vehicle rotations and orientation relative to the orbital plane.

6.9.4.1.3 Model. The philosophy adopted in this assessment was to model, as thoroughly as possible, the thermal-fluid response of the coolant, the transport of heat through the aeroshell thickness, and the consequent radiant heat balance of the aeroshell surface with the extraterrestrial environment. The conceptual construction began with the subdivision of the aeroshell into 12 equivalent rectangular panels, approximately 80 by 46 cm on a side, as shown in Figure 6.9-3. Each panel represented 30° of vehicle circumference, and the combined areas matched that of the actual conic's midsection minus the aft skirt and nose cap. Each panel consisted of a 2.286 cm lay-up of ESM (the aeroshell thermal protection material) over a 0.145 cm substrate of aluminum into which coolant passages were integrated as shown in Figure 6.9-4. This was an approximation of the actual substrate that will be aluminum honeycomb with aluminum coolant tubes bonded to the inner surface of the outboard facing sheet. However, the mass of the solid aluminum plate

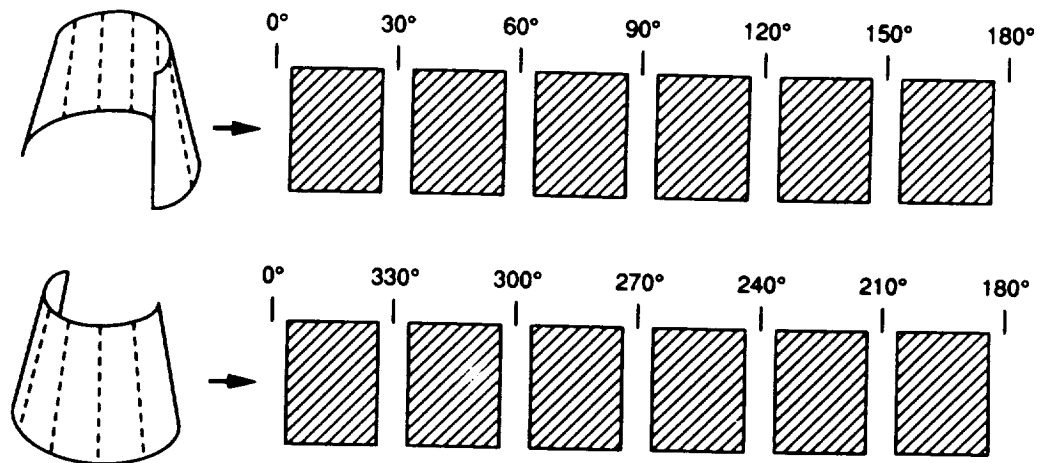


Figure 6.9-3. Subdivision of Aeroshell Radiator Into 12 Equivalent Panels

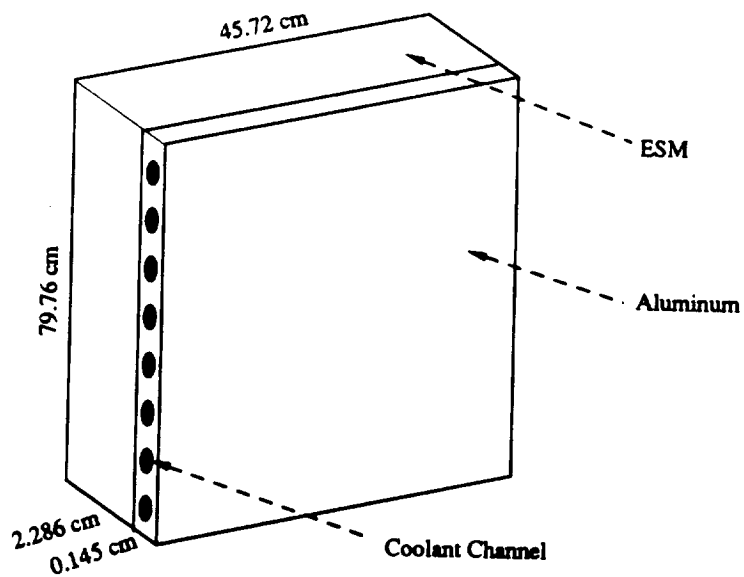


Figure 6.9-4. Detail of Aeroshell Radiator Panel Model

modeled replicated the anticipated mass of the actual substrate. Although the number and size of the coolant tubes were arrived at iteratively as part of the assessment process, it is noted at this time that the TCS design requires eight coolant tubes, 0.899 cm in diameter, spaced 5 cm apart.

The aeroshell ESM surface was coated with a low absorptivity white paint to enhance the dissipative efficiency of the system. A solar absorptance of 0.2 and a hemispherical emissivity of 0.9 were used in the assessment.

Following the HYSTAM modeling approach, a fluid network model of the cooling loop and its various components was constructed. A schematic of the network and a list of the component descriptions are presented in Figure 6.9-5 and Table 6.9-3, respectively. The network model consisted of a 1 liter reservoir, a pump, the ECLSS heat exchanger, an inlet manifold which branched the flow, two sets of six panels representing 180° of vehicle circumference, a collection manifold which merged the flow, and 3 meters of miscellaneous tubing. Loss coefficients were applied to the heat exchanger and both manifolds. The pump characteristic curve used in the analysis, which was postulated, is presented in Figure 6.9-6.

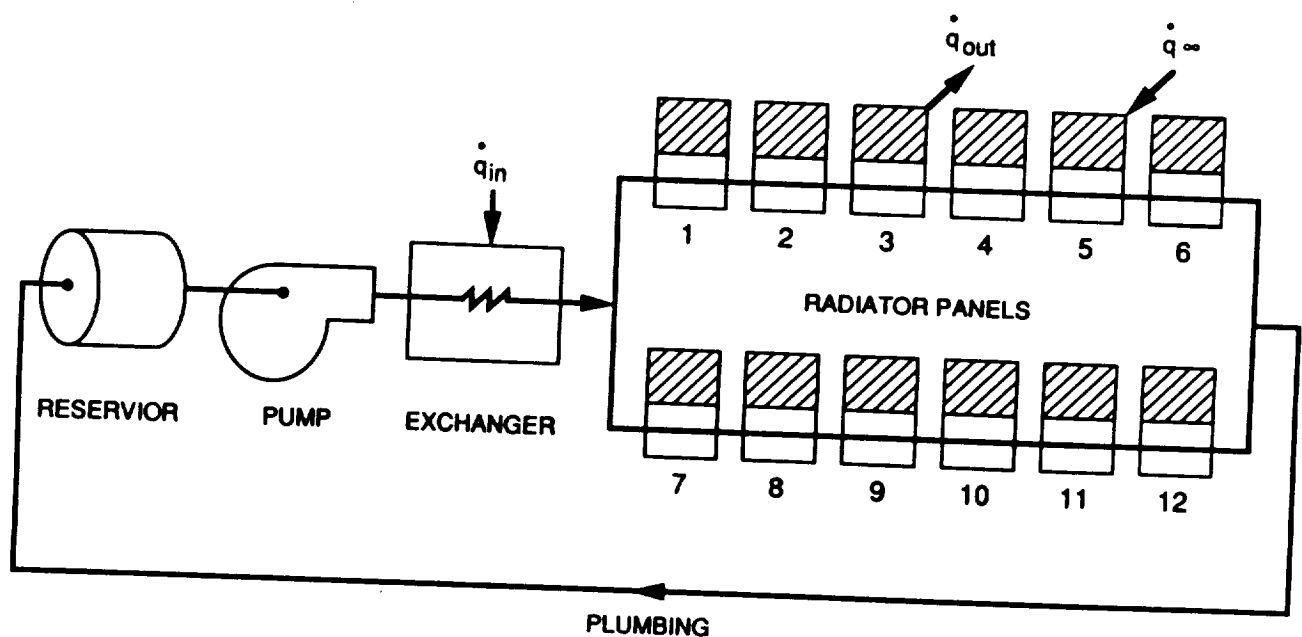


Figure 6.9-5. ECLSS Heat Exchanger TCS Coolant Loop Fluid Network Model

Table 6.9-3. ECLSS Heat Exchanger TCS Coolant Loop Fluid Network Components

Reservoir	Volume Pressure Material	= 0.001 m ³ = 14.7 psia = Aluminum
Pump	See Figure 5-8	
Heat Exchanger	120 W continuous	
Radiator Panel (see Figure 5-6)	Surface: Backface:	$\epsilon_H = 0.9$ $\alpha_S = 0.2$ Adiabatic
Coolant Tube (see Figure 5-6)	Number Diameter Material	= 8 / panel = 0.889 cm = Aluminum
Plumbing (assorted tubing)	Total Length Diameter Material	= 304.8 cm = 1.27 cm = Aluminum
Coolant	Ethylene Glycol	

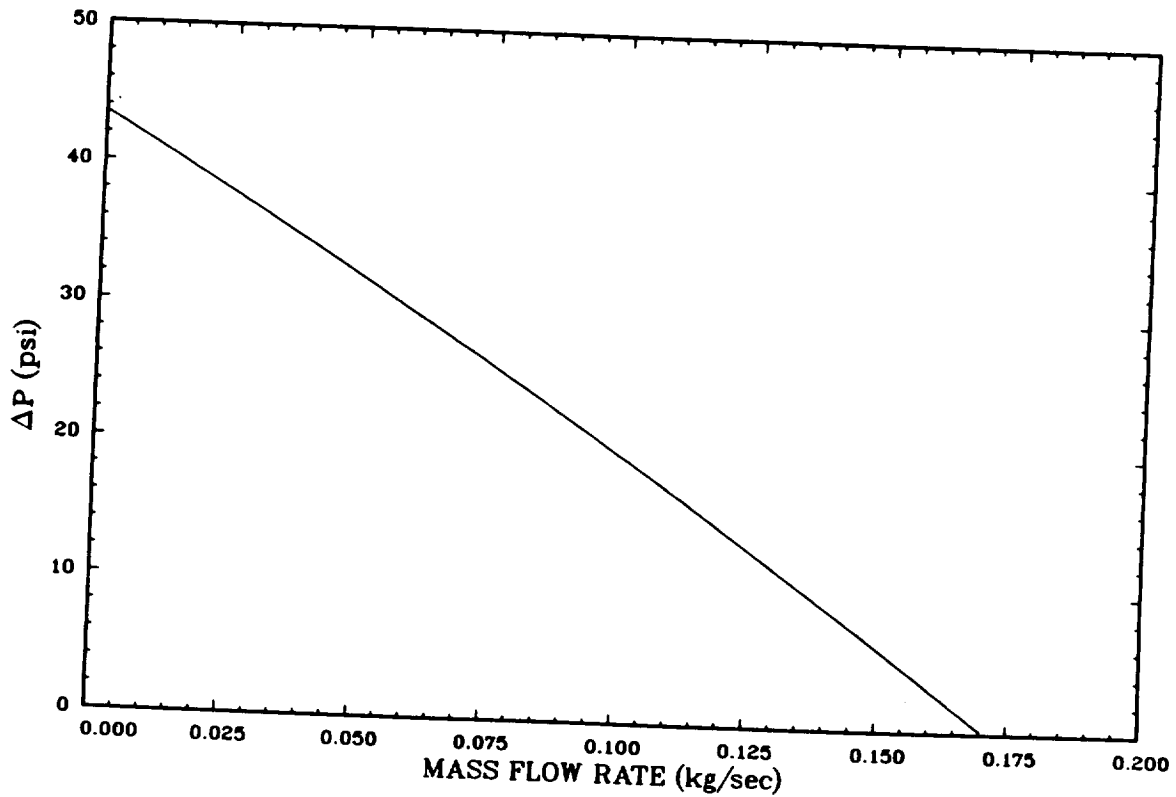


Figure 6.9-6. ECLSS Heat Exchanger TCS Pump Characteristic Curve

6.9.4.1.4 Assumptions. In developing the TCS concept model, several assumptions and simplifications were necessary to adhere to the multi-one-dimensional modeling limitation in HYSTAM. The surface area of each aeroshell radiator panel was modeled exactly; however, the additional surface area provided by the aft skirt and nose sections was neglected. The spherical geometry of the nosecap and the complex radiant heating and exchange experienced by the skirt's backface present situations HYSTAM could not model. Intuitively, one may surmise that the additional area will enhance the overall efficiency of the radiator.

In the model, the backface of the aeroshell substructure was treated as a perfectly adiabatic boundary. A low density insulation will cover the substructure surface to minimize heat transfer with vehicle's internals, but some radiant exchange will still take place. As noted above, HYSTAM is not configured to model the complex radiant exchange between the insulation and the satellite's internals. However, the temperature differences between the various internal surfaces and the substructure insulation will be small and, therefore, the consequent radiant transfer of heat should be negligible.

With regard to the ECLSS heat exchanger, no attempt was made to model the time variant nature of the heat load or the transport of heat from the incoming PM air to the coolant. For this analysis, the heat exchanger control volume served as a continuous 120 W source term in the fluid's thermal energy balance.

Lastly, since the HYSTAM approach is multi-one-dimensional, no structural thermal communication was permitted between panels. However, the heating loads about the aeroshell's circumference will be essentially uniform because of the vehicle's constant axial rotation. This will result in a fairly uniform temperature distribution, consequently negating circumferential conduction.

6.9.4.1.5 Results. Prior to exercising HYSTAM, a preliminary set of computations was conducted to ascertain which of the 30 possible DRM/vehicle orientation/season combinations (five DRMs, three seasons, two vehicle orientations) subjected the aeroshell's surface to the most stressing thermal environments. The goal was to economize the required number of HYSTAM runs by concentrating on the scenarios that produced the highest and lowest aeroshell heating rates and, therefore, the hottest and coldest aeroshell surface temperatures. The orbital geometry and vehicle orientation and rotation modes considered in the analysis are portrayed in Figure 6.9-7. The same orbital heat loads model used for the aft cover and aeroshell heat balance computations described previously was used. For this investigation, however, surface reradiation was not computed.

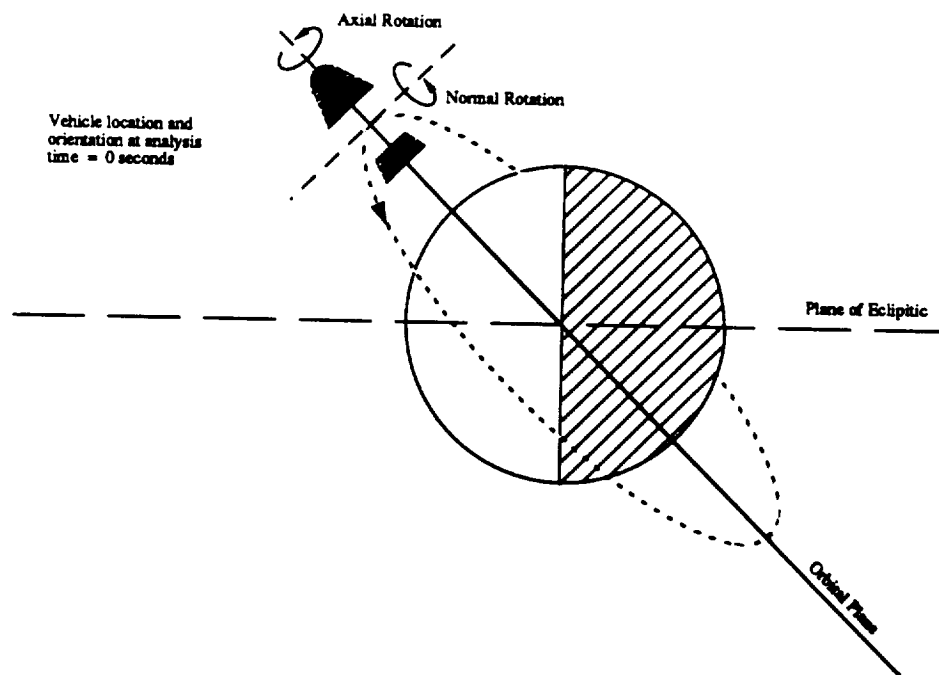


Figure 6.9-7. Orbital Geometry and Vehicle Orientation and Rotation Modes Considered in Total Absorbed Flux Computations

For the analysis, total absorbed flux computations were performed for DRMs 1 through 5, considering both normal rotation (7 rpm, see Figure 6-9-7) and microgravity vehicle orientations with a constant axial rotation rate of 0.14 rpm. Orbit inclination angle relative to the ecliptic was adjusted to account for Vernal/Autumnal Equinox, Summer Solstice, and Winter Solstice seasonal variations. The analysis location corresponded to the aeroshell's 15° circumferential station which translated to the center of panel 1 in the coolant loop fluid network model.

Based on the results of this preliminary investigation for the 30 possible combinations, the average absorbed flux at the aeroshell's surface during one orbital period ranged between 76 and 103 W/m². These extremes corresponded to the DRM-5, Summer Solstice and the DRM-3, Vernal/Autumnal Equinox orbits with the vehicle in a 7 rpm normal rotation mode. Table 6.9-4 depicts the parameters that define these two orbits. The total absorbed flux witnessed by aeroshell panel 1, as a function of time for these two orbits, is presented in Figure 6.9-8.

Table 6.9-4. DRM-3, Vernal/Autumnal Equinox and DRM-5, Summer Solstice Orbit Definitions

Designation	DRM-3 Vernal/Autumnal Equinox	DRM-5 Summer Solstice
Orbit Inclination (relative to ecliptic)	98°	5°
Orbital Period	6176 sec	5492 sec
Occultation Period	0 sec	2177 sec
Altitude	897 km	350 km
Normal Rotation	7 rpm	7 rpm
Axial Rotation	0.14 rpm	0.14 rpm

Having defined a TCS network model and identified the most stressing orbits, the thermal/hydraulic response of the fluid network and space radiator was assessed using HYSTAM. Figure 6.9-9 shows the predicted hydraulic response of the subsystem at steady-state conditions for both orbits. The computed pump power, assuming an efficiency of 65%, is a continuous 7.4 W. The pump produces approximately 5 psia of head, a coolant mass flow rate of 0.153 kg/sec, and a coolant velocity of 0.137 m/sec within the radiator coolant tubes.

The predicted thermal response of the coolant for both orbits is presented in Figure 6.9-10. The temperatures correspond to that of the fluid as it enters the ECLSS heat exchanger. The initial system temperature for the DRM-3 orbit was set at 300 K and was designated the hot orbit/hot start condition. The initial system temperature for the DRM-5 orbit was set at 280 K and was designated the cold orbit/cold start condition. The intent was simply to derive some insight into how initial temperature influenced the time required for the subsystem to reach a steady-state operating condition.

The hot orbit/hot start condition requires the coolant loop to bypass the heat exchanger for approximately 3600 seconds. The bypass permits the residual heat within the subsystem to dissipate allowing the temperature of the coolant to drop below the 291 K maximum allowable for ECLSS heat exchanger. For the analysis, the bypass was simulated by switching the 120 W source term in the ECLSS heat exchanger control volume on at 3600 seconds into the calculation. This is evidenced in Figure 6.9-10 by the burp in the coolant temperature response curve. For the DRM-3 orbit, the coolant temperature stabilizes at 284 K.

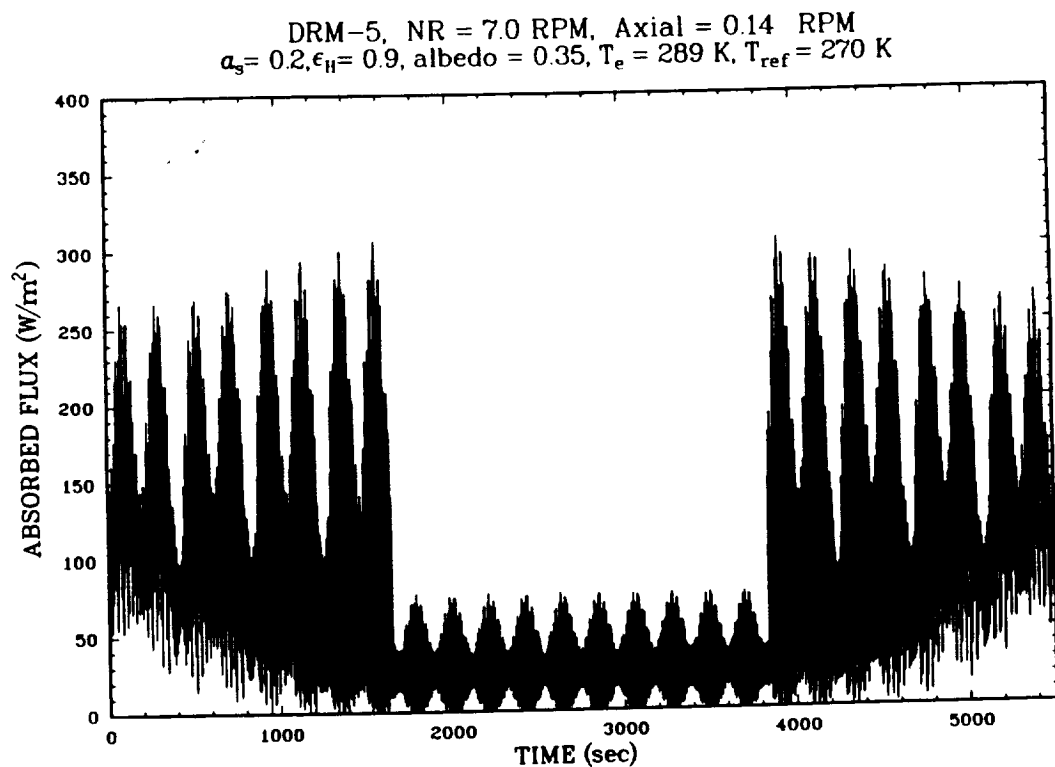
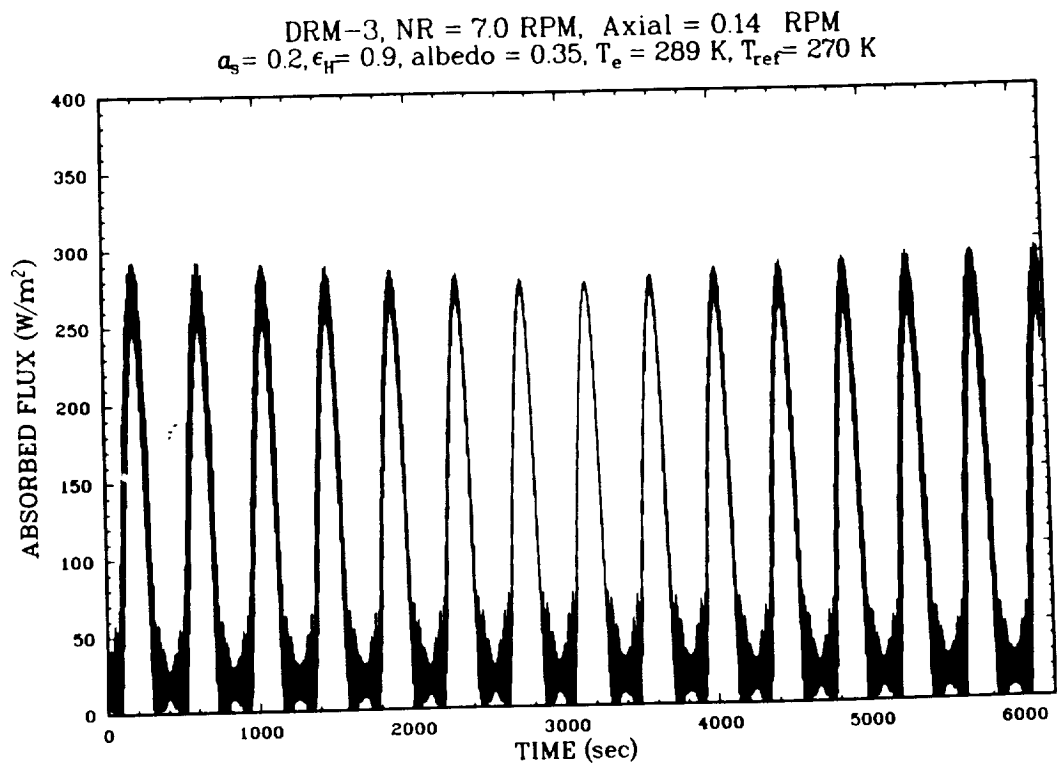


Figure 6.9-8. Total Absorbed Flux (Solar + Albedo + Earth IR) at Radiator Panel 1 Surface During One Orbital Period for DRM-3, Vernal/Autumnal Equinox and DRM-5, Summer Solstice With Vehicle Normal and Axial Rotation Rates of 7.0 and 0.14 rpm, Respectively

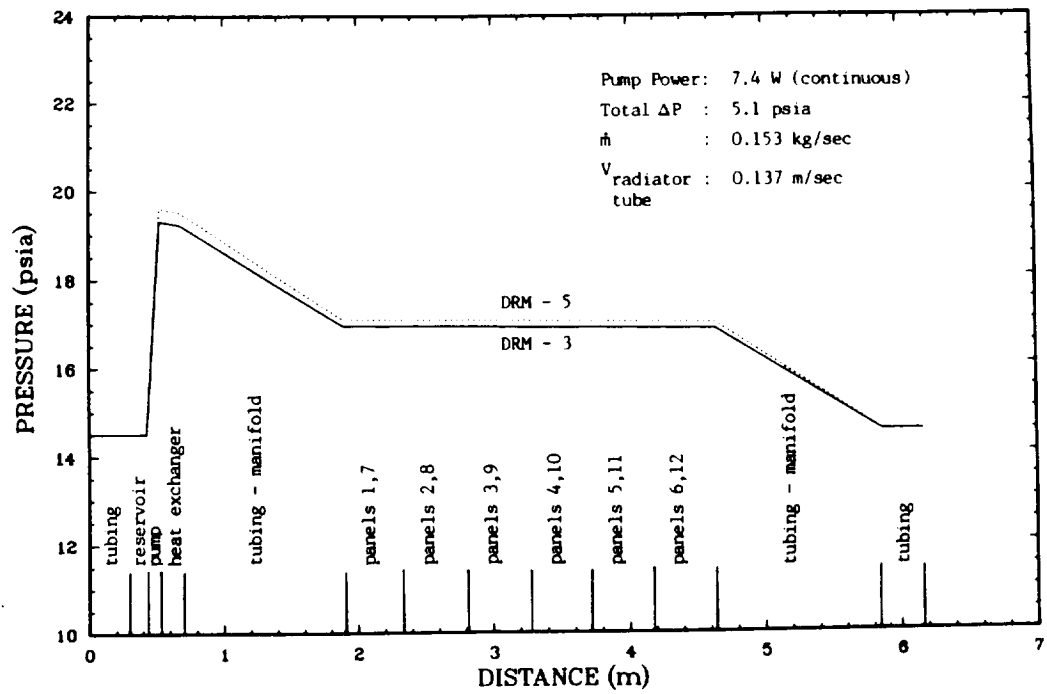


Figure 6.9-9. Fluid Network Hydraulic Response

Fluid Temperature at Heat Exchanger Inlet

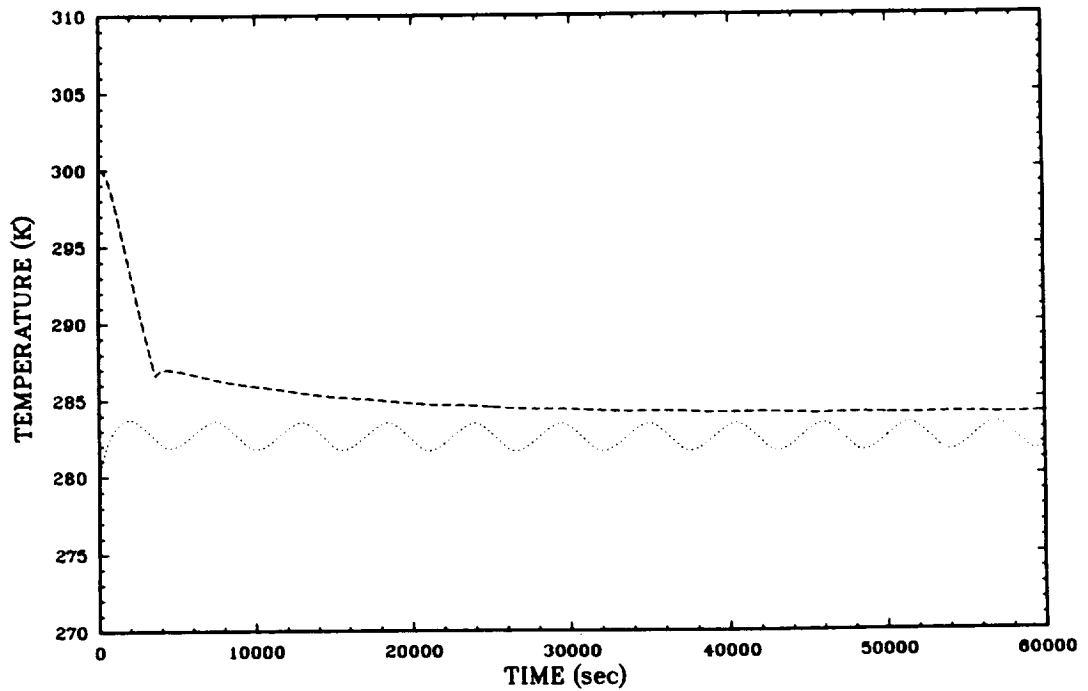


Figure 6.9-10. Coolant Thermal Response

Considering the cold orbit/cold start condition, the prediction indicates that the coolant temperature quickly equilibrates to a pseudo-steady-state condition between 282 and 284 K. The periodic oscillation in the coolant temperature response is the result of the 2177 second occultation period that occurs during the DRM-5 orbit. Note that the coolant temperatures achieved for both orbits fall between the maximum and minimum allowable coolant temperatures of 291 and 273 K identified previously.

The required number and diameter of coolant tubes in the space radiator were arrived at iteratively by performing successive sets of HYSTAM computations. The above coolant temperatures were achieved using eight 0.889 cm diameter tubes per panel spaced 5 cm apart.

Figure 6.9-11 permits a comparison of the thermal response of the coolant relative to that of the aeroshell surface. The temperature response at the surface of radiator panels 1 and 4 (15° and 105°) are shown in relation to the coolant temperature as a function of time for both DRM-3 and DRM-5. The aeroshell surface temperature ranges between 260 to 280 K. In addition, the results indicate that the maximum temperature difference between adjacent panels does not exceed 3 K. Therefore, circumferential conduction about the aeroshell is negligible, as assumed originally.

Having arrived at a viable concept, a weight estimate of the proposed TCS was made assuming a construction entirely of aluminum. The complete breakdown for the subsystem is given in Table 6.9-5. The total weight calculated, excluding the ECLSS heat exchanger and the aeroshell and its substructure, is 38.4 lbs (17.4 kg).

Table 6.9-5. PM ECLSS TCS Weight Budget

Component	Mass lbs (kg)
Coolant	10.8 (4.9)
Tubing	15.6 (7.1)
Pumps	5.5 (2.5)
Reservoir	3.1 (1.4)
Valves and fittings	2.2 (1.0)
Structure	1.1 (0.5)
TOTAL	38.4 (17.4)

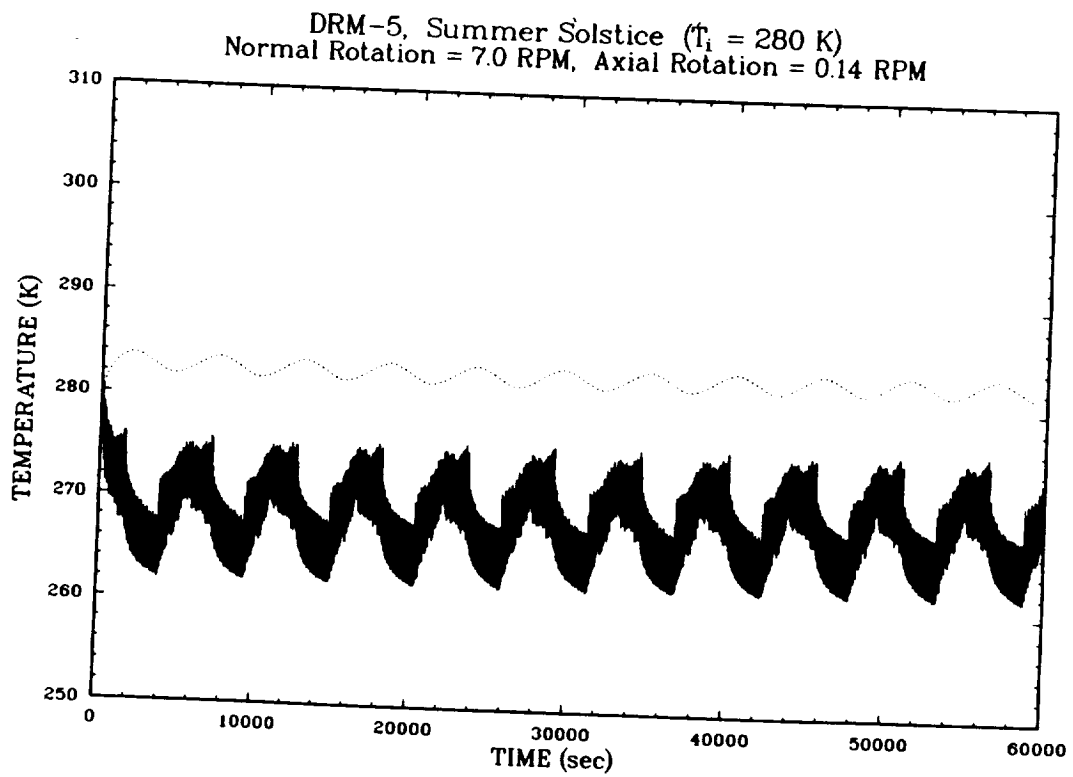
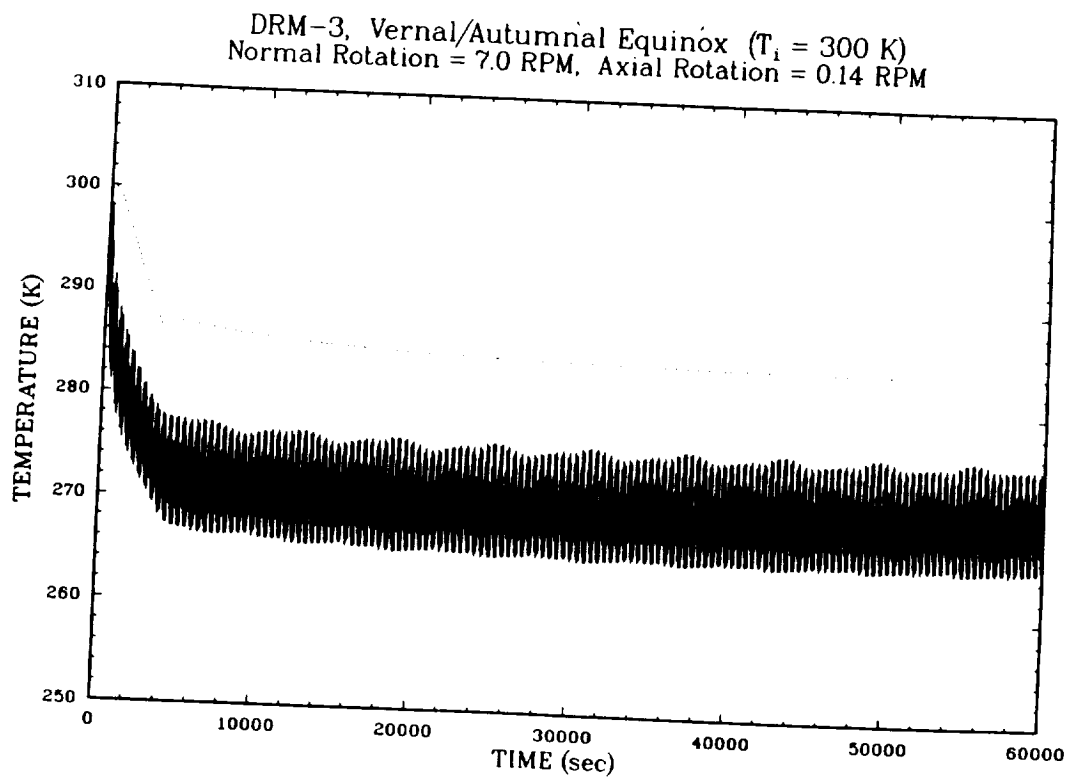


Figure 6.9-11. Aeroshell Surface and Coolant Thermal Response, DRM-3 and DRM-5

6.9.4.1.6 Conclusions. Based on results reported in the Ames Reusable Reentry Satellite Design Study and the current trade study, it was concluded that an active TCS, consisting of a fluid network coupled with a space radiator, was a viable thermal control concept for the SAIC RRS Payload Module's ECLSS heat exchanger. A preliminary thermal response calculation indicated that the RRS aeroshell would serve as an acceptable location for the TCS space radiator. Based on the subsystem's projected operating pressure and temperature, the liquid coolant ethylene glycol was chosen as the TCS working fluid.

A thermal-fluid response assessment of the proposed TCS was performed using the HYSTAM computer code. The analysis considered the two RRS orbit/vehicle orientation/seasonal combinations that subjected the aeroshell to the most stressing thermal environments. The aeroshell surface was coated with a low absorptivity white paint to enhance its dissipative efficiency. The coating was assumed to have a solar absorptance of 0.2 and a hemispherical emissivity of 0.9. The results indicated that eight 0.889 cm diameter coolant tubes integrated into the aeroshell's substructure effectively dissipated the heat exchanger's 120 W heat load while maintaining the coolant within the mandated temperature range of 273 to 291 K.

The pump power requirement for the TCS was estimated to be a continuous 7.4 W. The projected weight of the complete subsystem is 38.4 lbs (17.4 kg).

6.9.4.2 Extended Module Propellant Thermal Response

6.9.4.2.1 Introduction. The RRS Extended Module contains six spherical tanks fabricated from titanium in which hydrazine propellant is stored. Current system requirements dictate that the temperature of the propellant must be maintained between 275 and 330 K to ensure its safe containment. The tanks are almost completely enclosed by surrounding surfaces and thereby shielded from direct extraterrestrial exposure; however, because of the wide array of orbit types and vehicle orientations the RRS might encounter, thermal exchange with these externally exposed structures will still take place. Therefore, it is probable that under certain conditions the temperature of the tanks and their accompanying propellant will violate the above requirement if corrective measures, such as insulations, spectrally selective coatings, or heaters, are not imposed. This section describes the thermal assessment of the Extended Module that was performed to ascertain which corrective measures, if any, were necessary.

6.9.4.2.2 Modeling Tool. The Extended Module presents a relatively complex three dimension geometry that experiences radiant exchange with its extraterrestrial environment as well as radiant and conductive exchange between its component parts. The SAIC-developed Thermal Analyzer for Systems Components (TASC) computer code is well suited for this application. TASC is a lumped-capacitance, electrical resistor-capacitor network analog-based code for analyzing time-dependent thermal response of arbitrarily configured, multi-material, one, two, and three dimensional systems. A routine for computing direct solar insolation, Earth-reflected solar insolation, and Earth IR radiation on an arbitrarily oriented surface was integrated into the code which computed the magnitudes of these radiant components exactly as a function the Extended Module's time variant orbital position and orientation. This routine was an adaptation of the model used in the ECLSS TCS heat balance and HYSTAM computations described in Section 6.9.4.

6.9.4.2.3 Model. A pictorial representation of the Extended Module model developed for this assessment is presented in Figure 6.9-12. The model consisted of a truncated cone composed of a solar array over a substrate of aluminum honeycomb, two circular aluminum honeycomb disks serving as forward and aft covers, and six tanks, half full of hydrazine (nominal condition), suspended within the resulting enclosure. The entire model experienced rotations as prescribed by the particular orbital mission under consideration. The solar array and the external surfaces of the covers were exposed to direct solar insolation, Earth-reflected solar insolation, and Earth IR radiation and experienced radiant exchange with the Earth and deep space.

Before developing a TASC electrical network analog for the Extended Module model, a set of preliminary calculations was undertaken to assess the thermal response of the module's solar array. The motivation was to obtain an estimate of temperature gradients about the module's circumference and guide the model nodalization process.

As described above, solar panels cover the entire exterior surface of the module's truncated cone perimeter. A simple TASC model of the array was developed by dividing the truncated cone into six equivalent circumferential sections. Each section consisted of a lay-up of quartz over a substrate of aluminum honeycomb. Each panel was permitted to communicate with its neighbors via conduction, however, no radiant exchange across the cone's interior was considered. The thermal mass and response of the remaining Extended Module's structure was ignored.

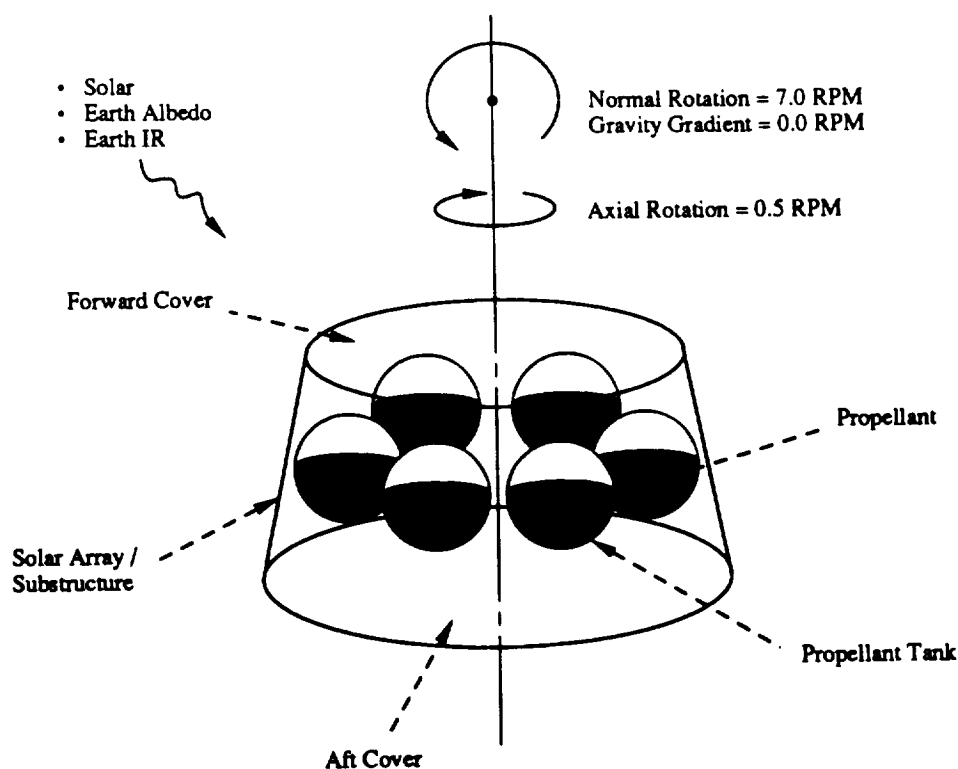


Figure 6.9-12. RRS Extended Module Model

The TASC code was exercised for the DRM-3 orbit at Vernal/Autumnal Equinox with the vehicle in the gravity gradient orientation (no vehicle rotation, vehicle's axis is perpendicular to the Earth's surface, and vehicle nose facing outward). From analyses discussed in Section 6.9-4, this scenario was determined to impose the highest heat loads on vehicle conic surfaces. Figure 6.9-13 presents a pictorial representation of the orbital geometry and vehicle orientation considered.

The results are presented in Figure 6.9-14 which plots the temperature response at the centroid of each panel versus time. The temperatures experienced by the sun facing panels ($\sim 120^\circ$ - 180° - $\sim 240^\circ$) cause a substantial degradation in the array's overall efficiency and a consequent loss in power production that is unacceptable.

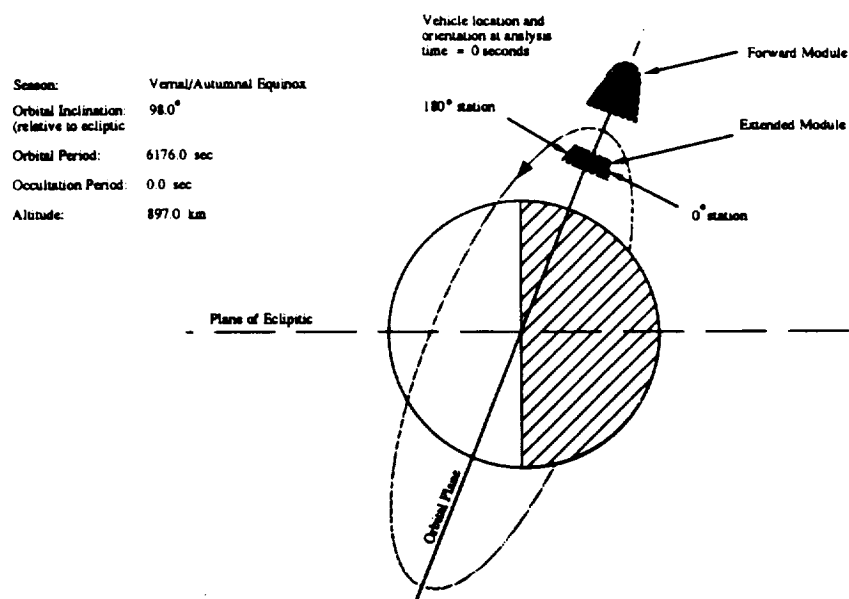


Figure 6.9-13. DRM-3 Orbital Geometry and RRS Vehicle Orientation Considered in Extended Module Solar Array Thermal Response Analysis

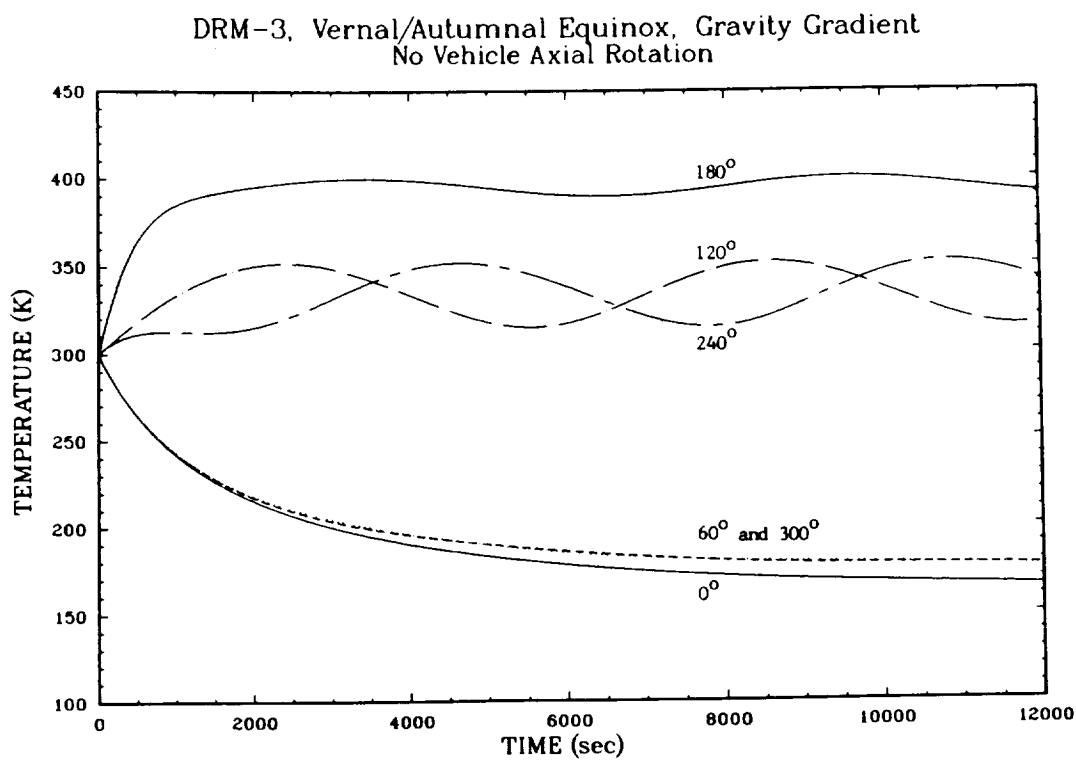


Figure 6.9-14. Extended Module Solar Array Thermal Response for DRM-3 Orbit

An obvious solution for eliminating the large nonuniformity in temperature about the module's circumference is to impose an axial rotation on the entire vehicle. However, the loads induced by such a rotation must not produce an acceleration greater than 10^{-5} g as set forth in the RRS System Design Study Statement of Work. A simple calculation sets the maximum allowable axial rotation rate at 0.14 rpm. This rotation produces an acceleration of 10^{-5} g at the PM's 44.5 cm outer radius. This results in an acceptable 0.8×10^{-5} g at the maximum rodent cage radius of 35.6 cm.

Repeating the previously described TASC analysis with a vehicle axial rotation rate of 0.14 rpm results in the circumferential temperature distribution presented in Figure 6.9-15. The rotation is sufficient to effectively smooth the nonuniformity and results in an array temperature of 300 K +/- 10 K.

The above results were used to develop the electrical network analog for the Extended Module model shown in Figure 6.9-16. Because of geometric and thermal symmetry, the solar array, array substructure, and forward and aft covers were modeled as single nodes. In addition, the six propellant tanks and their resident propellant were also treated as single nodes. The surface areas, masses, and conductive contact areas between each of these structures, however, were all computed based on the Extended Module's actual geometry. The radiation view factors between the array substructure, forward cover, aft cover, and propellant tanks were calculated assuming no intervening obstructions.

Table 6.9-6 describes the material, mass, and radiant properties for each of the six network nodes. The external surfaces of the forward and aft covers were coated with a high absorptivity black paint. The coating was assumed to have a solar absorptance and hemispherical emissivity of 0.9. For the DRM-3 polar orbit, the mass of the node representing the propellant was set to zero. Since the heating environments induced by this orbit are relatively uniform, the temperatures of the various surfaces which constitute the module's exterior will not fluctuate broadly over each orbit. Since the temperatures of these surfaces in turn drive the thermal response of the propellant tanks, the tanks themselves will experience even smaller fluctuations and as a consequence equilibrate to a steady-state condition. As a result, the additional mass provided by the propellant only serves to lengthen the system's equilibrium time constant. By eliminating the mass of the propellant when considering the DRM-3 orbit, the system reaches its equilibrium condition more rapidly thereby reducing the required computation time interval.

DRM-3, Vernal/Autumnal Equinox, Gravity Gradient
Vehicle Axial Rotation = 0.14 RPM

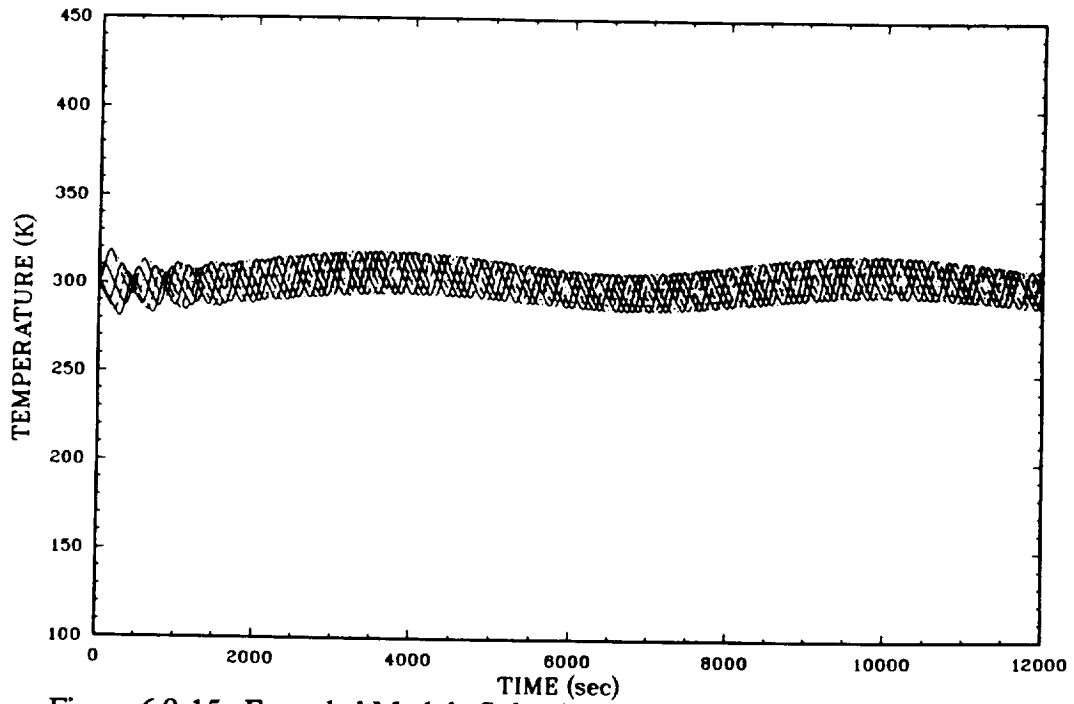
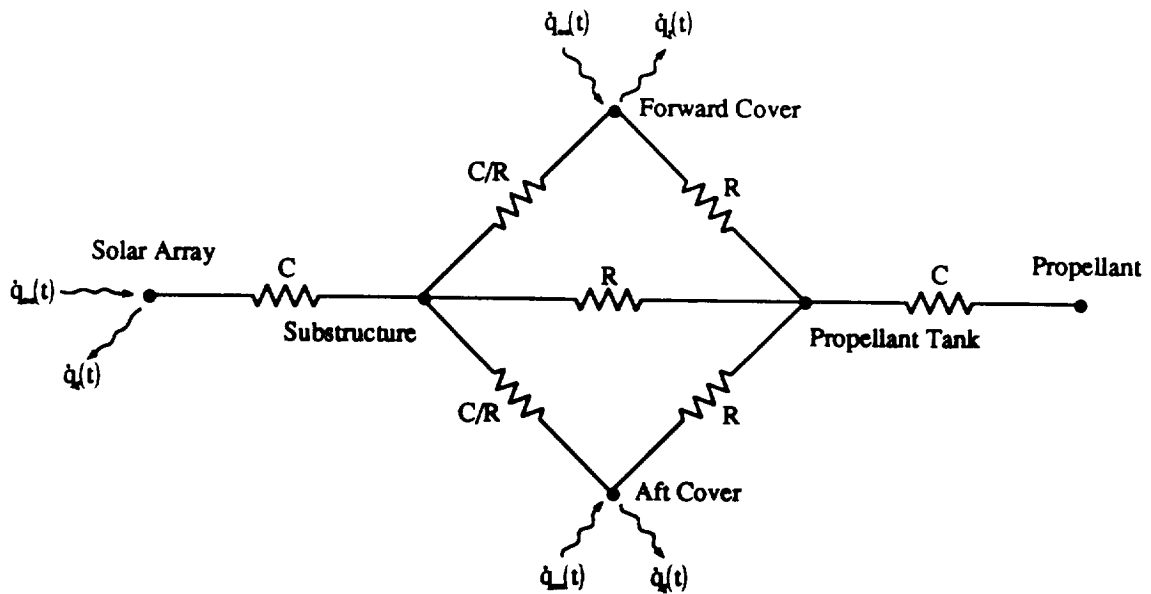


Figure 6.9-15. Extended Module Solar Array Thermal Response for DRM-3
Orbit With and Axial Rotation of 0.14 rpm



$\dot{q}_t(t)$: Radiation to environment (Deep Space, Earth)

$\dot{q}_r(t)$: Radiation from environment (Solar, Earth Albedo, Earth IR)

C : Conduction

R : Radiation

Figure 6.9-16. Extended Module Model Electrical Network Analog

Table 6.9-6. Extended Module Model Electrical Network Analog Nodal Descriptions

Node	Material Modeled	Nodal Mass (kg)	Radiant Surface Properties *
Solar Array	Quartz	3.15	$\alpha_s = 0.86 \ \epsilon_H = 0.80$
Substructure	Aluminum Honeycomb	20.10	$\alpha = 0.80 \ \epsilon = 0.80$
** Forward Cover	Aluminum Honeycomb	8.23	$\alpha_s = 0.90 \ \epsilon_H = 0.90$ $\alpha = 0.80 \ \epsilon = 0.80$
** Aft Cover	Aluminum Honeycomb	15.41	$\alpha_s = 0.90 \ \epsilon_H = 0.90$ $\alpha = 0.80 \ \epsilon = 0.80$
Propellant Tank	[†] Titanium	44.91	$\alpha = 0.80 \ \epsilon = 0.75$
Propellant	Hydrazine	DRM-3 0.0 DRM-5 154.20	

- * α_s and ϵ_H correspond to vehicle external surfaces, α and ϵ correspond to vehicle internal surfaces
- ** External surfaces coated with black paint
- [†] External surfaces coated, but uninsulated

6.9.4.2.4 Assumptions. As is evident from the inspection of Figures 6.9-12 and 6.9-16, the model representing the Extended Module resulted from several simplifying assumptions that assisted in economizing the analysis without sacrificing the integrity of the predictions. Several of these assumptions have been discussed previously. The remainder are addressed here.

Since struts and/or flanges with relatively small cross-sectional areas will be used to secure the tanks within the module, it was assumed that radiative rather than conductive exchange would be the dominant mechanism of heat transfer between the module's shell and the tank surfaces. Also, it was assumed that the tanks are completely shielded from direct exposure to the external environment. This, in fact, is not the case since the forward cover is penetrated by the portion of the PM which protrudes from the forward module when the vehicle is in the retracted position. This requires an 88.9 cm diameter opening in the cover that exposes a portion of the tankage surface to the extraterrestrial environment. However, the placement of a cylindrical radiation shield of a diameter equivalent to that of the opening and extending into the module (to the aft cover if necessary) would suffice in completely isolating the tanks.

Additional assumptions were adopted in order to impart some degree of conservatism into the overall analysis. The tanks were assumed to be coated with a surface preparation, but were left uninsulated. The analysis neglected the 67 W of heat rejected from the various electronics, batteries, and hardware located within the module (a conservative estimate when considering minimum predicted temperatures). Also, as noted previously, the view factors between the tanks and the inner surfaces of the solar array and covers were computed assuming that there were no intervening obstructions.

6.9.4.2.5 Results. As was the case in the ECLSS heat exchanger TCS thermal response assessment described in Section 6.9.4, prior to executing the TASC code, a set of preliminary calculations was performed to determine which DRM/vehicle orientation/season combinations subjected the module's surfaces to the most stressing thermal environments. As before, the goal was minimize the number of code computations necessary to adequately assess the module's thermal performance. Figure 6.9-7 shows the orbital geometry and RRS vehicle orientation and rotation modes considered in the analysis. The orbital heat loads routine described in Section 6.9.1.5 was used to perform the computations in conjunction with the surface radiative properties given in Table 6.9-6.

The results from the above investigation indicated that the DRM-3, Vernal/Autumnal Equinox and DRM-5, Summer Solstice orbits in combination with a vehicle normal rotation rate of 7 rpm produced the lowest and highest heat loads on the module. The forward cover was the exception. This surface received the lowest and highest absorbed fluxes for the above orbits, but in combination with the gravity gradient vehicle orientation. Examples of the computed total absorbed fluxes at the surface of the Extended Module aft cover are presented in Figures 6.9-17 and 6.9-18 for the above scenarios.

Having identified the most thermally stressing orbits, the TASC code was exercised on the previously described Extended Module model. Figure 6.9-19 shows the predicted temperature responses of the solar array substructure, the forward and aft covers, and the propellant tank for DRM-3. Since the solar array was treated as a single node and the thermal heat balance was performed at only a single circumferential station on the conic, the 0.14 axial rotation produces an oscillatory temperature response for this surface. For both the normal rotation and gravity gradient vehicle orientations, the propellant tank equilibrates to approximately 280 K.

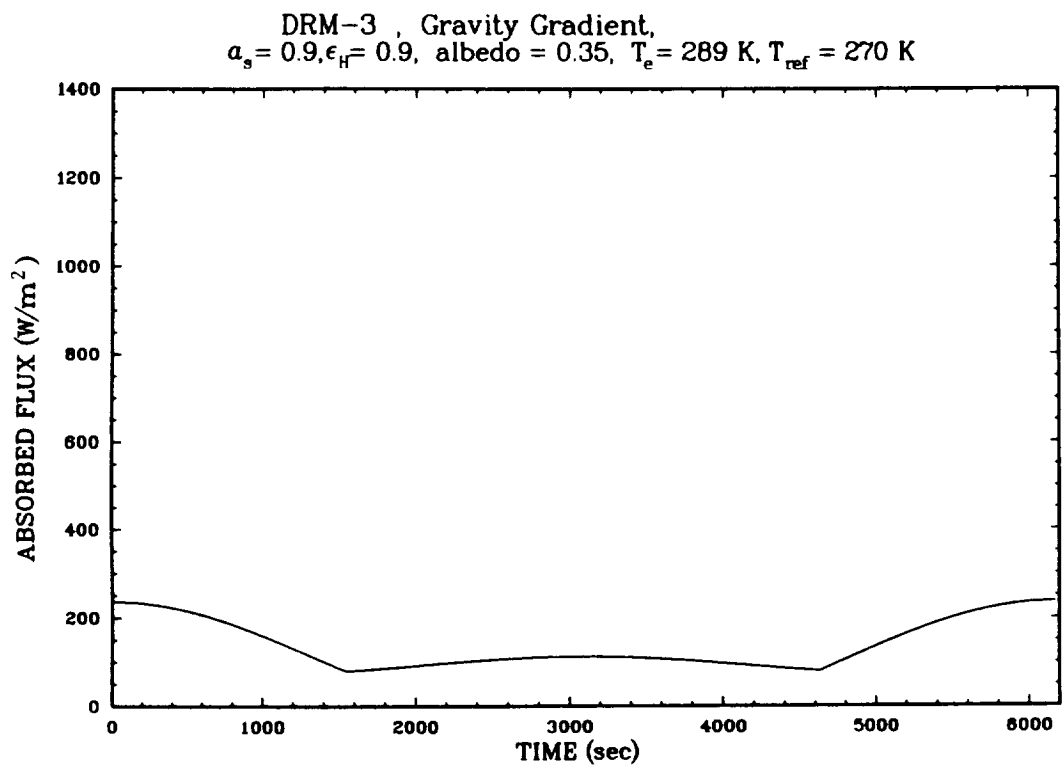
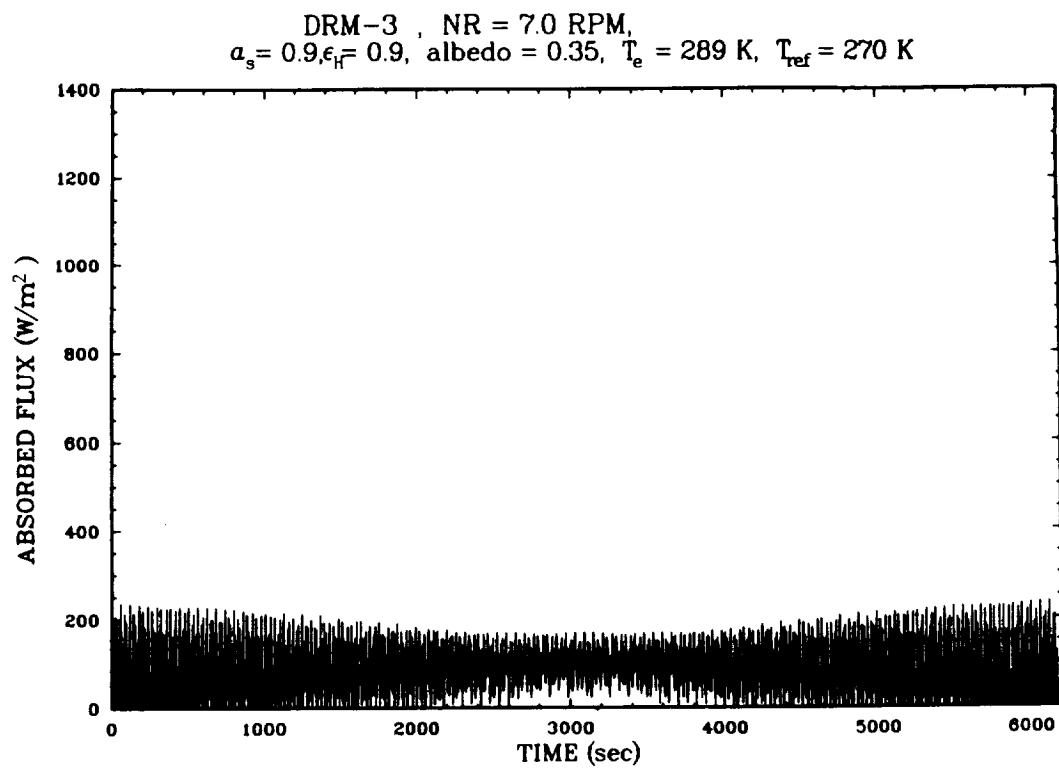


Figure 6.9-17. Total Absorbed Flux (Solar + Albedo + Earth IR) at Extended Module Aft Cover Surface During One Orbital Period for DRM-3, Vernal/Autumnal Equinox, Normal Rotation and Gravity Gradient Vehicle Orientations

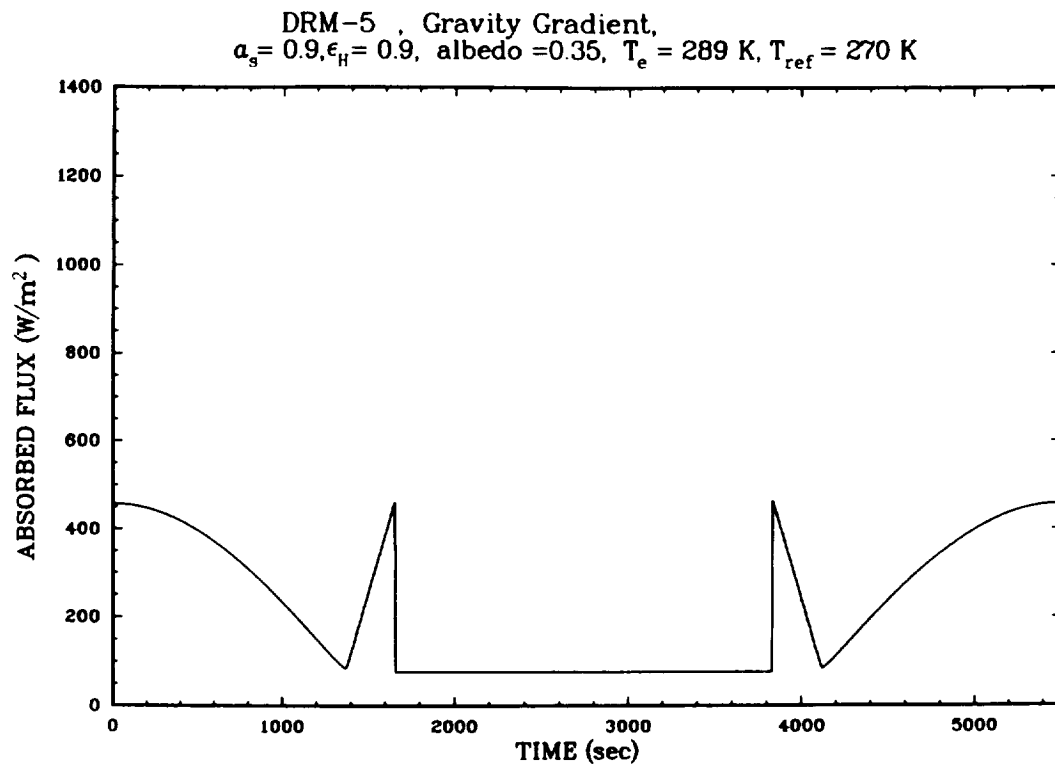
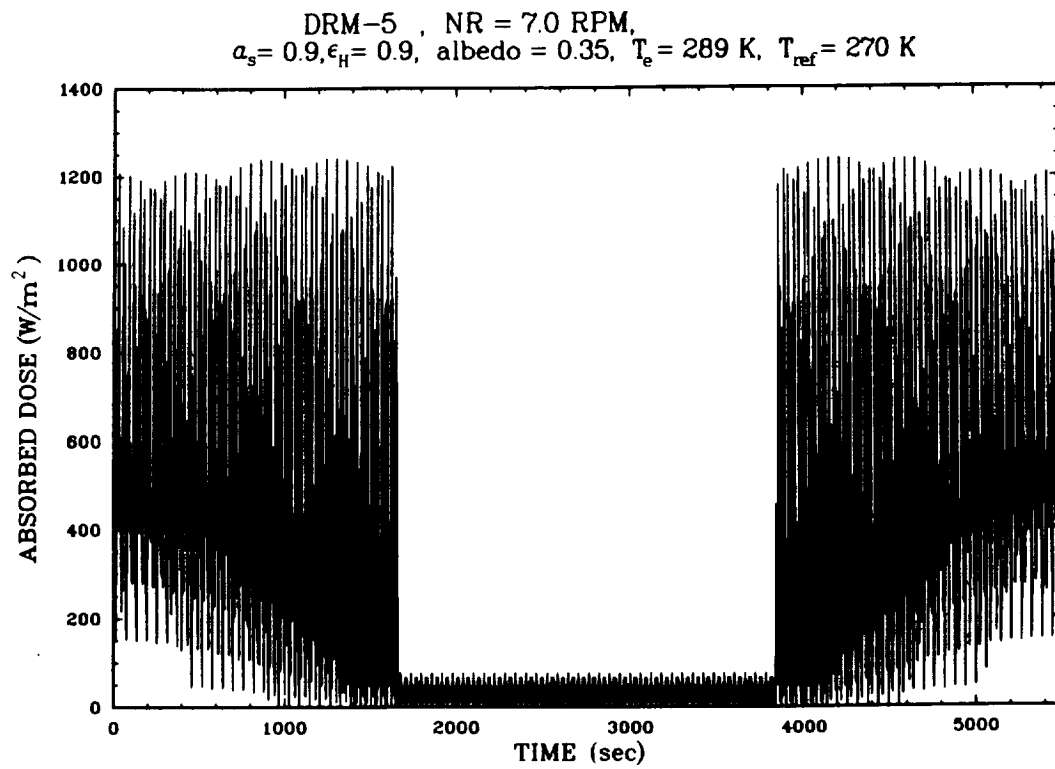


Figure 6.9-18 . Total Absorbed Flux (Solar + Albedo + Earth IR) at Extended Module Aft Cover Surface During One Orbital Period for DRM-5, Summer Solstice, Normal Rotation and Gravity Gradient Vehicle Orientations

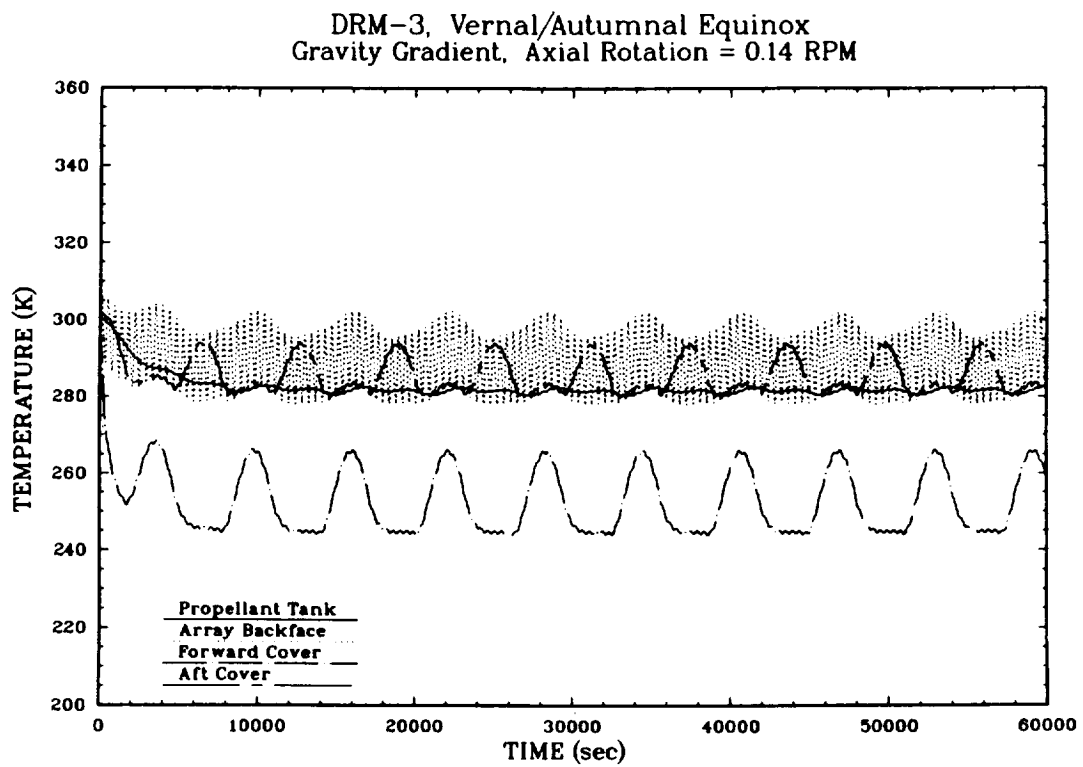
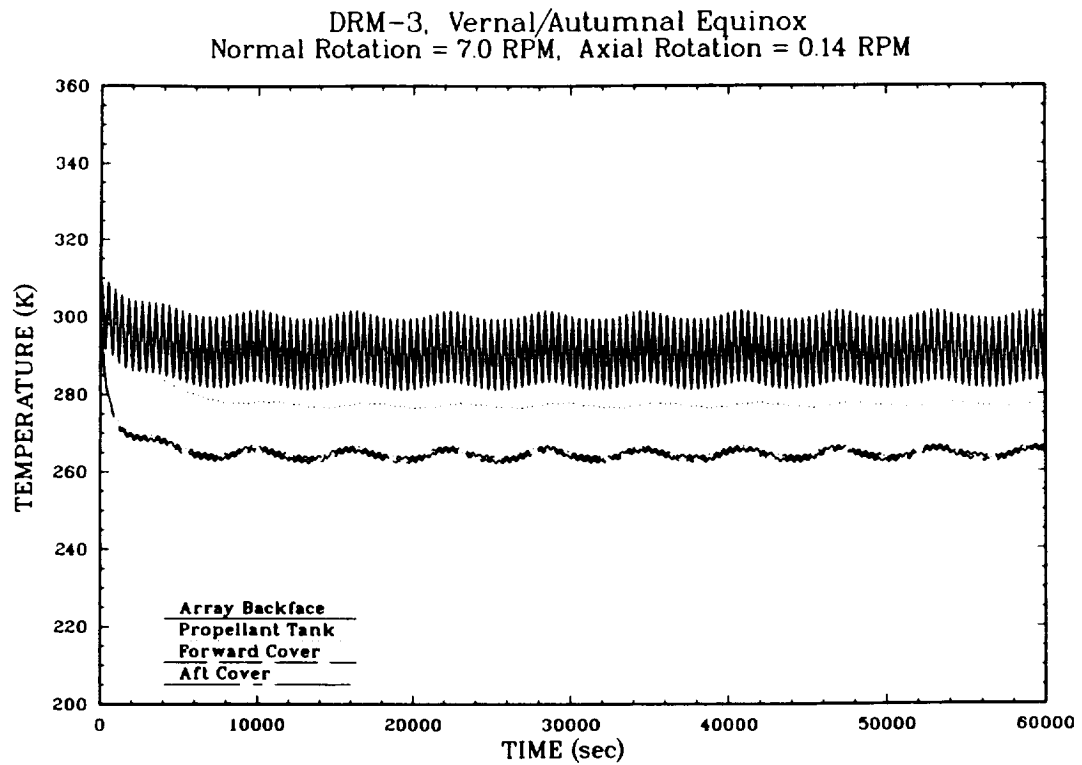


Figure 6.9-19. Predicted Temperature Response of Extended Module for DRM-3, Vernal/Autumnal Equinox, Normal Rotation and Gravity Gradient Vehicle Orientations

Figure 6.9-20 shows the predicted temperature responses of the solar array substructure, forward and aft covers, the propellant tank, and propellant for the DRM-5 orbit. For this orbit, the nodal temperature fluctuations are more pronounced because of the 2177 second occultation period. Although the temperature variations of the module's external surfaces fall well below the minimum propellant allowable of 275 K, the radiant coupling between these surfaces and the tank is sufficiently damped to prevent the tank temperature from dropping below 280 K. The bulk temperature of the propellant remains relatively steady, equilibrating to about 295 K for both the normal rotation and gravity gradient vehicle orientations.

Subsequent to the analysis performed for the microgravity mission with the RRV in the plane of the orbit as shown in Figure 6.9-13, it was determined that placing the vehicle in an orientation perpendicular to the plane of the ecliptic, as shown in Figure 6.9-21, would be preferred for all orbital inclinations. This orientation optimizes power available from the solar panels and provides good antenna coverage for the GPS and TDRSS links. The results of the analysis, as shown in Figure 6.9-20, for the DRM-5 mission provide the temperature extremes on the Extended Module containing the propulsion system. The temperature of the Extended Module in the new orientation will not reach the cold extremes as indicated in Figure 6.9-20 because the Extended Module will see more Earth during the eclipse mode. This result is more than acceptable since the propellant tanks will benefit from the warmer temperature. The temperatures of the Extended Module, as indicated for the DRM-3 mission and shown in Figure 6.9-19, will be somewhat warmer with the new orientation. In the new orientation, the RRS will be more exposed to the Earth and less exposed to deep space. The time constant of the heat shield material is approximately 1/2 that of the orbital period which may marginally increase the temperature extremes. The temperatures should be quite acceptable but a more detailed analysis should be performed.

6.9.4.2.6 Conclusions. An assessment of the on-orbit thermal response of the SAIC RRS Extended Module has shown that the propellant housed within its interior should remain between 280 to 300 K for all anticipated RRS missions. The analysis indicates that shielding the tanks from exposure to the external environment and coating the exterior surfaces of the forward and aft covers with a high absorptivity black paint are adequate measures for maintaining the propellant above its minimum allowable of 275 K. At present, it appears that no active thermal control measures will be necessary.

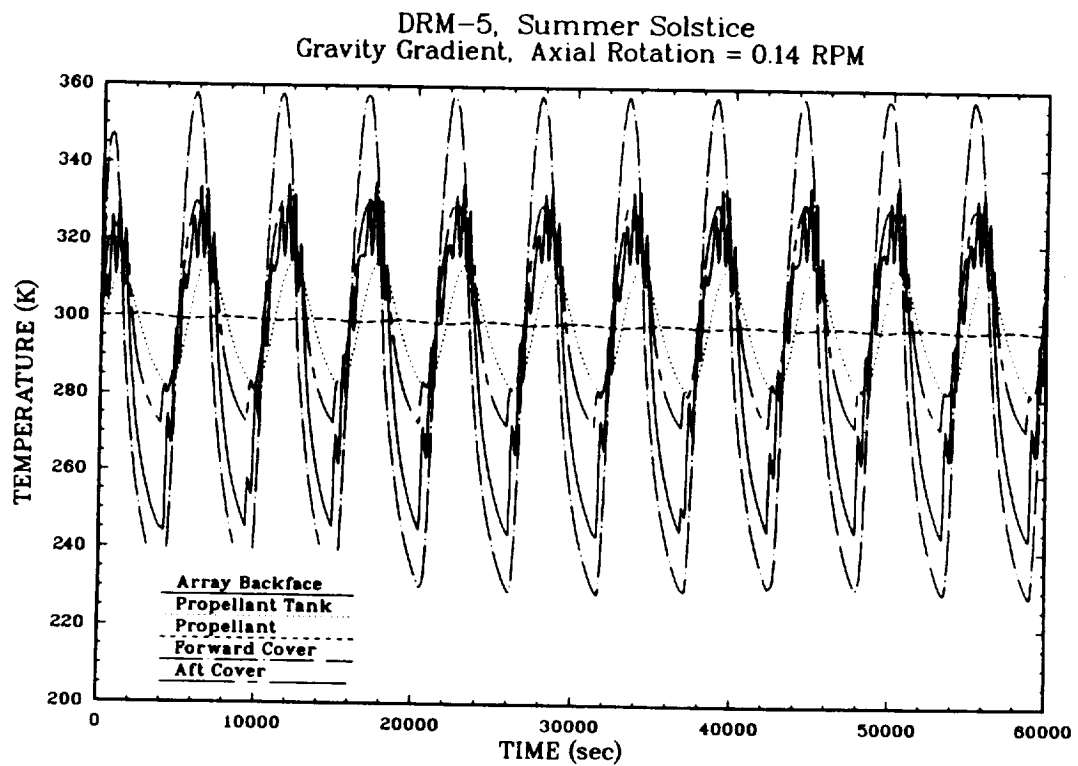
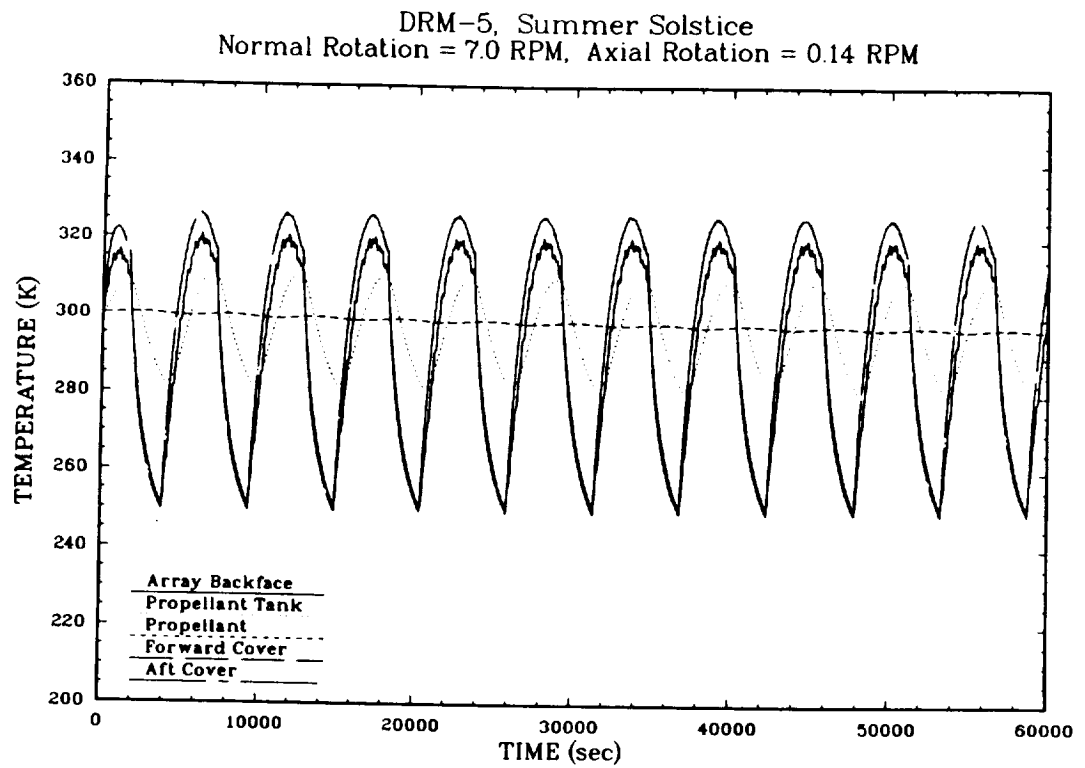


Figure 6.9-20. Predicted Temperature Response of Extended Module for DRM-5, Summer Solstice, Normal Rotation and Gravity Gradient Vehicle Orientations

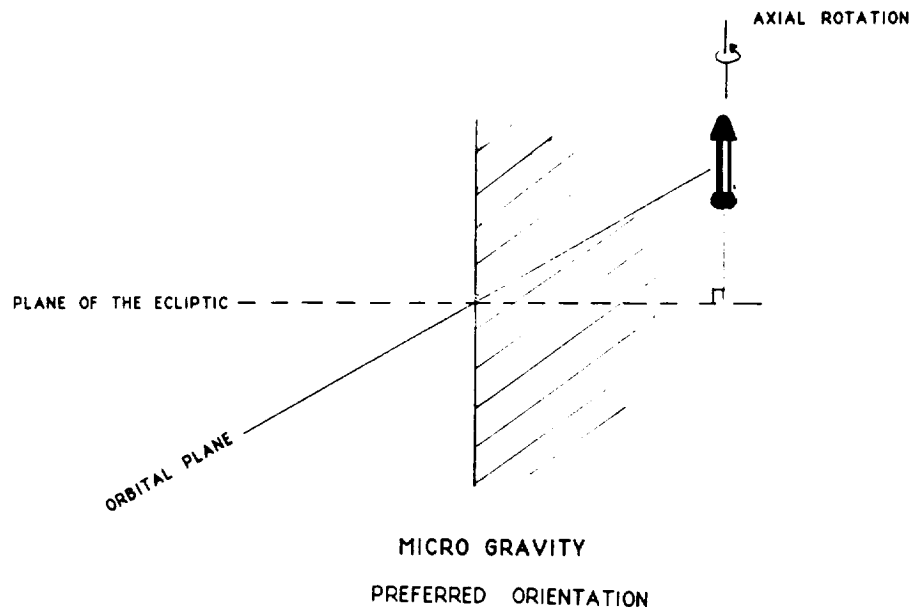


Figure 6.9-21. Microgravity Preferred Orientation

6.9.4.3 Payload Module Water Supply Thermal Response

Three cylindrical tanks reside within the RRS Main Module, each containing approximately 20 kilograms of water. The tanks are situated concentrically about the PM, as shown in Figure 6.9-22. The total quantity of water stored is sufficient to sustain a population of 18 rodents for 60 days. Since the water is stored in liquid form, it must remain above 273 K throughout all anticipated RRS missions. The following addresses the design issue of whether or not active heaters are required to maintain the water above this temperature.

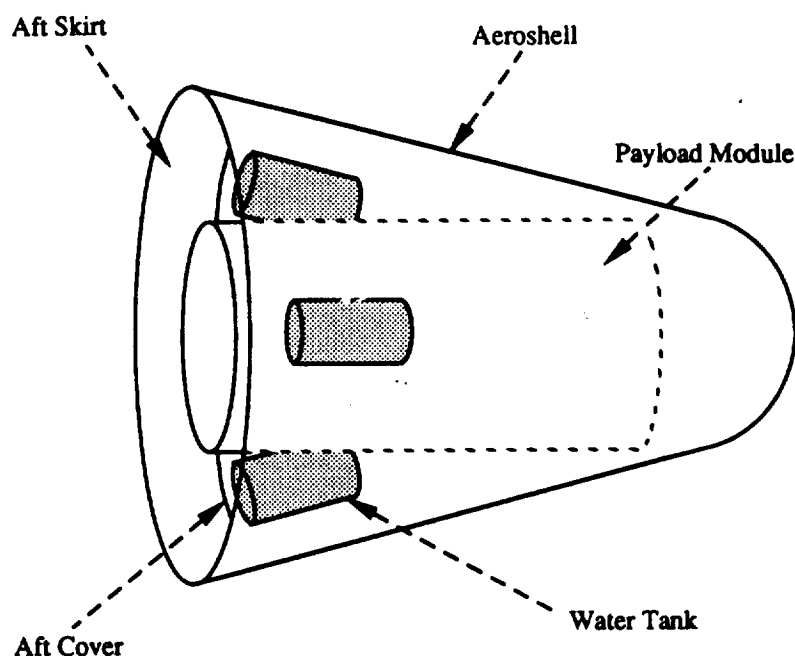


Figure 6.9-22. Water Storage Tank Locations Within Forward Module

While in orbit, the tanks experience both radiative and conductive exchange with their surroundings. However, conductive heat transfer will be minimized because of the relatively small cross-sectional areas of the brackets used to secure the tanks to the aeroshell substructure. Therefore, it may be assumed that radiative, rather than conductive exchange, will be the dominant mode of heat transfer for the water tanks.

An examination of Figure 6.9-22 shows that the primary radiating surfaces, which constitute the Main Module's internal cavity and experience some form of thermal forcing function, whether it be internal (rodents and electronics) or external (solar insolation), are the exterior of the Payload Module and the insulated backface of the aeroshell substructure. The oxygen and air tanks that bound each water tank can be ignored since they experience the same thermal environment as the water tanks and will, therefore, equilibrate to the same temperature, thus neutralizing radiant exchange.

Mission requirements dictate that the temperature of the PM interior range between 299 and 291 K. The analysis described in Section 6.9.4 indicates that the temperature of the aeroshell substructure will fall somewhere between 284 and 281 K. Since radiative exchange is dominant, and the PM and aeroshell substructure surfaces essentially encompass the water tanks, the temperature of the tanks will equilibrate between these two limits. Since the lower limit, the substructure temperature, is well above 273 K, it is concluded that no active heating of the water tanks will be necessary.

6.9.4.4 Mass/Power Summary. Table 6.9-7 presents the mass and power summary for the thermal subsystem.

6.9.5 Command and Control

The thermal subsystem is designed to operate semi-autonomously with commanding limited to subsystem configuration and heater (propellant, battery) on/off control. Although the thermal telemetry measurements listed in Table 6.9-8 will be used to monitor thermal operations, the only action to be taken in the case of a thermal malfunction not correctable by subsystem redundancy is mission termination and early recovery.

Table 6.9-7. Thermal Subsystem Mass and Power

Component	Unit Mass (lbs)	POWER (Watts)	#	Total Mass (lbs)	TOTAL MASS	MASS VALUE (lbs)	UNCERTAINTY %	UNCERTAINTY (lbs)
COOLANT	10.8		1	10.8	50	10.8	20	2.2
TUBING	15.6		1	15.6		15.6	20	3.1
PUMPS	2.8	7 WATTS EACH	2	5.5		5.5	20	1.1
RESERVOIR	3.1		1	3.1		3.1	10	0.3
SQUIB VALVES	0.3	5A@20 MSEC	5	1.3		1.3	2	0.0
MISCELLANEOUS FITTINGS	0.3		6	1.5		1.5	20	0.3
FILTERS	0.3		1	0.3		0.3	2	0.0
PRESSURE TRANSDUCERS	0.5		1	0.5		0.5	10	0.1
QUICK DISCONNECTS	0.3		4	1.0		1.0	5	0.1
FILL/DRAIN	0.3		2	0.5		0.5	2	0.0
SENSORS	0.1	.1 WATT	4	0.4		0.4	2	0.0
INSULATION	10.0		1	10.0		10.0	50	5.0
							TOTAL	12.1

Table 6.9-8. Telemetry Measurements

- AFT Solar Panel Temperature
- Battery Base Plate Temperature
- Payload Temperature
- Propellant Temperature
- Coolant Temperature
- Discharge Controller Temperature
- GNC Computer Temperature
- Thermal Radiator Temperature
- Temperature of Heat of Fusion Heat Sink

References

1. "A Conceptual Design Study of the Reusable Reentry Satellite," NASA Technical Memorandum TM 101043, NASA Ames Research Center, Moffet Field, California, October 1988.
2. "Statement of Work for a Phase B Study of a Reusable Reentry Satellite", NASA Request for Proposal 9-BE2-23-8-48P, NASA Johnson Space Center, Houston, Texas, January 10, 1989.
3. Wassel, A. T., D. C. Bugby, A. L. Laganelli, and C. E. Wallace, "Hypersonic-Vehicle Structural, Thermal and Acoustic Management (HYSTAM) Program," SAIC Report No. SAIC-90/1208, SAIC, Torrance, California, 1989.
4. Duncan, T. C., J. L. Farr, F. T. Makowski, and A. T. Wassel, "Satellite Laser Vulnerability Model: Thermal Analysis Module," SAIC Report No. SAI-060-80R-073-LA, SAIC, Torrance, California, 1980.

6.10 Recovery

6.10.1 Operations

The terminal recovery system performs final deceleration of the vehicle for a CONUS (White Sands) or water recovery. The system is operated by the GNC system which uses GPS position and velocity data to determine release points for the chutes. The first chute is deployed by an explosive mortar that ensures that the chute clears the major slipstream of the RRV before beginning deployment. The second and main chutes are deployed by the chute before.

6.10.2 Requirements

The terminal recovery system is responsible for decelerating the RRV from approximately Mach 2.5 at 60,000 feet to 20 feet per second at touchdown. The RRV mass is estimated at 3,700 lbs, and the touchdown location is White Sands Missile Range, which is at an altitude of approximately 5,500 feet. The system initial deployment requirement is driven by stability requirements of the RRV design. Below Mach 5, the RRV center of pressure (CP) moves forward as the velocity decreases. The CP reaches minimum at about Mach 1, at which time the baseline RRV would have about 9.8% stability margin. The supersonic drogue deployment alleviates this by stabilizing the vehicle and slowing it sufficiently for pilot chute and main chute deployment.

6.10.3 Trade Study Summary

The terminal recovery trade study considered four designs: a) air snatch with conventional parachute, b) conventional chute with terminal retro rockets, c) conventional parachute and impact attenuation system, d) gliding parafoil with impact attenuation system.

The advantages and disadvantages of these systems, as reviewed for the RRV, are summarized in Table 6.10-1. The results of the trade study rejected the air snatch and terminal retrofire on the basis of cost for the air snatch, and design complexity for the terminal retrofire system. The trade summary is given in Table 6-10-2.

Table 6.10-1. Preliminary Screening of Landing Systems

Screening Criteria	Passive Attenuation	Air Recovery	Terminal Retrofire	Gliding Parachute
Design Philosophy <ul style="list-style-type: none"> - Minimum Safety Risks - Low Life-Cycle Costs - Flight Proven Technology - Existing Hardware Design - Redundancy Necessary for Safety and Mission Success 	Good Excellent Excellent Excellent Excellent	Good Poor Excellent Excellent Poor	Poor Fair Fair Fair Fair	Good Excellent Fair Fair Good
Landing Point Dispersions <ul style="list-style-type: none"> - Dispersion Range 	Good	Good	Good	Excellent
G Loads <ul style="list-style-type: none"> - Atmospheric Braking - Ground Impact <10G 	Fair Good	Fair Excellent	Fair Good	Fair Excellent
Post Landing Access <ul style="list-style-type: none"> - Access to PM in 2 Hours - GSE Within TBD Minutes 	Good Good	Excellent Fair	Good Good	Excellent Good

TWP37/01.08
RRS-036

Table 6.10-2. Landing System Downselect

<ul style="list-style-type: none"> • DROP AIR RECOVERY LANDING SYSTEM <ul style="list-style-type: none"> - High Operational Cost <ul style="list-style-type: none"> -- Requires Continued Availability of Highly Trained Helicopter Flight Crews for Project Life -- Requires Continued Availability of Specially Configured Helicopters for Project Life - Mission Success Reliability <ul style="list-style-type: none"> -- Demonstrates Mission Success in Recovery is Approximately 96% -- Mission is Affected by Weather and Night • DROP TERMINAL RETROFIRE LANDING SYSTEM <ul style="list-style-type: none"> - RRS Project Safety Risk <ul style="list-style-type: none"> -- Design Approach Requires the Addition of Multiple Landing Rockets and Initiators - Hardware Design and Development <ul style="list-style-type: none"> -- Landing System Design Requires Some Development of Hardware and Sensors to Meet RRS Mission Reliability Goals • PERFORM FINAL COMPARISON OF CONVENTIONAL PARACHUTE WITH PASSIVE ATTENUATION AND GLIDING PARACHUTE LANDING SYSTEM
--

This left the conventional and gliding parafoil designs. Detailed design data was obtained from three manufacturers as shown in Table 6.10-3.

Table 6.10-3. Source Data from Parachute Industry

Manufacturer	Representative	Gliding Parachute		Conventional Parachute	
Para-Flight, Inc.	Troy Laney	X			
Pioneer Aerospace Corp.	William Everett		X	X	
Irving Parachute Co.	Phil Delurglo				X
Estimated System Weight		120 lbs.*	90 lbs.**	130 lbs.	160.6 lbs.
Estimated System Volume		2.75 cu. ft.	2.6 cu. ft.	3.7 cu. ft.	3.14 cu. ft.
Estimated DDT&E Costs		\$1.2-1.4M	\$1.16M	\$0.78M	\$1.28M
Estimated DDT&E Time		—	2 Years	1.5 Years	—
Estimated Hardware Cost		\$100,000	\$38,000	\$17,500	\$40,000
Estimated Refurbishment Cost		\$15,000	\$8,500	\$5,800	—
Anticipated Test Program		1 Year	1 Year	0.5 Year	—
Number of Drops to Qualify System		25-30	15	10	10

* Weight and volume do not include power source.

** Cost, weight, and volume do not include guidance, navigation, and control equipment, onboard sensing, steering actuators, or power source.

TWP37/01.10
RRS-036

The gliding parafoil offered several key advantages over a conventional parachute. These included:

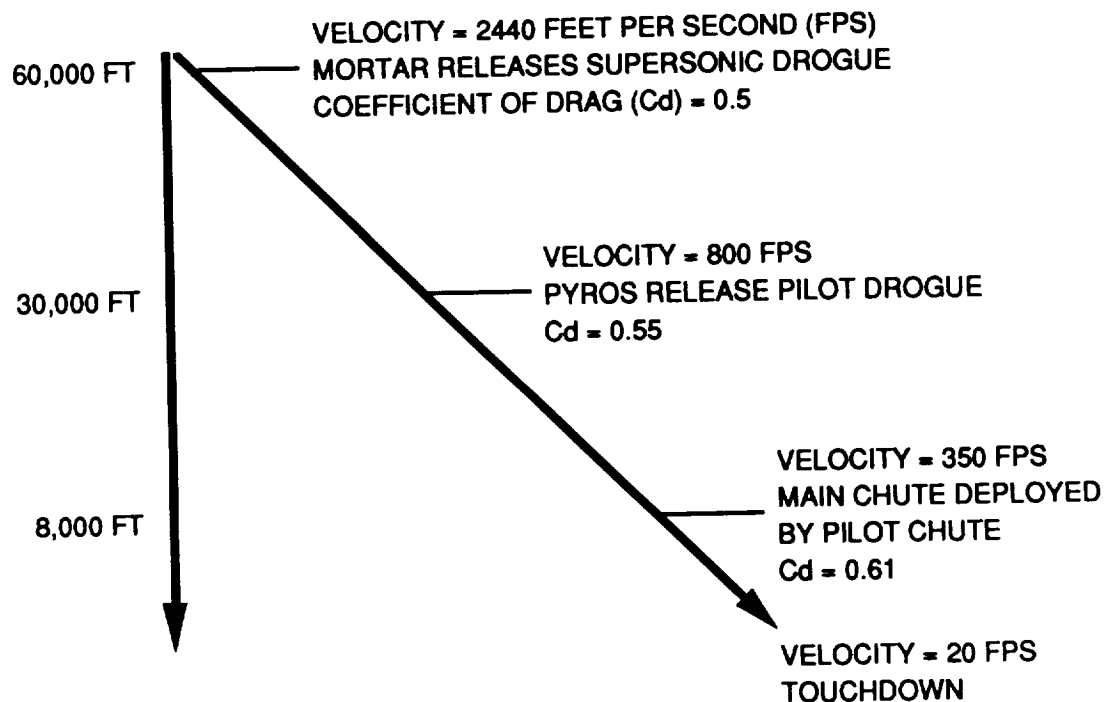
- a. Landing Recovery Dispersion Minimization - The gliding parachute has a glide ratio of >2.5:1. This, coupled with use of GPS to determine absolute position and relative position to a desired landing point, allows the gliding parachute to decrease landing dispersions caused by upper atmospheric density variations and wind drift at lower altitudes.

- b. Soft Landing Flare - The gliding parachute has the capability to eliminate most of the vehicle's forward and vertical motion just before touchdown. This landing "flare" operation can be automated using a GPS-based system, or can be manually controlled by ground personnel.

The major disadvantage of the gliding parachute is its lack of design maturity. For this reason, the gliding parachute is considered a design option for the RRV, with a conventional parachute as the baseline design.

6.10.4 Baseline Design

The baselined terminal recovery system design consists of two ribbon parachutes and a main final descent parachute. Figure 6.10-1 shows the sequence of events during the recovery cycle.



TOR42I/26

Figure 6.10-1. Recovery Sequency

6.10.4.1 Supersonic Drogue. The supersonic drogue deploys at approximately 60,000 feet for the nominal DRM-1 mission descent profile. This corresponds to a velocity of approximately 2,440 feet per second. This parachute is 12 feet in diameter, is a ribbon design, and weighs 10 lbs. The design has a coefficient of drag (C_d) of 0.5. This chute decelerates the vehicle to 800 fps at approximately 30,000 feet, at which point pyros release the main parachute drogue, which is pulled out by the supersonic drogue.

6.10.4.2 Pilot Drogue. The pilot drogue is a ribbon type design with a 15 foot diameter and a C_d of 0.55. This parachute decelerates the vehicle to 350 fps, where it serves as the pilot parachute used to pull out the main chute. This unit weighs 15 lbs.

6.10.4.3 Main Parachute. The main parachute is a ring sail design with a C_d of 61. The parachute has a 127 foot diameter and weighs 150 lbs. The design implies single stage reefing to limit opening shock less than 6 g's. This system decelerates the vehicle from 350 fps to 20 fps at touchdown.

6.10.4.4 Ancillary Hardware. Ancillary hardware includes the mortar for initial supersonic parachute deployment, pyrotechnic bolts for release of covers and sequential parachutes, and the cover itself. Total weight for these items is 18 lbs. A weight breakdown of the system is provided in Table 6.10-4.

Table 6.10-4. Terminal Reentry Mass and Power

Component	Unit Mass (lbs)	#	Total Mass (lbs)	POWER (Watts)	TOTAL MASS	MASS VALUE (lbs)	UNCERTAINTY %	UNCERTAINTY (lbs)
COVER	5.0	1	5.0		193	5.0	10	0.5
MAIN CHUTE (127")-20fps	150.0	1	150.0			150.0	5	7.5
DROUGE(15")	15.0	1	15.0			15.0	10	1.5
SUPERSONIC DROUGE (12")	10.0	1	10.0			10.0	20	2.0
MORTAR	7.0	1	7.0	5A@ 20 MSEC		7.0	10	0.7
PYRO'S	0.5	12	6.0	5A@20 MSEC		6.0	5	0.3
						TOTAL		12.5

6.10.5 Command and Control

Command signals for parachute deployment are provided by the GNC subsystem. The GNC calculates altitude and velocity, and releases the parachutes based on a stored set of parameters. Release can also be commanded from the ground, if required. The optional gliding parachute requires additional commanding to two control motors. The motors control flaps on the parachute that control the direction of the glide. In addition, operation of both flaps "stalls" the chute for final touchdown. The flight direction would be determined by a homing beacon equipped with a GPS receiver, and the GPS on the vehicle. The computer could then fly the RRV as close as possible to the beacon. The final landing flare would nominally be automatic, based on the differential GPS between the beacon and the RRV. However, manual control override is provided via the TT&C system.

7.0 COST SUMMARY

The cost analyses for the RRS are contained in the System Cost Estimates Document. These analyses were performed based upon a set of ground rules and assumptions (Table 7-1) made at the beginning of the program and used in the preliminary report. This section contains a brief summary of the results.

Table 7-1. Key Ground Rules and Assumptions

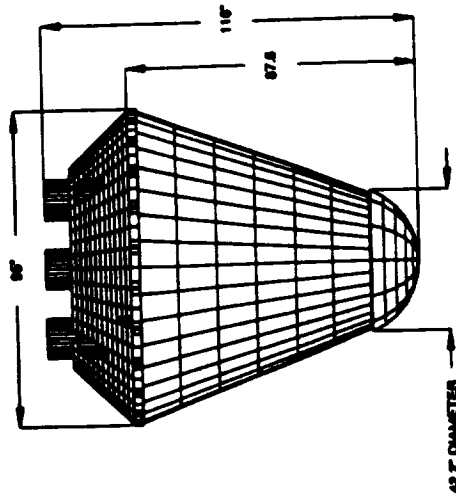
- SAIC'S TECHNICAL BASELINE FOR RRS AS PRESENTED AT FINAL REVIEW
- DELTA 6920 LAUNCH VEHICLE COSTED
- COSTED IN CONSTANT FY90 DOLLARS (FY90\$)
- A 100% LEARNING CURVE
- THE O&S LIFE CYCLE COSTED IS TEN YEARS
- ALL ELV LAUNCHES ARE COSTED AS DEDICATED RRS LAUNCHES
- SEALED VEHICLE COSTS ARE RELATIVE

7.1 Scalability

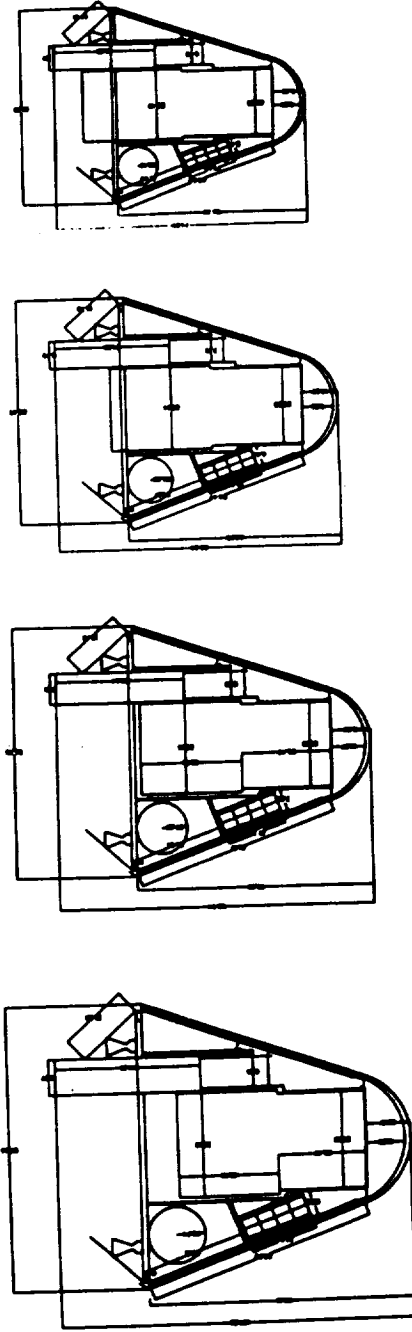
One of the key issues addressed in the cost analyses was the possibility of achieving cost savings via the use of the newer, smaller commercial boosters. To assess the smaller vehicle approach, the basic design was scaled down to several smaller sizes (Figure 7-1), the smallest being roughly the size required for a Taurus launch. This analysis resulted in the following observations:

- a. The smaller booster is cost inefficient on a per unit payload basis. For example, three Taurus launches (approximately \$81M) are required to achieve the same number of rodent-days that a single RRS Delta launch (approximately \$45M) can provide. Furthermore, since the Delta has a dual-launch capability for the orbits accessible to the Taurus, the Taurus is effectively over three times more expensive than the Delta.
- b. The smaller vehicle required for a Taurus class launch will not easily accommodate off-the-shelf equipment, resulting in less redundancy (a public safety issue) and/or the need to develop more compact components at higher development cost and cost/schedule risk.

RRV EXTERNAL DIMENSIONS



LESS REDUNDANCY - MORE RISK



600 GM RODENTS
WEIGHT

18
219
2/DELTA

6
356
≤1/TAURUS

9
277

12
254

15
240

- FOR SINGLE LAUNCH
45M DELTA EQUIVALENT TO 27M TAURUS
- FOR DUAL (OR SHARED) LAUNCH, OR DOUBLED PAYLOAD
45M DELTA EQUIVALENT TO 14M TAURUS
- SMALLER BOOSTER CANNOT ACCOMMODATE HIGHER GROUP PRIMATES

TOR42/18A

Figure 7-1. Relative Scaled Vehicle Cost

7.2 Approach

The GE (RCA) Price H Cost Model (Table 7-2) was used for estimating the cost of the development and manufacture of the RRS. The inputs were provided at the unit level and basic cost runs made for the individual unit, single-flight vehicle, and two-flight vehicle cases. Fifty percent spares were then added to the 2-vehicle case to approximate the 2-vehicle operating case, and a 4-vehicle run was made to investigate the cost increment for a few additional vehicles. Table 7-3 describes the quantities used in the two-vehicle case. The development and manufacturing breakout is presented for each case in Table 7-4.

Table 7-2. Price H Cost Estimating Approach

- PERFORMED BY CO\$T, INC THROUGH FAIRCHILD SPACE
- WEIGHT/VOLUME/COMPLEXITY/SCHEDULE BASED INPUT AT SUBSYSTEM/BOX LEVEL
 - Manufacturing Complexity Calibrated By Co\$T, Inc.
- OUTPUT PROVIDES SUBSYSTEM/SYSTEM VISIBILITY ENGINEERING, MANUFACTURING, INTEGRATION, AND TEST
- RUN SEQUENCE
 - Single Unit Development Cost
 - Program With:
 - 1 Flight Vehicle
 - 2 Flight Vehicles
 - 2 Flight Vehicles with Spares
 - 4 Flight Vehicles with Spares
 - With and Without Schedule Constraints

7.3 Summary

In summary (Table 7-5), the proven Delta/Atlas boosters are cost competitive with the newer, smaller commercial boosters if viewed on a total program requirements basis. A total cost of about \$200M for the development and production of two flight vehicles is split roughly 50-50 between development and production, and the \$50M per vehicle cost compares reasonably with recent GPS IIR (a comparable sized vehicle) experience. When viewed on a Life Cycle basis, the cost of the four-vehicle program is less than a 5% increase and would appear to be a good investment against unforeseen booster failure, especially if dual launches are used to decrease the overall program cost.

Table 7-3. RRS Subsystem Quantities (Definitions)

Quantity:	2	Flight Reusable Reentry Vehicles (RRV) Consisting of 1 Main Model (MM) and 1 Deployed Module (DM)
	1	Engineering Test Vehicle (ETV) Selected Flight Quality Subsystems + Thermal/Mass Models (TMM)
	1	Vehicle Emulator (VE) Complete Working/Tested MM Model Except for Selected Subsystems. Full Interface Support to PM
	2	Flight Payload Modules Consisting of 1 Support Module (SM) and 1 Experiment Module (EM)
	1	Payload Module Emulator Complete Working/Tested SM Model Except for Selected Subsystems. Full Interface, Mass and Thermal Emulation
	1	Ground Control Experiment Model Consisting of 1 VE and 1 Non-Flight PM (Ground Test Module (GTM))
		Refurbishment/Spares Concept Is to Have Sufficient Spares to Pull and Replace Any Item Subject to Test Failure and/or Needing Replacement Following Flight (e.g., Heat Shield). Redundant Items Are Dual Spared
	3	Flight Payload Adapters
	6	Partial Payload Adapters Support Structure and RRV Interface Only. 2 for Factory Test, 2 for Field (ETV/Launch, Recovery) Operations, 2 for VEs
Quality:	F - Flight P - Partial Prototype E - Engineering Model -- Not Applicable	
	C - Complete Working and Tested Model B - Brassboard	

Table 7-4. Pre-Calibration Price H Results (\$M)

RUN	DEVELOPMENT	MANUFACTURING	TOTAL	INCREMENT
Single Unit	75	31	106	--
1 Flight	89	76	165	59
2 Flight	92	100	192	26
2 Flight With Spares	95	121	216	25
4 Flight With Spares	101	166	267	51
QUICK-LOOK CALIBRATION—35 PERCENT LOW				

Table 7-5. LCC Summary

PROVEN BOOSTERS (DELTA/ATLAS) PROVIDE COMPETITIVE EXPERIMENT VALUE			
Small Boosters Cost More Per Unit Experiment			
Larger Vehicle Higher Value Per Launch			
PRE-CALIBRATION PRICE H COST ESTIMATE, VEHICLE AND RODENT MODULE			
Development	\$105M		
Vehicle 1	60		
Vehicle 2	26	50% Spares	26
Vehicles 3 and 4	51		
4-Vehicle Average	34	(\$50M Based Upon GPS IIR)	
TOTAL, BASED ON PRE-CAL PRICE-H FOR 2-FLIGHT VEHICLES WITH 50% SPARES, IS \$217M			
PRELIMINARY LCC ESTIMATE FOR 30 DELTA FLIGHTS, 10 YEARS			
Includes SAIC O&S Estimate of \$1682M			
	Total (\$M)	Per Launch	
		Single	Dual
2 Flight, 50% Spares	2001	67	43
4 Flight, 50% Spares	2075	69	45

8.0 CONCLUSIONS AND RECOMMENDATIONS

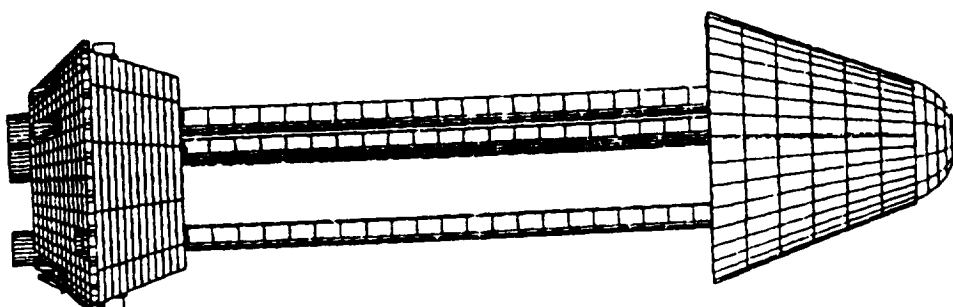
The primary intent of the Phase B study for the Resuable Reentry Satellite was to evolve the NASA Phase A concept into a preliminary design. Specific subsystem and booster tradeoff studies were identified to be completed in Part I, with the preliminary design to be developed during Part II. However, SAIC proposed a unique design, significantly different in concept from the Phase A approach, tailored to maximize the available support for the wide range of scientific objectives. As a result, the SAIC effort includes both the basic effort required by the SOW and the additional studies and design efforts needed to evolve the new concept into a comparable level of development. These additional efforts included a risk analysis to determine the degree of redundancy needed to ensure public safety for CONUS recovery operations, the GNC/propulsion approach required to fulfill the de-orbit requirements identified in the risk analysis, and an independently verified evaluation of the unique deployable tri-mast approach.

8.1 Key Features

The SAIC design (Figure 8-1) provides a flexible, science friendly approach that can be readily launched on existing boosters. The centralized payload volume can accommodate up to six STS Mid-Deck Lockers (Figure 4-2), each having a near-uniform gravitational environment. Furthermore, a large fraction of the Payload Module can be exposed to free-space radiation (Figure 4-3), minimizing the modification of the free-space spectrum and the potential for secondary radiation. The design also allows exact replication of the on-orbit 1 g operation in ground control experimentation, significantly aiding the correlation of the two sets of data.

The split vehicle design that makes the radiation exposure possible also allows the use of solar arrays as the primary power source, eliminating power as a restriction on mission duration and capable of providing over 300 watts (sun-synchronous orbit) of continuous payload power, enough to support the EBM simultaneous micro-G/1-g experiment.

The split vehicle concept also allows modularizing to provide the parallel manufacturing and test flows needed to reduce the overall manufacture/refurbishment time. This parallel flow approach also minimizes the potential impact of test failures, significantly reducing both schedule and cost risk.



TOR421/04

- **SCIENCE FRIENDLY**
Can Accommodate:
 - From 18 Rodents to a Squirrel Monkey
 - Up to 6 Mid-Deck Lockers
 - Extensive Free Space Radiation Spectral Exposure
 - Variable Gravity Environment:
 - As Low As 1% Gravity Gradient Across Experiment
 - Minimal Coriolis Effects
- **VEHICLE FLEXIBILITY**
 - 0-100 Foot Length Deployment Provides Added Power, Radiation Exposure, Low G Experimentation
 - Solar Power Allows Extended (>60 Day) Missions
 - Restartable Propulsion Provides
 - Precision Reentry Trimburn, Multiorbit Missions
- GNC Provides For:
 - All Orientation Attitude Determination
 - Precision Reentry Thrust Alignment, ΔV
 - Precision Timing, Orbit Determination
- Common G Vector Mission Profile
- **ADAPTS EXISTING LAUNCH VEHICLE HARDWARE**
Dual Payload Configuration

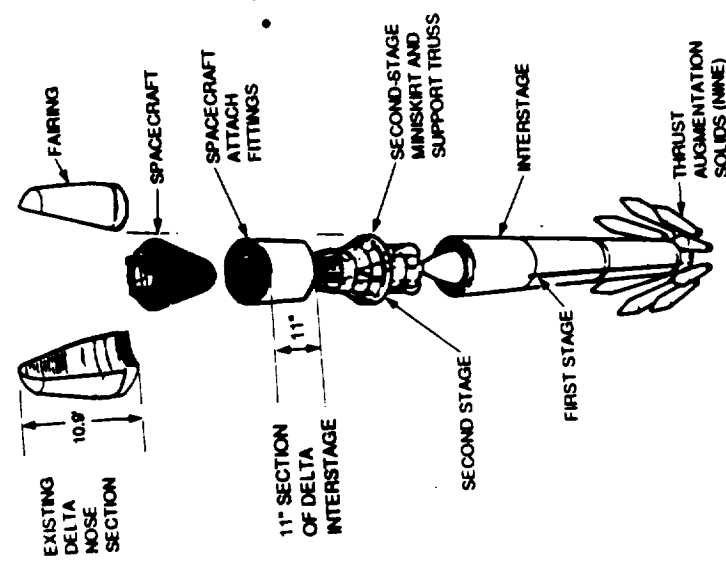


Figure 8-1. Key SAIC Design Features

The "Fail Operational" GNC/propulsion configuration (Table 8-1) provides an autonomous, decision-based, self-correcting de-orbit capability to ensure public safety both during normal operations and by precluding any viable possibility of an uncontrolled "dead vehicle" reentry. The restartable propulsion configuration also provides the capability to vary the orbit during a mission.

Table 8-1. Propulsion System Trade

Item	Pros	Cons	Comments
Solid Motor for De-Orbit Burn With Liquid Attitude Control System	Simple-Low Cost	Single Burn Single-Point Failure Requires High Spin Rate for Thrust Averaging (20-50 rpm) Impulse/Velocity Error of 0.5% High g Burn Not Flexible	Nonreusable Relies on Reliability Science Desires Not Met Major Contributor to Landing Inaccuracy Science Desires Not Met Changes of Motor Propellant Load Difficult to Perform in Timely Manner
All Liquid System	Flexible Multi-Burn System Highly Accurate Impulse Delivery Reusable Low g Deorbit	Higher Nonrecurring Cost	Trim Burn Capability Minimizes Landing Dispersion Errors

BASELINED LIQUID SYSTEM

**FAIL OPERATIONAL CONFIGURATION
MINIMIZES PUBLIC SAFETY CONCERNS**

The Global Positioning System is used for orbit determination, "any orientation" attitude determination, precision de-orbit control, and precision recovery via a gliding parachute and/or providing landing coordinates to within a fraction of a meter to the recovery forces.

The RRS can be mounted on a Delta launch vehicle, in either a single or dual configuration, using a modified version of the existing second stage interstage and fairing nose section. The dual

launch version can also be readily used for shared launches to minimize booster cost.

8.2 Conclusions

The basic conclusion of this study (Table 8-2) is that the SAIC design is a viable, effective means of fulfilling the NASA LifeSat requirements. Given SAIC's requirements driven approach, the RRS SRD did not create any significant design problems. Furthermore, the risk evaluation indicates that the design can mitigate all of the public safety concerns involved in a CONUS recovery operation.

Table 8-2. Conclusions

- RRS SRD DID NOT CREATE DESIGN PROBLEMS
- FAIL OPERATIONAL DESIGN MEETS PUBLIC SAFETY REQUIREMENTS FOR WHITE SANDS OPERATIONS
- VEHICLE DESIGN CAN PROVIDE
 - Controllable, Uniform Environment
 - Near-Free Space Radiation Spectrum
 - Exact 1 g Ground Control Experiment
 - Simple STS Mid-Deck Locker Use
 - Significant, Long Duration Power
 - Orbit Maneuver Capability
- BOOST — USE OF PROVEN BOOSTER HARDWARE
 - Single Launch — Delta to All Orbits
 - Radiation Mission Compatible
 - Dual Launch — Delta/Atlas — Primary Cost Saving
 - New, "Low Cost" Boosters Not Cost Effective

The vehicle design provides a highly flexible scientific environment for the investigation of radiation/gravity issues as well as a wide range of other life sciences and technology experimentation. The vehicle can virtually replicate the operating parameters of any centrifuge proposed for long mission space vehicles, and can accommodate specimens up to a small primate for such experimentation.

Although other boosters are potentially available, the use of the proven Delta/Atlas booster families provides the lowest cost per unit payload, and the proposed dual launch capability can reduce the per vehicle cost of the Delta to approximately the cost of the theoretically less expensive new boosters.

8.3 Recommendations

The primary recommendation (Table 8-3) is that key areas of the RRS SRD should be further quantified to more definitize the program requirements. Additional quantification of the public safety issue is especially critical since the safety requirements can be a major design driver and lack of agreement on those requirements represents a major cost/schedule risk. In addition, the vehicle requirements should be refined to reflect the degree of payload environmental uniformity required and the amount of vehicle shielding acceptable for the radiation experimentation. Any need for a single mission multi-orbit capability and/or missions beyond the current SRD requirements should be quantified. Last, but not least, the relative importance of development vice life cycle (and/or O&M) cost should be identified to permit the Phase C/D effort to be properly scoped.

Table 8-3. Recommendations

- KEY REQUIREMENTS ISSUES SHOULD BE CLEARLY SPECIFIED
- FAIL OPERATIONAL DESIGN SHOULD BE REQUIRED FOR PUBLIC SAFETY IN WHITE SANDS OPERATIONS
- VEHICLE REQUIREMENTS SHOULD SPECIFY
 - Payload Environment Uniformity
 - Acceptable Vehicle Shielding
 - Degree of Ground Control Experiment Replication
 - Simple STS Mid-Deck Locker Use
 - Significant, Long Duration Power
 - Orbit Maneuver Capability
 - Dual Launch and Elliptic Orbit Compatibility
 - Flexible Operations (Configuration/Mission)
 - Reliability
- MINIMIZE LIFE-CYCLE COST

8.4 Summary

In summary (Table 8-4), SAIC has determined that the unique split vehicle concept is a viable, science friendly, operationally flexible approach to meeting LifeSat and other recoverable experimentation requirements. Furthermore, the highly modularized design approach allows a parallel manufacturing (and refurbishment) flow that should minimize overall program cost. However, several key requirements need further quantification to ensure cost-effective development and operations efforts.

Table 8-4. Summary

- KEY SAIC FEATURES
 - Science Friendly, Operationally Flexible
 - Dual Launch, Inter-Orbit Maneuvering
- INTEGRATED MANAGEMENT APPROACH
 - SAIC — Payload, Overall System Integration
 - Fairchild — Vehicle Manufacture and Test
 - Subsystems — SAIC, Fairchild, and Others
- CONCLUSIONS — ALL REQUIREMENTS CAN BE MET
 - Safe and Flexible Operations
 - Parallel Manufacturing and Dual Launch Save Cost
- RECOMMENDATIONS — SPECIFY KEY REQUIREMENTS
 - Fail Operational Reentry for Public Safety
 - Science — Shielding Limits, Environment Uniformity
 - Operations — Flexibility, Power, Reliability